UNIVERSITY OF CALIFORNIA SAN DIEGO

# Copper, Culture, and Collapse: Modeling the Trajectory of Iron Age Copper Production in Faynan, Jordan

A dissertation submitted in partial satisfaction
of the requirements for the degree Doctor of Philosophy

in

Anthropology

by

Brady Liss

Committee in charge:

Prof. Thomas E. Levy, Chair
Prof. James M.D. Day
Prof. Paul S. Goldstein
Prof. Jürgen P. Schulze

2022

The dissertation of Brady Liss is approved, and it is acceptable in quality and form for publication on microfilm and electronically.

University of California San Diego

2022

DEDICATION

*To my mom and dad.*

# EPIGRAPH

I’m on the pursuit of happiness, and I know
Everything that shine ain’t always gonna be gold, hey.
I’ll be fine once I get it.
I’ll be good.

Scott Mescudi

TABLE OF CONTENTS

Dissertation Approval Page....iii

Dedication....iv

Epigraph....v

Table of Contents....vi

List of Figures....x

List of Tables....xviii

Acknowledgements....xx

Vita....xxiv

Abstract of the Dissertation....xxvii

Chapter 1 – Introduction....1
1.1 Research Questions and Goals....1
1.2 Research Approach and Methods....4
1.3 Chronology....6
1.4 Historical Context: The Late Bronze Age Collapse and Iron Age in the Southern Levant....7
1.4.1 The Late Bronze Age Collapse....8
1.4.2 Iron Age in the Southern Levant....10
1.4.3 Evidence of Edom in Ancient Texts....11
1.5 Outline of Dissertation....15

Chapter 2 – Theoretical Framework: Technology, Culture, and the Environment....20
2.1 Introduction....20
2.2 Anthropology of Technology....21
2.3 Anthropology of Production....25
2.4 The Culture System: Technology as a Subsystem of Culture....28
2.5 Social-Ecological Systems: Resilience Theory and the Adaptive Cycle....31
2.6 Pastoral Nomadism and Precarity: Copper Production as Adaptation and Exploitation (r to K) ....44
2.7 Overshoot: A Possible Explanation of Collapse (K to Ω) in the Archaeological Record....47
2.8 Copper, Culture, and Collapse?....51

Chapter 3 – Background: Faynan, Edom, and the Wadi Arabah in the Iron Age....53
3.1 Introduction....53
3.2 Geography – The Wadi Arabah, Faynan, and Edom....53

3.2.1 Geography of the Wadi Arabah and Faynan....53
3.2.2 Geography of Edom....56
3.3 Current and Past Climate of Faynan....59
3.4 The Geology of Faynan and its Implications for the Archaeological Record....65
3.5 History of Research....71
3.5.1 Early Explorations, Surveys, and Excavations in Faynan and Edom....71
3.5.2 Archaeology of Faynan: Surveys, Excavations, and Debates....75
3.5.3 Archaeometallurgical Research of Iron Age Faynan....82
3.5.4 Current Understandings of Copper Smelting in the Iron Age Wadi Arabah....85
3.6 Iron from Copper? Investigating the Origins of Iron Production in the Eastern Mediterranean....90
3.7 Summary: Foundations for the Current Research....99

Chapter 4 – Excavations of Iron Age Faynan....103
4.1 Introduction....103
4.2 Excavation Methods for the 2014 Season at Khirbat al-Jariya....107
4.3 Khirbat al-Jariya....111
4.3.1 Overview and Previous Research....111
4.3.2 The 2006 Excavation Season....113
4.3.3 The 2014 Excavation Season....117
4.3.3.1 Site Survey and Mapping....117
4.3.3.2 Area B – Building 2....120
4.3.3.3 Area C – Slag Mound....124
4.3.3.4 Slag Processing Installations....125
4.3.3.5 Radiocarbon Dates....127
4.3.3.6 Paleobotanical Analyses....129
4.3.3.7 Interpretation of Area B....129
4.3.3.8 Comparison of the Area A and Area C Slag Mounds....134
4.3.4 Summary....135
4.4 Khirbat en-Nahas....137
4.4.1 Previous Research....138
4.4.2 ELRAP Excavations at Khirbat en-Nahas....139
4.4.2.1 Area A – Fortress Gatehouse....140
4.4.2.2 Area T – Elite Residence and Tower....142
4.4.2.3 Area W – Residential and Storage Complex....143
4.4.2.4 Area F – Metallurgical Workshop....144
4.4.2.5 Area S – Slag Processing Workshop....147
4.4.2.6 Area R – Central Elite/Supervision Residence....149
4.4.2.7 Area M – Slag Mound Probe....153
4.5 Khirbat al-Ghuwayba....163
4.6 Other Iron Age Sites....167
4.6.1 Khirbat Faynan....167
4.6.2 Khirbat Hamra Ifdan....169
4.6.3 The Ras al-Miyah Fortresses and Archaeological Complex....172
4.6.4 Rujm Hamra Ifdan....174

4.6.5 Wadi Fidan 40....176
4.6.6 Wadi Dana 1....178
4.6.7 Ras en-Naqb and Barqa al-Hetiye....178
4.7 Relevant Mining Sites....179
4.8 Summary/Discussion....182

Chapter 5 – Analytical Examination of Iron Age Metal from Faynan: Methods and Results....186
5.1 Introduction and Research Questions....186
5.2 Isotope and Highly Siderophile Element Analysis of Iron Objects and Chunks....187
5.2.1 Introduction....187
5.2.2 Sample Selection....190
5.2.3 Methods....192
5.2.3.1 Scanning Electron Microscopy....192
5.2.3.2 Mass Spectrometry Analysis....193
5.2.4 Results....201
5.2.4.1 Copper Ores....201
5.2.4.2 Iron-Copper Chunk and Iron Object Compositions....202
5.2.4.3 SEM-EDX of Metal Chunks and Iron Objects....208
5.2.5 Discussion....212
5.2.6 Future Directions....220
5.3 Sediment Analysis for Iron Production Residues at Khirbat an-Nahas....221
5.3.1 Introduction....221
5.3.2 Sample Selection....224
5.3.3 Methods....228
5.3.3.1 Magnetic Collection....228
5.3.3.2 X-Ray Fluorescence....229
5.3.4 Results....232
5.3.4.1 Magnetic Material....232
5.3.4.2 X-Ray Fluorescence....236
5.3.5 Discussion....240
5.3.6 Future Directions....245
5.4 A Diachronic Analysis of Iron Age Copper Metal: Scanning Electron Microscopy....246
5.4.1 Introduction....246
5.4.2 Sample Selection....249
5.4.3 Methods....257
5.4.3.1 Scanning Electron Microscopy-Energy Dispersive X-Ray Spectroscopy....257
5.4.3.2 Limitations of SEM-EDX....261
5.4.4 Results....262
5.4.4.1 Copper Content in Prills....262
5.4.4.2 Other Elements in Copper Prills....281
5.4.4.3 Iron Inclusions....282
5.4.4.4 SEM-EDX and XRF Comparison....285
5.4.5 Discussion....288

5.4.6 Future Directions....296
5.5 Summary....297

Chapter 6 – Data Dissemination and Record Keeping: 3-D Modeling at Khirbat al-Jariya and Khirbat en-Nahas....301
6.1 Introduction....301
6.2 3-D Modeling at Khirbat al-Jariya....304
6.3 3-D Modeling at Khirbat en-Nahas....308
6.3.1 Methods and Workflow....311
6.3.2 Results and Discussion....314
6.4 Summary....322

Chapter 7 – Synthesis and Discussion: The Cycle and "Collapse" of Iron Age Copper Production in Faynan....324
7.1 Introduction....324
7.2 Release (Ω) in the Middle Bronze Age: 22nd-14th Centuries BCE....330
7.3 Reorganization (α) in the Late Bronze Age: 13th-Early 12th Centuries BCE....331
7.4 The Nested Hierarchy: Faynan and the Late Bronze Age Collapse as an Example of "Revolt" and "Remember"....332
7.5 Exploitation and Growth (r) in the Early Iron Age: 12th to Early 10th Centuries BCE....338
7.5.1 Explaining Growth in the r-phase: The Multiplier Effect and Political Economy....342
7.6 Transition from r to K: A Punctuated Leap or Gradual Growth?....346
7.7 Conservation and Consolidation (K) in the Iron Age: Late 10th to 9th Centuries BCE....348
7.7.1 Resilience and Rigidity: Copper production as a Rigidity Trap....350
7.8 Transition from K to Ω: Collapse or Abandonment?....353
7.8.1 Overshoot or Otherwise? Identifying the Triggering Agent....356
7.9 Release or "Collapse" (Ω) in the Late Iron Age: 8th Century BCE....360
7.10 A Failed Reorganization (α) in the Late Iron Age: 7th-6th Centuries BCE....363

Chapter 8 – Conclusion....366
8.1 Copper....366
8.2 Culture....369
8.3 Collapse....372

References....375

LIST OF FIGURES

**Figure 2.1:** Model of the human cultural system including subsistence, technology (craft production), symbolic, trade/communication, and social organization subsystems based on Renfrew 1972: Figure 21.1.....30

**Figure 2.2:** Diagram of the adaptive cycle (modeled after Holling and Gunderson 2002: Figure 2-1).....33

**Figure 2.3:** To display "resilience" in the adaptive cycle requires a three-dimensional model. Note that in the K phase (which precedes a collapse) connectedness and potential for change are high whereas resilience is low (modeled after Holling and Gunderson 2002: Figure 2-2).....35

**Figure 2.4:** Diagram of the "nested hierarchy" of adaptive cycles functioning on different scales of time and space with the interactions between them (modeled after Holling, Gunderson, and Peterson 2002: Figure 3-10).....42

**Figure 3.1:** Location of Faynan in modern Jordan on the northeastern side of the Wadi Arabah. Shaded relief base layer copyright Esri 2014. Map produced by Brady Liss.....54

**Figure 3.2:** Boundaries of Edom in the Iron Age following Rainey and Notley 2006: 162.....58

**Figure 2.3*:*** Rainfall data for modern Jordan. The average annual rainfall in Faynan is ca. 50-60 millimeters with significant seasonal variability. Rainfall data and layer from Fick and Hijmans 2017. Shaded relief base layer copyright Esri 2014. Map produced by Brady Liss.....61

**Figure 3.3:** Geology of Faynan in the immediate area around Khirbat en-Nahas, Khirbat al-Jariya, and Khirbat al-Ghuwayba. Note the presence of Dolomite Limestone Shale or Burj Dolomite-Shale (BDS) near the smelting sites.....67

**Figure 3.4:** The new chronology for biblical Edom and Faynan established through the work of the ELRAP in comparison to the old chronology based on Bennett's excavations (figure modeled after Levy et al. 2014: Figure 1.1). Some radiocarbon dates suggest an occupation at Khirbat en-Nahas prior to 1200 BCE, but they are less secure.....79

**Figure 4.1:** Map of the Iron Age industrial landscape in Faynan including all sites mentioned in the text.....104

**Figure 4.2:** Aerial photograph of Khirbat al-Jariya. Photograph credit: Rebecca Banks, APAAME 2015 (APAAME_20151013_REB-0107).....112

**Figure 4.3:** Area A excavations at Khirbat al-Jariya including the probe into a slag mound and Structure 276. Photograph credit: Thomas E. Levy, UCSD Levantine and Cyber Archaeology Lab.....114

**Figure 4.4:** Modeled radiocarbon dates from Khirbat al-Jariya Area A excavations. Uncalibrated and calibrated dates are available in Table 4.1.....116

**Figure 4.5:** Map of Khirbat al-Jariya produced in 2014 using the ELRAP balloon photography platform.....119

**Figure 4.6:** Building 2 at Khirbat al-Jariya following its excavation during the 2014 ELRAP season. Photograph credit: Matthew D. Howland, UCSD Levantine and Cyber Archaeology Lab.....121

**Figure 4.7:** Intentionally blocked doorways in the central north-south wall of Building 2 at Khirbat al-Jariya. Photograph credit: Thomas E. Levy, UCSD Levantine and Cyber Archaeology Lab.....122

**Figure 4.8:** Completed excavation probe into the Area C slag mound at Khirbat al-Jariya. Photo credit: Thomas E. Levy, UCSD Levantine and Cyber Archaeology Lab.....124

**Figure 4.9:** Bedrock mortars likely dedicated to slag crushing found north of Building 2 and associated with large mounds of crushed slag at Khirbat al-Jariya. Photograph credit: Thomas E. Levy, UCSD Levantine and Cyber Archaeology Lab.....126

**Figure 4.10:** Modeled radiocarbon dates from Khirbat al-Jariya Areas B and C. Uncalibrated and calibrated dates are available in Table 4.1 and Liss et al. 2020.....128

**Figure 4.11:** Aerial image of Khirbat en-Nahas with excavation areas labeled. Note the large square fortress on the right side of the photo and the significant amount of black slag mounds. Image credit: Matthew D. Howland, UCSD Levantine and Cyber Archaeology Lab.....137

**Figure 4.12:** Area A at Khirbat en-Nahas after excavation. Note the interior entrance into the fortress on the left side of the photograph was intentionally blocked. Photograph credit: Thomas E. Levy, UCSD Levantine and Cyber Archaeology Lab.....141

**Figure 4.13:** Area T at Khirbat en-Nahas after excavation. Photograph credit: Thomas E. Levy, UCSD Levantine and Cyber Archaeology Lab.....142

**Figure 4.14:** Area W at Khirbat en-Nahas after excavation including the structures and the alley separating them. The western structure is partially cut off by the edge of the photograph. Photograph credit: Thomas E. Levy, UCSD Levantine and Cyber Archaeology Lab.....144

**Figure 4.15:** Area F at Khirbat en-Nahas after excavation. Note the unique “cells” on the back wall, and the excavated portion of the fortress wall at the top of the photo. Photograph credit: Thomas E. Levy, UCSD Levantine and Cyber Archaeology Lab.....145

**Figure 4.16:** Modeled radiocarbon dates from Khirbat en-Nahas Area F. Uncalibrated and calibrated dates are available in Table 4.1 and Levy et al. 2014: 130-131.....146

**Figure 4.17:** Area S at Khirbat en-Nahas during excavation. The four-room structure is visible, along with the deposits of slag on the right and left sides of the photo. Photograph credit: Thomas E. Levy, UCSD Levantine and Cyber Archaeology Lab.....147

**Figure 4.18:** Modeled radiocarbon dates from Khirbat en-Nahas Area S. Uncalibrated and calibrated dates are available in Table 4.1 and Levy et al. 2014: 168-169.....148

**Figure 4.19:** Area R at Khirbat en-Nahas after excavation including the substantial building (center), metallurgical complex (bottom), and perimeter wall. Photograph credit: UCSD Levantine and Cyber Archaeology Lab.....149

**Figure 4.20:** The metallurgical complex of Area R at Khirbat en-Nahas with the large structure in the background. This area yielded a substantial number of mixed iron-copper chunks. Photograph credit: Thomas E. Levy, UCSD Levantine and Cyber Archaeology Lab.....151

**Figure 4.21:** Modeled radiocarbon dates from the metallurgical complex of Area R at Khirbat en-Nahas. Uncalibrated and calibrated dates are available in Table 4.1 and Levy et al. 2014: 223-228.....153

**Figure 4.22:** Area M at Khirbat en-Nahas after excavation. The completed excavation was over six meters in depth. The wall of the structure in Area M is visible on the bottom edge of the photo. Photograph credit: Thomas E. Levy, UCSD Levantine and Cyber Archaeology Lab.....154

**Figure 4.23:** Modeled radiocarbon dates from Khirbat en-Nahas Area M. Uncalibrated and calibrated dates are available in Table 4.1 and Levy et al. 2014: 150-151.....161

**Figure 4.24:** Aerial photograph of Khirbat al-Ghuwayba. The ELRAP excavations are visible in the center of the photo.....164

**Figure 4.25:** Aerial photograph of Khirbat Faynan. The substantial tel site (center) is primarily known as the largest Roman-Byzantine copper smelting site in Faynan but includes Iron Age slag mounds. Photograph credit: Dr. Robert Bewley, APAAME 2015 (APAAME_ 20151013_RHB-0032).....168

**Figure 4.26:** Aerial photograph of Khirbat Hamra Ifdan. The site is located atop an inselberg in the Wadi Fidan. Photograph credit: Rebecca Banks, APAAME 2015 (APAAME_ 20151013_REB-0040).....170

**Figure 4.27:** Aerial photograph of the Ras al-Miyah fortresses (center) and archaeological complex. Photograph credit: Dr. Robert Bewley, APAAME 2015 (APAAME_ 20151013_RHB0134).....172

**Figure 4.28:** Completed excavations at Rujm Hamra Ifdan. The completed lower probe is visible in the bottom right. Photograph credit: Thomas E. Levy, UCSD Levantine and Cyber Archaeology Lab.....176

**Figure 4.29:** Aerial photograph of Wadi Fidan 40 cemetery located along the Wadi Fidan (top of photo). Photograph credit: Rebecca Banks, APAAME 2015 (APAAME_20151013 _REB-0058).....177

**Figure 4.30:** Photograph of the Jabal al-Jariya Minefields. The depressions across the landscape are the remains of ancient mining pits. Photograph credit: Erez Ben-Yosef, UCSD Levantine and Cyber Archaeology Lab.....181

**Figure 5.1:** Representative materials analyzed for HSE abundances and osmium isotopes. (a) An iron-copper mixed chunk at Khirbat en-Nahas.....188

**Figure 5.2:** Locations of samples analyzed for HSE abundances and osmium isotopes. All iron objects and mixed iron-copper chunks originated from Khirbat en-Nahas, and one ore sample was analyzed from each of the labeled mining sites.....191

**Figure 5.3:** Rare earth element patterns for ore samples from the DLS normalized to conventional CI-chondrite (normalization values from McDonough and Sun 1995).....202

**Figure 5.4:** Normalized trace element diagram for iron from the mixed metal chunks and objects measured by LA-ICP-MS. CI-chondrite normalization from McDonough and Sun (1995). Figure produced by Dr. James M.D. Day.....203

**Figure 5.5:** Highly siderophile element abundance patterns for (a) iron from iron-copper chunks and (b) iron objects from the Khirbat en-Nahas site normalized to CI-chondrite composition.....205

**Figure 5.6:** Comparison of Re, Pd, Pt, Ru, Ir, and Os concentration measurements for objects (black symbols) and iron from iron-copper chunks (yellow symbols) using Isotope Dilution ICP-MS and N-TIMS versus LA-ICP-MS.....206

**Figure 5.7:** Rhenium-osmium isotope diagrams for (a) the full range of samples including chunks, objects, and ores and (b) expanded view for $^{187}Re/^{188}Os$ = <400 for objects (black circles), iron from chunks (yellow circles) and local DLS ores (unfilled circles).....208

**Figure 5.8:** SEM image of iron from chunk Sample 5636 with results of EDS analysis (presented in wt.%). The identification of iron-phosphide inclusions reiterates that the chunks were produced by smelting.....209

**Figure 5.9:** SEM image and associated EDS results (presented in wt.%) for iron-copper chunk Sample 680 with evidence for P-rich iron.....210

**Figure 5.10:** SEM image and associated EDS results (presented in wt.%) for iron-copper chunk Sample 16356. The presence of significant carbon is likely a product of peak overlap.....211

**Figure 5.11:** SEM image and associated EDS analysis (presented in wt.%) from sample 7179. The results support a reinterpretation of this object as potentially a mixed iron-copper chunk (although there was no visible copper) or other waste product. The sample contains only inclusions of iron-oxides and a low iron content.....212

**Figure 5.12:** Methodology for collecting magnetic material from a sediment sample. The sample is spread into a thin layer and the magnet is dragged through the sediment to collect any magnetic material. Photograph credit: Brady Liss, UCSD Levantine and Cyber Archaeology Lab.....229

**Figure 5.13:** Magnetic collection from sediment Sample 1256, Area F, Khirbat en-Nahas. Note the abundant amount of magnetic material including bits of slag and other material. Photograph credit: Brady Liss, UCSD Levantine and Cyber Archaeology Lab.....233

**Figure 5.14:** Representative slag prills and possible hammerscales collected with the magnet from Areas F, R, and S at Khirbat en-Nahas. Note that the scale on the bottom image is 0.5 centimeter and 1 centimeter in the top images.....236

**Figure 5.15:** Overlay of all XRF spectra for analyzed possible hammerscales and slag prills from Area F (n=6). Note the dominant iron peak for all samples; the smaller peak between iron and copper is a secondary iron peak (see also Table 5.9).....239

**Figure 5.16:** Overlay of all XRF spectra for analyzed possible hammerscales and slag prills from Area R (n=11). Note the dominant peak varies between manganese and iron (see also Table 5.9).....239

**Figure 5.17:** A slag prill collected from Area S sediment Sample 5993 along with its XRF spectrum. While magnetic, the iron peak is small, and almost entirely hidden by the manganese peaks.....240

**Figure 5.18:** The basin (left) and an associated stone installation (right) from Cell 9 in Area F. A fragment of a bellow pipe (a unique material culture of Area F) can be seen just above the basin (white arrow).....242

**Figure 5.19:** Section drawing and orthophoto of the southern section in the Area M slag mound at Khirbat en-Nahas. The red labels are samples analyzed as part of this research.....250

**Figure 5.20:** Section drawing and orthophoto of the eastern section in the Area M slag mound at Khirbat en-Nahas. The red labels are samples analyzed as part of this research.....252

**Figure 5.21:** Section drawing of the northern section in the Area A slag mound at Khirbat al-Jariya. The red labels are samples analyzed as part of this research. Section drawing modified from Ben-Yosef 2010: 5.67a.....254

**Figure 5.22:** Section drawing of the northern section in the Area A slag mound at Khirbat al-Jariya. The red labels are samples analyzed as part of this research. Section drawing modified from Ben-Yosef 2010: 5.65a.....255

**Figure 5.23:** Image of a slag sample using the scanning electron microscope showing the charging phenomenon. The bright white streaks represent sample charging, making imaging and analysis impossible.....256

**Figure 5.24:** Representative SEM image of a slag sample (Sample 3278 from Khirbat al-Jariya, Area A) with copper prills (bright white circles). The backscatter sensor shows elements with higher atomic numbers as brighter. Images of every sample are available upon request from the author.....259

**Figure 5.25:** Image of an SEM-EDX point analysis on a copper prill (orange crosshairs). Points were analyzed from the center of the prills to keep the interaction volume within the prill.....260

**Figure 5.26:** Graph of the average copper content in prills per slag sample from Area M at Khirbat en-Nahas.....276

**Figure 5.27:** Graph of the average copper content in prills per slag sample from Area A at Khirbat al-Jariya.....277

**Figure 5.28:** Graph of the average copper content in prills by stratigraphic context in Area M at Khirbat en-Nahas. Vertical error bars represent the standard deviation of copper content.....278

**Figure 5.29:** Graph and associated data table of the average copper content in prills by context and Production Phase following the model developed by Ben-Yosef et al. 2019.....279

**Figure 5.30:** SEM image showing a copper prill encapsulated within a copper-sulfide inclusion (Sample 3281, Area A, Khirbat al-Jariya).....280

**Figure 5.31:** Graph of the average iron content in prills by stratigraphic context in Area M at Khirbat en-Nahas.....282

**Figure 5.32:** SEM image of an iron prill from Sample 10314, Area C, Khirbat al-Jariya. The prill contained 89.45 wt.% Iron.....283

**Figure 5.33:** Line fit plots for the copper content in prills (SEM-EDX) and bulk composition elements of slags (XRF) – A) Copper, B) Iron, C) Calcium, and D) Silicon.....288

**Figure 6.1**: Screenshot of the Khirbat al-Jariya Area C slag mound probe model. The stratigraphy is clearly visible showing the layers of crushed slag at the bottom, an occupation horizon (note the pottery sherd), and uppermost layer of large slag fragments. Model by Brady Liss and photography by Thomas E. Levy.....305

**Figure 6.2:** Screenshot of Khirbat al-Jariya Area C model produced using the balloon photography system. The model captures the entire slag mound and the modern mining road cutting its northern edge, providing context for the excavation probe (also visible). Photography by Matthew D. Howland and model produced by Kendra Scheer.....306

**Figure 6.3:** Screenshot of a model of a crushed slag mound on the southeastern outskirts of Khirbat al-Jariya (Locus 523). A bedrock mortar filled with crushed slag is visible in the center of the model (arrow). Photography by Thomas E. Levy and model produced by Kendra Scheer.....307

**Figure 6.4:** Photograph of the collapsed Area M excavation at Khirbat en-Nahas in 2014. Photograph credit: Brady Liss.....308

**Figure 6.5:** Screenshot of the 3-D model of Khirbat en-Nahas from 2014. For scale, the large square fortress on the left side of the models is ca. 73x73 meters. The photographs were taken using the ELRAP balloon platform. Photography and model by Matthew D. Howland.....310

**Figure 6.6:** Screenshot of the Area M and Khirbat en-Nahas site model being aligned in Blender (free to use, 3-D model editing software).....313

**Figure 6.7:** Screenshot of Khirbat en-Nahas Area M 3-D model produced using the original excavation photographs. Photography by the UCSD Levantine and Cyber Archaeology Lab and model produced by Brady Liss and Matthew D. Howland.....314

**Figure 6.8:** Orthophotographs of the south (left) and east (right) sections of the Area M slag mound excavation at Khirbat en-Nahas.....316

**Figure 6.9:** Comparison of Area M in the site model before (left) and after (right) the new Khirbat en-Nahas Area M model was integrated, and the collapsed portion was removed.....318

**Figure 6.10:** Screenshot of SketchFab showing the position and height of the viewer when they enter the virtual reality view on the Khirbat en-Nahas Area M model. This position orients the viewer towards the archaeological record and maintains a realistic experience by "standing" on the ground and looking down into the excavation.....319

**Figure 6.11:** Screenshot of SketchFab showing the Khirbat en-Nahas Area M model with added annotation providing a link to the original section drawing. The annotation is selected so the model automatically oriented to view the section.....321

**Figure 7.1:** The complete adaptive cycles for the Middle Bronze to Late Iron Ages for society and copper production in Faynan. The red arrows represent the "beginning" and "end" of the cycles from the perspective of this research. See Chapter 2 and Table 2.1 for detailed descriptions of each phase.....326

**Figure 7.2:** The "nested hierarchies" of adaptive cycles situating the social-ecological system of Faynan in a larger geographical and temporal context in the Late Bronze and Early Iron Ages.....334

LIST OF TABLES

**Table 1.1:** Local Iron Age chronology of ancient Jordan following Herr and Najjar 2001.....7

**Table 2.1:** Descriptions of the phases of the adaptive cycle along with their associated properties (connectedness, potential, and resilience). Table is modeled after Méndez et al. 2005: Table 2 and Holling and Gunderson 2002.....36

**Table 4.1:** Complete list of all radiocarbon dates collected from contexts excavated or sampled as part of this research.....105

**Table 4.2:** Complete stratigraphy for the 2006 and 2014 excavations at Khirbat al-Jariya with associated radiocarbon dates.....130

**Table 4.3:** Complete stratigraphy of the Area M slag mound excavation at Khirbat en-Nahas. Includes correlation between the 2002 and 2006 excavations. Table modeled off Levy et al. 2014: Table 2.8.....157

**Table 5.1:** Archaeological details for isotope analysis samples.....190

**Table 5.2:** Elemental composition of the ore samples from Faynan – WAG-57, WAJ-458, and JAJ-1 – and standard rock reference materials (BHVO-2, BCR-2, and BIR1a) in parts per million (ppm) .....195

**Table 5.3**: Blank measurements for HSE abundances and their percentage contribution to the sample measurements.....197

**Table 5.4:** Results in parts per million (ppm) of the Laser Ablation-ICP-MS analysis of artifacts, iron-copper chunks, and standard reference materials.....199

**Table 5.5:** Comparison between Isotope Dilution (ID) and Laser Ablation ICP-MS (LA-ICP-MS) analysis in parts per billion (ppb).....204

**Table 5.6:** Highly siderophile element abundance (in parts per billion - ppb) and Re-Os isotope systematics of Faynan samples.....207

**Table 5.7:** Archaeological details for sediment samples analyzed for iron production residues. FX and FLOT are codes used by ELRAP excavations to designate a sediment sample collected for flotation.....226

**Table 5.8:** The weight (Wt.) of magnetic material collected from all analyzed sediment samples and the magnetic percentage = magnetic weight/total sample weight. Note that the total weight is presented in kilograms and the magnetic weight in grams (total weight was converted to grams for determining the magnetic percentage).....234

**Table 5.9:** Net photon counts from XRF analysis of representative hammerscales and prills collected from Khirbat en-Nahas sediment samples. Photon counts provide semi-quantitative amounts for the elements present in the sample. The letter under the element symbol is the electron shell.....237

**Table 5.10:** Analyses of copper metal from Iron Age Faynan by Hauptmann (2007: Table A17 and Hauptmann et al 1992: Table 6).....248

**Table 5.11:** SEM-EDX results for copper prills in the slag thin-sections. All results are presented in weight%.....264

**Table 5.12**: The average and standard deviation copper content of all prills per sample analyzed with SEM-EDX All results are presented in weight%.....272

**Table 5.13**: The average and standard deviation copper content of all prills analyzed with SEM-EDX by stratigraphic layer. All results are presented in weight%.....275

**Table 5.14:** SEM-EDX results for iron prills and inclusions in the slag thin-sections. All results are presented in weight%.....284

**Table 5.15:** Pearson Correlation Coefficient for the elemental contents of slags analyzed by XRF (Ben-Yosef et al. 2019: Table S3) and the Copper content of prills from the same samples analyzed by SEM-EDS.....286

**Table 7.1:** Descriptions of each phase of the adaptive cycles for the social-ecological system of Faynan along with their archaeological evidence and correlation to Ben-Yosef's phases of copper production.....328

ACKNOWLEDGEMENTS

Throughout my academic experience, I have been very fortunate to research, work, discuss, and become friends with many people that directly and indirectly contributed to this project. While I am the sole author of this dissertation, it would not have been possible without their help and support, and I am grateful to each of them.

First and foremost, I want to thank my advisor and committee chair Dr. Thomas E. Levy. Tom quite literally made this research possible and shaped my development as a scholar. When applying to graduate school, Tom was one of the only professors who responded to my inquiring email, and his support has been unwavering since then. His constant availability and dedicated guidance were essential in making my graduate experience intellectually fulfilling. Tom created an ideal balance of the necessary freedom for me to explore and develop original ideas and thinking while also providing encouragement and guidance to make this project possible and worthwhile. I will always look to Tom as a mentor.

Similarly, I need to thank the rest of my committee, Dr. James Day, Dr. Paul Goldstein, and Dr. Jürgen Schulze, for all their support and dedication to my research. This dissertation would not have been possible without their guidance and input. Through classes, meetings, research collaborations, emails, and casual conversations, they opened my eyes to new ways of thinking and exploring archaeology. Their influence is weaved throughout all aspects of this research, from the methods to the theoretical perspectives.

I am truly indebted to Dr. Erez Ben-Yosef. Erez played a critical role throughout my graduate education at UCSD. Following Tom, Erez was one of the first people I spoke to about my research as a first-year student – a conversation which provided foundational ideas for this dissertation years later. Erez generously hosted me in his lab at Tel Aviv University allowing me

to begin my investigations into the relationships between copper and iron which is further explored here. Working with Erez on a research article was a wonderful and insightful experience, and I can confidently say it helped make me the scholar I am today.

A very special thank you is necessary for Dr. Ann Killebrew. Dr. Killebrew introduced me to the world of Levantine archaeology and provided the opportunity for my first field experience at Tel Akko. Between classes at Penn State and four excavation seasons at Akko, Dr. Killebrew was truly a mentor and guided me in pursuing a graduate education in archaeology. I still remember the meeting in her office when she suggested reaching out to Tom and applying to UCSD. Without her, I would not be where I am today, and I owe her my deepest gratitude.

During my second excavation season at Tel Akko, I was introduced to archaeometallurgy for the first time under the guidance of Dr. Adi Eliyahu-Behar, a pivotal moment in my interest in archaeology. Adi graciously welcomed me at the Weizmann Institute for two weeks of archaeometallurgical research, and I haven't looked back since. Adi continued to provide invaluable opportunities throughout graduate school including participation in her iron metallurgy workshop and a research fellowship. She has been a kind and formative mentor as well as an intellectual role model. Thank you for everything.

I also want to thank all the members of the UCSD Levantine and Cyber Archaeology Lab for not only all their help and support in my education and research but also their friendship. The countless conversations in the lab and elsewhere shaped my graduate school experience. Thank you to Dr. Kyle Knabb, Dr. Aaron Gidding, Dr. Ian Jones, Dr. Sowparnika Balaswaminathan, Kathleen Bennallack, Craig Smitheram, Anthony Tamberino, Jackson Reece, Loren Clark, and Andrew Johnson.

Also, thanks to Dr. Barbara Porter of the American Center of Oriental Research (ACOR)

in Amman and Dr. M. Jamhawi, Director General of the Department of Antiquities of Jordan. Without the generous opportunity for research collaboration and loaning of materials from the Department of Antiquities, this research would have been impossible.

Thank you to the people of Faynan and Qirayqira. Not only for their essential assistance in the field and lab, but for their hospitality and kindness to a stranger.

All the fieldwork and materials analyzed for the dissertation were part of the UC San Diego-Department of Antiquities of Jordan Edom Lowlands Regional Archaeology Project (ELRAP), directed by Thomas E. Levy and Mohammad Najjar. I am grateful to both of them for the kind permission to use materials from ELRAP projects in this research.

I would also like to thank the staff at Nano3 – Dr. Ryan Nicholl, Dr. Jeff Wu, Marquez Balingit, and Natalie Toon – for all their training and assistance with the SEM. I similarly need to thank Scott McAvoy of the UCSD Library for his critical and substantial help with the 3D visualization components of this research.

Thank you to the UCSD Department of Anthropology staff – Veri Chavarin, Nikki Gee, Debbie Kelly, and Nancy Lee.

A special thank you to Matt Howland. From Penn State to UCSD and beyond, you have been a mentor, a colleague, a collaborator, a peer, but most importantly, a friend. My graduate school experience truly would not have been the same without your friendship (and Mindy's).

Finally, thank you to my parents, brothers, and friends. This work was only made possible through your love and support. And, of course, Ellen. Through thick and thin, highs and lows, you carried me through this process.

My research has received generous support from a number of sources: the UCSD Jewish Studies Program Katzin in Perpetuity (KIP) Fellowship, the Wenner-Gren Foundation

(Dissertation Fieldwork Grant - #9872), the Rust Family Foundation (Archaeology Grant - RFF-2019-87), the National Science Foundation Integrative Graduate Education and Research Traineeship – Training, Research and Education in Engineering for Cultural Heritage Diagnostics (IGERT-TEECH - #DGE-0966375), and the UCSD Department of Anthropology (Graduate Student Research Fellowship, F.G. Bailey Dissertation Research Fellowship, and George G. Haydu Prize for the Study of Culture, Behavior, and Human Values).

With all of that said, any errors in the present work must be attributed to only me.

Chapter 4, in part, is a reprint of the material as it appears in Brady Liss, Matthew D. Howland, Brita Lorentzen, Craig Smitheram, Mohammad Najjar, and Thomas E. Levy 2020 Up the Wadi: Development of an Iron Age Industrial Landscape in Faynan, Jordan. *Journal of Field Archaeology* 45(6): 413-427. The dissertation author was the primary investigator and author of this paper.

Chapter 5, in part, is a reprint of the material as it appears in Brady Liss, Thomas E. Levy, and James M.D. Day 2020 Origin of Iron Production in the Eastern Mediterranean: Osmium isotope and highly siderophile element evidence from Iron Age Jordan, *Journal of Archaeological Science* 122: 105227. The dissertation author was the primary investigator and author of this paper.

## VITA

| | |
|---|---|
| 2012 | Bachelor of Arts, Classics and Ancient Mediterranean Studies, Pennsylvania State University |
| 2012 | Bachelor of Science, Archaeological Sciences, Pennsylvania State University |
| 2015 | Master of Arts, Anthropology, University of California San Diego |
| 2017 | Candidate of Philosophy, Anthropology, University of California San Diego |
| 2022 | Doctor of Philosophy, Anthropology, University of California San Diego |

## PUBLICATIONS

Levy, Thomas E., Brady Liss, Ho Jung S. Yoo, Ioannis Liritzis, and Margie M. Burton
2022 From the Field to the CAVE: a Workflow for Collecting, Storing and Sharing Archaeological Data. In *Preserving Cultural Heritage in The Digital Age: Sending Out an S.O.S*, edited by Nicola Lercari, Willeki Wendrich, Benjamin W. Porter, Margie M. Burton, and Thomas E. Levy, pp. 57-78. Equinox, Sheffield and Bristol.

Liss, Brady, Thomas E. Levy, and James M.D. Day
2020 The Origin of Iron Production in the Eastern Mediterranean: Osmium isotope and highly siderophile element evidence from Iron Age Jordan. *Journal of Archaeological Science* 122: 105227.

Howland, Matthew D., Brady Liss, Mohammad Najjar, and Thomas E. Levy
2020 Integrating Digital Datasets into Public Engagement through ArcGIS StoryMaps. *Advances in Archaeological Practice* 8(4): 351-360.

Liss, Brady, Matthew D. Howland, Brita Lorentzen, Craig Smitheram, Mohammad Najjar, and Thomas E. Levy
2020 Up the Wadi: Development of an Iron Age Industrial Landscape in Faynan, Jordan. *Journal of Field Archaeology* 45(6): 413-427.

Levy, Thomas E. and Brady Liss
2020 *Cyber-archaeology*. In *Encyclopedia of Global Archaeology*, edited by C. Smith. Springer New York.

Ben-Yosef, Erez, Brady Liss, Omri Yagel, Ofir Tirosh, Mohammad Najjar, and Thomas E. Levy
2019 Ancient technology and punctuated change: Detecting the emergence of the Edomite Kingdom in the Southern Levant. *PLoS ONE* 14(9): e0221967.

Liss, Brady and Thomas E. Levy
2018 Metallurgy in the World of the Bible. In *Behind the Scenes of the Old Testament:*

*Cultural, Social, and Historical Contexts*, edited by Jonathan S. Greer, John W. Hilber, and John H. Walton, pp. 438-445. Baker Academic, Grand Rapids.

Levy, Thomas E., A. Sideris, Matthew D. Howland, Brady Liss, G. Tsokas, P. Tsourlos, G. Vargemezis, A. Georgopoulos, E. Stambolidis, I. Fikos, Georg Papatheodorou, M. Garaga, D. Christodoulou, Richard D. Norris, Isabel Rivera-Collazo and Ioannis Liritzis
2017 At-Risk World Heritage, Cyber, and Marine Archaeology: The Kastrouli – Antikyra Bay Land and Sea Project, Phokis, Greece. In *Cyber-Archaeology and Grand Narratives - Digital Technology and Deep-Time Perspectives on Culture Change in the Middle East*, edited by T. E. Levy and I. W. N. Jones, pp. 143-234. Springer New York.

Liss, Brady and Samantha Stout
2017 Materials Characterization for Cultural Heritage: XRF Case Studies in Archaeology and Art. In *Heritage and Archaeology in the DigitalAge: Acquisition, Curation, and Dissemination of Spatial Cultural Heritage Data*, eds. by Matthew L. Vincent et al., 49-65. Springer International.

Liritzis, Ioannis, George Pavlidis, Spyros Vosniakis, Anestis Koutsoudis, Pantelis Volonakis, Matthew D. Howland, Brady Liss, and Thomas E. Levy
2017 Delphi4Delphi: Data Acquisition of Spatial Cultural Heritage Data for Ancient Delphi, Greece. In *Heritage and Archaeology in the DigitalAge: Acquisition, Curation, and Dissemination of Spatial Cultural Heritage Data*, eds. by Matthew L. Vincent et al., 151-165. Springer International.

Liss, Brady, Matthew D. Howland, and Thomas E. Levy
2017 Testing Google Earth Engine for the automatic identification and vectorization of archaeological features: A case study from Faynan, Jordan. *Journal of Archaeological Science: Reports.* 15: 299-304.

Sideris, Athanasios, Ioannis Liritzis, Brady Liss, Matthew D. Howland, and Thomas E. Levy
2017 At-Risk Cultural Heritage: New Excavations and Finds from the Mycenaean Site of Kastrouli, Phokis, Greece. *Mediterranean Archaeology and Archaeometry* 17(1):271-285.

Liritzis, Ioannis, George Pavlidis, Spyros Vosynakis, Anestis Koutsoudis, Pantelis Volonakis, Nikos Petrochilos, Matthew D. Howland, Brady Liss, and Thomas E. Levy
2016 Delphi4Delphi: first results of the digital archaeology initiative for ancient Delphi, Greece. *Antiquity* 90(354): 1-6.

Levy, Thomas E., Mohammad Najjar, Brady Liss, Matthew D. Howland, Craig Smitheram, and Neil Smith
2016 Khirbat al-Jariya. *American Journal of Archaeology: Archaeology in Jordan Newsletter* 120(4): 654-655.

Liss, Brady and Thomas E. Levy
2015 One Man's Trash: Using XRF to Recreate Ancient Narratives from Metallurgical

Waste Heaps in Southern Jordan. In *Proceedings of the 2015 Digital Heritage International Conference (Volume 1)*, eds. by Gabriele Guidi et al., 27-34. IEEE.

Howland, Matthew D., Brady Liss, Mohammad Najjar, and Thomas E. Levy
2015 GIS-Based Mapping of Archaeological Sites with Low-Altitude Aerial Photography and Structure from Motion: a Case Study from Southern Jordan. In *Proceedings of the 2015 Digital Heritage International Conference (Volume 1)*, eds. by Gabriele Guidi et al., 91-94. IEEE.

ABSTRACT OF THE DISSERTATION

Copper, Culture, and Collapse: Modeling the Trajectory of Iron Age Copper Production in Faynan, Jordan

by

Brady Liss

Doctor of Philosophy in Anthropology

University of California San Diego, 2022

Professor Thomas E. Levy, Chair

During the Iron Age (ca. 1200-800 BCE), society in the Faynan region of southern Jordan experienced intertwined technological and cultural revolutions, transforming from opportunistic copper production by segmentary tribes of pastoral nomads to industrial-scale metallurgy connected to a regional polity. Previous research in Faynan identified a pinnacle in metallurgy in terms of scale and efficiency during the 10$^{th}$-9$^{th}$ centuries BCE; yet these advancements were followed by an abrupt industry abandonment by the end of the 9$^{th}$ century BCE with no associated evidence of natural or human intervention such as drought or warfare. Furthermore, while Iron Age Faynan and its copper industry have been the subject of numerous studies and

publications, most previous archaeometallurgical research has focused on slag (the waste byproduct of metal production), other components of the metallurgical *chaîne opératoire*, or only included limited investigations concerning the actual metal. This dissertation aims to fill these scholarly lacunae by investigating the final phases of copper smelting in Iron Age Faynan from the perspective of the metal produced to test if a failure in the metallurgical industry drove a societal collapse. To do so, a combination of theoretical perspectives from anthropology, ecology, and sociology is applied to an original dataset produced using methods from the social, natural, and computer sciences. At the core of this dissertation is the application of the adaptive cycle from Resilience Theory to construct a holistic model of the trajectory of society and copper production across the entire Iron Age sequence with particular emphasis on its "collapse" phase. Using archaeological excavation, scanning electron microscopy and mass spectrometry, this possible "collapse" was investigated with a robust dataset of elementally analyzed copper and iron metal from Khirbat al-Jariya and Khirbat en-Nahas, two of the largest Iron Age copper smelting centers in Faynan. Together, the analytical results and the theoretical approach reveal a "collapse" in the Iron Age social-ecological system of Faynan that was likely driven by socio-economic factors in the greater Eastern Mediterranean rather than internal disruptions to the metallurgical industry.

# Chapter 1 – Introduction

## 1.1 Research Questions and Goals

As a field of study, anthropological archaeology generally explores transformations in human society and culture. Along with the origins of social complexity, societal collapse is one such transformation of particular interest. Understanding how and why societies collapse is critical for both interpreting the archaeological record and analyzing trends in modern society. This dissertation examines the possible relationship between anthropogenic natural resource degradation/depletion and societal collapse through an archaeological case study in the Faynan region of modern Jordan. Faynan offers a rich archaeological record spanning the Neolithic to Islamic Periods, but during the Iron Age (ca. 1200-800 BCE), society in Faynan witnessed intertwined technological and cultural revolutions, transforming from opportunistic copper production by segmentary pastoral nomadic tribes to industrial-scale metallurgy connected to a regional polity - the biblical Edomites (Levy, Najjar, and Ben-Yosef 2014). Previous research identified a pinnacle in metallurgy in terms of scale and efficiency during the $10^{th}$-$9^{th}$ centuries BCE; yet these advancements were followed by an abrupt industry abandonment by the end of the 9th century BCE with no associated evidence of human or natural intervention such as warfare or drought (Ben-Yosef 2010). It is hypothesized here that society in Faynan's significantly developed metallurgical technologies over-exploited diminishing copper ores during the Iron Age, causing a failure of metallurgy, a subsequent breakdown of economic networks, and a societal collapse – leading to a return to more predominantly pastoral nomadic lifeways.

This dissertation aims to address three interrelated research questions in pursuit of understanding the abandonment of copper smelting in Faynan during the $9^{th}$ century BCE:

1. Can the depletion or degradation of copper ores be identified in the archaeological record of Iron Age Faynan?
2. How does the appearance of iron artifacts in the archaeological record of the 10th-9th centuries BCE contribute to current understandings of metal production during this final phase?
3. Should the abandonment of copper smelting in Iron Age Faynan be interpretated as a "collapse"?

To address these questions, this dissertation combines a new theoretical lens with an original and robust dataset to investigate four inter-linked hypotheses: 1) the advanced metallurgical technologies of the 10-9th centuries BCE degraded/exhausted copper ore resources in Faynan; 2) the iron artifacts from this period represent a local and developmental production of the metal, perhaps to supplement the copper industry; 3) diminishing returns from the copper smelting industry strained economic connections between Faynan and agricultural settlements/societies reducing imports of critical subsistence goods and wealth finance which supported the political economy and culture system; and 4) economic breakdowns rendered the cultural system in Faynan generally unsustainable due to the harsh terrain and climate of the region causing a return or "collapse" to mainly pastoral nomadism (evidenced by the abandonment of major smelting sites). In other words, this research suggests the collapse of the metallurgical industry was a catalyst for a societal collapse in Faynan rather than a consequence.

Specifically, this research draws on Resilience Theory and the "adaptive cycle" for a more nuanced approach to collapse (Holling and Gunderson 2002). Resilience Theory highlights the dynamic integration/interactions between humans and the environment and treats collapse as a "transformation" in a complex system, avoiding catastrophic biases that associate collapse with

destruction and/or population loss (Gunderson and Holling 2002; Redman 2005; Faulseit 2016a). However, the mechanisms and processes of collapse need to be identified and grounded in archaeological evidence within specific systems and cycles. To do so, this dissertation explores the "overshoot" paradigm which connects societal collapse with exhaustion of essential resources (Catton 1980; Malthus 1798; Rees 2002). Overshoot has proliferated in scholarly literature since first proposed by Malthus (1798), but few (if any) concrete archaeological examples exist, partially due to the difficulties in identifying natural resource depletion in the archaeological record (Tainter 2006; cf., Redman 2005: 74-75). Faynan can potentially function as a case study to substantiate overshoot as a possible cause of collapse in any number of contexts (both Old and New World) in a "case-by-case situation" as suggested by Redman (2005: 75). Finally, perspectives are drawn from the anthropology of technology (Lechtman and Steinberg 1979; Pfaffenberger 1988, 1992; Lemonnier 1986, 1992; Hamilton 1996), the culture system model (Renfrew 1972; Binford 1965), and political economy (Hirth 1996; Brumfiel and Earle 1987) to investigate the intersection of technology (metallurgy) and the social, political, and economic trajectory of Iron Age Faynan.

These theoretical approaches are applied to an original analytical dataset. The potential collapse of society in Faynan is investigated here from the perspective of the metal produced during the Iron Age. First, an innovative methodology combining slag thin-sections and scanning electron microscopy is used to elementally analyze copper metal from Faynan which will function as a proxy for evaluating copper ore quality and availability. Second, the iron artifacts from Faynan are investigated using a suite of mass spectrometry methodologies to test if excavated iron objects were locally produced or imported. Iron artifacts from Faynan can contribute to current understandings of both metallurgical technologies and economic

connections. Investigation of iron production in Faynan is supplemented with an analysis of sediments collected from copper smelting sites to test for characteristic residues of iron smelting/smithing. In following, this dissertation contributes to three standing scholarly lacunae concerning of the Iron Age copper smelting industry in Faynan: 1) the copper metal actually produced during the Iron Age is largely understudied and limited to only a few analyses (Hauptmann 2007; Ben-Yosef 2010); 2) the excavated iron materials are currently enigmatic as they were only briefly analyzed by Ben-Yosef (2010) and lack systematic investigation; and 3) the abandonment of the industry at the end of the Iron Age has not been considered from the perspective of natural resource depletion and does not have a clear explanation.

## 1.2 Research Approach and Methods

This dissertation combines a variety of research methods from the social, natural, and computer sciences to investigate the archaeological record, analyze collected material culture, and share the produced data. First, new excavations were conducted at Khirbat al-Jariya, an Iron Age copper smelting center in Faynan, as part of the Edom Lowlands Regional Archaeology Project (ELRAP – directed by Thomas E. Levy and Mohammad Najjar) for this research. The excavations included an exploratory probe into a slag mound (the waste byproduct from smelting) at the site which provided samples for this dissertation. Critically, to investigate metallurgical transitions and developments in Faynan, the ELRAP previously excavated large slag mounds at Khirbat al-Jariya and Khirbat en-Nahas, the largest Iron Age copper smelting site. Additional materials from these excavations afforded a larger sample collection of slag with a greater chronological and geographical extent. All the slag mound excavations discovered bedrock, and they were dated with radiocarbon samples (Levy, Ben-Yosef, and Najjar 2014).

The radiocarbon results span the 12th-9th centuries BCE suggesting the slag mounds represent a complete record of metallurgical activity during the Iron Age.

These slag mound excavations provided a chronological scaffold for the selection and analysis of slag samples. This dissertation uses an innovative methodology combining the slag mound excavation with thin-sectioning and scanning electron microscopy (SEM) to expose and elementally analyze copper prills trapped within slag. As prills are often microscopic, slags were sectioned, mounted in epoxy, and polished to cleanly expose the copper droplets for microscopy (Eliyahu-Behar et al. 2012). Scanning electron microscopes offer a powerful combination of high magnification with spot elemental analysis; an ideal functionality for examining the chemical composition of copper prills. Each slag sample was sectioned and inspected with the SEM to analyze all identifiable prills. The elemental analysis in combination with stratigraphic excavation provides a diachronic record of copper purity through the Iron Age, reflecting ore quality/availability.

While copper was the primary metal produced in Faynan, the iron artifacts of the 10th-9th centuries BCE raise questions of possible iron production or exchange. Iron artifacts in the Faynan region were excavated at Khirbat en-Nahas in the form of mixed copper-iron chunks (amorphous conglomerates of what appeared to be a mixture of the two metals) and select iron objects (small pins/rods and possible arrowheads) (Ben-Yosef 2010; Levy et al.2014). Here, iron from both the chunks and objects was analyzed with mass spectrometric methods to determine their isotopic signatures and highly siderophile element abundances. Osmium isotope analysis is a cutting-edge method for iron provenance, and it is used here to determine if the mixed copper-iron chunks were purified to extract iron and produce objects, or if the iron objects represent a medium of exchange (Liss, Levy, and Day 2020). To further investigate possible iron

production, sediment samples collected from Khirbat en-Nahas were examined for magnetic residues. Iron production results in magnetic materials (hammerscales and prills) in the archaeological record that are often overlooked during excavations. Some of the magnetic material collected was further analyzed with x-ray fluorescence to consider its elemental composition. Here, the primary goal was to look for representative evidence of iron production.

Finally, this dissertation is committed to using 3-D modeling for the sampled excavations to facilitate the preservation of the archaeological contexts and for novel methods of data sharing. As such, the 2014 excavations at Khirbat al-Jariya employed a rigorous 3-D recording methodology of every locus, including the slag mound excavation. However, as many of the samples originated in previously excavated contexts, a new technique of using archived excavation photographs for photogrammetry is tested for the slag mound excavation at Khirbat en-Nahas. This approach also allows for generating orthophotographs of the stratigraphic sections based on the produced model. Additionally, a method for combining models of excavation areas with lager site-scale models is also introduced, and the models are uploaded to SketchFab for access by scholars and the general public.

The results of these methods created the largest dataset of analyzed metal from Faynan to date which can be viewed in conjunction with the archaeological context through photorealistic 3-D models.

## 1.2 Chronology

The archaeological sites and materials investigated in this dissertation are primarily dated to the Iron Age (1200-500 BCE). The chronology of the Iron Age in the Southern Levant is vehemently debated in the scholarly discourse with no clear consensus (Mazar 2005, 2011;

Finkelstein 2005a; Finkelstein and Piasetzky 2011 for overviews). These discussions have resulted in three separate dating schemes for the Iron Age in the region – the "conventional" or "high" chronology, the "low" chronology, and the "modified conventional" chronology (Mazar 2005; Lee, Ramsey, and Mazar 2013). The implications of each system are largely in the potential representations of the biblical narrative within the archaeological record. While discussions of Faynan and its substantial copper smelting industry are occasionally included in the conversation (e.g., Levy et al. 2008, Mazar 2011: Table 2), this dissertation is not intended to contribute to the debate. Rather, it primarily relies on the significant collection of radiocarbon dates specifically from Faynan to chronologically situate the excavations discussed and in turn the analytical results. As such, a more localized chronology can be applied for this research (following Herr and Najjar 2001). However, terms such as "Early Iron Age" are used throughout, and it is therefore important to define the chronology (Table 1.1). Specific century ranges are frequently applied when discussing the archaeological record, but the below table can be referenced when more general chronological periods are mentioned.

**Table 1.1:** Local Iron Age chronology of ancient Jordan following Herr and Najjar 2001. The "General Terminology" column refers to common terms used in this dissertation. This table should be referenced for the more specific date ranges for these terms.

| Period | Sub-Period | Local Dates (BCE) | General Terminology |
|---|---|---|---|
| **Late Bronze Age** | - | 1550-1200 | Late Bronze Age |
| **Iron Age I** | Iron Age IA | 1200-1100 | Early Iron Age |
| | Iron Age IB | 1100-1000 | |
| **Iron Age II** | Iron Age IIA | 1000-900 | |
| | Iron Age IIB | 900-700 | |
| | Iron Age IIC | 700-500 | Late Iron Age |

## 1.4 Historical Context: The Late Bronze Age Collapse and Iron Age in the Southern Levant

The historical context of the Southern Levant during the Late Bronze and Iron Ages provides a foundation for understanding the developments of industrial copper smelting and

social complexity in Faynan. Specifically, the collapse at the end of the Late Bronze Age in the Eastern Mediterranean created the necessary sociopolitical and economic space for burgeoning polities like the Edomites and Israelites. The interregional dynamics of these Early Iron Age sociopolitical units shaped the trajectory of Faynan through new economic relationships, political rivalries, and by facilitating processes of ethnogenesis. The development of an Edomite polity during the Iron Age plays a particularly significant role in this dissertation. Here, Biblical and Egyptian texts provide additional insight concerning the formation of an Edomite kingdom (Knauf-Belleri 1995; Edelman 1995; Ben-Yosef 2016; Bartlett 1992; Avishur 2007; Kitchen 1992; Ward 1992). As will be discussed in Chapter 3, Faynan was likely within the territory of the biblical kingdom of Edom. As such, this dissertation must similarly be situated within this broader context. This section briefly reviews the history of the Southern Levant during the Late Bronze and Iron Age, primarily from the perspectives of Faynan, Edom, and copper production.

### 1.4.1 The Late Bronze Age Collapse

The Late Bronze Age (ca. 1550-1200 BCE) in the Eastern Mediterranean was characterized by a "world" economy dominated by the local empires including New Kingdom Egypt and the Hittites in the Levant. This economic interconnectivity is best captured by the international cargo of the Late Bronze Age Uluburun and Cape Gelidonya shipwrecks (Bass 2005; Pulak 2005; Cline 1994; Sherratt and Sherratt 1991; see also Yahalom-Mack et al. 2022). Along with various goods from Egypt, Greece, and the Levant was an abundance of raw copper from Cyprus, the primary supplier of the metal to the Eastern Mediterranean during this period (Bass 2005). Cyprus maintained a monopoly over copper production throughout the Late Bronze Age as emphasized by the wide distribution of the characteristic oxhide ingots and further

corroborated by lead isotope analysis studies (Kassianidou 2013; Muhly 1989; Lo Schiavo et al. 2009; Yahalom-Mack et al. 2014a). A small-scale copper smelting industry was also identified in Late Bronze Age Timna in southern Israel, but the region was under Egyptian hegemony at this time (Rothenberg 1988; Ben-Yosef et al. 2019; Yagel, Ben-Yosef, and Craddock 2016). Excavations in Faynan have only yielded minimal evidence for inhabitation and copper production in the Late Bronze Age (discussed further below and in Chapter 4). Thus, during the Late Bronze Age, Faynan was a marginal zone to the powerful empires and likely unable to compete with Cypriot dominance over copper exchange.

However, this international world system came to a dramatic end in ca. 1200 BCE when the region experienced a cataclysmic combination of climatic fluctuations, pandemics, invasions, internal uprisings, and warfare (among other possible factors) – the Late Bronze Age collapse (Knapp and Manning 2016; Drews 1993; Cline 2014; Weiner 2018; Carpenter 1966; Langgut et al. 2015; Drake 2012; Kaniewski et al. 2013). While the exact causes and chronology of this collapse are debated, the Southern Levant unquestionably experienced a series of destructive forces around 1200 BCE attested by destruction layers at archaeological sites throughout the region and an unprecedented sociopolitical breakdown with the dissolution of the major empires (Knapp and Manning 2016; Drews 1993; Cline 2014). Hittite and Egyptian control (along with its industry in Timna) withdrew from the Levant and the economic connections sustained by these empires similarly broke down (Bietak 2007; Yakar 2006; Ben-Yosef et al. 2012). Cyprus, now cut off from Levant, shifted focus to exchange with the western Mediterranean, creating an unfilled demand for copper (Kassianidou 2012, 2014; Zaccagnini 1990; Yahalom-Mack et al. 2014a; Knauf 1991). The resulting sociopolitical and economic void allowed for the emergence and development of the Iron Age polities of the Southern Levant.

### 1.4.2 Iron Age in the Southern Levant

The Iron Age (ca. 1200-500 BCE) in the Southern Levant is a period of growth and ethnogenesis associated with the appearance of "kingdoms" or "ethnic states" such as the Edomites, Israelites, Moabites, Philistines, etc. (Levy 2008, 2009; Finkelstein 1988; Faust 2006; LaBianca and Younker 1995; Killebrew 2005; Joffe 2002 for an overview). The simultaneous development of these polities likely facilitated their ethnogenesis through processes of resistance and peer-polity interactions (discussed further below; Joffe 2002; Levy 2009; Faust 2006). The origins of the Israelites have been extensively discussed in the scholarly literature, particularly in the light of the biblical narrative (e.g., Finkelstein and Silberman 2002). Edom has also been a focus of significant archaeological discourse especially recently following the paradigmatic shift in its dating to the Early Iron Age based on discoveries in Faynan and Timna and in juxtaposition to Israel as its rival (discussed in Chapter 3; Maeir 2021; Levy 2008, 2009; Levy et al. 2008; Ben-Yosef et al. 2012). Specifically, the new evidence for industrial scale copper production possibly connected to the Edomites introduced new interpretations concerning their development.

As mentioned, the Late Bronze Age collapse caused an economic disconnect between Cyprus and the Southern Levant, preventing the import of copper. Based on this understanding, Knauf (1991: 185) contextualized copper production in Edom (although attributing it to King Solomon) in relation to production in Cyprus, suggesting smelting in the Wadi Arabah only "flourished" when "the Cypro-Phoenician copper supply failed". Levy (2009) further builds on this idea suggesting that this "political ecology" of exploiting the local copper ores was integrated into the "practice and ideology" of the local nomadic Edomites during the formation

of a complex chiefdom in the Early Iron Age. In the context of the broader Levant, he continues that the formation of an Edomite identity and polity was likely driven by "resistance to the other" – in this case, the Israelites as exemplified in the biblical text (discussed further in Chapter 3; Levy 2009: 156; 2008; see also Faust 2006). In summary, the economic and sociopolitical conditions of the Late Bronze Age created an opportunity for local Edomites to develop a substantial copper industry (focused in Faynan and Timna) that was intimately integrated into their ideology and ethnic identity, partially also as a mode of resistance towards the other emerging groups. This formation of an Edomite polity during the Iron Age and the associated archaeological evidence are discussed further in Chapters 3 and 4.

It is important to note that despite the change in nomenclature from the "Bronze" to "Iron" Age, copper/bronze remained the metal *par excellence* for the first few centuries of the Iron Age (Waldbaum 1980, 1999; Yahalom-Mack and Eliyahu-Behar 2015). The transition from the Bronze Age to the Iron Age should not be interpreted as a complete replacement of bronze with iron in antiquity or in the archaeological record. Thus, the appearance of a large-scale copper production industry in Faynan during the Early Iron Age fulfilled this continued need and demand for the metal. However, "Edomites" were likely already present in Faynan in the Wadi Arabah prior to the Iron Age as evidenced by the ancient texts.

### 1.4.3 Evidence of Edom in Ancient Texts

While the nature and identifiers of an Edomite ethnicity in the Early Iron Age are somewhat debated (e.g., Beherec 2011, Ben-Yosef et al. 2019), Edom and its territory/inhabitants frequently appear in ancient texts dated to or describing the Late Bronze and Iron Ages, providing additional insight regarding society in Faynan. The main text sources

dealing with Edom are Egyptian letters/reports and topographical lists as well as the Hebrew Bible (Ward 1992; Kitchen 1992; Bartlett 1992; Levy and Najjar 2006a). The Egyptian sources suggest a possible Edomite polity as early as the Late Bronze Age. Specifically, the Papyrus Anastasi VI, a field report from the eastern frontier of Egypt (and potentially a model letter used to teach school children), provides a representative description of Late Bronze Age Edom (Wilson 1969: 259). Dated to the end of the 13th century BCE, the document mentions the "*Shasu* tribes of Edom" (Wilson 1969: 259). This line is significant in both mentioning "Edom" for the first time in historical records, suggesting the existence of some social/political entity as early as the end of the Late Bronze Age, and also by indicating the presence of "tribes" signifying a possible nomadic social organization (Levy and Najjar 2006a: 28; Avner 2021). *Shasu*, which likely translates "to wander", was probably not an ethnic identifier, but rather a general reference to a social class of nomads, similar to the modern term Bedouin (Ward 1992: 1165; Levy, Adams, and Muniz 2004: 66; Avner 2021). The papyrus goes on to mention that the *Shasu* of Edom were allowed "to pass…to the pools…to keep them alive, and keep their cattle alive", further reiterating they were pastoral nomads keeping livestock (Wilson 1969: 259).

Additional Egyptian texts, while not directly mentioning Edom, further reiterate the presence of *Shasu* in the land of Edom in the Late Bronze Age and Early Iron Age. Several texts reference Seir (the term also used in the Hebrew Bible to refer to the Edomite territory, discussed below) or the Seirites (Kitchen 1992). While debated, a 14th century BCE temple of Amenhotep III in Nubia (modern Sudan) includes a list of place names referencing the "*Shasu*-lands" and a possible mention of Seir (Kitchen 1992: 26; Ward 1992: 1165-1166). In the 13th century BCE, Ramesses II mentions Seir and the *Shasu* on an obelisk at Tanis and a stela from Tell er-Retabeh (Kitchen 1992: 28, 31). The Harris Papyrus, dated to the 12th century BCE and describing the

conflict between Ramesses III and the Sea Peoples, pronounces the pharaoh's destruction of the Seirites and the *Shasu* clans, pillaging their tents and livestock (Kitchen 1992: 27). Kitchen (1992: 27) suggests the copper industry of Timna may have been the impetus for Ramesses II campaign in Seir.

In summary, Egyptian texts depict the Edomites/Seirites as pastoral nomads, termed *Shasu*, inhabiting the region of Seir. While only one text references Edom directly, Ward (1992: 1165) concluded that "From the Egyptian viewpoint, then, the *Shasu* were a prominent part of the Edomite population" based on the entire corpus. The dating of these documents as early as the 14$^{th}$ century BCE as well as the 13$^{th}$-12$^{th}$ centuries BCE indicates an early Edomite existence with a presence significant enough to warrant Egyptian attention and officials' reference (Kitchen 1992: 27). Thus, while archaeological evidence for Late Bronze Age populations in Faynan is largely lacking (discussed further in Chapter 4), this is not necessarily an indication that Faynan was uninhabited (Kitchen 1992; Ward 1992; Levy, Adams, and Muniz 2004). The current absence of archaeological evidence for Late Bronze Age habitation in Faynan is potentially (at least partially) attributable to the pastoral nomadic social organization as described in the Egyptian texts, lacking permanent sites and stone architecture – a "tented kingdom" (Kitchen 1992: 27; Levy, Adams, and Muniz 2004: 68-71; Ben-Yosef 2021; Finkelstein 1992a; see also Ben-Yosef 2019a for additional discussion of the "Architectural Bias"). Ben-Yosef et al. (2019) further suggest that the tribes of Edom remained pastoral and nomadic in the Iron Age, but their engagement in industrial copper production during this period, requiring smelting centers and producing slag mounds, allowed archaeologists to identify them in the archaeological record.

Edom also appears frequently in the Hebrew Bible where it is first referenced in the Book of Genesis (Levy and Najjar 2006a: 26; Bartlett 1992). Edom's story begins in Genesis 25 with Jacob and Esau's birth, the children of Isaac and Rebekah (Genesis 25: 21-24). Esau was described as red at birth, most likely connecting to his designation as "Edom", the Semitic word for red (Genesis 25: 24; Levy and Najjar 2006a: 26). Jacob and Esau are described as two nations within the womb of Rebekah, a prophecy realized through Jacob's Israelites and Esau's Edomites (Genesis 25:23). Following selling his birthright to Jacob in exchange for red stew, Esau moves his family line of Edomites to the hill country known as Seir (Genesis 36: 9). Genesis 36:1 also describes Edomite kings that reigned over this region prior to any Israelite kings; an important textual reference for interpretations of Edom's origins. Subsequently, Edom is a consistent point of contention for the Israelite kings of the United Monarchy (Numbers 20:17; 1 Samuel 14:47; 2 Samuel 8:13–14; 1 Kings 11:14). King David had a particularly tumultuous relationship with Edom: "And David became famous after he returned from striking down eighteen thousand Edomites in the Valley of Salt. He put garrisons throughout Edom, and all the Edomites became subject to David" (8 Samuel: 13-14). Edom also appears in conflict with Judah during the Late Iron Age (Ezekiel 16:57, 25:12 provide two examples). A particularly insightful reference appears in the Book of Jeremiah (49:7-16) in the "Judgement Concerning Edom": "You may make your home in the cleft of the rocks; you may occupy the highest places in the hills. But even if you made your home where the eagles nest, I would bring you down from here". Here, the Edomites are described as living on cliffs and hills, likely referring to the Edomite Plateau of the Late Iron Age – the center of the Edomite polity following the abandonment of the copper smelting industry.

To summarize the biblical account, the Edomites were the bloodline of Esau, brother of Jacob, and inhabited a hill country known as Seir. The Edomites were regularly in contact with the Israelites during both the United Monarchy and the Divided Kingdom; however, these interactions were typically quarrelsome and violent. The reference to Edomite kings prior to Israelite kings alludes to an Edomite kingdom existing prior the United Monarchy, although this is debated (cf., Finkelstein 1992a, 2005b; LaBianca and Younker 1995; Levy 2008, 2009). The later texts describing the location of the Edomites in the hills likely reflects the reality of the Late Iron Age location of the Edomites on the plateau. Neither the biblical nor the Egyptian texts make any direct reference to copper production in Edom.

Taken together, these texts and the broader historical context suggest Faynan and Edom were inhabited by pastoral nomads in the Late Bronze Age and developed into a polity in the Early Iron Age, filling the economic and sociopolitical space created by the Late Bronze Age collapse. Industrial copper production, centered in Faynan and Timna, likely played an integral role in the developing Edomite polity, both to extract power from the political ecology and as a mode of resistance against the other Iron Age societies. This context provides the backdrop for this dissertation.

## 1.5 Outline of Dissertation

Following this Introduction, Chapter 2 discusses the theoretical framework used to interpret the produced data. The theoretical perspectives draw from anthropology, ecology, and sociology with an emphasis on the intersections of technology, society/culture, and the environment. As metallurgy is inherently a technology, this section begins with an overview of anthropological approaches and understandings of technology. Moreover, metallurgy is a

productive technology (in the sense that the result is a material object), so additional perspectives are drawn from the anthropology of production with an emphasis on political economy. Political economy in turn introduces connections between technology and other societal structures; these intersections are further discussed by contextualizing technology more broadly in society/culture using the culture system approach with technology representing one subsystem. However, the culture system also needs to be situated in its ecological context. To do so, the adaptive cycle from Resilience Theory is introduced. The adaptive cycle further provides a model for diachronically examining the trajectory of this social-ecological system. Finally, the section concludes with a discussion of pastoral nomadism and the "overshoot" model of societal collapse to provide a basis for examining critical transitions between the phases of the adaptive cycle.

Chapter 3 provides the necessary background information to contextualize this dissertation both within the physical environment and within the scholarly discourse. The chapter begins with an overview of the geography, climate, and geology of Faynan. The geography and climate of Faynan has shaped the lifeways of its inhabitants (both past and present) and thus requires consideration when examining the archaeological record. Similarly, understanding the geology of Faynan, more specifically its abundant copper ores, provides critical insights from the perspective of archaeometallurgy. The chapter then transitions to a review of the history of archaeological research in Faynan from the early explorations up through recent excavations and archaeometallurgical investigations. Finally, an overview of the possible relationship between the origins of iron production and copper smelting is provided as a foundation for the isotope analysis discussed in Chapter 5.

Chapter 4 is dedicated to the relevant archaeological excavations of Iron Age Faynan by the Edom Lowlands Regional Archaeology Project. The chapter begins with a detailed

discussion of the 2014 excavation season at Khirbat al-Jariya as this excavation was completed as part of this research. The 2006 season at Khirbat al-Jariya is also described as it included one of the slag mound excavations that were sampled for this dissertation. The excavations at Khirbat en-Nahas are then detailed, again with particular emphasis on the slag mound excavation which was also sampled. While not directly analyzed as part of this project, the small excavations at Khirbat al-Ghuwayba are also discussed as they play an important role in understanding the industrial landscape of the region. The chapter then provides brief overviews of excavations at other Iron Age sites that are less significant in terms of this dissertation before mentioning relevant mining sites (most of which have only been surveyed).

With the necessary background and excavations discussed, the dissertation then moves into analytical examinations of Iron Age metal from Faynan in Chapter 5. After a brief introduction and overview of the research questions, this chapter essentially discusses in detail three studies that provide the original analytical data of the dissertation. The first two studies focused on investigating possible iron production in Faynan. Iron objects and unique mixtures of copper and iron excavated at Khirbat en-Nahas were analyzed with mass spectrometry to examine their isotopic signatures and highly siderophile element abundances. The goal was to determine if the copper-iron mixtures were purified to extract metal iron which could be used to produce objects, and in turn, to investigate if iron production could have developed directly from copper smelting. The second study focused on sediment samples previously collected at Khirbat en-Nahas. As iron production results in magnetic residues in the archaeological record that are often overlooked during excavations, sediment samples from metallurgical areas at the site were tested with a magnet for such byproducts. Some of the magnetic material collected was further analyzed with x-ray fluorescence to consider its elemental composition. Here, the primary goal

was to look for representative evidence of iron production. Finally, the chapter transitions to a focus on copper with a diachronic analysis of produced metal using scanning electron microscopy. This section focuses on the elemental analysis of copper prills trapped in slags using samples collected from the slag mound excavations at Khirbat en-Nahas and Khirbat al-Jariya. By using the slag mound excavations and their associated radiocarbon dates as chronological scaffolds, this study examined the quality of produced copper through time to determine if degradation or exhaustion of copper ores impacted the Iron Age metallurgical industry.

Chapter 6 discusses the methods of data dissemination and record keeping used for this project with particular emphasis on 3-D modeling. The chapter first discusses 3-D modeling at Khirbat al-Jariya, particularly the 2014 excavation season where every locus was modeled. A larger portion of the chapter is dedicated to Khirbat en-Nahas where a new methodology of re-purposing archived excavation photographs for 3-D modeling was developed. A method for combining models of excavation areas with lager site-scale models is also discussed, and the process for uploading these models to SketchFab for access by scholars and the general public is detailed. This 3-D dataset is now freely available to view in tandem with the data produced here.

Chapter 7 provides a synthesis and discussion of the dissertation overall, combining the analytical data of Chapter 5 with the theoretical perspectives from Chapter 2. This chapter is organized chronologically and by phases of the adaptive cycle. To provide a holistic perspective of Iron Age society in Faynan, the adaptive cycle is extended back to the Middle Bronze Age and continues into the Late Iron Age. Each phase is discussed in detail and the theoretical perspectives introduced in Chapter 2 are drawn on when relevant. Thus, the chapter begins with a brief discussion of the Middle Bronze Age before moving into the critical foundations of the Late Bronze Age. The Late Bronze Age collapse is then contextualized using the “nested

hierarchy" from resilience theory to set up the developments of the Early Iron Age copper smelting industry in Faynan. The growth and exploitation phase of the 12th-10th centuries BCE is combined with the multiplier effect of the culture system model and political economy to understand the intricacies of this phase. The critical transition in copper smelting technology in the late 10th century BCE is highlighted before discussing the resilience and rigidity of the 9th century BCE. Particular emphasis is placed on the transition to the 8th century BCE when the metallurgical industry is abandoned. Overshoot is discussed here in evaluating if this industrial abandonment should be characterized as a societal collapse. The chapter concludes with the Late Iron Age (7th-6th centuries BCE) and the attempts to reorganize a copper production industry.

Finally, Chapter 8 functions as the conclusion for the dissertation, focused primarily on the overall goals and contributions of the research. Returning to the title, the conclusion is divided into three sections: copper, culture, and collapse. The analytical and theoretical contributions are discussed in relation to each.

## Chapter 2 - Theoretical Framework: Technology, Culture, and the Environment

### 2.1 Introduction

From an archaeological perspective, society in Iron Age Faynan and its metallurgical industry experienced a rapid trajectory of formation, growth, and collapse (as will be shown in the following chapters). Over the course of approximately 400 years, tribes of pastoral nomads founded a regional kingdom (the Biblical Edomites), established large-scale smelting centers, produced thousands of tons of copper, traded metal as far as the Mediterranean coast, and deserted the industry by the end of the 9$^{th}$ century BCE (Levy, Ben-Yosef, and Najjar 2014). Previous research determined the abundant copper ore resources in Faynan as the likely *raison d'etre* for the development of an Iron Age polity in the region (particularly considering the preceding Late Bronze Age Collapse, Ben-Yosef 2010; Levy, Ben-Yosef, and Najjar 2014); however, the abandonment of copper production, the associating smelting centers, and the complex society/kingdom more generally remains enigmatic. This dissertation suggests society in Faynan was uniquely dependent on sustained copper production during the Iron Age, and the abandonment of the industry should be reinterpreted as a 'collapse'.

In turn, this research tests if a failure within the metallurgical industry was an impetus for a societal collapse in Faynan rather than a consequence. This shift in thinking requires a theoretical framework that recognizes the significant interconnections between society, technology, and the environment - an anthropology of technology (Lechtman and Steinberg 1979; Pfaffenberger 1988, 1992; Lemonnier 1986, 1992; Hamilton 1996). The anthropology of technology can also be expanded to include anthropological perspectives of production more generally (Polanyi 1944: 46; Roseberry 1989; Hirth 1996). Here, political economy will be emphasized to highlight the impact technology/production can have on sociopolitical structures

(Hirth 1996; Brumfiel and Earle 1987). Technology also needs to be situated within a social-ecological system that accounts for the dynamic interactions between technology, society, and the ecosystem. To do so, society in Iron Age Faynan will be treated as a cultural system (Renfrew 1972; Binford 1965), and it will be examined from the perspective of the "adaptive cycle" from Resilience Theory (Holling, Gunderson, and Ludwig 2002). The adaptive cycle can holistically model the complete trajectory of Iron Age society in Faynan from the development of a regional kingdom founded on metallurgical technologies, through the 'collapse' of the industry and societal structures, to subsequent periods of continuity and reorganization. Moreover, the adaptive cycle of Faynan in the Iron Age can be embedded within the "nested hierarchy" of adaptive cycles representing copper production in the Eastern Mediterranean more generally to examine Faynan within a longer temporal sequence and larger geographic region (i.e. the *longue durée*) (Holling, Gunderson, and Ludwig 2002b). Finally, collapse as a concept is critically considered in light of recent paradigmatic shifts in anthropological understandings of the collapse process (Tainter 1988; Renfrew 1984; Eisenstadt 1988; McAnany and Yoffee 2010a; Faulseit 2016b), and a possible "triggering agent" is presented for the perspective of "overshoot" (Catton 1980; Redman 2005).

## 2.2 Anthropology of Technology

As the locus of analysis here is copper production/metallurgy, a theoretical framework built on anthropological understandings of "technology" is necessary. In the past, technology has often been reductively "portrayed as something fundamentally extraneous to human life and a force to which communities and beliefs are obliged to adapt" (Pfaffenberger 1988: 236). Anthropological perspectives work towards dismantling this monolithic view by treating

technology as a system that interacts with and is influenced by culture and *vice versa*. In other words, an anthropological approach to technology rejects the "standard view" of technology – an unsophisticated treatment that assumes "necessity is the mother of invention", "desocializes" the meanings of artifacts to only function with residual considerations of style, and accepts a "unilinear progression" of technology from simple to complex (Pfaffenberger 1992: 493-495; see also Erb-Satullo 2021 for an archaeological example against the "unilinear progression" of technology). Moreover, recognizing that technology is entangled within a socio-cultural 'web' requires a definition that is not simply concerned with the manipulation of the material world, but includes a cultural component (Hughes 1986). Lechtman and Steinberg (1979) provide an early example of viewing technology through an anthropological lens, suggesting it is a subsystem of culture interrelated to other subsystems such as religion, art, and social structure. Their definition of technology claims "technologies are the cultural traditions developed in human communities for dealing with the physical and biological environment… [they] are important not only because they affect social life but also because they constitute a major body of cultural phenomena in their own right" (Lechtman and Steinberg 1979: 136). This definition appropriately acknowledges the reciprocal relationship between society/culture and technology; technology is both a "cultural phenomena" in itself and capable of affecting social life.

This assimilation of culture and technology was further developed by Lemonnier (1986, 1989, 1992) in his call for an "anthropology of technology". According to Lemonnier (1986: 147-149), simplistic approaches to technology focusing on objects and forms (in line with a culture-history approach to archaeology) are a burden to anthropological/archaeological questions and thought as they fail to consider "all facets of human technical activity". In order to study the relationship between technological systems and society (i.e., an anthropology of

technology), Lemonnier (1992: 5-6) proposed a five-component definition of technology. Technological activities or techniques (any action involving a physical intervention resulting in the transformation of matter) are comprised of matter, energy (forces of movement/transformation), objects (artifacts, tools, and means of work), gestures (physical actions and movements known as the operational sequence or *chaîne opératoire*), and specific knowledge (Lemonnier 1992: 5-6). Deconstructing technology into these components provides a more complete perspective beyond 'objects and forms' and creates new opportunities for anthropological archaeologists to discern reciprocal influences between society and technology, particularly within the *chaîne opératoire*.

Pfaffenberger (1988, 1992), in a similar fashion calling for a "social anthropology of technology", suggested that "technological determinism" and "technological somnambulism" (the diagnostic term for sleepwalking) in Western discourse have inhibited an anthropological engagement with technology. Technological somnambulism inappropriately simplifies technology to just "making" and "using" in which "the human choices and decisions are masked, so the technology seems to operate beyond human control and appears to embody the result of automatic, inevitable process"; the role of humans is reduced to sleepwalking through a technological world (Pfaffenberger 1988: 238). In contrast, technological determinism treats technology as "a powerful and autonomous agent that dictates the patterns of human social and cultural life", reducing humans to simply "helpless spectators" and history to just "a chain of technological events" (Pfaffenberger 1988: 239). Both ideas inappropriately remove human actors and decision making from technology, and in turn, limit anthropological approaches.

In order to properly consider the use and creation of technology as a social behavior, Pfaffenberger (1992: 497) relies on the concepts of "technique" and the "sociotechnical system".

"Techniques" are in line with Lemonnier's definition, composed of the matter, energy, objects, gestures, and specific knowledge involved in producing material culture, and the "sociotechnical system" is the collection of technological activities that connect techniques and the produced material culture to the social coordination of labor (Pfaffenberger 1992: 497). In other words, the "sociotechnical system" considers "the social, economic, legal, scientific, and political context of the technology" which coordinate the relationships between humans and technology, similar to the culture system model discussed below (Pfaffenberger 1992: 497-498). This idea builds on Hughes' (1986: 112) "seamless web" approach to technology: "the social is indissolubly linked with the technological and the economic". These sociotechnical systems produce more than just materials, but also meaning and power in order to ensure that society and technology "work together harmoniously" (Pfaffenberger 1992: 498-502). In sum, this broad perspective of technology incorporates techniques, material culture, and sociotechnical systems to emphasize its social components. In doing so, it further reiterates the interconnections between society and technology as will be emphasized here in the case study from Faynan.

Building on these theoretical foundations, Hamilton (1996: 3, 8) attempted to construct a definition that regards technology as a "seamless part of culture" while being "more useful for analytical purposes". For Hamilton (1996: 3), technology is a system defined as "that corpus of material, knowledge, behaviors, and values that comprise, affect, or are affected by an individual's or a society's manipulations of the physical environment". This definition directly incorporates all aspects of technological processes (material, knowledge, behaviors, and values) while stressing the relationships between technology, society, and the physical environment; many technologies such as metallurgy are inherently reliant on natural resources (although not always the case). Moreover, the role of human agency and the individual within technology is

not ruled out *a priori*, alleviating the issues of technological determinism and somnambulism. As such, this definition best suits the research presented here and will be applied throughout. Through the development of an anthropology of technology, definitions of technology have become more nuanced and emphasize the complex connections between technology and society.

## 2.3 Anthropology of Production

In the case of Faynan, the anthropology of technology, focusing on the production of metal, can be expanded as an anthropology of production[1]. Moreover, treating metallurgy as a productive technology (c.f. non-material technologies like the internet, for example) enables application of generalized models dealing with modes and relations of production to elaborate on the interactions between technology and the other components in the cultural system. In other words, the anthropology of production can highlight and describe the interactions between technology and sociopolitical changes. Here, borrowing from Godelier (1978: 60, 71) and in line with Ben-Yosef (2010: 45), production will be defined as:

> "…the totality of the operations aimed at procuring for a society its material means of existence…In the end we see that all production is a twofold act subject to the technical norms of a certain relation between [humans] and nature and to the social norms governing the relations between [humans] and their use of the factors of production".

This definition draws attention to the importance of social/cultural influences on production and its organization and *vice versa*. The conceptualization of production's role in social structures was previously developed by Marx (1904[1859]) along with Engels (Marx

[1] Any discussion of an anthropology of production should acknowledge the paramount work by Cathy Costin (1991, 1998, 2001). However, Costin's theoretical perspectives have been previously applied to Iron Age Faynan in Ben-Yosef's (2010) dissertation. His successful and detailed application remains accurate in light of any new excavations and data. As such, a reapplication would yield limited if any novel theoretical insight and will not be undertaken here.

and Engels 1947) (and by many other scholars since – see Hirth 1996 for an overview). Marx (1904[1859]: 11-12) emphasized the control over means of production and the ensuing wealth differential (relations of production) in understanding the organization of society – i.e., historical materialism. According to Marx (1904[1859]: 11-12), the resulting societal structure is composed of two parts: base and superstructure. The base consisted of the means and relations of production whereas the superstructure, resting on the base, included political and ideological institutions that provided a veiled justification for the existing relations of production (Marx (1904[1859]: 11-12, Marx and Engels 1947: 23, 39). However, the relegation of social, political, and ideological processes to the 'superstructure' in Orthodox Marxism as a unidirectional outgrowth of class relations results in economic determinism and neglects the reciprocal nature of the relationship between technology and the society in which it functions (Marx 1904[1859]: 11-12). Engels (1934[1890]: 84) subsequently disputed this deterministic aspect of historical materialism in a series of letters in 1890 (also discussed by Althusser 1969 [1965]: 117-128, 255):

> "The political, legal, philosophical, religious, literary, artistic, etc., development rest upon the economic. But they all react upon one another and upon the economic base. It is not the case that the economic situation is the *cause, alone active,* and everything else only a passive effect. Rather there is a reciprocal interaction with fundamental economic necessity which *in the last instance* always asserts itself" (emphasis original)

Despite Engels' (1934[1890]: 84) clarification, the economic 'base' remained predominant in structuring society: "the economic relations, no matter how much they are influenced by relations of a political or ideological order, are ultimately decisive". Thus, the Marxist perspective remains problematic in its undermining of social influences in productive technologies, yet it offers linkages between production and social evolution.

For a more holistic approach, the relations of production can be considered through the recent reevaluations of political economy largely from the substantivist school of economic anthropology (Polanyi 1944: 46; Roseberry 1989; Hirth 1996). As generally defined by Roseberry (1989: 44), political economy is "an analysis of social relations based on unequal access to wealth and power" (Hirth 1996: 204-205). With this in mind, archaeological applications of political economy typically consider differential control of scarce resources in the development of social complexity (Hirth 1996: 205). This "control" was frequently focused on either production or exchange in practice, but Hirth (1996: 205, 207) argues these are two sides of the same coin; elites leverage control over *both* production and exchange in order to exercise sociopolitical power.

Additional debate followed concerning the role of agricultural/subsistence production versus nonperishable commodities including craft items (Brumfiel and Earle 1987; Hirth 1996: 208). Archaeologically, political economy originally emphasized control over staple goods, but Brumfiel and Earle (1987: 3-5, 9) stressed luxury items (wealth finance) suggesting these craft goods are "politically charged" and thereby reinforce the sociopolitical systems in which they exist and circulate (see also Goldstein 2000). Again, Hirth (1996: 208) calls for mutual considerations. Finally, political economy witnessed a shift away from Marxist rationale prioritizing economic foundations in the creation and perpetuation of political systems; new ideational approaches emphasized religious and social structures in resource mobilization (Hirth 1996: 209). Hirth (1996: 209) agreeably suggests that a middle ground between these perspectives is necessary: "While economic control provides the material means to support political bureaucracies, ideational systems provide the structure

and justification that allow them to operate". Treating political economy in the fashion fits with the definitions of technology and production described above.

This work follows Hirth (1996) in suggesting political economy should (when possible) incorporate control over both agricultural and craft production along with their exchange, but this approach has limited feasibility in Faynan. First, the agricultural circumstances of Faynan remain complex and ambiguous; the harsh terrain and climate begs the question of agricultural practicality and viability in the region as is discussed in Chapter 3 (See Barker, Gilbertson, and Mattingly 2007; LaBianca and Younker 1995; Knabb et al. 2016 for discussion). Second, the exchange networks along with the means and modes of exchange for produced copper are under investigation for the Ion Age (e.g., Ben-Yosef and Sergi 2018; Yahalom-Mack et al. 2014a; Martin and Finkelstein 2013; Martin et al. 2013; Kiderlen et al. 2016; Ben-Dor Evian 2017; Ben-Dor Evian et al. 2021; Vaelske, Bode, and Loeben 2019). While it is clear that copper was traded over regional economic networks, the specific goods returned in exchange for copper remain enigmatic; there is limited evidence for imports/foreign material culture in the Iron Age archaeological record of Faynan. It is suggested here that copper was exchanged for perishable goods as will be discussed in Chapter 7. In this sense, copper functions as a "politically charged" commodity through its production and exchange which potentially provided elites with a means to accumulate wealth and power in combination with a process of ethnogenesis, the processes and transformations of creating a social identity (Weik 2014; Levy and Holl 2002), that placed a cultural importance on copper smelting (Chapters 4 and 7).

## 2.4 The Culture System: Technology as a Subsystem of Culture

In order to consider the relationship between technology (more specifically, mining and

metallurgy) and societal change, technology needs to be contextualized within the specific cultural context drawing from the archaeological record. To do so, culture will be treated as a broader system[2] in which technology functions as one subsystem following Binford (1965), Renfrew (1972), and Lechtman and Steinberg (1979). Renfrew (1972: 19) treats culture as a system composed of artifacts including non-material artifacts like language and religion, the humans that produce/use them, and the inhabited environment, all of which are "inextricably bound" and interrelated. Within the human-artifact-nature framework, the archaeologist is free to determine the significant interacting elements or subsystems that constitute a specific cultural system as well as its spatial and chronological boundaries based on the specific archaeological context and record (Renfrew 1972: 20-22). Following Renfrew (1972: 22, Figure 21.1), the culture system model applied here includes subsistence, social, projective/symbolic (e.g., religion and ritual), trade/communication, and technological subsystems (Figure 2.1). Population, as in the number of people living within a cultural system, and the environment are considered basic parameters of the system, rather than individual subsystems (Renfrew 1972: 23). This systemic approach to culture recognizes the connections between technology and the other subsystems (in line with the definitions above), and it provides a model for archaeologists that can be derived from material culture and the archaeological record.

Using the culture system model, Renfrew (1972: 23) also proposes it is possible to

[2] Using Systems Theory in archaeology has been criticized as being mechanistic, discounting agency, and descriptive rather than explanatory (e.g., Hodder and Hutson 2004; Hodder 1994; Salmon 1978). This research does not dismiss these critiques nor does it strictly adhere to "General Systems Theory" which uses computer simulations and mathematical equations to model societies and social processes, but rather it is employing a "systemic approach to archaeological data" – examining "artifacts and so forth, not as isolated individual entities, but as parts of a larger system with social, cultural, ecological, technological, and other components" to enhance understanding (Salmon 1978: 178). Cowgill (1988: 252), while critiquing Systems Theory more generally, also suggested archaeologists need to "look at social phenomena in this broadly systemic way if we are to understand them".

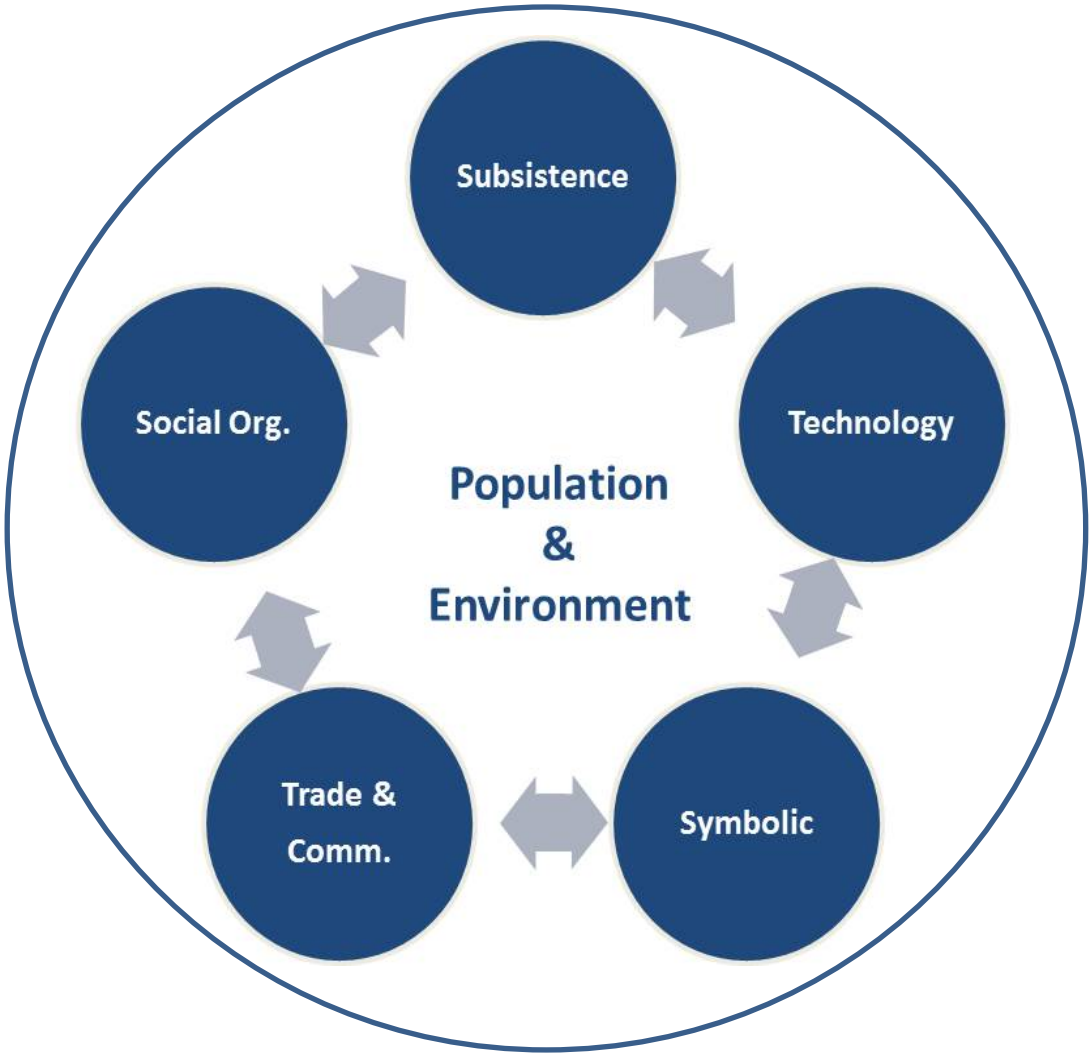


**Figure 2.1:** Model of the human cultural system including subsistence, technology (craft production), symbolic, trade/communication, and social organization subsystems based on Renfrew 1972: Figure 21.1.

identify processes of culture change through the "multiplier effect" - when "changes in one area of human experience [one subsystem] lead to developments in another. In this way the created environment is enlarged in many dimensions, and itself becomes more complex". In other words, the subsystems of culture can be related through positive feedback loops that facilitate growth/development: "innovation [in one subsystem] produces effects [in other subsystems] which favour the further development of the innovation" (Renfrew 1972: 38). While

invention/development within one subsystem can initiate the multiplier effect, at least two subsystems of the culture are inherently involved through the feedback relationships. For example, technological developments in metallurgy can produce new agricultural tools impacting the subsistence subsystem, and in turn, growth within subsistence production will require continued production and/or additional metal tools. If the multiplier effect impacts "most or all" of the subsystems, the entire system experiences a "cultural take-off" and "the subsystems of the society will then undergo marked structural change" (the Industrial Revolution provides a straightforward example) (Renfrew 1972: 39-43). The result of the multiplier effect and cultural take-off is the "emergence of civilization" (Renfrew 1972: 38-39). Treating culture as a system in this way highlights the intricate relationships between technology and society. The culture system model and multiplier effect can be applied to the interrelated developments of metallurgy and complex society in Faynan. However, complex systems such as cultures/societies do not exist in permanent stability or equilibrium. As described below, the adaptive cycle from Resilience Theory offers a theoretical perspective to consider the additional processes and stages of a complex system.

## 2.5 Social-Ecological Systems: Resilience Theory and the Adaptive Cycle

A cultural system inherently exists within a particular environment or ecological niche. It needs to be considered within its environmental context in a similar approach to examining technology from the perspective of the culture system. The relationships between humans/society and the environment are somewhat paradoxical; population growth and industrialization place mounting stresses and pressure on the environment to sustain human activities (both today and in antiquity), and yet collective society continues to function and avoid wide-scale collapse despite

Malthusian-style predictions of environmental limitations (Holling, Gunderson, and Ludwig 2002: 15; Malthus 1798). Resilience Theory, originating in ecology, attributes this contradiction to the adaptive capacity of humans and the resiliency of social-ecological systems - the complex integration of humans and nature (Holling, Gunderson, and Ludwig 2002: 15-18). Resilience is a system's "ability to absorb change and disturbance and still maintain the same relationships between populations or state variables" - in other words, the vulnerability of a system to unexpected changes (Holling 1973: 14). This is not to say that resilient systems exist in a perpetual and static equilibrium of stability, but rather they experience episodic changes on different scales that allow multiple states of equilibria (Holling, Gunderson, and Ludwig 2002: 18). Resilience Theory was developed to investigate these transformational changes that occur within social-ecological systems and to create "theories for sustainable futures" (Holling, Gunderson, and Ludwig 2002: 21). Through a comparative approach, resilience theorists discovered ecosystems pass through a series of cyclical transformations which can be modeled as the "adaptive cycle" (Figure 2.2).

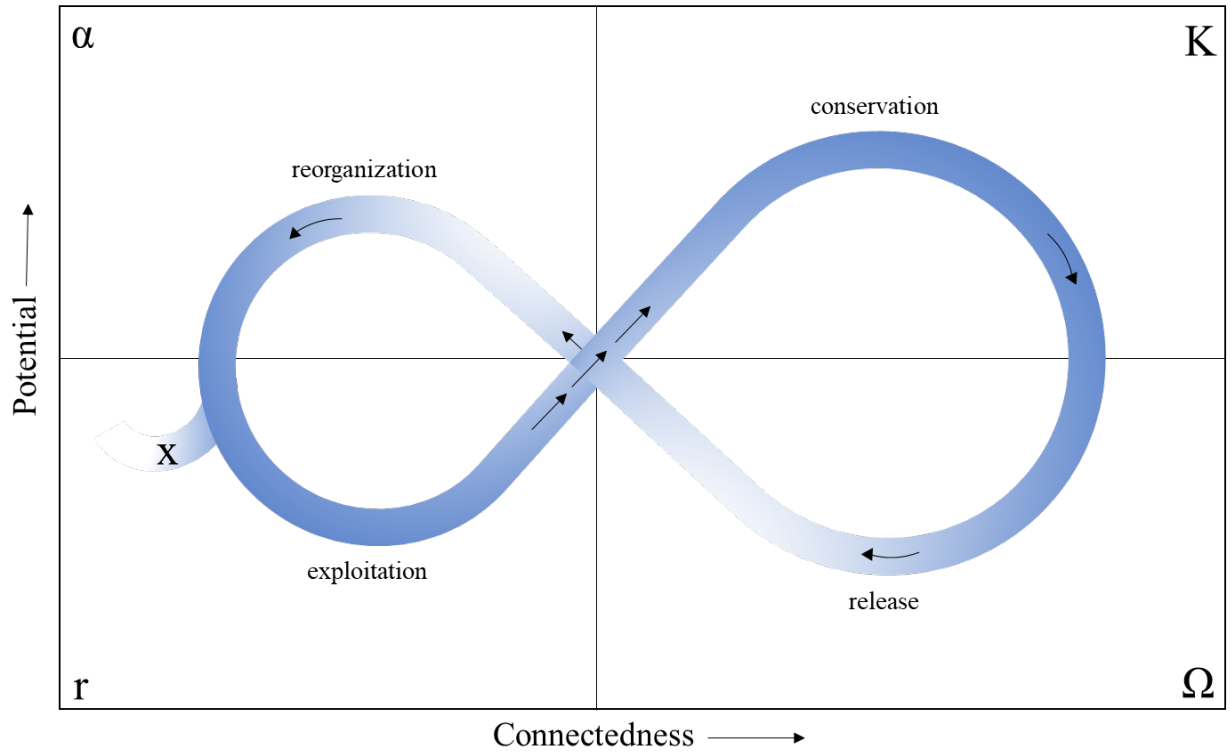


**Figure 2.2:** Diagram of the adaptive cycle (modeled after Holling and Gunderson 2002: Figure 2-1). The X represents an exit from the cycle when "potential can leak away and where a flip into a less productive and organized system is most likely" (Holling and Gunderson 2002: 34).

However, the adaptive cycle is not limited to only ecosystems, but it can model the trajectory of any complex system (Holling and Gunderson 2002: 62). Within Resilience Theory, the adaptive cycle functions as "a fundamental unit for understanding complex systems from cells to ecosystems to societies to cultures" (Holling and Gunderson 2002: 62). Recently, archaeologists have expanded applications of the adaptive cycle to include ancient societies as well (e.g., Redman 2005; Faulseit 2016a; Rosen and Rivera-Collazo 2012; Bradtmöller, Grimm, and Riel-Salvatore 2017; Mourad 2021), and therefore, it can provide an important model for the changing social-ecological system of Iron Age Faynan, i.e., to situate the cultural system within its specific environment and consider its transformational changes/developments. In turn, archaeological research can also contribute to resilience theory by providing deep-time

perspectives capable of holistically examining adaptive cycles to inform ‘theories for sustainable futures’.

The adaptive cycle (Figure 2.2) suggests that complex systems pass through a series of four phases: exploitation (r-phase), conservation (K-phase), release (Ω-phase), and reorganization (α-phase) (Holling and Gunderson 2002: Figure 2-1). These phases are modeled as a “figure eight” representing the cyclical/recurring nature of the adaptive cycle; a system “flows” through all four phases before the process repeats with the development of a reorganized or new system (Holling and Gunderson 2002: 32-52). Two of the main controlling variables for when a system moves from one phase to another are presented on the x- and y-axes: connectedness and potential, respectively (Figure 2.2). Connectedness refers to the connections or relationships internal to a system that allow it to control for external influences, and potential is the potential for change available in the accumulated resources, said otherwise, the range of available options for the future (Holling and Gunderson 2002: 34, 49-50). The third characteristic or variable of the cycle is resilience (defined above); in order to depict resilience on the adaptive cycle diagram, a third dimension is added (Figure 2.3). Together, these three variables control how and when a system moves through the phases of the adaptive cycle.

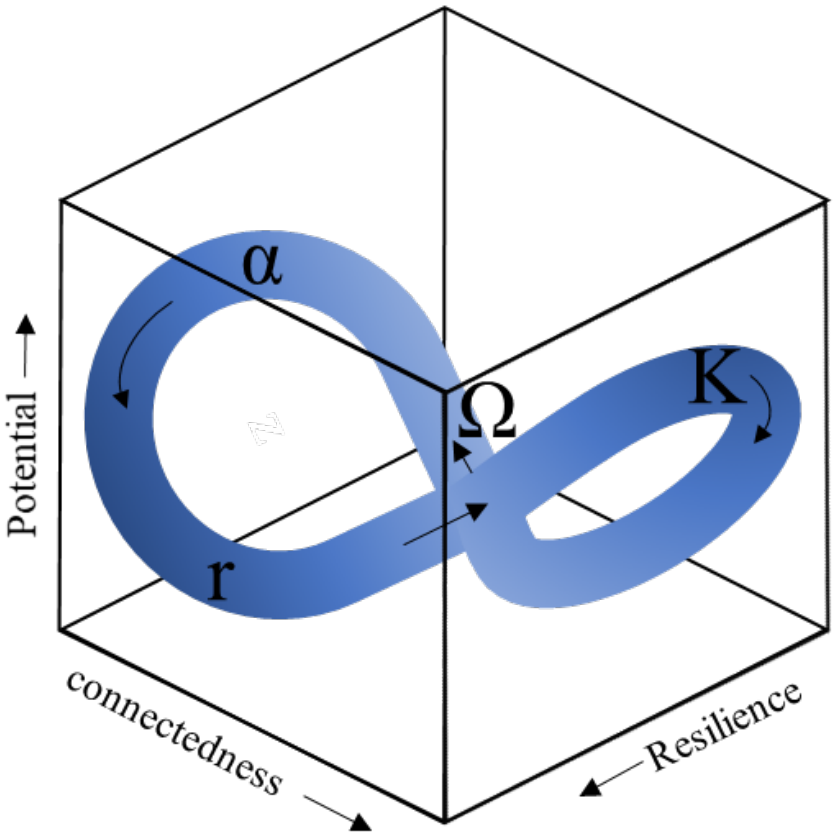


**Figure 2.3:** To display "resilience" in the adaptive cycle requires a three-dimensional model. Note that in the K phase (which precedes a collapse) connectedness and potential for change are high whereas resilience is low (modeled after Holling and Gunderson 2002: Figure 2-2).

Each phase of the adaptive cycle is associated with particular processes and developments within a complex system. As Resilience Theory was established in ecology, the phases are often presented from an ecological perspective; however, their application to societies and economic systems is also considered (Holling and Gunderson 2002). Here, each phase will be considered primarily from the perspective of change in Iron Age society and economy, as these are very much interconnected and can create feedback loops in the development of complex systems as seen in the culture system model described above. Descriptions of all of the phases of the adaptive cycle and their associated properties are available in Table 2.1.

**Table 2.1:** Descriptions of the phases of the adaptive cycle along with their associated properties (connectedness, potential, and resilience). Table is modeled after Méndez et al. 2005: Table 2 and Holling and Gunderson 2002.

| Phases and Properties of the Adaptive Cycle | | | | |
|---|---|---|---|---|
| **Phase** | **Description** | **Potential for Change** | **Connectedness** | **Resilience** |
| **α - Reorganization** | - System widely open to reorganization.<br>- Experimentation and initial establishment of actors, organizations, and institutions, strongly subjected to evolutionary forces (i.e. competition, failure, survival).<br>- Uncertainty about options for the future and chance for unexpected forms of renewal. | - Relatively high for future development. | - Low. Very much influenced by external variability such as opportunities to exploit or constraints. | - High. Stability in the region with a "welcoming" environment for experimentation with limited competition (Holling and Gunderson 2002: 41). |
| **r - Exploitation and Growth** | - Incremental exploitation of available resources and growth.<br>- Innovators perceive unlimited opportunity.<br>- External variability remains, and is favorable to entities adapted to it.<br>- Future becomes more predictable. | - Declines as resources continue to be exploited. | - Remains low, but starts to increase as actors develop systems of relationships to "control external variability and reinforce their own expansion" (Holling and Gunderson 2002: 44). | - Remains high due to adaptation to the high variability of the environment or through the ability of producers to capture open markets. |
| **K - Conservation and Consolidation** | - Growth rate sloes down.<br>- Reduced opportunity and difficulties for new entrants.<br>- Future seems more determined and certain.<br>- Increasing returns from efficiency (e.g. streamlining, minimizing costs).<br>- Organizations become bureaucratized, rigid, and internally focused (i.e. can be blind to external changes). | - Becomes high again in terms of stored resources and capital. | - Increases as the system becomes highly stable and more inter-connected in structure and organization i.e. more rigid. | - Rapidly declines. Vulnerability to external disturbance starts to increase. Systems in the K-phase are "accidents waiting to happen" (Holling and Gunderson 2002: 45). |
| **Ω - Release** | - Extreme structural rigidity that may trigger sudden change or collapse.<br>- Creates sources for reorganization and opportunity for new systems. | - Suddenly declines as resources that were previously accumulated and bound within the system are abruptly released but increases as "exotic" agents can take action. | - High, but connections and control over the system suddenly break. | - Low, but increases as the system moves towards a new reorganization phase. |

The exploitation/growth or r-phase is described as the "rapid colonization of recently disturbed areas" (Holling and Gunderson 2002: 33). Said otherwise, this phase is characterized by the 'exploitation' of available resources in unexploited areas such as an environmental zone or even an economic market by human actors (Holling and Gunderson 2002: 43). Exploitation is considered a phase of "unlimited opportunity…in which producers of new products can aggressively capture…newly opened markets" (Holling and Gunderson 2002: 43). The capturing of this potential or capital results in rapid growth within the system. With the growth and accumulation of resources, the social-ecological system increases in the potential (accumulated resources within the system) and the connectedness begins to increase (control and exploitation of resources start to become bound within the system) (Holling and Gunderson 2002: 43). Resilience during the exploitation phase is high as the succeeding agents and actors are adapted to the unique conditions of the time and ecological niche; i.e. they can capture the opportunity and grow in the face of any competition (Holling and Gunderson 2002: 33, 43). From the perspective of archaeology and this research, this phase can be characterized by the growth/development within a subsystem, or multiple subsystems, resulting in positive feedback and growth in the entire culture system. The system moves towards the K-phase as it "expand[s], grow[s], and accumulate[s] potential from resources acquired" (Holling and Gunderson 2002: 43).

The K-phase, or conservation and consolidation phase, is associated with the accumulation of "capital" or "resources" which are general terms used in the "broadest sense" to be identified based on the specific social-ecological system (Holling 2001: 394; Holling and Gunderson 2002: 43). For example, social/economic capital can include materials, wealth, or natural resources collected by human populations (Holling 2001: 394). As the K-phase continues

to develop, this capital becomes increasingly bound within the system, and the components of the social-ecological system become gradually more interdependent, similar to the subsystems of the cultural system becoming interconnected by positive feedback loops (Holling 2001: 394). The K-phase is associated with increased connectedness within the system as it becomes more stable and structured; in other words, the system has firm control over available resources, and it is little influenced by external variability (Holling and Gunderson 2002: 44-45, 50). With control over external variability, the system can focus inward and increase "efficiency for utilizing energy, minimizing costs, and streamlining operations" (Holling and Gunderson 2002: 44). However, high connectedness does not correlate with high resiliency (Figure 2.2, Holling and Gunderson 2002: 50). In contrast, a social-ecological system in the K-phase is increasingly rigid due to the interconnectedness of key elements causing resiliency to actually decrease; it is more "vulnerable to surprise", "brittle", and susceptible to unexpected disturbances (Holling and Gunderson 2002: 33, 41, 44). As such, the potential for change is similarly high (Table 2.1).

Systems in the K-phase are susceptible to unpredicted events or disturbances caused by "triggering agents" (such as drought, fire, labor strikes, revolutions, etc.) which can result in the accumulated resources being "released" from the tight control of the current system (Holling 2001: 394-395). This "release", which in a culture system or society could be described as a collapse (discussed further below), represents the Ω-phase (See Holling 2001: 395 for an example based on the Soviet Union in which a sociopolitical system became increasingly connected and rigid before a triggered collapse). The Ω or release phase can affect a system quickly and unexpectedly which correlates with some examples of collapse in the archaeological record (Redman 2003: 73). During this phase, potential drops as the previously accumulated resources are abruptly released (they are no longer actively involved in system growth and

maintenance), but it begins to increase as agents take action in capturing these resources (Holling and Gunderson 2002: 45). Similarly, resilience is also low as the system loses its structure (destabilizing) and essential function (Holling and Gunderson 2002: 45). In contrast, connectedness initially remains high through the established connections of the K-phase as the feedback loops between system elements allow the release phase to run its course (Holling and Gunderson 2002: 45). These connections are subsequently broken, resulting in a decrease in connectedness as the cycle transitions to the next phase.

After the system "releases" or "collapses", the cycle moves into the α-phase or "reorganization". The reorganization phase "is essentially…one of innovation and restructuring in an industry or in a society…at times of economic recession or social transformation" (Holling and Gunderson 2002: 35). The α-phase has low connectedness as any existing capital/resource is freely available and relatively high potential for change, for development of a new system (Holling and Gunderson 2002: 40). Resilience, however, is high as the system now exists in a "wide, loosely regulated domain of stability" with weak connections between actors and functions (Table 2.1) (Holling and Gunderson 2002: 46). These conditions create an opportunity for experimentation and the "initial establishment of entities that otherwise would be out-competed" (Holling and Gunderson 2002: 40-41). The "legacies of past cycles" such as physical architecture left behind from the previous release provide potential for future growth (Holling and Gunderson 2002: 45). In this way, the reorganization phase is the foundation for a future exploitation phase, and the creation of a new system of resource accumulation (Holling and Gunderson 2002: 46). By extending the system cycle beyond collapse in which enduring traditions and "legacies" shape the future, resilience theory provides a nuanced understanding of the collapse process avoiding catastrophic assumptions and allowing for post-collapse processes

(discussed further below). With the transition from the α-phase to a new r-phase, the adaptive cycle is simultaneously completed and beginning again.

The final component of the adaptive cycle is the "nested hierarchy" (Holling, Gunderson, and Peterson 2002: 68-76). Resilience theory expands the scale of its model by suggesting adaptive cycles "nest in one another in a hierarchy" across both time and space; smaller and faster adaptive cycles are "nested" or situated within larger and slower cycles (Holling, Gunderson, and Peterson 2002: 72) (Figure 2.4). There are critical interactions and connections between the smaller and larger adaptive cycles that compose a nested hierarchy known as "revolt" and "remember" (Holling, Gunderson, and Peterson 2002: 68-76) (Figure 2.4). "Revolt" occurs when an Ω-phase or collapse "cascade[s] up to the next larger and slower level by triggering a crisis, particularly if that [higher] level is at the K phase, where resilience is low" (Holling, Gunderson, and Peterson 2002: 75). For example, "revolt" in a social system could include local activists facilitating changes in regional institutions through disruptive actions such as labor strikes (the triggering agent and subsequent release phase) driving a higher minimum wage policy (a reorganization of the system). The "remember" process follows a release or collapse in a small and fast cycle, and it "facilitates renewal by drawing on the potential that has been accumulated and stored in a larger, slower cycle" (Holling, Gunderson, and Peterson 2002: 75). The "remember" process has recently been archaeologically applied to examine how subsistence practices reacted to climate change in the Southern Levant over several millennia (Rosen and Rivera-Collazo 2012). Rosen and Rivera-Collazo (2012) suggest periods of colder and dryer climates caused a release in sedentary/agricultural societies (smaller scale cycles) which would transition to hunting-gathering strategies to draw on the new resource base (the "remember" process) provided by the climatic and environmental changes (the larger cycle) (see

also Rivera-Collazo et al. 2018). Recognizing that these interactions between cycles exist, an individual adaptive cycle cannot be fully understood from examination on a single geographical or temporal scale, but it needs to be considered from the perspective of the nested hierarchy (Holling, Gunderson, and Peterson 2002: 68-76).

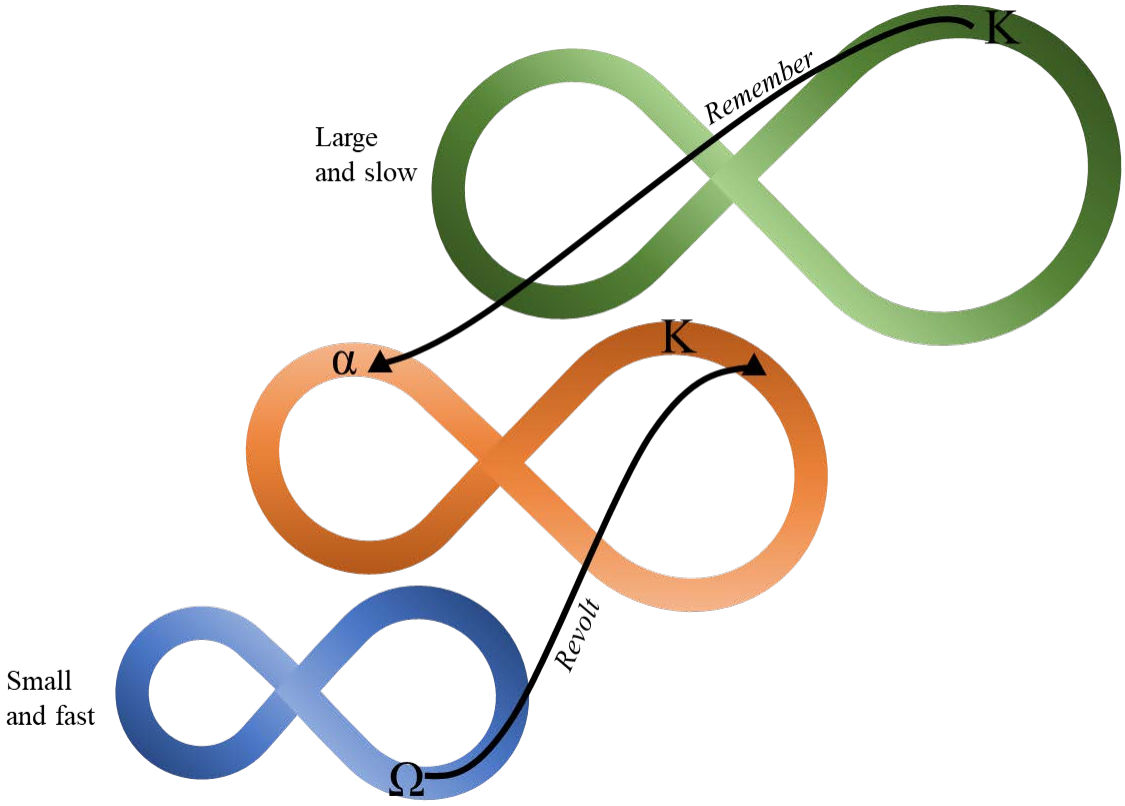


**Figure 2.4:** Diagram of the "nested hierarchy" of adaptive cycles functioning on different scales of time and space with the interactions between them (modeled after Holling, Gunderson, and Peterson 2002: Figure 3-10).

The adaptive cycle will be applied[3] on three scales here to construct the nested hierarchy: within Faynan specifically, the larger scale political entities of the Levant, and the Eastern Mediterranean world more generally. In doing so, Faynan will be situated within a larger geographical region and longer temporal sequence (comparable to using the adaptive cycle to understand changes in subsistence practices by Rosen and Rivera-Collazo 2012). Nested adaptive cycles can successfully model the intricacies of copper production within Faynan and situate it within the broader Eastern Mediterranean as the locus of production and economic networks shifted through time primarily between Faynan and Cyprus during the Late Bronze and Iron Ages. In doing so, the nested hierarchy can provide a more holistic and nuanced understanding of the processes and dynamics involved in the development and subsequent abandonment[4] of industrial-scale copper production in Iron Age Faynan particularly from the perspective of "revolt" and "remember" interactions.

[3] Previously, Knabb (2015) applied resilience theory and the adaptive cycle to archaeological research in Faynan as part of his dissertation. Knabb (2015: Figure 4.16), focusing on the environmental impacts of copper production, successfully identified two consecutive adaptive cycles extending from the Late Bronze Age to the Late Roman and Byzantine Periods. This dissertation adjusts his identification of the various phases of the cycle within the Iron Age, and also introduces multiple levels of geographical scale by applying a nested hierarchy, which was not used in his research. In doing so, it also introduces the notions of "revolt" and "remember" for integrating the various adaptive cycles within the nested hierarchy which will play an important role in understanding both the beginning and end of copper production during the Iron Age. Finally, the newly established production phases of copper smelting through the Iron Age are integrated into the adaptive cycle for the first time here (Ben-Yosef 2010; Ben-Yosef et al. 2019) (discussed in Chapters 3 and 4).

[4] There is some overlap between Resilience Theory and General Systems Theory in its application for archaeology and understanding collapse (Faulseit 2016b). For example, Renfrew (1984: 372-377), a proponent of General Systems Theory, discusses the "high measure of interdependence" in his "cusp catastrophe" model for collapse which more or less correlates with "connectedness" and "release" within Resilience Theory (Faulseit 2016b: 10-12). However, General Systems Theory treats collapse as an "inevitable outcome of sociopolitical evolution" (Faulseit 2016b: 11; Yoffee 1988). In contrast, Resilience Theory allows "more nuanced and complex understandings of societal transition" through its dynamic and episodic approach to societal transformation including "non-collapse outcomes" (see the discussion of the "nested hierarchy") (Faulseit 2016b: 11-12).

2.6 Pastoral Nomadism and Precarity: Copper Production as Adaptation and Exploitation (r to K)

To appropriately apply the adaptive cycle, the environmental conditions and their impact on the socioeconomic organization of Iron Age Faynan also need to be considered (e.g., Rivera-Collazo et al. 2018). Faynan is in the harsh and marginalized environmental context of the Saharo-Arabian desert of the Arabah Valley. Current paleoclimate data while highly variable suggests the environment and climate of Iron Age Faynan were possibly similar to today during at least the 10th-9th centuries BCE, characterized by a hot and dry climate (discussed further in Chapter 3) (Levy, Ben-Yosef, and Najjar 2014: 22-23; Ben-Yosef 2010: 123 for an overview, cf. Langgut et al. 2015). Smith et al. (2007: 7) suggest archaeological investigations into past desert peoples must address two inherent complexities: 1) that the present environment and climate is not necessarily representative of the past and 2) that we must consider the adaptive and economic strategies that prepared populations for life in the desert. In other words, "how do societies in marginal environments actually deal with risk in either a reactive or strategic sense?" (Smith et al. 2007: 2). In the case of Faynan, the first complexity is alleviated at least based on current evidence; however, surviving the harsh climate and terrain still required specific adaptive and economic strategies. Addressing the second complexity requires certain attention to the social and economic organization of Iron Age Faynan – a unique combination of pastoral nomadism and industrial-scale copper production.

Despite the wide coverage of excavations and surveys in Faynan (see Levy, Ben-Yosef, and Najjar 2014 for an overview), evidence for extensive Early Iron Age (ca. 1200-800 BCE) domestic settlement (i.e., household architecture) is largely lacking from the archaeological record suggesting more mobile lifeways (Ben-Yosef 2019a, 2020, 2021). In addition, excavations at Khirbat al-Jariya, an Iron Age copper smelting center, discovered potential tent-

post holes connecting nomadism and copper production, and the material culture from the Wadi Fidan 40 Iron Age cemetery site was in line with a society of pastoral nomads (Ben-Yosef et al. 2010: 736-738; Beherec 2011; Beherec, Najjar, and Levy 2014; Levy 2009). Ancient Egyptian texts also indicate that the region of Edom was inhabited by nomadic populations which likely provided the foundations for the Edomite polity (Chapters 1 and 3) (Kitchen 1992: 27; Beherec 2011; Levy and Najjar 2006a). As will be discussed in the following chapters, Faynan developed from these pastoral nomadic groups into a kingdom/chiefdom in the Early Iron Age; however, subsistence and economic strategies in Faynan remained generally pastoral and nomadic based on the archaeological evidence (Levy 2008, 2009). Following Marx (2006: 93; cf. Khazanov 1994: 16-17), pastoral nomadism describes "groups for whom the mobile production of animals and animal products is a significant way of making a living". This definition adequately accounts for the significance of mobile herding in pastoral nomadism without inappropriately precluding other possible subsistence and/or economic endeavors *a priori*. Society in Iron Age Faynan was probably a form of "*semi*-nomadic pastoralism" or a "mixed economy" based on animal herding but including some horticulture (around local springs), cultivation[5], and exchange (Khazanov 1994: 20-21; Bar-Yosef and Khazanov 1992: 2; Marx 2006: 86; Beherec 2011: 129; Barker 2012). This mixed economy included large-scale copper production, providing access to additional economic networks and in turn creating connections with settled societies.

Both historic and ethnographic sources have shown that pastoral nomadic populations "cannot function in isolation" from the settled world (Khazanov 1998, 1994: 198-212; Marx

[5] It is generally accepted that rain-fed agriculture was impossible in Iron Age Faynan due to the dry climate (Palmer et al. 2007; Hunt et al. 2004; Mithen and Black 2011), but Iron Age populations potentially practiced some forms of dry agriculture possibly using water management techniques (Mattingly et al. 2007; Knabb et al. 2016). Botanical remains from Khirbat al-Jariya are currently being investigated (by Brita Lorentzen and Jade d'Alpoim Guedes) for possible evidence of agricultural practices during the Iron Age.

2006: 78-82; Bar-Yosef and Khazanov 1992; Barker 2012; Bienkowski and van der Steen 2001; Finkelstein 1995; Anfinset 2010; Levy 2009). This interaction often occurs through trade relationships; production within pastoral nomadic societies is frequently oriented towards subsistence, but it can be "directed to quite a considerable extent towards exchange" (Khazanov 1994: 203). Even pastoral nomads practicing some small-scale agriculture often require additional grains from agricultural societies, especially in times of drought (Bar-Yosef and Khazanov 1992: 5)[6]. These relationships between societies with different modes of subsistence production have also been called "specialized complex systems" in which participant groups "buffer" subsistence variability through "exchange across ecological boundaries" – commonly between agricultural and nomadic societies (O'Shea 1989: 60). Furthermore, specialization in a specific craft/industry among pastoral groups (like copper production in Faynan) increases their dependency on sedentary populations for exchange, i.e., investing in non-subsistence practices can decrease resilience (Khazanov 1998: 9; Bar-Yosef and Khazanov 1992: 5). Iron Age Faynan was potentially reliant on metal production and trade networks exchanging copper for resources to survive the environment. In following, copper production can be viewed as an adaptive strategy - addressing the second complexity of examining desert peoples in the archaeological record. With this in mind, this dissertation will use the adaptive cycle to model the process through which the more mobile pastoral nomads of the Late Bronze Age transitioned to a more settled, mixed-economy in the Early Iron Age characterized by the development of adaptive strategies exploiting natural resources. Using copper production and exchange as an adaptation

[6] Written records and ethnographic evidence suggest that agricultural products "have always formed an important portion of [pastoral nomads'] diet" (Bar-Yosef and Khazanov 1992: 5; Khazanov 1994; Marx 2006). For example, diet among the Rendile (a pastoralist group in East Africa) was found to include 50-80% of caloric intake from maize over a five year study – emphasizing the role of agricultural products, purchased or otherwise produced (Marx 2006: 83-84 and citations there within).

also likely made society precariously dependent on the availability of copper ores/metal (increased connectedness), economic outlets for exchange, and potentially vulnerable to overshoot and collapse (decreased resilience).

## 2.7 Overshoot: A Possible Explanation of Collapse in the Archaeological Record (K to Ω)

Societal collapse has a longstanding interest extending over decades of research in numerous fields including anthropology, archaeology, economics, sociology, and history (Malthus 1798; Jevons 1906; Tainter 1988; Yoffee and Cowgill 1988; Chew 2001; Diamond 2005; McAnany and Yoffee 2010a; Faulseit 2016a). Over the past thirty years, collapse has been redefined to avoid misplaced expectations connecting collapse to wide-spread destruction or population loss, and explanations have been reformulated to highlight the intricacies of the collapse process (discussed further below) (Tainter 1988, 2016; Yoffee and Cowgill 1988; Butzer 2012). Critically, a recent paradigmatic shift has also created a new space for examining post-collapse processes of resilience, regeneration, and reorganization (McAnany and Yoffee 2010b; Faulseit 2016a; Schwartz and Nichols 2006; Gunderson and Holling 2002). Even in catastrophic cases, there is often evidence for enduring cultural and social continuity following collapse (in line with the adaptive cycle) (Faulseit 2016b; Hoggarth and Awe 2016). In general, this new thinking suggests collapse needs to be holistically examined with considerations of proximate causes, the collapse process, and post-collapse continuity. Archaeology is uniquely suited through its deep-time perspectives to provide this encompassing approach.

Novel understandings of collapse are largely founded on more generalized definitions (Tainter 1988; Renfrew 1984; Eisenstadt 1988; McAnany and Yoffee 2010a, 2010b; Faulseit 2016b). For example, Tainter (2012; 1988: 4) broadly proposed that “Collapse is a rapid

transformation to lower social, political, and economic complexity" [7]. This definition appropriately avoids any calamitous assumptions, and it necessitates more refined understandings of collapse and its impacts (Tainter 1988: 4-5): e.g., what level of complexity is exhibited before and after collapse? How does the collapse manifest (economically, socially, and/or politically)? Was the process rapid and severe? In other words, Tainter (2016: 37) suggests asking "What causes societies to vary and change in complexity?" is "more productive" and "anthropological" than "What went wrong?" when dealing with collapse. More recently, Faulseit (2016b: 5) presented a similarly expansive definition of collapse, building on Eisenstadt (1988): "Collapse is probably best understood as the fragmentation or disarticulation of a particular political apparatus". Both definitions afford a broad perspective of collapse, avoid eliminating possible causes of collapse *a priori*, and describe processes identifiable in the archaeological record (See Renfrew 1984: 367-369). Moreover, characterizing collapse as a "transformation" or "fragmentation" in this way invokes the possibility of social/cultural continuity (see also Ben-Yosef 2020). In line with Tainter's thinking, this research attempts to answer the anthropological question: what caused society in Faynan to experience a rapid change, transformation, or disarticulation in its social, economic, or political complexity at the end of the 9$^{th}$ century BCE?

Theories attempting to explain societal collapse in the archaeological record (or the transition from the K to Ω phase in the adaptive cycle) are abundant and diverse (e.g., Tainter 1988, 2006, 2014; Yoffee and Cowgill 1988; Yoffee 2005; Manning et al. 2020). While clear, event-based explanations such as famine or warfare are possible, collapse is more often

[7] This definition of collapse could also be interpreted as the "decomposition" of a complex system following Simon (1962: 473-475). The "decomposition" concept similarly treats collapse as a transformation, avoiding assumptions connecting collapse to catastrophe.

attributed to complex, multivariate processes involving interrelated factors - frequently a combination of human influences and natural forces/conditions (Butzer 2012). Environmental factors can take a variety of forms (e.g., drought, climate change, deforestation, etc.), and they can be paired with growing population pressure following the Malthusian paradigm of "overshoot" (Malthus 1798; Rees 2004; Tainter 2006; Catton 1980). Malthus (1798) suggested human populations grow exponentially whereas subsistence production only grows linearly; humans would out-run or 'overshoot' available resources in the foreseeable future. While Malthus was specifically looking at subsistence resources, a more generalized definition of "overshoot" following Tainter (2006: 60) building on Catton (1980) is better suited for archaeological investigations: "the outcome when a trajectory is unsustainable for environmental, technical, or social reasons". The 'trajectory' in this case is the development/growth of society (the α, r, and K phases in the adaptive cycle), and the 'outcome' of overshoot is a form of collapse (the Ω phase). Based on this understanding, overshoot can provide a possible triggering agent in the adaptive cycle, and a potential explanation for collapse in the archaeological record.

Overshoot is inherently based on carrying capacity, and, therefore, it needs to be contextualized within a "particular habitat" (the social-ecological system) (Catton 1980: 272,278). Furthermore, Catton (1980: 158) advocates that carrying capacity is not only limited by biological essentials such as food and water, but any substance or resource that is "indispensable but inadequate". These "indispensable" resources could also be interpreted as "limiting factors" – the "one or two critical resources" for human survival "in any given context" (Halstead and O'Shea 1989: 2). In other words, society along with its political and economic structures – the cultural system – can become dependent on *any* crucial resource within its

particular habitat for system 'survival' and overshooting its availability can potentially cause a collapse. However, carrying capacity can be supplemented with trade relationships through the process of "scope enlargement"; essentially, exchange for food or other vital goods that are locally unavailable (Catton 1980: 158). Through trade, a society or population is no longer limited to proximate resources but the "composite carrying capacity" of resources from diverse areas, mitigating potential collapse from exhausting the local carrying capacity (Catton 1980: 158). In other words, scope enlargement and exchange provide a "buffer mechanism" against variability in food supply (Halstead and O'Shea 1989). Critically, with scope enlargement comes increased vulnerability, or decreased resilience, because any disruption to this trade can have significant repercussions (Catton 1980: 159)[8]. As such, to evaluate a possible case of overshoot and collapse, both the particular habitat and exchange relationships of a culture system require consideration.

A limited number of examples of overshoot and collapse have been identified in the archaeological record (e.g., Diamond 2005; Chew 2001; Jacobsen and Adams 1958; Hughes and Thirgood 1982; Catton 1980: 214-216), but Tainter (2006: 71) recently reinterpreted and undermined many of these case studies (See also McAnany and Yoffee 2010b: 5-8 and Redman 2005: 74-75 for additional discussion on applying overshoot to the archaeological record). It is proposed that situating overshoot within resilience theory and treating it as a triggering event in a highly connected social-ecological system supports the overshoot and collapse theory which can also be understood as modeling the transition from the K to Ω phase. Redman (2005: 75) briefly

[8] While not using the theoretical perspectives of "overshoot", Finkelstein (1995: 38) described a similar phenomenon where pastoral-nomadic societies can become overly dependent on sedentary people; "A crisis in the settled land, with a decrease in its agricultural production, would undermine these symbiotic relationships (no grain surplus for the nomads)". Finkelstein (1995: 38) suggests pastoral nomads would then be forced to shift to a more agropastoral subsistence and further sedentarization.

considered overshoot as a possible triggering agent for collapse in the adaptive cycle, but also (correctly) acknowledged the debate in the archaeological discourse over the relationship between environmental degradation and societal collapse. He concluded that overshoot and collapse need to be treated as a "case-by-case situation" (Redman 2005: 75). Furthermore, Redman (2005: 74) suggests "a triggering event causing release and collapse also can occur as the result of an internal change in the system, often having inadvertently developed as part of the strategy to maintain the system in K". In combination with the overshoot model, intensive mining and over-exploitation of copper ores in Iron Age Faynan, which likely "developed as part of the strategy to maintain the system", could provide this event which drove collapse. In this way, Iron Age Faynan can function as one such "case" of overshoot and collapse in the archaeological record. This dissertation tests this possibility.

## 2.8 Copper, Culture, and Collapse

In summary, this dissertation proposes a new theoretical framework drawing from the anthropology of technology, systems approach to culture, and resilience theory to holistically examine the formation, growth, and collapse of Iron Age society in Faynan. A redefining of technology that avoids inaccurate assumptions of technological determinism or somnambulism provides the foundations. Treating technology as a system of techniques within a sociocultural framework allows archaeologists to identify and examine the reciprocal relationships between technology and culture. Furthermore, positioning technology as a subsystem within a larger cultural system properly recognizes technology as a critical component of a functioning society. Technology is "inextricably bound" to the other subsystems of culture, and *vice versa*. Consequently, technological developments can facilitate growth of the entire system through

positive feedback loops (the multiplier effect). However, growth is only an initial stage of the culture system which experiences transformational changes on different geographical and temporal scales. Resilience Theory provides a model for understanding such complex systems as they move through the various phases of the adaptive cycle which represent the origins, development, collapse, and post-collapse continuity of a social system[9]. Moreover, the "release" phase of the adaptive cycle affords a new theoretical perspective for examining collapse in the archaeological record. Resilience Theory suggests "release" is often driven by trigger agents within a highly connected system making overshoot a logical and plausible example. Overshoot is particularly pertinent in the Faynan case where Iron Age society was probably precariously reliant on the copper to maintain the cultural system, especially considering the pastoral nomadic social and economic organization. Finally, the adaptive cycle of Iron Age Faynan must be "nested" within the larger and slower cycles of the Eastern Mediterranean more generally to identify the "remember" and "revolt" interactions that could have impacted the trajectory of Iron Age society and copper production in the region. In doing so, Faynan will be temporally and geographically contextualized within the *longue durée*. Through this combined theoretical lens, this dissertation will identify, examine, and model the significant interrelationships between culture, copper, and collapse in Iron Age Faynan.

[9] The transitions between Ω to α and α to r phases, while not emphasized in this chapter, will also be discussed, see Chapter 7.

# Chapter 3 - Background: Faynan, Edom, and the Wadi Arabah in the Iron Age

## 3.1 Introduction

This chapter provides the foundational information and background which the forthcoming chapters rely and build upon. An overview of the region of interest is first provided, focusing on the Wadi Arabah, Faynan, and Edom. To situate this research in the environmental context, this chapter discusses current understandings of the climate (present and past) and geology (particularly in reference to its copper ore resources) of Faynan in order to establish the "ecological niche" of the Iron Age in this part of the Southern Levant. Furthermore, as the natural characteristics of the copper ores in Faynan directly impact the archaeological record and our interpretations of it – they are taken into consideration and described here. This dissertation builds on a long and rich history of research in Faynan over the past ca. 100 years. The various explorations, surveys, and excavations in Faynan provide critical foundations that allow this research to function, and they are reviewed in detail. A final section focuses on the origins of iron production and its possible connection to copper smelting, a primary research question of this dissertation. The chapter is concluded by describing how the remaining chapters both rely and build on this previous research.

## 3.2 Geography – The Wadi Arabah, Faynan, and Edom

### 3.2.1 Geography of the Wadi Arabah and Faynan

This research is focused on the Faynan region of modern Jordan. Faynan is located ca. 30 kilometers south of the Dead Sea on the northeastern edge of the Wadi Arabah/Aravah (Figure 3.1). The Wadi Arabah is a large depression stretching ca. 160 kilometers from the Gulf of Aqaba/Eilat in the south to the southern tip of the Dead Sea in the north, and it

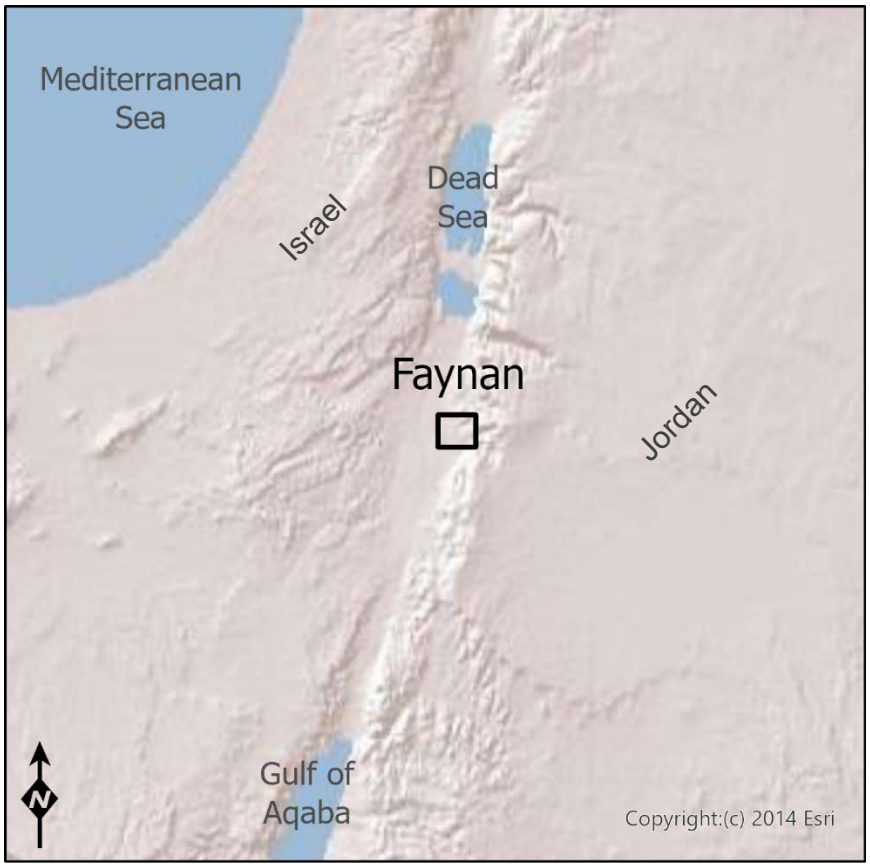


**Figure 3.1:** Location of Faynan in modern Jordan on the northeastern side of the Wadi Arabah. Map produced by Brady Liss.

functions as a natural border between modern Israel and Jordan. The Arabah is part of the Dead Sea Transform or Dead Sea Rift which is the border of the Arabian and African tectonic plates; movement between these plates created the Arabah Valley. Furthermore, uneven geological uplifting on both sides of the valley resulted in varying environmental characteristics (especially between the lowlands in Faynan and the Jordanian Plateau) and geological exposures from east to west across the Arabah (Levy, Ben-Yosef, and Najjar 2014: 8-9, Figure 1.2, 1.14). Critically, this uneven uplifting shaped the exposure and availability of copper ores in Faynan and Timna. Timna is a smaller copper ore zone with a rich archaeological record of copper production in modern Israel and also located within the Wadi Arabah roughly 110 kilometers to the southwest (Rothenberg 1990a, 1990b). Faynan and Timna were originally part of the same copper ore

resource zone, but they were subsequently separated by the tectonic shift of the Dead Sea Rift (see Hauptmann 2007: Figure 4.3). The eastern side of the Wadi Arabah including Faynan experienced a more drastic uplifting which exposed the characteristic red sandstone of the region (discussed below) and the Dolomite-Limestone-Shale, the main copper ore horizon, in Faynan (Levy, Ben-Yosef, and Najjar 2014: 9). These geological phenomena of the Wadi Arabah provided the foundations for copper producing societies in the Faynan region from late prehistory to Islamic times.

Today, Faynan is considered to cover an area of ca. 300 square kilometers (Levy, Ben-Yosef, and Najjar 2014: 9). Within Faynan are two main wadi basins which drain into the Wadi Arabah to the west (Levy, Ben-Yosef, and Najjar 2014: Figure 1.3). In the north, the Wadi al-Ghuwayba catchment with its tributaries is the primary research area for this dissertation. Located along the Wadi al-Ghuwayba are major Iron Age smelting sites including Khirbat en-Nahas and Khirbat al-Ghuwayba. The Wadi al-Jariya is a tributary of the Wadi al-Ghuwayba; Khirbat al-Jariya and various mining sites are located along this wadi. To the south, the Wadi Fidan which transitions into the Wadi Faynan as it moves east is the major wadi (Levy, Ben-Yosef, and Najjar 2014: Figure 1.3). The Wadi Dana and Wadi Ghuweir provide its main tributaries, and many significant Iron Age sites are located along the Wadi Fidan/Faynan including Wadi Fidan 40, Rujm Hamra Ifdan, Khirbat Hamra Ifdan, and the eponymous Khirbat Faynan (Levy, Ben-Yosef, and Najjar 2014: 9). Each catchment also contains a perennial spring, ‘Ain al-Ghuwayba and ‘Ain Fidan, which likely provided a critical water source in antiquity (other springs may also have been active in the past) (Levy, Ben-Yosef, and Najjar 2014: 9).

The Faynan region is named after Khirbat Faynan, one of the main copper smelting centers from antiquity, which draws its name from ancient texts (Levy, Ben-Yosef, and Najjar

2014: 8; Najjar and Levy 2011; Edelman 1995: 4-5). “Faynan” is the modern Arabic spelling of the various names used for the region in the past including Pinon, Punon, Phinon, Phaeno, Fenum, Fin, Fenon, Phaison, and Feinan (Najjar and Levy 2011: 32). The earliest Biblical mention of Faynan is Genesis 36:41 where “Pinon” is listed as one of the regions within Edom (discussed below); note that P and F are the same letter in most Semitic languages (Najjar and Levy 2011: 32). This same reference to Pinon appears again in 1 Chronicles 1:52, and “Punon” is mentioned as one of the places the Israelites camped during their Exodus from Egypt in Numbers 33:42-43 (Najjar and Levy 2011: 32; Edelman 1995: 4-5). In later periods during the Roman and Byzantine Empire, Faynan is mentioned in texts describing the punishments for criminals and Christians – being condemned to the mines of Faynan (Najjar and Levy 2011). For example, Eusebius describes a bishop sent to “the copper mines of Phaeno” and the Christian historian Theodoret mentions monks being tortured and subsequently “sent to the *metalla* of Phenneusus [Faynan]” (quoted in Najjar and Levy 2011: 36). The local Bedouin communities who live there today still refer to the region as Faynan, although they derive the name from a variety of traditions and stories (“What’s In a Name? The Many Names of Feynan”). Critically, the Biblical text places Faynan within “Edom”, which plays a more significant role in texts associated with the Late Bronze and Iron Ages.

### 3.2.2 Geography of Edom

Edom, a term used to refer to both a land and a group of people, is a polity that likely arose in the Late Bronze and Iron Ages alongside other nascent sociopolitical entities such as the Israelites, Moabites, Ammonites, etc. (discussed in Chapter 1, Avishur 2007). Generally located in the southeastern Transjordan, the borders of ancient Edom have been theoretically identified

through a combination of text and archaeological evidence (Levy, Ben-Yosef, and Najjar 2014: 9-12; Glueck 1936a; Edelman 1995; Zucconi 2007; Avishur 2007; Rainey and Notley 2006: 162). However, they are debated, and should not be considered completely secure; border zones also changed and fluctuated during the Late Bronze and Iron Ages (Levy, Ben-Yosef, and Najjar 2014: 9-12). A particularly questioned issue is how far the Edomite territory may have extended into the southern Negev and when such an expansion may have occurred (Zucconi 2007; Edelman 1995: 2-3; Glueck 1936a; c.f. Rainey and Notley 2006: 162). Regardless, the currently identified and generally accepted borders of Early Iron Age Edom encompass Faynan and the highlands of Edom in the Shara mountains to the east (Figure 2.2) (Avishur 2007; Edelman 1995; Glueck 1936a). According to the Biblical narrative, the northern border of Edom, which it shared with Moab, was the Zered River which has been identified with the Wadi al-Hesa (Avishur 2007: 151). The eastern border was naturally delineated by the deserts of eastern Jordan, potentially inhabited by the Kedemites of the Hebrew Bible, and the southern border was mainly identifiable by the Gulf of Aqaba and the Biblical port city of Ezion-Geber (Avishur 2007: 151). The southern border extending to the Gulf of Aqaba was recently reiterated by Ben-Yosef's (2010; Ben-Yosef et al. 2019) research which suggests Timna was also part of Edom (some scholars suggested Edom did not extend this far south, see Edelman 1995: 2-3). As mentioned, the western boundary during the Iron Age is more convoluted and potentially was never fixed (Avishur 2007: 151). with some scholars suggesting Edom did not extend beyond the Arabah (Glueck 1936a: 152; Edelman 1995: 3) and others proposing an extension into the Negev during certain periods (Zucconi 2007; Rainey and Notley 2006: 162; Levy, Ben-Yosef, and Najjar 2014: 12). In sum, Faynan, Timna, and the Iron Age copper industry of the Wadi Arabah were likely within the Edomite territory of the Iron Age (Figure 3.2) (Ben-Yosef et al. 2019).

This geographic location also shapes the climate of the region, both past and present, and impacts the lifeways of its inhabitants to this day.

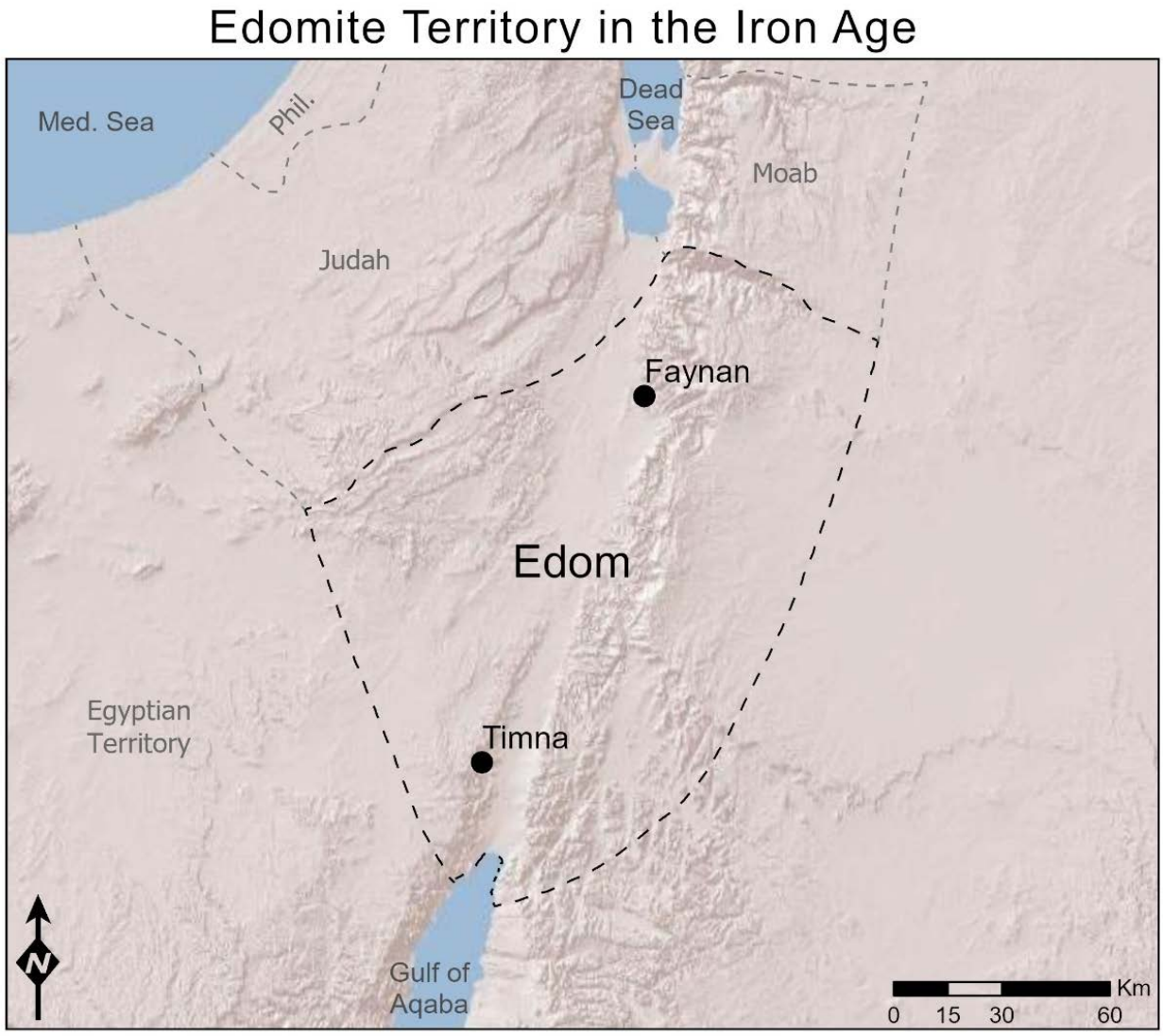


**Figure 3.2:** Territorial boundaries of Edom in the Iron Age following Rainey and Notley 2006: 162. Phil. – Philistia. The extent and chronology of the territory are debated (particularly with regards to the western extent into the Negev, see text), but Ben-Yosef's (2010; Ben-Yosef et al. 2019) research further reiterates that at least Faynan and Timna were part of a unified sociopolitical entity. The eastern border of Edom is determined by the desert, possibly inhabited by the biblical Kedemites (Avishur 2007: 151). Shaded relief base layer copyright Esri 2014. Map produced by Brady Liss.

## 3.3 Current and Past Climate of Faynan

As mentioned, the culture system model includes environment as one of the inherent parameters of a society, and the adaptive cycle models the trajectory of social-ecological systems requiring consideration of the particular ecology. Faynan today is also characterized by its harsh climate and environment which play a role the adaptive strategies and lifestyles of the current populations warranting further investigation of the past climate and environment. The copper production industry of the Iron Age introduces further complexities in requiring fuel sources and subsistence resources to sustain a population of miners, smiths, laborers, etc. (Ben-Yosef 2010: 110-126). The climate of the Iron Age was briefly touched on in Chapter 2, suggesting that it was similar to today; this section will further unpack this claim to provide additional discussion of the current paleoclimatic data and interpretations. A complete and detailed review of all the paleoclimate studies for the Eastern Mediterranean is outside the scope of this dissertation; however, the general overview presented here sufficiently considers the likely paleoclimatic reconstruction for the Iron Age in Faynan. It is important to note that paleoclimatic data is highly variable, often localized, and occasionally lacks the high-resolution dating required to make secure connections between the climate and societal/cultural processes at the sub-century level that is so important for studies like the one presented here (for further discussion, see Knapp and Manning 2016; Finné et al. 2011; Ben-Yosef 2010: 110-126 for Faynan specifically). Finally, monocausal explanations of climatic/environmental determinism need to be avoided, while still recognizing the important role of environment and climate on the trajectory and history of a society (Rosen 2007: 1-16; e.g., McGovern 1980: 245-246, 268-272). Thus, the paleoclimatic reconstructions reviewed here should be considered critically as a “parameter” of the cultural system, and not necessarily the determining cause in sociocultural processes in Iron Age Faynan.

The current climate and environment of Faynan is used as a reference point and as such needs to be clarified. Faynan is located in the Saharo-Arabian desert zone, characterized by a hot and arid climate (Palmer et al. 2007: 25-27; Cordova 2007: Figure 2.9; Bruins 2006: 29-30). Most of the rain falls in the winter months, between December and March, and there is almost no precipitation during the summer months from June to September (Palmer at al. 2007: 27). The average rainfall for Faynan is ca. 50-60 millimeters per year, and it is highly variable (Figure 3.3) (Bruins 2006: Figure 2.1; Hunt et al. 2004: 922; Ababsa 2013: 64, Figure 1.12; Palmer et al. 2007: 27). This amount is below the required minimum for rain-fed agriculture (barley requires ca. 200 millimeters per year, for example), and modern populations rely on drip-irrigation systems using plastic pipes and above-ground cisterns to collect and store flood/rainwater to support some agriculture (Knabb 2015: 204; Knabb et al. 2016: 88). The average temperature for the lowlands of the Wadi Arabah is around 23-24°C with hot summers and warm winters (Bruins 2006: 30, Table 1). The vegetation of the region is primarily desert shrubs and other xeromorphic plants adapted to the dry landscape such as acacia and tamarix (Palmer et al. 2007: Figure 2.11 and 2.12). Some perennial springs, such as ‘Ain al-Ghuwayba, provide enough for water for small orchards and fruit trees (discussed further in Chapter 4). Despite the limited vegetation, it is still sufficient for the seasonal grazing herds of the local Bedouin (Palmer et al. 2007; Ben-Yosef 2010: 117). In sum, Faynan is currently a hot and dry desert environment with limited rainfall that has made it marginal for agriculture until the advent of modern agro-technology.

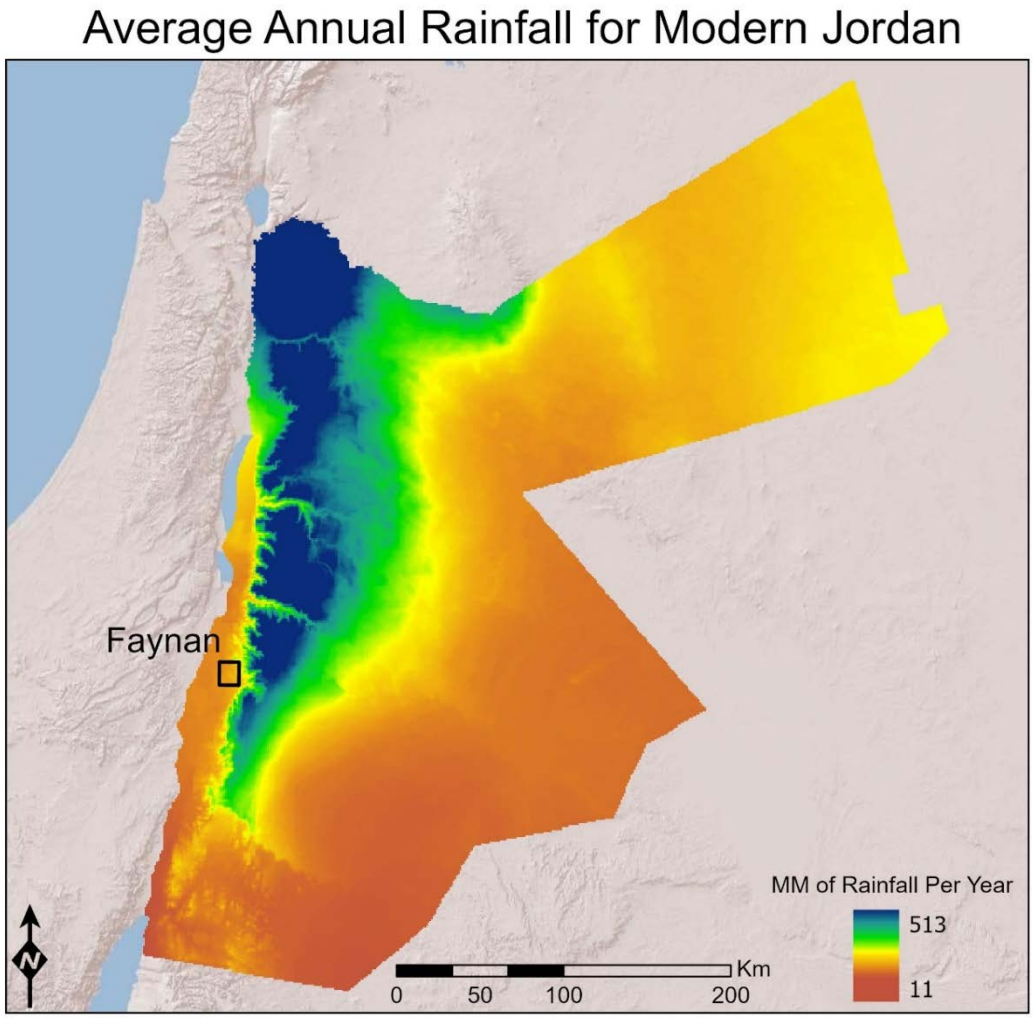


**Figure 3.3*:*** Rainfall data for modern Jordan. The average annual rainfall in Faynan is ca. 50-60 millimeters with significant seasonal variability. Rainfall data and layer from Fick and Hijmans 2017. Shaded relief base layer copyright Esri 2014. Map produced by Brady Liss.

Paleoclimatic reconstructions in the Eastern Mediterranean have been a focus of significant scholarly research. At the local scale, paleoclimatic and environmental reconstructions in Faynan were addressed by the Wadi Faynan Landscape Survey (Barker, Gilbertson, and Mattingly 2007; Hunt et al. 2007, 2004; el-Rishi et al. 2007). Using a combination of modern biogeographical data, palynology, geomorphology, and charcoal evidence from Wadi Faynan, this project reconstructed the environment and climate of Faynan

for the entire Holocene (el-Rishi et al. 2007; Gilbertson et al. 2007; Hunt et al. 2004, 2007). Based on the evidence, they concluded that the Iron Age in Faynan had "essentially the modern climate and geomorphic regime" (Gilberston et al. 2007: Table 13.4: el-Rishi et al. 2007: Figure 3.17). However, the authors also point out some of the methodological difficulties in their reconstruction such as the "patchy and discontinuous" evidence and the limited temporal resolution (Gilbertson et al. 2007: 404, 407). Regardless, this research provides the only current climatic reconstruction based on evidence directly from Faynan. On a slightly larger scale, Cordova (2007) reconstructed the past environments of Jordan more generally using geoarchaeological and cultural ecological approaches. While the Iron Age does not receive specific attention, he does suggest "it is possible that even the people who inhabited Transjordan during the Iron Age faced an already deteriorated environment" in comparison to a moister Early Bronze Age (Cordova 2007: 195).

Previous studies have also reconstructed the climate of the Southern Levant on a regional scale. The climate data comes from a variety of sources including water levels in seas and lakes, palynological data from sediment cores, and isotopic analyses from cores and speleothems among others (Kaniewski et al. 2019; Frumkin and Elitzur 2002; Migowski et al. 2006; Langgut et al. 2015; Schilman et al. 2001; Bar-Matthews, Ayalon, and Kaufman 1997). Using geomorphological evidence, Fumkin and Elitzur (2002) suggest the Dead Sea was relatively high from ca. 1500-1200 BCE and low from 1200-500 BCE representative of a dry climate during the Iron Age (they also draw support from the archaeological and historical records). While their data differs slightly for the Late Bronze Age, Migowski et al. (2006: Figure 4) similarly identified a relative low period in the Dead Sea during the Iron Age using sediment cores. They suggest the climate deteriorated starting in ca. 1450 BCE and a drier climate persisted until 200

BCE (Migowski et al. 2006: 426-427, Figure 4). In contrast, using marine core sediments off the coast of Israel and oxygen isotope analysis, Schilman et al. (2001) suggest there was a humid period between 1550-1050 BCE followed by more arid conditions until ca. 50 BCE in the Eastern Mediterranean. Isotope analysis of speleothems from the Soreq Cave in Israel yielded somewhat different results indicating the climate was similar to today from ca. 5050 BCE to 950 CE with some short periods of variation (Bar-Matthews, Ayalon, and Kaufman 1997: 161-166, Table 2). Isaar and Zohar (2007: Figure 3a and 3b, 193-194) synthesized some of these data sets (including the levels of the Dead Sea, levels of the Mediterranean Sea, and the Soreq Cave isotopes) to suggest a colder and humid period at the beginning of the Iron Age, which became more arid as the Iron Age continued. The Water, Life and Civilization Project also investigated the past, present, and future climates of the "Middle East", similarly using an aggregate of data from a variety of regional climatic reconstructions (Mithen and Black 2011; Rambeau and Black 2011). Based on their interpretations, Rambeau and Black (2011: 99, Figure 7.2) also suggest the Iron Age was an arid period possibly starting with a wetter climate; however, they point out the conflicting nature of the data (discussed further below).

A team lead by David Kaniewski has published extensively on the Late Bronze and Iron Age paleoclimate in the Eastern Mediterranean focusing primarily on identifying paleoclimatic drivers connected to the Late Bronze Age collapse (Kaniewski et al. 2019, 2020, and citations there within). Contributing sediment cores and pollen analysis from Syria, Cyprus, and Israel, Kaniewski et al. (2020, 2019, 2013, and 2010) identified a drying period or drought around the Late Bronze to Iron Age transition. From two cores extracted at Gibala-Tell Tweini on the coast of modern day Syria, Kaniewski et al. (2010: 210, Figure 3) identified low percentages of pollen from cultivated plant species and grasses associated with a 350 year period dated from ca. 1210-

860 BCE with a short spike in moisture around 1000 BCE. Similarly, their results from a single core collected from Larnaca Salt Lake near the Hala Sultan Tekke in Cyprus identified a drying event around 1200 BCE based on pollen analysis (Kaniewski et al. 2013). These cores also suggest some improvement in the climate following the extreme drying around 1200 BCE and moving towards the 1000 BCE moisture spike mentioned above (Kaniewski et al. 2019: Figure 5). They also draw support from cores at Tel Dan and Tel Akko in modern Israel which provide additional evidence for a drying period at the end of the Late Bronze Age (Kaniewski et al. 2019: Figure 5). In general, the evidence suggests drought may have been a major contributing factor in the Late Bronze Age collapse, and conditions might have improved slightly during the first centuries of the Iron Age.

Finally, the climate of the Southern Levant was also recently reconstructed by Langgut et al. (2015; Langgut, Finkelstein, and Litt 2013) using cores and palynological data from several locations in Israel. The authors combined their core from the Sea of Galilee with three other climate reconstructions from Birkat Ram, ‘Ein Freshka, and Ze’elim Gully, all of which are located along a north-south transect across Israel, to investigate the Early Bronze through Iron Ages (Langgut et al. 2015). Relevant here, the pollen records indicated an extremely dry period at the end of the Late Bronze Age before conditions improved in the Early Iron Age with a more humid climate (Langgut et al. 2015: 228-231). The data suggests the climate remained humid through the $10^{th}$-$9^{th}$ centuries BCE before a shift towards a more moderate climate in the $8^{th}$-$7^{th}$ centuries BCE (Langgut et al. 2015: 229-231, Figure 5). With that said, there was some acknowledged inconsistency in the data with the Birkat Ram core not indicating similar climatic fluctuations, possibly due to its location which receives significant annual rain fall (Langgut et al. 2015: 230). It should also be noted that the authors identified most vegetation changes within

the Mediterranean and semi-arid zones; Faynan is in the Saharo-Arabian desert zone which perhaps needs further investigation and was potentially less impacted by the identified climatic changes (Langgut et al. 2015: 230). In general, the pollen evidence suggests the Southern Levant was more humid in the Early Iron age, and slightly drier in the later periods of the Iron Age.

While brief, it is apparent from this overview that there are some inconsistencies and disagreements in the paleoclimatic data for the Southern Levant during the Late Bronze and Iron Ages. This issue has been generally highlighted by Finné et al. (2011) who aggregated data from 80 paleoclimate records to review the last 6000 years in the Mediterranean region. Their results show variations in the data across the Bronze and Iron Ages for temperature and aridity reconstructions (Finné et al. 2011: Figures 2 and 5). Knapp and Manning (2016: 111) similarly emphasized the inconsistency across paleoclimate reconstructions. Both groups cite poor chronological resolution as a likely cause for these discrepancies with Knapp and Manning (2016: 111, 117) concluding that "we lack any usefully defined (in temporal terms) climatic data from the Eastern Mediterranean region" (also Finné et al. 2011: 3169). Given the current state of the evidence, it is difficult to make any solid claims concerning the climate of Faynan during the Iron Age. However, from the above data, it is generally agreed upon that the beginning of the Iron Age was relatively wetter in comparison to the Late Bronze Age which may have experienced a drying event. The climate then seems to become more arid and dry as the Iron Age continues (especially by ca. 1050 BCE), likely similar to the modern climate and environment in Faynan.

## 3.4 The Geology of Faynan and its Implications for the Archaeological Record

The geology of Faynan, as a resource zone, plays an especially important role in understanding the archaeological record, particularly from an archaeometallurgical perspective (Figure 3.4) (for detailed reviews of the geology of the entire Eastern Mediterranean, see Hauptmann 2007, Palmer et al. 2007, and citations there within, see also Rabba' 1991). The presence of abundant copper ores was likely a primary incentive for periods of more sedentary habitation in the region, and the ability to successfully exploit the natural resources was critical to the sociopolitical trajectory of the Iron Age. This section provides an overview of the processes that resulted in the rich mineralization of copper in Faynan, along with the important details concerning the copper ores in relation to this research.

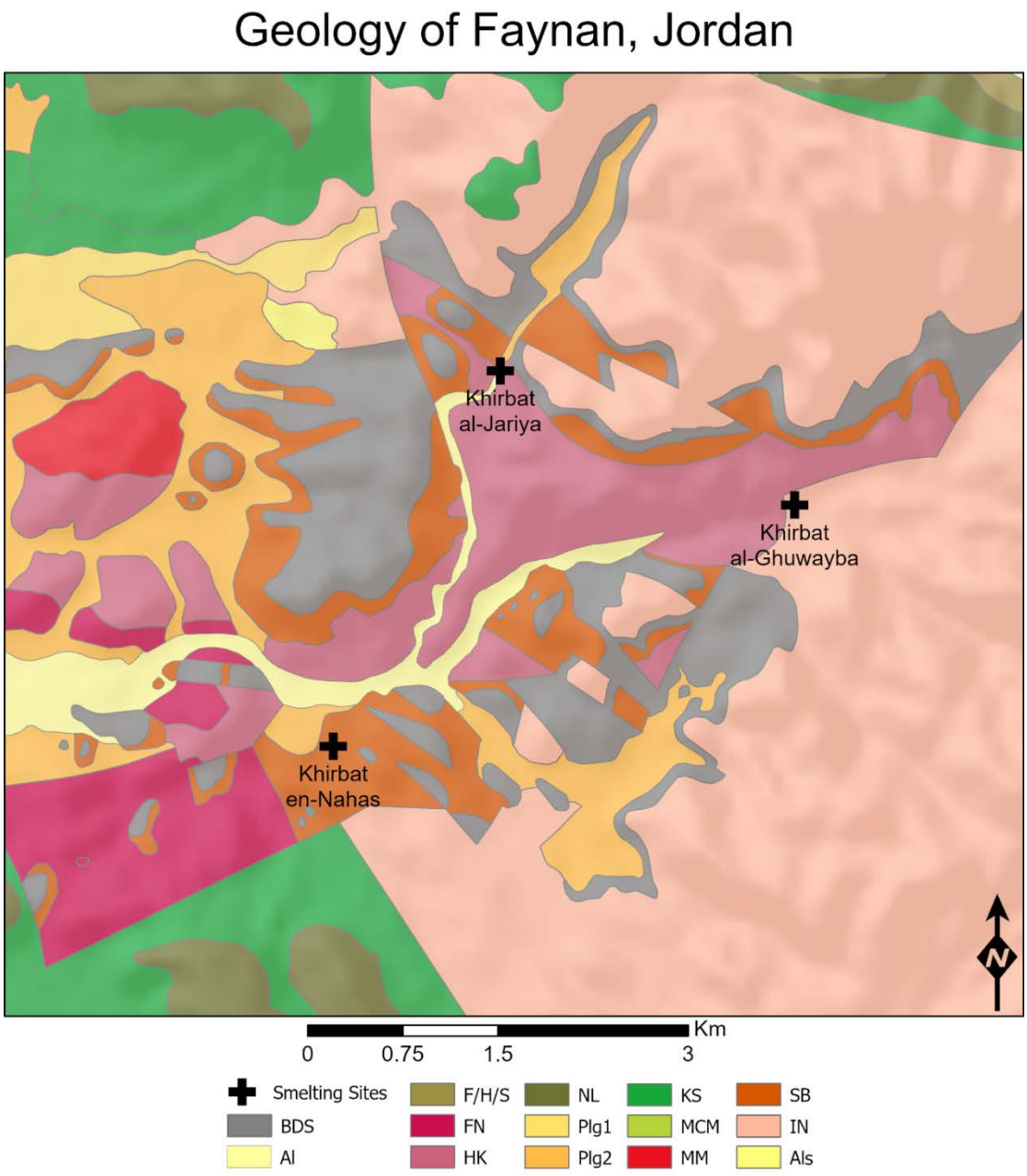


**Figure 3.4:** Geology of Faynan in the immediate area around Khirbat en-Nahas, Khirbat al-Jariya, and Khirbat al-Ghuwayba. Note the presence of Dolomite Limestone Shale or Burj Dolomite-Shale (BDS) near the smelting sites. Legend: BDS - Burj Dolomite-Shale, Al - Alluvium Sands, F/H/S - Fuhays Hummar Shuayb, FN - Finan Granitic, HK - Hunayk Monzogranite, NL - Na'ur Limestone, Plg1 - Wadi Araba Fluviatile Sand and Gravel, Plg2 - Fluviatile Gravel, KS - Kurnub Sandstone, MCM - Muwaqqar Chalk Marl, MM - Minshar Monzogranite, SB - Salib Arkosic Sandstone, IN - Umm Ishrin Sandstone, Als - Aeolian Sand. Map and legend based on Rabba' 1991. Map produced by Matthew D. Howland, Brady Liss, and Tyler Tucker. Shaded relief base layer copyright Esri 2014

As noted above, the copper mineralization of Faynan and Timna were the result of the same processes, and they were subsequently separated through tectonic shift (Hauptmann 2007: 64, Figure 4.3). The genesis of these copper ores was simplified into a three-stage process: (1) The formation of primary copper-iron sulfide mineralizations in Late Precambrian volcanic rocks roughly 500 million years ago; (2) The erosion of these volcanic rocks in the Lower Cambrian period resulting in copper-rich dolostones in marine environments. This stage was also associated with the migration and redeposition of copper as chlorides and the mineralization of manganese ores; (3) Finally, the formation of the Rift Valley, its erosion/weathering, and faulting/fracturing created a karst formation (shaped by erosion and characterized by irregularities like caves and sinkholes). The karst formation was subsequently filled by residual sandy-clayey components which provided the host sediments for an enrichment of secondary copper and manganese ores. The result of these processes was the copper ore bearing Cambrian unit of the Dolomite-Limestone-Shale (DLS), also known as the "Burj Limestone" (Hauptmann 2007: 67-68, Figure 4.4). The copper and manganese ores of the DLS are stratabound, being limited to narrowly defined stratigraphic levels, and composed primarily of copper oxides and silicates (abundant Chrysocolla and Malachite) (Hauptmann 2007: 68). While the thickness of the DLS formation ranges from twenty to forty meters in total, the most substantial copper and manganese mineralizations are found in the upper shale formations that are roughly 1-1.5 meters thick (Hauptmann 2007: 65-66). These dark mineralization layers of the DLS are easily recognizable throughout Faynan in the form of cliffs, terraces, and plateaus (Hauptman 2007: 65). Thus, they were easily identifiable by past populations.

The characteristics of the DLS copper ores have significant implications for copper smelting. It is important to note that the copper oxides and silicates of Faynan do not require

roasting prior to smelting; sulfide ores, such as those in Cyprus, do require this preliminary step (Hauptmann 2007: 68-69; see also Kassianidou and Knapp 2005). Additionally, the copper ores in Faynan were found to contain 15-45% copper, and likely did not require further beneficiation (Hauptmann 2007: 71). Finally, the inter-growth of substantial manganese among the copper ores of the DLS, an average manganese content of 41-43%, provided an intrinsic fluxing agent - an additive that assists in purifying the metal and liquefying slag, resulting in smelts with purer metallic yields (Hauptmann 2007: 70-71, 234; Ben- Yosef 2010: 100; Ben-Yosef et al. 2019). Fluxes were commonly a secondary additive to a smelt and required an additional procedure in the copper production *chaîne opértoire* (Tylecote 1992: 189). Moreover, other fluxes used in copper smelting include iron minerals, as is seen in Timna, but manganese is more efficient in purifying the copper (Ben-Yosef 2010: 100). Consequently, manganese-rich copper ores of the DLS afford a twofold advantage: they are self-fluxing eliminating the need and procurement of secondary additives, and the manganese is a superior flux in comparison to other minerals.

As this dissertation also investigates possible iron production in Faynan, it is important to examine possible sources of iron. While the copper ores of the DLS are relatively low in iron content, the intergrown manganese ores can be rich in iron. These ores were found to contain an average of 8-10% iron oxide with enrichments in hematite and goethite in some areas (Hauptmann 2007: 71; Basta and Sunna 1972). One such area of enriched iron was identified to the southeast of Khirbat en-Nahas, the El-Furn mines (El-Furn is an Islamic Period smelting site also known as Khirbat Nuqayb al-Asaymir) (Hauptmann 2007: 71; Jones, Levy, and Najjar 2012). As these mines were exploited in antiquity, the iron-rich copper-manganese ores were potentially smelted in the Iron Age. While not a source of iron, the DLS formation also includes nodules and layers of phosphorite (Hauptmann 2007: 66). In his study of copper slags from Iron

Age Faynan, Hauptmann (2007: 209, Figure 6.4) found iron phosphide dendrites associated with prills of α-Fe within copper inclusions trapped in slag; phosphorus has a stronger affinity for iron than copper. He further suggested that this is a unique quality of copper produced in Faynan, and it could potentially be used for provenance studies (Hauptmann 2007: 210-211). Thus, smelting charges using DLS ores during the Iron Age at least occasionally contained iron and phosphorus, likely from the manganese flux and phosphorite inclusions respectively (discussed further in Chapter 5).

Based on the geology, Hauptmann's (2000, 2007) extensive archaeometallurgical surveys of Faynan recognized developmental stages in ore procurement through antiquity. By analyzing the elemental composition of chronologically controlled slag samples, Hauptmann (2007: 184) discovered a dichotomy in the ores used between the Early Bronze Age and Iron Age in Faynan. In the Early Bronze Age, slags contained a broad range of chemical compositions, whereas the Iron Age slags showed less variation in elemental content and a prominent tendency for being rich in manganese – connecting these slags to the DLS ores (Hauptmann 2007: 184). Along with mining evidence from this period, he determined that the DLS provided the principal ore source for Faynan copper production during the Iron Age (the intensive copper smelting of the Roman-Byzantine Period exploited ores from the Massive Brown Sandstone formation) (Hauptmann 2007; Ben-Yosef 2010: 98-99). This understanding is reiterated by the outcrops of ore-bearing DLS around the main Iron Age smelting centers including Khirbat en-Nahas, Khirbat al-Jariya, and Khirbat al-Ghuwayba (Figure 3.4; Hauptmann 2007: 64; Rabba' 1991). In addition, Hauptmann (2007: 184, 251) further suggested the Iron Age miners deliberately and carefully selected manganese-rich ores for their self-fluxing properties, representing a technological development from previous periods.

To summarize, the geology and geological history of Faynan resulted in rich outcrops of copper ores in the DLS unit exposed throughout the region. The nature of the copper ores, oxide and silicate ores with high copper and manganese contents, allowed for a streamlined smelting *chaîne opértoire*; they did not require roasting, beneficiation beyond manual sorting, or secondary fluxes. Smelting DLS ores results in slags with similarly elevated manganese contents, and copper inclusions containing iron phosphides due to the presence of phosphorite in the DLS formation. The rich copper ores of Faynan provided a significant incentive for more sedentary or semi-nomadic habitation in the region, and the Iron Age smelting and mining sites focused on the DLS ores. The dry climate described above and the lack of modern mining helped preserve these smelting centers which are still visible on the surface and drew the attention of exploders and archaeologists visiting the region.

## 3.5 History of Research

### 3.5.1 Early Explorations, Surveys, and Excavations in Faynan and Edom

Early research in Faynan was largely limited to explorations and surveys by archaeologists, orientalists, and colonial and military topographers. In 1883, Major Horatio H. Kitchener (1884) surveyed Faynan during his expeditions from the Dead Sea to Aqaba, providing the first report of a major smelting site in the area, Khirbat al-Jariya (Ben-Yosef and Levy 2014a:179). In the report chronicling his expedition into the Wadi Arabah, Kitchener (1884: 213-214) describes a day of exploration after pitching camp in the Wadi al-Ghuwayba. Roughly 10 kilometers from the camp one of Kitchener' s associates, found "the ruins of a small town in a valley" with "ruined walls" and "some black heaps resembling slag heaps" which was later identified as Khirbat al-Jariya (Kitchener 1884: 214; Ben-Yosef and Levy 2014a: 180, 183).

The Czech orientalist and explorer Alois Musil (1907: 298) subsequently surveyed Faynan (as well as Timna) recording other smelting sites in the region including Khirbat en-Nahas. According to Glueck (1935: 29), Faynan was also visited by British scholars including Alec Kirkbride, George Horsfield, and R.G. Head, but they did not keep significant records of their visits (Ben-Yosef 2010: 130). Fritz Frank (1934: 221-224, Plan 16), a German Templar, later surveyed the metal producing regions of the Arabah including Faynan in the early 1930s, and he provided an early and accurate sketch of Khirbat en-Nahas (see also Hadas 2006).

The Edomite territory and its prominence in the biblical narrative also drew early attention from biblical archaeologists. Following Frank, dedicated archaeological research in the Arabah also began in the 1930s. As director of the American School of Oriental Research (now W.F. Albright Institute of Archaeological Research) in Jerusalem during the "Golden Age" of biblical archaeology, Nelson Glueck (1934, 1935, 1940a) headed extensive, systematic surveys of the Transjordan region in pursuit of archaeological substantiations of the biblical narrative. During his surveys of the Wadi Arabah and the Southern Negev desert of modern Israel, Glueck (1935) detailed the presence of significant archaeological remains in immediate proximity to abundant copper ores in Edom around Timna and Faynan. Glueck (1935: 138) reported major copper smelting centers in Faynan including Khirbat en-Nahas, Khirbat al-Jariya, and Khirbat al-Ghuwayba which he attributed to the 13$^{th}$-8$^{th}$ centuries BCE based on ceramic typology (he would later further narrow this date range to primarily the 10$^{th}$ century BCE to fit his Solomonic narrative, Glueck 1940a: 50-88). In light of these substantial sites with significant evidence of copper smelting and the large fortress at Khirbat en-Nahas, Glueck (1935: 137-139) concluded that Edom developed into a powerful kingdom in the Early Iron Age through its accessibility to copper ores proclaiming, "The civilization of Esau was certainly not inferior to that of Jacob [i.e.

the Israelites]". The predominant role of copper in Edom's evolution was further corroborated by Glueck's excavations at Tell el-Kheleifeh on the Gulf of Aqaba (Glueck and Albright 1938). He believed Tell el-Kheleifeh to be the biblically identified port city of King Solomon, Ezion-geber, and he interpreted the site as a massive copper refinery deeming it the "Pittsburgh of Old Palestine" (although, this is now refuted – Glueck misinterpreted what was likely a storage facility for a large refinery) (Glueck 1940b; Glueck and Albright 1938: 12; Ben-Yosef 2010: 136). Based on his excavations and surveys, Glueck (1940a: 50-88, 1935: 28, 50) posited that King Solomon with an Edomite workforce was the paramount controller of copper exports from Faynan, "the first great copper king", a point of continued scholarly intrigue and contention (cf. Muhly 1987; Pratico 1985; Kafafi 2014; Najjar 2015; Knauf and Lenzen 1987). In general, Glueck's conclusions upheld the biblical text identifying the Edomites as an Iron Age kingdom and secured their place in the scholarly discourse.

Following the paramount work of Glueck with his biblical assertions, the focus of archaeological research shifted to just the hilltops above Faynan – the Edomite plateau – which was also part of his survey (Glueck 1935: 82-83). Glueck (1935: 82-83) had identified several biblical sites on the plateau including Umm el-Biyara, Tawilan, and Buseirah. In the 1960s, Crystal-Margaret Bennett (1966, 1977, 1983) set out to test Glueck's identification of these biblical sites in the highlands. Based on her excavations at all three sites, the Edomite polity and its copper industry in Faynan were chronologically shifted, away from Glueck's conclusions, to the Late Iron Age - the 8$^{th}$-6$^{th}$ centuries BCE (Bienkowski 1990). All three sites yielded single-phase Iron Age settlements dated by ceramic typology (Bienkowski 1990). Umm el-Biyara functioned as a chronological anchor based on the discovery of the Qos-Gabr seal (Bienkowski 1995, 1992a: 99). This small seal included two lines of text translated as "Qos-Gabr, King of

Edom"; this name is also mentioned in Assyrian texts dated to the early 7th century BCE (Bienkowski 1992a: 99). The textual correlates provided a relative chronology for the pottery excavated from Umm el-Biyara and a comparative typology for other Edomite sites.

Following these excavations, John Bartlett (1972) called for a reevaluation of Glueck's interpretations. With the chronological shift for Edom essentially initiated by the Qos-Gabr seal, a new impetus for Edomite development became plausible: Assyrian involvement. By dating the zenith of the highland Edomite cities to the 7th-6th centuries BCE, they fall within the period associated with Assyrian hegemony. Bartlett (1989: 31), along with Bennett (1983), attributed Edom's development as a kingdom to the ascension of the Assyrian empire in the 8th-6th centuries BCE. Assyrian texts further indicate the existence of an Edomite polity during this period. The annals of Adid-nirari III, who reigned from 810-785 BCE, mention Edom as a subdued country forced to pay tribute (Bartlett 1972: 32). Tiglath-pileser III similarly received tribute from an Edomite king, Kaush-malaku (Bennett 1983: 16). As aforementioned, texts from Essarhadon and Ashurbanipal mention King Qos-Gabr of Edom, requesting tributary materials and troops respectively (Bartlett 1972: 33). In addition, Assyrian influenced architecture identified at the acropolis of Buseirah potentially reiterated Assyrian investment in Edom (Bienkowski 1990: 103). In short, following Bennett's excavations, Edom and the associated copper production Faynan were chronologically shifted to the Late Iron Age and attributed to Assyrian hegemony; this understanding became the accepted wisdom (cf. Weippert 1982). However, these investigations and their resulting interpretations were based entirely on research and excavations on the Edomite plateau.

Surveys in Edom and Faynan continued into the 1970s and 1980s, and again identified material culture believed to be Iron Age I in date (Weippert 1982; MacDonald 1992, Hauptmann

2007). Moreover, Hauptmann (2007: Table 5.1) collected radiocarbon dates from Khirbat en-Nahas which calibrated to approximately 1200-950 BCE (Bienkowski 1992a: 110). Following the influx of Early Iron Age material culture from the various survey projects, James Sauer (1986) returned to Glueck's original findings. Sauer (1986:16) did not deny Edom's presence in the Late Iron Age, but he was reluctant to accept that Early Iron Age material would not be found at Tawilan, Umm el-Biyara, and Buseirah, claiming some Early Iron Age pottery had already been excavated and misidentified from these sites. Israel Finkelstein (1992a) supported this assertion with a reevaluation of pottery from Bennett's excavations. Finkelstein (199a2: 159-163) identified approximately 30 Early Iron Age sites in Edom that were previously misinterpreted based on the ceramics. According to Finkelstein (1992a: 164), Edom was populated by the *Shasu* nomads of Egyptian sources in the Late Bronze Age, and after the collapse, there was settlement in the region dating to the Iron I. In following, an Edomite monarchy was established as a result of conflict with the United Monarchy in Israel, as demonstrated in the biblical narrative (Finkelstein 1992a: 164). With the ascension of the Assyrian Empire, and possibly through economic control of Arabian trade and copper production, the Edomite kingdom then culminated in the 8$^{th}$ century BCE (Finkelstein 1992a: 164). However, Bienkowski (1992b) immediately responded to Finkelstein's proclamations, calling into question his stratigraphic analysis, pottery typology, and methodology. Thus, the chronology and origins of the Edomite polity remained debated and convoluted, but Faynan and the copper-rich lowlands were still largely untouched by archaeological investigations.

### 3.5.2 Archaeology of Faynan: Surveys, Excavations, and Debates

Research in Faynan in the 1970s-1980s remained primarily limited to surveys (Raikes

1980, MacDonald 1992, Hauptmann 2007). In the late 1970s, Thomas Raikes (1980) surveyed the Wadi Fidan with particular interest in flint artifacts, but he noted several metallurgical sites and the abundance of slag. Manfred Weippert (1982: 157) also surveyed the "homeland of ancient Edomites" in 1974, and he produced evidence for Iron I inhabitation at seven sites in Edom, following a noticeably unrepresented Late Bronze Age. He also identified an increase in settlement through the Iron Age II (Weippert 1982: 156). In the early 1980s, Burton MacDonald (1992) explored the western margins of Faynan, and Andreas Hauptmann (2007) initiated a long-term archaeometallurgical investigation of the entire Faynan region. Under the auspices of the German Mining Museum, Hauptmann (2007, 2006, 1989, Hauptmann and Weisgerber 1987) lead intensive geological and metallurgical surveys, which included some archaeological probing, of Faynan between 1983 and 1993, contributing immensely to its archaeometallurgical narrative (discussed below). In 1985, MacDonald (1992) returned and surveyed the northeastern Arabah Valley and the area around Faynan as part of the Southern Ghors and Northeast 'Arabah Archaeological Survey with no particular focus on metallurgical remains. MacDonald (1992: 73-77, 119, Figure 15) identified 13 sites with Iron Age I pottery and visited Khirbat en-Nahas and Khirbat al-Ghuwayba, assigning an Early Iron Age date for each based on pottery; additionally, he provided a sketch of the northern portion of Khirbat en-Nahas. In 1996, Wadi Faynan and the environs surrounding Khirbat Faynan (a massive Roman and Byzantine smelting center) were thoroughly surveyed by Graeme Barker et al. (1997; Barker, Gilbertson, and Mattingly 2007) as part of the Wadi Faynan Landscape Survey and the Center for British Research in the Levant. This multidisciplinary project emphasized desertification processes in Faynan and their impact on human populations (Barker, Gilbertson, and Mattingly 2007). Additional topics explored by British groups in Faynan included the agricultural revolution and the impact of pollution from

ancient copper smelting (Finlayson and Mithen 2007; Grattan, Gilbertson, and Hunt 2007; and citations there within). Together, these modern projects surveyed much of the Faynan landscape and acknowledged the significant metallurgical nature of the archaeological record, but they lacked the deep time perspective of stratigraphic excavation.

In 1997, Thomas E. Levy (PI) of the University of California San Diego (UC San Diego), Mohammad Najjar of the Department of Antiquities of Jordan, and Russell Adams of the University of Bristol initiated an archaeological investigation into Faynan utilizing systematic survey and stratigraphic excavations - The Jabal Hamrat Fidan Project (JHFP) (Levy, Adams, and Najjar 2001; Levy, Adams, and Shafiq 1999). Developing from the Wadi Fidan Project (Adams 1991), the main incentive for the JHFP was examining the procurement of copper ore throughout Faynan and its sociopolitical implications from a social archaeology perspective (Levy, Adams, and Najjar 2001: 442). Initially focused on the Pre-Pottery Neolithic and Early Bronze Age, the project transitioned under Levy and Najjar in 2002 towards an emphasis on the Iron Age and the associated Edomites (Levy, Ben-Yosef, and Najjar 2014: 1). Titled the Edom Lowlands Regional Archaeology Project (ELRAP) in 2006, the new project used anthropological archaeology and cyber-archaeological approaches to discern the nuances between technology (metallurgy) and social evolution. Ongoing archaeological expeditions have investigated predominant Iron Age copper producing sites throughout Faynan including Khirbat en-Nahas, Khirbat al-Jariya, and Khirbat al-Ghuwayba (See Ben-Yosef, Najjar, and Levy 2014a for a complete review). In doing so, the ELRAP fostered the most complete understanding of the profound relationship between copper production and social transformations in Faynan/Edom.

ELRAP's contribution to understanding the emergence of Edomite society was founded on a full commitment to systematic surveys, absolute dating methodologies, the first large open-

air excavation strategies, and cyber-archaeology (Levy 2013, Levy, Najjar, and Ben-Yosef 2014; Ben-Yosef and Levy 2014b; Knabb et al. 2014a; Ben-Yosef, Najjar, and Levy 2014a, 2014b; Ben-Yosef 2010). Contrary to Bennett and her reliance on pottery typology and relative dating schemes, ELRAP employed intensive radiocarbon sampling for absolute dating at all excavated sites. Excavations at Khirbat en-Nahas functioned as a chronological anchor (the excavations and radiocarbon samples at Khirbat en-Nahas are fully described in detail in Chapter 4) (Levy et al. 2008; Higham et al. 2005). Excavations in the gatehouse of the site's formidable fortress yielded a collection of 28 radiocarbon samples dated to the 10$^{th}$ through 9$^{th}$ centuries BCE (Levy et al. 2014a: 113-120). Metallurgical contexts (including slag mounds) from Khirbat en-Nahas, Khirbat al-Jariya, and Khirbat al-Ghuwayba, similarly dated to the Early Iron Age by radiocarbon indicating intense copper production during this period (discussed further below but also see Ben-Yosef et al. 2014). The total suite of radiocarbon dates from Faynan now totals over 100 samples providing a secure chronological framework with clear connections to the Early Iron Age – the 12$^{th}$-9$^{th}$ centuries BCE (Levy et al. 2008; Levy et al. 2005). Thus, the Edomite lowlands were populated with Early Iron Age sites, including the most substantial copper smelting centers, suggesting an early emergence of the Edomite polity as originally suggested by Glueck in 1935. This reevaluation fostered a paradigmatic shift in the accepted chronology for Edom and its copper industry (Figure 3.5).

Despite the new reliance on stratigraphic excavation and absolute dating methods, the results were similarly debated (Finkelstein 2005b, 2020). Finkelstein (2005b) questioned the analyses of the collected radiocarbon dates while also proposing an alternative model for the control of Iron Age copper production in Edom. The validity of the radiocarbon samples was reexamined based on their contexts from industrial fills and wastes (i.e., slag mounds), and their

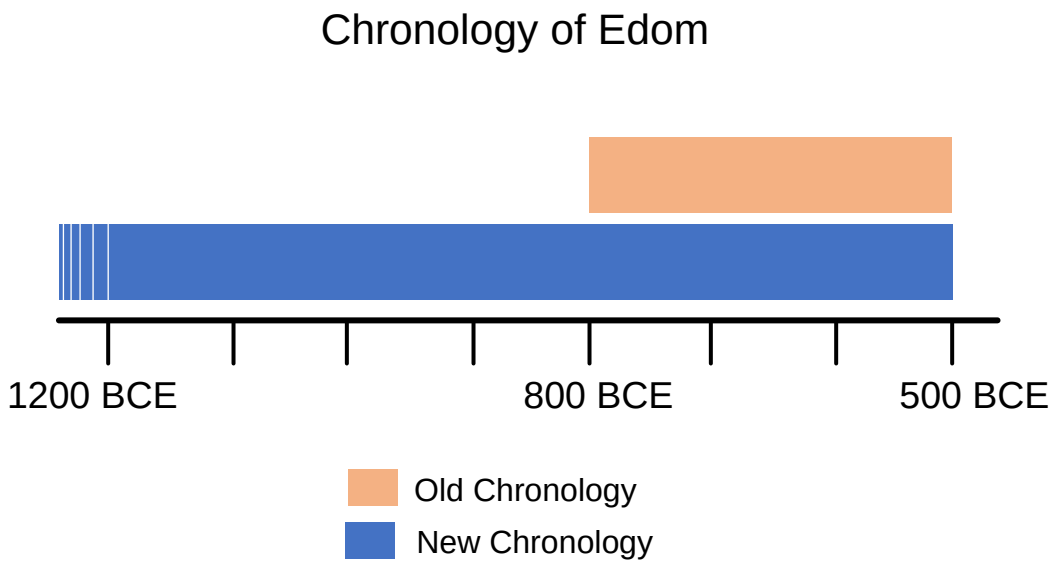


**Figure 3.5:** The new chronology for biblical Edom and Faynan established through the work of the ELRAP in comparison to the old chronology based primarily on Bennett's excavations (figure modeled after Levy, Ben-Yosef, and Najjar 2014: Figure 1.1). Some radiocarbon dates suggest an occupation at Khirbat en-Nahas prior to 1200 BCE, but they are less secure.

attribution to the 12th century BCE was doubted due to the majority falling within the 11th-9th centuries BCE (Finkelstein 2005b: 120). Along with proposing that copper production should be more accurately dated to only the 11th-9th centuries BCE, the dating of the Khirbat en-Nahas fortress was also reevaluated. Finkelstein (2005b: 123), through an examination of aerial photographs and top plans, concluded that the fortress cuts the surrounding slag piles dated to the 9th century BCE; thus, it must date to a later period. Additionally, the similar architectural layout between the fortress and other Edomite fortresses dated to the 8th-7th centuries BCE, specifically Ein Hazeva and Tell el-Khelefeh, reiterated his adjusted dating (Finkelstein 2005b: 123). Finkelstein's interpretations placed the Khirbat en-Nahas fort firmly back within the Assyrian influence theory for the Edomite polity. However, this shift in the dating caused a chronological disconnect between the fortress and the intense phase of copper production at Khirbat en-Nahas in the 10th-9th centuries BCE; the fortress post-dated the industrial production (Finkelstein 2005b:

124). This potential issue was solved by attributing Tel Masos with control of the copper industry (Finkelstein 2005b: 121). Tel Masos, located in the Beersheba Valley of Israel and along major trade routes through the region, witnessed a period of prosperity coinciding with this early copper production at Khirbat en-Nahas (Finkelstein 2005b: 121-122). Additionally, excavations at Tel Masos discovered copper objects and pottery similar to that found in Faynan ('Negebite' Pottery) (Finkelstein 2005b: 121-122). According to Finkelstein (2005b: 121), this situation of growth and prosperity in the Beersheba Valley in the 10$^{th}$-9$^{th}$ centuries BCE contrasted with Faynan which had limited occupation/sites during this period, apart from Khirbat en-Nahas. By controlling the trade routes on which copper would be exported from Faynan, Tel Masos was essentially able to extend control over production and capitalize.

Levy and Najjar (2006b: 3-6; also Levy, Najjar, and Higham 2007; and more recently, Levy, Ben-Yosef, and Najjar 2018 and Ben-Yosef 2020) responded and contradicted the claims posed by Finkelstein, pointing out misinterpretations, the forcing of data into models, and ignoring the total publication corpus. An additional 27 radiocarbon dates corroborating the initial findings from the 2002 excavation season at Khirbat en-Nahas were posited as an antithesis to Finkelstein's reading of the dates (Levy and Najjar 2006b: 4). The relationship between the fortress and the surrounding slag mounds was clarified as well; the slag mounds accumulated around and within the fortress during the second copper production phase and are not actually cut by the fortress (Levy and Najjar 2006b: 8). Additional excavation projects from the region similarly contrasted Finkelstein's assertion that the limited Iron Age record in Faynan only accounts for the first half of the copper production sequence at Khirbat en-Nahas (Levy and Najjar 2006b: 6). Focusing primarily on the Wadi Fidan 40 cemetery and its ca. 3,500 Iron Age graves, Levy and Najjar (2006b: 6-7) suggested Faynan had a significant population during the

10th-9th centuries BCE, even if sites and/or architecture dating to this period was lacking. Levy and Najjar (2006b: 10) believed that Finkelstein's suggestion for Tel Masos control is based on an unjustified belief that control of such large-scale production required a complex sedentary population (see also Ben-Yosef 2019a for the "Architectural Bias"). Accepting the possibility of a nomadic power, conceivably in the form of a chiefdom, allowed for new avenue of explanation for the development of an Edomite polity[1].

With the new chronology determined by ELRAP, focus shifted towards a local social evolutionary process for the development of an Edomite polity (Levy et al. 2004: 867). Using anthropological archaeology and historical perspectives, Levy and Najjar (2006b: 13) responded to Finkelstein's Tel Masos theory with a new model for the origins of the Edomites. Building on the tribal kingdom model for Edom proposed by LaBianca and Younker (1995), Levy and Najjar (2006a; Levy 2009) suggested an "oscillating tribal segmentary system model" using a tribal mechanism and the associated copper production to understand the formation of an Edomite chiefly confederacy (see also Maeir 2021). As reiterated by the Wadi Fidan 40 excavations, the Faynan region was likely inhabited by the nomadic *Shasu* in the Late Bronze Age (Kitchen 1992:27; Beherec 2011). Levy (2008, 2009:156) suggested these populations provided the foundation for an Edomite polity; ethnogenesis of the local pastoral nomads into an Edomite identity was an initial step towards social complexity. The segmentary tribes identifying with Edomite ethnicity would fuse to form chiefdoms or diffuse into nomadic tribes in order to adapt to natural and cultural environments – the oscillating tribal segmentary system (Levy 2009: 158). The final component of the model is political ecology - the effects access to natural resources have in the political and economic structures of societies (Levy 2009: 158). The political ecology

[1] These debates remain ongoing and were most recently discussed in Finkelstein 2020 and Ben-Yosef 2020 as well as Tebes 2021.

for Edom/Faynan is highlighted by the availability of abundant copper resources, providing a possible driver towards a more complex social and political organization. In summary, following the Late Bronze Age collapse, the segmentary *Shasu* tribes coalesced into a complex chiefdom, filling the political void created by the fall of the major empires. The lack of extant evidence for an archaic state (as described in Marcus and Feinman 1998) reiterates a chiefdom level society (Levy and Najjar 2006b: 10; Beherec 2011). The local ecology supported the development of a complex society through accessible copper ores which were in high demand due to the economic collapse. The other growing polities in the region (such as the Israelites) facilitated ethnogenesis of the Edomites with strong connections to metallurgy (Levy 2009: 156; Finkelstein 1992a). The result of these interrelated processes was a socially complex Edomite kingdom/chiefdom in the Early Iron Age, founded on the copper ore sources of Faynan. As will be discussed further below, this dissertation follows this line of thinking, accepting that a nomadic society was capable of controlling the industrial copper production of Iron Age Faynan/Edom.

### 3.5.3 Archaeometallurgical Research of Iron Age Faynan

The rich and largely undisturbed record of copper production in Faynan also provided an unprecedented opportunity for archaeometallurgical research. Investigations into the archaeometallurgy of Iron Age Faynan was a main focus of Hauptmann's (2007) surveys and also ELRAP, primarily as Ben-Yosef's (2010) dissertation research. As discussed above, Hauptmann and a team from the German Mining Museum (GMM) lead geological and archaeometallurgical surveys throughout Faynan which were absolutely critical in establishing an understanding of the archaeometallurgy of copper production both in general and in Faynan specifically. While not directly focused on the Iron Age, Hauptmann (2007) and the GMM team

surveyed the major Iron Age smelting centers (Khirbat en-Nahas, Khirbat al-Jariya, Khirbat Faynan, etc.), evaluated the mining regions and ore sources, provided details concerning the smelting technologies (tuyère shape and size, slag shape and size, furnaces, etc.), and also considered the trade of produced copper (the results of the surveys for relevant sites to this research are discussed in Chapter 4). However, aside from the small probes excavated at Khirbat en-Nahas and Khirbat Faynan, the project almost exclusively relied on surveys focused on metallurgy, technology, and geology; the project lacked a stratigraphic investigation of specific sites and the historical and archaeological interpretation/implications (Ben-Yosef 2010: 159). The ELRAP focused on combining archaeometallurgical research with anthropological/social archaeology to holistically investigate copper production and its impact on society in Faynan during the Iron Age.

Building on the foundations of the GMM surveys, the archaeometallurgy of the Iron Age in particular and its relationship to socio-political oscillations in Faynan were more recently investigated by Ben-Yosef (2010; Ben-Yosef et al. 2019). His research focused on the technological developments in the smelting process through time while maintaining an anthropological lens (Ben-Yosef 2010). Along with new excavations and surveys in both Faynan and Timna, his research applied analytical techniques including x-ray fluorescence, x-ray diffraction, scanning electron microscopy, and archaeomagnetism to examine the microscopic details of copper production (Ben-Yosef 2010: 769-829). Moreover, by combining research in both Faynan and Timna, Ben-Yosef created an unparalleled dataset for examining copper production in the Wadi Arabah more generally. Critically, Ben-Yosef (2010; Ben-Yosef et al. 2012) successfully adjusted the chronology of copper production in Timna to the end of the Late Bronze Age and continuing into the Early Iron Age (it was previously attributed to only the Late

Bronze Age, Rothenberg 1972), making it contemporaneous with Faynan, and he also identified technological consistencies between the two regions. The archaeometallurgical material assemblages from Faynan and Timna are almost identical, and witnessed similar changes over the course of the Iron Age (Ben-Yosef et al. 2012: 59; Ben-Yosef 2010: 622-763; Ben-Yosef and Levy 2014b: 952-953: Ben-Yosef et al. 2019: Figure 5). There were two phases of copper smelting technologies which are primarily identifiable by changes in tuyères and slags (Ben-Yosef and Levy 2014b: 952). The tuyères fall into two distinct categories, small and large, and the transition between them is contemporaneous between the two regions, in the 10$^{th}$ century BCE (Ben-Yosef and Levy 2014b: 923-927; Ben-Yosef et al. 2019). The slags similarly fit a typological scheme. Large tap slag plates are only found in the most advanced phases of copper production in Timna and Faynan seen in only the uppermost layers of the slag mounds during the 10$^{th}$-9$^{th}$ centuries BCE. In light of the new chronology for copper production at Timna, the temporal and technological parallels between Timna and Faynan suggest a unity between them (Ben-Yosef 2010: 1053; Ben-Yosef et al. 2019).

In conjunction with the archaeometallurgical material culture, the analytical findings of the Ben-Yosef's (2010) dissertation provide another major contribution by diachronically examining slags excavated from Faynan and Timna using x-ray fluorescence to determine their elemental composition. Using the copper content of slags as a proxy for smelting efficiency, Ben-Yosef (2010; Ben-Yosef et al. 2019) identified improvements in copper smelting technologies over the course of the Iron Age. Copper in slag is essentially metal lost during the smelting process, and as such, a lower copper content in the slag is representative of a more successful smelt. His research discerned a pinnacle in metallurgy in the 10$^{th}$-9$^{th}$ centuries BCE based on slags from this period in both regions having the lowest average copper content and the

tightest standard deviation suggestive of consistently efficient smelts (Ben-Yosef 2010: Figures 8.22,8.23, and 8.25; Ben-Yosef et al. 2019). Finally, Ben-Yosef (2010: 881-953; Ben-Yosef et al. 2019: Figure 5) was able to combine the excavation and laboratory results with the historical context and an anthropological perspective to construct unique *chaînes opértoire* for copper production during the Iron Age in the Wadi Arabah. These *chaînes* provide the foundations for the current understanding of the coinciding developments in copper production and the Edomite polity during the Iron Age.

### 3.5.4 Current Understandings of Copper Smelting in the Iron Age Wadi Arabah

Following the work of Levy, Najjar, and Ben-Yosef, the copper production industries of Faynan and Timna can be considered two components of a broad, integrated industrial landscape in the Wadi Arabah, probably associated with the biblical Edomites (Levy, Najjar, and Ben-Yosef 2014; Ben-Yosef et al. 2019; Ben-Yosef 2010, 2020, 2021). The trajectory and development of this unified system over the Late Bronze and Early Iron Ages was further detailed and divided into four phases by Ben-Yosef – Phases 0-4 (Ben-Yosef et al. 2019; cf. Luria 2021). Phase 0 represents the beginning of Late Bronze Age copper production in the Arabah in Timna under the hegemonic control of the Egyptian New Kingdom, with no contemporaneous production in Faynan (Ben-Yosef et al. 2019: 8). Despite Egyptian control, the workforce appears to have been composed primarily of the local population (Ben-Yosef et al. 2019: 8). Following the collapse of the Egyptian New Kingdom, copper production continued in Timna, but also began in Faynan in the Iron Age (ca. 1140 BCE), representing the transition to Phase 1 (Ben-Yosef et al. 2019: 8). Phase 1 in both regions is characterized by limited architecture and unwalled sites dedicated to copper smelting – the local tribes began

collaborating in copper production, the ethnogenesis stage of Levy's model above (Ben-Yosef et al. 2019: Figure 5). Phase 2 is identified by the introduction of defensive elements (such as the fortress at Khirbat en-Nahas) and abandonment of unprotected smelting sites in both regions at roughly the beginning of the 1st millennium BCE (Ben-Yosef et al. 2019: 8, Figure 5). Phase 3, beginning approximately around 925 BCE following the campaign of Sheshonq I, is associated with major reorganizations of metal production, a new archaeometallurgical assemblage (including the large tuyères and tap slags described above), and an improved efficiency in smelting (Ben-Yosef et al. 2019; Luria 2021[2]). Finally, Phase 4 represents the limited evidence for Late Iron Age ($7^{th}$-$6^{th}$ centuries BCE) copper mining in Faynan. This unique phase seems to completely lack smelting sites and potentially is a failed attempt to renew copper production activities (Ben-Yosef 2010: 886, Figure 9.5A and 9.6A). These phases and their manifestations in the archaeological record of Faynan will be further discussed in Chapter 4.

While copper production in Faynan reached an industrial peak in the $10^{th}$-$9^{th}$ centuries BCE, these advancements were followed by an enigmatic and abrupt abandonment of the industry and its smelting centers at the end of the $9^{th}$ century BCE with no associated evidence of natural or human intervention, such as a drought or warfare. Ben-Yosef and Sergi (2018) recently proposed an explanation for this industry abandonment based on the contemporaneous

[2] Luria (2021) recently argued against the five-phase model proposed by Ben-Yosef et al. 2019 in favor of a two "technological phase" organization for copper production in the Iron Age Arabah. He also proposed for more gradual developments in copper smelting technology driven by indigenous populations rather than Egyptian influence as suggested by Ben-Yosef et al. 2019 (Luria 2021). However, as he acknowledges these gradual changes would be "invisible in the archaeological record" and thus provide no additional explanatory power to understanding the archaeological record in comparison to the Ben-Yosef et al. 2019 model (Luria 2021). Either explanation (two phases of gradual developments versus five phases with a punctuated leap) is viable; however, the simplicity of Luria's two phase model which only focuses on the metallurgy disregards the larger archaeological context and developments in the archaeological record. Thus, the more nuanced and holistic perspective presented by Ben-Yosef et al. 2019 is given preference here.

destruction of Tell es-Safi/Gath, an Iron Age settlement in modern Israel (building on a theory first introduced by Fantalkin and Finkelstein 2006, Finkelstein 2014: 99; cf. Bienkowski 2021). They suggest Tell es-Safi/Gath likely functioned as a main hub for the export of copper produced in Faynan (Ben-Yosef and Sergi 2018). Indeed, lead isotope analysis of copper materials from the site identified the origins of the metal to Arabah reiterating this connection (Eliyahu-Behar and Yahalom-Mack 2018a). With its destruction at the end of the 9$^{th}$ century BCE, as attested to in the Hebrew Bible (Hazael's Conquests, 2 Kings 12:17-18) and identified in the archaeological record, they believe Faynan was essentially cut off from the market, preventing an economic outlet for copper, and forcing an abandonment of the industry (Ben-Yosef and Sergi 2018: 474). This theory is interesting and plausible, but it is essentially circumstantial and difficult to substantiate.

Bienkowski (2021) raised doubts concerning this theory by undermining what he perceived as four essential but unsupported assumptions: 1) that Tell es-Safi/Gath was central to the Arabah copper trade; 2) that the end of copper production in Faynan and the Arabah coincided with the destruction of Tell es-Safi/Gath; 3) that Hazael's primary motivation in destroying the site was to disrupt the copper trade; and 4) the Cypriot copper replaced the Arabah industry as a result of this disruption. In contrast, he suggests Gaza was likely the primary hub of exchange due to its coastal location, the end of copper production in Faynan was a more drawn out process resulting from "internal issues of control, stability and management" based on the lack of administrative contexts in the final phases of production, Hazael's rationale for destroying Tell es-Safi/Gath was to disrupt the olive oil and metallurgical industries and to attack a strategic rival, and Cyrpiot copper production was revived prior to the end of the Arabah industry based on a reinterpretation of the radiocarbon dates (Bienkowski 2021: 3-9).

Bienkowski (2021) raises valuable critiques, but the alternative model he proposes similarly relies on certain assumptions. As he acknowledges, the archaeological evidence from Gaza is "extremely meager, and we lack definitive evidence for its existence as a major port in the 9th century BCE"; thus, its role the Arabah copper trade is assumed (Bienkowski 2021: 3). Concerning the lack of administration in Faynan prior to the abandonment of the industry, Bienkowki (2021: 5-6) suggests "there was a decrease in administrative complexity and control decades before the final cessation of copper production" based on the monumental buildings at Khirbat en-Nahas going out of use. Here, monumentality is used as the primary correlation for complexity and administration which inherently requires some assumption i.e., the architectural bias (Ben-Yosef 2019). Moreover, it was previously identified that the copper production industry experienced a reorganization in the late 10th century BCE when many of these buildings went out of use. Thus, the decommissioning of these buildings could be a result of this reorganization and not necessarily a decrease in "administrative complexity". This understanding is further reiterated by the changes in the metallurgical technology. The peak in copper production and the appearance of a new metallurgical repertoire similarly occurs in the late 10th century BCE. It seems unlikely the pinnacle of production (which would also inherently require the complex organization required for long distance exchange) would correlate with a period of "internal issues of control, stability and management". Finally, the construction of the Area F workshop within the walls of the fortress suggests some level of authority over production was still present in the late 10th to early 9th centuries BCE. While there is some evidence to suggest authority and control over the industry waned near the end of production in the 9th century BCE (see Chapter 7), it is difficult to accept that this process began in the late 10th century BCE with the industrial peak in production. Bienkowski's (2021: 8-9) claim that Cypriot copper was likely

already reviving prior to the end of the Arabah copper industry is valid, and copper production likely continued in Cyprus throughout the Iron Age (Kassianidou 2014, 2013, 2012; Yahalom-Mack et al. 2014a). However, evidence for exchange of Cypriot copper with the Levant during the early 9th century BCE is limited, currently relying only on an Assyrian text and a single ingot from Hazor based on lead isotope analysis (Bienkowski 2021: 9; Kassianidou 2013: 69-71; Kassianidou 2014: 266; Yahalom-Mack et al. 2014a). This lack of evidence is particularly challenging in light of the current understanding that Cyprus focused exchange to the west during the Early Iron Age until the 9th century BCE (as acknowledged by Bienkowski 2021: 12; Kassinidou 2013, 2014). While it may be the case that Cypriot copper was traded with the Levant already in the late 10th to early 9th centuries BCE, this suggestion requires further evidence, particularly from the archaeological record and ideally through provenance studies (e.g., Yahalom-Mack et al. 2014a).

There are other possible hypotheses concerning the abandonment of copper production, but they currently lack archaeological evidence. Ben-Yosef (2010: Table 10.1) previously proposed military conquest in the Northern Arabah (also possibly by Hazael) as a potential cause, but this is only based on the Hebrew Bible; he acknowledges there is "no clear evidence of destruction" in the archaeological record of Faynan. Exhaustion of charcoal resources (the main fuel source for copper smelting) could similarly drive the abandonment of the metallurgical industry, but botanical investigations in Faynan indicate "that during the Iron Age the wood source was managed (harvested) such that the fuel supply would be constant" (Ben-Yosef 2010: 938; Engel 1993: 210; Liss et al. 2020: 8-11). Finally, while not directly suggested, climatic fluctuations could possibly have caused the abandonment, but paleoclimatic data from Israel indicates that the end of the 9th century BCE was characterized by a "moderate climate" with no

extreme changes (Langgut et al. 2015: 231). This dissertation investigates exhaustion of natural resources as a possible explanation for the abandonment.

## 3.6 Iron from Copper? Investigating the Origins of Iron Production in the Eastern Mediterranean

During the pinnacle of copper smelting in Faynan in the $10^{th}$-$9^{th}$ centuries BCE, unique but limited iron artifacts also appear in the archaeological record, particularly at Khirbat en-Nahas and Wadi Fidan 40 (Levy et al. 2014; Beherec 2011). A principal objective of this dissertation is to investigate these iron artifacts, and in turn, critically evaluate the proposed theory that smelted iron was first produced as an unintentional byproduct of advanced copper smelting technologies. The development of iron production and the coming of the "Iron age" represents one of the most critical technological advances in human history, with archeological evidence suggesting its innovation as early as 1500 to 1200 BCE in parts of Anatolia and southwest Asia (Tylecote 1992; Erb-Satullo 2019). However, the origin of this technological advance in the Eastern Mediterranean is poorly understood, and numerous theories have attempted to explain it (Erb-Satullo 2019; Wertime and Muhly 1980; Waldbaum 1980, 1999). The deterministic and unilineal idea that iron was a logical technological progression from bronze has been largely dismissed (Eliyahu-Behar and Yahalom-Mack 2018b; Pleiner 1979), but there is still little agreement in the scholarly discourse on an adequate model. One theory suggests that iron production was adventitiously discovered as a byproduct from developed copper smelting technologies (Wertime 1980; Pigott 1982; Moorey 1994; Charles 1980; Avery 1982; Tylecote and Boydell 1978; Gale et al. 1990). Here, sophisticated copper smelting furnaces created the necessary reducing conditions to extract metallic iron from a furnace charge abundant in iron oxides in the form of iron-enriched copper ores or fluxes (Tylecote and Boydell

1978; Cooke and Aschenbrenner 1975). The result of this process could potentially be metallic iron and slag formed at the bottom of the furnace (an iron bloom) or a product of iron-rich copper which would need to be purified by experienced metalsmiths in order to separate the two metals. Workable iron would then be recovered and used to produce early iron objects - the discovery of iron production. This idea has a long history of research, and it remains debated.

Early investigations concerned with iron in copper metallurgy were focused on the removal of the element during smelting, and its presence in copper/bronze objects was often discounted to simply iron-rich slag inclusions (Cooke and Aschenbrenner 1975: 215). Cooke and Aschenbrenner (1975) facilitated an initial shift in understanding the presence of iron in copper/bronze objects. Based on a sample size of 193 copper/bronze artifacts from various contexts and dates in the Mediterranean region, they found iron in significant amounts (based on magnetism) to be present in copper/bronze more frequently than previously believed (Cooke and Aschenbrenner 1975: 254-255). From their results (including more in-depth analyses on five particularly magnetic samples), the iron found in copper/bronze artifacts was attributed to a general improvement in furnace construction and operation (Cooke and Aschenbrenner 1975: 264). Specifically, “increased sophistication in pyrometallurgy led to higher temperatures and increased reducing conditions in copper smelting” resulting in the reduction of excess iron oxides present in the furnace charge (Cooke and Aschenbrenner 1975: 264). For Cooke and Aschenbrenner (1976: 264), this understanding was “a valid explanation for the occurrence of many high-iron coppers from the Bronze Age down through the Iron Age”. This study provided preliminary evidence for a relationship between copper smelting technology and iron.

Tylecote and Boydell (1978) subsequently contributed to the discussion through experimental archaeology. Using excavations in Timna as a reference, furnaces similar to those

dating to the Chalcolithic and Iron Age were constructed and used in smelting experiments (Tylecote and Boydell 1978: 29-30). The Iron Age style furnace produced copper containing significant amounts of iron (up to 28.9%), and it was the main impurity found in the metal (Tylecote and Boydell 1978: 44-45). Moreover, Tylecote and Boydell (1978: 45, 47-48) were able to separate an "iron product which can be forged" from a crucible containing a load of copper and iron, and they suggested that it "is possible some of the earlier iron finds arise from this process" (reiterated by Gale et al., 1990: 185; Kassianidou 1994: 77; see also Tylecote's comment in Snodgrass 1982: 295). Timna is a particularly important and frequently referenced case study due to the exceptional presence of iron objects in a region with sophisticated copper smelting technologies, but without direct evidence of iron production (c.f. Tylecote and Boydell 1978; Gale et al. 1990; Merkel and Barrett 2000). Tylecote and Boydell's experiments gave credibility to the possibility that these iron objects were locally produced from iron that was the byproduct of copper smelting.

Following these findings, that idea that iron produced in a sophisticated copper smelting furnace was a possible origins for iron production became more popular in the scholarly discourse (Wertime 1980: 13; Moorey 1994: 279-280; Charles 1980: 164-167,180; Avery 1982: 206; Kassinidou 1994; Erb-Satullo 2019 for overview). Some additional support was provided by Craddock and Meeks (1987) who found iron content to increase in copper alloys with the adoption of more sophisticated techniques, cross-culturally. Craddock and Meeks (1987: 188-189), however, were primarily concerned with the unworkable nature of copper that contains significant iron (Papadimitriou 2001). Similarly using Timna as a case study and in agreement with Tylecote and Boydell (1978), it was suggested that secondary refining of iron-rich copper was essential for subsequent casting and hammering to produce functioning copper objects;

however, the presence of iron in copper artifacts including ingots excavated in Timna suggests the refining process may have occurred elsewhere (Craddock and Meeks 1987: 192, Craddock 1988: 179; Roman 1990). In summary, the iron content in copper/bronze objects appeared to be a cross-cultural phenomenon, and considerable quantities of iron were typically contemporaneous with advanced metallurgical technologies.

Craddock (1988) touched on this issue again in a larger quantitative analysis of 346 metal artifacts from Timna (the vast majority of which were from Site 200 – the "Hathor Temple"). Using atomic absorption spectrometry to analyze the elemental contents of the objects, the results found copper artifacts in Timna to occasionally contain significant iron (several percent) (Craddock 1988: 178-179, Diagram 1). Craddock (1988: 178-179) suggested iron oxide flux, which was typical in Timna, was likely reduced to iron metal which was subsequently dissolved into the copper during the smelting/melting process. The copper was possibly exported with appreciable iron only to be purified and manufactured into finished products in secondary production centers (Craddock 1988: 179). Unfortunately, the iron objects found in Timna were not specifically addressed, and it was not determined if the artifacts could have produced using this methodology. As such, this study corroborated the noticeable existence of iron in copper produced in Timna, but the removal and possible production of metallic iron remained somewhat enigmatic.

Building on the work of Craddock and also focusing on material from Timna, Gale et al. (1990) used archaeometallurgical analysis of iron objects to evaluate the possible production of iron from copper smelting. Iron objects excavated from Timna Site 2 (n=1) and Site 200 (n=11) were analyzed with X-ray Fluorescence (XRF), lead isotope analysis, and scanning electron microscope (Gale et al. 1990: 186). Based on a lack of nickel in the XRF results from the iron

objects, a primary indicator of meteoritic iron, they were all considered to be smelted material (Gale et al. 1990: 186). The copper content was found to be somewhat variable across the artifacts, but its presence and significant range led Gale et al. (1990: 186) to suggest copper was a primary component in the iron used to produce the objects. A bent iron rod from Site 200 was further analyzed with scanning electron microscope; copper was distributed homogeneously across the section which provided evidence that the iron was a by-product of copper smelting (discussed further below) (Gale et al. 1990: 187-188). The lead isotope analysis, which included copper ores, iron ores, manganese ore, along with artifacts of iron, copper, and lead, revealed a distinct group including the majority of the ores and artifacts suggesting the iron objects were produced from Timna ores (Gale et al. 1990: 188, Graph 1). Based on the presence of copper in noticeable amounts in the iron objects and the lead isotope analysis, Gale et al. (1990: 189-190) concluded: “it seems that in Timna metallic iron was truly born in a copper smelting furnace”.

Along with Timna, the possibility of producing iron in a copper smelting furnace was similarly considered in Cyprus (Snodgrass 1982; Pickles and Peltenburg 1998; Kassinidou 1994; Muhly and Kassianidou 2012). The archaeological and metallurgical record of Cyprus during the Late Bronze to Iron Ages were very similar to Timna; there is archaeological evidence for advanced copper smelting, numerous iron objects and artifacts, but no direct evidence for iron production (Snodgrass 1982; Kassianidou 1994). Snodgrass (1982: 293), using the high iron content in copper slags from Cyprus as evidence, suggested “the material circumstances in Cyprus would be exceptionally favourable to the accidental discovery of the properties of iron, in the course of copper smelting”. In a similar fashion, Maddin (1982: 303) proposed that the metalsmiths in Iron Age Cyprus actually recycled/remelted the copper slags with the intention of extracting the iron content (a slightly different variation on discovering iron production through

copper smelting). Kassianidou (1994: 77-79) subsequently dismissed the recycling of copper slags as a means of iron production, but she maintained that iron could have been produced in Cyprus as an accidental byproduct of copper smelting perhaps through adding iron oxide fluxes. However, Kassianidou (1994: 79) also pointed out that iron ores were available in Cyprus in various forms (including ochres and umbers) which could have provided the raw material for direct iron production. Pickles and Peltenberg (1998: 87) reiterated this possibility in the broader examination of the Bronze/Iron Age transition in the Eastern Mediterranean: "we believe that the metal [iron] may have been produced as a by-product of copper scavenging in the course of current smelting operations…we can only state that copper smelting seems to us to remain a plausible source for early iron". Muhly, also looking at the Eastern Mediterranean more broadly, proposed that Cyprus potentially refocused on iron production in response to Faynan dominating the copper market in the Early Iron Age (while also acknowledging the source of iron is unclear) (Muhly and Kassianidou 2012: 125). In sum, Cyprus presents another possible locus for iron production being discovered as a byproduct of copper smelting.

Following the research in Timna and Cyprus, iron originating from copper smelting gained some acceptance, but doubts were also raised (Craddock 1995; Merkel and Barrett 2000). The difficulties in working a mixed copper-iron alloy were once again considered by Craddock (1995: 255-256). Because iron with small amounts of copper would be difficult to manipulate, it was proposed that the copper content found in iron objects from Timna was a result of post-depositional processes i.e. copper entered the iron due to its burial in a copper-rich context, not during its production (Craddock 1995: 255-256). Building on this idea, Merkel and Barrett (2000) reexamined the same iron objects (and others) investigated by Gale et al. (1990) to elucidate the presence of copper. Merkel and Barrett (2000: 61-65) raised several important

critiques of previous work by Gale et al. (1990): 1) the XRF analysis sampled the corroded surface of the iron objects; 2) a fresh break was examined in the scanning electron microscope when considering the distribution of copper within the artifact; and 3) three samples contained no copper. In this renewed investigation, twelve iron objects from Site 200 were analyzed with electron probe microanalysis (EPMA) (Merkel and Barrett 2000: 62). When focused on the limited remaining metallic iron (rather than a corroded surface), the objects were found to contain concentrations of copper usually less than 0.1% by EPMA (Merkel and Barrett 2000: 62). Moreover, the distribution of copper did not appear homogeneous, but rather, concentrated on the edges of the objects and decreasing towards the interior (Merkel and Barrett 2000: 63, Figure 4, 5). Merkel and Barrett (2000: 64) subsequently claimed the copper in the corroded iron objects should be interpreted as "contamination from burial alongside larger quantities of copper and copper alloy artefacts". This hypothesis was further supported by the corrosion properties of metallic iron and copper; if the copper was soluble in the groundwater, it would be electrochemically attracted to the metallic iron (Merkel and Barrett 2000: 64). To account for the presence of iron objects in Timna, it was proposed that these artifacts represent the very beginnings of iron smelting in the region, *not* a byproduct of copper smelting (Merkel and Barrett 2000: 65). Merkel and Barrett (2000: 65) acknowledged that metallic iron was likely produced during copper smelting in Timna based on its presence in copper ingots (see Roman 1990), but this iron was not separated and utilized. Furthermore, the lead isotope analysis, and in turn, the local origins of the iron artifacts, was also questioned based on the significant corrosion on the iron (Merkel and Barrett 2000: 65). Between the potential inability to separate and produce workable iron and the possibility that accumulation of copper in the iron artifacts was

post-depositional, the idea that iron production originated as a copper smelting byproduct lost ground in the archaeological literature.

More recently, archaeological excavations in the Southern Levant reiterate at least a possible relationship between iron and copper metallurgy. Following its innovation, iron metallurgy was often closely associated with copper working (primarily re-melting or alloying) in the Iron Age, even occurring in shared workshops, suggestive of a possible connection between the two metals or a generalized metallurgical knowledge by the metalsmiths (Workman et al. 2020; Rabinovich et al. 2019; Erb-Satullo and Walton 2017; Eliyahu-Behar et al. 2012; Yahalom-Mack and Eliyahu-Behar 2015; Gottlieb 2010)[3]. The occasional discovery of mixed iron-copper chunks (sometimes referred to as "bears") in the archaeological record also raised the question as to whether iron production was discovered in this way; it has been suggested that "[d]irect evidence for the extraction of iron from mixed copper-iron deposits would provide a crucial link between iron and copper production" (Erb-Satullo 2019). Critical to this research, recent finds in Faynan also reintroduce the issue of iron produced in a copper smelting furnace into scholarly discourse. At Khirbat en-Nahas, excavations discovered amorphous chunks of mixed copper and iron (see Chapter 4 and 5) (Ben-Yosef 2010: 736-737). Preliminary analyses indicated significant concentrations of iron (up to 70%) in these materials, but their function was unclear (Ben-Yosef 2010: 822-824). Ben-Yosef (2010: 824) suggested these mixed metals were secondarily processed to extract copper (and potentially iron) based on their significant number and association with the most advanced smelting technologies seen in Faynan in the 10$^{th}$-9$^{th}$ centuries BCE at Khirbat en-Nahas. In contrast, Hauptmann (2007: 207-208) treated similar finds from the Mamluk period in Faynan as simply waste products from failed smelts based on

[3] A similar phenomenon was recently discovered in the Iron Age Caucasus where iron and bronze metallurgy were occurring even within the same hearth (Erb-Satullo et al. 2020).

their predominance in the archaeological record. To date, however, these artifacts have not been the focus of systematic investigation.

While not directly related to the idea of producing iron from copper smelting, Glueck (1936b: 4) discussed additional "nondescript" sites in a separate publication from his report that he believed provided evidence of iron production in Faynan. East-southeast of Khirbat en-Nahas and south of Buseirah, Glueck (1936b: 4-5) reported discovering "large areas strewn with specimens of iron ore, which even to the eye of the layman seemed to be extraordinarily rich" near a site called Qa'ir which he was unable to date. Based on his findings and the chemical analysis of two samples from the area around Qa'ir, he concluded that "Just as much iron as copper may been produced" in the Wadi Arabah (Glueck 1936b: 5). G.M. Enos, who completed the chemical analysis, further suggested that "frequently an alloy may have been produced from ores which contained respectable quantities of both iron and copper" – like the mixed chunks found at Khirbat en-Nahas (Glueck 1936b: 6). However, as the article describes iron ores in Faynan and also in the Wadi es-Sabrah which is roughly 45 kilometers to the south and associated with the Nabateans, it is difficult to evaluate exactly which periods Glueck (1936b: 5; 1935: 80-81) is associating with iron production. Regardless, it is interesting to note the discovery of rich iron near Faynan and the suggestion that both metals could have been produced along with mixed alloys. As direct evidence for iron production Faynan is currently lacking (discussed in Chapter 5), these ideas require further investigation.

Thus, as research currently stands, the mixed iron-copper chunks from Faynan and, more generally, the origins of iron production in the Eastern Mediterranean remain puzzling, but these distinctive materials along with the complete record of copper production in Iron Age Faynan

afford an ideal opportunity to examine the possible origins of iron production from copper smelting.

## 3.7 Summary: Foundations for the Current Research

The previous research in Faynan and the ensuing debates have established a strong understanding of the Iron Age and provide the foundations for this dissertation. To summarize, Faynan was likely populated by pastoral nomads in the Late Bronze Age (Phase 0) who coalesced into an Edomite chiefdom following the collapse of the major powers in the region. Capitalizing on the sustained economic demand for copper and possibly ameliorated climatic conditions in the Eastern Mediterranean, Faynan and Timna became copper smelting hubs for a unified industrial system under Edomite control in the Wadi Arabah during the Early Iron Age ($12^{th}$-$11^{th}$ centuries BCE) (Phase 1). Copper production continued to develop and the local populations invested further in the industry by building substantial architecture at the smelting centers such as the fortress and elite structures at Khirbat en-Nahas (Phase 2). The climate of Faynan during this time potentially became more arid, and it was becoming more similar to the current environmental conditions. Following a disruption and reorganization in the $10^{th}$ century BCE, possibly attributed to Pharaoh Shoshenq I, the industry reached a peak with a new smelting toolkit and improved efficiency (Phase 3, see also Levy, Münger, and Najjar 2014). Along with the new metallurgical tools and methods, mixed iron-copper chunks and select iron objects appear in the archaeological record of Khirbat en-Nahas. This sophisticated technology was used until the abandonment of copper production in Faynan at the end of the $9^{th}$ century BCE. The exact impetus and reasoning behind the cessation of copper smelting requires further research, but it can potentially be correlated to military campaigns disrupting the economic connections

between Faynan and the Eastern Mediterranean. At this time, the center of the Edomite polity shifted to the highlands at sites like Busayra, Umm el-Biyara, and Tawilan as identified by Bennett and Bienkowski.

Despite the abundant research in Faynan, certain components of the copper smelting industry still require further investigation. Along with the end of the copper production, the actual produced copper is also a currently understudied component of Iron Age Faynan. Ben-Yosef and Hauptmann provided critical research into the archaeometallurgy of Faynan, but analysis of produced copper was not a focus of Ben-Yosef's (2010: 734-737) research, and, as he acknowledges, it requires further investigation to discern the quality of copper in the Iron Age. Hauptmann (2007; Hauptmann et al. 1992: Table 6) did examine the purity of copper from the Early Bronze and Iron Ages in Faynan, but on a small scale, only analyzing 10 samples from the Iron Age. Today, the limited research on copper metal and/or artifacts remains a notable and detrimental lacuna to a complete understanding of the technological, economic, and socio-political arc of Iron Age society in Faynan. Also, a possible relationship between the abandonment of Faynan and industrial-scale metallurgy is still unexamined i.e. is it possible that the Iron Age industry depleted available natural resources?

Previous research briefly considered the possibility that ancient mining exhausted copper ores in Faynan; however, this issue is debated (Hauptmann 2007: 69; Ben-Yosef 2010: 471; Weisgerber 2006: 15, 21). Hauptmann (2007: 69-71) suggests ore sources remained sufficient in antiquity based on their availability today. In contrast, Ben-Yosef (2010: 98, 471) proposed that mining activities were "exhaustive" in the Iron Age in specific regions based on new evidence from the Jabal al-Jariya minefield. Ben-Yosef (2010: 98) also addresses the present availability of copper ores as "representing the minimum quality of the available ore in antiquity" inferring

that ancient mining depleted the highest quality ores. This possibility is reiterated by renewed mining activities in Faynan in the 7th century BCE which are currently considered "unsuccessful" possibly because "the yield in copper ore there did not meet expectations" (Weisgerber 2006: 15)[4]. This later phase of Iron Age mining also currently lacks any evidence of copper smelting "in the entire Faynan region" further indicating that the mining was a failed endeavor despite significant efforts (Ben-Yosef 2010: 420). This research will adopt a nuanced understanding of "exhaustion" in line with Ben-Yosef; exhausting the highest quality ores (rather than the totality) could similarly disrupt copper production in Faynan.

Copper metal is currently understudied partially because Faynan functioned as a primary smelting center focused on casting metallic ingots intended for trade and export, leaving limited copper in local archaeological record (Yahalom-Mack et al. 2014a; Martin and Finkelstein 2013; Martin et al. 2013; Kiderlen et al. 2016; Ben-Dor Evian 2017; Ben-Dor Evian et al. 2021; Vaelske, Bode, and Loeben 2019). However, the abundance of slag in Faynan affords a comparatively massive collection of metal through the copper prills trapped in the slag matrix – a common phenomenon of ancient metal production. Furthermore, this assemblage of slag-entrapped copper is ideal for diachronic investigations; the slag mound excavations provide a complete record of copper smelting activities with secure chronological control through radiocarbon dating (discussed in detail in Chapter 4). Prills from well-dated contexts can be elementally analyzed to detect temporal changes in the purity of produced copper, the basis for this project's hypotheses and methods. Similarly, the mixed copper-iron chunks excavated from Khirbat en-Nahas have not been the focus of systematic research. Ben-Yosef (2010: 736-737,

[4] Copper mining and smelting were successfully renewed in the Roman Period, but mining in this period exploited a different ore source possibly after finding "that the much richer mineralization…had been completely exhausted during the Bronze and Iron Ages" (Weisgerber 2006: 21; Hauptmann 2007: 155).

822-824) completed some initial elemental analysis and interpretation, but acknowledged that further research is needed. In particular, it is not clear if these artifacts were an intended smelting product (for copper and/or iron production) or if they were simply a failed smelt.

In the following chapters, this dissertation fills these scholarly lacunae concerning the quality of copper produced during the Iron Age in Faynan, the function of the mixed copper-iron chunks, and investigates the possibility that the industry exhausted available copper ores.

## Chapter 4 - Archaeological Excavations: Methods and Results

### 4.1 Introduction

As presented above, there is a rich history of archaeological research in the Faynan region by the ELRAP and other projects. This dissertation relies both on these previous research endeavors and new excavations in Faynan to contextualize, archaeologically and chronologically, the produced archaeometallurgical analyses. Along with an overview of the excavation and survey methods employed during the 2014 season at Khirbat al-Jariya (the most recent excavations and conducted as part of this research during which the author functioned as a field supervisor under the directorship of Thomas E. Levy and Mohammad Najjar), the following chapter provides more detailed elaborations on the surveys and excavations at sites relevant to and investigated for this dissertation (Figure 4.1). The main sites of focus in this dissertation are Khirbat al-Jariya and Khirbat en-Nahas. The slag mound excavations at these sites are discussed in detail as they provide the context and chronological scaffold for all the samples analyzed. While not directly examined, Khirbat al-Ghuwayba also plays an important role in understanding the industrial landscape during the Iron Age, especially considering the new excavations and data from Khirbat al-Jariya. When possible, both old and new radiocarbon dates are presented and modeled for the sites/excavations relevant to this dissertation to chronologically situate it. Dates are presented in two forms: 1) a complete table of relevant radiocarbon dates including calibrated and modeled year ranges (Table 4.1) and 2) as multiple-plot Bayesian models as previously presented by the original excavators (citations are provided in figure captions). In order to holistically present the Iron Age industrial landscape, other relevant Iron Age sites related to the metallurgical industry in Faynan are briefly overviewed (Figure 4.1). Finally, a brief discussion of certain mining regions is provided as a foundation for the isotope analyses presented in

Chapter 5. Where relevant, the production phase (discussed in Chapter 3) will be provided for each site. A summary discussion concludes the chapter to situate these excavations within the broader research project. The locations of all sites are available in Figure 4.1.

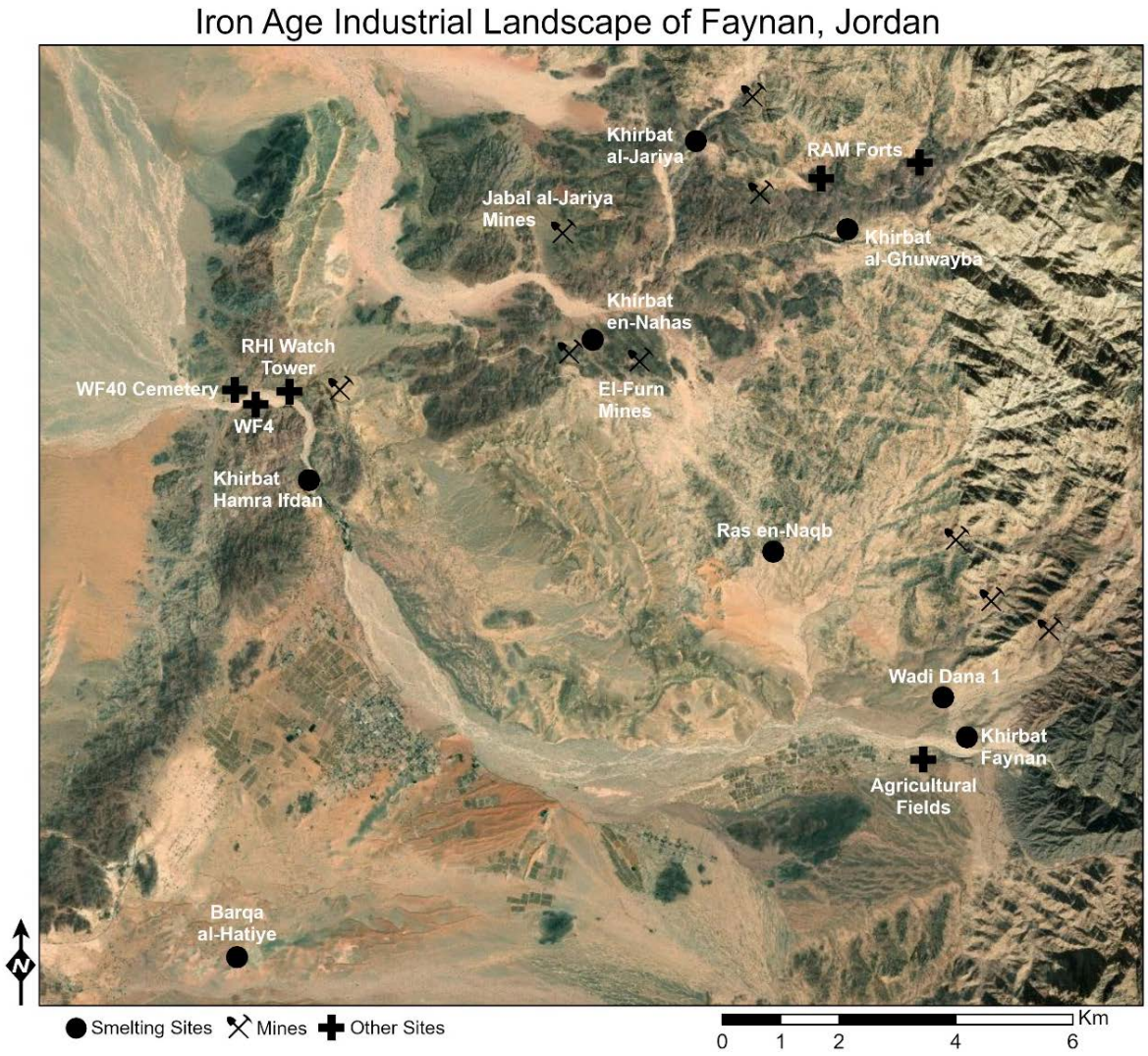


**Figure 4.1:** Map of the Iron Age industrial landscape in Faynan including all sites mentioned in the text. WF – Wadi Fidan, RHI – Rujm Hamra Ifdan, RAM – Ras al-Miyah. Wadi Fidan 4 is included here but not discussed in the text as it is primarily an Early Bronze Age smelting site; however, some Iron Age graves were excavated there, and it is thus marked as an "Other Site" (Ben-Yosef 2010: Table 5.1). Satellite imagery base layer source: Esri, Maxar, GeoEye, Earthstar Geographics, CNES/Airbus DS, USDA, USGS, AeroGRID, IGN, and the GIS User Community. Map produced by Brady Liss.

**Table 4.1:** Complete list of all radiocarbon dates collected from contexts excavated or sampled as part of this research.

| Complete Radiocarbon Data from Relevant Excavation Areas | | | | | | | | | | | | | | | |
|---|---|---|---|---|---|---|---|---|---|---|---|---|---|---|---|
| | | | | | | | Calibrated/Unmodeled | | | | Calibrated/Modeled | | | | |
| | | | | | | | 1σ (68.2%) | | 2σ (95.4%) | | 1σ (68.2%) | | 2σ (95.4%) | | |
| Site | Year | Strat. | Lab # | Sample Type | Material | Age BP | From | To | From | To | From | To | From | To | Source |
| KEN | 2002 | M1 | OxA-12346 | Charcoal | Tamarix sp. | 2659±32 | 895 | 830 | 923 | 805 | 871 | 842 | 883 | 831 | Levy et al. 2014 |
| KEN | 2002 | M1 | OxA-12347 | Charcoal | Tamarix sp. | 2746±35 | 917 | 839 | 976 | 815 | 872 | 847 | 886 | 837 | Levy et al. 2014 |
| KEN | 2002 | M1 | OxA-17630 | Charcoal | Retama raetam | 2764±25 | 969 | 846 | 977 | 835 | 867 | 838 | 882 | 826 | Levy et al. 2014 |
| KEN | 2006 | M2a | OxA-17631 | Charred Seed | Phoenix dactylifera | 2676±26 | 894 | 826 | 906 | 809 | 902 | 883 | 906 | 861 | Levy et al. 2014 |
| KEN | 2006 | M2b | OxA-17632 | Charred Seed | Phoenix dactylifera | 2713±26 | 898 | 839 | 923 | 817 | 910 | 892 | 917 | 868 | Levy et al. 2014 |
| KEN | 2006 | M2a | OxA-17633 | Charred Seed | Phoenix dactylifera | 2734±25 | 900 | 841 | 925 | 819 | 911 | 895 | 921 | 867 | Levy et al. 2014 |
| KEN | 2006 | M2b | OxA-17634 | Charcoal | Haloxylon persicum | 2783±25 | 974 | 858 | 998 | 842 | 906 | 889 | 911 | 864 | Levy et al. 2014 |
| KEN | 2006 | M2b | OxA-17635 | Charcoal | Haloxylon persicum | 2777±25 | 976 | 860 | 1000 | 844 | 906 | 889 | 911 | 864 | Levy et al. 2014 |
| KEN | 2006 | M2b | OxA-17636 | Charred Seed | Phoenix dactylifera | 2732±25 | 899 | 840 | 923 | 819 | 909 | 892 | 915 | 867 | Levy et al. 2014 |
| KEN | 2006 | M1 | OxA-17637 | Charcoal | Phoenix dactylifera | 2836±26 | 999 | 926 | 1036 | 902 | 876 | 851 | 889 | 842 | Levy et al. 2014 |
| KEN | 2006 | M2b | OxA-17638 | Charred Seed | Phoenix dactylifera | 2814±25 | 1001 | 928 | 1038 | 904 | 915 | 896 | 927 | 867 | Levy et al. 2014 |
| KEN | 2006 | M2a | OxA-17639 | Charred Seed | Phoenix dactylifera | 2678±26 | 841 | 804 | 896 | 801 | 880 | 855 | 892 | 846 | Levy et al. 2014 |
| KEN | 2006 | M3 | OxA-17640 | Charcoal | Tamarix sp. | 2770±25 | 969 | 846 | 944 | 835 | 936 | 913 | 975 | 907 | Levy et al. 2014 |
| KEN | 2006 | M3 | OxA-17641 | Charcoal | Acacia sp. | 2767±25 | 974 | 896 | 1001 | 844 | 930 | 908 | 971 | 899 | Levy et al. 2014 |
| KEN | 2006 | M3 | OxA-17642 | Charcoal | Tamarix sp. | 2781±25 | 976 | 898 | 1003 | 846 | 932 | 911 | 972 | 904 | Levy et al. 2014 |
| KEN | 2006 | M4 | OxA-17643 | Charcoal | Tamarix sp. | 2813±26 | 1001 | 927 | 1041 | 903 | 972 | 917 | 978 | 912 | Levy et al. 2014 |
| KEN | 2006 | M5a | OxA-17644 | Charcoal | Tamarix sp. | 2824±25 | 1008 | 932 | 1047 | 912 | 977 | 920 | 995 | 914 | Levy et al. 2014 |
| KEN | 2006 | M4 | OxA-17645 | Charcoal | Tamarix sp. | 2747±25 | 913 | 843 | 972 | 827 | 926 | 906 | 970 | 895 | Levy et al. 2014 |
| KEN | 2006 | M3 | OxA-17646 | Charcoal | Tamarix sp. | 2871±26 | 1112 | 1005 | 1129 | 936 | 1077 | 997 | 1115 | 943 | Levy et al. 2014 |
| KEN | 2006 | M5a | OxA-17647 | Charcoal | Haloxylon persicum | 2764±25 | 904 | 839 | 970 | 814 | 973 | 919 | 984 | 913 | Levy et al. 2014 |
| KEN | 2006 | M2 | OxA-17702 | Charcoal | Retama raetam | 2740±30 | 906 | 841 | 972 | 816 | 904 | 885 | 908 | 864 | Levy et al. 2014 |
| KEN | 2006 | M3 | OxA-17703 | Charred Seed | Phoenix dactylifera | 2792±30 | 993 | 906 | 1013 | 845 | 941 | 915 | 975 | 911 | Levy et al. 2014 |
| KEN | 2006 | M5a | OxA-19040 | Charcoal | Retama raetam | 2942±27 | 1371 | 1258 | 1389 | 1133 | 1215 | 1126 | 1257 | 1078 | Levy et al. 2014 |
| KEN | 2006 | M5b | OxA-19041 | Charcoal | Indeterminate | 3026±27 | 1373 | 1260 | 1391 | 1135 | 1287 | 1214 | 1378 | 1131 | Levy et al. 2014 |
| KEN | 2006 | F1a | OxA-19897 | Charcoal | Indeterminate | 2710±26 | 895 | 824 | 906 | 811 | 901 | 841 | 910 | 820 | Levy et al. 2014 |
| KEN | 2006 | F1a | OxA-18988 | Charcoal | Indeterminate | 2765±26 | 970 | 846 | 979 | 835 | 906 | 849 | 917 | 837 | Levy et al. 2014 |
| KEN | 2006 | F2a | OxA-18989 | Charcoal | Indeterminate | 2782±25 | 976 | 899 | 1004 | 846 | 937 | 900 | 976 | 870 | Levy et al. 2014 |
| KEN | 2006 | F2b | OxA-18990 | Charcoal | Indeterminate | 2831±26 | 1014 | 932 | 1071 | 907 | 983 | 916 | 1016 | 906 | Levy et al. 2014 |
| KEN | 2006 | F2a | OxA-19061 | Charcoal | Phoenix dactylifera | 2728±28 | 899 | 837 | 923 | 814 | 921 | 883 | 937 | 855 | Levy et al. 2014 |
| KEN | 2006 | R2b | OxA-18979 | Charcoal | Tamarix sp. | 2766±26 | 970 | 847 | 980 | 836 | 932 | 905 | 970 | 897 | Levy et al. 2014 |
| KEN | 2006 | R3a | OxA-18978 | Charcoal | Phoenix dactylifera | 2812±27 | 999 | 928 | 1042 | 902 | 963 | 908 | 969 | 904 | Levy et al. 2014 |
| KEN | 2006 | R3a | OxA-19045 | Charcoal | Tamarix sp. | 2799±28 | 994 | 914 | 1019 | 850 | 966 | 914 | 971 | 910 | Levy et al. 2014 |
| KEN | 2006 | R3a | OxA-19046 | Charcoal | Phoenix dactylifera | 2821±28 | 1006 | 930 | 1049 | 906 | 966 | 911 | 970 | 907 | Levy et al. 2014 |
| KEN | 2009 | R3a | OxA-23245 | Charcoal | Haloxylon persicum | 2772±24 | 973 | 854 | 996 | 842 | 968 | 916 | 973 | 911 | Levy et al. 2014 |
| KEN | 2009 | R3a | OxA-23155 | Charcoal | Tamarix sp. | 2753±28 | 921 | 844 | 976 | 827 | 969 | 918 | 975 | 912 | Levy et al. 2014 |
| KEN | 2009 | R3a | OxA-23246 | Charcoal | Tamarix sp. | 2783±25 | 976 | 900 | 1004 | 847 | 971 | 920 | 976 | 914 | Levy et al. 2014 |
| KEN | 2009 | R3a | OxA-23153 | Charcoal | Tamarix sp. | 2781±27 | 977 | 898 | 1003 | 846 | 974 | 921 | 980 | 916 | Levy et al. 2014 |
| KEN | 2009 | R3a | OxA-23154 | Charcoal | Tamarix sp. | 2858±27 | 1071 | 945 | 1114 | 932 | 977 | 921 | 987 | 917 | Levy et al. 2014 |
| KEN | 2009 | R3a | OxA-23156 | Charcoal | Retama raetam | 2770±27 | 972 | 851 | 996 | 839 | 977 | 922 | 992 | 918 | Levy et al. 2014 |
| KEN | 2009 | R3a | OxA-23157 | Charcoal | Retama raetam | 2801±28 | 996 | 916 | 1023 | 852 | 979 | 922 | 999 | 918 | Levy et al. 2014 |
| KEN | 2002 | S1 | GrA 25324 | Charcoal | Indeterminate | 2720±35 | 898 | 831 | 930 | 806 | 846 | 815 | 877 | 806 | Levy et al. 2014 |
| KEN | 2002 | S1 | GrA 25325 | Charcoal | Indeterminate | 2700±35 | 895 | 813 | 911 | 804 | 854 | 823 | 879 | 814 | Levy et al. 2014 |
| KEN | 2002 | S1 | GrA 25326 | Charcoal | Indeterminate | 2735±35 | 906 | 836 | 972 | 811 | 860 | 831 | 885 | 821 | Levy et al. 2014 |
| KEN | 2002 | S1 | GrA 25328 | Charcoal | Indeterminate | 2670±35 | 887 | 801 | 898 | 797 | 867 | 837 | 890 | 827 | Levy et al. 2014 |
| KEN | 2002 | S1 | GrA 25342 | Charcoal | Indeterminate | 2795±45 | 1009 | 898 | 1056 | 829 | 871 | 846 | 895 | 836 | Levy et al. 2014 |
| KEN | 2002 | S2a | GrA 25329 | Charcoal | Indeterminate | 2705±40 | 898 | 826 | 969 | 803 | 885 | 860 | 900 | 850 | Levy et al. 2014 |
| KEN | 2002 | S2a | GrA 25331 | Charcoal | Phoenix dactylifera | 2820±35 | 1011 | 923 | 1108 | 896 | 878 | 853 | 896 | 844 | Levy et al. 2014 |
| KEN | 2002 | S2a | GrA 25332 | Charcoal | Tamarix sp. | 2715±40 | 898 | 826 | 969 | 803 | 892 | 868 | 905 | 856 | Levy et al. 2014 |
| KEN | 2002 | S2a | GrA 25343 | Charcoal | Tamarix sp. | 2720±45 | 904 | 823 | 975 | 802 | 897 | 876 | 909 | 863 | Levy et al. 2014 |
| KEN | 2002 | S2a | OxA 12274 | Charcoal | Indeterminate | 2683±34 | 892 | 804 | 901 | 801 | 903 | 883 | 915 | 871 | Levy et al. 2014 |
| KEN | 2002 | S2b | GrA 25344 | Charcoal | Tamarix sp. | 2770±45 | 975 | 844 | 1017 | 818 | 913 | 891 | 926 | 878 | Levy et al. 2014 |
| KEN | 2002 | S2b | GrA 25345 | Charcoal | Tamarix sp. | 2780±45 | 996 | 856 | 1042 | 827 | 921 | 898 | 936 | 886 | Levy et al. 2014 |
| KEN | 2002 | S2b | OxA 12168 | Charcoal | Indeterminate | 2747±26 | 912 | 844 | 972 | 827 | 928 | 906 | 946 | 892 | Levy et al. 2014 |
| KEN | 2002 | S3 | GrA 25347 | Charcoal | Tamarix sp. | 2830±45 | 1043 | 922 | 1121 | 851 | 942 | 915 | 964 | 903 | Levy et al. 2014 |
| KEN | 2002 | S3 | GrA 25353 | Charcoal | Tamarix sp. | 2820±50 | 1041 | 910 | 1116 | 844 | 956 | 921 | 979 | 911 | Levy et al. 2014 |
| KEN | 2002 | S3 | OxA 12342 | Charcoal | Indeterminate | 2830±27 | 1014 | 932 | 1071 | 906 | 967 | 927 | 991 | 918 | Levy et al. 2014 |
| KEN | 2002 | S4 | GrA 25348 | Charcoal | Tamarix sp. | 2770±45 | 975 | 844 | 1017 | 818 | 981 | 934 | 1001 | 922 | Levy et al. 2014 |
| KEN | 2002 | S4 | GrA 25349 | Charcoal | Tamarix sp. | 2790±45 | 1006 | 896 | 1050 | 831 | 1002 | 957 | 1011 | 926 | Levy et al. 2014 |
| KEN | 2002 | S4 | GrA 25352 | Charcoal | Tamarix sp. | 2800±45 | 1010 | 901 | 1073 | 833 | 1014 | 941 | 1029 | 930 | Levy et al. 2014 |
| KEN | 2002 | S4 | OxA 12169 | Charcoal | Indeterminate | 2899±27 | 1121 | 1027 | 1195 | 1004 | 1032 | 944 | 1060 | 932 | Levy et al. 2014 |

**Table 4.1:** Complete list of all radiocarbon dates collected from contexts excavated or sampled as part of this research (Continued).

| Complete Radiocarbon Data from Relevant Excavation Areas | | | | | | | | | | | | | | | |
|---|---|---|---|---|---|---|---|---|---|---|---|---|---|---|---|
| | | | | | | | Calibrated/Unmodeled | | | | Calibrated/Modeled | | | | |
| | | | | | | | 1σ (68.2%) | | 2σ (95.4%) | | 1σ (68.2%) | | 2σ (95.4%) | | |
| Site | Year | Strat. | Lab # | Sample Type | Material | Age BP | From | To | From | To | From | To | From | To | Source |
| KAJ | 2006 | A1A | OxA-19033 | Charcoal | Tamarix sp. | 2864±28 | 1113 | 997 | 1127 | 924 | 996 | 943 | 1011 | 936 | Ben-Yosef et al. 2010 |
| KAJ | 2006 | A3 | OxA-19035 | Charred Seed | Phoenix dactylifera | 2799±26 | 994 | 915 | 1016 | 854 | 1010 | 980 | 1019 | 960 | Ben-Yosef et al. 2010 |
| KAJ | 2006 | A3 | OxA-19030 | Charred Seed | Phoenix dactylifera | 2815±36 | 1108 | 934 | 1083 | 850 | 1004 | 969 | 1016 | 951 | Ben-Yosef et al. 2010 |
| KAJ | 2006 | A4 | OxA-19036 | Charcoal | Tamarix sp. | 2803±26 | 995 | 919 | 1025 | 859 | 1015 | 990 | 1031 | 970 | Ben-Yosef et al. 2010 |
| KAJ | 2006 | A5 | OxA-19037 | Charred Seed | Phoenix dactylifera | 2902±27 | 1128 | 1026 | 1207 | 1006 | 1031 | 1003 | 1064 | 993 | Ben-Yosef et al. 2010 |
| KAJ | 2006 | A6 | OxA-19038 | Charcoal | Phoenix dactylifera | 2880±26 | 1113 | 1012 | 1189 | 945 | 1056 | 1011 | 1103 | 1004 | Ben-Yosef et al. 2010 |
| KAJ | 2006 | A6 | OxA-19089 | Charcoal | Indeterminate | 2884±27 | 1114 | 1016 | 1192 | 949 | 1044 | 1008 | 1081 | 1001 | Ben-Yosef et al. 2010 |
| KAJ | 2014 | C1 | AA105765 | Whole Seed | Phoenix dactylifera | 2749±47 | 968 | 832 | 1001 | 813 | 997 | 876 | 1012 | 827 | Liss et al. 2020 |
| KAJ | 2014 | C2 | AA105764 | Entire Twig | Tamarix sp. | 2852±30 | 1054 | 940 | 1112 | 928 | 1037 | 942 | 1067 | 922 | Liss et al. 2020 |
| KAJ | 2014 | C3 | AA105756 | Entire Twig | Retama raeta | 2873±33 | 1111 | 1005 | 1130 | 931 | 1088 | 1001 | 1127 | 942 | Liss et al. 2020 |
| KAJ | 2014 | B2a | AA105758 | Whole Seed | Phoenix dactylifera | 2821±32 | 1009 | 927 | 1083 | 898 | 974 | 941 | 996 | 931 | Liss et al. 2020 |
| KAJ | 2014 | B2a | AA105759 | Whole Seed | Phoenix dactylifera | 2896±28 | 1118 | 1027 | 1196 | 1001 | 961 | 931 | 994 | 923 | Liss et al. 2020 |
| KAJ | 2014 | B2a | AA105760 | Seed Fragment | Phoenix dactylifera | 2786±29 | 979 | 901 | 1007 | 846 | 968 | 935 | 996 | 926 | Liss et al. 2020 |
| KAJ | 2014 | B2a/b | AA105757 | Whole Seed | Phoenix dactylifera | 2763±34 | 970 | 844 | 997 | 832 | 990 | 947 | 1000 | 933 | Liss et al. 2020 |
| KAJ | 2014 | B2b | AA105761 | Whole Seed | Phoenix dactylifera | 2819±34 | 1009 | 924 | 1107 | 896 | 991 | 955 | 1003 | 937 | Liss et al. 2020 |
| KAJ | 2014 | B2b | AA105762 | Whole Seed | Phoenix dactylifera | 2836±30 | 1026 | 931 | 1107 | 912 | 1005 | 960 | 1016 | 936 | Liss et al. 2020 |
| KAJ | 2014 | B2b | AA105763 | Whole Seed | Phoenix dactylifera | 2779±29 | 978 | 895 | 1002 | 845 | 997 | 960 | 1007 | 937 | Liss et al. 2020 |

## 4.2 Excavation Methods for the 2014 Season at Khirbat al-Jariya

The most recent ELRAP excavation was the 2014 season at Khirbat al-Jariya. The excavation season ran from August 20-September 12, and it focused on two areas - one structure and a slag mound (discussed in greater detail below). In order to establish a complete exposure of the building, excavations used a single-context strategy; trenches were informed by the architectural remains at the site rather than arbitrary square boundaries. Where architecture was lacking, such as the probe into the slag mound, baulks were established to track the stratigraphy of the excavation. All excavation areas used a 100% sieving strategy (three-millimeter mesh) and a rigorous flotation sampling method. A sediment sample (one full bucket of ca. 15 liters) for flotation was collected from every opened locus in an archaeologically significant context (i.e., not modern fill/debris). To record all the relevant archaeological data and to document the excavation thoroughly, the 2014 season used a *cyber-archaeology* methodology.

Since its inception, ELRAP has employed fully digital, archaeological recording tools to maximize the amount of data that could be brought back from the field to the research institution,

in other words, paperless recording of archaeological data (Levy et al. 2012). This commitment to digital methods led to the development of a *cyber-archaeology* approach that continues to be used on ELRAP excavations (Levy 2013, 2015, 2017; Jones and Levy 2018; Levy and Liss 2020). *Cyber-archaeology* is the integration of the latest developments in computer science, engineering, the natural sciences, and archaeology organized into four main domains or phases for archaeological research – data capture (the phase associated with excavation), data analysis, data curation, and data dissemination (Levy 2013, 2015; Levy and Liss 2020). Essentially, the *cyber-archaeology* methodology uses digital tools in every step of archaeological research to facilitate and maximize the amount of data that can be recorded, transported, stored, and shared.

For digital data capture in the field, the 2014 season primarily relied on a Leica TS02 total station. All artifact locations and locus perimeters were recorded with the total station to document geospatial locations (X, Y, and Z coordinates) with the highest possible resolution. However, the total station alone is somewhat limited in its ability to record data associated with artifacts/loci such as number identifiers, artifact/locus types, classifications, descriptors, etc. To supplement the total station, the UCSD team developed a custom software called *ArchField* (developed by Neil Smith – Smith and Levy 2014). *ArchField* integrates the digital surveying of the total station with digital data entry using a laptop computer or tablet to streamline recording of artifact and locus locations with their associated descriptions in the field (Smith and Levy 2012). To do so, the total station is directly connected to a laptop with *ArchField* using its serial cable; all coordinates collected with the total station are immediately captured by *ArchField* which provides additional fields for the relevant archaeological information - numbers, types, descriptors, notes, etc. In this way, *ArchField* handled collecting all the main elements of archaeological data in real-time, in the field, and through a single platform. In addition, all the

geospatial data was exported from *ArchField* as shapefiles at the end of each day for storage and later analysis/manipulation in GIS (Geographic Information System).

To digitally document the more detailed contextual information associated with loci (e.g., sediment descriptions, periodization, stratigraphic relationships, etc.), the team used a Microsoft Access database. The ELRAP had previously created this custom database to handle the types of locus information relevant to excavations in Faynan, essentially providing digital locus sheets. As a sheet was completed and saved, Access would also keep a running table of all opened loci and generate a new empty sheet for the next locus. These sheets could be populated while in the field using the same computer running *ArchField* or completed at the end of an excavation day using a supervisor's daily notebook. The finished product at the end of the season was a single Microsoft Access file containing all the locus sheets which could be easily stored and brought back to UCSD in comparison to sheets of paper. Moreover, using a digital format for this data helped to mitigate some of the issues typically associated with hand-written notes such as illegible writing.

For digital data curation and storage, the 2014 season used *ArchaeoSTOR*– a custom web-based database developed at UCSD by Aaron Gidding specifically for digital storage, management, and curation of archaeological data (Gidding et al. 2013, Gidding, Levy, and DeFanti 2014; Levy et al. 2012; Levy and Liss 2020). *ArchaeoSTOR* provides digital forms for text-based artifact data/metadata and geographic information which can be associated with photographs. It is deployed using a localized network and field server housed in an on-site lab, and users simply access the platform through personal laptops connected to the local network; this was run through Mac Mini desktop computer at the field lab in 2014. The Mac Mini also stored all the produced data which could be easily brought back to UCSD due to its small size.

Once back from the field, the collected data can be easily moved to more permanent storage (see below) for continued post-excavation management and analysis.

The 2014 season also employed an intensive 3-D recording strategy to document the site over the course of excavation. Using Structure from Motion (SfM, digital photogrammetry), the ELRAP team produced photorealistic 3-D models on various scales throughout the excavation season (see Chapter 6 for additional discussion of the 3-D models for data sharing and outreach). From the terrestrial perspective, every locus was photographed for photogrammetry on opening; some loci were photographed and modeled more than once based on the excavations and what was found. In addition, a balloon platform with attached camera was used to capture models of excavation areas daily. This aerial perspective was also used to construct a 3-D model of the entire site (Howland et al. 2015; Liss et al. 2020: 4-5). Critically, the site-wide 3-D model was used to generate a georeferenced orthophoto which provided a basis for remapping the site in GIS (discussed below and see Howland et al. 2015). This dual-approach of using combined terrestrial and aerial perspectives along with the high temporal and spatial resolution extensively documented the site and excavation with 3-D models.

At the conclusion of the season, all data was returned to UCSD on portable hard-drives and uploaded to the UCSD Levantine Archaeology Lab server for perpetual storage (the server is also regularly backed up to separate server in the UCSD Levantine Archaeology Pottery Lab for disaster protection). In addition, the Department of Antiquities of Jordan generously allowed the bulk of non-museum quality artifacts (e.g., pottery sherds, slag, botanicals, etc.) to be shipped to UCSD for research and storage in the Levantine Archaeology Lab facilities on permanent loan. Together, the ELRAP's use of *cyber-archaeology* and the accommodations from the Department

of Antiquities of Jordan essentially allowed the excavations to be brought back to the lab, making this dissertation possible.

## 4.3 Khirbat al-Jariya

### 4.3.1 Overview and Previous Research

Khirbat al-Jariya (KAJ) is a copper smelting center in Faynan with an estimated 15,000-20,000 tons of copper slag (Figure 4.2) (Ben-Yosef et al. 2010; Ben-Yosef 2010; Hauptman 2007: 131-132; Ben-Yosef and Levy 2014a; Liss et al. 2020). This amount of slag makes KAJ potentially the second largest Iron Age copper smelting site in the region (pending further research at Khirbat Faynan, discussed below). The site is located roughly three kilometers northeast of Khirbat en-Nahas (KEN), nestled among the rocky terrain and outcrops of the Faynan landscape. Khirbat al-Jariya currently covers an area of approximately 4.8 hectares with archaeological features including collapsed architecture and slag mounds visible on the surface straddling the Wadi al-Jariya; the central portion of the site has likely been eroded over time due to the deepening and changing course of the wadi (Ben-Yosef et al. 2010; Liss et al. 2020). As mentioned, the location of KAJ was first reported by Kitchener (1884) during his explorations of the Faynan region (Ben-Yosef and Levy 2014a). Following Kitchener, Glueck (1935: 23-26; 1940a: 61-63) described the site during his regional surveys, characterizing the site as a “copper mining and smelting center”. Glueck (1935: 23-26) also provided the first archaeological dating of the site, attributing KAJ to the Early Iron Age based on ceramic typology. Hauptmann (2007: Table 5.1, 131-132) subsequently surveyed the site providing an evaluation of the archaeometallurgy and dating KAJ to the early Iron Age, corroborating Glueck, based on three radiocarbon dates and the size of the tuyères at the site. The small tuyères found at KAJ were

**Figure 4.2:** Aerial photograph of Khirbat al-Jariya. Photograph credit: Rebecca Banks, APAAME 2015 (APAAME_20151013_REB-0107).

considered part of a technological assemblage associated with the Late Bronze Age and Early Iron Age (in comparison to the larger tuyères found at sites like KEN – discussed below) (Hauptmann 2007: Figure 5.10). Finally, a topographic and architectural map of KAJ was produced for the first time by the Jabal Hamrat Fidan Project (JHFP - directed by Thomas E. Levy, Russell B Adams, and Mohammad Najjar) as part of their surveys of the Wadi al-Ghuwayba and Wadi al-Jariya (Levy et al. 2003: Figure 16). Overall, these surveys situated KAJ as a principal component of the Early Iron Age copper industry in Faynan.

### 4.3.2 The 2006 Excavation Season

Khirbat al-Jariya was excavated for the first time in 2006 by ELRAP with Erez Ben-Yosef as the field supervisor (Ben-Yosef 2010: 340-373; Ben-Yosef et al. 2010). The excavations covered a small area of four, 5x5 meter excavation units (Area A) including a probe into a slag mound and an associated rectangular structure (Structure 276) on the eastern bank of the wadi (Figure 4.3) (Levy et al. 2003; Ben-Yosef et al. 2010). Structure 276 was a small construction of 6.5 meters long and 3.2 meters wide with walls of a single course (Ben-Yosef et al. 2010: 738-740). It was excavated down to an ephemeral floor surface of hardened earth with limited material culture including pottery sherds, grinding stones, and a patch of pavement constructed of tap slags (Ben-Yosef et al. 2010: 740). The limited archaeological material made the function of the building and its relationship with the adjacent slag mound difficult to interpret (Ben-Yosef, Najjar, and Levy 2014a: 810). Worth noting, the doorway to the structure appeared to be intentionally blocked in antiquity (Ben-Yosef et al. 2010: Figure 7); this phenomenon will be discussed further below based on the results of the 2014 excavation season.

The probe into the slag mound was excavated for a temporal investigation of copper production at KAJ. The excavation discovered bedrock sandstone beneath the slag at a depth of 2.4 meters (Ben-Yosef et al. 2010: 735). An initial occupation phase (Layer A6) was identified directly above the basal sediments with some evidence of metallurgical activity including a thin layer of finely crushed slag, pits dug into the bedrock, ash, and fragments of copper ore (Ben-Yosef et al. 2010: 736). The metallurgical remains directly above bedrock reiterate the understanding that KAJ was established for copper smelting from its outset (Ben-Yosef et al. 2010; Liss et al. 2020). Following the initial occupation layer, approximately 70 centimeters of primarily domestic refuse were excavated with only limited metallurgical evidence; this layer

**Figure 4.3:** Area A excavations at Khirbat al-Jariya including the probe into a slag mound and Structure 276. Photograph credit: Thomas E. Levy, UCSD Levantine and Cyber Archaeology Lab.

(A5) was attributed to waste deposition for domestic activities (Ben-Yosef, Najjar, and Levy 2014a: 803). The area appeared to be subsequently leveled out and used for a habitation based on the excavation of pottery, stone installations, stone pavement patches, and possible tent-stake holes (Layer A4) (Ben-Yosef et al. 2010: 737-738). A thick accumulation of metallurgical debris comprised of tap and furnace slags, charcoal, furnace fragments, tuyères, and copper metal embedded in an ashy and clay sediment was excavated above the habitation phase (Layer A3) (Ben-Yosef et al. 2010: 738). The final and uppermost layers of excavation were similarly a horizon of metallurgical debris; however, the slags were generally larger in diameter (Layers A2-A1a) (Ben-Yosef, Najjar, and Levy 2014a: 810). These top layers likely represent the final

copper production phase, potentially contemporaneous with occupation in Structure 276 (For a complete stratigraphy of Area A at KAJ, see Ben-Yosef, Najjar, and Levy 2014a: Table 12.3).

To refine the chronology at KAJ and build on the interpretations of Hauptmann and Glueck, the excavations were supplemented with a suite of radiocarbon dates. In total, nine charcoal samples were collected from various stratigraphic contexts. The radiocarbon analysis indicated the site was likely established in the early 11$^{th}$ century BCE and abandoned in the mid- to late-10$^{th}$ century BCE, situating KAJ within the Early Iron Age (Figure 4.4). The radiocarbon dates were further supported with a geomagnetic archaeointensity study which reiterated this chronology primarily by identifying consistencies in the archaeomagnetism between the KAJ slag mound and the slag mound excavation at KEN (Ben-Yosef et al. 2010: 740; Ben-Yosef et al. 2009, 2008). To summarize, the geomagnetism yielded similar results from slag samples radiocarbon dated to the Early Iron Age (11$^{th}$-10$^{th}$ centuries BCE) in both contexts (Ben-Yosef et al. 2010: 740; Ben-Yosef et al. 2009: Figure 4). These parallels in archaeointensity are indicative of contemporaneity, reaffirming the chronology at both sites.

Considering the excavations and the chronology, KAJ was interpreted as an opportunistic smelting center established to capitalize on the new markets created by the Late Bronze Age Collapse and the reduced availability of Cypriot copper (Ben-Yosef, Najjar, and Levy 2014a: 813-814). The site was likely situated along the wadi for access to the nearby mines, and potentially also for the protection provided by the surrounding terrain (Figure 4.1, 4.2, Ben-Yosef 2010: 370). Over the course of habitation, copper manufacture gradually developed from small-scale to industrial (as indicated by the thick layers and larger cakes of slag at the top of the slag mound excavation) along with the appearance of stone-built architecture (Ben-Yosef 2010: 370: Ben-Yosef et al. 2010). Based on the dating of the abandonment of the site in the mid- to

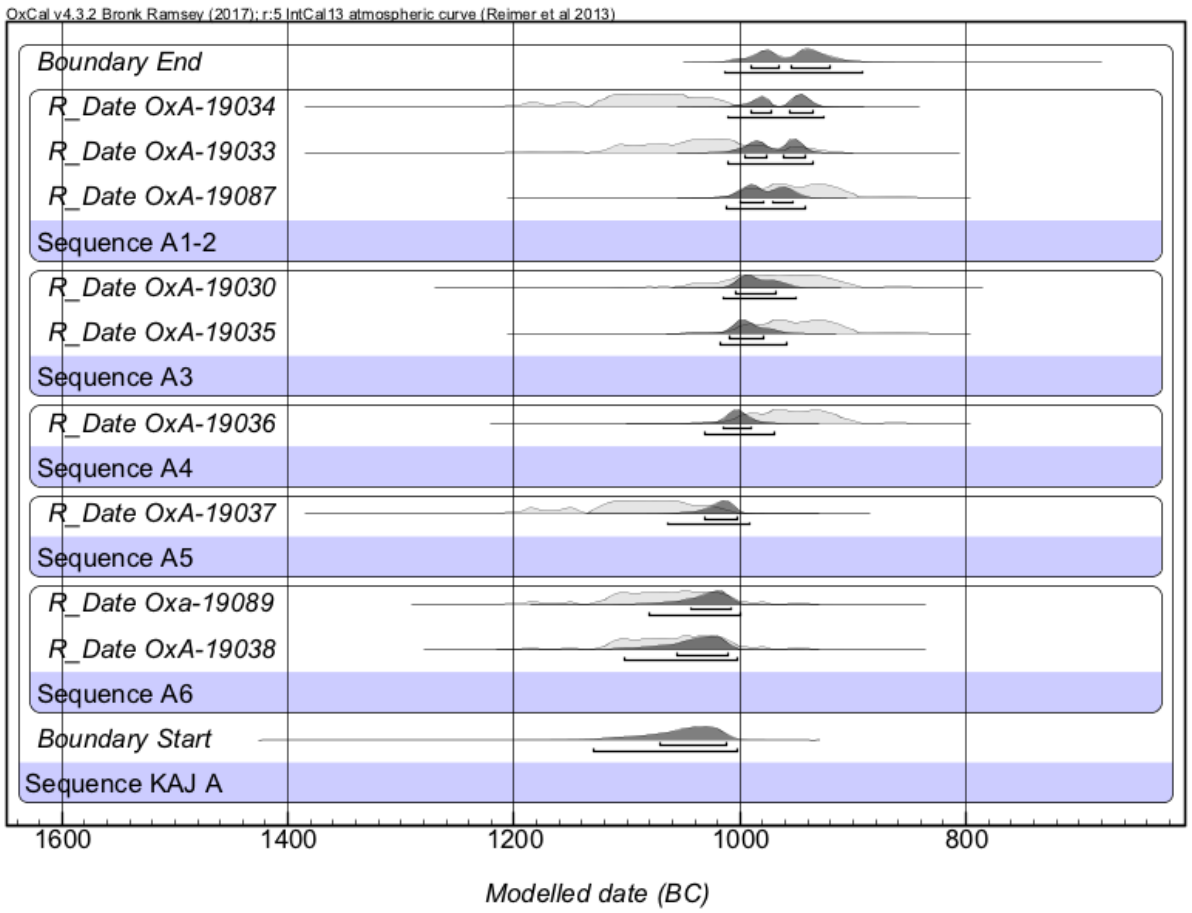


**Figure 4.4:** Modeled radiocarbon dates from Khirbat al-Jariya Area A excavations. Uncalibrated and calibrated dates are available in Table 4.1 and Ben-Yosef et al. 2010.

late-10th century BCE, it is hypothesized that the campaigns of Pharaoh Sheshonq I were the cause, which is corroborated by a coeval disruption to copper production at KEN and the Sheshonq scarab found at Khirbat Hamra Ifdan, another smelting center in Faynan (Ben-Yosef, Najjar, and Levy 2014a: 815; Ben-Yosef et al. 2019; Levy, Münger, and Najjar 2014). In sum, the 2006 excavation situated KAJ in the early phases (Phases 1 and 2 of Ben-Yosef's model) of copper smelting in Faynan; however, the results were based on somewhat limited excavations, which warranted a second excavation season in 2014.

#### 4.3.3 The 2014 Excavation Season

The 2014 excavation season at KAJ aimed to build on the results from 2006 by investigating the control and organization of the copper industry and to further examine the archaeometallurgical record (Liss et al. 2020; Liss and Levy 2015; Liss 2015). To do so, excavations focused on a potentially administrative or residential complex (Area B) and excavated another test probe into a slag mound (Area C). In order to identify and examine possible relationships between metallurgical and administrative/residential areas, the site was also comprehensively remapped. Finally, sieving and flotation of excavated sediment produced a substantial botanical collection, providing new data about fuel selection for smelting and preliminary evidence concerning subsistence practices. The integration and analysis of these diverse datasets in conjunction with the 2006 excavations contributes to a more holistic understanding of the site. The 2014 season was directed by Levy and Najjar with the present author, Matthew D. Howland, and Craig Smitheram functioning as field supervisors.

##### 4.3.3.1 Site Survey and Mapping

The first goal when returning to KAJ was to methodically remap the site, since existing maps (e.g., Levy et al. 2003: Figure 16) lacked a complete representation of the distribution and layout of archaeological and archaeometallurgical remains, based on a comparison of the map to what could be seen on the ground. The ELRAP team used a balloon platform with an attached camera to produce georeferenced 3-D models and orthophotos for a comprehensive and spatially accurate representation of KAJ (Howland, Kuester, and Levy 2014; Howland et al. 2015). In turn, these orthophotos were used to create site maps through vectorization in GIS.

The results of the aerial photography and mapping project shed new light on the distribution of archaeological remains at KAJ (Figure 4.5) (Howland et al. 2015). The produced orthophoto, providing an aerial perspective with ca. 2 cm resolution, facilitated detailed vectorization of all site features in GIS. The new map (Figure 4.5) affords a more accurate depiction of the density of copper slag mounds and concentrations at the site, revealing 19 new slag deposits and scatters that were not present on the previous map generated by total station survey (cf. Levy et al. 2003: Figure 16). The new map also differentiates slag deposits by type, including slag mounds, mounds of crushed slag, and slag scatters (all of which were ground-truthed), providing a more nuanced representation of the spatial distribution of the copper smelting remains. Moreover, it was possible to identify dozens of architectural features that were not previously mapped, which also facilitates greater understanding of the scale of the industry and site use. Finally, the new map also helped guide excavation decisions over the course of the field season, such as identifying the most centrally located structure for excavation.

In general, the newly discovered features fall within the original spatial boundaries defined for the site and conform to what is seen at other smelting sites in Faynan, with slag being primarily deposited along the outskirts with some smaller deposits among the architecture. While the identification of new slag mounds inherently suggests a larger scale of production at KAJ than previously believed, it is difficult to estimate the amount of slag without excavations, as slag mounds can contain 40% or less slag (Ben-Yosef 2010: 338). The mounds of crushed slag at KAJ were previously mentioned by Hauptmann (2007) but were mapped for the first time here. In antiquity, slags were frequently crushed to extract extraneous bits and prills of metallic copper trapped in the slag matrix during smelting, and it is considered a standard step in the ancient metal production *chaîne opératoire* in Faynan and beyond (Hauptmann 2007: 245-246;

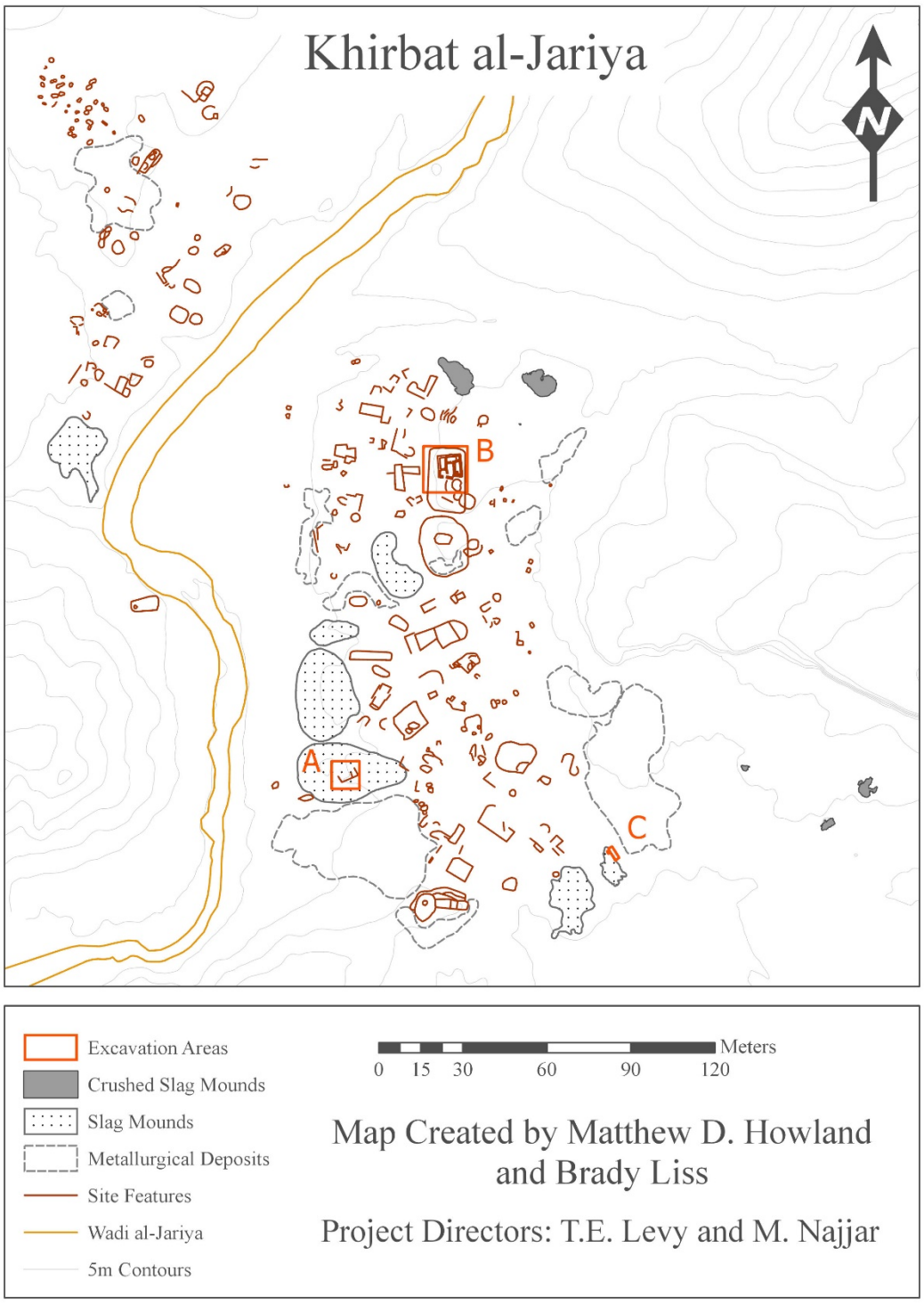


**Figure 4.5:** Map of Khirbat al-Jariya produced in 2014 using the ELRAP balloon photography platform.

Hauptmann and Löffler 2013: 80; Ben-Yosef 2010: 929). Crushed slag served additional functions, such as pottery temper (including in ceramics from KAJ), a metallurgical flux, and as foundations for structures (Martin et al. 2013; Smith, Goren, and Levy 2014; Smith and Levy 2008; Ben-Yosef, Najjar, and Levy 2014a: 810-812). Crushed slag mounds at KAJ are towards the furthest extent of the site (on its northeastern and southeastern boundaries), similar to KEN (Ben-Yosef 2010: 329-331). Some of these mounds are near the excavations at Area B and possibly provide some indication of the function of the building.

#### 4.3.3.2 Area B – Building 2

In order to investigate the social organization of copper production at KAJ, the ELRAP project directors decided to excavate half of the largest architectural complex visible on the surface, located in the northern part of the site with a central position on a high, natural bedrock outcrop (Area B). The building was selected based on the potential for uncovering a possible elite residence/administrative context like those seen at KEN (such as Areas R and T - see Levy et al. 2014). Excavation revealed a structure (Building 2) measuring approximately 7.5 x 7.5 meters with between four and seven possible rooms - it was difficult to determine the room organization on the eastern side of the building, as it was not fully excavated (Figure 4.6). The building was likely accessible through two entrances in its southern wall connecting the building to a central alley which separated it from another potentially related but unexcavated structure immediately to its south. Excavations discerned seven unique strata associated with the building's occupation and abandonment.

Building 2 was constructed directly on the local bedrock, which likely functioned as the surface for the initial occupation (Stratum B2c). All the major walls on the perimeter and interior

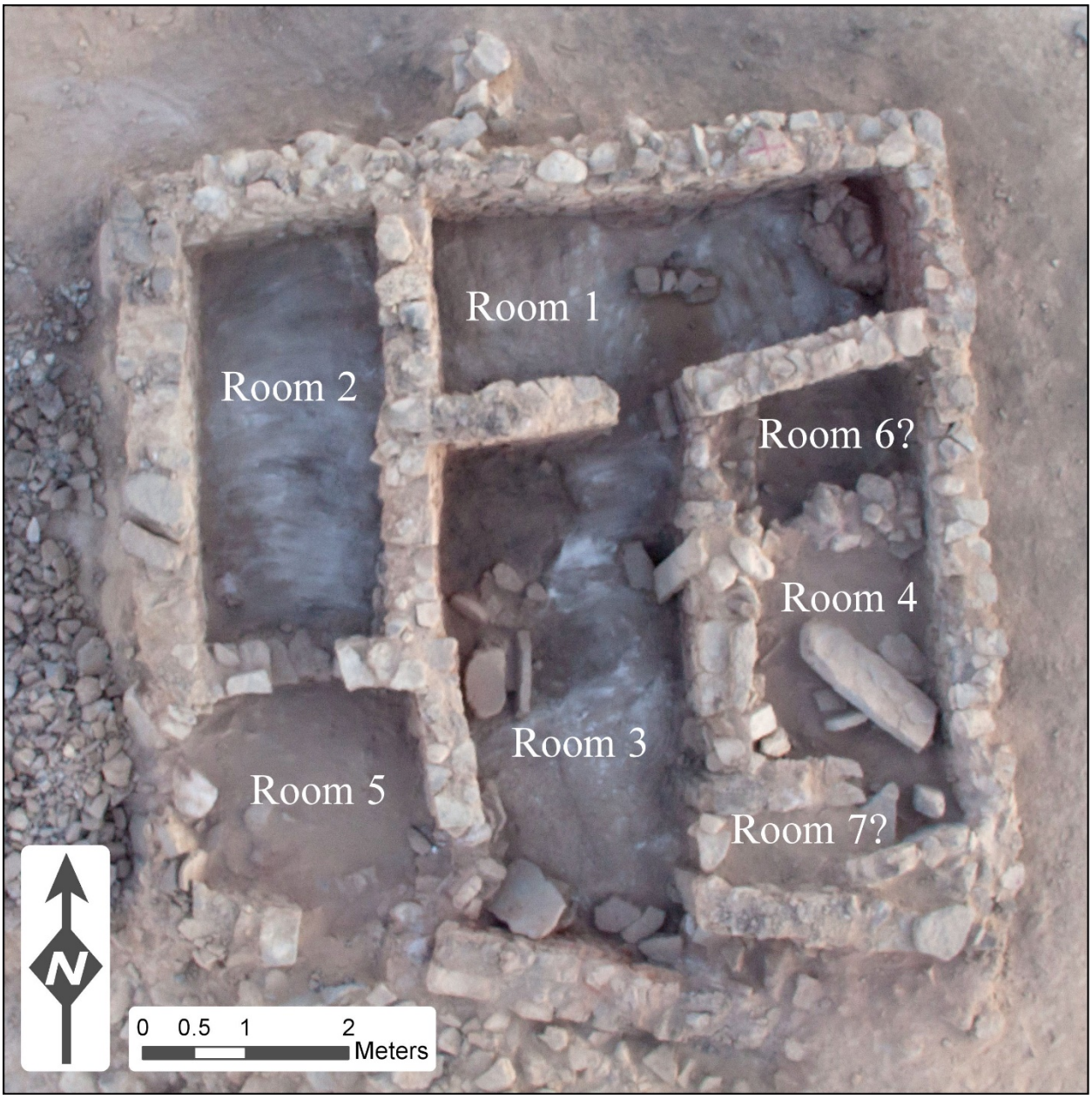


**Figure 4.6:** Building 2 at Khirbat al-Jariya following its excavation during the 2014 ELRAP season. Photograph credit: Matthew D. Howland, UCSD Levantine and Cyber Archaeology Lab.

of the building, which are adjoining, were constructed at the beginning of this stratum. The end of the first occupation is identified by the entrances to Rooms 4, 6, and 7 being intentionally blocked, after which they went out of use for the remainder of the site's habitation, creating an undisturbed context (Figure 4.7). As the building likely experienced a second occupation on the

**Figure 4.7:** Intentionally blocked doorways in the central north-south wall of Building 2 at Khirbat al-Jariya. Photograph credit: Thomas E. Levy, UCSD Levantine and Cyber Archaeology Lab.

bedrock surface (discussed further below), during which the floors were presumably cleaned as part of normal habitation/use, artifacts associated with the first occupation would only be excavated in these blocked eastern rooms of the structure (4, 6, and 7); however, as previously mentioned, these rooms were not completely excavated. Thus, material culture from the initial occupation of Building 2 is extremely limited, and the stratum is primarily identifiable by the construction of the building.

Following the blocking of the interior doorways, there was a second occupation in Building 2 (Stratum B2b), which probably also used bedrock as a surface in the structure, indicated by the blockages also being built directly on bedrock. Finds relating to this occupation were excavated immediately above the bedrock, with small patches of beaten earth possibly

representing a floor in Rooms 1, 2, and 3. In addition, a semicircular stone installation faced with mudbrick was excavated in the eastern end of Room 1; the interior of the installation was left unexcavated. Artifacts collected from the floors in Rooms 1 and 2 were primarily ground stone artifacts, including hammerstones and grinding slabs, as well as some pottery (see Howland 2021 for analysis of the pottery). Room 3, the central space of Building 2, was unique in the discovery of a grinding feature with a finely crafted grinding slab and associated grinding stone in situ. The ground stones were immediately adjacent to a possible bedrock mortar but separated by a standing stone slab. In addition, crushed slag was found within and around the bedrock mortar (similar to mortars and mounds of crushed slag found northeast of Building 2, discussed further below). A possible crushed slag floor surface was excavated in the northwestern corner of the room and likely connects to the grinding feature. Following the end of this second occupation period, a layer of fill (Stratum B2a/b) accumulated on the bedrock. The excavated material from the fill was difficult to definitively attribute to a particular occupation (B2a or B2b) and was classified as belonging to its own stratum (B2a/b).

The subsequent and final occupational phase (Stratum B2a) in Building 2 included a significant accumulation of ceramics on top of the preceding fill. A small north-south partition wall excavated on top of the fill in Room 1 was also associated with this stratum. The excavation of some hammerstones and grinding slabs similarly indicated the presence of an occupation horizon. Following this final phase, the structure went out of use, as represented by the wall collapse embedded in aeolian sediment (Stratum B1b and B1c) both within and surrounding the standing architecture. Some of the collapsed stone was repurposed in modern times (Stratum B1a) to construct circular structures (approximately 2–5 meters in diameter). These installations were potentially animal pens built by the local Bedouin community.

#### 4.3.3.3 Area C – Slag Mound

To build on the metallurgical narrative constructed from the 2006 excavations and to collect additional samples for analyses conducted in this dissertation, a large slag mound on the southeastern extent of the site was selected for a small excavation probe (Area C) (see also Liss 2015; Liss and Levy 2015; Liss and Stout 2017; Ben-Yosef et al. 2019). The slag mound was identified based on a visible scatter of broken slags on the surface, and a cut by a mining road from the 1960s on its northeastern edge revealed additional metallurgical remains below the surface. A 1x1 meter sounding was excavated to a depth of ca. 1.75 meter, where local bedrock was discovered (Figure 4.8).

**Figure 4.8:** Completed excavation probe into the Area C slag mound at Khirbat al-Jariya. Photo credit: Thomas E. Levy, UCSD Levantine and Cyber Archaeology Lab.

Above the bedrock was a significant accumulation of crushed slag, roughly 80 centimeters thick (Stratum C2d). The excavated material from this stratum was almost entirely crushed slag with only some bits of charcoal and a few pottery sherds. Above the slag, there was a drastic transition in material culture; this new layer of ashy sediment yielded significant domestic refuse, including pottery, charcoal, charred date seeds, burnt bones, and a ground stone artifact (Stratum C2c). A stone feature consisting of four stones in a line was excavated as well; however, its function was indeterminable, as it continued into the section. Atop this stratum was a thin, compact layer of tan sediment, possibly from weathered technical ceramics related to metal production, such as furnace fragments and/or tuyères (Stratum C2b). The associated artifacts included pottery sherds, possible pieces of technical ceramic, and a broken copper ring. The final layer of the slag mound was another metallurgical phase dominated by large fragments of both tap slag (ranging from 5–25 centimeters in diameter) and furnace slag embedded in a dark-brown, ashy sediment totaling about 50 centimeters thick (Stratum C2a). Charcoal, broken technical ceramics, and some pottery sherds were also collected. This second layer of metallurgical waste was probably the final period of copper production prior to the abandonment of KAJ.

#### 4.3.3.4 Slag Processing Installations

The new map and excavations at KAJ confirmed the significant role of secondary slag processing at the site originally identified by Hauptmann (2007: 131-132). Hauptmann's (2007: 131) survey of KAJ located a notable presence of crushed slag (estimated 100 tons) on the southern edge of the site. In addition to mapping these mounds (three in total), the 2014 ELRAP expedition identified and mapped two additional crushed slag mounds northeast of Building 2 on the northern limits of KAJ (see also Chapter 6 for 3-D models). Further exploration of these

features revealed bedrock mortars associated with the mounds (like those described by Hauptmann [2007: 125] at Ras en-Naqb) which were not previously reported on at KAJ (Figure 4.9). Ten bedrock mortars were identified and mapped near the two heaps of crushed slag in the northeast, and one additional mortar was discovered by the crushed slag in the south. One of the northern mortars was still filled with crushed slag, clearly connecting them to the grinding process. The excavations from Building 2 also corroborate the importance of crushing activities at the site. Artifacts collected from the bedrock surface in the building were dominated by hammerstones and grinding slabs (potentially used for slag), and a possible bedrock mortar was centrally located in Room 3. The northwestern corner of this room was also surfaced with a layer of crushed slag.

**Figure 4.9:** Bedrock mortars likely dedicated to slag crushing found north of Building 2 and associated with large mounds of crushed slag at Khirbat al-Jariya. Photograph credit: Thomas E. Levy, UCSD Levantine and Cyber Archaeology Lab.

As indicated from the survey results and previous excavations, only some of the slag at KAJ was crushed, which is also the case at KEN. This phenomenon is possibly the result of later slags being produced from a more efficient smelting technology. As smelting technologies improved, less copper would be lost/trapped in the slag. The decreased amount of copper, or even a reduced amount of visible copper, could potentially render the slag crushing process ineffective or inefficient. This understanding is further supported by the excavations and stratigraphy in Areas B and C, where crushed slag is only directly associated with the early occupation phases of the site. There is also substantial evidence for the gradual improvement of copper production over the course of habitation at KAJ and in Faynan more generally (Ben-Yosef et al. 2019; Liss and Levy 2015; Liss and Stout 2017). Given the site seems to have been abandoned, it is also possible the inhabitants simply did not reach the crushing step for some of the slag prior to leaving KAJ. However, this explanation is less likely, given the similar phenomenon at KEN, which continued to produce copper after KAJ.

#### 4.3.3.5 Radiocarbon Dates

Ten new radiocarbon samples were selected from both the slag mound and building excavations to further contextualize KAJ in the Iron Age, bringing the total number to 19 from the site (Figure 4.10). Based on the dates and stratigraphy, the construction and initial occupation of Building 2 likely begins approximately in the mid-11th century BCE (elaborated on in greater detail below), and the structure was most likely abandoned with the site in the mid–late 10th century BCE. The radiocarbon results from the slag mound similarly indicate that the site was established in the mid-11th century BCE, contemporaneous with the construction of Building 2. Samples from the main production phase (Stratum C2a) at the top of the mound correlate with

the last occupation of Building 2 in the late 10th century BCE. In general, this new suite of radiocarbon dates matches with those collected from Area A (Ben-Yosef et al. 2010), securely placing KAJ within the Early Iron Age between the 11th and 10th centuries BCE.

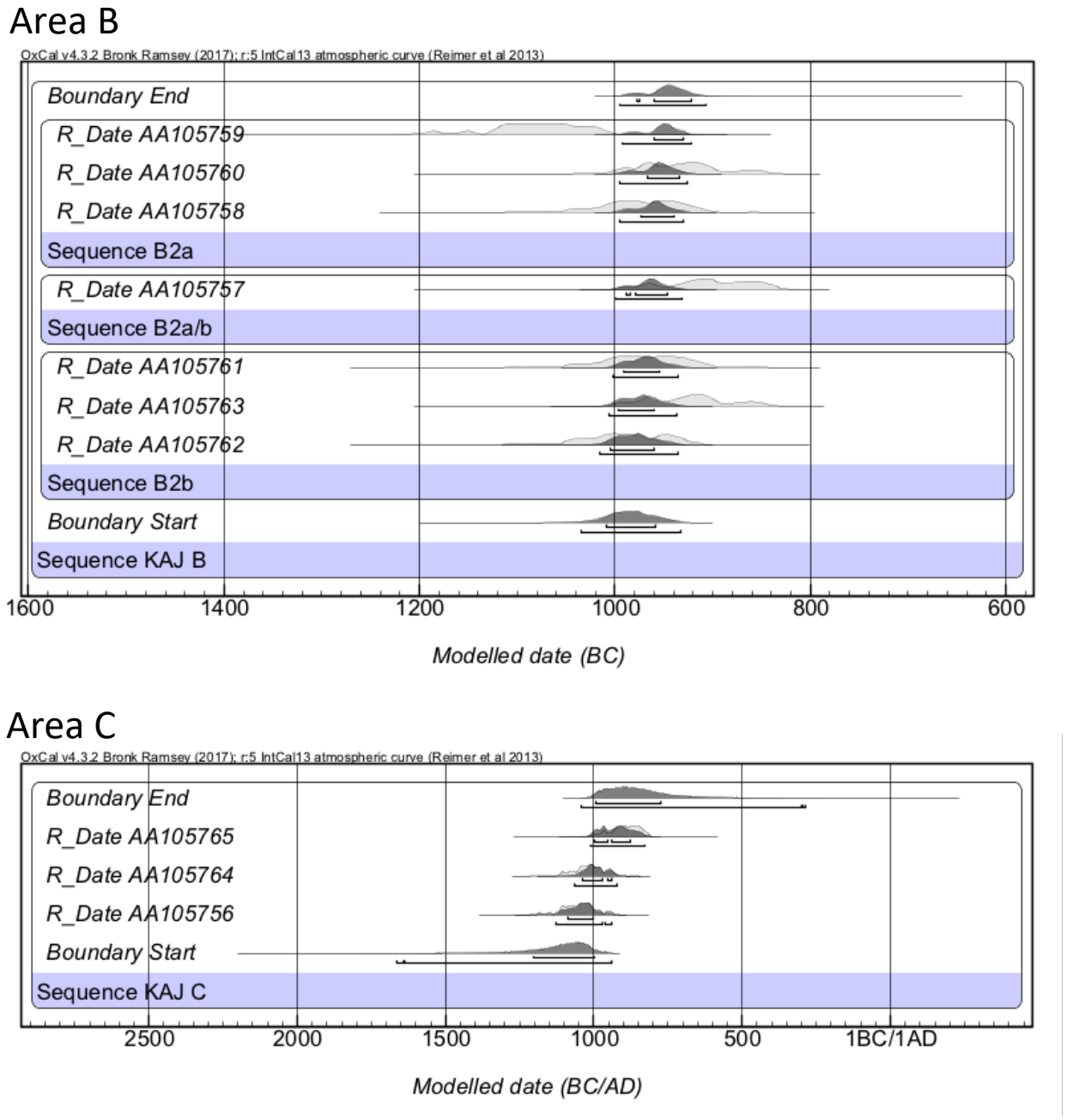


**Figure 4.10:** Modeled radiocarbon dates from Khirbat al-Jariya Areas B and C. Uncalibrated and calibrated dates are available in Table 4.1 and Liss et al. 2020.

#### 4.3.3.6 Paleobotanical Analyses

This section will provide only a brief overview of the paleobotanicals from the 2014 season which were collected by Rosemary Yuka Hoshino and analyzed by Dr. Brita Lorentzen (for a more detailed discussion, see Liss et al. 2020: 420-422). Thus far, only the wood charcoal and botanicals collected from the dry sieve have been analyzed, a total of 3,305 fragments from 10 contexts (Liss et al. 2020: 420). In general, the assemblage (90% of which was successfully identified) was similar with other Iron Age copper smelting centers in Faynan including plant taxa typical of the dry environment and its wadis with Tamarisk being the most abundant (Liss et al. 2020: Table 3). The assemblage also included wood from fruit trees including carob, date palm, fig, grape, olive, and pomegranate from contexts in both Area B and Area C. Both the Tamarisk and the fruit tree wood were likely used as a fuel source in smelting, a practice also seen at KEN (Liss et al. 2020: 421-422). The presence of wood from fruit trees along with fruit remains such as date seeds indicates that the inhabitants of KAJ had access to fruit trees despite the harsh terrain immediately surrounding the site. Nearby KAJ, however, is the Wadi Ghuwayba al-Ghani ("al-Ghani" is a descriptor meaning "the moist one") where modern Bedouin grow fruit tress including olive and pomegranate (Liss et al. 2020: 422). Thus, the fruits and wood cuttings likely came from orchards or fields located in a water-rich location such as the Wadi Ghuwayba al-Ghani; an Iron Age site, Khirbat al-Ghuwayba, is located adjacent to a spring with this wadi (discussed further below).

#### 4.3.3.7 Interpretation of Area B

The complicated stratigraphy of Area B required careful consideration when dating the construction of the building (Table 4.2).

**Table 4.2:** Complete stratigraphy for the 2006 and 2014 excavations at Khirbat al-Jariya with associated radiocarbon dates.

| Complete Stratigraphy and Correlation from KAJ 2006 and 2014 Excavation Seasons | | | | | | | | | | |
|---|---|---|---|---|---|---|---|---|---|---|
| **Strat.** | **Description** | **Radiocarbon Area A (1σ)** | **Area A** | **Description** | **Radiocarbon Area B (1σ)** | **Area B** | **Description** | **Radiocarbon Area C (1σ)** | **Area C** | **Description** |
| I | Post-Occupation | 1113-997 BCE | A1a | Top sediments of slag mound, copper production debris and aeolian loess | N/A | B1a | Modern, repurposed stones | N/A | | Not present |
| | | 1125-1026 BCE | A1b | Fill inside Structure 276, large boulders and stones | N/A | B1b<br>B1c | Stone collapse<br>Stone collapse with loess fill | N/A | | |
| II | Final occupation and copper production phase | 995-912 BCE | A2 | Occupation phase of Structure 276,<br>copper production debris at top of mound | 1009-927 BCE<br>979-901 BCE<br>1118-1027 BCE<br>970-844 BCE | B2a<br>B2a/b | Final occupation phase in Building 2<br>Ambiguous loci associated with 2a or 2b | 932-832 BCE | C2a | Thick accumulation of copper production debris |
| III | Occupation following architectural restructuring of Building 2 | 994-915 BCE<br>1108-934 BCE | A3 | Accumulation of copper production debris in slag mound | 1009-924 BCE<br>1026-931 BCE<br>978-895 BCE | B2b | Second occupation phase in Building 2 following architectural restructuring | N/A | | Not present |
| IV | Initial Occupation of Site | 995-919 BCE | A4 | Occupation phase with stone installations,<br>floors, and tent dwelling? | N/A | B2c | Construction and initial occupation in Building 2 | N/A | C2b | Thin debris accumulation |
| | | 1128-1026 BCE | A5 | Accumulation of domestic debris mixed with industrial remains | | | | 1054-940 BCE | C2c | Occupation phase with domestic refuse |
| | | 1113-1012 BCE<br>1114-1016 BCE | A6 | Occupation phase above bedrock with<br>fine crushed slag, ore, ash, and pits | | | | 1111-1005 BCE | C2d | Superimposed layers of crushed slag, nearby mounds of crushed slag |
| **Bedrock** | | | | | | | | | | |

Based on the stratigraphy indicating two occupation phases on bedrock floors chronologically separated by the blocking of doorways, excavated radiocarbon samples from the bedrock must relate to the second occupation phase. These dates therefore post-date the first occupation of Building 2 and function as a *terminus ante quem* for its construction. As such, Building 2, the largest extant stone-constructed building at KAJ, was likely built in the mid-11th century BCE, at the very beginnings of the settlement. The function of the building is not clear; however, it seems to have served a combination of industrial and potentially elite functions based on the central grinding feature and high-quality ceramics, respectively (Howland 2021). The significance of this early and possible elite construction at the site suggests KAJ was an integral part of the Early Iron Age Faynan copper production network from the outset of its settlement, representing development early in Production Phase 1 in Faynan.

Following the initial construction and occupation in Building 2, the structure was architecturally modified by the aforementioned door blockages. The reason for this alteration is currently unclear. It may be associated with a change in function and/or control of the building, but it is impossible to determine from the current state of the archaeological record, based on the understanding that material culture from the first occupation was no longer present at the time of excavation, except in the minimally excavated eastern rooms. As mentioned, the doorway to the small structure excavated in 2006 was also intentionally blocked (Ben-Yosef et al. 2010: Figure 7); it is difficult to situate chronologically, but it was potentially associated with the same event in Building 2. A similar phenomenon was discovered at KEN, in which the guard chambers of the gatehouse connected to the fortress were intentionally narrowed (Levy et al. 2014: 96). However, this event has been attributed to the campaign of Sheshonq I, which has also been connected to the synchronous abandonment of KAJ (and the transition to Production Phase 3)

(Ben-Yosef et al. 2010: 744; Levy, Münger, and Najjar 2014; Ben-Yosef et al. 2019). Thus, these blocked doorways at KAJ are unique in their early date, and they are potentially evidence of a localized event. Future excavation in the unexcavated eastern rooms could provide additional insight.

Based on the material culture in Building 2 and the proximity of the two crushed slag mounds, the building might have been connected to slag processing and/or supervision of the operations; this draws a possible parallel to Area S at KEN, which also included a building rich with stone tools that was associated with slag crushing (Levy et al. 2014: 151-169; Levy, Bettilyon, and Burton 2016). The connection between a large, central building at the site and slag processing suggests it was a crucial component of metal production at KAJ. Secondary slag processing also links the metallurgical process at KAJ and KEN. Similar mounds of crushed slag were found on the outskirts of KEN, suggesting both sites employed a comparable *chaîne opératoire* (Ben-Yosef 2010: 329-331). These crushed slag deposits at KEN were initially difficult to date precisely within the Iron Age or to associate with a specific Production Phase, given the long and continuous copper smelting at the site from the 12th–9th centuries BCE. (Ben-Yosef 2010: 930). The crushed slag at KAJ can help refine the chronological attributions for these features, as KAJ was only inhabited during the 11th–10th centuries BCE (during Production Phase 1 and 2). Furthermore, slag processing seems to stop during the later phases of copper production in Iron Age Faynan (Ben-Yosef 2010). Thus, it is possible to date the crushed slag mounds more generally at KEN to an early production phase in the 11th–10th centuries BCE (Production Phase 1 and/or 2), contemporaneous with KAJ.

#### 4.3.3.8 Comparison of the Area A and Area C Slag Mounds

In general, the Area A and Area C slag mounds are similar in both dating and stratigraphy (Table 4.2). Both excavations discovered crushed slag directly above bedrock associated with the initial occupation of the site. The crushed slag in the first layer reiterates the hypothesis that KAJ was established for the direct purpose of producing copper and exploiting the local mines, especially given the presence of ancient mines near the site, the Wadi al-Jariya mines, and the lack of nearby water or other natural resources (Ben-Yosef et al. 2010: 736; Knabb et al. 2014a). However, the Area C mound had a much larger accumulation of crushed slag (roughly 80 centimeters) suggesting a more intensive early production period than seen at the bottom of the Area A slag mound, where there was only a thin layer of crushed slag (ca. 10 centimeters). Based on the radiocarbon dates, this earliest production is contemporaneous with the construction of Building 2 in the mid-11th century BCE. As such, along with the immediate construction of significant architecture, the inhabitants of KAJ were likely producing copper on a substantial scale early in the site's occupation, suggesting a more rapid development of copper production within Production Phase 1.

Above the layer of crushed slag, Area C transitioned to a possible domestic/habitation function, reflecting what was seen in Area A. Material culture from this layer was indicative of domestic refuse related to cooking, based on the bones and date seeds, and completely lacking slag. Following the unique and somewhat ambiguous deposit of compact tan sediment, the area once again functioned as a metallurgical dump. Here, the material record diverges slightly from Area A in the size of slag fragments found within this layer; tap slags with diameters up to 25 centimeters were collected, whereas previously excavated tap and furnace slags were typically less than 10 centimeters in diameter, with some samples reaching 15 centimeters (Ben-Yosef et

al. 2010: 738; Ben-Yosef and Levy 2014b: 941-943). These slags are possibly indicative of intensification in production not represented by the Area A slag mound. From the radiocarbon dates and its presence on the surface of the site, it is possible to suggest that this thick metallurgical layer represents the final phase of intense copper production associated with Phase 2 before the abandonment of KAJ, and it is likely linked with the final occupation in Building 2.

#### 4.3.4 Summary

Overall, the results from KAJ show organization and coordination in the development of the site. The excavations from both Areas B and C build on Area A, indicating that KAJ was a significant copper production site from its initial establishment during Production Phase 1. Taking into consideration the contemporaneous copper production at KEN (discussed below), which likely began producing copper at the very beginning of Phase 1, settlement at KAJ should be reinterpreted as an organized expansion of the already active metallurgical industry in Faynan. The reason for this expansion is probably connected to the location of KAJ up the wadi from KEN, providing a greater proximity to the copper resources in this area of Faynan (Knabb et al. 2014a: Figure 1). The consistencies in the copper production *chaîne opératoire* between KAJ and KEN also support this conclusion; inhabitants of both sites dedicated significant efforts to slag crushing, depositing mounds on the perimeter of the site, and used similar strategies/resources for charcoal. Thus, it is possible a subset of metalworkers from KEN with a shared technical knowledge established KAJ for easier access to the Wadi al-Jariya mines.

The extension of copper smelting to KAJ also indicates that the demand for copper in the mid-11th century BCE was significant enough to justify/incentivize an intensification of production, as KEN also continued to smelt copper during this period. This understanding fits

within the broader context of copper production in the eastern Mediterranean as discussed above. Ultimately, the Wadi Arabah would develop into the main source of copper to the region following the Late Bronze Age collapse until the end of production in the Late Iron Age (Levy, Ben-Yosef, and Najjar 2014; Ben-Yosef et al. 2019). The metal produced in Faynan reached the Mediterranean via the Negev Desert, as evidenced by pottery analysis at sites in the Negev and a submerged copper cargo found at Neve Yam (Yahalom-Mack et al. 2014a Martin and Finkelstein 2013; Martin et al. 2013; Yahalom-Mack and Segal 2018; Ben-Yosef and Sergi 2018). Moreover, this copper seems to have been available to a wide market at least as far as Greece and Egypt (Kiderlen et al. 2016; Vaelske, Bode, and Loeben 2019; Ben-Dor Evian et al. 2021). The role of Faynan in the eastern Mediterranean economy and the demand for copper could also have contributed to the gradual technological developments seen over the course of production at KAJ, such as the larger slags in the final phases of copper smelting and the transition to Production Phase 2 (this is also evidenced through x-ray fluorescence analysis of slag samples from the site [Ben-Yosef et al. 2019; Ben-Yosef 2010; Liss and Levy 2015; Liss and Stout 2017]). The new map of KAJ also reiterates the significant scale of production based on the identified slag deposits. Increases in technological sophistication, efficiency, and scale to maximize copper extraction could have been driven by the potential economic profits or other socio-political factors. Situating the excavation results within the context of Iron Age Faynan and the economy of the southern Levant in this way can help explain the reinterpretation of KAJ as a calculated expansion of the existing copper smelting industry and part of the development of the Iron Age industrial landscape.

4.4 Khirbat en-Nahas

Khirbat en-Nahas (KEN) is the largest Iron Age copper smelting center in the Southern Levant and the cornerstone for understanding the development of both metallurgy and social complexity in Faynan during this period (Levy et al. 2014; Levy et al. 2008; Ben-Yosef 2010: 245-339; Hauptmann 2007: 127-130). Covering an area of more than 10 hectares, KEN includes the remains of over 100 structures and an estimated 50,000-60,000 tons of copper slag (Figure 4.11) (Levy, Ben-Yosef, and Najjar 2018; Hauptmann 2007: 127). The large, square fortress, measuring 73x73 meters, is also a testament to the significance of the site – the largest extant structure from Iron Age Faynan (Levy et al. 2014: 93-122; Glueck 1940a: 60). In addition, with a total of 108 radiocarbon dates, KEN is the chronological anchor of Iron Age society and copper production in Faynan (as discussed in Chapter 3).

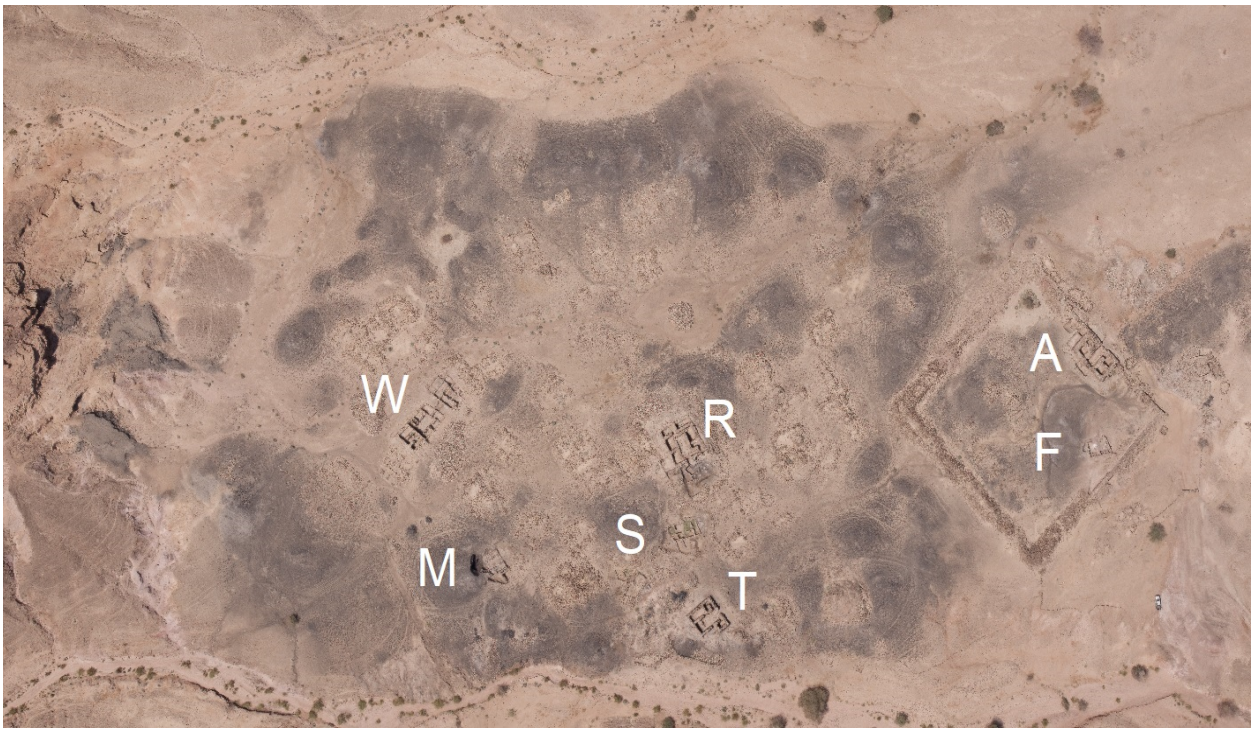


**Figure 4.11:** Aerial image of Khirbat en-Nahas with excavation areas labeled. Note the large square fortress on the right side of the photo and the significant amount of black slag mounds. Image credit: Matthew D. Howland, UCSD Levantine and Cyber Archaeology Lab.

The site was the primary focus of ELRAP excavations for the 2002, 2006, and 2009 seasons opening seven excavation areas (Levy et al. 2014). As the largest and most intensively excavated site from Iron Age Faynan, this section will provide overviews of all the excavation areas, and more comprehensive descriptions of the areas relevant to this dissertation (full descriptions for every excavation area are available in Levy et al. 2014). Emphasis and detail will be provided for the Area M slag mound excavation as the majority of the analyzed slag samples originated from this context. For each area relevant to this dissertation, a plot of the radiocarbon dates is provided, and a table (Table 4.1) at the start of the chapter provides a comprehensive record of all the radiocarbon dates including modeled and unmodeled data.

### 4.4.1 Previous Research

Khirbat en-Nahas was first reported by Alois Musil (1907: 298) in 1898 during his explorations throughout the region (Levy et al. 2014: 90; Glueck 1935: 29). The site was also visited by Kirkbride, Horsfield, Head, and Fritz Frank (1934: 221-224, Plan 16) during their surveys of the Arabah Valley (Glueck 1935: 29; Levy et al. 2014: 90). Frank (1934: Plan 16) provided a detailed sketch of the site with future excavation Areas A, F, and R clearly visible (see below). Glueck (1935: 26-29, 166; 1940a: 57-61) subsequently surveyed and sketched KEN describing the “great heaps of copper slag”, the large fortress, and dating the site to the Early Iron Age based on the pottery. Hauptmann (2007: 127-130 and citations there within) and the team from the German Mining Museum (GMM) also examined KEN as part of their archaeometallurgical investigations of Faynan. Along with mapping the site, they excavated small soundings into one of the buildings visible on the surface and sampled three of the slag mounds (Levy et al. 2014: 90; Hauptmann 2007: 127-130, Figure 5.33b). Using charcoal

collected from the soundings, they dated the site with radiocarbon for the first time and conducted an analysis of fuel used in the smelting process (Hauptmann 2007: 128; Engel 1993). Nine radiocarbon samples were analyzed (one from the probe into the building and eight from the slag mounds) providing dates primarily between the 12th-9th centuries BCE (Hauptmann 2007: Table 5.1). Lastly, MacDonald (1992: 73-77, Figure 15) surveyed the site, dating it to the Early Iron Age based on pottery, and provided a sketch of its northern portion mainly around the large fortress. Together, these explorations, surveys, and small excavations brought scholarly attention to KEN and chronologically situated the site in the Early Iron Age.

### 4.4.2 ELRAP Excavations at Khirbat en-Nahas

Intensive excavations at KEN began in 2002 as part of the ELRAP; the site was the focus for the project's investigation into the Iron Age (Levy et al. 2014). In 2002, excavations began with the gatehouse attached to the large fortress (Area A) focusing on delineating the structure and excavating two of its interior chambers. Excavations also opened a rectangular building adjacent to metallurgical deposits near the GMM excavations (Area S) and began excavating the initial layers (ca. 1.2 meters) of the slag mound probe (Area M). The 2006 excavations continued in Area A excavating an additional "guard room" and the interior passage[1], excavated Area M down to local bedrock, and also opened three new excavation areas: a small structure on the interior of the fortress (Area F), a structure on the eastern edge of the site (Area T) that Glueck (1935: 27, 166) potentially identified as a tower, and a large, centrally located building complex (Area R) which is also visible on Glueck's (1935: 166) map of the site. Finally, in the 2009 season, excavations focused on a large structure located in the southern portion of the site (Area

[1] One chamber was intentionally left unexcavated for future researchers (Ben-Yosef 2010: 253).

W) which did not appear to be directly associated with any slag mounds (Levy et al. 2014: 184). Excavations also continued in Area R, fully excavating the building except for its central courtyard and also excavating the extramural courtyard dedicated to copper production (Levy et al. 2014: 202). The excavations were supplemented with rigorous collection of radiocarbon samples and archaeometallurgical material culture providing the basis of Ben-Yosef's (2010) dissertation and a significant portion of this dissertation.

#### 4.4.2.1 Area A – Fortress Gatehouse

Excavations in Area A revealed the gatehouse's four-chamber construction plan, like other Iron Age sites in the Levant, and three occupation phases (Figure 4.12) (Levy et al. 2014: 93-122). The construction of the gatehouse was dated to the 10$^{th}$ century BCE based on radiocarbon, and it initially served as a defended entryway to the fortress and likely a more general military function of protecting/controlling the site (the beginning of Phase 2) (Levy et al. 2014: 119). This initial phase was associated with limited material culture due to the repurposing of the gatehouses in later phases (Levy et al. 2014: 119). The gatehouse transitioned in function in the early 9$^{th}$ century BCE; following its decommissioning as a military structure, the building was most likely used for domestic purposes by the local inhabitants (Levy et al. 2014: 119). This repurposing was identifiable by an architectural restructuring and a shift in material culture (the transition to Phase 3) (Levy et al. 2014: 119). Specifically, the doorways into the chambers were intentionally narrowed, the gateway entrance was partially blocked to potentially prevent wheeled vehicles or large animals, and the opposite entrance into the fortress itself was completely blocked essentially turning the gatehouse into a residence/public building (Figure 4.12) (Ben-Yosef 2010: 253-254; Levy et al. 2014: Figure 2.23-2.26).

**Figure 4.12:** Area A at Khirbat en-Nahas after excavation. Note the interior entrance into the fortress on the left side of the photograph was intentionally blocked. Photograph credit: Thomas E. Levy, UCSD Levantine and Cyber Archaeology Lab.

In its last phase, the structure was repurposed possibly for a metallurgical function as there was significant industrial waste (Levy et al. 2014: 120). While there was no direct evidence of smelting within the gatehouse, the probe outside its southern wall (and within the fortress wall) discovered significant slag along with tuyère and furnace fragments (Ben-Yosef 2010: 255-256; Levy et al. 2014: Figure 2.7, "Probe 6"). Dated to the 9$^{th}$ century BCE, this phase might also be associated with the industrial remains in Area F and the various slag scatters within the fortress walls as part of a general repurposing of the entire fortress for a metallurgical function (Levy et al. 2014: 120). In total, 28 radiocarbon dates situate the gatehouse to the 10$^{th}$-9$^{th}$ centuries BCE (Levy et al. 2014: 113-119, Figure 2.43). The fortress and gatehouse provide significant evidence for the complex organization of the copper smelting industry in Iron Age Faynan.

#### 4.4.2.2 Area T – Elite Residence and Tower

The Area T excavation focused on a structure located on the eastern edge of the site to test Glueck's (1935: 27, 166) interpretation that the building was a tower and its possible relationship with Areas A and R (Figure 4.13) (Levy et al. 2014: 169-184).

**Figure 4.13:** Area T at Khirbat en-Nahas after excavation. Its location on the edge of the site (note the wadi on the right side of the photo), two levels, and robust construction indicates the structure might have functioned as a watch tower (as suggested by Glueck 1935: 27, 166). Photograph credit: Thomas E. Levy, UCSD Levantine and Cyber Archaeology Lab.

The structure included thick exterior walls and measured 11 x 12 meters (Levy et al. 2014: 169, Figure 2.124). The interior included five rooms surrounding a courtyard and a stairwell to a second floor or possible tower, all of which were excavated during the 2006 season (Levy et al. 2014: 169-184). The initial construction and occupation of the building was on a layer of crushed slag, and a second occupation phase was identifiable by a mud surface over paving stones (Ben-Yosef 2010: 266-267). Only limited evidence of potential metallurgy was discovered in Area T

(Room 5) – although the metallurgical debris could be fill to level the surface, and the other rooms likely served storage and living/administrative functions (Ben-Yosef 2010: 268-269). Along with the evidence for a possible tower/lookout, this structure is assumed to be an elite residence (similar to Area R) based on its robust construction and limited if any metallurgical function (Levy et al. 2014: 184). Eight radiocarbon samples date the building the 10$^{th}$-early 9$^{th}$ centuries BCE (Levy et al. 2014: 181-183). Based on the dates, the structure is like associated with Production Phases 2-3 and provided additional control/security for the copper smelting activities.

#### 4.4.2.3 Area W – Residential and Storage Complex

Area W consisted of three building complexes (two of which shared a wall) located in the southern portion of the site (Figure 4.14) (Levy et al. 2014: 184-201). The buildings were excavated to investigate the stratigraphy of this part of the site, and because of the distinct absence of slag in direct connection with them (Levy et al. 2014: 184). It was also initially considered that Area W might be an administrative complex due to its size (Levy et al. 2014: 200). A total of 18 rooms, including two courtyards, were excavated in the two constructions which were separated by an alley (Levy et al. 2014: 184-201, Figure 2.154). The evidence suggests that these complexes were used for residential and cultic functions (Levy et al. 2014: 200-210). The eastern building included three probable storage rooms with an attached seven room structure (Ben-Yosef 2010: 278-279). These smaller rooms surrounded a courtyard associated with cultic finds and architecture, such as pillars, standing stones, and figurines (Ben-Yosef 2010: 278-279). The western structure consisted of seven rooms around a courtyard and appeared to be domestic in function based on material culture including a tabun and food

**Figure 4.14:** Area W at Khirbat en-Nahas after excavation including the structures and the alley separating them. The western structure is partially cut off by the edge of the photograph. Photograph credit: Thomas E. Levy, UCSD Levantine and Cyber Archaeology Lab.

processing tools/installations (Ben-Yosef 2010: 279; Levy et al. 2014: 201). Thus, Area W likely served cultic and domestic functions, potentially for non-elites, rather than an administrative role as originally believed (Ben-Yosef et al. 279). Area W was loosely dated to the 11$^{th}$-9$^{th}$ centuries BCE based on two radiocarbon dates (Levy et al. 2014: 199-202). While two dates are limited, they fit with the general chronology of the site, but it is difficult to determine which production phase Area W was associated with, potentially Phases 1-3.

#### 4.4.2.4 Area F – Metallurgical Workshop

Area F was a small building (ca. 7 x 9 meters) within the defensive walls of the site's fortress, and the excavations included a small portion of the fortress wall itself (Figure 4.15) (Levy et al. 2014: 123-131). The building had foundations constructed on crushed slag and an

**Figure 4.15:** Area F at Khirbat en-Nahas after excavation. Note the unique "cells" on the back wall, and the excavated portion of the fortress wall at the top of the photo. Photograph credit: Thomas E. Levy, UCSD Levantine and Cyber Archaeology Lab.

unusual angle in comparison to the fortress walls indicating that it likely post-dated the construction of the fortress (Levy et al. 2014: 123-130, Figure 2.46). The interior of the structure included two rooms and seven smaller cells/installations around a central courtyard (Levy et al. 2014: 123). These cells currently represent a unique architectural feature at KEN, and the material culture (bellow pipes, slag, furnace fragments, etc.) excavated within four of the cells suggested a metallurgical function (Levy et al. 2014: 123). Finds from within the two larger rooms also indicated metallurgical activities including bellow pipes, copper metal, slag, large basins, and installations (Ben-Yosef 2010: 261-262). Based on the evidence for copper production, the exceptional architectural, and the archaeometallurgical record (e.g., the high concentration of bellow pipes), the excavation supervisors determined Area F to be a copper refining/casting workshop (Levy et al. 2014: 131). Radiocarbon dates (n=5) point toward a

primarily late-10th to early-9th century BCE dating, and the shallow excavations suggested a single use-phase for the structure during Phase 3 (Figure 4.16) (Levy et al. 2014: 130-131). As such, Area F is associated with the industrial peak of production during the Iron Age.

Area F is particularly relevant to this research due to its dating and its interpretation as a refining workshop. The Area F workshop is contemporaneous with the appearance of unique iron-copper mixtures in the archaeological record of KEN (mainly recovered from Areas R and S, discussed further below) (Ben-Yosef 2010: 736-737). Ben-Yosef (2010: 736-737) has suggested that Area F might have been dedicated to refining these mixed metallic chunks to remove the iron and to produce copper ingots. While Ben-Yosef (2010: 822-825) was primarily focused on extracting copper from the mixtures, it is also possible that metallic iron was recovered. Area F could have functioned as a refining workshop where both metallic iron and copper were separated from these chunks and recovered. This possibility is a focus of Chapter 5 and is discussed at length there.

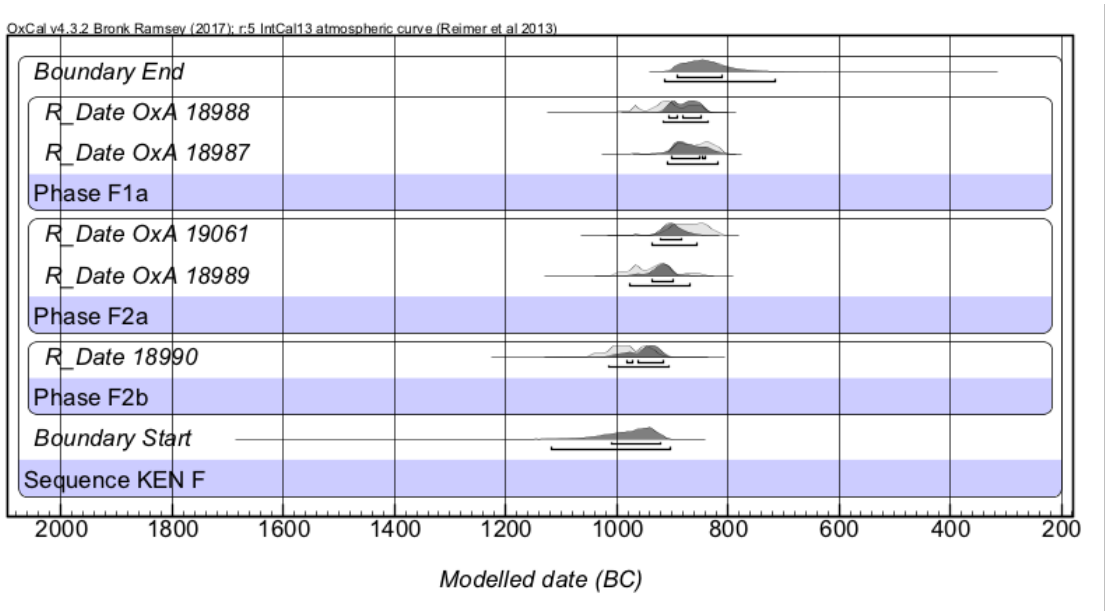


**Figure 4.16:** Modeled radiocarbon dates from Khirbat en-Nahas Area F. Uncalibrated and calibrated dates are available in Table 4.1 and Levy et al. 2014: 130-131.

#### 4.4.2.5 Area S – Slag Processing Workshop

Excavations in Area S focused on a rectangular structure (ca. 15 x 8 meters) composed of four rooms (one of which is possibly a courtyard) and the metallurgical deposits surrounding the building (Figure 4.17) (Levy et al. 2014: 151-169).

**Figure 4.17:** Area S at Khirbat en-Nahas during excavation. The four-room structure is visible, along with the deposits of slag on the right and left sides of the photo. Photograph credit: Thomas E. Levy, UCSD Levantine and Cyber Archaeology Lab.

The building was constructed on a leveled layer of crushed slag which was also present in thick layers outside its walls (Levy et al. 2014: Figures 2.112, 2.115). In addition, over 350 ground stone implements were collected from the excavations suggesting the building may have served as a slag crushing facility to extract copper (Levy et al. 2014: 151-154). There was also some evidence of metallurgy in the later phases of Area S around the building to the north and south

including significant slag, tuyère fragments, furnace fragments, and a possible furnace (Levy et al. 2014: 162-163). Other metallurgical materials collected included a casting mold, copper chunks/prills, and some metal objects (Levy et al. 2014: Figure 2.96-297; Ben-Yosef 2010: 266). Based on these remains, Area S was likely a slag processing workshop, and some melting/casting may have also occurred. The structure was dated to the 9th century BCE by 20 radiocarbon samples and is likely part of Production Phase 3 (Figure 4.18) (Levy et al. 2014: 168-169, Figure 2.120). Area S is also relevant to this dissertation because the excavations found both iron objects (Levy et al. 2014: Figure 2.93, 2.97) and mixed copper-iron chunks. In connection with the building possibly functioning as a melting/casting workshop in its later phases, Area S also could have played a role in potential iron production at KEN.

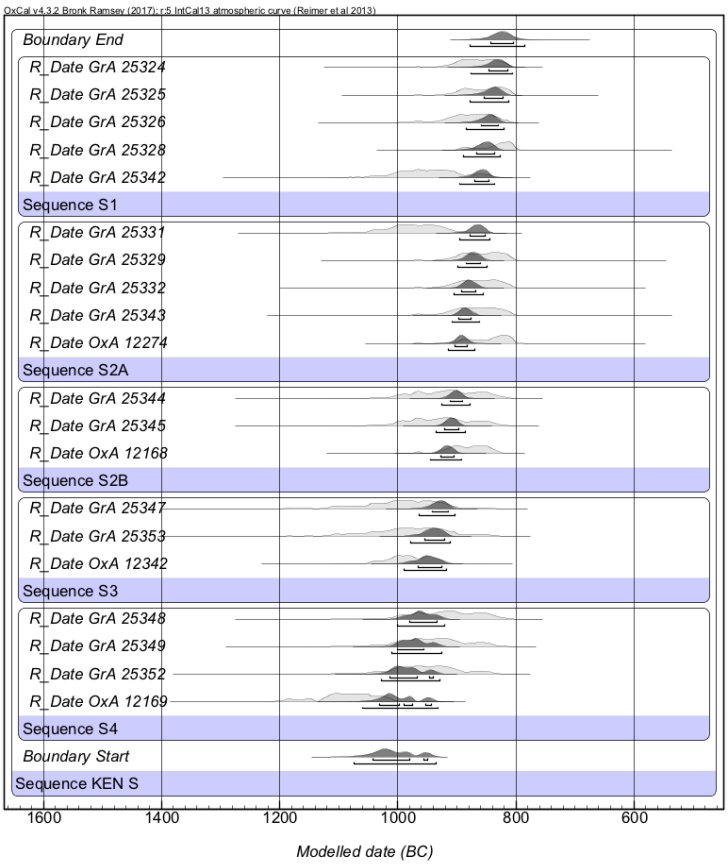


**Figure 4.18:** Modeled radiocarbon dates from Khirbat en-Nahas Area S. Uncalibrated and calibrated dates are available in Table 4.1 and Levy et al. 2014: 168-169.

#### 4.4.2.6 Area R – Central Elite/Supervision Residence

Area R consisted of a large building located roughly at the center of the site and surrounded by a stone perimeter wall (Figure 4.19) (Levy et al. 2014: 202-232; Glueck 1935: 166).

**Figure 4.19:** Area R at Khirbat en-Nahas after excavation including the substantial building (center), metallurgical complex (bottom), and perimeter wall. Photograph credit: UCSD Levantine and Cyber Archaeology Lab.

The structure is 12.7 x 15 meters, contained six rooms surrounding a courtyard, and included a second floor as indicated by a well-preserved staircase (Levy et al. 2014: Figure 2.196). The 2006 season probed the courtyard between the monumental structure and the perimeter wall discovering metallurgical layers and excavated one of the interior rooms (Levy et al. 2014: 203). The 2009 excavations revealed all the interior rooms of the main structure except for the central courtyard and also further probed the metallurgical levels discovered beneath and in front of the structure (Levy et al. 2014: 204). The structure in Area R was founded on layers of crushed slag (similar to Area S), and the material assemblage from within the building included beads, pendants, scarabs, and amulets along with metal weapons (Ben-Yosef 2010: 272; Levy et al. 2014: 231). There was also a unique stone bench attached to the northeastern exterior wall of the building; it may have functioned as a seat for an elite in control as its elevation would allow someone to see over the perimeter walls (Levy et al. 2014: 212, Figure 2.214). Based on its location with a commanding view of the rest of the site, monumental construction, the stone bench, and the special finds, the Area R building is believed to have been an elite residence, possibly for those controlling the copper production. Radiocarbon analysis dates the building in Area R to the late $10^{th}$-$9^{th}$ centuries BCE based on six samples (Levy et al. 2014: 223-228). Thus, Area R was likely part of the increased investment in the copper industry during Phase 2 and continued into Phase 3.

Relevant to this dissertation is the substantial evidence for industrial copper smelting that was found in the courtyard between the structure and its perimeter wall (Figure 4.20) (Levy et al. 2014: Figures 2.234-2.248). The excavation of this area was dominated nearly entirely by material culture associated with copper production (Ben-Yosef 2010: 276). Almost immediately beneath the surface, excavations discovered intact metallurgical installations and bases of

**Figure 4.20:** The metallurgical complex of Area R at Khirbat en-Nahas with the large structure in the background. This area yielded a substantial number of mixed iron-copper chunks. Photograph credit: Thomas E. Levy, UCSD Levantine and Cyber Archaeology Lab.

installations that were probably furnaces (Ben-Yosef 2010: 275). Excavations also revealed several roughly constructed walls that seem to be directly related to copper production as some had furnaces built against them and a “round chamber” that was constructed for slag disposal (Ben-Yosef 2010: 275-276; Levy et al. 2014: 218-219). Another wall seemed to delineate an area dedicated to crushed slag (Ben-Yosef 2010: 274). The material culture also included hundreds of furnace and tuyère fragments with some large tuyères that were still intact (Ben-Yosef 2010: 274). Along with two furnace bottoms, the Area R excavation also discovered the best-preserved furnace installation at the site (Ben-Yosef 2010: 661-670; Levy et al. 2014: 221-222). Finally, mixed chunks of iron and copper were excavated from the smelting complex, and they are

currently interpreted as the immediate product of copper smelting in the area (Ben-Yosef 2010: 735-736). The copper smelting complex of Area R was an organized space and well-planned workshop associated with the most sophisticated smelting technology in Iron Age Faynan (Ben-Yosef 2010: 278). It is important to note that this advanced technology is contemporaneous with the appearance of the copper-iron chunks in the archaeological record, to be discussed further in Chapter 5.

The stratigraphic relationship between copper production and the occupation in the building is convoluted (Ben-Yosef 2010: 272; cf. Levy et al. 2014: 204, 218-222). The copper smelting complex is located directly in front of the entrance to the structure, and it is also lower than the walls suggesting it predates the construction of the building (Ben-Yosef 2010: 272, Figure 5.30). The radiocarbon dates collected from the copper smelting area also slightly overlap with the building, dating to the late 10$^{th}$ and mainly the 9$^{th}$ century BCE based on 11 samples (Figure 4.21) (Levy et al 2014: 223-228). However, the archaeometallurgical assemblage from the copper smelting complex - including large tuyères, large tap slags, and sophisticated furnaces/installations - is the most advanced from Faynan and is associated with the final phases of copper production in the Iron Age during the 9$^{th}$ century BCE (Ben-Yosef 2010: 272). As such, it is more likely that the smelting complex post-dates the final occupation of the structure in Area R, and its lower elevation may be the result of the Iron Age inhabitants digging pits for disposal of metallurgical waste (Ben-Yosef 2010: 272). This stratigraphic interpretation can still work with the radiocarbon dates as well (Ben-Yosef 2010: 272). In sum, the smelting complex of Area R represents the pinnacle of smelting technologies during the final phases of production at KEN (Phases 2-3) and Faynan more generally in the Iron Age.

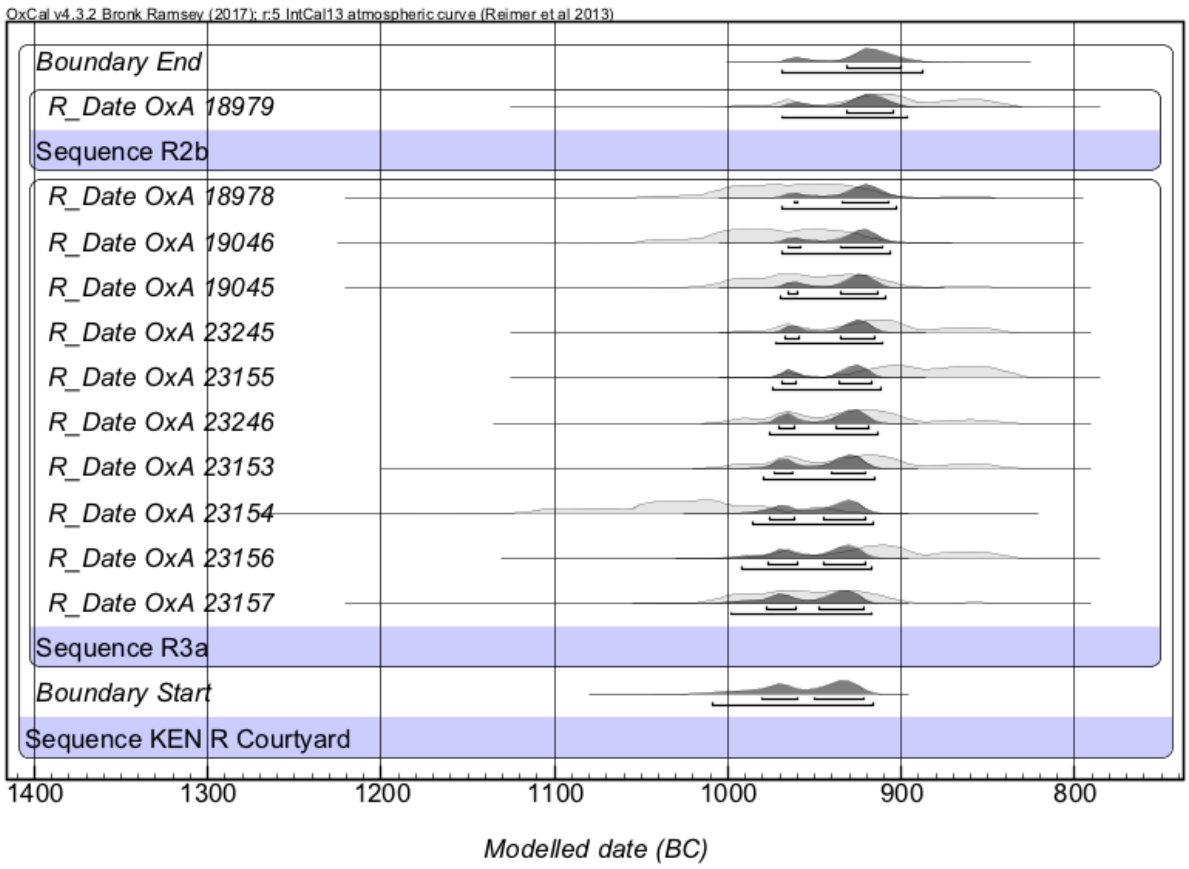


**Figure 4.21:** Modeled radiocarbon dates from the metallurgical complex of Area R at Khirbat en-Nahas. Uncalibrated and calibrated dates are available in Table 4.1 and Levy et al. 2014: 223-228.

#### 4.4.2.7 Area M – Slag Mound Probe

Area M was an excavation into one of the large slag mounds at the site, the first systematic and stratigraphic excavation of a slag mound in the region (Figure 4.22) (Levy et al. 2014: 131-151; Ben-Yosef 2010: 280-328). The goals of the excavation were to investigate the complete stratigraphy of the slag mound, to collect radiocarbon samples to chronologically situate metal production, and to diachronically examine the copper smelting technology at KEN (Levy et al. 2008, 2014: 131; Ben-Yosef 2010: 280). The excavation began in the 2002 season (supervised by E. Monroe) which excavated the initial layers of the mound (ca. 1.2 meters) and

**Figure 4.22:** Area M at Khirbat en-Nahas after excavation. The completed excavation was over six meters in depth. The wall of the structure in Area M is visible on the bottom edge of the photo. Photograph credit: Thomas E. Levy, UCSD Levantine and Cyber Archaeology Lab.

exposed a corner of a structure (Ben-Yosef 2010: 280-281; Levy et al. 2014: 131-136). The excavation continued in 2006 under the supervision of Ben-Yosef (2010: 292-324) and M. Beherec which completed the probe down to bedrock and excavated the entire structure (Levy et al. 2014: 136-149). Both seasons employed rigorous sampling of archaeometallurgical material culture providing the foundation of the current understanding of copper production in Faynan during the Iron Age (Ben-Yosef 2010; Ben-Yosef et al. 2019). Once the excavation was completed, Ben-Yosef (2010: Figures 5.55 and 5.56) sampled the stratigraphic sections for slag samples for additional analyses, many of which were analyzed as part of this dissertation. In turn, the Area M slag mound provides a chronological scaffold for most of the samples analyzed here.

#### 4.4.2.7.1 The 2002 Excavation Season

The 2002 excavation was critical in providing a record of the final phases of copper production at KEN (Levy et al. 2014: 136). The excavation was divided into contexts (essentially equivalent to layers) and further subdivided into horizons which were believed to represent individual smelting cycles (Levy et al. 2014: 131). A new horizon was determined by the appearance of large tap slags; however, the correlation between tap slags and a smelting cycle is tenuous (Levy et al. 2014: 132). In total, three contexts and seven metallurgical horizons were distinguished (Levy et al. 2014: Figures 2.62, Table 2.6, 2.8). Context Ia is only represented by two small stone installations visible on the surface which were likely intrusive and post-date the metallurgical layers (Levy et al. 2014: 132). Context Ib contains the seven metallurgical horizons with the last one being a layer of crushed slag (not necessarily a "smelting cycle") (Levy et al. 2014: 135-136). The other six horizons were characterized by their rich archaeometallurgical remains including tuyère and furnace fragments, slag, and ash (Levy et al. 2014: 135; For detailed descriptions of each metallurgical horizon, see Levy et al. 2014: Table 2.6). Beneath the seventh horizon of crushed slag was a layer of fill based on the limited metallurgical remains and higher concentrations of pottery and bone (Levy et al. 2014: 135).

Context IIb and II were associated with the excavation of the structure. Context IIb represented the occupation surface, and Context II was the collapse inside the room (Levy et al. 2014: 135). The occupation layer was approximately one meter lower than the production horizons, and collapse from the structure was found in the fifth horizon suggesting the room predated the smelting horizons (Context Ib) (Levy et al. 2014: 135). Limited material was excavated from within the structure as only the corner of what was named Room 1 was exposed (Levy et al. 2014: 135-136). Both the exterior of the walls, which faced the slag mound, had

evidence of burning suggesting smelting activities were conducted just outside the building and up to it (Levy et al. 2014: 135). In addition, a compact, reddish sediment possibly decomposed mudbrick was excavated along the walls, perhaps the remains of a layer placed to protect the building from smelting (Levy et al. 2014: 135-146, Figure 2.65). Radiocarbon samples were collected in 2002, and they will be discussed below along with the samples form 2006. In general, the 2002 Area M excavations identified the final production phases at KEN, associated with the most advanced technology represented by large tap slags and tuyère fragments.

#### 4.4.2.7.2 The 2006 Excavation Season

The 2006 excavations continued the slag mound probe to bedrock, fully exposed the structure associated with the corner discovered in 2002 (Structure 1), and partially excavated an adjacent structure (Structure 2) (Levy et al. 2014: 136-151; Ben-Yosef 2010: 292-324). The system of dividing the stratigraphy into contexts and horizons was also abandoned for a more standardized approach of dividing the excavation into layers (Levy et al. 2014: 136, see also Table 4.3). Five major layers were identified in the stratigraphy of the slag mound, and they are discussed below separately from the Structure 1 and 2 excavations which follow.

The bottommost layer of the slag mound (M5) likely represents the earliest occupation at the site as it is founded directly on basal sediments (the transition from Phase 0-1) (Levy et al. 2014: 146, Figure 2.79). Layer M5 is divided into M5a and M5b based on the discovery of two installations that were separated by a thin layer of sediment (Levy et al. 2014: 146). The bottom layer (M5b) consisted of a rectangular installation of flat limestones covered with plaster to form raised edges (Levy et al. 2014: 146, Figure 2.79). The southern side of the installation included a small wall with a plastered corner stone that had the appearance of a horn (similar to four-horned

**Table 4.3:** Complete stratigraphy of the Area M slag mound excavation at Khirbat en-Nahas. Includes correlation between the 2002 and 2006 excavations. Table modeled off of Levy et al. 2014: Table 2.8.

| Complete Stratigraphy of Area M Slag Mound at Khirbat en-Nahas | | |
|---|---|---|
| **2006 Layer** | **2002 Context** | **Description** |
| M1a1 | Ia | Surface slag and installations |
| M1a | Ib | Post building abandonment, Aeolian sediment, some metal production |
| M1b | Ib-IIa | Post building abandonment, wall collapse and Aeolian sediment, some metal production |
| M2a | IIb | Last occupation phases of structures, plastered exterior work area, metal production |
| M2b | IIb | "Slag Mound" leveled, Structures 1 and 2 built |
| M3 | III | Remains of intensive metal production beneath structures |
| M4 | - | Intensive metal production, installation construction, possible abandonment horizon |
| M5a | - | Decommissioning of earliest installation and construction of new installation |
| M5b | - | Earliest site occupation. Installation construction and thin layer of crushed slag |

altars), indicating the installation might have functioned as an altar (Levy et al. 2014: 146, Figure 2.79). The installation in Layer M5a was likely a hearth or oven; it consisted of a circle of stones with ash and bones but no slag (Levy et al. 2014: 146, Figure 2.78). The installation continued into the section preventing a complete exposure (Levy et al. 2014: 146). Limited evidence of metallurgy was found in this earliest layer, but there was crushed slag in the sediments suggesting some metallurgy in the early occupation of the site (Ben-Yosef 2010: 319). To summarize, Layer M5 represents the earliest occupation at KEN with probably some limited metallurgy, perhaps in connection with an altar installation.

Layers M4 and M3 represent horizons of more intense metallurgical production at KEN during the later periods of Phase 1 (Levy et al. 2014: 146). Layer M4 began with an accumulation of crushed slag before transitioning into a layer of compact sediment containing

mud, clay, furnace fragments, and crushed slag (Levy et al. 2014: 146). Atop this dense layer was a thick accumulation of ashy, sandy Aeolian sediment without significant material culture, perhaps representing a brief abandonment of the area at the end of Layer M4 (Levy et al. 2014: 146). Layer M3 is a phase of intense copper smelting beneath Structure 1 (Levy et al. 2014: 146). The entire layer is composed of deposits of metallurgical debris (slag, ash, charcoal, tuyères, furnace fragments, etc.) and stone installations likely connected to copper production (Levy et al. 2014: 146). Some surfaces were also identified which potentially represent an episode of smelting activity prior to more slag being dumped in the area (Ben-Yosef 2010: 316). Layer M3 was truncated and leveled to provide a foundation for Structure 1 and its initial occupation Layer M2b – a distinct surface with a layer of Aeolian dust; this is one of the main identifiers for the transition from Phase 2 to 3 (Levy et al. 2014: 140). Within the structure, Layer M2a represents a second occupation phase (Levy et al. 2014: 139).

From the perspective of the slag mound, Layer M2a represents another significant accumulation of copper smelting waste (Levy et al. 2014: 144-146). Critically, it is in the transition from Layer M3 to M2 that we see the changes to a more sophisticated smelting technology associated with Phase 3 (discussed in Chapter 3, see also Ben-Yosef 2010; Ben-Yosef et al. 2019). The material culture from M2 is almost entirely metallurgical including large tap slags and furnace fragments (Levy et al. 2014: 139). This period of metal production resulted in the accumulation of slag that would later cause the walls of Room 1 to cave in (Levy et al. 2014: 137, 139). The uppermost layers of the slag mound, Layers M1b, M1a, and M1a1, post-date the final occupation of the structure (Levy et al. 2014: 139). Layers M1b and M1a both represent phases of metal production; they are distinguished by the presence of wall collapse with Structure 1 which is considered Layer M1b (Levy et al. 2014: 139, Table 2.8). Layer M1a1

is the surface of the slag mound identifiable by the presence of huge tap slags unique the KEN in Faynan (Levy et al. 2014: 139). From the initial layers above the bedrock sands to the surface, the complete excavation was over six meters in depth.

Briefly returning to the structures of Area M, the exact function of Structure 1 was not clear, but the finds from within the structure were mostly domestic (Levy et al. 2014: 140). Structure 1 was possibly connected to copper smelting based on its proximity to the slag mound and the damaged exterior walls. There were also many ground stone objects in the courtyard of the structure, perhaps related to ore or slag processing (Levy et al. 2014: 140). Structure 1 consisted of three rooms and a courtyard space (Levy et al. 2014: Figure 2.66). Room 1 was fully exposed in the 2006 season revealing an intentionally blocked doorway into the remainder of the structure (Levy et al. 2014: 136-137). The walls of Room 1 were damaged from both fire (as previously mentioned) and the pressure of accumulating slag and production debris on its northeastern and southeastern walls (Levy et al. 2014: 136-137). It seems Room 1 was intentionally sealed after it was damaged and became a dumping space for metallurgical waste (Levy et al. 2014: 137). A beaten earth floor, spindle whorl, and date seeds were excavated from the room, but its function was unclear; Room 1 was removed following its excavation in order to expose the metallurgical layers beneath it (Levy et al. 2014: 140). The other rooms were also fully excavated, but similarly did not provide much indication of the building's function (see Levy et al. 2014: 136-151 for details concerning the excavations of the other rooms). Structure 2 was only partially excavated, but it appeared to be larger than Structure 1 (Levy et al. 2014: 144, Figure 2.66, 2.70). The exact nature of Structure 2 was difficult to determine based on the limited excavations, but the finds suggest it was potentially industrial (Levy et al. 2014: 144-145). It is important to note that Structure 1 was constructed directly on top of a thick accumulation of slag

that was leveled to provide a foundation – Layer M3 (Levy et al. 2008: 16461); this will be discussed further in the Summary section below.

#### 4.4.2.7.3 Absolute Dating

Area M provides a chronological anchor for copper production in Faynan with 24 radiocarbon dates presented in Figure 4.23 and Table 4.1 (Levy et al. 2014: 150-151; Levy et al. 2008). The results indicate that the original occupation at KEN began in the latest phases of the Late Bronze Age and the beginning of the Early Iron Age (Layers M5a and M5b were dated to the 13$^{th}$-12$^{th}$ centuries BCE) (Levy et al. 2014: 151, Figure 2.86, Table 2.9). Layer M4, the first substantial accumulation of copper smelting debris, was dated to the 11$^{th}$ century BCE (Levy et al. 2014: 151). The intense production phase evidenced in Layer M3 was dated to the 10$^{th}$ century BCE, and it was flattened/truncated in the late 10$^{th}$ century BCE (Levy et al. 2014: 151). Layers M2 and M1, the final phases of metal production associated with the most advanced technologies, were dated to the 9$^{th}$ century BCE with copper production stopping at the end of the same century (Levy et al. 2014: 151). In addition, the slag mound was also sampled for geomagnetic archaeointenstiy which further secured the dating of the mound to the Iron Age (briefly mentioned above in the chronology of KAJ; for a full discussion of this method and the results, see Ben-Yosef et al. 2008, 2009; Shaar et al. 2010). To summarize, the Area M slag mound securely situates copper production at KEN between the Late 13$^{th}$/12$^{th}$-9$^{th}$ centuries BCE.

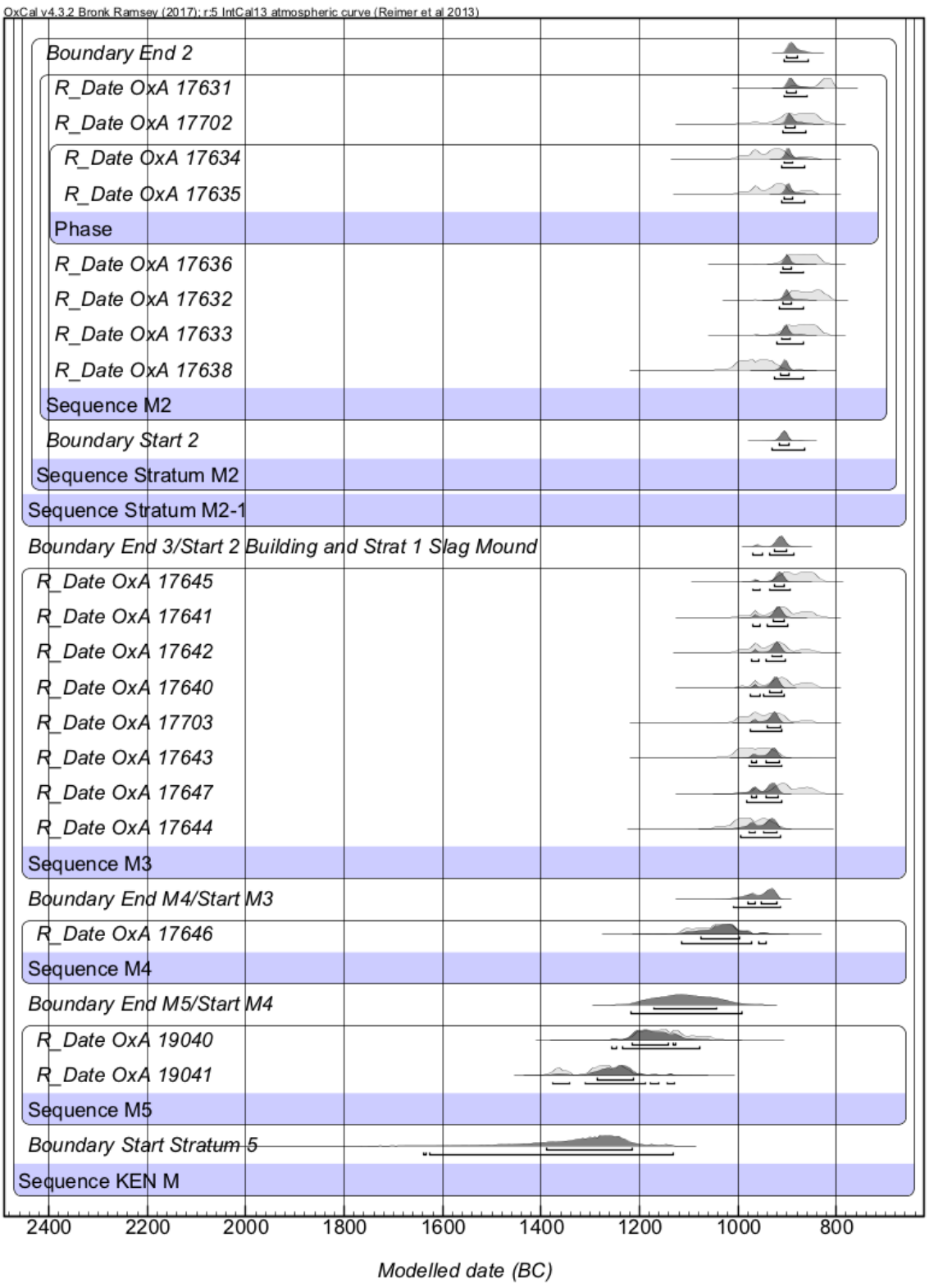


**Figure 4.23:** Modeled radiocarbon dates from Khirbat en-Nahas Area M. Uncalibrated and calibrated dates are available in Table 4.1 and Levy et al. 2014: 150-151.

#### 4.4.2.7.3 Summary

Khirbat en-Nahas provides critical insight into understanding the development and trajectory of copper smelting during the Iron Age in Faynan. Not only is KEN the largest Iron Age smelting site in the region, but its occupation also spans the entire duration of copper production during the Iron Age. The Area M slag mound provides a continuous sequence of metal production debris concretely dated with absolute methodologies. While copper production was likely modest and opportunistic in its earliest stages (as seen by the limited crushed slag at in Layer M5 – Phase 1), the industry at KEN continually developed (Phase 2) with the most sophisticated copper smelting technologies only apparent here (Phase 3) in the 10$^{th}$-9$^{th}$ centuries BCE (the large tuyères and tap slags are lacking from other Iron Age smelting sites like KAJ and Khirbat al-Ghuwayba) (Ben-Yosef 2010; Ben-Yosef et al. 2019). This transition to an advanced technology was also associated with the leveling of the slag mound in Area M and the architectural reorganization of Area A, possibly attributed to the campaigns of Sheshonq I. In the final stages of copper production at KEN, Area F seems to have functioned as a recycling/melting workshop, interestingly located within the walls of the fortress, possibly as an expression of control over this specialized metallurgy (Ben-Yosef 2010: 334). The main occupation of Area S is also dated to the 10$^{th}$ century BCE when it was likely dedicated to slag processing; however, these excavations also discovered iron objects and mixed copper-iron chunks (discussed further in Chapter 5). Area W, which has slightly less secure dating, probably functioned as a storage complex and possible cultic area for the inhabitants of KEN during this period. While KEN reached its metallurgical and architectural zenith in the 10$^{th}$-9$^{th}$ centuries BCE, it is important to note that all the excavated structures were founded on layers of metallurgical debris and/or crushed slag, reiterating the continuity of copper production through

the Iron Age (Levy et al. 2014: Table 2.1). In following, these excavations have come to play a significant role in historical reconstructions of the Iron Age Levant and are continually debated (see Chapters 1 and 3, e.g., Ben-Yosef 2019; Ben-Yosef et al. 2019; Maeir 2021; Tebes 2021; Bienkowski 2021; Finkelstein 2020). The excavations at KEN play a critical role in this dissertation as the iron materials from Areas R and S and the copper slags from Areas M, R, and F were analyzed here (discussed in the follow chapters).

## 4.5 Khirbat al-Ghuwayba

Khirbat al-Ghuwayba (KAG) is a ca. seven hectare Iron Age smelting site located about four kilometers east of KEN and approximately 2.5 kilometers southeast from KAJ (Figure 4.24) (Ben-Yosef 2010: 430-450; Ben-Yosef, Najjar, and Levy 2014a: 840-850). Despite its relatively large size, the site is composed of somewhat limited archaeological material including some architectural collapse and thin scatters of broken slag, stretching across both sides of the Wadi Ghuwayba al-Ghani (Ben-Yosef 2010: 432). Khirbat al-Ghuwayba is also located adjacent to a perennial spring, ‘Ain al-Ghuwayba, which supports the growth of fruit trees as seen by the modern Bedouin orchards (Ben-Yosef 2010: 432; Ben-Yosef, Najjar, and Levy 2014a: Figure 12.29; Glueck 1935: 164). The archaeological site was first reported and drawn by Glueck (1935: 22-23, 164; 1940a: 61) who characterized KAG as an Early Iron Age smelting center based on ceramics, though he also identified some Nabatean sherds. Subsequently, KAG was surveyed by McDonald (1992: 76) who dated the site to the Early Iron Age based on pottery, Hauptmann (2007:132-133), and Ben-Yosef (Ben-Yosef, Najjar, and Levy 2014b: 525) prior to the first stratigraphic excavations by ELRAP.

**Figure 4.24:** Aerial photograph of Khirbat al-Ghuwayba. The ELRAP excavations are visible in the center of the photo. Note the substantial vegetation in the wadi as a result of the perennial spring, ‘Ain al-Ghuwayba, and also the limited amount of slag in comparison to Khirbat en-Nahas and Khirbat al-Jariya. Photograph credit: Dr. Robert Bewley, APAAME 2015 (APAAME_20151013_RHB-0127).

The ELRAP completed a limited excavation at KAG during the 2009 season, also under the field supervision of Ben-Yosef (2010: 430-450). The excavations focused on a small structure and a probe into one of the more significant accumulations of slag at the site in order to investigate the copper production technology and the relationship between the structure and the slag (Ben-Yosef 2010: 432). The site was also remapped (topographic and architectural) and dated using two radiocarbon dates in conjunction with the technical ceramics and pottery (discussed below, Ben-Yosef 2010: Figure 5.100). Based on the mapping, most of the archaeological features are on the northern bank of the wadi, and the slag scatters are not directly associated with substantial architecture (Ben-Yosef 2010: 433). There were also some smaller installations on the southern bank of the wadi (though not mapped) and the spring is located between the banks (Ben-Yosef 2010: 433, Figure 5.100; Glueck 1935: 164).

The excavation of the small structure revealed a room and exposed a floor surface containing hearths and some small finds (Ben-Yosef 2010: 435). Based on the pottery, a large amount of glass, and a playing die, the floor and the structure more generally were dated to the Roman-Nabatean periods (Ben-Yosef 2010: 435). A probe was excavated in a corner of the building to check the relationship between the wall foundations and the floor; some copper production debris were discovered beneath the floor (Ben-Yosef, Najjar, and Levy 2014a: 842). A second probe outside of the building excavated to basal sediments also found a thin layer of copper production remains (mostly crushed slag), indicating that there was a distinct layer of metallurgical debris beneath the structure which was dated to the Iron Age (Ben-Yosef 2010: Figure 5.108; Ben-Yosef, Najjar, and Levy 2014a: 842). The excavation continued to the south of the structure into a dense accumulation of metallurgical debris (Ben-Yosef, Najjar, and Levy 2014a: 842-846). The excavation discovered limited metallurgical remains just above the basal wadi sediments (Ben-Yosef, Najjar, and Levy 2014a: 845). The sparse layer was topped with a richer accumulation of copper production remains including slag, tuyère fragments, hammer stones, pottery, and charcoal (Ben-Yosef, Najjar, and Levy 2014a: 845-846). Above this layer of metallurgical material was an additional layer of copper production debris along with three stone installations (Ben-Yosef, Najjar, and Levy 2014a: 843-845, Figure 12.62). The function of the installations, two of which were circular and appeared to be filled with metallurgical material such as crushed slag, was not clear from the excavations (Ben-Yosef, Najjar, and Levy 2014a: 843-845). Finally, the uppermost layers of the metallurgical deposit included layers of dust and the surface slag scatter (Ben-Yosef, Najjar, and Levy 2014a: 842-843). In total, the excavation was just over one meter from the surface to the basal sediments (based on Ben-Yosef, Najjar, and Levy 2014a: Figure 12.64), a shallow “slag mound” in comparison to KAJ and KEN.

The two charcoal samples collected from the metallurgical remains for radiocarbon analysis yielded dates of 1192-1051 BCE and 1608-1526 BCE with 68.2% probability (Ben-Yosef 2010: 447-448). While only one of these dates fits the Early Iron Age, the ceramics and archaeometallurgical assemblage, both of which share typological similarities with KAJ, reiterate an Early Iron Age date for copper production at KAG, situating the site within Production Phase 1 (Ben-Yosef, Najjar, and Levy 2014a: 848; Ben-Yosef 2019: Figure 5). The limited amount of slag in comparison to KAJ and KEN suggests the site was producing copper on a much smaller scale (Figure 4.24) (Ben-Yosef, Najjar, and Levy 2014a: 849-850). However, the paleobotanical and anthracological data from the 2014 season at KAJ help to frame KAG in a regional context as part of an interconnected industrial landscape. While KAG might not have been a substantial smelting center, it potentially served an additional function of controlling the spring and growing fruit trees (Liss et al. 2020: 423-425). Evidence of fruits and cultivated fruit trees in the archaeological record at KAJ indicates that subsistence for workers at the site likely depended on a provisioning network operating on a regional scale. The nearest area capable of growing such trees would be around ʻAin al-Ghuwayba and KAG. Thus, the settlements of KAJ and KAG, with comparable dating and material culture, are likely two components of an organized network centered at KEN in Production Phase 1 and possibly Phase 2 (further dating is required). These three sites are also interconnected by wadis and within four kilometers of each other, facilitating movement between them (Figure 4.1). As such, KAG may have served a dual purpose as a small-scale smelting site and a provisioning center moving fruits, wood, and water along the wadis to the other smelting sites. It is interesting to note that during his visit to KEN, Glueck (1935: 29) acknowledged the lack of available water and said, “We were compelled to send for

water to ‘Ain el-Gheweibeh” and further suggested that “…water being brought to various camps must also be borne in mind” in reference to the Iron Age.

Slag samples from KAG were not included in the analysis for this dissertation as the slag mound excavation was shallow and limited in its absolute dating. In the future, additional excavations and radiocarbon sampling from the site could make it a valuable comparative dataset. It would be particularly interesting to examine potential differences in smelting technologies based on the relatively small scale of production at the site. However, KAG still plays an important role in this dissertation as it contributes to current understandings of the trajectory of Iron Age society in Faynan. The development of the site and its connections to KAJ and KEN are critical to consider in construction the adaptive cycle of Iron Age Faynan.

## 4.6 Other Iron Age Sites in Faynan

There are many other Iron Age sites in Faynan that have only been the focus of limited investigation or play a smaller role in this dissertation, and as such, will only be briefly summarized here. This is not an extensive list, but it covers the major sites relevant here. Not all these sites functioned as smelting centers or metallurgical sites, but they were likely connected to the copper production industry in Faynan in various ways, as will be discussed. For a complete list of all known Iron Age sites surveyed in Faynan with descriptions, see Ben-Yosef 2010: Table 5.1 and Ben-Yosef, Najjar, and Levy 2014a.

### 4.6.1 Khirbat Faynan

Khirbat Faynan (KF) is primarily known as the largest Roman-Byzantine copper smelting site in Faynan, but there is also evidence for an Iron Age presence (Figure 4.25) (Barker et al.

**Figure 4.25:** Aerial photograph of Khirbat Faynan. The substantial tel site (center) is primarily known as the largest Roman-Byzantine copper smelting site in Faynan but includes Iron Age slag mounds. The archaeological remains extend on both sides of the Wadi Faynan. Photograph credit: Dr. Robert Bewley, APAAME 2015 (APAAME_20151013_RHB-0032).

1997, 2007; Mattingly et al. 2007; Hauptmann 2007: 94-110). Located about eight kilometers southeast of KEN as the crow flies, KF and associated archaeological remains including agricultural fields and slag mounds span both sides of the Wadi Faynan (Hauptmann 2007: 94-110). The site and its surroundings were surveyed by the early explorers/researchers in the region (Glueck 1935: 32-33; Musil 1907) as well as by Hauptmann (2007: 94-110), and it has since been a primary research focus for Graeme Barker and the Centre for British Research in the Levant (Barker et al. 1997, 2007). These projects assigned unique site identifiers to the archaeological features around KF such as slag mounds; however, contemporaneous features were all likely part of an associated archaeological complex centered at KF (Hauptmann 2007: 94-110; Ben-Yosef 2010: Table 5.1). For example, slag mounds identified as sites Faynan 3, 4,

5, 7, and 14 and all date to the Iron Age along with some agricultural terraces (Mattingly et al 2007; Knabb et al. 2016). However, identifying an Iron Age settlement/site at KF itself is difficult due to it being a tel; much of the Iron Age is probably covered by the later periods of habitation.

The slag mounds around KF were dated using ceramic and slag typologies, technical ceramics, as well as a few radiocarbon dates (Hauptmann 2007: 97-103). Of particular interest here is Faynan 5, a large slag mound to the east of KF (Hauptmann 2007: 97; for complete descriptions of the other Iron Age slag mounds see Hauptmann 2007: 94-110 and Ben-Yosef 2010: Table 5.1). The Faynan 5 slag mound was dated based on pottery and three radiocarbon dates to the $10^{th}$-$9^{th}$ centuries BCE, overlapping with the period of peak production at KEN (Phase 2-3) (Hauptmann 2007: 97). Hauptmann (2007: 97-98) estimated Faynan 5 contains as much as 30,000 tons of slag, and he suggested it is part of a larger production center including mounds Faynan 3, 4, and 7; this would make Faynan 5/KF the second largest Iron Age copper smelting center following KEN. However, as Hauptmann points out (2007: 97), a complete understanding of Iron Age KF and the slag mounds requires additional excavation. Further research is especially warranted following Ben-Yosef's (2010: 338) discovery that slag mounds can contain 40% or less of actual slag. Regardless, KF likely functioned as a significant copper smelting site in the Iron Age.

### 4.6.2 Khirbat Hamra Ifdan

To the southwest of KEN along the Wadi Fidan is a primarily Early Bronze Age metallurgical site called Khirbat Hamra Ifdan (KHI) (Figure 4.26). Located on a defensive plateau, the site was visited/reported by some of the various projects described above (Levy et al.

**Figure 4.26:** Aerial photograph of Khirbat Hamra Ifdan. The site is located atop an inselberg in the Wadi Fidan. Photograph credit: Rebecca Banks, APAAME 2015 (APAAME_20151013_REB-0040).

2002 and citations there within; Raikes 1980: “Site F”; Hauptmann 2007: 134-136) identifying architecture and slag mounds before being excavated for the first time by Russell Adams (1992, 1999; see also Friedman et al. 2020). Khirbat Hamra Ifdan was systematically excavated as part of the JHFP which secured the site’s identification as the largest Early Bronze Age copper manufactory in the region (Levy et al. 2002; Gidding and Levy 2020). While excavations and radiocarbon dates confirmed an Early Bronze Age settlement at the site (Levy et al. 2002), Hauptmann (2007: 134-136) also described the presence of Iron Age slag typologies. The ELRAP continued excavations at KHI in 2007 to both further investigate the Early Bronze Age remains and to probe one of the large slag mounds at the site (Area E) for a possible Iron Age

presence (Ben-Yosef, Najjar, and Levy 2014a: 850-856). Along with excavating the slag mound, samples were collected for an archaeomagnetic intensity study to further refine its chronology.

The slag mound probe began at the highest point of the mound and continued down to the local bedrock (Ben-Yosef, Najjar, and Levy 2014a: 850-853, Table 12.10). The only architecture discovered was directly above basal sediments and dated to the Early Bronze Age III (Ben-Yosef, Najjar, and Levy 2014a: 852). Following a possible brief abandonment identifiable by a fill, excavations discovered a crushed slag layer which was similarly followed by a possible abandonment (Ben-Yosef, Najjar, and Levy 2014a: Table. 12.10). A final layer of large tap slags with abundant charcoal representing the main smelting phase was excavated just beneath the surface; the total depth of the excavation was just over one meter (Ben-Yosef, Najjar, and Levy 2014a: 852). The archaeointensity results indicated an Iron Age date for the slags from Area E (Ben-Yosef, Najjar, and Levy 2014a: 855; Ben-Yosef 2010: 460-464; Ben-Yosef et al. 2016). In conjunction with some pottery evidence and the tap slags which are unique to the Iron Age, the slag mound was dated to the $12^{th}$-$10^{th}$ centuries BCE (Phases 1-2). As such, the slag layers were interpreted as two smelting phases, not associated with substantial architecture (Ben-Yosef, Najjar, and Levy 2014a: 855). Thus, during the Iron Age, it seems KHI functioned as a small-scale smelting site. Slag samples from KHI were not analyzed here to avoid any potential problems with mixing of Early Bronze Age and Iron Age contexts; all sites analyzed were single context, Iron Age sites. Careful selection of Iron Age samples from KHI dated either through archaeomagnetism or radiocarbon of embedded charcoal would be worth pursuing in the future.

4.6.3 The Ras al-Miyah Fortresses and Archaeological Complex

Located in the cliffs above KAG to the north and northeast are the Ras al-Miyah (RAM) Fortresses and the Ras al-Miyah archaeological complex (Figure 4.27) (Ben-Yosef, Najjar, and Levy 2014a: 816-840; Ben-Yosef, Levy, and Najjar 2009a).

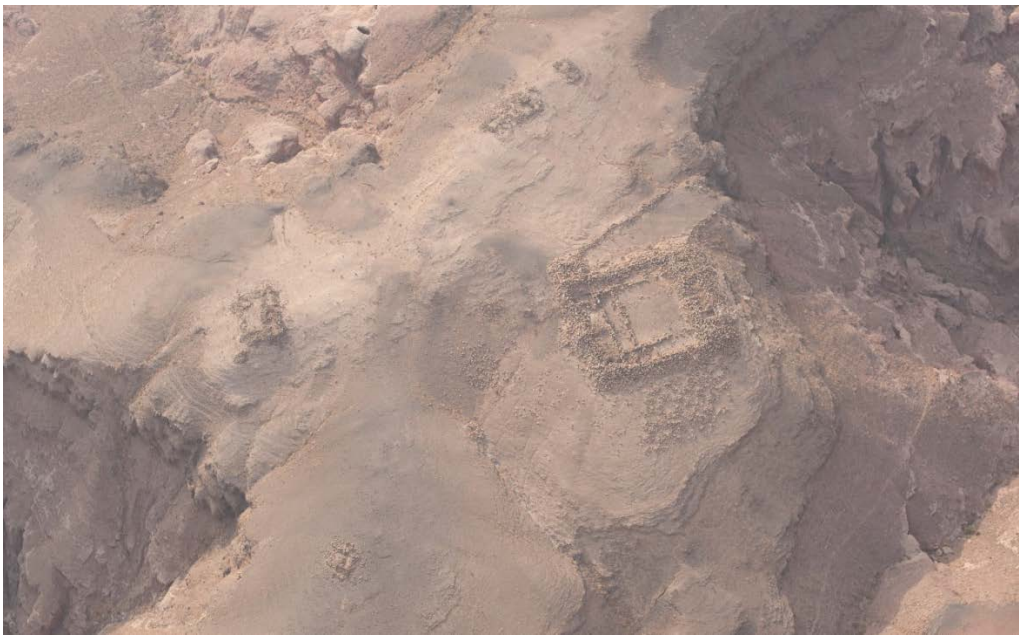

**Figure 4.27:** Aerial photograph of the Ras al-Miyah fortresses (center) and archaeological complex. Photograph credit: Dr. Robert Bewley, APAAME 2015 (APAAME_20151013_RHB-0134).

The two fortresses, which are associated with other archaeological remains making a kind of complex, were identified by Hauptmann (2007: 132) and the GMM team who suggested they were intended to control the primary route between Faynan and the Edomite Plateau along the Wadi al-Ghuwayba as well as the nearby mines (Weisgerber 2006: 13; Ben-Yosef, Najjar, and Levy 2014a: 816). The RAM fortresses and the surrounding area were subsequently surveyed in detail as part of ELRAP by Ben-Yosef (Ben-Yosef, Najjar, and Levy 2014b: 514-520; Ben-Yosef, Levy, and Najjar 2009a) and small probes were excavated into the eastern fortress (Ben-Yosef, Najjar, and Levy 2014a: 816). The surveys revealed dense collections of ceramics

associated with the fortresses and the other archaeological features in the area; interestingly, the ceramic typologies were distinct from those found at smelting sites in Faynan and were typical Edomite forms of the Iron Age IIB-C – the 7th-6th centuries BCE (Phase 4) (Ben-Yosef, Najjar, and Levy 2014a: 816). Given that the mines near the RAM complex are the closest to Busayra in the highlands, the fortresses could have controlled these mines and the main road during a Late Iron Age smelting phase in Faynan (Ben-Yosef, Najjar, and Levy 2014a: 816-817). Based on their proximity, it was originally thought that KAG might have functioned as the primary smelting center associated with the RAM fortresses and mines; given the new dating of KAG to the Early Iron Age, however, this idea has been dismissed and evidence for any smelting during this period in Faynan is currently lacking (Ben-Yosef, Najjar, and Levy 2014a: 816, 836-837). The other architectural features around the fortresses potentially provided housing or other functions for the Iron Age miners or builders working on the fortress (Ben-Yosef, Najjar, and Levy 2014a: 833-834).

The ELRAP excavations at RAM included two probes in the eastern fortress (42x35 meters) investigating one of the chambers of the casemate wall around the fortress and the corridor entrance (Ben-Yosef, Najjar, and Levy 2014a: 830-835, Figure 12.41). Critically, the excavations seemed to indicate the construction of the fortress was never completed based on several lines of evidence including an unfinished water system, unfinished filling and fortifications in the casemate walls, incomplete divisions of casemate walls, massive foundations with only small superstructure walls, and a complete lack of a significant occupation layer (Ben-Yosef, Najjar, and Levy 2014a: 833). In summary, the RAM fortresses (one of which was incomplete) represent a 7th-6th century BCE occupation in Faynan associated with intensive mining activities, but currently lack any contemporaneous smelting sites. In following, they

potentially provide support for the claim by Weisgerber (2006: 15) that copper production in Late Iron Age Faynan was a failed endeavor (Ben-Yosef, Najjar, and Levy 2014a: 836-837). This idea will be further discussed in Chapter 7.

#### 4.6.4 Rujm Hamra Ifdan

Rujm Hamra Ifdan (RHI) is a small site about five kilometers to the southwest of KEN on the northern bank of the Wadi Fidan (Smith, Najjar, and Levy 2014: 724). Located on an elevated conglomerate, RHI provides a look-out point at the junction of Wadi Fidan and a secondary drainage that provides access to the Wadi al-Ghuwayba (which leads to KEN, KAG, and the Wadi al-Jariya/KAJ) (Smith, Najjar, and Levy 2014: 724, Figure 10.16). Based on its strategic location, the site is believed to have been a watchtower (as suggested by Glueck) or small habitation intended to monitor the entrance to the main copper smelting sites and mines along the wadis (Smith, Najjar, and Levy 2014: 725, Figure 10.16). The site was first surveyed by Glueck (1935: 20-22), but there was initially some confusion in his reports; he seems to have conflated his descriptions of RHI and KHI (Adams 1992; Smith, Najjar, and Levy 2014: 724). Glueck (1935: 20) reported arriving at "Rujm Hamra Ifdan…a small ruined watch tower…on the south bank of the Wadi Ifdan [Fidan]" which he believed to be Nabatean. However, RHI is located on the northern side of the wadi. He precedes to describe another site, "Khirbat Hamra Ifdan", but the description is more in line with RHI. For example, when describing KHI, Glueck (1935: 21) says "No slag was found", but slag is visible on the surface of KHI to this day (Adams 1992: 180-181). Perhaps most revealing of Glueck confusing the two sites is his drawing of "Khirbat Hamra Ifdan" which depicts a site similar in shape and location to RHI – on the *northern* bank of the Wadi Fidan (Glueck 1935: 163; Adams 1992: 180-181). In following, RHI

was referred to as “Glueck’s Khirbet Hamra Ifdan” in subsequent surveys (MacDonald 1992) until excavations by ELRAP in 2004 when the site was renamed Rujm Hamra Ifdan (Smith, Najjar, and Levy 2014: 724).

The ELRAP excavations at RHI included two soundings, one at the summit of the site and another on the lower slopes, with the goal of testing Glueck’s suggestion that it was a watchtower (Figure 4.28) (Smith, Najjar, and Levy 2014: 725). Together, the probes revealed a large wall encircling the site, a sampling of pottery and radiocarbon dates, and some small-scale metallurgy (Smith, Najjar, and Levy 2014: 725-726). Both the radiocarbon dates (n=5) and the pottery indicated two phases at the site; an initial occupation in the 10$^{th}$-9$^{th}$ centuries BCE and a second phase in the 7$^{th}$-6$^{th}$ centuries BCE (Smith, Najjar, and Levy 2014: 735). The excavations at the summit revealed a small habitation area dated to the 10$^{th}$-9$^{th}$ century BCE, perhaps functioning as a form of look-out or watchtower, which is potentially reiterated by the view shed analysis (Smith, Najjar, and Levy 2014: 736-737, Figure 10.16). The soundings at the bottom of the slopes revealed domestic rubbish and a larger settlement dated to the 7$^{th}$-6$^{th}$ centuries BCE (Smith, Najjar, and Levy 2014: 736). While the excavations were limited, they identified the only known site in the lowlands with habitation in both the Iron IIA and Iron IIB-C[2] (Smith, Najjar, and Levy 2014: 7237-738). As such, RHI plays an important role in investigating the development of ceramics and social transformations in the region during the peak in habitation in both the lowlands and highlands of Edom (Smith, Goren, and Levy 2014). The 10$^{th}$-9$^{th}$ century BCE occupation phase was likely intended to provide additional control over access to the copper ores.

[2] Khirbat Faynan may also have a complete Iron Age sequence, but this requires further investigation (Ben-Yosef 2010: Table 5.1).

**Figure 4.28:** Completed excavations at Rujm Hamra Ifdan. The completed lower probe is visible in the bottom right. Photograph credit: Thomas E. Levy, UCSD Levantine and Cyber Archaeology Lab.

4.6.5 Wadi Fidan 40

Wadi Fidan 40 (WF40) is an Iron Age cemetery site in Faynan covering an area of ca. 3450 square meters with an estimated 1300 individual graves (Figure 4.29) (Beherec, Najjar, and Levy 2014: 678; Beherec 2011). The site was surveyed by Raikes (1980: "Wadi Fidan Gorge Site D"), MacDonald (1992: "Site 14"), and Adams (1991: "Wadi Fidan Site 009") prior to being excavated by the Wadi Fidan Project (Adams 1991), JHFP (Levy, Adams, and Najjar 2001), and ELRAP (Beherec, Najjar, and Levy 2014). Wadi Fidan 40 is approximately six kilometers west of KEN at the entrance of the Wadi Fidan, and it is characterized entirely by its mortuary features, lacking any other extant archaeological remains or architecture (Beherec, Najjar, and Levy 2014: 665). In total, over 400 grave features (including 245 cist graves) were excavated as

**Figure 4.29:** Aerial photograph of Wadi Fidan 40 cemetery located along the Wadi Fidan (top of photo). Photograph credit: Rebecca Banks, APAAME 2015 (APAAME_20151013_REB-0058).

part of the JHFP and ELRAP (Beherec, Najjar, and Levy 2014; Levy, Adams, and Shafiq 1999). Based on eight radiocarbon dates and artifact typologies, WF40 was dated to the 11$^{th}$-9$^{th}$ centuries BCE (Beherec, Najjar, and Levy 2014: 678). Research at the site did not identify material culture directly representative of an "Edomite ethnicity", but the consistency in burial structures suggests use by a single population which in combination with its location and dating suggests it is an Iron Age Edomite cemetery (Beherec 2011: 1415; Beherec, Najjar, and Levy 2014). Moreover, the distribution of wealth objects (varying greatly with potentially competing familial lines) reaffirmed that Iron Age Edom was likely a chiefdom of pastoral nomads (Beherec 2011: 1399-1400). Finally, recent isotope analysis of human remains excavated at the

site suggest at least some of the interred population was involved in the copper smelting industry (Beherec et al. 2016). Additionally, some iron objects including a bracelet and a ring were found in some of the excavated graves, but it was a rare metal only found in graves associated with other wealth objects and a unique burial position (extended body) (Beherec, Najjar, and Levy 2014: 687). These iron finds will be touched on in Chapters 5 and 7. Generally, WF40 likely served a dual function as a cemetery for the populations of Iron Age Faynan and possibly also as an ethnic and territorial marker.

#### 4.6.6 Wadi Dana 1

Wadi Dana 1 is a smelting site based on the identification of slag scatters and heaps in the Northwest Cemetery of KF (Hauptmann 2007: 122; Ben-Yosef 2010: Table. 5.1). The site was surveyed by Hauptmann (2007: 120-122) who dated it to the Late Bronze Age based on the small tuyères and its proximity to a mine, Wadi Kahlid 42, also dated to the Late Bronze Age by radiocarbon (a wood sample from the backfill). However, Ben-Yosef (2010: 191, Table 5.1) suggests the site might also be dated to the Iron Age as his research determined that small tuyères were also used in the Early Iron Age – $12^{th}$-$10^{th}$ centuries BCE. Further research is needed at Wadi Dana 1, but it is included here as it may represent Late Bronze Age activity in Faynan, and possibly a continuation into the Early Iron Age.

#### 4.6.7 Ras en-Naqb and Barqa el-Hetiye

Ras en-Naqb and Barqa el-Hetiye are two sites primarily dated to the Early Bronze Age, but also containing evidence of Iron Age smelting activity (Hauptmann 2007: 123-136, 141-143; Ben-Yosef 2010: Table 5.1). Ras en-Naqb is a small site located roughly between KEN and KF

along the route connecting them (Hauptmann 2007: 123-126). A slag mound there was dated to the Early Bronze Age based on the technical ceramics and a radiocarbon sample. However, a previously bulldozed slag mound was dated to the Iron Age II based on pottery and slag typologies; Hauptmann (2007: 123) suggests the Early Bronze Age slag was reprocessed to extract copper during the Iron Age. This understanding is further reiterated by the cup marks in the local bedrock, similar to those seen at KAJ, which were likely used for slag crushing (Hauptmann 2007: 124, Figure 5.30). The collected copper was subsequently remelted, producing the Iron Age slag mound. Barqa el-Hetiye was an Early Bronze smelting settlement where ingots were produced, similar to KHI, located about 10 kilometers southwest of KEN (somewhat distant from other smelting sites and ore sources) (Hauptmann 2007: 141-143). The site was excavated by Fritz in the early 1990s revealing four houses and copper production remains despite erosion by shifting sand dunes (Hauptmann 2007: 142). Two of the houses were excavated; one house dated to the Early Bronze Age based on pottery and radiocarbon dating, and the other was considered Iron Age I based on pottery (Hauptmann 2007: 142). These sites, along with KHI, provide important evidence of reusing the Early Bronze Age copper smelting infrastructure in the Iron Age.

## 4.7 Relevant Mining Sites

While ancient mines are notoriously difficult to interpret and date due to a lack of material culture and destruction by later industrial activities (Craddock 1995: 8-11; Stöllner 2014: 151), there is significant evidence of Iron Age mining activities in Faynan aside from the smelting centers (see Hauptmann 2007; Knabb et al. 2014a; Ben-Yosef, Najjar, and Levy 2014b; Ben-Yosef, Levy, and Najjar 2009b for detailed descriptions of the Iron Age mining sites in

Faynan). Various surveys have documented mining camps and sites based on identifiable shafts and tailing piles, and some have been dated to the Iron Age based on pottery and occasionally radiocarbon (Hauptmann 2007: 85-156; Levy et al. 2003; Knabb et al. 2014a; Ben-Yosef, Najjar, and Levy 2014b). This dissertation is primarily concerned with two mining areas within Faynan: the Jabal al-Jariya Mine Fields and the El-Furn Mines.

During surveys of the region in 2007, Ben-Yosef investigated a valley plane of about 30 hectares nestled among the Jabal al-Jariya mountains approximately 1.5 kilometers north of KEN (Ben-Yosef, Levy, and Najjar 2009b). Within the valley there were hundreds of plate-like depressions of about seven meters in diameter on average that Ben-Yosef identified to be blocked pit mines - the Jabal al-Jariya (JAJ) Mine Fields (Figure 4.30) (Ben-Yosef, Levy, and Najjar 2009b: 98). Three fields of the blocked pit mines were identified – JAJ 1 (the largest), 2, and 3 – along with some associated architectural remains likely for miners and/or controlling the mines (Ben-Yosef, Levy, and Najjar 2009b: 99; Ben-Yosef, Najjar, and Levy 2014a: Figure 12.78). The JAJ mines were initially dated to the Iron Age based on their proximity to KEN and KAJ, and a small excavation in 2009 tested this dating (Ben-Yosef, Levy, and Najjar 2009b: 99; Ben-Yosef 2010: 466-499; Ben-Yosef, Najjar, and Levy 2014a: 856-874). The excavations focused on one of the well-defined pits at JAJ 1 and included sample collection for optically stimulated luminescence (OSL) dating (Ben-Yosef, Najjar, and Levy 2014a: 864-874). Excavations yielded almost no material culture and only limited ore that appeared to be of an exceptionally high quality (Ben-Yosef, Najjar, and Levy 2014a: 864-871). Five OSL dating samples, which along with the stratigraphy and field observations, indicated an Early Iron Age date, but further research is required (Ben-Yosef, Najjar, and Levy 2014a: 871-874).

**Figure 4.30:** Photograph of the Jabal al-Jariya Minefields. The depressions across the landscape are the remains of ancient mining pits. Photograph credit: Erez Ben-Yosef, UCSD Levantine and Cyber Archaeology Lab.

Critically, the small amount of ore found in surveys and excavation at JAJ 1 led Ben-Yosef (2010: 471) to conclude that the mines were completely exhausted in antiquity.

Mines that could be possible sources of iron are also of particular interest for this research. While there are reports of iron ores found around the region (Glueck 1936b), direct iron metallurgy currently seems unlikely in Faynan (discussed further in Chapter 5). Rather, it is more probable that a copper ore with a high iron content could result in an iron-rich furnace charge. Thus, mining sites associated with iron-rich ores are important to consider. Two copper mines near KEN were discovered to contain enriched iron contents, named the El-Furn mines by

Hauptmann (2007: 71). These two clusters of mines, subsequently designated WAG 57 and WAG 58 by Knabb et al. (2014a: 603), were surveyed for material culture, and WAG 58 contained only Iron Age pottery suggesting activity during this period. However, it is likely they also served as an ore source during the Islamic period based on their proximity to the Middle Islamic smelting site, Khirbat Nuqayb al-Asaymir, also known as El-Furn (Knabb et al. 2014a: 603; Jones, Levy, and Najjar 2012: 74; Hauptmann 2007: 126-127). It is possible this later mining destroyed the record from previous periods, particularly at WAG 57 where only one pottery sherd was discovered and tentatively dated to the Islamic period (Jones, Levy, and Najjar 2012: 74). Based on the material culture (although limited) and location, Iron Age mining at these iron-enriched mines seems probable and potentially provided the iron discovered in the mix chunks at KEN. As such, two ore samples collected from these mines were included in the isotope analysis for this dissertation (discussed further in Chapter 5).

## 4.8 Summary/Discussion

Based on all the excavation and survey projects, it is possible to describe a general timeline of events and developments for Iron Age Faynan. While the "phases of production" were already described in Chapter 3, this summary will integrate the sites and excavation areas not mentioned there, include the new results from KAJ, and include sites not directly related to copper smelting. In general, the evidence for early copper production at the beginning of the end of the Late Bronze and Early Iron Ages is only present at KEN and potentially Wadi Dana 1. The bottommost layers of the Area M slag mound are dated to the Late Bronze-Early Iron Age, representing an early and opportunistic period of production (a possible Phase 0 and the beginning of Phase 1 in the 13$^{th}$-12$^{th}$ centuries BCE). Copper production continues at KEN into

the 12th-11th century BCE with increased evidence for smelting in Area M (Layer M4). During the 11th century BCE, KAJ was established as an additional smelting center as evidenced by the crushed slag at the bottom of the Areas A and C slag mounds, likely to access the mines of the Wadi al-Jariya and potentially also the Jabal al-Jariya Mine Fields (Phase 1). The dating of the Area B structure and the significant accumulation of crushed slag at the bottom of Area C at KAJ suggests a rapid development with early and substantial architecture. As such, KAJ was likely an organized expansion of the growing industry at KEN; this is reiterated by similarities in the *chaîne opértoire*. While the dating is less secure, KAG was likely also built in the 11th century BCE to control the spring, grow fruit trees, and perform small-scale smelting. At this point, there was likely a regional network in Faynan, centered at KEN with additional smelting at KAJ and provisioning from KAG (Phase 1). As the industry grew, the WF40 cemetery site was established at the entrance of the Wadi Fidan in the 11th century BCE possibly as a territorial marker. Finally, remaining Early Bronze Age sites and slag were repurposed during this period for additional copper smelting as seen at KHI, Ras en-Naqb, and Barqa el-Hetiye.

As the copper industry continued to develop, the local inhabitants invested further in the smelting sites. In the 10th century BCE, the fortress and Area A gatehouse were built at KEN along with elite architecture such as Areas R and T (Phase 2). Copper smelting also intensified as seen in the Area M slag mound (Layer M3) at KEN and the Area C slag mound at KAJ (Layer C2a). It is possible that KAG was abandoned at this time for the more defensible centers at KAJ and KEN, but further research is required, and this seems unlikely given ‘Ain al-Ghuwayba would be an important water source. Copper production continued at KEN and KAJ into the 10th century BCE until a disruption event identified in the Area M slag mound (flattened and construction of the structure), Area A gatehouse (decommissioned, reorganized, and blocked

doorways), and the abandonment of KAJ - the transition to Phase 3. Currently, this event is attributed to the Shoshenq I campaigns around 925 BCE, possibly for the direct intention of disrupting the significant copper industry in the Arabah. All copper production is now centered at KEN (and possibly KF), a small habitation and possible watchtower are built at RHI to watch over the entrance to Faynan, and a new metallurgical toolkit including larger tuyères and furnaces appears for the first time as seen in Area R. The new sophisticated technology produces the largest tap slags (only seen at KEN) and copper with a high iron content as seen in the mixed copper-iron chunks from Area R and Area S – possibly as a result of exploiting iron-rich copper at the WAG 57 and 58 mines. However, the copper-iron mixtures required further refining (discussed in Chapter 5) and casting into ingots for export; Area F, with its unique archaeometallurgical assemblage, was potentially constructed for this purpose. As Area F was built within the walls of the fortress, the technology, knowledge, and products were likely considered significant and worth protecting. If Area F produced metallic copper, iron, or both is discussed in Chapter 5.

During the 10$^{th}$-9$^{th}$ centuries, copper is being produced on an industrial scale at KEN and possibly also KF. However, by the end of the 9$^{th}$ century BCE, KEN, the last remaining smelting site was abandoned and the copper production industry along with it; potentially a result of disrupted economic connections based on the contemporaneous destruction of Tell es-Safi/Gath (this issue is investigated further in this research) (Ben-Yosef and Sergi 2018). In the 7$^{th}$-6$^{th}$ centuries BCE, there is an attempt to renew copper exploitation in the region with the appearance of new mines and the Ras al-Miyah archaeological complex (Phase 4). However, there is no evidence of copper smelting, and one of the fortresses is never completed, suggesting this is a failed endeavor. By this time, the Edomite polity has shifted to the highlands, and copper

smelting doesn't appear in Faynan again until the Roman Period. This dissertation uses new analytical evidence and theoretical approach to explore what occurred in these crucial centuries and to understand why copper smelting was abandoned in the 9th century BCE.

Chapter 4, in part, is a reprint of the material as it appears in Liss, Brady, Matthew D. Howland, Brita Lorentzen, Craig Smitheram, Mohammad Najjar, and Thomas E. Levy 2020 Up the Wadi: Development of an Iron Age Industrial Landscape in Faynan, Jordan. *Journal of Field Archaeology* 45(6): 413-427. The dissertation author was a primary investigator and author of this paper.

## Chapter 5 – Analytical Examination of Iron Age Metal from Faynan: Methods and Results

### 5.1 Introduction and Research Questions

The Iron Age industrial landscape of Faynan has been intensively researched including extensive surveys and excavations at major smelting centers; however, the actual metal produced is largely understudied in comparison. Thus, a primary goal of this dissertation is to fill this scholarly lacuna using a variety of analytical techniques to examine the metal from Iron Age Faynan. In general, this chapter aims to produce a robust dataset for investigating four research questions: 1) Was iron produced in Faynan as an adventitious byproduct of sophisticated copper smelting? 2) How can we interpret the mixed iron-copper chunks excavated from Khirbat en-Nahas? 3) Does the quality of copper produced in Faynan change through time? and 4) Does the quality of copper in the final phases of the Iron Age industry suggest the industry over-exploited the highest quality copper ores? The answers to these questions provide the foundation for answering the broader research questions introduced in Chapter 1.

The chapter begins by examining the first two questions presented using a sophisticated methodology of osmium isotope and highly siderophile element abundance analyses focusing on iron objects and the mixed metal chunks from Khirbat en-Nahas. This section is supplemented by a related study of sediment samples from Khirbat en-Nahas looking for iron production residues using magnetism and x-ray fluorescence. The chapter then moves into the next two research questions relying primarily on a large-scale scanning electron microscopy examination of copper prills trapped in slag samples from Khirbat an-Nahas and Khirbat al-Jariya. Together, the results of these analyses produced the largest analytical dataset of metal from Iron Age Faynan to date. In combination with the new theoretical lens presented in Chapter 2, this dataset helps to inform current understandings of copper production through the Iron Age, its

relationship to sociopolitical structures in Faynan, as well as the end of the industry in the 9th century BCE (Chapter 7).

## 5.2 Isotope and Highly Siderophile Element Analysis of Iron Objects and Chunks

### 5.2.1 Introduction

As discussed above, a standing theory concerning the origins of iron production in the Eastern Mediterranean is that iron was produced as an adventitious byproduct of sophisticated copper smelting. To reiterate, this hypothesis suggests advanced copper smelting furnaces created the necessary reducing conditions to extract metallic iron from a furnace charge abundant in iron oxides in the form of iron-enriched copper ores or fluxes (Tylecote and Boydell 1978; Cooke and Aschenbrenner 1975) (Chapter 3). While this theory has received limited scholarly attention since the work of Merkel and Barrett in 2000, the mixed iron-copper chunks and iron objects excavated at Khirbat en-Nahas draw back into question whether iron production was discovered as an unintended byproduct of copper smelting (Figure 5.1). Critically, the iron artifacts at Khirbat en-Nahas are contemporaneous with the pinnacle in smelting technologies during the 10th-9th centuries BCE (Ben-Yosef et al. 2019). Thus, Iron Age Faynan yields coeval evidence of both sophisticated copper smelting technologies and iron artifacts. In this way, while not the earliest appearance of iron in the Levant, Faynan provides an ideal case study for examining a possible connection between copper smelting and iron production i.e., to examine if the mixed copper-iron chunks were purified to extract metallic iron for producing objects.

The iron in the mixed chunks provides evidence that iron of some kind was produced in Faynan (discussed further below), but it is currently unknown if they were used to make objects (Figure 5.1). As such, these materials have been interpreted in multiple ways: 1) as potential

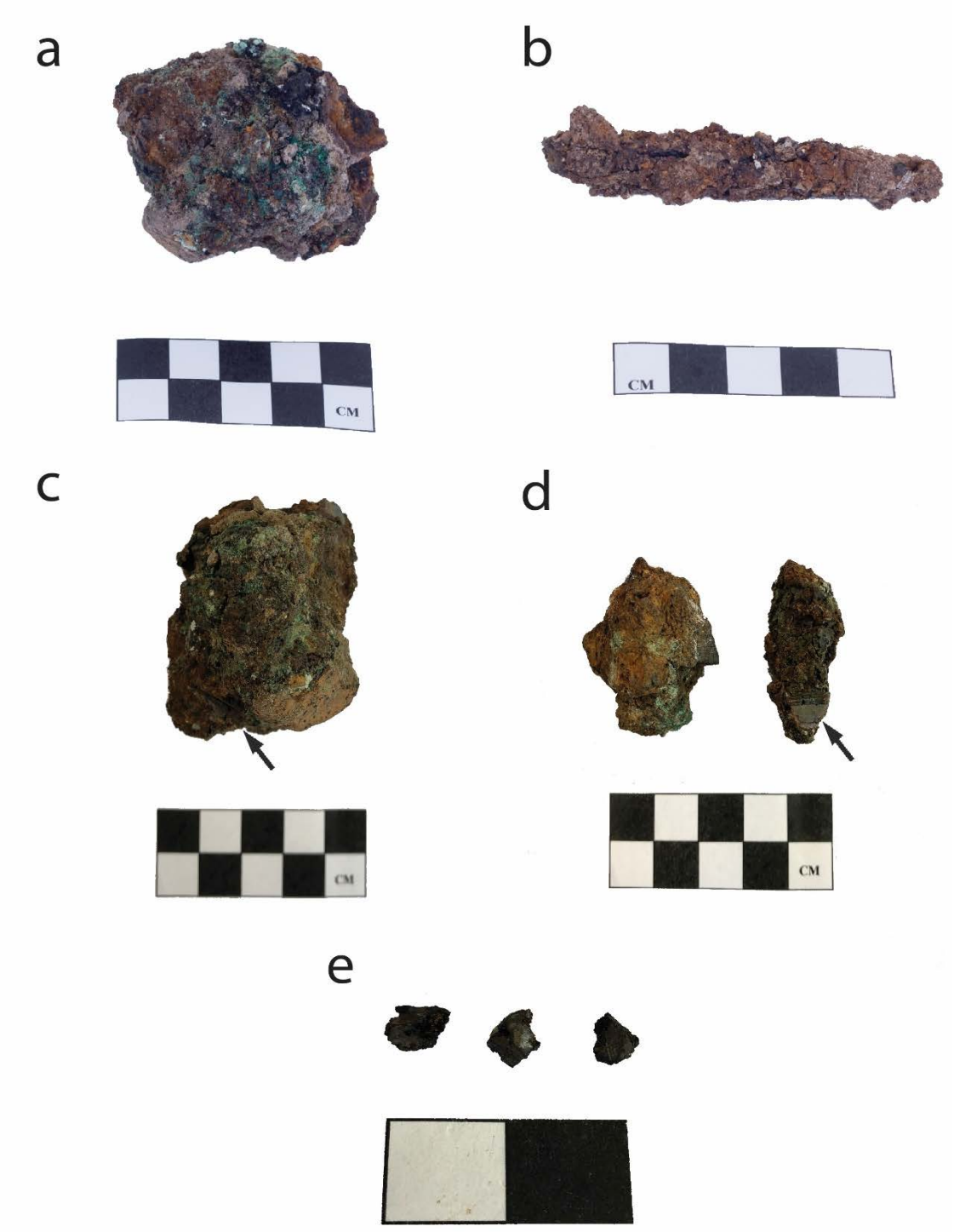


**Figure 5.1:** Representative materials analyzed for HSE abundances and osmium isotopes. (a) An iron-copper mixed chunk at Khirbat en-Nahas. (b) An example of an iron object excavated at Khirbat en-Nahas. (c-d) Additional examples of iron-copper chunks with arrows pointing to where sample iron material was extracted for isotope analysis. (e) Sample iron extracted from the chunks and used in the isotope analysis.

evidence for iron production stemming from the advanced copper smelting technologies in Faynan during the $10^{th}$-$9^{th}$ centuries BCE, supporting the theory introduced above; 2) as waste materials from failed smelts resulting in unworkable metal; or 3) as a raw product from copper smelting that required further refinement to extract copper metal (For overview see Erb-Satullo 2019 and citations there within; Hauptmann 2007: 208; Ben-Yosef 2010: 711). To address these interpretations, this research used highly siderophile element abundances and osmium (Os) isotope analysis. Highly siderophile elements (HSE) abundances and Os isotopes can act as arbitrators in the provenance of iron production techniques due to their strong affinity for metallic iron (siderophile literally means "iron-loving"). Using experimental archaeology and Re-Os isotope analysis, Brauns et al. (2013, 2020) discovered limited isotopic differences between iron ore and bloom in archaeological materials from southern Germany, indicating that these long-lived isotopic variations, generated from radioactive decay of $^{187}Re$ to $^{187}Os$ ($\lambda = 1.67 \times 10^{-11}$ $a^{-1}$ [cf., Day, Brandon, and Walker 2016]) are predictably unaffected by smelting processes (see also Schwab et al. 2022). Part of the success with Os isotope analysis is due to the iron ores being the primary source of the HSE through the entire smelting process (Brauns et al. 2013). Other materials that could potentially cause contamination, such as furnace linings that contribute to Sr isotopic variations, have negligible Os and other HSE compared with the ore (Brauns et al. 2013). As such, HSE abundances and Os isotopes can be used to identify a possible connection between the metal chunks and iron objects excavated in Faynan; a consistent isotopic signature as well as relative and absolute abundances of the HSE between the chunks and objects would indicate the mixed metals were being purified to recover iron for producing objects.

### 5.2.2 Sample Selection

For a holistic study, samples (n=15) were selected and analyzed from each phase of the metallurgical *chaîne opératoire*: Faynan copper ores (n=3), iron from the metal chunks (n=6), iron objects (n=5), and also a sample of unknown provenance (7179) originally believed to be an object (discussed further below) (Table 5.1). The ore samples were selected from three different mines exploiting the DLS near Khirbat al-Jariya and Khirbat en-Nahas (Figure 5.2). It is difficult to securely date these mines to the Iron Age (Stöllner 2014: 151), but their proximity to Iron Age smelting sites is possibly suggestive of their use during this period. Moreover, ores from mines to the southeast of Khirbat en-Nahas (WAG 57 or the El Furn mines) were strategically sampled as geological surveys reported these mines as enriched in iron (Hauptmann 2007: 71), providing a possible source for the iron seen in the chunks and objects.

**Table 5.1:** Archaeological details for isotope analysis samples.

| Samples for Isotope Analysis | | | | | |
|---|---|---|---|---|---|
| **Year** | **Site** | **Area** | **Locus** | **Basket** | **Artifact Type** |
| 2002 | KEN | S | 316 | 6740 | Iron Object |
| 2002 | KEN | S | 317 | 6849 | Iron Object |
| 2002 | KEN | S | 317 | 6391 | Iron Object |
| 2002 | KEN | S | 339 | 6953 | Iron Object |
| 2006 | KEN | M | 727 | 10367 | Iron Object |
| 2002 | KEN | S | 312 | 7179 | Unknown |
| 2002 | KEN | S | 270 | 5636 | Iron-Copper Chunk |
| 2009 | KEN | R | 141 | 1514 | Iron-Copper Chunk |
| 2006 | KEN | M | 721 | 10228 | Iron-Copper Chunk |
| 2009 | KEN | R | 64 | 680 | Iron-Copper Chunk |
| 2009 | KEN | R | 64 | 722 | Iron-Copper Chunk |
| 2006 | KEN | R | 1834 | 16356 | Iron-Copper Chunk |
| 2009 | JAJ | 1 | - | - | Copper Ore |
| 2002 | WAG | 57 | - | - | Copper Ore |
| 2002 | WAJ | 548 | - | - | Copper Ore |

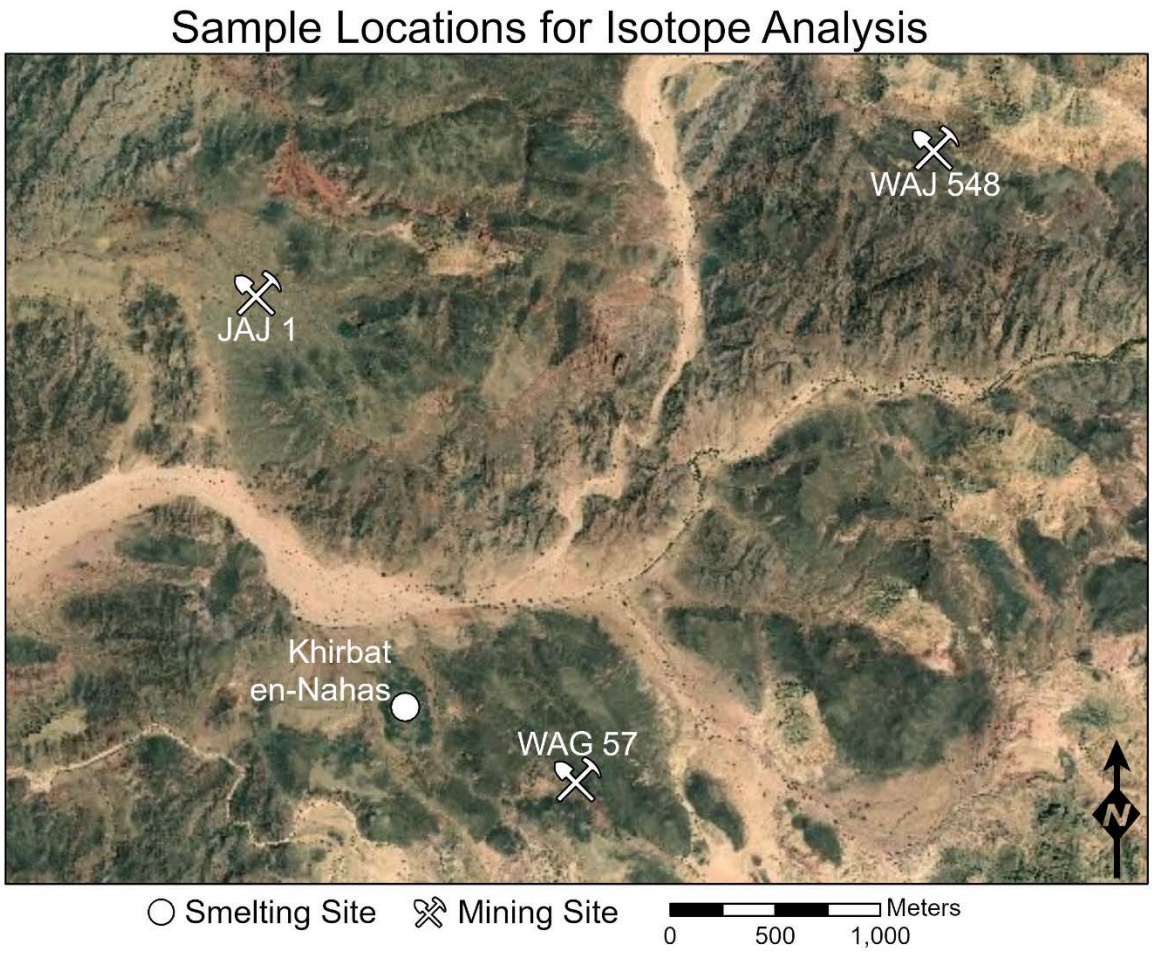


**Figure 5.2:** Locations of samples analyzed for HSE abundances and osmium isotopes. All iron objects and mixed iron-copper chunks originated from Khirbat en-Nahas, and one ore sample was analyzed from each of the labeled mining sites. Satellite imagery base layer source: Esri, Maxar, GeoEye, Earthstar Geographics, CNES/Airbus DS, USDA, USGS, AeroGRID, IGN, and the GIS User Community. Map Produced by Brady Liss.

The mixed iron-copper chunks are abundant at Khirbat en-Nahas in the time-interval of study (radiocarbon dated at 10$^{th}$-9th centuries BCE), and six were sampled for analysis. A small selection of iron was extracted by using a low-speed saw to physically separate Fe-rich material from heterogeneous metallic chunks (copper and iron were often visually separated – Figure 5.1). The sample size for iron objects was inherently limited by the small number of these artifacts excavated at the site. The corrosion of the iron also prevented secure identification of

object type, but their clear shapes, in contrast to the chunks/lumps of metal, supported their classification as artifacts/objects as opposed to amorphous iron (Figure 5.1). The objects were similarly excavated from layers dated to the 10th-9th centuries BCE, primarily from Area S at Khirbat en-Nahas.

Some of the samples are highly oxidized, from metallic to ferric iron, forming hematite, siderite, and other byproducts. It is possible that this alteration led to mobility of some of the HSE. The closest proxies to these objects that have been studied for alteration effects on the HSE are metal grains in meteorites, with the mobility of the HSE being generally low, with the possible exception of Re (Hyde et al. 2014; Day, Brandon, and Walker 2016). Furthermore, mobility of the HSE during weathering and alteration will have no effect on $^{187}Os/^{188}Os$, as this ratio is controlled by time-integrated $^{187}Re$ decay, rather than any other process. In other words, $^{187}Os/^{188}Os$ ratios are consistent through the smelting process and are not impacted by the weathering and oxidations processes.

### 5.2.3 Methods

#### 5.2.3.1 Scanning Electron Microscopy

The oxidation of the iron objects and chunks warranted further investigation of their microstructure to test if the chunks represented geological/corroded minerals rather than smelting products. To investigate this issue, samples were imaged and analyzed with a scanning electron microscope (Phenom XL) equipped with an energy dispersive spectrometer (SEM-EDX) without any coating (SEM-EDX is discussed in greater detail below)[1]. In order to expose potential iron metal and reduce further destruction of the artifacts, the same portions of the sample removed for

[1] Scanning electron microscopy was done in the UCSD Paleoethnobotany Laboratory (Director and PI: Dr. Jade d'Alpoim Guedes) with the assistance of Jacques Lyakov.

LA-ICP-MS were used for examination with the SEM. As such, these samples were primarily iron based on visual inspection. Since the samples were not highly polished, the primary goal was to use SEM-EDX to identify metallic iron and textural features if possible.

#### 5.2.3.2 Mass Spectrometry Analysis

Mass spectrometry is an analytical method for determining the elemental and/or isotopic composition of a sample. While there are a variety of types of mass spectrometry instruments (three different mass spectrometers were used here), they have the same main components and follow the similar scientific principles. The three general components of a mass spectrometer are an ionization source, a mass analyzer, and a detector (Gross 2011: 6-7, Figure 1.3). To simplify, the ionization source (which differs by instrument type – such as inductively coupled plasma or thermal ionization, for example) ionizes the molecules of a sample to create charged ions (Gross 2011: 21-22). These ions are subsequently focused into a beam which is directed through a magnetic field – the mass analyzer. The magnetic field forces the path of the ions to curve and separate in space based on their mass-to-charge ratio; as the magnetic force is consistent across all ions, their mass-to-charge ratio essentially determines the curvature of their path. In other words, lighter ions will experience a more curved trajectory in comparison to heavier ions.

The mass analyzer then directs the ions to a detector. As the ions reach the detector, they create a signal based on their mass-to-charge ratio and the relative abundance (Gross 2011: 9-11). The signal from the detector is read by the computer which produces as a mass spectrum. This mass spectrum can then be interpreted to understand what elements/isotopes are present in a sample by correlating the identified masses (plotted along the x-axis) to known masses or by identifying a characteristic pattern. The spectrum also provides the relative abundance of the ion

(the height of a peak in the spectrum) which is used to quantitatively determine the amount of each element/isotope. While mass spectrometry is destructive in the sense that the sample is consumed in the process, only a very small amount of sample material (often micrograms) is typically needed, making it a valuable technique for archaeological applications.

Due to the variability in the composition and nature of samples that were examined, we took a two-stage analytical approach to analyzing ores, objects, and iron-copper chunks to ensure optimum spiking for isotope dilution (ID) measurements. All protocols and measurements were conducted at the *Scripps Isotope Geochemistry Laboratory* (*SIGL*) under the supervision of Dr. James Day. In the first stage, for the ores, 100 mg of sample powder was precisely weighed and digested in a 1:4 mixture of Teflon-distilled $HNO_3$:HF for >96 Hrs at 150˚C on a hotplate using methods outlined in Day (2019). Rock standards (BHVO-2, BIR-1, BCR-2, AGV-2) and total procedural blanks were prepared along with the samples (Tables 5.2 and 5.3). After drying down and sequential $HNO_3$ dry-down steps to break-down fluorides, clear sample solutions, free from any residual solid material (e.g., complete dissolution of zircon and other refractory phases), were diluted by a factor of 5000 in 2% $HNO_3$ and doped with a 1 part per billion (ppb) In solution to monitor instrumental drift. Solutions were measured using a *Thermo Scientific* iCAPq c quadrupole inductively coupled plasma mass spectrometer (ICP-MS). Reproducibility of the reference materials was generally better than 5% (relative standard deviation - RSD), and element abundances were generally within error (1σ standard deviation) of recommended values (Table 5.2). The nickel and cobalt concentrations from these measurements were used to inform optimum spiking for ID measurements of the HSE in the ore samples, as these siderophile elements and the HSE generally positively correlate.

**Table 5.2:** Elemental composition of the ore samples from Faynan – WAG-57, WAJ-458, and JAJ-1 – and standard rock reference materials (BHVO-2, BCR-2, and BIR1a) in parts per million (ppm). GEOREM – GeoReM database of reference materials, Av – Average, St Dev – Standard Deviation, RSD – Relative Standard Deviation, USGS – United States Geological Survey reference material. Table prepared by Dr. James M.D. Day and modified from Liss, Levy, and Day 2020: Table S1.

| Compositions of local ores and standard reference materials (BHVO-2, BCR-2, BIR1a) in parts per million (PPM) | | | | | | | | | | | | | | | |
|---|---|---|---|---|---|---|---|---|---|---|---|---|---|---|---|
| | WAG-57 | WAJ-458 | JAJ-1 | BHVO-2 | | | BHVO-2 | BCR-2 | | | BCR-2 | BIR1a | | | BIR1a |
| | BL-1 | BL-2 | BL-3 | Av | St Dev | RSD | GEOREM | Av | St Dev | RSD | GEOREM | Av | St Dev | RSD | USGS |
| **Cu** | 126709 | 440932 | 163584 | 129 | 2 | 1% | 129 | 23 | 0 | 1% | | 115 | 2 | 1% | |
| **Al** | 26390 | 2959 | 11312 | 71130 | 943 | 1% | 71130 | 69793 | 925 | 1% | | 78641 | 1043 | 1% | |
| **Mg** | 2755 | 10887 | 3488 | 43762 | 402 | 1% | 43762 | 21347 | 196 | 1% | | 56278 | 517 | 1% | |
| **Ca** | 4875 | 24499 | 4157 | 81479 | 1099 | 1% | 81479 | 50323 | 679 | 1% | | 90955 | 1227 | 1% | |
| **Mn** | 19587 | 1237 | 451 | 1309 | 13 | 1% | 1309 | 1516 | 15 | 1% | | 1283 | 12 | 1% | |
| **Fe** | 6275 | 851 | 1107 | 86300 | 1043 | 1% | 86300 | 95372 | 1152 | 1% | | 76622 | 926 | 1% | |
| **Na** | 739 | 68 | 3119 | 16462 | 125 | 1% | 16462 | 23015 | 175 | 1% | | 12930 | 98 | 1% | |
| **P** | 161 | 71 | 104 | 1172 | 42 | 4% | 1172 | 1553 | 56 | 4% | | 122 | 4 | 4% | |
| **K** | 4431 | 783 | 2852 | 4259 | 72 | 2% | 4259 | 14307 | 243 | 2% | | 163 | 3 | 2% | |
| **Ti** | 504 | 45 | 196 | 16368 | 211 | 1% | 16368 | 13352 | 172 | 1% | | 5506 | 71 | 1% | |
| **Cr** | 8 | 1 | 3 | 287 | 5 | 2% | 287 | 232 | 4 | 2% | | 100 | 2 | 2% | |
| **V** | 4 | 47 | 26 | 318 | 4 | 1% | 318 | 414 | 5 | 1% | | 312 | 4 | 1% | |
| **Co** | 96 | 380 | 20 | 45 | 0 | 1% | 45 | 37 | 0 | 1% | | 51 | 1 | 1% | |
| **Ni** | 15 | 224 | 11 | 120 | 1 | 1% | 120 | 13 | 0 | 1% | | 166 | 2 | 1% | |
| **S** | 67 | 148 | 125 | 164 | 41 | 25% | 164 | 112 | 28 | 25% | | 210 | 52 | 25% | |
| | | | | | | | | | | | | | | | |
| **Li** | 16.40 | 1.24 | 3.16 | 4.50 | 0.18 | 4% | 4.50 | 9.57 | 0.38 | 4% | 9.13 | 3.14 | 0.13 | 4% | 3.6 |
| **B** | 34.6 | 24.0 | 48.2 | 3.0 | 0.4 | 12% | 3.0 | 6.4 | 0.8 | 12% | 4.4 | 1.1 | 0.1 | 12% | |
| **Sc** | 2.6 | 0.9 | 0.7 | 31.8 | 2.0 | 6% | 31.8 | 34.9 | 2.2 | 6% | 33.5 | 45.9 | 2.8 | 6% | 44 |
| **Zn** | 122.4 | 632.0 | 35.3 | 103.9 | 3.9 | 4% | 103.9 | 134.3 | 5.0 | 4% | 129.5 | 68.0 | 2.5 | 4% | 70 |
| **Ga** | 6.1 | 1.9 | 3.9 | 21.4 | 0.5 | 2% | 21.4 | 22.7 | 0.5 | 2% | 22.1 | 15.4 | 0.4 | 2% | 16 |
| **Ge** | 1.0 | 0.5 | 0.8 | 1.6 | 0.0 | 3% | 1.6 | 1.8 | 0.1 | 3% | 1.5 | 1.1 | 0.0 | 3% | |
| **Se** | 0.24 | 0.12 | 0.05 | 0.18 | 0.12 | 69% | 0.18 | 0.26 | 0.18 | 69% | 0.08 | 0.05 | 0.03 | 69% | |
| **Rb** | 19.3 | 2.4 | 8.6 | 9.3 | 0.2 | 2% | 9.3 | 48.3 | 1.1 | 2% | 46.0 | 0.2 | 0.0 | 2% | |
| **Sr** | 333.2 | 39.0 | 450.3 | 394.1 | 5.2 | 1% | 394.1 | 344.1 | 4.5 | 1% | 337.4 | 109.1 | 1.4 | 1% | 110 |
| **Y** | 8.1 | 1.8 | 4.6 | 25.9 | 0.4 | 1% | 25.9 | 36.1 | 0.5 | 1% | 36.1 | 15.5 | 0.2 | 1% | 16 |
| **Zr** | 81.9 | 6.7 | 73.6 | 171.2 | 2.4 | 1% | 171.2 | 188.4 | 2.6 | 1% | 186.5 | 14.8 | 0.2 | 1% | 18 |
| **nb** | 0.9 | 0.3 | 1.0 | 18.1 | 0.3 | 2% | 18.1 | 12.4 | 0.2 | 2% | 12.4 | 0.6 | 0.0 | 2% | 0.6 |
| **Mo** | 0.5 | 1.3 | 0.5 | 4.1 | 1.9 | 47% | 4.1 | 272.3 | 126.8 | 47% | 250.6 | 0.1 | 0.0 | 47% | |
| **Sn** | 0.16 | 0.05 | 0.18 | 1.78 | 0.04 | 2% | 1.78 | 2.12 | 0.05 | 2% | 2.28 | 0.69 | 0.01 | 2% | |
| **Te** | 0.01 | 0.00 | 0.01 | 0.01 | 0.00 | 28% | 0.01 | 0.01 | 0.00 | 28% | 0.00 | 0.00 | 0.00 | 28% | |
| **Cs** | 2.8 | 0.2 | 0.4 | 0.1 | 0.0 | 3% | 0.1 | 1.2 | 0.0 | 3% | 1.2 | 0.0 | 0.0 | 3% | |
| **Ba** | 5773 | 327 | 17097 | 130.9 | 1.3 | 1% | 130.9 | 672.6 | 6.9 | 1% | 683.9 | 6.2 | 0.1 | 1% | 7 |
| **La** | 5.6 | 1.2 | 5.3 | 15.2 | 0.2 | 1% | 15.2 | 25.1 | 0.3 | 1% | 25.1 | 0.6 | 0.0 | 1% | 0.63 |
| **Ce** | 21.1 | 2.7 | 9.8 | 37.5 | 0.4 | 1% | 37.5 | 53.0 | 0.6 | 1% | 53.1 | 1.9 | 0.0 | 1% | 1.9 |
| **Pr** | 1.4 | 0.3 | 0.9 | 5.3 | 0.1 | 2% | 5.3 | 6.8 | 0.1 | 2% | 6.8 | 0.4 | 0.0 | 2% | |
| **Nd** | 5.7 | 1.2 | 3.1 | 24.3 | 0.4 | 2% | 24.3 | 28.6 | 0.5 | 2% | 28.3 | 2.3 | 0.0 | 2% | 2.5 |
| **Sm** | 1.4 | 0.3 | 0.7 | 6.0 | 0.1 | 2% | 6.0 | 6.5 | 0.1 | 2% | 6.5 | 1.0 | 0.0 | 2% | 1.1 |
| **Eu** | 1.5 | 0.1 | 4.0 | 2.0 | 0.0 | 2% | 2.0 | 2.1 | 0.0 | 2% | 2.0 | 0.5 | 0.0 | 2% | 0.55 |
| **Gd** | 1.6 | 0.3 | 0.9 | 6.2 | 0.1 | 2% | 6.2 | 6.9 | 0.1 | 2% | 6.8 | 1.6 | 0.0 | 2% | 1.8 |
| **Tb** | 0.2 | 0.0 | 0.1 | 0.9 | 0.0 | 2% | 0.9 | 1.1 | 0.0 | 2% | 1.1 | 0.3 | 0.0 | 2% | |
| **Dy** | 1.4 | 0.3 | 0.7 | 5.3 | 0.1 | 2% | 5.3 | 6.3 | 0.1 | 2% | 6.4 | 2.5 | 0.1 | 2% | 4 |
| **Ho** | 0.3 | 0.1 | 0.1 | 1.0 | 0.0 | 2% | 1.0 | 1.3 | 0.0 | 2% | 1.3 | 0.6 | 0.0 | 2% | |
| **Er** | 0.7 | 0.2 | 0.4 | 2.5 | 0.0 | 2% | 2.5 | 3.6 | 0.1 | 2% | 3.7 | 1.6 | 0.0 | 2% | |
| **Tm** | 0.1 | 0.0 | 0.1 | 0.3 | 0.0 | 2% | 0.3 | 0.5 | 0.0 | 2% | 0.5 | 0.2 | 0.0 | 2% | |
| **Yb** | 0.7 | 0.2 | 0.5 | 2.0 | 0.0 | 2% | 2.0 | 3.3 | 0.1 | 2% | 3.4 | 1.6 | 0.0 | 2% | 1.7 |
| **Lu** | 0.1 | 0.0 | 0.1 | 0.3 | 0.0 | 2% | 0.3 | 0.5 | 0.0 | 2% | 0.5 | 0.2 | 0.0 | 2% | 0.26 |
| **Hf** | 2.1 | 0.2 | 1.9 | 4.5 | 0.1 | 2% | 4.5 | 4.9 | 0.1 | 2% | 5.0 | 0.6 | 0.0 | 2% | 0.6 |
| **Ta** | 0.0 | 0.0 | 0.1 | 1.2 | 0.0 | 2% | 1.2 | 0.8 | 0.0 | 2% | 0.8 | 0.0 | 0.0 | 2% | |
| **W** | 0.4 | 0.0 | 0.3 | 0.3 | 0.0 | 3% | 0.3 | 0.5 | 0.0 | 3% | 0.5 | 0.1 | 0.0 | 3% | |
| **Pb** | 601.7 | 9.5 | 18.6 | 1.7 | 0.0 | 3% | 1.7 | 11.3 | 0.3 | 3% | 10.6 | 3.1 | 0.1 | 3% | 3 |
| **Th** | 2.9 | 0.3 | 2.0 | 1.2 | 0.0 | 2% | 1.2 | 5.9 | 0.1 | 2% | 5.8 | 0.0 | 0.0 | 2% | |
| **U** | 46.9 | 5.0 | 22.3 | 0.4 | 0.0 | 2% | 0.4 | 1.6 | 0.0 | 2% | 1.7 | 0.0 | 0.0 | 2% | |

**Table 5.3**: Blank measurements for HSE abundances and their percentage contribution to the sample measurements. All HSE abundance data were blank corrected, with the blanks, on average, representing less than 2% of the HSE, with the exception of Ru and Os in some ore samples (up to 35%), and Pt in Sample 6391 (16%). Ng – nanogram. Table prepared by Dr. James M.D. Day and modified from Liss, Levy, and Day 2020: Table S2.

| Blank and blank percentages as a function of total analyte for isotope dilution measurements | | | | | | | | | |
|---|---|---|---|---|---|---|---|---|---|
| **Blank in ng** | | **Re** | **Pd** | **Pt** | **Ru** | **Ir** | **Os** | **$^{187}Os/^{188}Os$** | **2SE** |
| | | 0.00016 | 0.00169 | 0.00532 | 0.00530 | 0.00089 | 0.00013 | 0.65 | 0.04 |
| **Sample** | **Lab ID** | **%Blk Re** | **%Blk Pd** | **%Blk Pt** | **%Blk Ru** | **%Blk Ir** | **%Blk Os** | | |
| **6740** | BL1-2 | 0.03% | 1.60% | 5.06% | 1.27% | 0.50% | 7.6% | | |
| **7179** | BL1-3 | 0.02% | 0.42% | 0.28% | 1.51% | 0.54% | 2.9% | | |
| **6849** | BL1-4 | 0.02% | 6.53% | 4.16% | 2.29% | 0.86% | 6.3% | | |
| **6391** | BL1-5 | 0.02% | 1.13% | 16.4% | 2.84% | 2.36% | 7.1% | | |
| **6953** | BL1-6 | 0.02% | 0.99% | 13.6% | 2.27% | 1.79% | 6.2% | | |
| **10637** | BL1-7 | 0.05% | 0.61% | 7.5% | 2.15% | 1.31% | 5.6% | | |
| **5636** | BL1-8 | 0.005% | 0.04% | 0.03% | 1.47% | 0.10% | 0.2% | | |
| **10228** | BL1-9 | 0.01% | 1.08% | 0.31% | 3.07% | 0.45% | 0.7% | | |
| **1514** | BL1-10 | 0.02% | 0.36% | 1.33% | 5.22% | 2.34% | 5.3% | | |
| **722** | BL1-11 | 0.01% | 0.04% | 0.04% | 1.71% | 0.26% | 0.3% | | |
| **680** | BL1-12 | 0.00% | 0.03% | 0.05% | 2.25% | 0.52% | 0.4% | | |
| **16356** | BL1-13 | 0.01% | 0.61% | 0.21% | 1.50% | 0.25% | 0.4% | | |
| **WAG-57** | BL1 | 0.3% | 2.1% | 0.1% | 32% | 5.2% | 16% | | |
| **WAJ-458** | BL2 | 1.2% | 2.4% | 4.1% | 21% | 5.2% | 35% | | |
| **JAJ-1** | BL3 | 0.3% | 2.9% | 7.4% | 30% | 7.0% | 15% | | |

The first stage of analysis for the iron from the mixed chunks and objects involved analysis by laser ablation ICP-MS using a *New Wave Research* UP213 (213 nm) laser-ablation system coupled to an iCAP Qc ICP-MS (LA-ICP-MS). Analyses were done on fragments of iron material with visible metallic luster using ~0.5 mm long rasters with a 100 μm beam diameter, a laser repetition rate of 5 Hz, and a photon fluence of ~3 to 3.5 J/cm$^2$. Ablation analysis took place in a 3 cm$^3$ ablation cell. The cell was flushed with a He-gas flow to enhance production and transport of fine aerosols and was mixed with an argon carrier-gas flow of ~1 L/min before reaching the torch. Each analysis consisted of ~60 second data collection. Backgrounds on the sample gas were collected for ~20 second, followed by ~40 second of laser ablation. Washout time between analyses was >120 seconds. Data were collected in time-resolved mode so effects of inclusions, mineral zoning, and possible penetration of the laser beam to underlying phases

could be evaluated. Plots of counts per second versus time were examined for each analysis, and integration intervals for the gas background and the sample analysis were selected. Standardization was performed using standard reference material metal standards Hoba, Coahuila and Filomena, and sulfide standard MASS-1 using protocols outlined in Day et al. 2018. Reproducibility of the reference materials was generally better than 4% (RSD) for standards for the HSE, and element abundances were generally within error (1σ standard deviation.) of recommended values (Table 5.4).

The second stage of analysis involved Os isotope and HSE abundance determination by digesting samples in sealed borosilicate Carius tubes, with isotopically enriched multi-element spikes ($^{99}$Ru, $^{106}$Pd, $^{185}$Re, $^{190}$Os, $^{191}$Ir, $^{194}$Pt), and 11 mL of a 1:2 mixture of multiply Teflon distilled HCl and $HNO_3$, with the latter purged with $H_2O_2$ to eradicate Os. Optimal spiking of metals was performed using the LA-ICP-MS abundance data to estimate bulk-rock HSE compositions. Samples were digested in Carius tubes to a maximum temperature of 270˚C in an oven for 72 hours. Osmium was triply extracted from the acid using $CCl_4$ and then back-extracted into HBr, prior to purification by micro-distillation, with the other HSE being recovered and purified from the residual solutions using anion exchange separation (Day et al. 2016). Isotopic compositions of Os were measured in negative-ion mode using peak jumping on the central secondary electron multiplier of a *Thermo Scientific* Triton thermal ionization mass spectrometer (N-TIMS). Rhenium, palladium, platinum, ruthenium, and iridium were measured using a *Cetac Aridus II* desolvating nebulizer coupled to an iCAP Qc ICP-MS. Offline corrections for Os involved an oxide correction, an iterative fractionation correction using $^{192}$Os/$^{188}$Os = 3.08271, a $^{190}$Os spike subtraction, and finally, an Os blank subtraction. Precision for $^{187}$Os/$^{188}$Os, determined by repeated measurement of the UMCP Johnson-Matthey standard

**Table 5.4:** Results in parts per million (ppm) of the Laser Ablation-ICP-MS analysis of artifacts, iron-copper chunks, and standard reference materials. Av. – Average, St Dev – Standard Deviation, IC – Iron from Chunk, Unk. – Unknown Sample Type. Hoba, Coahila, Filomena, and MASS-1 are standard reference materials. Table prepared by Dr. James M.D. Day and modified from Liss, Levy, and Day 2020: Table S3.

| Laser Ablation-ICP-MS analyses of artifacts and iron-copper chunks with standard reference materials (in ppm) | | | | | | | | | | | | | | | | | | | | | | | | | | | | | | | | | | | |
|---|---|---|---|---|---|---|---|---|---|---|---|---|---|---|---|---|---|---|---|---|---|---|---|---|---|---|---|---|---|---|---|---|---|---|---|
| | | Obj. | 6470 | Obj. | 6849 | Obj. | 6391 | Obj. | 6953 | Obj. | 10637 | Unk. | 7179 | IC | 5636 | IC | 10228 | IC | 1514 | IC | 722 | IC | 680 | IC | 16356 | Hoba (n = 8) | | Coahuila (n = 8) | | Filomena (n = 8) | | MASS-1 (n = 10) | |
| Ele. | Iso. | Av. | St Dev | Av. | St Dev | Av. | St Dev | Av. | St Dev | Av. | St Dev | Av. | St Dev | Av. | St Dev | Av. | St Dev | Av. | St Dev | Av. | St Dev | Av. | St Dev | Av. | St Dev | Av. | St Dev | Av. | St Dev | Av. | St Dev | Av. | St Dev | Av. | St Dev |
| S | [34] | 554 | *78* | 716 | *44* | 683 | *51* | 713 | *229* | 545 | *40* | 5982 | *4304* | 2569 | *396* | 2108 | *833* | 1550 | *125* | 2633 | *190* | 692 | *93* | 1484 | *64* | 1011 | 248 | 637 | 102 | 311 | 73 | 294744 | 12015 |
| Co | [59] | 112 | *25* | 211 | *84* | 23 | *5* | 33 | *1* | 129 | *58* | 4965 | *1076* | 11514 | *1391* | 20307 | *610* | 6842 | *1621* | 15120 | *378* | 9875 | *450* | 18622 | *1351* | 5707 | 52 | 2962 | 12 | 3387 | 81 | 219 | 17 |
| Ni | [60] | 44 | *3* | 339 | *187* | 83 | *7* | 24 | *8* | 62 | *20* | 1281 | *233* | 5223 | *1122* | 7384 | *727* | 1824 | *668* | 6826 | *357* | 4056 | *351* | 3572 | *957* | 146014 | 2465 | 39558 | 470 | 52931 | 10547 | 368 | 18 |
| Cu | [63] | 53 | *13* | 54 | *1* | 56 | *29* | 30 | *14* | 153 | *77* | 12868 | *10633* | 7455 | *1473* | 7906 | *1521* | 7118 | *2608* | 6920 | *1018* | 2650 | *257* | 5775 | *339* | 201 | 316 | 40 | 6 | 25 | 26 | 142834 | 4528 |
| Zn | [66] | 0.1 | *5.8* | 32 | *15* | 86 | *71* | 73 | *47* | 73 | *83* | 451 | *304* | 46 | *6* | 12 | *2* | 15 | *2* | 37 | *3* | 50 | *9* | 44 | *31* | 17 | 30 | 22 | 15 | 14 | 8 | 223927 | 3336 |
| Se | [77] | 11.5 | *2.1* | 3.4 | *1.8* | 4.8 | *0.2* | 1.8 | *2.3* | 3.9 | *1.9* | 19.3 | *9.4* | 2.8 | | 0.7 | | 9 | *7* | 1.5 | *1.2* | 0.72 | *0.56* | 5.4 | *0.2* | 3.3 | 3.7 | 1.6 | 2.6 | 2.5 | 6.2 | 1164 | 71 |
| Mo | [95] | 90.7 | *37.2* | 1.6 | *1.7* | 18.5 | *10.1* | 6.7 | *0.9* | 24.6 | *29.9* | 37.9 | *5.7* | 354 | *158* | 552 | *19* | 195 | *268* | 683 | *5* | 586 | *162* | 310 | *6* | 34.3 | 1.2 | 6.8 | 0.7 | 12.6 | 5.0 | 364 | 14 |
| Ru | [101] | | | 0.002 | | 0.002 | | 0.004 | | 0.003 | | 0.026 | *0.018* | 0.019 | *0.002* | 0.022 | *0.002* | 0.014 | *0.005* | 0.023 | *0.007* | 0.013 | *0.008* | 0.015 | *0.003* | 29.3 | 0.5 | 17.7 | 2.5 | 20.2 | 2.3 | 0.1 | 0.0 |
| Pd | [105] | 0.03 | *0.01* | 0.03 | *0.02* | 0.06 | *0.02* | 0.13 | *0.01* | 0.05 | *0.06* | 4.83 | *2.77* | 1.933 | *0.004* | 1.78 | *0.45* | 1.64 | *0.71* | 2.08 | *0.45* | 0.90 | *0.03* | 1.79 | *0.03* | 10.7 | 0.2 | 2.4 | 0.2 | 3.2 | 0.4 | 34.5 | 2.3 |
| Ag | [107] | 0.06 | *0.01* | 0.63 | *0.84* | 0.25 | *0.06* | 4.02 | *5.65* | 0.07 | *0.04* | 2.12 | *1.31* | 0.7 | *0.2* | 0.026 | *0.002* | 0.063 | *0.004* | 20 | *9* | 12 | *16* | 1.65 | *0.63* | 0.8 | 0.5 | 0.2 | 0.1 | 0.03 | 0.04 | 53.3 | 1.3 |
| Sn | [118] | 11.43 | *5.09* | 0.06 | *0.02* | 13.09 | *5.40* | 0.824 | *0.004* | 1.00 | *0.34* | 0.65 | *0.15* | 0.394 | *0.004* | 0.56 | *0.10* | 0.32 | *0.03* | 0.53 | *0.32* | 0.39 | *0.11* | 5.07 | *2.52* | 97.6 | 190.9 | 0.24 | 0.17 | 0.08 | 0.04 | 63.0 | 2.3 |
| Te | [125] | 0.003 | | 0.001 | *0.001* | 0.006 | *0.006* | 0.009 | *0.002* | 0.016 | *0.004* | 0.002 | | 0.006 | *0.001* | 0.003 | | 0.003 | | 0.005 | *0.005* | 0.005 | *0.001* | 0.015 | *0.007* | 0.001 | 0.008 | 0.031 | 0.015 | 0.004 | 0.009 | 10.7 | 0.4 |
| W | [182] | 372 | *264* | 0.19 | *0.25* | 15 | *8* | 2.19 | *0.52* | 0.85 | *0.60* | 68 | *54* | 55 | *26* | 116.34 | *0.03* | 45 | *64* | 67 | *12* | 67 | *16* | 106 | *19* | 3.48 | 0.06 | 2.82 | 0.46 | 3.27 | 0.34 | 91.7 | 3.1 |
| Re | [185] | 0.011 | *0.006* | 0.010 | *0.006* | 0.008 | *0.001* | 0.005 | *0.002* | 0.011 | *0.002* | 0.007 | *0.006* | 0.067 | *0.019* | 0.20 | *0.05* | 0.02 | *0.02* | 0.062 | *0.014* | 0.3 | *0.3* | 0.123 | *0.091* | 2.81 | 0.06 | 0.99 | 0.14 | 0.21 | 0.01 | 0.004 | 0.003 |
| Os | [189] | 0.002 | *0.000* | 0.002 | *0.002* | | | 0.002 | *0.002* | 0.001 | *0.001* | 0.008 | | 0.007 | *0.002* | 0.012 | *0.002* | 0.002 | *0.001* | 0.010 | *0.002* | 0.004 | *0.000* | 0.008 | *0.001* | 38.5 | 1.4 | 8.0 | 1.2 | 1.0 | 0.1 | 0.010 | 0.003 |
| Ir | [193] | 0.004 | *0.005* | 0.009 | *0.012* | 0.10 | *0.10* | 0.04 | *0.03* | 0.009 | *0.002* | 0.081 | *0.103* | 0.048 | *0.016* | 0.036 | *0.003* | 0.002 | *0.003* | 0.048 | *0.027* | 0.063 | *0.025* | 0.030 | *0.003* | 27.9 | 0.3 | 13.4 | 1.8 | 3.8 | 0.4 | 290 | 5 |
| Pt | [195] | 0.000 | *0.001* | 0.0048 | *0.0004* | 0.080 | *0.069* | 0.031 | | 0.015 | *0.011* | 0.064 | *0.002* | 0.42 | *0.02* | 0.264 | *0.075* | 0.018 | *0.024* | 0.633 | *0.085* | 0.700 | *0.247* | 0.231 | *0.063* | 29.4 | 0.6 | 25.4 | 3.3 | 26.7 | 2.7 | 291 | 17 |
| Au | [197] | 0.02 | *0.02* | 0.22 | *0.11* | 0.03 | *0.02* | 0.29 | *0.41* | 10 | *14* | 2 | *3* | 0.090 | *0.071* | 0.007 | | | | 3.5 | *4.5* | 12 | *17* | 0.054 | *0.018* | 0.13 | 0.15 | 0.33 | 0.18 | 0.19 | 0.03 | 111 | 48 |
| Pb | [208] | 2 | *1* | 36 | *27* | 1 | *1* | 22 | *2* | 29 | *17* | 370 | *44* | 327 | *243* | 105 | *92* | 303 | *26* | 4.3 | *1.8* | 10 | *2* | 483 | *211* | 2.46 | 1.21 | 4.42 | 2.95 | 0.63 | 0.09 | 73 | 5 |

was better than ±0.2% (2 St. Dev.; 0.11372 ±22; n = 9). The highly radiogenic nature of some samples ($^{187}Os/^{188}Os$ up to 19) means we report uncertainties on the internal precision of the measurements at the two-sigma error of uncertainty. Measured rhenium, palladium, platinum, ruthenium, and iridium isotopic ratios for sample solutions were corrected for mass fractionation using the deviation of the standard average run on the day over the natural ratio for the element. External reproducibility on HSE analyses using our method was better than 0.5% for 0.5 ppb solutions and all reported values are blank corrected. The total procedural blank run with the samples had $^{187}Os/^{188}Os = 0.65 \pm 0.04$, with average quantities (in picograms [$10^{-12}$]) of 0.2 [Re], 1.7 [Pd], 5.3 [Pt], 5.3 [Ru], 0.9 [Ir], and 0.13 [Os]. All data are blank corrected, with the blanks, on average, representing less than 2% of the HSE, with the exception of ruthenium and Os in some ore samples (up to 35%), and platinum in 6391 (16%) (Table 5.3).

### 5.2.4 Results

#### 5.2.4.1 Copper Ores

The local ores of Faynan are copper rich (12.6 to 44 wt.%) with high zinc and lead, variable manganese (0.05 to 2 wt.%), relatively low iron (0.08 to 0.6 wt.%), and are characterized by light rare earth element enriched patterns and positive europium anomalies (Figure 5.3). These ores are likely derived from a marine source with enrichment through Mississippi Valley type ore deposit processes. The ore samples have low Os (0.001 to 0.004 ppb) and total HSE abundances (ΣHSE = 0.2-1.5 ppb), and are relatively enriched in rhenium, palladium, and platinum relative to ruthenium, iridium, and Os (Table 5.1). They have high $^{187}Re/^{188}Os$ (1330 to 2570) and variably radiogenic $^{187}Os/^{188}Os$ (2 to 19).

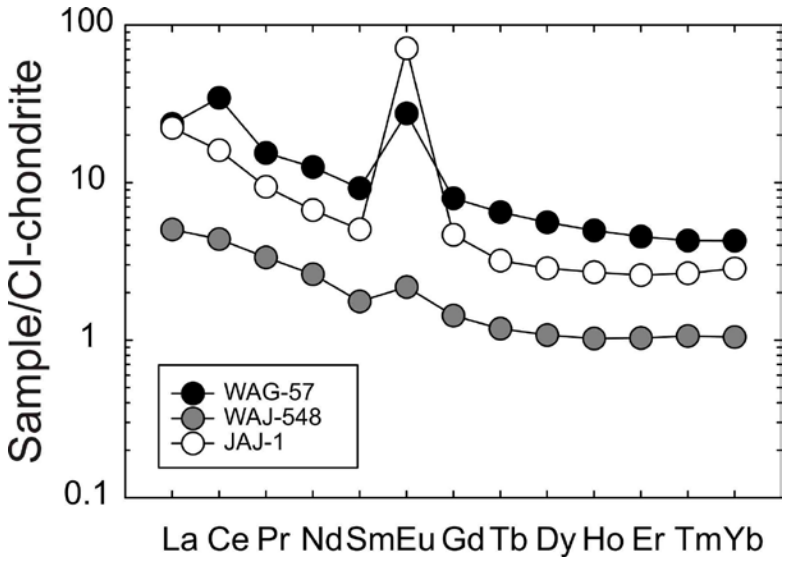


**Figure 5.3:** Rare earth element patterns for ore samples from the DLS normalized to conventional CI-chondrite (normalization values from McDonough and Sun 1995). CI-chondrites are meteorites typically used to normalize rock composition values due to their similarity to the solar nebula (McDonough and Sun 1995: 224). The ore samples are characterized by light rare earth element enriched patterns and positive Eu anomalies. Figure produced by Dr. James M.D. Day.

#### 5.2.4.2 Iron-Copper Chunk and Iron Object Compositions

Laser ablation-ICP-MS was performed on iron from the chunks and iron objects to assess a wide variation in major (iron), minor, and trace element abundances (S, Co, Ni, Cu, Zn, Se, Mo, Ag, Sn, Te, W, Pb) as well as the full variation in HSE abundances (Os, Ir, Ru, Rh, Pt, Pd, Re, Au). Objects were found to be dominantly iron (99.9%), with minor cobalt (23-211 parts per million - ppm), nickel (24-339 ppm), and copper (30-153 ppm). In contrast, iron chunks are dominantly iron (>96%), with higher abundances of cobalt (0.7-2 wt.%), nickel (0.2-0.7 wt.%), and copper (0.3-0.8 wt.%). The sample of unknown identification (7179) has iron, cobalt, nickel, and copper contents more similar to the iron chunks than to the objects. The objects also have generally lower and more variable lead than the chunks, but have higher zinc and selenium, and more variable tungsten (Figure 5.4).

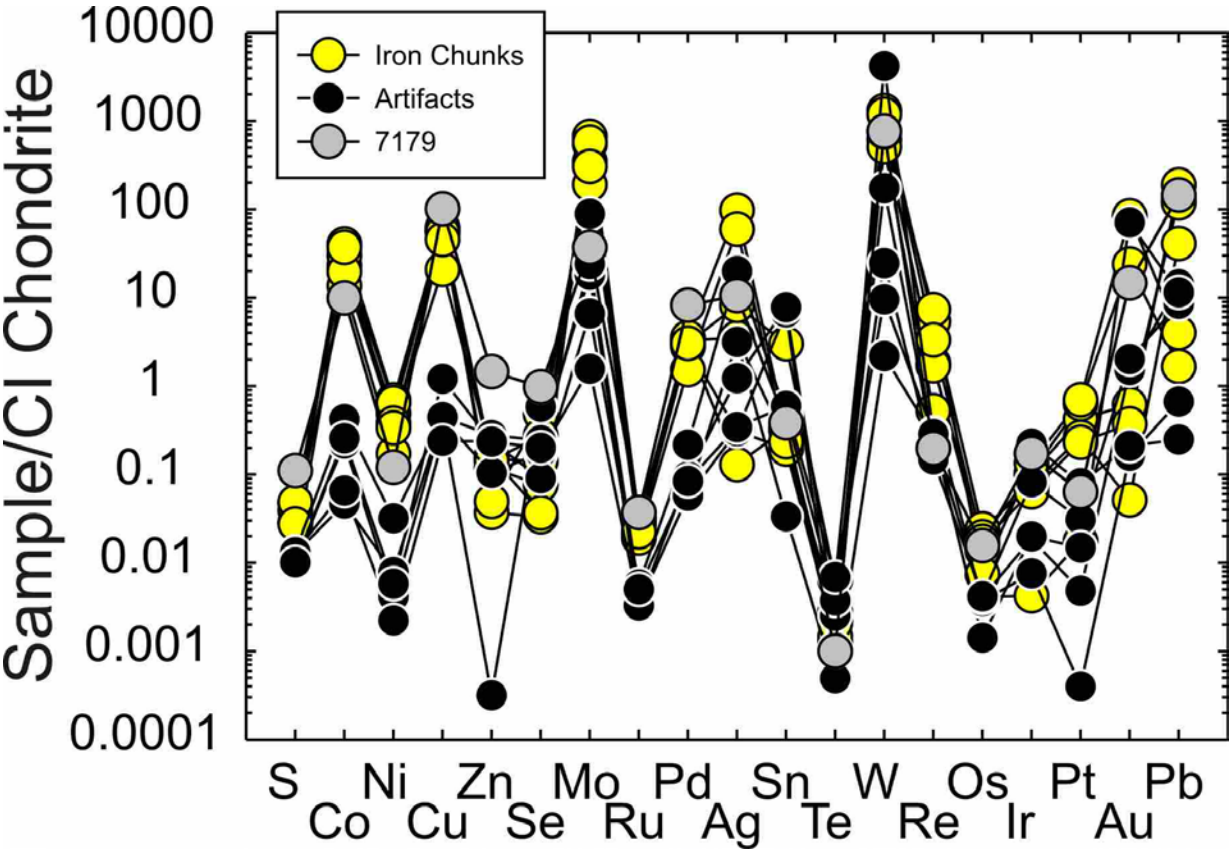


**Figure 5.4:** Normalized trace element diagram for iron from the mixed metal chunks and objects measured by LA-ICP-MS. CI-chondrite normalization from McDonough and Sun (1995). Figure produced by Dr. James M.D. Day.

The LA-ICP-MS data were obtained primarily to achieve accurate ID 'spiking' for high-precision Os isotope and HSE abundance measurements by N-TIMS and solution ICP-MS. Despite this effort, LA-ICP-MS analyses gave consistently higher HSE abundances than solution isotope dilution ICP-MS analyses (Table 5.5 and Figure 5.5). There are three causes for the differences. The first cause are nugget heterogeneities within the altered samples (Figure 5.6 and Table 5.4), where LA-ICP-MS analyses sample inherently smaller sample volumes than ID digestion methods (μg vs 100's mg). Second, LA-ICP-MS raster lines were performed on the 'cleanest' portions of metal observed in the samples, where there was metallic luster on the

**Table 5.5:** Comparison between Isotope Dilution (ID) and Laser Ablation ICP-MS (LA-ICP-MS) analysis in parts per billion (ppb). LA-ICP-MS analyses generally gave consistently higher HSE abundances than solution isotope dilution ICP-MS analyses (see also Figure 5.6). Table prepared by Dr. James M.D. Day and modified from Liss, Levy, and Day 2020: Table S4.

| LA-ICP-MS versus ID HSE data for artifacts and iron chunks (in ppb) | | | | | | | | |
|---|---|---|---|---|---|---|---|---|
| **Sample ID** | **Sample Type** | **Method** | **Re** | **Pd** | **Pt** | **Ru** | **Ir** | **Os** |
| **6740** | **Object** | ID | 6.20 | 1.06 | 1.05 | 4.18 | 1.80 | 0.16 |
| | | LA-ICP-MS | 10.9 | 32.9 | 0.40 | | 3.56 | 1.78 |
| **6849** | **Object** | ID | 10.23 | 0.26 | 1.28 | 2.32 | 1.04 | 0.18 |
| | | LA-ICP-MS | 10.10 | 33.72 | 4.83 | 2.31 | 8.81 | 1.96 |
| **6391** | **Object** | ID | 7.18 | 1.50 | 0.32 | 1.87 | 0.38 | 0.16 |
| | | LA-ICP-MS | 7.79 | 55.8 | 79.9 | 2.27 | 104.8 | |
| **6953** | **Object** | ID | 7.10 | 1.71 | 0.39 | 2.34 | 0.50 | 0.19 |
| | | LA-ICP-MS | 5.47 | 127.8 | 30.9 | 3.92 | 38.3 | 2.03 |
| **10637** | **Object** | ID | 3.04 | 2.76 | 0.71 | 2.47 | 0.68 | 0.23 |
| | | LA-ICP-MS | 10.6 | 49.4 | 14.9 | 3.46 | 9.32 | 0.69 |
| **7179** | **Unknown** | ID | 9.33 | 4.06 | 18.79 | 3.51 | 1.67 | 0.47 |
| | | LA-ICP-MS | 7.29 | 4.83 | 63.8 | 25.68 | 81.1 | 7.58 |
| **5636** | **Iron Chunk** | ID | 34.92 | 45.12 | 167.35 | 3.60 | 9.13 | 6.76 |
| | | LA-ICP-MS | 67.3 | 1933 | 423 | 18.9 | 48.2 | 6.6 |
| **10228** | **Iron Chunk** | ID | 21.17 | 1.57 | 17.36 | 1.73 | 1.98 | 1.80 |
| | | LA-ICP-MS | 199 | 1776 | 264 | 22 | 36 | 12 |
| **1514** | **Iron Chunk** | ID | 7.94 | 4.67 | 4.00 | 1.02 | 0.38 | 0.25 |
| | | LA-ICP-MS | 19.4 | 1638 | 17.6 | 14.5 | 2.0 | 2.0 |
| **722** | **Iron Chunk** | ID | 30.28 | 46.21 | 120.78 | 3.10 | 3.41 | 4.89 |
| | | LA-ICP-MS | 62.4 | 2080 | 633 | 22.5 | 48.5 | 9.5 |
| **680** | **Iron Chunk** | ID | 48.11 | 53.76 | 106.94 | 2.36 | 1.70 | 3.05 |
| | | LA-ICP-MS | 271 | 901 | 700 | 13.2 | 63.3 | 3.6 |
| **16356** | **Iron Chunk** | ID | 31.11 | 2.78 | 25.70 | 3.54 | 3.56 | 3.32 |
| | | LA-ICP-MS | 123 | 1786 | 231 | 15.5 | 29.9 | 8.5 |

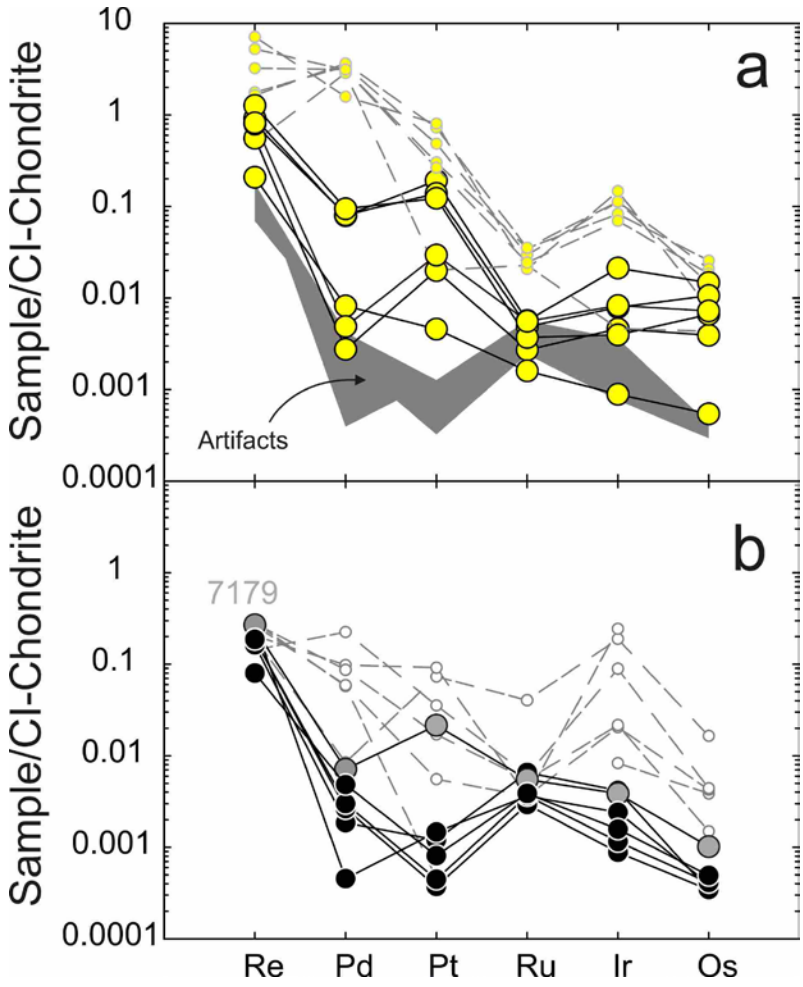


**Figure 5.5:** Highly siderophile element abundance patterns for (a) iron from iron-copper chunks and (b) iron objects from the Khirbat en-Nahas site normalized to CI-chondrite composition. Sample 7179 is shown in grey in (b). Dashed lines denote LA-ICP-MS analyses and solid lines denote isotope-dilution solution analyses of samples. CI-chondrite normalization from Day et al. 2016. Figure produced by Dr. James M.D. Day.

exposed interior of the sample, whereas ID work was performed on fragments without this discrimination. Finally, many of the analyses reached limits of detection (LOD) for LA-ICP-MS (1-10's ppb) yet are well above LOD for ID methods (typically 0.001 ppb). The HSE patterns obtained by LA-ICP-MS and ID for the iron chunks are also distinct from one another, with the LA-ICP-MS data being consistently elevated in palladium, suggesting possible mobilization of this element within the iron chunks during alteration.

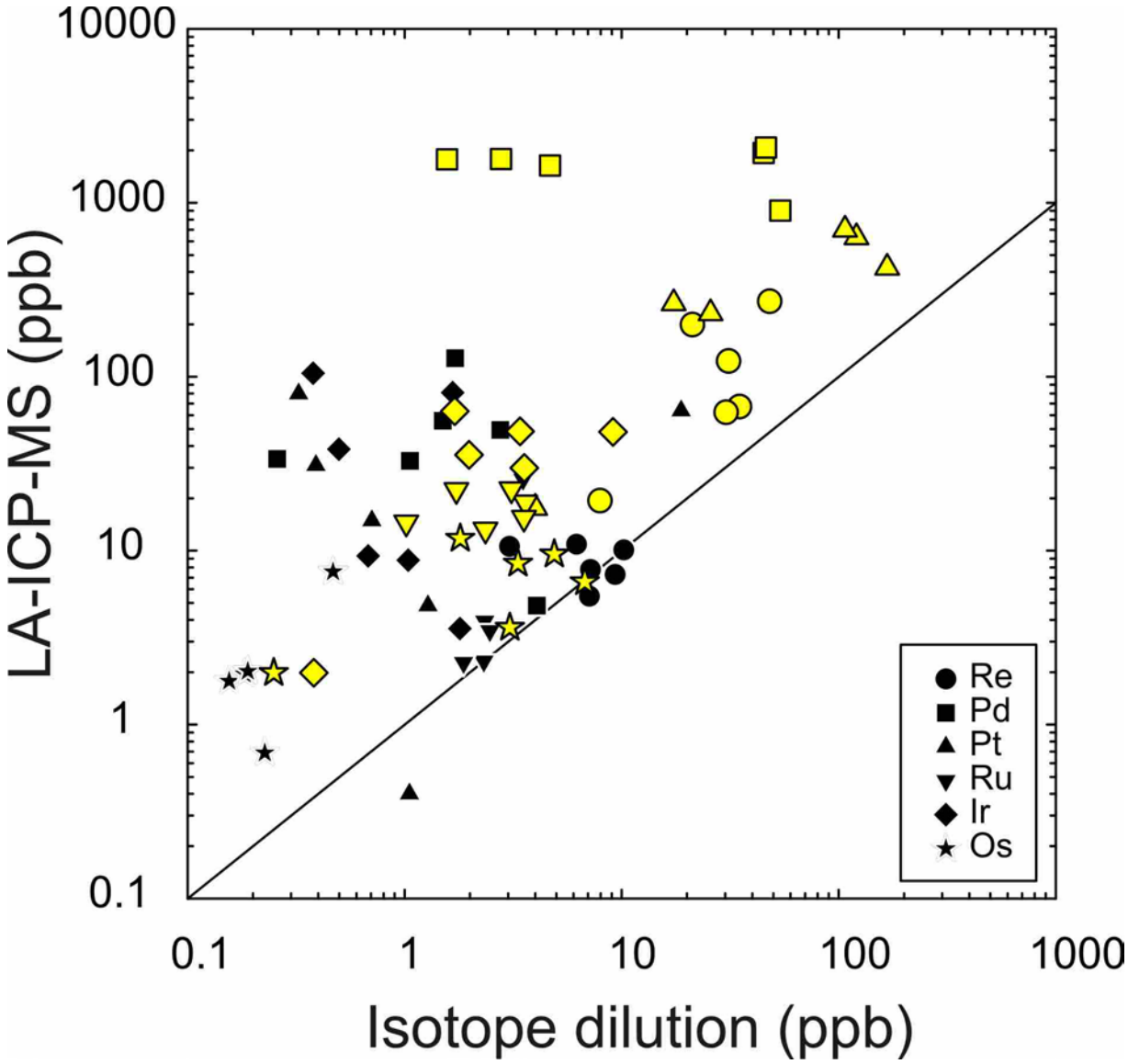


**Figure 5.6:** Comparison of Re, Pd, Pt, Ru, Ir, and Os concentration measurements for objects (black symbols) and iron from iron-copper chunks (yellow symbols) using Isotope Dilution ICP-MS and N-TIMS versus LA-ICP-MS. The line show in 1:1 – the LA-ICP-MS generally yielded higher concentration measurements. Here, Sample 7179 is included with the objects. Figure produced by Dr. James M.D. Day.

The iron objects measured by ID have lower absolute HSE abundances (ΣHSE = 10-15 ppb) compared with the iron from the chunks (ΣHSE = 18-265 ppb) (Table 5.6) and have both higher Ru/Ir and lower Os/Ir. Iron chunks have higher Pt/Ru (4-47) and have $^{187}Re/^{188}Os$ (46-194) generally lower than the objects (Pt/Ru = 0.2-0.6; $^{187}Re/^{188}Os$ = 83-353). Osmium isotopic

**Table 5.6:** Highly siderophile element abundance (in parts per billion - ppb) and Re-Os isotope systematics of Faynan samples. SE – Standard Error. Blank contributions are listed in Table 5.3 and a comparison of isotope dilution versus LA-ICP-MS data is available in Table 5.5. Table prepared by Dr. James M.D. Day.

| **Highly siderophile element abundance (ppb) and Re-Os isotope systematics of Faynan samples** | | | | | | | | | | |
|---|---|---|---|---|---|---|---|---|---|---|
| **Sample** | **Re** | **Pd** | **Pt** | **Ru** | **Ir** | **Os** | **$^{187}$Re/$^{188}$Os** | **2SE** | **$^{187}$Os/$^{188}$Os** | **2SE** |
| **Objects** | | | | | | | | | | |
| 6740 | 6.20 | 1.06 | 1.05 | 4.18 | 1.80 | 0.16 | 227.0 | 0.2 | 1.5119 | 0.0032 |
| 6849 | 10.2 | 0.26 | 1.28 | 2.32 | 1.04 | 0.18 | 352.8 | 0.3 | 2.4997 | 0.0042 |
| 6391 | 7.18 | 1.50 | 0.32 | 1.87 | 0.38 | 0.16 | 247.0 | 0.2 | 1.1463 | 0.0053 |
| 6953 | 7.10 | 1.71 | 0.39 | 2.34 | 0.50 | 0.19 | 215.2 | 0.2 | 1.5884 | 0.0047 |
| 10637 | 3.04 | 2.76 | 0.71 | 2.47 | 0.68 | 0.23 | 83.0 | 0.1 | 2.316 | 0.015 |
| **Unknown Identification** | | | | | | | | | | |
| 7179 | 9.33 | 4.06 | 18.79 | 3.51 | 1.67 | 0.47 | 162.6 | 0.2 | 5.419 | 0.026 |
| **Iron Chunks** | | | | | | | | | | |
| 5636 | 34.9 | 45.1 | 167 | 3.60 | 9.13 | 6.76 | 45.6 | 0.9 | 6.5068 | 0.0027 |
| 10228 | 21.2 | 1.57 | 17.4 | 1.73 | 1.98 | 1.80 | 104.0 | 0.5 | 6.5682 | 0.0054 |
| 1514 | 7.94 | 4.67 | 4.00 | 1.02 | 0.38 | 0.25 | 193.7 | 0.2 | 2.148 | 0.038 |
| 722 | 30.3 | 46.2 | 121 | 3.10 | 3.41 | 4.89 | 51.3 | 0.8 | 5.6466 | 0.0022 |
| 680 | 48.1 | 53.8 | 107 | 2.36 | 1.70 | 3.05 | 163.4 | 1.2 | 8.9684 | 0.0046 |
| 16356 | 31.1 | 2.78 | 25.7 | 3.54 | 3.56 | 3.32 | 84.6 | 0.8 | 6.8335 | 0.0036 |
| **DLS Ores** | | | | | | | | | | |
| WAG-57 | 0.593 | 0.850 | 7.48 | 0.135 | 0.049 | 0.003 | 1348 | 20 | 3.4463 | 0.0042 |
| WAJ-458 | 0.179 | 0.775 | 0.125 | 0.218 | 0.052 | 0.001 | 2568 | 39 | 19.82 | 0.02 |
| JAJ-1 | 0.772 | 0.624 | 0.068 | 0.151 | 0.038 | 0.004 | 1327 | 20 | 2.0349 | 0.0030 |

compositions are distinct between the iron chunks, objects, and ores. Iron chunks ($^{187}$Os/$^{188}$Os = 2.15-8.97) are generally more radiogenic than the objects ($^{187}$Os/$^{188}$Os = 1.15-2.50). On a $^{187}$Re/$^{188}$Os-$^{187}$Os/$^{188}$Os diagram (Figure 5.7), objects are consistent with generation from a less radiogenic initial source composition compared with the iron chunks. In general, iron objects and metal chunks have distinct geochemical compositions and Re-Os isotope systematics, with the exceptions of artifact 7179, which lies close to the majority of metal chunks, and metal chunk 1514, which lies within the field of objects (discussed below).

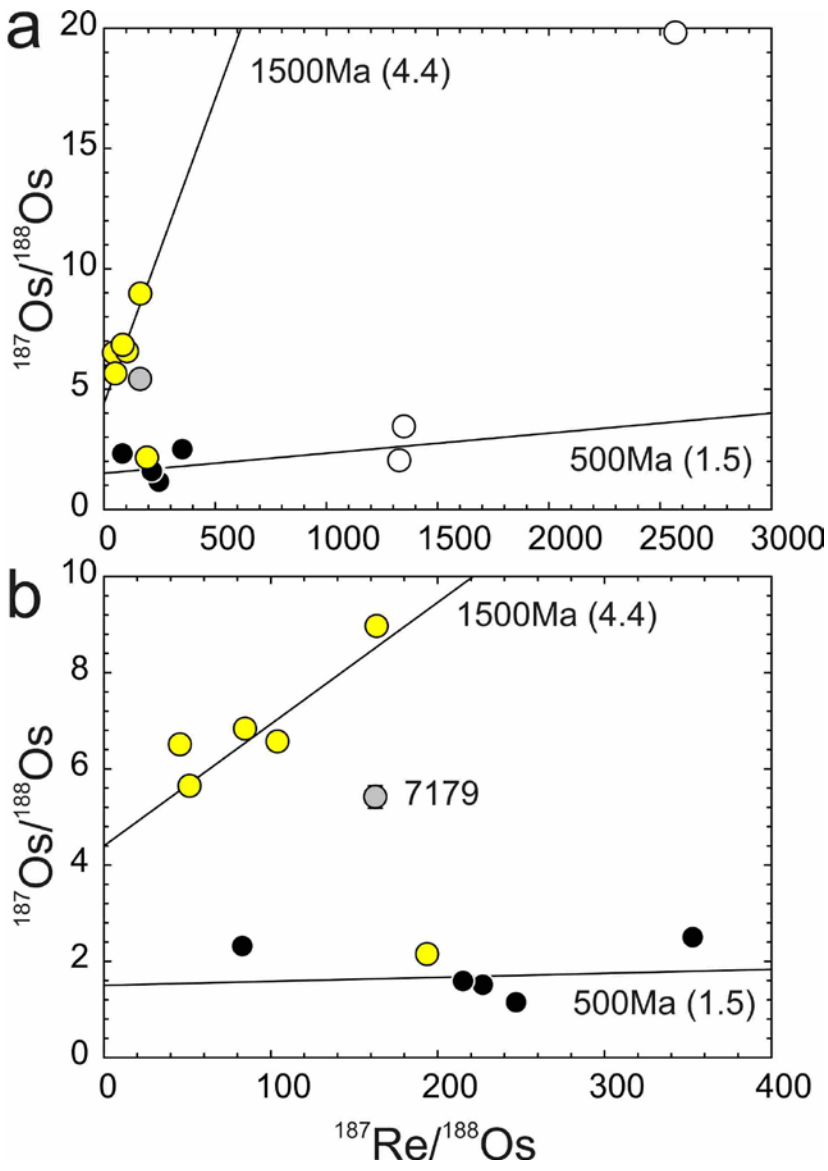


**Figure 5.7:** Rhenium-osmium isotope diagrams for (a) the full range of samples including chunks, objects, and ores and (b) expanded view for $^{187}Re/^{188}Os$ = <400 for objects (black circles), iron from chunks (yellow circles) and local DLS ores (unfilled circles). Shown for illustration are isochrons conforming to a ~500 Ma source with initial $^{187}Os/^{188}Os$ = 1.5 and a 1500 Ma source with $^{187}Os/^{188}Os$ = 4.4. Figure produced by Dr. James M.D. Day.

5.2.4.3 SEM-EDX of Metal Chunks and Iron Objects

The SEM-EDX was used to analyze several spots throughout each of the iron samples from the chunks and objects. Analyses revealed portions of the unpolished iron-copper chunks

had iron contents as high or equal to the LA-ICP-MS analyses (Figures 5.8-5.11). In some cases, the high iron content was also associated with an elevated phosphorous content – as high as 14 wt.% in the iron from the chunks. Copper was also identified in one of the iron-copper chunk samples (Sample 1514) reiterating that the samples can be mixtures of these two metals. Copper was not identified in all the samples (as might be expected) due to using the same samples from the LA-ICP-MS study; these samples were intentionally selected as they were primarily iron. The copper inclusion also had a high sulfur and iron content (16 wt.% and 8.6 wt.% respectively). The analysis of the iron objects indicated that they were primarily composed of iron-oxides.

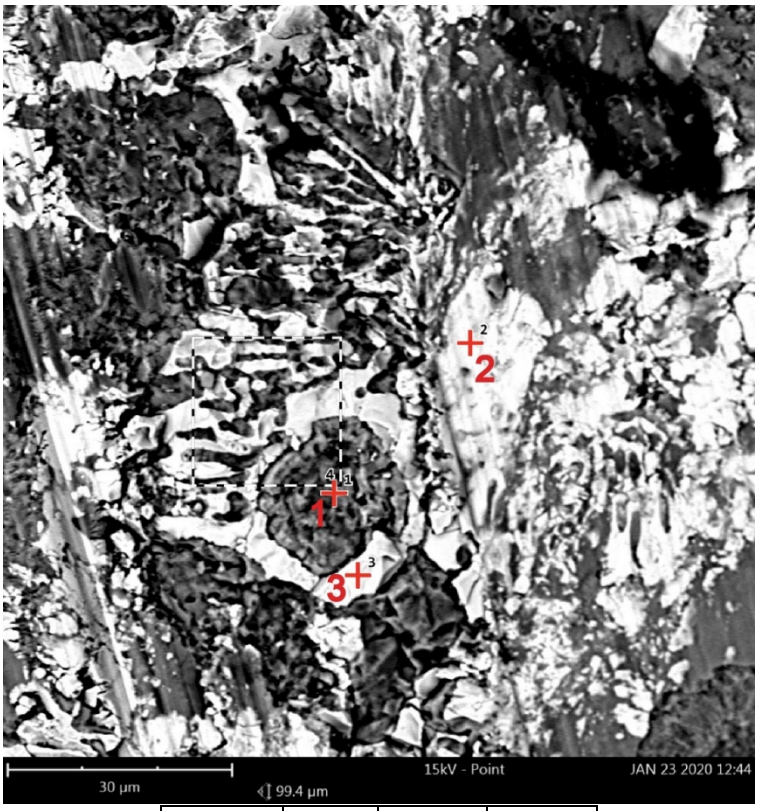


| Spot # | O | P | Fe |
|---|---|---|---|
| **2** | 6.42 | 12.32 | 81.25 |
| **3** | 2.46 | 12.73 | 84.80 |

**Figure 5.8:** SEM image of iron from chunk Sample 5636 with results of EDS analysis (presented in wt.%). The identification of iron-phosphide inclusions reiterates that the chunks were produced by smelting.

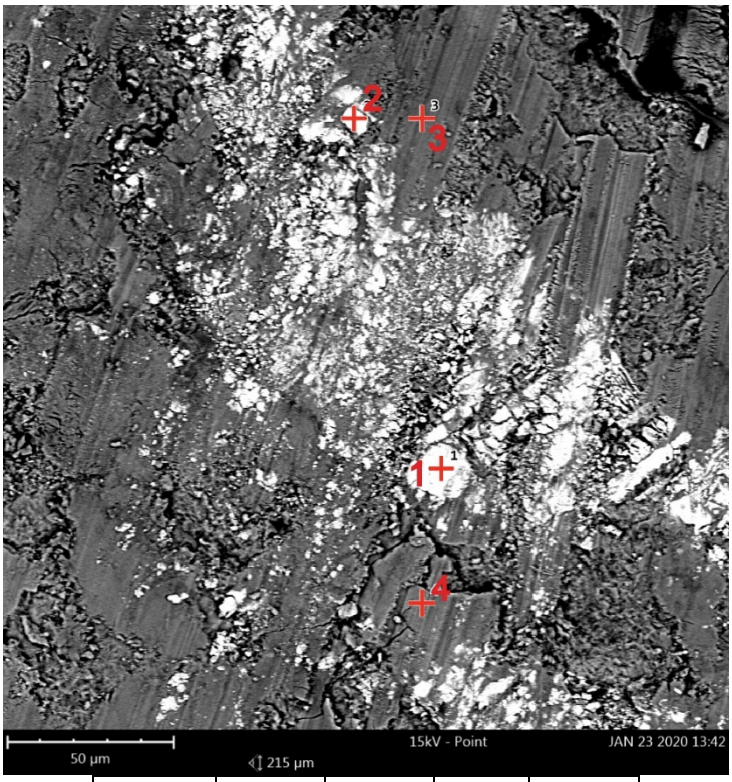


| Spot # | O | P | K | Fe |
|---|---|---|---|---|
| **1** | 9.26 | 10.99 | - | 79.75 |
| **3** | 9.91 | 10.88 | - | 80.21 |
| **4** | 37.65 | 2.92 | 1.18 | 58.25 |
| **5** | 37.82 | 2.42 | - | 59.66 |

**Figure 5.9:** SEM image and associated EDS results (presented in wt.%) for iron-copper chunk Sample 680 with evidence for P-rich iron.

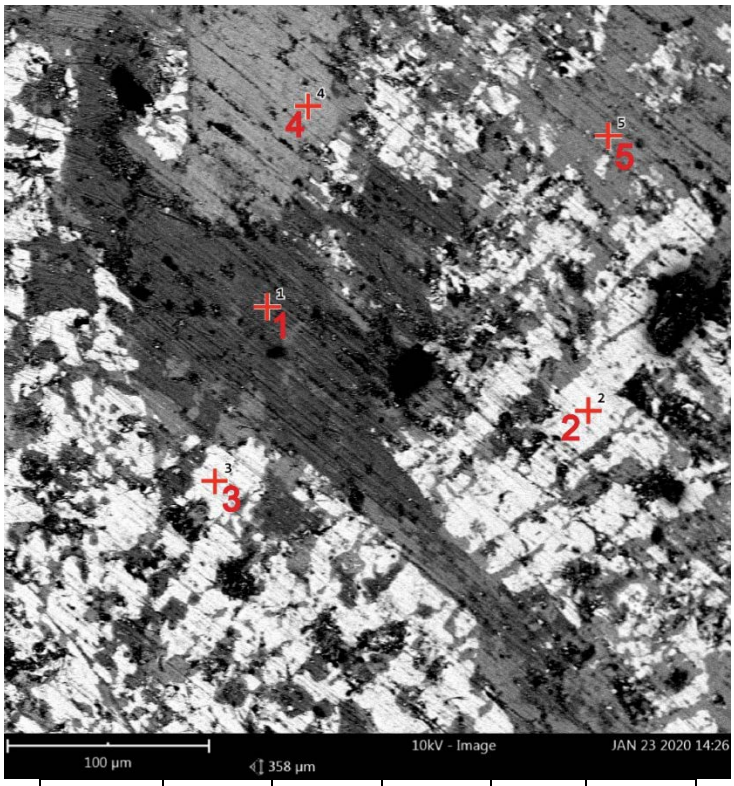


| Spot # | C | O | P | K | Fe |
|---|---|---|---|---|---|
| **1** | 10.32 | 47.08 | 8.80 | 4.15 | 29.66 |
| **2** | 13.11 | 2.98 | 11.41 | - | 72.51 |
| **3** | 15.68 | 5.87 | 11.51 | - | 66.95 |
| **4** | 10.88 | 26.57 | - | - | 62.54 |
| **5** | 9.58 | 35.75 | - | - | 45.32 |

**Figure 5.10:** SEM image and associated EDS results (presented in wt.%) for iron-copper chunk Sample 16356. The presence of significant carbon is likely a product of peak overlap.

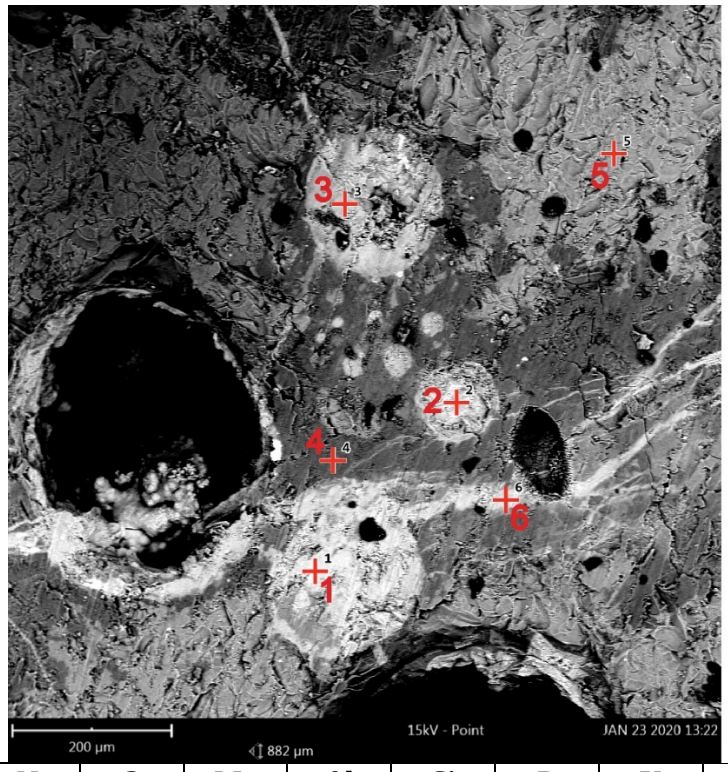


| Spot # | C | N | O | Mg | Al | Si | P | K | Ca | Mn | Fe |
|---|---|---|---|---|---|---|---|---|---|---|---|
| **1** | - | - | 45.54 | - | - | 2.73 | 1.37 | - | - | - | 50.36 |
| **2** | - | - | 48.54 | - | - | 7.47 | 1.37 | - | - | - | 41.61 |
| **3** | 6.32 | 5.40 | 47.63 | - | - | 2.15 | - | - | 1.25 | - | 37.31 |
| **4** | - | - | 49.20 | - | 4.19 | 17.13 | 4.96 | 3.06 | 5.63 | - | 15.83 |
| **5** | - | - | 46.15 | 1.27 | 2.22 | 12.71 | 5.07 | 1.98 | 8.96 | 5.31 | 16.32 |
| **6** | - | 5.00 | 45.77 | - | - | 4.60 | 2.31 | - | 1.89 | - | 40.42 |

**Figure 5.11:** SEM image and associated EDS analysis (presented in wt.%) from sample 7179. The results support a reinterpretation of this object as potentially a mixed iron-copper chunk (although there was no visible copper) or other waste product. The sample contains only inclusions of iron-oxides and a low iron content.

### 5.2.5 Discussion

As discussed in Chapter 3, the principal copper ore source mined in Faynan during the Iron Age was the Dolomite Limestone Shale (DLS) geological unit (See Hauptmann, 2007 for detailed discussion). The copper ores of the DLS formation were abundant and accessible in the Iron Age, and they are also characterized by an intergrowth of substantial manganese ores (Hauptmann 2007; Basta and Sunna 1972). Critically, the manganese ores in the DLS formation

were found to contain an average of 8-10 wt.% iron oxide ($Fe_2O_3$) with enrichments in hematite and goethite in some areas (Hauptmann 2007: 71; Basta and Sunna 1972). In contrast, the three copper ore samples analyzed here are poor in iron (Table 5.1), similar to eight samples of copper ore or ore bearing stone from the DLS analyzed previously that contained an average of only 0.98 wt.% iron oxide (Hauptmann 2007: Table 4.1). Thus, the manganese ores in the DLS seem to have a higher iron content in comparison to the copper ores.

Intentionally selecting copper ores with significant manganese from the DLS formation (as suggested by Hauptmann 2007: 251) would have introduced iron along with copper into the smelting furnaces – perhaps in the form of iron phosphides, discussed below. Moreover, an enrichment in iron oxides was identified in the DLS ores to the southeast of Khirbat en-Nahas, sampled here (WAG 57) (Hauptmann 2007: 71). Based on the results of our isotopic and abundance analysis, there are affinities in the Os isotopic compositions between some of the ore samples (particularly WAJ 548) and the iron and copper chunks. However, there are also key differences between the ore samples and metal chunks, the most prominent being high ruthenium and Os in the chunks and more radiogenic $^{187}Os/^{188}Os$ in the ores. These phenomena most likely reflect that the ore samples that we analyzed and those used in production of the iron chunks were not the same. Comparing HSE contents for average ore and iron chunk samples shows they have similar relative abundances of rhenium, palladium, platinum, ruthenium, and iridium but different Os, supporting the fact that the ores used to make the iron chunks and those that we measured, were different. This understanding is also reiterated by the rather low iron content in the sampled ores (Table 5.1). As the copper ores themselves do not appear to be the source for iron, we suggest that the mixed iron-copper chunks were a product of an iron-rich manganese fluxing agent within copper ores mined during the Iron Age. The DLS ores were exploited

throughout the Iron Age, so the appearance of the iron-copper mixtures only during the 10th-9th century BCE is likely a result of the technological advancements discussed above and the availability of Mn-rich materials; only during this period did the furnaces create the necessary reducing conditions to produce metallic iron from an Mn- and Fe-rich copper ore.

The combination of LA-ICP-MS and SEM-EDX analysis supports the understanding that the iron-copper chunks are smelting products rather than geological mixtures or other corroded minerals. The identification of iron phosphide fits with previous studies of copper produced in Faynan (Figure 5.8, Hauptmann 2007: 208-211). The DLS formation includes nodules and layers of phosphorite resulting in iron phosphide inclusions in Faynan copper (Hauptmann 2007: 209). In his study of copper slags from Iron Age Faynan, Hauptmann (2007: 209, Figure 6.4) found iron phosphide dendrites (with similar composition to what is seen in our study, Figure 5.8) associated with prills of α-Fe within copper inclusions trapped in slag. He further suggested that this is a unique quality of copper produced in Faynan and could potentially be used for provenance studies (Hauptmann 2007: 210-211). As such, the results here connect the iron chunks to smelting in Faynan. The identification of a copper sulfide inclusion in chunk Sample 1514 possibly reiterates that these artifacts are smelting products; copper sulfide inclusions also appear in slags excavated from Faynan (Ben-Yosef 2010: Figure 8.37). The presence of iron-oxides in the iron chunks is most likely the result of post-depositional corrosion, but it may also suggest that the success in producing metallic iron and the reducing conditions of the furnaces were variable. The LA-ICP-MS analyses support the dominance of iron in samples, whereas SEM-EDX analyses of the iron objects identified primarily iron-oxides, reiterating that the objects were strongly corroded (e.g., Figure 5.1).

The iron objects yield different Os isotopic ratios and distinct HSE patterns compared with the ores and the iron chunks (Figures 5.5 and 5.7), suggesting that they were not locally produced by separating/purifying the iron-copper mixtures. The best fit isochron for the objects would be ~500 Ma with initial $^{187}Os/^{188}Os$ of ~1.4. This is close to a Pan African age, possibly suggesting they were produced using ores from iron deposits similar to this age. In contrast, the best-fit for five of the six iron chunks is significantly older with initial $^{187}Os/^{188}Os$ of ~4.4; clearly distinct from the objects. Furthermore, although two of the ores measured have relatively low $^{187}Os/^{188}Os$ similar to the objects, their HSE patterns are distinct, having similar rhenium, platinum, and palladium enrichment to the mixed metal chunks. These results demonstrate that the iron objects were likely imports to Khirbat en-Nahas. The exception to the rule is object 7179, which appears similar in composition to the iron chunks, and iron chunk 1514 which falls in the composition of objects. This overlap is likely due to misidentification in morphology of materials (in the case of Sample 7279) or the possibility of far-field sourcing of ore. For example, Sample 7179 contains inclusions of iron-oxide and has much higher copper, cobalt, and nickel than the objects (Figure 5.11). As such, Sample 7179, which was originally interpreted as an object based on its unique shape, is more likely an iron chunk or other waste product. This reinterpretation explains the distinct Os isotopic and HSE composition of 7179 relative to the objects (Figures 5.5 and 5.7).

The idea that the majority of iron objects found at Khirbat en-Nahas are in fact imports is supported both by the scale of copper smelting in Faynan, and the evidence for iron production elsewhere in the Southern Levant during this time period. Copper production in Faynan during the Iron Age far exceeded local consumption; estimates suggest as much as 33,000-36,000 tons of metallic copper were produced during the $12^{th}$-$9^{th}$ centuries BCE, and most of the metal was

cast into ingots and exported from the region, which is reiterated by the lack of copper metal in the archaeological record of Faynan (Ben-Yosef 2010: 936; Yahalom-Mack et al. 2014a). The produced copper moved along trade routes to the west through the Negev Desert of modern Israel and beyond through ports along the Mediterranean coast reaching at least as far as Greece (Martin et al. 2013; Martin and Finkelstein 2014; Kiderlen et al. 2016; Ben-Dor Evian 2017; Ben-Dor Evian et al. 2021; Yahalom-Mack et al. 2014a; Vaelske, Bode, and Loeben 2019). Excavations in modern Israel and Jordan have also found several iron production sites dating to the Iron Age, during the $10^{th}$-$9^{th}$ centuries BCE when iron was becoming a more popular metal of use (Workman et al. 2020: Table 5; Ilani, Lederman, and Bunimovitz 2020; Rabinovich et al. 2019; Eliyahu-Behar et al. 2012, 2013; Yahalom-Mack and Eliyahu-Behar 2015; Veldhuijzen and Rehren 2007; Veldhuijzen 2009; Yahalom-Mack et al. 2014b). Among the sites producing iron during this period was Tell es-Safi/Gath, which was previously suggested to play a key role as an economic hub for the exchange of copper from Faynan (Workman et al. 2020: 229-230; Eliyahu-Behar et al. 2012; Ben-Yosef and Sergi 2018). Thus, copper could have been traded for iron objects at Tell es-Safi/Gath or other known iron-producing sites such as Tell Hammeh and returned to Faynan; this understanding is further supported by the presence of iron jewelry in a few Iron Age graves in Faynan, suggesting a value attached to the metal (Beherec 2011). Recent analysis of iron ores from the Aljoun region of Jordan (where Tell Hammeh is located) may provide additional support to these claims (Personal communication, Dr. Adi Eliyahu-Behar; Brauns et al. 2020). The $^{187}Os/^{188}Os$ ratio of the iron objects from Faynan are similar to those from the Aljoun ores, although this requires further investigation (Brauns et al. 2020: Table 3). Regardless, the import of iron objects produced from a different ore source would explain the Os isotopic differences between the objects and metal chunks in Faynan.

Returning to the mixed iron-copper chunks and the possible interpretations introduced above, our geochemical results critically counter the possibility that they were refined to extract iron and in turn support the claims that these mixed metals were either failed smelts treated as waste or an initial product of copper smelting that required purification to recover copper metal (as discussed in Ben-Yosef 2010: 736-737). Without separating the metals, the difficulty in working a mixture of iron and copper would render the chunks useless in their current state, perhaps supporting the interpretation that they were a waste material. The large number of these chunks excavated in Faynan could be additional evidence for this understanding (Ben-Yosef 2010: 823-824); excavations at Khirbat en-Nahas discovered many of these artifacts, but only limited copper artifacts and no ingots have been excavated from Iron Age smelting sites in the region to date (Ben-Yosef 2010). While Tylecote and Boydell (1978) successfully extracted metallic iron from a copper-iron mixture, it is possible this technological knowledge did not exist in Iron Age Faynan (especially considering the required ideal furnace charge and conditions to produce workable metal [Gale et al. 1990: 185]), or they otherwise lacked the necessary desire/stimulus to pursue iron production further (e.g., Snodgrass 1982: 292-293). It is also still plausible that the iron chunks were an initial smelting product that were subsequently refined to recover copper, rather than iron (Ben-Yosef 2010: 736-737, 822-824). This interpretation could similarly be supported by the abundance of these artifacts; they are associated with a sophisticated period of production perhaps unlikely to produce so many failed smelts (Ben-Yosef 2010: 824). Further support potentially comes from the Area F excavations at Khirbat en-Nahas which discovered a contemporaneous workshop which could have been dedicated to refining the mixed chunks (Ben-Yosef 2010: 257-265, 823-824). This area included a unique archaeometallurgical assemblage with a high number of bellows pipes (in comparison to other

areas at the site) and architectural installations or “cells” dedicated to metallurgy (Ben-Yosef 2010: 257, 265).

This data set provides additional evidence against the theory that iron objects were first produced using iron obtained from a copper smelt. While the iron in the chunks suggests the furnaces in Faynan created the required reducing conditions to produce metallic iron (which is a generally accepted phenomenon), the mixture of iron and copper was not used to create the excavated objects based on the isotope analysis. This conclusion does not completely rule out the production of iron objects in Faynan, but it is more likely that this would be a separate process not occurring in a copper smelting furnace (i.e., iron smelting), if at all. However, evidence to support this possibility is largely lacking based on current excavations which have yet to discover direct evidence for iron production such as smithing-hearth bottoms or other unambiguous iron smithing/smelting slags. It is also unlikely that direct iron smelting in Faynan would produce different HSE inter-element fractionations and especially Os signatures from the mixed chunks due to the high metal-silicate, metal-sulfide partition coefficients for these elements. Returning to the research question introduced at the beginning of this chapter, iron was not likely produced in Faynan as an adventitious byproduct of sophisticated copper smelting.

The production of the iron-copper chunks should probably be interpreted as an unintended result of an iron-rich furnace charge, not as innovative iron production. As such, this research is in line with the original issue raised by Merkel and Barrett (2000) that there is a lack of evidence for iron produced in a copper smelt being used to forge objects. However, Faynan is a singular case study, and the possibility of producing adventitious iron from copper smelting may still be identified in other regions of advanced copper metallurgy such as Timna (Gale et al. 1990; Craddock 1988) and Cyprus (Snodgrass 1982; Pickles and Peltenburg 1998; Kassianidou

1994; Muhly and Kassianidou 2012). Both regions have been considered possible candidates for the discovery of iron from copper smelting, and it remains debated (see previous citations and Erb-Satullo 2019: 575-576 for an overview). Notwithstanding and in consideration of the presented evidence, sites with direct and early evidence of iron smelting regardless of a presence of copper metallurgy should also maintain a focus of investigation (Erb-Satullo 2019). Worth noting are the excavations at Tell Hammeh that revealed one of the earliest iron production sites in the Levant to date (Veldhuijzen and Rehren 2007). Critically, the site currently lacks any evidence of copper production, and "the nature of [iron] production [at Tell Hammeh] contrasts markedly with contemporary Levantine copper production" (Erb-Satullo 2019: 584). Recent investigations at Tel Beth-Shemesh, another site in modern Israel with evidence of Iron Age iron production, suggest locally available iron-oxide concretions provided the raw material for iron smelting, providing additional evidence for direct iron smelting (Ilani, Lederman, and Bunimovitz 2020). Thus, it is also plausible that iron production in the Eastern Mediterranean was an independent discovery not directly associated with copper smelting.

Finally, within the framework of this dissertation, the results indicate that the iron objects excavated in Faynan should likely be interpreted as wealth finance that was exchanged for copper (reiterated by their discovery in wealthy graves at Wadi Fidan 40). While few in number, this provides new evidence for trade with the broader region during the Iron Age as other foreign imports are limited in the archaeological record in Faynan. In following, the results also support the claim that an elite class in Faynan controlled the political economy through the production and also the exchange of copper metal. It also highlights the feedback loops between the trade and technology subsystems for the culture system. As these iron objects are primarily associated with the final phase of copper smelting, their import may provide additional evidence that copper

was still being produced at a high enough quality to exchange for valuable exotica until the very end of the industry.

### 5.2.6 Future Directions

There are several possibilities for future directions to build on these results and continue investigating the origins of the iron artifacts in Faynan. First, a more detailed study of the mixed iron-copper chunks, using optical and scanning electron microscopy for metallography, could provide additional insight into the composition and function of these materials. While SEM was performed here, the samples were very small and not polished. A detailed study of larger samples including both iron and copper could be particularly beneficial in identifying if these materials could have been purified for copper metal. Second, a larger scale osmium isotope study of iron artifacts from the Southern Levant could help reveal the movement of the metal between sites. Specifically examining any iron materials excavated at Tell es-Safi/Gath to test for possible isotopic consistencies with the iron objects from Khirbat en-Nahas could potentially support the existence of exchange networks between these sites. Finally, additional iron material from Faynan could also be isotopically analyzed to broaden this unique dataset. As is discussed in the next section, possible slag prills and hammerscales enriched in iron were collected from sediment samples at Khirbat en-Nahas. Analyzing these remains could potentially test for evidence of working or experimentation with the iron-copper chunks if their isotopic signatures are comparable (discussed below). In general, the origins and development of iron production in the Levant remains enigmatic, but a broad dataset of Os isotope and HSE abundance analyses from sites throughout the region can contribute to answering this longstanding question.

## 5.3 Sediment Analysis for Iron Production Residues at Khirbat en-Nahas

### 5.3.1 Introduction

The metallurgical process to produce iron is sufficiently different than copper production to impact the way it is investigated in the archaeological record. While copper and bronze were typically heated into a liquid form in antiquity, iron, requiring a significantly higher melting temperature (ca. 1500°C in comparison to for ca. 1100°C copper), was only heated until malleable (Eliyahu-Behar et al. 2012: 255-256, 2013: Figure 2). In turn, the iron production *chaîne opértoire* required more manipulation and hammering of the metal at various stages. Specifically, early iron production, from ore to finished product, required at least three steps: 1) smelting ore to produce a bloom - a conglomerate of metal and slag that forms at the bottom of the furnace; 2) refining the bloom into a more compact and pure metal through hammering known as primary smithing; and 3) forging or secondary smithing to produce a final product (Eliyahu-Behar et al. 2013: 4319, Figure 2). Each step of this process results in residues and byproducts which can found in the archaeological record.

Iron slags are produced during each phase of iron production including tap and furnace slags. Tap slags are typically only associated with smelting, and furnace slags which often take the shape of the furnace/hearth bottom, known as smithing hearth or plano-convex bottom slags, can be produced during any step (Eliyahu-Behar et al. 2013: 4320). Thus, while slags are primary evidence for iron metallurgy, they are less indicative of the stage of production, i.e., smelting vs. smithing. In contrast, hammerscales and slag prills (also called spheroidal hammerscales or slag spheres) are formed only during smithing (Eliyahu-Behar et al. 2013: 4320, Figure 2; Starley 1995; Dungworth and Wilkes 2007). Hammerscales are produced when hot iron is struck with a hammer. The surface of hot iron is partially oxidized forming brittle

scales (resembling fish scales) that flake off during hammering (Starley 1995; Dungworth and Wilkes 2007: 7, Figures 11 and 15). Slag prills are solidified droplets of liquid slag that are similarly expelled from hot iron during working (Starley 1995; Dungworth and Wilkes 2007: Figure 17). Slag prills are identifiable by their spherical shape, occasionally also having a droplet tail, and they are typically associated with fire welding pieces of iron or refining a bloom (Starley 1995; Dungworth and Wilkes 2007). Both hammerscales and slag prills range in size from microscopic to a few millimeters in diameter/length, but they are very abundant in activity areas associated with primary and secondary smithing (e.g., around anvils in iron workshops). Despite their abundance, hammerscales and slag prills can be difficulty to identify in the archaeological record as they can often blend in with the sediment matrix. However, and perhaps most significant for archaeologists, hammerscales and slag prills are magnetic.

Recently, identification and collection of hammerscales and slag prills have become a primary focus of archaeological excavations in metallurgical contexts (Bayley, Dungworth, and Paynter 2001; Veldhuijzen and Rehren 2007; Veldhuijzen 2009; Eliyahu-Behar et al. 2012, 2013). Typically, these iron production residuals are collected by simply running a magnet through the sediment in metallurgical contexts and areas. This practice can be done in the field (as seen in Veldhuijzen and Rehren 2007) or in the lab by collecting sediment samples for this purpose. Identifying hammerscales and slag prills is beneficial in shedding light on the stage of iron production practiced in a given area and for identifying specific activity areas by mapping their locations and abundance (Veldhuijzen and Rehren 2007: Figure 11). As such, examining sediment samples from metallurgical contexts from Iron Age Faynan provides a valuable opportunity to test for possible iron working.

To date, no iron smelting slags have been identified in Faynan suggesting direct iron smelting was probably not a component of the metallurgical industry during the Iron Age (smithing slags also have not been excavated). However, excavations have not examined the sediments for other iron production residues such as hammerscales and slag prills. Given that the mixed iron-copper chunks might have provided iron metal without iron *smelting*, the archaeological record of Faynan might only include these residues and byproducts associated with *smithing*. In other words, if iron could be successfully extracted from the iron-copper chunks (although the isotope analysis above suggests otherwise), the forging of this iron into objects could produce hammerscales and slag prills. It is also possible that the evidence for iron smelting has not yet been discovered (especially considering Glueck's [1936b] suggestion that large-scale iron production was feasible in Faynan). As such, hammerscales and slag prills can provide tangible evidence of some working with iron despite the current lack of iron smelting/smithing slags.

Here, sediment samples from Khirbat en-Nahas were examined with a magnet and x-ray fluorescence to investigate for iron production residues. If iron smithing was occurring in Iron Age Faynan, Khirbat en-Nahas provides one of the most likely locations. As discussed, excavations at Khirbat en-Nahas yielded evidence for the most advanced copper smelting technologies, the mixed iron-copper chunks, iron objects, and the unique metallurgical assemblage of the Area F workshop (discussed further below). While the isotope analysis presented here indicates the mixed iron-copper chunks were not refined to produce iron objects, it is possible iron metal was collected/produced from another source. As such, examining the sediment samples from other iron production residues can provide further insight on this issue.

### 5.3.2 Sample Selection

Ideally, pristine sediment samples would be collected from small units across an excavation area and the magnetic portions would be extracted prior to any further sieving/analysis following the methodology established by Bayley, Dungworth, and Paynter (2001) and Veldhuijzen and Rehren (2007). However, this research relied on previously collected sediment samples, where this methodology was not employed[2]. Thus, samples were not collected across entire excavation areas or at a fine spatial resolution. During the 2002, 2006, and 2009 seasons at Khirbat en-Nahas, sediment samples were collected at various locations through the excavations periodically in random locations within an excavation area both in the fill and at floor levels, limiting the samples in the contextual extent and spatial resolution. Moreover, the primary goal for these sediment samples was originally for flotation to collect archaeobotanical material. As such, some samples were previously sieved and/or floated prior to being brought to UCSD for storage; this can be particularly problematic for identifying slag prills as they often contain air voids and can float (Starley 1995). Magnetic collection from the sediment samples was mainly used for identifying a presence or absence of magnetic material, and not for considering the distribution or comparative ratios of magnetic material across excavation areas/units. The magnetic percentage for individual samples (magnetic material weight/overall sediment sample weight) was still determined as it could be useful for identifying sediment samples that were particularly rich in magnetic material. Using the percentage of magnetic material rather than raw weight also avoids biases of particularly large or small sediment samples. In total, 46 sediment samples were examined from Khirbat en-Nahas. All available

[2] While a more rigorous sediment sampling strategy was used at Khirbat al-Jariya during the 2014 excavation season, the site predates the most advanced copper metallurgy in Faynan and is not a likely candidate for iron production (reiterated by the lack of mixed iron-copper chunks). As such, these sediment samples were not considered as part of this study.

sediment samples (i.e., currently in storage at UCSD) for contexts with possible connections to iron metallurgy including Area S (n=7), Area F (n=11), and Area R (n=27) were investigated (Table 5.7).

**Table 5.7:** Archaeological details for sediment samples analyzed for iron production residues. FX and FLOT are codes used by ELRAP excavations to designate a sediment sample collected for flotation. Yr. – Excavation Year, Ar. – Area, Loc. – Locus, Bask. – Basket, and Wt. – Weight in kilograms.

| Sediment Samples Analyzed for Iron Production Residues | | | | | | |
|---|---|---|---|---|---|---|
| **Yr.** | **Site** | **Ar.** | **Loc.** | **Bask.** | **Wt. (kg)** | **Notes and Visual Inspection** |
| 2002 | KEN | S | 279 | 5518 | 0.62 | FLOT 1/8 sample, dark brown and black |
| 2002 | KEN | S | 279 | 5519 | 0.71 | FLOT 1/8 sample, dark brown and black |
| 2002 | KEN | S | 331 | 7258 | 0.29 | 1/4 coarse flot soil sample, dark brown/black, slag bits |
| 2002 | KEN | S | 281 | 5520 | 0.36 | FLOT 1/4 sample, black and brown |
| 2002 | KEN | S | 303 | 5890 | 0.46 | FLOT 1/8 sample, dark brown and black, bits of slag |
| 2002 | KEN | S | 285 | 5773 | 0.55 | Coarse 1/4 sample flot, dark brown and black, crushed slag |
| 2002 | KEN | S | 275 | 5993 | 0.23 | Coarse 1/4 sample flot, soil sample from under B.5989, slag |
| 2006 | KEN | F | 880 | 1256 | 1.46 | Large mesh, significant copper |
| 2006 | KEN | F | 885 | 1282 | 0.47 | Soil sample, large mesh, copper bits, dark brown/black |
| 2006 | KEN | F | 890 | 1323 | 0.97 | Soil sample, large mesh, copper bits, slag bits |
| 2006 | KEN | F | 883 | 1298 | 0.40 | Soil sample, large mesh, bits of copper, slag bits |
| 2006 | KEN | F | 883 | 1298 | 23.00 | soil sample, fine mesh, dark brown |
| 2006 | KEN | F | 893 | 2328 | 0.46 | soil sample from installation, large mesh, dark, bits of slag |
| 2006 | KEN | F | 901 | 1407 | 0.69 | Large mesh, red color, bits of slag |
| 2006 | KEN | F | 893 | 1377 | 0.86 | Large mesh sample, ashy, tech ceramics?, tan, black |
| 2006 | KEN | F | 895 | 1366 | 0.46 | Soil sample large mesh, green in color, significant copper |
| 2006 | KEN | F | 876 | 1439 | 0.95 | Large mesh, light brown |
| 2006 | KEN | F | 860 | 1444 | 0.38 | Light brown, bits of slag |
| 2006 | KEN | R | 1842 | 16421 | 0.80 | Soil sample large mesh, black, lots of slag |
| 2006 | KEN | R | 1807 | 16050 | 1.46 | Soil sample, large mesh, lots of shell |
| 2006 | KEN | R | 1832 | 16357 | 2.45 | Large slag bits, charcoal, black and brown |
| 2006 | KEN | R | 1828 | 16263 | 0.69 | Black, large slag bits |
| 2006 | KEN | R | 1832 | 16316 | 0.89 | Soil sample large mesh, rocks, crushed slag, copper, bone |
| 2006 | KEN | R | 1828 | 16261 | 0.89 | Large mesh soil sample, black, lots of slag, charcoal, bone |
| 2009 | KEN | R | 53 | 397 | 3.56 | FX-soil sample, light brown, very fine, some stones |
| 2009 | KEN | R | 49 | 395 | 5.14 | FX- soil sample, ash layer, bits of rock, slag, and charcoal |
| 2009 | KEN | R | 49 | 362 | 9.11 | FX - soil sample, dark brown, bits of slag and rock |
| 2009 | KEN | R | 71 | 888 | 6.82 | FX, black, lots of large bits of slag, charcoal |
| 2009 | KEN | R | 135 | 1432 | 1.07 | FX, very dark brown/black, fine |
| 2009 | KEN | R | 135 | 1416 | 3.25 | FX, dark brown, fine, bits of slag |
| 2009 | KEN | R | 128 | 1385 | 5.80 | FX - soil sample, light brown/tan, bits of slag and stone |
| 2009 | KEN | R | 96 | 1153 | 6.25 | FX - soil sample, black, slag rich, charcoal |
| 2009 | KEN | R | 135 | 1479 | 4.22 | FX, technical ceramics, bits of slag and charcoal |
| 2009 | KEN | R | 134 | 1387 | 6.38 | FX - soil sample, light brown, rock and slag, copper bits |
| 2009 | KEN | R | 143 | 1526 | 1.41 | Soil sample - ash pocket, gray |
| 2009 | KEN | R | 135 | 1587 | 2.60 | FX - in furnace, dark brown/black, bits of slag and charcoal |
| 2009 | KEN | R | 33 | 149 | 12.7 | Soil sample, light brown, rocky, bits of slag |
| 2009 | KEN | R | 122 | 1329 | 7.54 | FX, black, slag rich - crushed and large bits |
| 2009 | KEN | R | 129 | 1386 | 8.75 | FX - soil sample, tan, rocky, small slag |
| 2009 | KEN | R | 144 | 1512 | 8.95 | FX, brown, rocky, bits of slag |
| 2009 | KEN | R | 59 | 454 | 4.98 | FX - soil sample, dark brown, small bits of slag, copper |

**Table 5.7:** Archaeological details for sediment samples analyzed for iron production residues. FX and FLOT are codes used by ELRAP excavations to designate a sediment sample collected for flotation. Yr. – Excavation Year, Ar. – Area, Loc. – Locus, Bask. – Basket, and Wt. – Weight in kilograms (Continued).

| Sediment Samples Analyzed for Iron Production Residues | | | | | | |
|---|---|---|---|---|---|---|
| **Yr.** | **Site** | **Ar.** | **Loc.** | **Bask.** | **Wt. (kg)** | **Notes and Visual Inspection** |
| 2009 | KEN | R | 55 | 451 | 5.96 | FX - soil sample, light brown, rocky |
| 2009 | KEN | R | 92 | 1050 | 2.71 | FX, dark brown/black, bits of slag and charcoal |
| 2009 | KEN | R | 93 | 1120 | 2.74 | FX - soil sample, dark brown/black, slag |
| 2009 | KEN | R | 97 | 1123 | 7.72 | FX - soil sample, tan, rocky |
| 2009 | KEN | R | 63 | 626 | 7.70 | FX, dark brown, rocky |

### 5.3.3 Methods

#### 5.3.3.1 Magnetic Collection

Collecting a magnetic fraction from a sediment sample is a straightforward process requiring only a strong magnet, a scale, and space to work. First, all samples were weighed prior to collecting/removing any material for determining the percentage of magnetic material and for posterity. After the weight was recorded, a small amount of sediment was removed and bagged to maintain an unaltered sub-sample for future investigations. The sediment sample was then spread into a thin layer (1-3 centimeters thick) across the workspace (Figure 5.12). Next, the magnet was simply dragged through the sediment in slightly overlapping transects across the entirety of the sample - repeating this step as many times as necessary to collect all the material. Any collected magnetic material was removed from the magnet, weighed, and bagged separately from the remaining non-magnetic sediment. The magnetic collection was then examined separately to identify any visible hammerscales and prills (using a low magnification optical microscope if necessary) as the magnet can collect other materials such as bits of slag, iron-rich fired clays, oxidized iron-rich stones, flakes/bits of corroded iron artifacts with some remaining

metal, etc. (Starley 1995). If identified, possible hammerscales and prills were also collected and bagged separately. Magnetic collection was completed for all 46 of the sediment samples.


**Figure 5.12:** Methodology for collecting magnetic material from a sediment sample. The sample is spread into a thin layer and the magnet is dragged through the sediment to collect any magnetic material (some collected material is visible on the magnet – black square in the top left corner). Photograph credit: Brady Liss, UCSD Levantine and Cyber Archaeology Lab.

#### 5.3.3.2 X-Ray Fluorescence

As mentioned, not everything collected with a magnet is necessarily a hammerscale or prill indicative of iron metallurgy. In the case of Faynan, it was also expected that the magnetic material would include small bits of iron-copper chunks and prills that were collected in the

sediment sample. To further investigate some of the identified magnetic material, a selection was analyzed with x-ray fluorescence (XRF). XRF is a technique for analyzing the elemental composition of materials based on atomic properties. The atoms of specific elements are characterized by a unique electron structure (Kaiser 2010: 4). These electrons orbit the nucleus in levels (or "shells") that are associated with a specific energy binding the electrons to the nucleus of the atom. The innermost electron shells must remain full for an atom to be stable. Should an electron be removed from an inner shell, the atom becomes unstable, and it will fill the vacancy with an electron from an outer shell (Kaiser 2010: 4). When an electron moves from an outer shell to one closer to the nucleus, less binding energy is required to maintain the electron's orbit; the excess energy from the shell transition is released. This process is known as fluorescence, and the amount of energy emitted is unique to each element (Kaiser 2010: 4).

The XRF measures elemental contents in essentially a two-step process: displacing the inner electrons in the atoms of a sample and detecting the fluorescing energies of the outer electrons. For the first stage, the XRF generates enough energy to penetrate the inner electron shells of elements. By bombarding the sample with sufficient energy to exceed the electron binding energies, the XRF instrument successfully excites and displaces the inner electrons of elements within the designated energy range. Second, as the vacancies are filled by higher orbiting electrons and fluorescing energies disperse from atoms, the instrument's detector registers these energies which in turn can be used to determine the present elements.

For this dissertation, a Bruker TRACeR III-V+ hand-held XRF was used (the same instrument used by Ben-Yosef [2010, et al. 2019]). The Bruker can generate energy up to 45 kV to penetrate the inner electron shells of elements between magnesium and uranium on the Periodic Table. The amount of energy emitted by the x-ray tube, and thus which elements are

excited/analyzed, can be controlled through the Bruker software and further refined with interchangeable filters. The energy is dispersed through a three-by-four millimeter window at the nose of the instrument, and the fluorescence energy from the sample is collected by a Si detector (Kaiser 2010: 8). In the case of this Buker TRACeR, the detector collects all the x-rays released by the sample and subsequently sorts them based on the number of electrons knocked free from the detector material; this is known as Energy Dispersive X-Ray Fluorescence (ED-XRF) (Kaiser 2010: 4). The processing system within the instrument converts the data into a spectrum which is visible on the attached laptop computer. The spectra represent the presence of elements within the analyzed sample and relative amounts can be roughly determined based on the location and heights of the peaks.

In total, 18 samples of potential hammerscales and prills were analyzed with the XRF to determine the elemental composition. Samples were selected from each of the excavation areas with sediment samples including Area F (n=6), Area R (n=11), and Area S (n=1). The main goal was to use the XRF results to help determine if the magnetic material was the residue of iron production. Samples were selected based on visual inspection for materials that appeared to be most similar to the expected morphology of an iron hammerscale or slag prill. In order to just generally examine what elements were present in the samples, the XRF was set to screen for any elements that can be identified with the instrument, without particular focus on any element/element class. Each sample was analyzed for 90 seconds at 40 kV and 15 μA without a filter or vacuum. Finally, to assist with interpreting the data, all the XRF spectra were converted into net photon counts (the number of counts recorded by the XRF for a particular energy level) using the Bruker Artax software. While the XRF spectra are beneficial for identifying the presence of an element, the heights of the peaks can be impacted by inter-elemental effects –

such as when the peaks of elements overlap, for example – and therefore are not necessarily indicative of the amount of an element present (Kaiser 2010: 9-10; Bloch 2015: 11). In contrast, the Artax software uses a Bayesian Deconvolution to correct such phenomena, and exports net photon counts which can be more reliably used as semi-quantitative data for the amounts of the elements present (Bloch 2015: 11). Together, the spectra and net photon counts provide a basis for understanding the elemental components of the hammerscales and slag prills.

### 5.3.4 Results

#### 5.3.4.1 Magnetic Material

After examining all the samples with the magnet, 40 of the 46 samples yielded some amount of magnetic material (at least one gram) totaling 1.35 kilograms. In general, the magnetic fraction from the sediment samples was much more abundant than expected, including more material than just hammerscales and/or prills such as small bits and chunks of iron-copper mixtures and slag (Figure 5.13). The average percentage of magnetic material in comparison to the total weight of a sediment sample was 1.66% across all samples; this number was used as the benchmark for determining particularly magnetic samples discussed further below (Table 5.8). Sample 1256 from Area F was very unique with 19.04% magnetic material; the next highest magnetic percentage was 3.96% also from Area F (Table 5.8). The examination of the separated magnetic material also identified what appeared to be hammerscales and slag prills in all areas, although in small numbers – approximately 5-20 individual scales and prills in any given sample (Figure 5.14).

**Figure 5.13:** Magnetic collection from sediment Sample 1256, Area F, Khirbat en-Nahas. Note the abundant amount of magnetic material including bits of slag and other material. Photograph credit: Brady Liss, UCSD Levantine and Cyber Archaeology Lab.

**Table 5.8:** The weight (Wt.) of magnetic material collected from all analyzed sediment samples and the magnetic percentage = magnetic weight/total sample weight. Note that the total weight is presented in kilograms and the magnetic weight in grams (total weight was converted to grams for determining the magnetic percentage).

| Magnetic Weights and Percentages for Analyzed Sediment Samples | | | | | | | |
|---|---|---|---|---|---|---|---|
| **Year** | **Site** | **Area** | **Locus** | **Basket** | **Total Wt. (kg)** | **Mag. Wt. (g)** | **Percentage** |
| 2002 | KEN | S | 279 | 5518 | 0.62 | 0.00 | 0.00 |
| 2002 | KEN | S | 279 | 5519 | 0.71 | 0.00 | 0.00 |
| 2002 | KEN | S | 331 | 7258 | 0.29 | 7.00 | 2.46 |
| 2002 | KEN | S | 281 | 5520 | 0.36 | 6.00 | 1.69 |
| 2002 | KEN | S | 303 | 5890 | 0.46 | 2.00 | 0.43 |
| 2002 | KEN | S | 285 | 5773 | 0.55 | 4.00 | 0.73 |
| 2002 | KEN | S | 275 | 5993 | 0.23 | 5.00 | 2.17 |
| 2006 | KEN | F | 880 | 1256 | 1.46 | 277.00 | 19.04 |
| 2006 | KEN | F | 885 | 1282 | 0.47 | 22.00 | 4.73 |
| 2006 | KEN | F | 890 | 1323 | 0.97 | 21.00 | 2.16 |
| 2006 | KEN | F | 883 | 1298 | 0.40 | 8.00 | 2.00 |
| 2006 | KEN | F | 883 | 1298 | 23.00 | 0.10 | 0.00 |
| 2006 | KEN | F | 893 | 2328 | 0.46 | 8.00 | 1.74 |
| 2006 | KEN | F | 901 | 1407 | 0.70 | 2.00 | 0.29 |
| 2006 | KEN | F | 893 | 1377 | 0.86 | 0.00 | 0.00 |
| 2006 | KEN | F | 895 | 1366 | 0.46 | 18.00 | 3.96 |
| 2006 | KEN | F | 876 | 1439 | 0.95 | 15.00 | 1.58 |
| 2006 | KEN | F | 860 | 1444 | 0.38 | 4.00 | 1.07 |
| 2006 | KEN | R | 1842 | 16421 | 0.80 | 18.00 | 2.25 |
| 2006 | KEN | R | 1807 | 16050 | 1.46 | 0.00 | 0.00 |
| 2006 | KEN | R | 1832 | 16357 | 2.45 | 17.00 | 0.70 |
| 2006 | KEN | R | 1828 | 16263 | 0.70 | 27.00 | 3.88 |
| 2006 | KEN | R | 1832 | 16316 | 0.90 | 25.00 | 2.79 |
| 2006 | KEN | R | 1828 | 16261 | 0.88 | 24.00 | 2.74 |
| 2009 | KEN | R | 53 | 397 | 3.56 | 13.00 | 0.37 |
| 2009 | KEN | R | 49 | 395 | 5.14 | 91.00 | 1.77 |
| 2009 | KEN | R | 49 | 362 | 9.11 | 18.00 | 0.20 |
| 2009 | KEN | R | 71 | 888 | 6.82 | 77.00 | 1.13 |
| 2009 | KEN | R | 135 | 1432 | 1.07 | 0.00 | 0.00 |
| 2009 | KEN | R | 135 | 1416 | 3.25 | 29.00 | 0.89 |
| 2009 | KEN | R | 128 | 1385 | 5.80 | 5.00 | 0.09 |
| 2009 | KEN | R | 96 | 1153 | 6.25 | 72.00 | 1.15 |
| 2009 | KEN | R | 135 | 1479 | 4.22 | 4.00 | 0.09 |
| 2009 | KEN | R | 134 | 1387 | 6.38 | 6.00 | 0.09 |
| 2009 | KEN | R | 143 | 1526 | 1.41 | 40.00 | 2.84 |
| 2009 | KEN | R | 135 | 1587 | 2.60 | 81.00 | 3.12 |
| 2009 | KEN | R | 33 | 149 | 12.65 | 10.00 | 0.08 |
| 2009 | KEN | R | 122 | 1329 | 7.54 | 169.00 | 2.24 |
| 2009 | KEN | R | 129 | 1386 | 8.75 | 14.00 | 0.16 |
| 2009 | KEN | R | 144 | 1512 | 8.95 | 11.00 | 0.12 |
| 2009 | KEN | R | 59 | 454 | 4.98 | 31.00 | 0.62 |

**Table 5.8:** The weight (Wt.) of magnetic material collected from all analyzed sediment samples and the magnetic percentage = magnetic weight/total sample weight. Note that the total weight is presented in kilograms and the magnetic weight in grams (total weight was converted to grams for determining the magnetic percentage) (Continued).

| Magnetic Weights and Percentages for Analyzed Sediment Samples (Continued) | | | | | | | |
|---|---|---|---|---|---|---|---|
| **Year** | **Site** | **Area** | **Locus** | **Basket** | **Total Wt. (kg)** | **Mag. Wt. (g)** | **Percentage** |
| 2009 | KEN | R | 55 | 451 | 5.96 | 1.00 | 0.02 |
| 2009 | KEN | R | 92 | 1050 | 2.71 | 38.00 | 1.40 |
| 2009 | KEN | R | 93 | 1120 | 2.74 | 82.00 | 2.99 |
| 2009 | KEN | R | 97 | 1123 | 7.72 | 1.00 | 0.01 |
| 2009 | KEN | R | 63 | 626 | 7.70 | 44.00 | 0.57 |

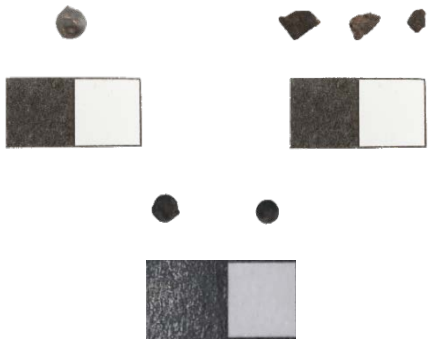

**Figure 5.14:** Representative slag prills and hammerscales collected with the magnet from Areas F, R, and S at Khirbat en-Nahas. Note that the scale on the bottom image is 0.5 centimeter and 1 centimeter in the top images.

5.3.4.2 X-Ray Fluorescence (XRF)

In general, the XRF results indicated the main elements in individual hammerscales and slag prills were iron and manganese (Table 5.9). Other elements identified included copper, lead, calcium, and potassium among smaller amounts of other metals such as zinc and titanium (Table 5.9). The XRF results for materials from Area F specifically revealed that these materials (both hammerscales and slag prills) were consistently and primarily iron, with some other elements

**Table 5.9:** Net photon counts from XRF analysis of possible hammerscales and prills collected from Khirbat en-Nahas sediment samples. Photon counts provide semi-quantitative amounts for the elements present in the sample. The letter under the element symbol is the electron shell.

| Net Photon Counts for Possible Hammerscales and Slag Prills from Khirbat en-Nahas | | | | | | | | | | | | | | | |
|---|---|---|---|---|---|---|---|---|---|---|---|---|---|---|---|
| **Sample** | **Si K12** | **K K12** | **Ca K12** | **Ti K12** | **Mn K12** | **Fe K12** | **Ni K12** | **Cu K12** | **Zn K12** | **Rb K12** | **Sr K12** | **Pb L1** | **Pb M1** | **Rh K12** | **Rh L1** |
| KEN_2002_AreaS_B5993_Prill | 2137 | 3729 | 18967 | 6313 | 577347 | 44245 | 313 | 6747 | 1178 | 120 | 8764 | 2708 | 600 | 6209 | 4684 |
| KEN_2006_AreaF_L860_B1440_Prill | 1604 | 933 | 13250 | 1406 | 4399 | 604512 | 775 | 38153 | 417 | 3808 | 1811 | 6125 | 111 | 4872 | 4061 |
| KEN_2006_AreaF_L876_B1439_Scales | 6313 | 9997 | 62911 | 4260 | 6171 | 195574 | 1465 | 61174 | 1906 | 2080 | 2843 | 74977 | 1702 | 7942 | 3814 |
| KEN_2006_AreaF_L883_B1298_Scale | 14749 | 32066 | 8472 | 9326 | 10394 | 270636 | 1986 | 24789 | 2074 | 3788 | 3853 | 2038 | 217 | 7747 | 5373 |
| KEN_2006_AreaF_L883_B1298_Scale2 | 13736 | 30236 | 12022 | 9316 | 14253 | 335297 | 1579 | 13678 | 2917 | 3586 | 5816 | 3264 | 112 | 8176 | 5330 |
| KEN_2006_AreaF_L885_B1282_Scales | 793 | 272 | 28619 | 651 | 46037 | 439937 | 621 | 62504 | 3852 | 1633 | 3356 | 28127 | 982 | 4987 | 4906 |
| KEN_2006_AreaF_L890_B1323_Prills | 304 | 446 | 5370 | 669 | 12973 | 211358 | 711 | 9237 | 1924 | 164 | 938 | 14468 | 186 | 5610 | 7838 |
| KEN_2006_AreaR_L1832_B16357_Scale | 7850 | 13970 | 12688 | 7388 | 114715 | 177739 | 1024 | 84504 | 7881 | 2725 | 4238 | 19569 | 1293 | 8912 | 4295 |
| KEN_2006_AreaR_L1842_B16421_Prill | 1720 | 5036 | 15616 | 2146 | 348485 | 177924 | 142 | 88213 | 3043 | 346 | 7894 | 4446 | 51 | 5624 | 4131 |
| KEN_2009_AreaR_L49_B395_Prill | 1621 | 3983 | 29855 | 1605 | 334534 | 201225 | 247 | 76190 | 1150 | 386 | 6902 | 3319 | 134 | 5473 | 2888 |
| KEN_2009_AreaR_L49_B395_Prill2 | 409 | 763 | 8793 | 303 | 129243 | 303919 | 310 | 3871 | 1181 | 299 | 766 | 1144 | 2 | 5203 | 6793 |
| KEN_2009_AreaR_L49_B395_Scales | 14342 | 32544 | 5174 | 7570 | 36783 | 319732 | 1487 | 39763 | 2542 | 2375 | 2300 | 4385 | 35 | 6432 | 5004 |
| KEN_2009_AreaR_L059_B0454_Prill | 1221 | 3507 | 11192 | 644 | 29518 | 407070 | 296 | 13512 | 3003 | 1765 | 1002 | 50041 | 308 | 5503 | 5250 |
| KEN_2009_AreaR_L059_B0454_Prill2 | 883 | 906 | 13002 | 1101 | 59291 | 325725 | 303 | 11207 | 1200 | 453 | 1715 | 2494 | 61 | 5907 | 6908 |
| KEN_2009_AreaR_L71_B888_Prills | 1164 | 1855 | 46674 | 1251 | 184895 | 74156 | 643 | 14564 | 7135 | 76 | 3751 | 5553 | 86 | 6185 | 7712 |
| KEN_2009_AreaR_L71_B888_Scale | 973 | 2889 | 5624 | 2167 | 435705 | 66920 | 11 | 53787 | 7877 | 145 | 5568 | 6658 | 56 | 3016 | 3383 |
| KEN_2009_AreaR_L096_B1153_Prill | 377 | 4806 | 11898 | 1819 | 429563 | 64502 | 261 | 14670 | 2217 | 55 | 3927 | 1217 | 107 | 6316 | 6233 |
| KEN_2009_AreaR_L096_B1153_Scale | 5128 | 14595 | 7681 | 3940 | 150820 | 144824 | 759 | 69823 | 8907 | 888 | 2701 | 14829 | 519 | 7901 | 6234 |

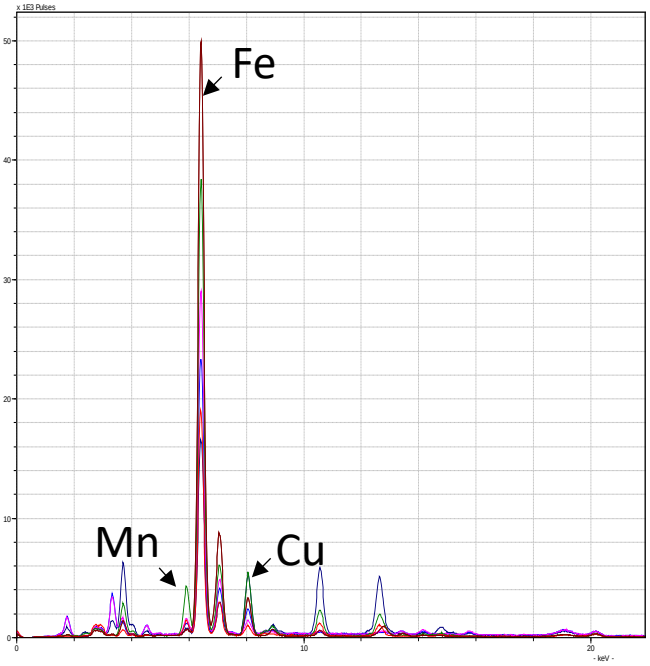


**Figure 5.15:** Overlay of all XRF spectra for analyzed possible hammerscales and slag prills from Area F (n=6). Note the dominant iron peak for all samples; the smaller peak between iron and copper is a secondary iron peak (see also Table 5.9).

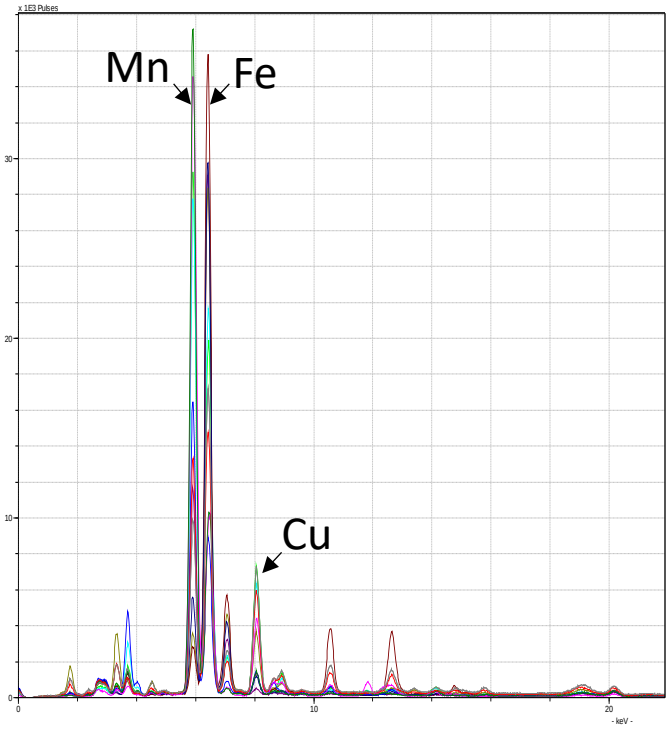


**Figure 5.16:** Overlay of all XRF spectra for analyzed possible hammerscales and slag prills from Area R (n=11). Note the dominant peak varies between manganese and iron (see also Table 5.9).

such as copper, manganese, and lead (Figure 5.15). In contrast, the hammerscales and slag prills from Area R were more variable in the dominant element with some being primarily iron and others manganese (Figure 5.16). The main element was also not correlated with the material type in Area R; both possible hammerscales and slag prills varied in iron or manganese being the abundant element (Table 5.9). The one possible slag prill examined from Area S was high in manganese with much less iron than the other samples analyzed (Figure 5.17).

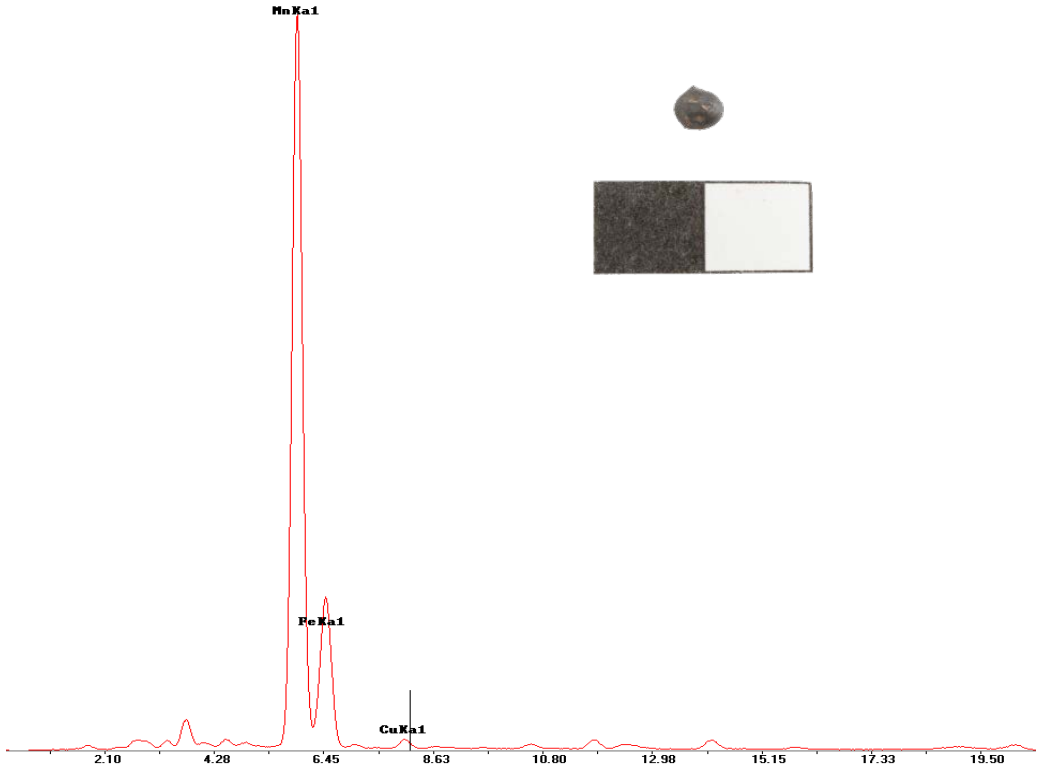


**Figure 5.17:** A slag prill collected from Area S sediment Sample 5993 along with its XRF spectrum. While magnetic, the iron peak is small, and almost entirely hidden by the manganese peaks.

### 5.3.5 Discussion

In general, the magnetic collection process revealed an abundance of magnetic material in the sediment samples from Khirbat en-Nahas. Moreover, the refined examination of the

magnetic fraction identified what appeared to be both hammerscales and slag prills. As previously mentioned however, it is important to remain critical as other materials resembling hammerscales can also be magnetic. In combination with the XRF results showing some of these to be primarily iron, the evidence suggests the possibility of at least some working/smithing of iron-rich materials occurring in the $10^{th}$-$9^{th}$ century BCE. The context of the samples provides additional insight.

Perhaps most significant are the results from Area F. This area yielded the sample with the largest magnetic percentage (Sample 1256), evidence for possible hammerscales and slag prills, and XRF results with the highest iron content (Table 5.9). Sample 1256, Sample 1366 (the second highest magnetic percentage of all samples at 3.96%), and Sample 1298 were all collected from Cell 9 in Area F which is an activity area associated with several installations connected to metallurgy (Levy et al. 2014: 126, Figure 2.51). Excavators described the loci from this cell as having the "best evidence for melting activity" with archaeometallurgical material culture including copper metal, slags, worked stone, and anvils (Levy et al. 2014: 126). Moreover, immediately adjacent to Cell 9 was a large basin and installation; the stone basin contained traces of copper and slag with complete bellows pipes next to it (Figure 5.18) (Levy et al. 2014: 126). Sample 1256 was collected from within this basin, Sample 1366 was collected from a compact mud layer in the cell, and Sample 1298 was from an ashy layer in the corner of Cell 9 where an anvil was found in the walls above. Both Sample 1256 and 1366 included significant copper in the magnetic fraction (likely bits and fragments of mixed iron-copper chunks, Figure 5.13). Sample 1298 had a small magnetic percentage, but it included possible hammerscales and a slag prill. The potential hammerscales were primarily iron based on the XRF (fitting with the other analyzed materials from Area F, Table 5.9). This finding contrasts

**Figure 5.18:** The basin (left) and an associated stone installation (right) from Cell 9 in Area F. A fragment of a bellow pipe (a unique material culture of Area F) can be seen just above the basin (white arrow). Sediment Sample 1256 (the sample with the highest magnetic percentage) was collected from within this basin, and Sample 1366 (second highest magnetic percentage of all samples) was also collected from this cell. Photograph credit: Thomas E. Levy, UCSD Levantine and Cyber Archaeology Lab.

with the typical copper slag of Iron Age Faynan which is rich in manganese rather than iron. Given the abundant magnetic fractions, the significant copper with the magnetic material, the iron-rich hammerscales, and the archaeometallurgical assemblage (including anvils and basins), perhaps Cell 9 functioned as an activity area for working iron-copper chunks including some mechanical separation or a kind of beneficiation and melting (discussed further below). This understanding is possibly reiterated by the presence of copper in all the analyzed samples with XRF from Area F.

Sediment samples from Area R also contained a significant amount of magnetic material which included some possible hammerscales and slag prills. The two samples with the highest magnetic percentage were Sample 16263 (3.88%) and Sample 1587 (3.12%). Sample 16263 was collected from a crushed slag layer during the excavation of the metallurgical complex adjacent the Area R structure. Sample 1587 was collected from within a possible furnace also during the excavation of the metallurgical complex. While both samples contained bits of slag and copper, no hammerscales or slag prills were identified. The potential hammerscales and prills from other samples in Area R varied in their elemental content with some being more manganese than iron, and vice versa (Table 5.9 and Figure 5.16). Given the high manganese content (typical of Iron Age slags from Faynan) and the context with abundant slag from copper smelting, some of these materials may be more directly related to copper smelting than any iron working. Based on the iron-copper chunks excavated here, it can already be assumed some amount of metallic iron was being produced in Area R. The iron-rich hammerscales may represent some attempt to separate the iron from the copper when removed from the furnace or other remains directly from the smelting process. Based on the small number of possible hammerscales and slag prills, it is unlikely that primary smithing was taking place in this area.

In contrast to Areas F and R, the magnetic material from Area S was somewhat limited, and there was only a small number of identified materials resembling hammerscales and slag prills. Sample 7258 had the highest percentage of magnetic material (2.46%) which was collected from above a slag crushing surface in an ashy layer with concentrations of crushed slag (Levy et al. 2014: 163). The sediment samples from Area S were generally characterized by bits of slag, and the one analyzed slag prill was rich in manganese, fitting with the elemental composition of copper slags from Faynan (Figure 5.17 and Table 5.9). As such, rather than an

iron slag prill, this prill is likely a small copper slag prill which fits with the overall function of the building as a slag crushing complex. In considering the context and function of Area S, the magnetic materials are more likely connected to copper slag processing rather than any form of iron working.

While some of the collected materials do seem to be hammerscales and slag prills connected to some kind of iron working, the small number contrasts with what is typical of an iron workshop. There are several possible explanations for this; 1) a large amount of this material was lost in any sieving or flotation of the sediment sample prior to examination with the magnet; 2) sediment samples were only collected near or adjacent to iron working activity areas but not directly within a workshop space; or 3) the hammerscales and slag prills are the product of a process not directly related to iron smithing, perhaps experimentation with the mixed iron-copper chunks or refining these materials to collect copper. At this stage, any of these explanations are possible.

Considering the first possibility, the nature of the samples remains a major detriment, but can only be solved by future investigations using a more metallurgical focused sampling strategy. However, the fact that at least some possible hammerscales and prills were identified perhaps suggests the previous sieving and flotation was not entirely detrimental (as a note, hammerscales will sink during flotation and thus were likely still collected in the heavy fraction, Starley 1995). The second explanation, when taken in consideration with the isotope analysis which provides evidence against iron production in Faynan, seems less likely as there might not have been any iron workshops or activity areas (also reiterated by the lack of iron slags). Moreover, the samples from Area F were collected directly from a metallurgical context connected to melting and hammering based on the material culture including anvils and worked

stones. In turn, the small number of scales and prills could be interpreted as further evidence against the possibility of iron production in Faynan. The isotope analysis could provide support of the third possibility. If the iron-copper chunks were not purified to produce iron objects, it is possible these materials were considered waste by the metallurgists of Iron Age Faynan. The limited hammerscales and prills may be the product of some experimentation or exploration (heating and hammering) to attempt to produce objects or metal from the chunks before determining they were useless given the difficulties in working an iron-copper mixture (discussed in Chapter 3).

Alternatively, the iron-copper chunks could have been purified to extract copper, and the hammerscales and prills were a byproduct of this process (Ben-Yosef 2010). This explanation seems most likely given the abundance of magnetic material from the basin in Area F and the hammerscales and slag prills from this area seeming to be primarily iron based on the XRF. The purification process would inherently require heating to extract the copper, and perhaps some hammering was also involved to produce the scales and prills. The context within Area F may further support this understanding, as the basin and adjacent bellow pipes might be directly related to the purification process. However, any of these hypotheses require further research. Based on the current evidence, these results also provide additional support that iron was probably not produced in Faynan as a byproduct of the copper smelting industry.

### 5.3.6 Future Directions

Outside of additional excavation and sampling, there are several opportunities for future research on the magnetic materials and possible iron production residues collected here. A more thorough analysis of the elemental composition of the hammerscales and slag prills using a

methodology that can yield quantitative results would be beneficial. Such an investigation would both help determine the exact nature of these remains (i.e., are they the result of iron working) and create new opportunities for comparing between areas and contexts. The possible relationship between the hammerscales/slag prills and the mixed iron-copper chunks could also be further investigated using the isotope and HSE analyses above. Examining the HSE abundances and Os isotopes could provide more concrete evidence that the scales/prills are or are not directly connected to working the mixed iron-copper chunks. A similar isotopic signature and HSE composition could link these materials directly. Finally, experimental archaeology to determine a possible method and process for purifying the iron-copper chunks would be insightful (building on Tylecote and Boydell 1978). This would allow the archaeologist to both determine the feasibility of such a process and identify any byproducts and residues.

## 5.4 A Diachronic Analysis of Iron Age Copper Metal using Scanning Electron Microscopy

### 5.4.1 Introduction

One of the main goals of this project was to test if the abandonment of copper smelting in Faynan at the end of the 9$^{th}$ century BCE was driven by natural resource degradation/depletion resulting in socio-political collapses following the overshoot paradigm. In the case of Iron Age Faynan, the "indispensable" or "limiting factor" natural resource for maintaining its culture system was copper (Chapters 2 and 3). Overly degraded/depleted ores would inhibit society in Faynan's ability to smelt and trade copper for critical wealth and subsistence resources (Chapter 2). This metallurgical and economic breakdown would undermine the interdependent socio-political structures of the social-ecological system, inducing a collapse. In other words, it is hypothesized here that the significantly developed metallurgical technologies in Faynan led to

over-exploitation of diminishing copper ores during the Iron Age, causing a collapse of the metallurgical industry, a subsequent breakdown of economic relationships, and a societal collapse - in this case, a return to predominantly pastoral nomadic lifeways. To support this hypothesis, evidence for human-driven resource exhaustion needs to be identified in the archaeological record.

Identifying copper ore exhaustion or degradation requires evidence from the mines (depleted shafts and galleries) or the copper produced (changes in elemental contents) during the Iron Age. Ancient mines are notoriously difficult to interpret due to a lack of material culture and destruction by later activities; accordingly, they are avoided here (Stöllner 2014: 151). Rather, copper metal produced in Faynan will provide a proxy for the availability/quality of ores. Unfortunately, only limited copper artifacts have been excavated in Faynan because the metal was primarily cast into ingots and exported, but massive amounts of slag accumulated in large mounds at smelting sites. This slag affords an abundant collection of metal through copper droplets or prills trapped in the slag matrix, a common phenomenon of ancient smelting. Hauptmann et al. (1992: 20, Table 6) previously extracted and analyzed prills from slags, but the analysis was limited in size and temporal scope with only 10 samples from the Iron Age (their results are provided in Table 5.10 for comparison). In contrast, the ELRAP slag mound excavations and the rigorous radiocarbon sampling strategies employed afford abundant slag samples with a secure chronological scaffold for sample selection. As such, the slag mound excavations in Faynan provide a unique opportunity to examine a ca. 400-year record of continuous copper smelting. By selecting slag samples throughout the stratigraphic section and analyzing the embedded prills, the purity of copper produced can be diachronically examined through the Iron Age to investigate for possible evidence of changes in ore quality.

**Table 5.10:** Analyses of copper metal from Iron Age Faynan by Hauptmann (2007: Table A17 and Hauptmann et al 1992: Table 6). Samples JD-2/23a and JD-2/23b were analyzed with Atomic Absorption Spectrometry and all others with Neutron Activation Analysis. The other elements present in the samples were analyzed but presented in parts per million and thus are not included here.

| Previous Analysis of Copper from Iron Age Faynan | | | | | |
|---|---|---|---|---|---|
| **Sample** | **Site** | **S** | **Fe** | **Cu** | **Pb** |
| JD-1/17 | Faynan 5 (Khirbat Faynan) | 0.29 | 1.82 | 92.8 | 2.43 |
| JD-2/19a | Khirbat en-Nahas | 0.53 | 2.42 | 90.7 | 2.96 |
| JD-2/19b | Khirbat en-Nahas | - | 2.19 | 95.3 | 0.71 |
| JD-2/19c | Khirbat en-Nahas | - | 2.34 | 64.0 | 2.43 |
| JD-2/19d | Khirbat en-Nahas | - | 2.61 | 92.9 | 3.11 |
| JD-2/19e | Khirbat en-Nahas | - | 2.28 | 92.8 | 0.73 |
| JD-2/23a | Khirbat en-Nahas | 0.68 | 0.82 | 83.1 | 6.38 |
| JD-2/23b | Khirbat en-Nahas | 0.49 | 2.06 | 89.7 | 1.49 |
| JD-11/1b | Khirbat al-Jariya | 0.42 | 2.41 | 92.7 | 0.66 |
| JD-11/3 | Khirbat al-Jariya | - | 1.67 | 77.9 | 0.27 |

The critical period of investigation is the century prior to the end of copper production – ca. the 10$^{th}$-9$^{th}$ century BCE. If natural resource exhaustion/degradation was a significant factor in the collapse of the industry, analyzed copper from samples dated to the end of this period could potentially yield evidence indicative of degrading/depleting copper ores such as changes in the elemental composition. Moreover, the previous investigations of the metallurgical technology in Faynan during the 10$^{th}$-9$^{th}$ centuries BCE afford essential variable control (Ben-Yosef et al. 2019). Ben-Yosef et al. (2019: 11) associated this period with consistent technology and smelts which continued "for more than a century with no discernible changes" based on analysis of the slags and the remains from technological equipment such as furnaces and tuyères. As such, fluctuations in the quality of produced metal during the final phases of copper smelting would not be the result of changing technological practices/knowledge, but rather the available ore resources. To investigate possible overshoot in Faynan, slag samples were selected from the slag

mound excavations at Khirbat en-Nahas and Khirbat al-Jariya for analysis with scanning electron microscopy.

### 5.4.2 Sample Selection and Preparation

The main goal for sample selection was to have a collection representative of Iron Age Faynan through both time and space. To do so, slag samples were selected from two main smelting sites, Khirbat en-Nahas and Khirbat al-Jariya, which include the entire Iron Age sequence of copper smelting in Faynan. For spatial representation and comparative purposes, slags samples were collected from five distinct excavation areas: Areas M, F, and R at Khirbat en-Nahas along with Areas A and C at Khirbat al-Jariya. Samples from the Area M at Khirbat en-Nahas were repurposed from Ben-Yosef's (2010) dissertation research. Reusing these previously analyzed samples prevented having to destroy additional archaeological material as they had all been previously cut/crushed to some extent and afforded the opportunity for comparing analytical techniques and results (see below). In addition, Ben-Yosef intentionally selected samples throughout the entire section providing a diachronic sequence which was also needed for this dissertation. In total, 66 slag samples from Area M were prepared for analysis (Figures 5.19 and 5.20). The same sampling strategy was used for Area A at Khirbat al-Jariya, using samples previously analyzed by Ben-Yosef (2010), and 15 samples were prepared from this context (Figure 5.21 and 5.22). Area C at Khirbat al-Jariya was unique as only one layer of slag was composed of slag cakes/chunks that could be sectioned (the bottom layer of the slag mound was entirely crushed slag) (Chapter 4). As such, only two samples were selected from this slag mound. Finally, Area R and Area F at Khirbat en-Nahas represent the final phases of Iron Age copper smelting in Faynan associated with the most sophisticated metallurgical

**Figure 5.19:** Section drawing and orthophoto of the southern section in the Area M slag mound at Khirbat en-Nahas. The red labels are samples analyzed as part of this research. White lines in the orthophoto are tape measures; the break in the lines and the shift in general coloring in the image was created by the unexcavated safety step. Section drawing modified from Ben-Yosef 2010: 5.55. See Chapter 6 for discussion of the orthophoto.

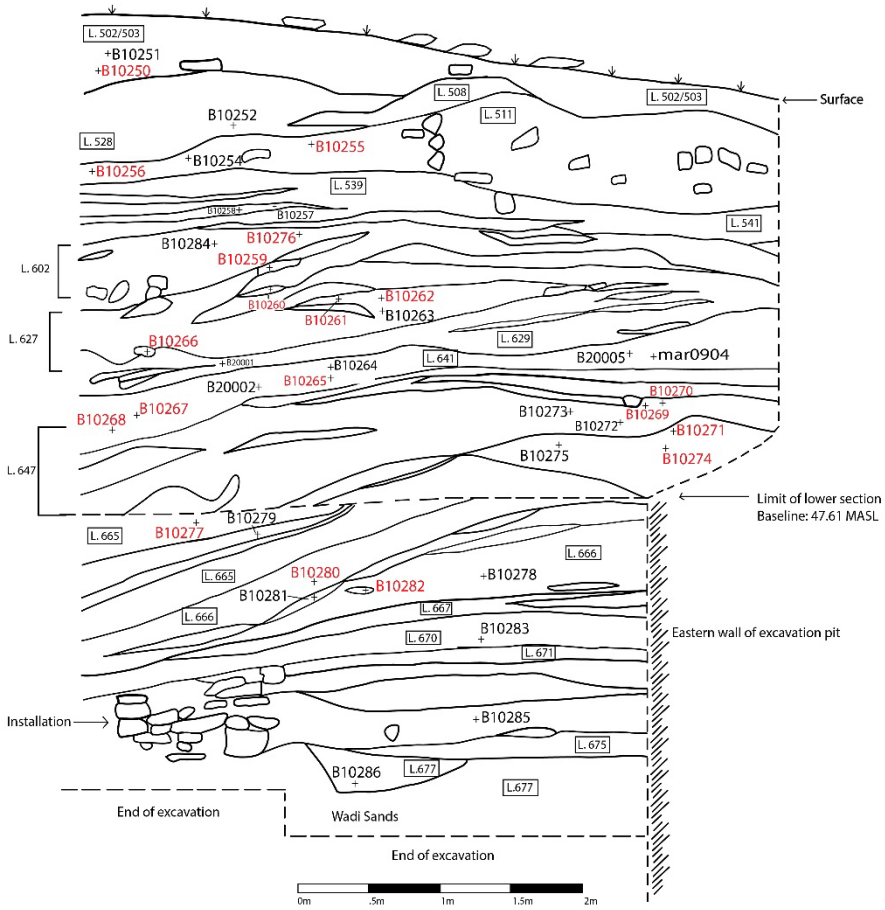
L. 502/503
+B10251
+B10250
B10252
L. 508
L. 511
L. 502/503
Surface
L. 528
+B10255
+B10254
+B10256
L. 539
B10258+
B10257
L. 541
B10284+
B10276+
B10259
L. 602
B10260
+B10262
+B10263
B10261
L. 627
B10266
L. 629
+B20001
+B10264
L. 641
B20005+
+mar0904
B20002+
B10265+
B10270
B10268
+B10267
B10273+
B10269
B10272+
+B10271
B10275
B10274
L. 647
Limit of lower section
Baseline: 47.61 MASL
B10279
L. 665
B10277
L. 666
L. 665
B10280
+B10278
B10281
B10282
L. 666
L. 667
B10283
L. 670
L. 671
Eastern wall of excavation pit
Installation
+B10285
L. 675
B10286
L.677
L.677
End of excavation
Wadi Sands
End of excavation
0m
.5m
1m
1.5m
2m

**Figure 5.20:** Section drawing and orthophoto of the eastern section in the Area M slag mound at Khirbat en-Nahas. The red labels are samples analyzed as part of this research. White lines in the orthophoto are tape measures. Section drawing modified from Ben-Yosef 2010: 5.56. See Chapter 6 for discussion of the orthophoto.

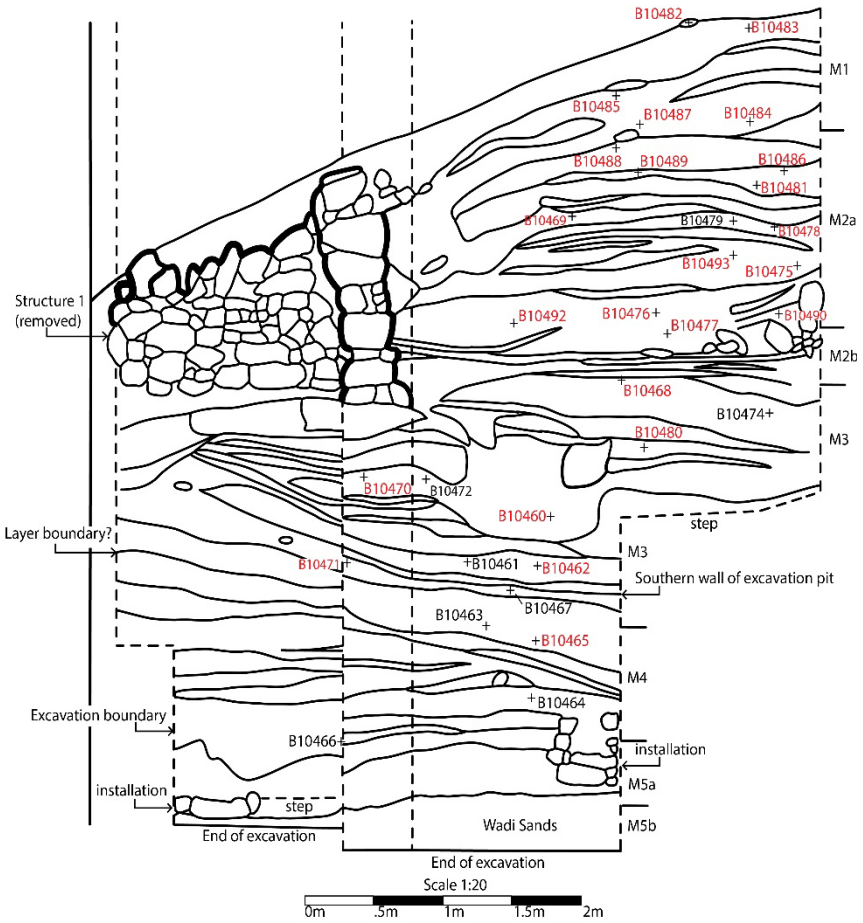
B10482
B10483
M1
B10485
B10487
B10484
B10488
B10489
B10486
B10481
B10469
B10479
M2a
B10478
B10493
B10475
Structure 1
(removed)
B10492
B10476
B10477
B10490
M2b
B10468
B10474
B10480
M3
B10470
B10472
B10460
step
Layer boundary?
B10471
B10461
B10462
M3
Southern wall of excavation pit
B10463
B10467
B10465
M4
B10464
Excavation boundary
B10466
installation
M5a
installation
step
End of excavation
Wadi Sands
M5b
End of excavation
Scale 1:20
0m
.5m
1m
1.5m
2m

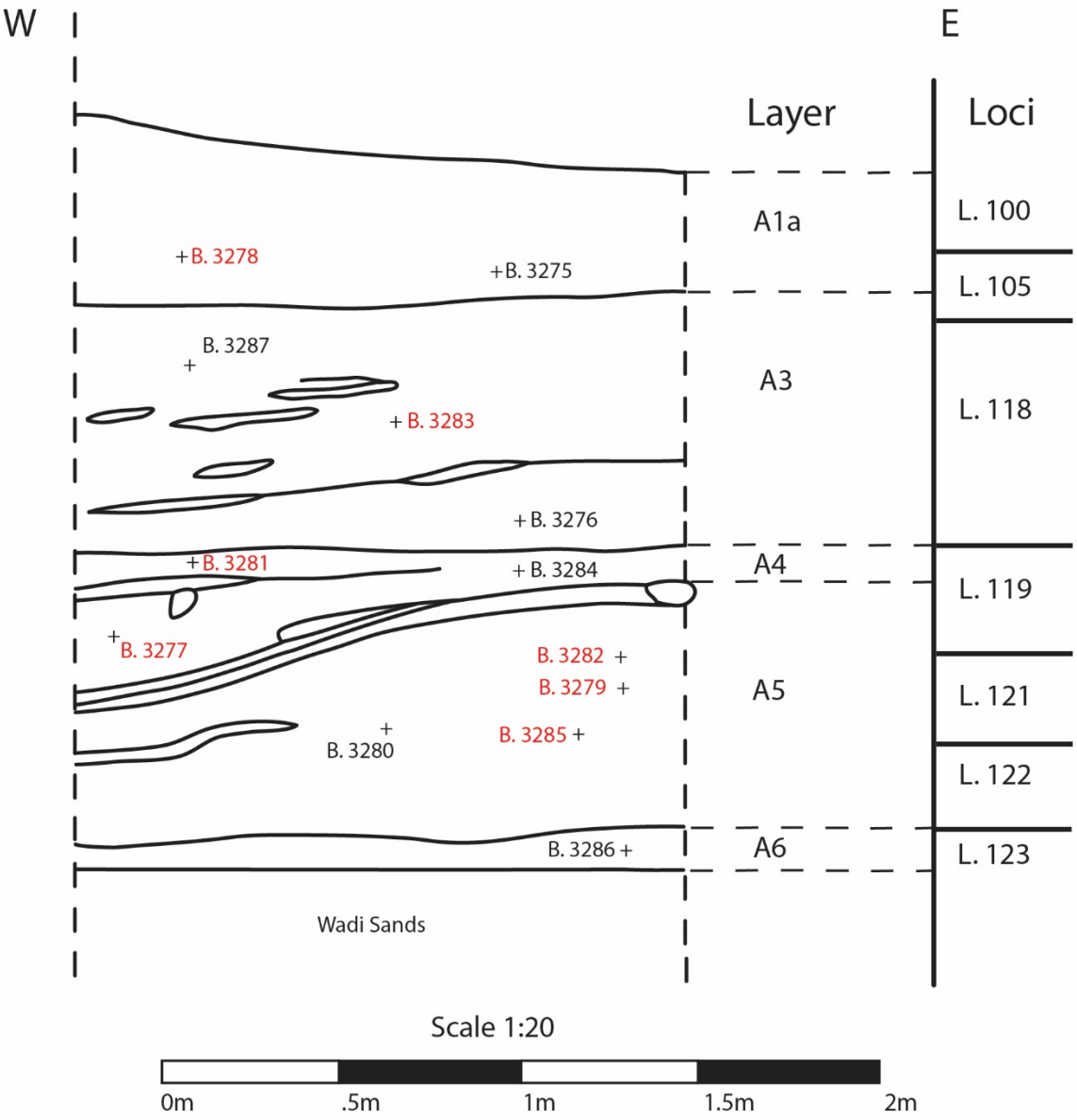


**Figure 5.21:** Section drawing of the northern section in the Area A slag mound at Khirbat al-Jariya. The red labels are samples analyzed as part of this research. Section drawing modified from Ben-Yosef 2010: 5.67a.

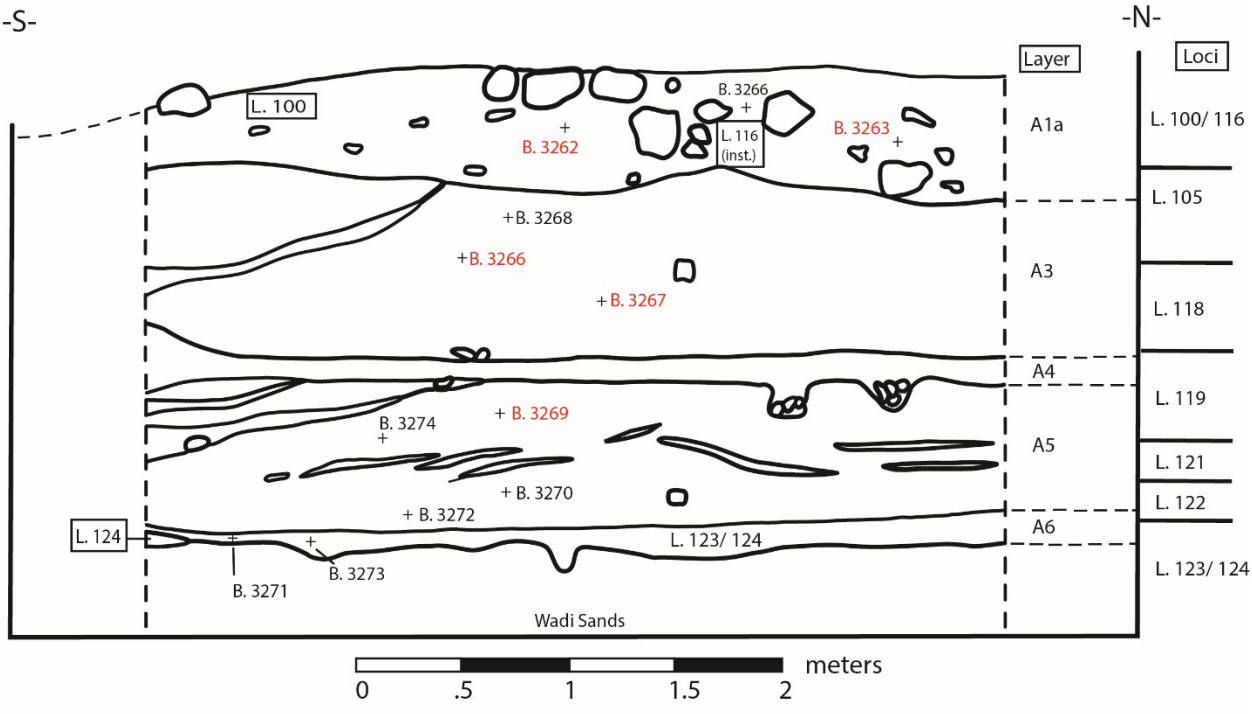


**Figure 5.22:** Section drawing of the northern section in the Area A slag mound at Khirbat al-Jariya. The red labels are samples analyzed as part of this research. Section drawing modified from Ben-Yosef 2010: 5.65a.

technology; eight and five samples were selected from these contexts respectively. Two thin-sections were produced from some of the slags when possible bringing the total collection to 96 samples.

To expose copper prills trapped in the slag, samples were thin-sectioned following a petrographic methodology. As the prills are often in the range of microns in diameter, a highly polished thin-section cleanly reveals the prills and provides an ideally flat surface for microscopic analyses. The slags also needed to be cut down to appropriate size to fit within the chamber of the scanning electron microscope (SEM) which can hold a maximum sample size of 122 millimeters in diameter depending on required stage travel and rotation. A thin-section (thickness of 35-45 microns) was removed from the larger sample and mounted in epoxy on a 25x75 millimeter glass slide. The thin-section was polished down to 0.5 micron high-purity

alumina polish powder ensuring a clean and level exposure of any prills. All thin-sections were professionally prepared by Texas Petrographic Inc. with funding from the UCSD F.G. Bailey Dissertation Research Fellowship and the Rust Family Foundation Archaeology Grant (RFF-2019-87).

While mounting the sample on a glass slide (or in an epoxy disk) is required for thin-sectioning and analysis, the glass and epoxy function as resistors for electrons bombarding the slag while imaging with the SEM (discussed further below). This effect causes the electrons produced by the SEM to gather on the sample and create a "charging" phenomenon. The charging makes imaging and analyzing the sample near impossible (Figure 5.23).

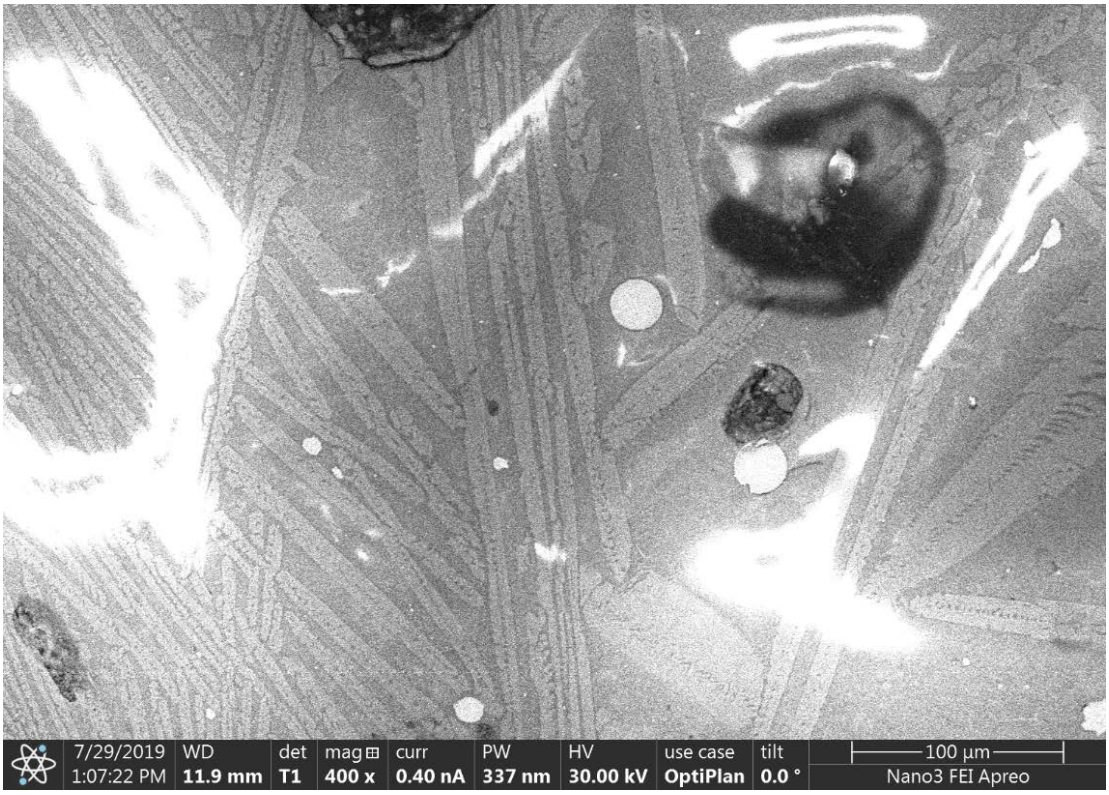


**Figure 5.23:** Image of a slag sample using the scanning electron microscope showing the charging phenomenon. The bright white streaks represent sample charging, making imaging and analysis impossible.

The first attempt at eliminating the charging was to run copper tape from the slag down to the stub mount (used to hold the sample on the SEM stage) to provide an exit path for the electrons; however, the slag continued to charge even at low magnifications. Instead, samples were sputter coated using an Emitech K575X Iridium Sputter Coater. The sputter coater deposits a thin film of iridium (particle sizes of 1-2 nanometers in diameter) on the sample to create a conductive surface which eliminates charging during SEM analysis and enables higher resolution imaging and greater sample stability for analysis[3]. Once coated, samples could be imaged even at high magnifications without charging.

### 5.4.3 Methods

#### 5.4.3.1 Scanning Electron Microscopy-Energy Dispersive X-Ray Spectroscopy

A scanning electron microscope (SEM) creates a high-resolution, magnified image of a sample by bombarding the sample with electrons rather than a light source as is the case in optical microscopes. Using an electron source, a beam of electrons is formed and accelerated towards the sample at a spot size of around 1 nanometer at an applied voltage known as the beam energy ("FEI Apreo SEM"). This beam scans the surface of the sample in a raster grid to produce various signals based on the electrons scattered off or emitted from the sample (secondary electrons and backscattered electrons) which are collected by the instrument detectors ("FEI Apreo SEM"). Based on the signal of electrons collected, the SEM can then create an image of the sample surface. When scanning a sample, the electron beam can also generate characteristic X-rays from the sample interaction. Some SEM instruments include an X-ray detector for collecting the generated X-rays and converting the energy into a signal to determine the

[3] While slag samples are typically coated with carbon to control for charging as the carbon content will not disrupt the analysis, a carbon sputter coater was not available at the time of conducting this research.

elemental composition of a sample, much like XRF described above. This process, known as SEM-EDX (Energy-Dispersive X-ray Spectroscopy), allows the user to also determine the elements present and their relative abundance at specific locations of interest on a sample. As such, SEM-EDX affords a combination of high-resolution imaging with elemental analysis.

In order to maintain consistency between samples, all slag samples were analyzed on the same SEM instrument using the same settings and parameters. Specifically, a *Thermo Scientific FEI Apreo* SEM was used for imaging and analysis. The *Apreo* includes three possible electron detectors (standard, backscatter, and secondary), a beam energy range from 1-30 kiloelectron volts (keV), and a beam current range of 1 picoamp (pA) to 400 nanoamps (nA). In addition, the system can be operated in three distinct modes depending on the required resolution – Standard, Opti-plan, and Immersion. The 340-millimeter-wide vacuum chamber includes a multi-purpose stage holder capable on hosting 18 stubs, depending on the stub and sample size. The *Apreo* used here is also outfitted with the optional EDX analyzer for elemental analysis with detection limits of ca. 0.1 wt.% (Dr. Ryan Nicholl, personal communication). For this research, the electron beam was set to 30.00 kV energy in order to excite all possible elements present in the sample[4]. The beam current was set to 0.8-1.0 nA to maintain a sufficient count rate (ca. 8-10k) during EDX analysis. In order to locate prills, the backscatter electron sensor (called T1 in the *Apreo* system) was used which creates elemental contrast in the image; elements with higher z-numbers are brighter making it easier to identify the copper prills in comparison to the silicate matrix of slag. The instrument was used in opti-plan mode for higher resolution imaging at a working

[4] Even at 30 kV, the penetration of the electron beam into the sample should not be greater than a few microns (see analysis by Wassilkowska et al. 2014: Figure 2 based on an iron sample). The thickness of the thin-sections was 35-45 microns.

distance of ca. seven millimeters (five to ten millimeters working distance is suggested when using opti-plan with the T1 sensor).

During each session on the SEM, the chamber was loaded with 1-3 slag thin-sections; only three samples mounted on stubs could fit on the stage at a time due to the size of the glass slide. In order to find prills for analysis, the navigation camera inside the SEM chamber was used to essentially run transects across each slag sample (one sample at a time). The navigation cam allows the user to see the spot on the sample currently being imaged and to move the SEM beam along the sample. A magnification between 200-800x was found to be the most efficient for finding prills which were typically a bright white due to the backscatter sensor and ranged in diameter from approximately 5-25 microns (μm) with larger prills sometimes reaching 100 μm (Figure 5.24).

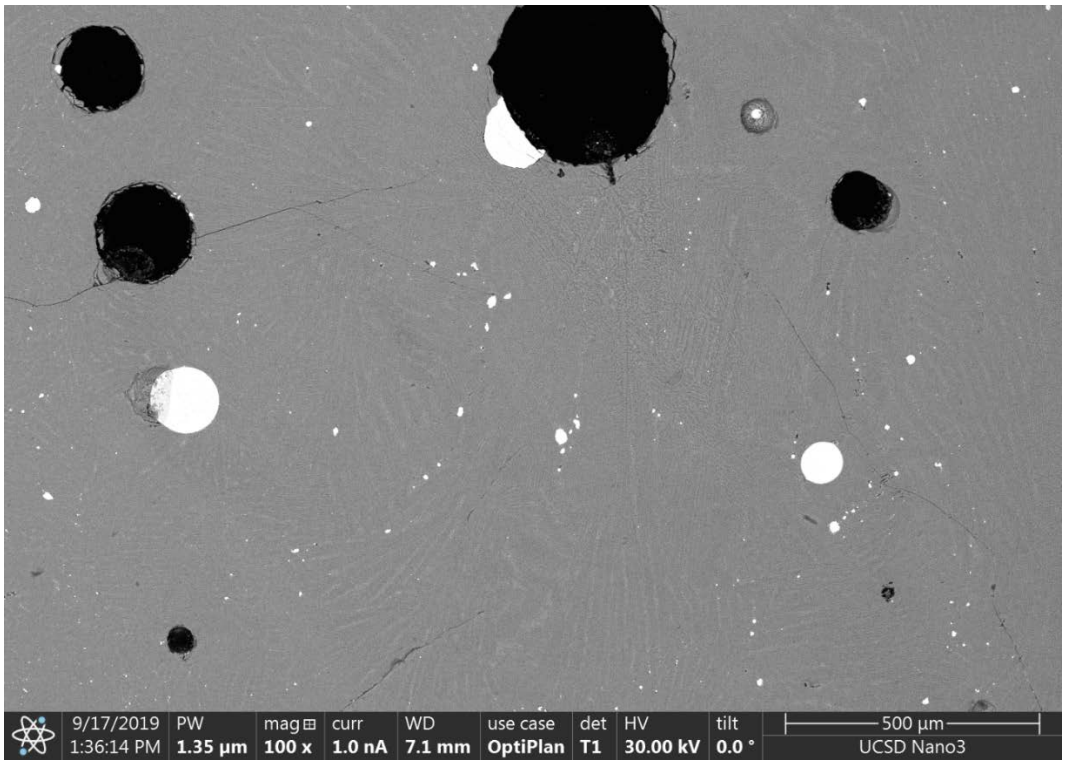


**Figure 5.24:** Representative SEM image of a slag sample (Sample 3278, Khirbat al-Jariya, Area A) with copper prills (bright white circles). The backscatter sensor shows elements with higher atomic numbers as brighter. Images of every sample are available upon request from the author.

When investigating a sample, all identifiable prills were analyzed with EDX. The point ID function which analyses one point with the size of the beam was used to avoid overflowing the size of the prill and analyzing the surrounding matrix given the high beam energy – minimizing the interaction volume (Figure 5.25). The point of analysis was set at the center of the prill, and each analysis was run for 90 second acquisition times. An image was also captured of every analysis location for record keeping. On the somewhat rare occasion that +10 prills were identified and analyzed in a sample, it was considered complete, and analysis moved to a new sample in order to maximize efficiency.

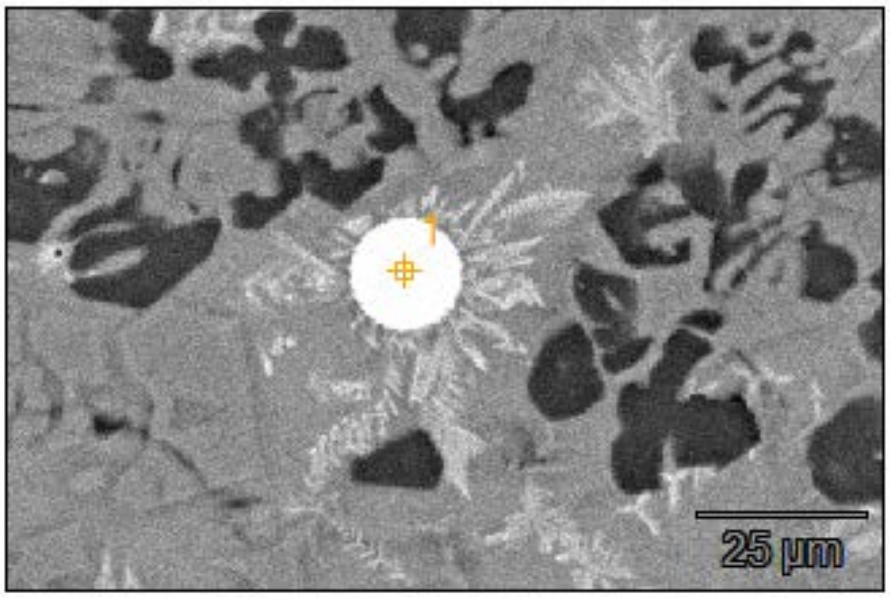


**Figure 5.25:** Image of an SEM-EDX point analysis on a copper prill (orange crosshairs). Points were analyzed from the center of the prills to try to keep the interaction volume within the prill.

All SEM analysis was completed at the UCSD Nano3 Cleanroom. The facility provides access to advanced fabrication and characterization equipment for UCSD students and faculty (with appropriate training and certifications) including the above-described SEM. The Nano3 facility is part of the San Diego Nanotechnology Infrastructure of UCSD which is a member of

the National Nanotechnology Coordinated Infrastructure that receives support from the National Science Foundation (Grant ECCS-1542148). The SEM analysis conducted for this dissertation was generously funded by the Wenner-Gren Foundation (Dissertation Fieldwork Grant - #9872), and the Rust Family Foundation (Archaeology Grant - RFF-2019-87)

#### 5.4.3.2 Limitations of SEM-EDX

Before moving into the results, some limitations of the current analysis should be noted. First, the sample chamber of the SEM always contains residual amounts of carbon due to carbon tape used to secure samples and the polymerization of hydrocarbons (Dr. Ryan Nicholl, personal communication). This phenomenon can create an incorrectly high carbon content in SEM-EDX analysis which can be further exacerbated by the higher beam energies used for EDX. This element was removed from the measurements and the remaining elements were adjusted through normalization (see below). Second, there is a peak overlap between phosphorus and iridium from the sputter coat at around 2 kV (Heu et al. 2019: 35). Thus, anywhere a phosphorous content was measured, the iridium coating may be contributing to this value; this is relevant for the analysis of iron inclusions which often included phosphorous. Third, the analysis was standardless and normalized to 100% using the internal system based on peak intensity ratios and the elements present. This method can create/hide some error, and some would argue makes EDX a semi-quantitative analysis technique (Goldstein et al. 2018: 296-297). Finally, any identified element with less than 1 wt.% content may be the within the error range, and thus, this technique is not ideal for identifying the trace elements within the samples. In general, these limitations should not be drastically impactful on the presented research as the samples were professionally prepared for SEM which helps to minimize inconsistencies in the analysis and the primary focus

was the main components of the sample including copper and other elements present in high percentages. Moreover, the conclusions drawn are based entirely on data using the same instrumentation and methodology giving them additional credibility.

### 5.4.4 Results

#### 5.4.4.1 Copper Content in Prills

In total, 360 copper prills were analyzed providing the largest analytical dataset for Iron Age copper from Faynan to date. All of the analytical data collected using SEM-EDX are presented in Table 5.11. In addition, Table 5.12 provides the average and standard deviation of copper content per sample (i.e., an average of all the prills within a sample), and Table 5.13 provides this data at the level of stratigraphic layers. Following Ben-Yosef (2010), standard deviation was used to measure the consistency of the smelting process. Across all prills from all contexts, the average copper content was 91.05 wt.% with a standard deviation (±) of 3.06. At the site level, the average and standard deviation were similar: Khirbat en-Nahas = 90.91±2.96 wt.% (n=272) and Khirbat al-Jariya = 91.50±3.30 wt.% (n=88). These values were fairly consistent down to the individual contexts as well: Area M = 91.10±2.94 wt.% (n=221), Area R = 90.56±2.71 wt.% (n=31), Area F = 89.34.12±3.32 wt.% (n=20), and Area A = 91.57±3.23 wt.% (n=85) (Area C only yielded three total analysis providing limited insight).

For diachronic considerations, the average copper content per sample (average of all the prills analyzed per slag sample) was plotted for Khirbat en-Nahas Area M and Khirbat al-Jariya Area A as they were selected from throughout these two slag mounds (Figures 5.26 and 5.27). In general, both slag mounds show a general though small increase in copper content through time based on the trend lines. Area M at Khirbat en-Nahas shows a tighter clustering in copper

**Table 5.11:** SEM-EDX results for copper prills in the slag thin-sections. All results are presented in weight%. Double-bottom borders indicate a change in the excavation area, and the table was divided to avoid splitting any samples across two pages. The letter following the elemental symbol represents the electron shell. The first letter in the Stratum (Strat.) represents the excavation area. Samples that did not include copper prills are not included in this table.

| Complete Data for Copper Prills analyzed with SEM-EDS | | | | | | | | | | | | | | | | | | | | |
|---|---|---|---|---|---|---|---|---|---|---|---|---|---|---|---|---|---|---|---|---|
| Year | Site | Area | Strat. | Loc. | Sample | O-K | Al-K | Si-K | S-K | K-K | Ca-K | Mn-K | Fe-K | Co-K | Ni-K | Cu-K | Zn-K | As-K | Ba-L | Pb-L |
| 2014 | KAJ | C | C1 | 533 | 10314 | 1.22 | 0.11 | 0.13 | - | - | 0.19 | 1.94 | 1.81 | 0.52 | 0.40 | 93.67 | - | - | - | - |
| 2014 | KAJ | C | C1 | 529 | 10338 | 9.49 | 0.59 | 0.55 | 2.87 | 0.12 | 0.22 | 2.45 | 0.51 | - | - | 83.21 | - | - | - | - |
| | | | | | | 2.93 | 1.20 | 0.55 | 0.44 | 0.19 | 0.32 | 2.12 | 0.58 | - | - | 91.66 | - | - | - | - |
| 2006 | KAJ | A | A1a | 100 | 3263 | 2.72 | - | 0.20 | 5.08 | - | - | 1.53 | 0.45 | 0.36 | 0.73 | 83.61 | - | - | - | 5.32 |
| | | | | | | 2.02 | - | 0.32 | 1.30 | - | 0.16 | 1.99 | 0.64 | 0.49 | 0.79 | 92.30 | - | - | - | - |
| | | | | | | 3.12 | - | 0.26 | 3.57 | - | 0.14 | 1.57 | 0.76 | 0.61 | 3.91 | 84.91 | - | 1.14 | - | - |
| | | | | | | 2.13 | 0.41 | 0.19 | 2.96 | - | 0.19 | 1.77 | 0.71 | 0.47 | 0.46 | 90.70 | - | - | - | - |
| | | | | | | 0.73 | 0.19 | 0.24 | 2.10 | - | - | 1.37 | - | 0.13 | 0.42 | 94.82 | - | - | - | - |
| 2006 | KAJ | A | A1a | 100 | 3278 | 1.66 | 0.33 | 0.27 | 1.12 | - | - | 0.39 | - | - | 0.29 | 95.94 | - | - | - | - |
| | | | | | | 1.76 | 0.68 | 0.51 | 0.36 | - | - | 0.87 | - | - | - | 95.83 | - | - | - | - |
| | | | | | | 2.72 | 0.44 | 0.62 | - | - | 0.11 | 0.97 | - | - | 0.36 | 94.78 | - | - | - | - |
| | | | | | | 1.88 | 0.27 | 0.37 | 0.32 | - | - | 0.56 | - | - | - | 96.59 | - | - | - | - |
| | | | | | | 4.73 | 0.46 | 0.52 | - | - | 0.25 | 2.18 | 0.48 | - | - | 91.38 | - | - | - | - |
| | | | | | | 5.26 | 0.71 | 0.87 | - | 0.13 | 0.24 | 2.82 | 0.42 | - | - | 89.55 | - | - | - | - |
| | | | | | | 5.17 | 0.43 | 0.36 | 3.60 | - | - | 0.86 | - | - | 0.36 | 89.20 | - | - | - | - |
| | | | | | | 7.10 | 0.33 | 0.37 | 1.81 | - | 0.11 | 1.32 | - | - | - | 88.95 | - | - | - | - |
| | | | | | | 3.29 | 1.28 | 0.61 | - | - | 0.21 | 2.45 | 0.39 | - | - | 91.77 | - | - | - | - |
| | | | | | | 1.78 | 0.44 | 0.52 | 0.12 | - | 0.11 | 1.41 | - | - | - | 95.62 | - | - | - | - |
| | | | | | | 2.89 | 0.36 | 0.48 | 1.47 | - | 0.07 | 0.54 | - | - | - | 94.20 | - | - | - | - |
| 2006 | KAJ | A | A1a | 100 | 3262 | 1.89 | 0.62 | 0.37 | 1.04 | 0.06 | 0.19 | 2.91 | 0.44 | - | 0.53 | 91.93 | - | - | - | - |
| | | | | | | 1.63 | 0.77 | 0.61 | 4.03 | 0.08 | 0.22 | 3.47 | - | - | 0.73 | 88.17 | - | - | 0.28 | - |
| | | | | | | 2.52 | 0.54 | 0.40 | 2.90 | - | 0.11 | 2.26 | 0.36 | - | 0.84 | 89.72 | - | 0.36 | - | - |
| 2006 | KAJ | A | A1a/A3 | 105 | 3265 | 2.11 | 0.46 | 0.54 | 0.21 | - | 0.26 | 2.05 | 0.32 | - | - | 94.05 | - | - | - | - |
| | | | | | | 4.47 | 0.54 | 1.13 | 1.69 | 0.14 | 0.44 | 2.34 | 0.43 | - | - | 88.82 | - | - | - | - |
| | | | | | | 4.24 | 0.83 | 1.33 | 1.17 | 0.21 | 0.66 | 2.60 | 0.48 | - | - | 87.95 | - | - | 0.52 | - |
| | | | | | | 4.42 | 0.54 | 0.49 | 1.31 | - | 0.26 | 2.00 | 0.33 | - | - | 90.65 | - | - | - | - |
| | | | | | | 2.16 | 0.73 | 0.46 | 0.13 | - | 0.23 | 2.10 | 0.38 | - | - | 93.80 | - | - | - | - |
| | | | | | | 2.59 | 0.66 | 0.67 | - | - | 0.22 | 1.63 | 0.28 | - | - | 93.95 | - | - | - | - |
| | | | | | | 2.68 | 0.39 | 0.36 | 1.09 | - | - | 0.29 | - | - | - | 95.19 | - | - | - | - |
| 2006 | KAJ | A | A1a/A3 | 105 | 3264 | 2.27 | - | 0.47 | - | 0.13 | 0.10 | 2.61 | 0.47 | - | - | 93.96 | - | - | - | - |
| | | | | | | 1.69 | 0.50 | 0.66 | 0.94 | 0.11 | 0.09 | 2.80 | 0.51 | - | - | 92.51 | - | - | 0.20 | - |
| | | | | | | 1.71 | 0.53 | 0.46 | 0.37 | 0.14 | 0.09 | 2.96 | 0.53 | - | - | 93.21 | - | - | - | - |
| | | | | | | 2.21 | 0.34 | 0.64 | 0.53 | 0.25 | 0.16 | 3.00 | 0.54 | - | - | 91.95 | - | - | 0.37 | - |
| | | | | | | 1.92 | 0.40 | 0.55 | 0.89 | - | 0.10 | 2.00 | 0.51 | - | - | 93.36 | - | - | 0.28 | - |
| | | | | | | 1.37 | 0.39 | 0.33 | 0.45 | 0.10 | 0.11 | 2.80 | 0.56 | - | - | 93.63 | - | - | 0.26 | - |
| | | | | | | 1.57 | 0.45 | 0.37 | 0.43 | 0.09 | 0.08 | 2.86 | 0.58 | - | - | 93.59 | - | - | - | - |
| | | | | | | 2.35 | 0.56 | 0.68 | - | 0.07 | 0.09 | 2.35 | 0.43 | - | - | 93.47 | - | - | - | - |
| 2006 | KAJ | A | A3 | 118 | 3267 | 1.52 | 0.12 | 0.18 | 5.63 | - | - | - | 0.51 | 0.37 | - | 91.67 | - | - | - | - |
| 2006 | KAJ | A | A3 | 118 | 3283 | 3.24 | 0.72 | 1.52 | 0.92 | 0.09 | 0.19 | 1.82 | - | - | - | 91.50 | - | - | - | - |
| | | | | | | 2.63 | 0.49 | 0.47 | 0.28 | - | - | 0.28 | 0.09 | - | - | 95.76 | - | - | - | - |
| | | | | | | 3.46 | 0.45 | 0.72 | 1.93 | - | 0.28 | 2.41 | 0.27 | - | - | 90.49 | - | - | - | - |
| | | | | | | 1.88 | 0.59 | 0.66 | 1.62 | 0.05 | 0.20 | 2.69 | - | - | - | 91.96 | - | 0.35 | - | - |
| | | | | | | 3.00 | - | 0.31 | - | - | 0.17 | 2.31 | - | - | - | 94.21 | - | - | - | - |
| | | | | | | 1.98 | 0.40 | 0.44 | 0.36 | - | 0.14 | 1.85 | - | - | - | 94.84 | - | - | - | - |
| | | | | | | 6.63 | - | 0.32 | 1.43 | - | 0.17 | 1.53 | - | - | - | 89.56 | - | 0.36 | - | - |
| | | | | | | 8.21 | 0.68 | 0.38 | 1.64 | - | 0.09 | 1.30 | - | - | - | 87.70 | - | - | - | - |
| | | | | | | 0.74 | 0.33 | 0.43 | 0.61 | - | - | 0.33 | - | - | 0.32 | 97.23 | - | - | - | - |
| | | | | | | 3.02 | 0.55 | 0.35 | 1.87 | - | - | 0.30 | - | - | 0.47 | 93.44 | - | - | - | - |
| | | | | | | 4.95 | - | 0.42 | - | - | 0.11 | 0.85 | - | - | - | 93.67 | - | - | - | - |
| 2006 | KAJ | A | A4 | 119 | 3281 | 3.18 | - | 0.37 | 4.40 | - | 0.09 | 1.52 | - | - | 0.37 | 90.07 | - | - | - | - |
| | | | | | | 4.76 | - | 0.36 | 4.67 | 0.09 | 0.15 | 2.12 | - | - | - | 87.85 | - | - | - | - |
| | | | | | | 2.37 | - | 0.28 | 1.26 | - | - | - | - | - | 0.16 | 95.93 | - | - | - | - |
| | | | | | | 5.07 | 0.21 | 0.33 | 4.75 | - | 0.13 | 1.72 | - | - | 0.40 | 87.39 | - | - | - | - |
| | | | | | | 2.44 | 0.24 | 0.24 | 0.95 | - | 0.07 | 1.09 | - | 0.14 | 1.40 | 87.20 | - | - | - | 6.23 |

**Table 5.11:** SEM-EDX results for copper prills in the slag thin-sections. All results are presented in weight%. Double-bottom borders indicate a change in the excavation area, and the table was divided to avoid splitting any samples across two pages. The letter following the elemental symbol represents the electron shell. The first letter in the Stratum (Strat.) represents the excavation area. Samples that did not include copper prills are not included in this table (Continued).

| Complete Data for Copper Prills analyzed with SEM-EDS (Continued) | | | | | | | | | | | | | | | | | | | | |
|---|---|---|---|---|---|---|---|---|---|---|---|---|---|---|---|---|---|---|---|---|
| Year | Site | Area | Strat. | Loc. | Sample | O-K | Al-K | Si-K | S-K | K-K | Ca-K | Mn-K | Fe-K | Co-K | Ni-K | Cu-K | Zn-K | As-K | Ba-L | Pb-L |
| 2006 | KAJ | A | A5 | 119 | 3282 | 6.72 | 0.37 | 0.36 | 1.57 | - | 0.09 | 1.18 | - | - | - | 89.71 | - | - | - | - |
| | | | | | | 5.49 | 0.51 | 0.33 | 2.94 | 0.08 | 0.30 | 2.28 | 0.37 | - | - | 87.70 | - | - | - | - |
| | | | | | | 5.20 | 0.52 | 0.51 | 1.73 | - | 0.08 | 0.69 | - | - | - | 91.29 | - | - | - | - |
| | | | | | | 5.50 | 0.72 | 0.32 | 1.45 | - | 0.10 | 0.99 | - | - | - | 90.91 | - | - | - | - |
| | | | | | | 3.20 | 1.36 | 0.34 | 2.95 | - | 0.10 | 1.12 | - | - | - | 90.93 | - | - | - | - |
| 2006 | KAJ | A | A5 | 121 | 3285 | 8.44 | - | 0.35 | - | - | 0.08 | 0.50 | - | - | - | 90.50 | - | - | 0.14 | - |
| | | | | | | 11.58 | - | 0.33 | 2.04 | - | 0.07 | 0.58 | - | - | - | 85.40 | - | - | - | - |
| | | | | | | 2.15 | - | 0.34 | 0.83 | - | 0.06 | 0.38 | - | - | - | 96.23 | - | - | - | - |
| | | | | | | 4.19 | 0.68 | 1.84 | - | 0.29 | 0.63 | 2.46 | 0.43 | - | - | 88.91 | - | - | 0.57 | - |
| | | | | | | 7.04 | 0.90 | 0.98 | 1.60 | 0.17 | 0.46 | 1.99 | - | - | - | 86.85 | - | - | - | - |
| | | | | | | 5.93 | - | 0.42 | 1.41 | - | 0.09 | 0.65 | - | - | - | 91.50 | - | - | - | - |
| | | | | | | 8.91 | 0.49 | 0.28 | 1.43 | - | 0.08 | 0.65 | 0.12 | - | - | 87.88 | - | - | 0.15 | - |
| | | | | | | 8.79 | - | 0.32 | - | - | 0.11 | 0.97 | - | - | - | 89.80 | - | - | - | - |
| | | | | | | 1.82 | 0.24 | 0.28 | - | - | 0.24 | 1.81 | - | - | - | 95.62 | - | - | - | - |
| | | | | | | 1.18 | - | - | - | - | 0.12 | 0.76 | - | - | - | 97.94 | - | - | - | - |
| | | | | | | 4.68 | 0.70 | 0.92 | 0.94 | 0.22 | 0.44 | 1.90 | 0.27 | - | - | 89.45 | - | - | 0.49 | - |
| | | | | | | 9.30 | 0.49 | 0.45 | 3.79 | 0.07 | 0.09 | 0.57 | - | - | - | 85.25 | - | - | - | - |
| 2006 | KAJ | A | A5 | 119 | 3269 | 2.27 | - | 0.47 | - | 0.13 | 0.10 | 2.61 | 0.47 | - | - | 93.96 | - | - | - | - |
| | | | | | | 1.69 | 0.50 | 0.66 | 0.94 | 0.11 | 0.09 | 2.80 | 0.51 | - | - | 92.51 | - | - | 0.20 | - |
| | | | | | | 1.71 | 0.53 | 0.46 | 0.37 | 0.14 | 0.09 | 2.96 | 0.53 | - | - | 93.21 | - | - | - | - |
| | | | | | | 2.21 | 0.34 | 0.64 | 0.53 | 0.25 | 0.16 | 3.00 | 0.54 | - | - | 91.95 | - | - | 0.37 | - |
| | | | | | | 1.92 | 0.40 | 0.55 | 0.89 | - | 0.10 | 2.00 | 0.51 | - | - | 93.36 | - | - | 0.28 | - |
| | | | | | | 1.37 | 0.39 | 0.33 | 0.45 | 0.10 | 0.11 | 2.80 | 0.56 | - | - | 93.63 | - | - | 0.26 | - |
| | | | | | | 1.57 | 0.45 | 0.37 | 0.43 | 0.09 | 0.08 | 2.86 | 0.58 | - | - | 93.59 | - | - | - | - |
| | | | | | | 2.35 | 0.56 | 0.68 | - | 0.07 | 0.09 | 2.35 | 0.43 | - | - | 93.47 | - | - | - | - |
| 2006 | KAJ | A | A5 | 121 | 3279 | 8.10 | 0.34 | - | 1.50 | - | 0.06 | 0.47 | - | - | 0.51 | 84.64 | - | 1.68 | - | 2.70 |
| | | | | | | 1.73 | 0.26 | - | 0.52 | - | 0.19 | 1.71 | - | - | - | 95.14 | - | 0.45 | - | - |
| | | | | | | 2.79 | 0.39 | 0.40 | 1.16 | 0.08 | 0.18 | 2.42 | - | - | - | 92.57 | - | - | - | - |
| | | | | | | 2.81 | 0.75 | 0.91 | 3.06 | 0.14 | 0.29 | 2.32 | 0.30 | - | - | 89.43 | - | - | - | - |
| | | | | | | 4.01 | 1.20 | 1.77 | 3.99 | 0.30 | 0.49 | 2.69 | 0.31 | - | - | 84.93 | - | - | 0.31 | - |
| | | | | | | 1.01 | 0.54 | 0.73 | 0.49 | 0.08 | 0.34 | 2.69 | - | - | - | 94.11 | - | - | - | - |
| | | | | | | 2.94 | 0.80 | 0.57 | 0.16 | - | 0.30 | 2.61 | 0.28 | - | - | 92.35 | - | - | - | - |
| | | | | | | 3.05 | 1.31 | 2.01 | - | 0.39 | 0.60 | 2.74 | - | - | - | 89.62 | - | - | 0.27 | - |
| | | | | | | 2.61 | 1.08 | 1.27 | 3.13 | 0.22 | 0.59 | 2.96 | - | - | - | 88.14 | - | - | - | - |
| 2006 | KEN | M | M1 | 502/3 | 10250 | 2.06 | 0.48 | 0.49 | 0.75 | - | 0.23 | 2.49 | 0.84 | - | 0.36 | 92.30 | - | - | - | - |
| | | | | | | 2.51 | 0.68 | 0.49 | 1.44 | - | 0.17 | 1.70 | 0.61 | - | 0.42 | 91.98 | - | - | - | - |
| | | | | | | 2.83 | 1.10 | 0.52 | 0.85 | - | 0.10 | 1.79 | 0.71 | - | 0.51 | 91.58 | - | - | - | - |
| | | | | | | 1.83 | 0.39 | 0.35 | 1.17 | - | - | 1.37 | 0.56 | - | 0.49 | 93.84 | - | - | - | - |
| | | | | | | 6.46 | 0.45 | 0.39 | 2.79 | - | - | 0.21 | - | - | 0.32 | 89.39 | - | - | - | - |
| | | | | | | 4.94 | 4.58 | 0.64 | - | 0.08 | 0.16 | 1.75 | 0.72 | - | 0.38 | 86.75 | - | - | - | - |
| | | | | | | 2.59 | 0.37 | 0.47 | 0.76 | 0.08 | 0.21 | 2.56 | 0.88 | - | 0.57 | 91.52 | - | - | - | - |
| | | | | | | 2.16 | 0.52 | 0.49 | 0.42 | - | - | 0.50 | 0.23 | - | 0.54 | 95.15 | - | - | - | - |
| | | | | | | 2.34 | 0.21 | 0.36 | 2.86 | - | 0.19 | 2.55 | 0.85 | - | 0.47 | 89.70 | - | 0.46 | - | - |
| | | | | | | 2.38 | 0.32 | 0.52 | 0.96 | - | 0.06 | 1.57 | 0.54 | - | 0.47 | 93.17 | - | - | - | - |
| | | | | | | 1.97 | 0.27 | 0.39 | 0.76 | - | 0.06 | 1.49 | 0.51 | - | 0.47 | 94.09 | - | - | - | - |
| 2006 | KEN | M | M1 | 502/3 | 10250-2 | 2.12 | 0.64 | 0.49 | 0.52 | - | 0.12 | 1.82 | 0.69 | - | 0.73 | 92.88 | - | - | - | - |
| | | | | | | 3.23 | 0.48 | 0.55 | 0.63 | - | 0.07 | 1.90 | 0.67 | 0.00 | 0.63 | 91.84 | - | - | - | - |
| | | | | | | 2.07 | - | 0.33 | 0.50 | - | - | 0.32 | 0.15 | - | 0.75 | 95.88 | - | - | - | - |
| | | | | | | 2.64 | 1.32 | 0.43 | 1.39 | - | 0.05 | 0.56 | 0.30 | - | 0.76 | 92.55 | - | - | - | - |
| | | | | | | 2.44 | 0.29 | 0.42 | 0.71 | - | - | 0.64 | 0.26 | - | 0.78 | 94.46 | - | - | - | - |
| | | | | | | 2.93 | 0.48 | 0.44 | 0.78 | - | 0.05 | 0.80 | 0.26 | - | 0.72 | 93.53 | - | - | - | - |

**Table 5.11:** SEM-EDX results for copper prills in the slag thin-sections. All results are presented in weight%. Double-bottom borders indicate a change in the excavation area, and the table was divided to avoid splitting any samples across two pages. The letter following the elemental symbol represents the electron shell. The first letter in the Stratum (Strat.) represents the excavation area. Samples that did not include copper prills are not included in this table (Continued).

| Complete Data for Copper Prills analyzed with SEM-EDS (Continued) | | | | | | | | | | | | | | | | | | | | |
|---|---|---|---|---|---|---|---|---|---|---|---|---|---|---|---|---|---|---|---|---|
| Year | Site | Area | Strat. | Loc. | Sample | O-K | Al-K | Si-K | S-K | K-K | Ca-K | Mn-K | Fe-K | Co-K | Ni-K | Cu-K | Zn-K | As-K | Ba-L | Pb-L |
| 2006 | KEN | M | M1 | - | 10482 | 1.82 | - | 0.22 | 1.85 | - | 0.08 | 2.04 | 0.31 | 0.68 | - | 93.00 | - | - | - | - |
| | | | | | | 3.23 | 0.33 | 0.23 | 2.82 | - | - | 1.65 | 0.33 | - | 0.50 | 90.91 | - | - | - | - |
| | | | | | | 2.48 | 0.26 | 0.33 | 3.90 | - | 0.12 | 3.00 | 0.44 | - | 2.32 | 87.15 | - | - | - | - |
| 2006 | KEN | M | M1 | - | 10482 | 1.63 | - | 0.23 | 3.22 | - | 0.13 | 3.33 | 0.47 | - | 1.40 | 89.59 | - | - | - | - |
| | | | | | | 1.45 | 0.27 | 0.25 | 2.25 | - | 0.13 | 3.59 | - | - | 1.23 | 90.83 | - | - | - | - |
| | | | | | | 0.89 | - | 0.25 | 2.71 | - | 0.14 | 3.39 | - | - | 0.98 | 91.64 | - | - | - | - |
| | | | | | | 0.94 | 0.57 | 0.52 | 1.06 | - | 0.08 | 1.26 | - | - | 0.81 | 94.75 | - | - | - | - |
| | | | | | | 2.32 | 0.15 | 0.15 | 3.27 | - | 0.08 | 1.38 | - | - | 2.40 | 90.25 | - | - | - | - |
| 2006 | KEN | M | M1 | - | 10482-2 | 2.83 | - | 0.38 | 0.64 | - | - | 1.98 | - | - | 0.85 | 93.31 | - | - | - | - |
| 2006 | KEN | M | M1/M2 | - | 10484 | 2.11 | 0.20 | 0.22 | 2.79 | - | 0.12 | 2.16 | 0.51 | - | 0.36 | 91.53 | - | - | - | - |
| | | | | | | 2.59 | - | 0.30 | 4.08 | - | 0.07 | 1.00 | 0.31 | - | 0.54 | 91.11 | - | - | - | - |
| | | | | | | 0.98 | 0.23 | 0.23 | 1.54 | - | - | 0.29 | - | - | 0.40 | 96.33 | - | - | - | - |
| | | | | | | 2.72 | 0.46 | 0.25 | 1.41 | 0.10 | 0.13 | 3.18 | 0.69 | - | 0.39 | 87.94 | - | - | - | 2.72 |
| 2006 | KEN | M | M1/M2 | - | 10484-2 | 1.67 | 0.21 | 0.29 | 0.86 | - | - | 0.57 | - | - | 0.78 | 95.62 | - | - | - | - |
| | | | | | | 3.55 | 0.20 | 0.22 | 0.47 | - | - | 0.83 | 0.49 | - | 0.52 | 90.90 | - | - | - | 2.82 |
| | | | | | | 1.63 | 0.23 | 0.12 | 0.94 | - | - | 1.34 | 0.45 | - | - | 92.57 | - | 0.00 | - | 2.72 |
| | | | | | | 2.81 | 0.28 | 0.32 | 0.93 | - | 0.10 | 1.65 | 1.35 | 0.12 | 0.76 | 91.69 | - | - | - | - |
| | | | | | | 3.54 | - | 0.29 | 1.32 | - | - | 1.01 | 1.56 | 0.06 | 0.59 | 91.63 | - | - | - | - |
| 2006 | KEN | M | M1/M2 | - | 10485-2 | 2.47 | 0.17 | 0.35 | 0.72 | - | 0.09 | 1.69 | 0.44 | - | 0.52 | 93.54 | - | - | - | - |
| | | | | | | 2.63 | 0.32 | 0.40 | 0.49 | - | - | 0.41 | 1.45 | 0.23 | 0.54 | 93.53 | - | - | - | - |
| | | | | | | 2.17 | 0.23 | 0.28 | 0.85 | - | - | 2.18 | 0.60 | - | 0.60 | 93.08 | - | - | - | - |
| | | | | | | 2.91 | 0.45 | 0.40 | 0.40 | - | - | 0.24 | 0.30 | 0.16 | 0.57 | 94.58 | - | - | - | - |
| | | | | | | 3.61 | 0.56 | 0.52 | 0.59 | - | - | 0.31 | 1.51 | 0.29 | 0.61 | 92.01 | - | - | - | - |
| | | | | | | 2.80 | 0.20 | 0.34 | 0.64 | - | - | 1.30 | 1.36 | 0.29 | 0.50 | 92.56 | - | - | - | - |
| | | | | | | 4.91 | - | 0.33 | 0.74 | - | - | 0.84 | 0.31 | - | 0.50 | 92.37 | - | - | - | - |
| | | | | | | 2.08 | 0.23 | 0.33 | 0.90 | - | - | 1.19 | 0.78 | - | 0.65 | 93.85 | - | - | - | - |
| 2006 | KEN | M | M1/M2 | - | 10485 | 2.44 | 0.27 | 0.54 | 0.72 | - | 0.07 | 0.89 | 0.36 | - | 0.37 | 93.04 | - | - | - | 1.31 |
| | | | | | | 2.50 | 0.61 | 0.82 | 0.91 | 0.09 | 0.23 | 3.52 | 1.04 | - | 0.25 | 90.04 | - | - | - | - |
| | | | | | | 2.02 | 0.53 | 0.59 | - | - | 0.14 | 2.30 | 0.75 | - | 0.29 | 93.38 | - | - | - | - |
| | | | | | | 2.60 | 0.15 | 0.35 | 3.33 | - | 0.18 | 2.48 | 0.93 | - | 0.46 | 89.52 | - | - | - | - |
| | | | | | | 1.89 | 0.31 | 0.39 | 1.76 | - | 0.10 | 2.47 | 0.84 | - | 0.42 | 91.82 | - | - | - | - |
| | | | | | | 2.60 | 0.34 | 0.65 | 0.52 | - | - | 1.18 | 0.63 | 0.28 | 0.37 | 93.43 | - | - | - | - |
| | | | | | | 3.05 | 0.54 | 0.53 | 0.39 | - | - | 0.31 | 2.93 | 0.10 | - | 92.14 | - | - | - | - |
| | | | | | | 2.89 | 0.51 | 0.58 | 0.39 | - | 0.08 | 1.53 | 0.62 | - | 0.29 | 93.11 | - | - | - | - |
| | | | | | | 1.88 | 0.36 | 0.43 | 0.64 | - | 0.10 | 2.52 | 0.78 | - | 0.18 | 93.11 | - | - | - | - |
| | | | | | | 2.24 | 0.51 | 0.44 | 1.56 | - | 0.17 | 2.15 | 0.79 | - | 0.19 | 91.95 | - | - | - | - |
| | | | | | | 2.57 | 0.29 | 0.40 | 0.44 | - | - | 1.50 | 0.41 | - | 0.35 | 91.83 | - | - | - | 2.22 |
| | | | | | | 1.96 | 0.41 | 0.56 | 0.83 | - | 0.09 | 2.18 | 0.53 | - | 0.31 | 93.13 | - | - | - | - |
| | | | | | | 3.01 | 0.64 | 0.55 | 1.06 | - | - | 2.08 | 0.56 | - | 0.30 | 90.20 | - | - | - | 1.60 |
| 2006 | KEN | M | M1/M2 | - | 10487 | 2.06 | - | 0.27 | 1.48 | - | - | 2.18 | 0.70 | - | 0.93 | 90.89 | 0.96 | 0.54 | - | - |
| | | | | | | 2.43 | - | 0.65 | - | 0.09 | 0.18 | 4.29 | 1.22 | - | 0.46 | 90.68 | - | - | - | - |
| | | | | | | 2.47 | 0.40 | 0.35 | - | - | 0.14 | 3.79 | 1.19 | - | 0.20 | 89.77 | 1.69 | - | - | - |
| | | | | | | 2.62 | 0.43 | 0.30 | 0.79 | - | 0.14 | 3.93 | 1.96 | 0.34 | 0.26 | 87.88 | 1.37 | - | - | - |
| | | | | | | 2.23 | - | 0.32 | 0.87 | 0.09 | 0.19 | 3.29 | 1.08 | 0.14 | 0.38 | 90.72 | - | 0.68 | - | - |
| | | | | | | 5.07 | - | 0.34 | 0.52 | - | 0.07 | 0.79 | 0.73 | - | 0.42 | 88.31 | - | - | - | 3.76 |
| 2006 | KEN | M | M2 (up) | - | 10488 | 4.44 | 0.19 | 0.30 | 7.78 | - | 0.11 | 0.86 | - | 0.13 | 1.40 | 84.80 | - | - | - | - |
| | | | | | | 3.29 | 0.20 | 0.33 | 3.73 | - | - | - | - | - | 0.37 | 92.08 | - | - | - | - |
| | | | | | | 3.30 | 0.75 | 0.27 | 1.50 | - | - | 0.53 | 0.29 | 0.24 | 0.91 | 92.21 | - | - | - | - |

**Table 5.11:** SEM-EDX results for copper prills in the slag thin-sections. All results are presented in weight%. Double-bottom borders indicate a change in the excavation area, and the table was divided to avoid splitting any samples across two pages. The letter following the elemental symbol represents the electron shell. The first letter in the Stratum (Strat.) represents the excavation area. Samples that did not include copper prills are not included in this table (Continued).

| Complete Data for Copper Prills analyzed with SEM-EDS (Continued) | | | | | | | | | | | | | | | | | | | |
|---|---|---|---|---|---|---|---|---|---|---|---|---|---|---|---|---|---|---|---|
| Year | Site | Area | Strat. | Loc. | Sample | O-K | Al-K | Si-K | S-K | K-K | Ca-K | Mn-K | Fe-K | Co-K | Ni-K | Cu-K | Zn-K | As-K | Ba-L | Pb-L |
| 2006 | KEN | M | M2 (up) | - | 10489 | 3.41 | 0.36 | 0.32 | 2.23 | - | 0.17 | 2.18 | 1.31 | 0.16 | 0.56 | 88.32 | 0.98 | - | - | - |
| | | | | | | 2.86 | 0.26 | 0.24 | 1.75 | - | - | 0.47 | 2.26 | 0.31 | 0.41 | 90.05 | 1.39 | - | - | - |
| | | | | | | 1.48 | 0.32 | 0.33 | 1.83 | - | 0.16 | 3.20 | - | - | 0.48 | 92.21 | - | - | - | - |
| | | | | | | 12.89 | 0.23 | - | 1.16 | 0.29 | - | 0.49 | 1.07 | 0.19 | 0.47 | 78.05 | 1.30 | 0.16 | - | 3.70 |
| | | | | | | 3.54 | 0.17 | 0.29 | 2.41 | 0.08 | 0.20 | 2.27 | 1.39 | 0.04 | 0.35 | 89.27 | - | - | - | - |
| | | | | | | 2.88 | 0.23 | 0.28 | 1.65 | - | 0.19 | 1.97 | 2.45 | 0.30 | 0.44 | 88.69 | 0.92 | - | - | - |
| | | | | | | 3.87 | 0.33 | 0.46 | 4.48 | - | 0.11 | 1.90 | 0.96 | 0.25 | 0.66 | 86.98 | - | - | - | - |
| | | | | | | 4.46 | - | 0.27 | 4.88 | - | 0.12 | 1.69 | 1.77 | 0.33 | 0.56 | 85.92 | - | - | - | - |
| 2006 | KEN | M | M2 (up) | 511 | 10255 | 1.67 | - | 0.15 | 1.26 | - | - | 0.72 | 0.49 | 0.29 | 0.43 | 94.99 | - | - | - | - |
| | | | | | | 4.77 | - | 0.37 | - | - | 0.14 | 2.42 | 0.81 | - | 0.40 | 91.09 | - | - | - | - |
| | | | | | | 4.57 | 1.92 | 0.62 | 1.62 | - | 0.15 | 2.78 | 0.78 | - | 0.28 | 87.28 | - | - | - | - |
| | | | | | | 4.98 | - | 0.40 | - | - | 0.16 | 2.81 | 0.77 | - | 0.37 | 90.52 | - | - | - | - |
| | | | | | | 2.61 | 0.32 | 0.23 | 2.09 | - | 0.07 | 1.49 | 0.39 | - | 0.38 | 92.41 | - | - | - | - |
| | | | | | | 2.65 | 0.24 | 0.24 | 1.39 | - | - | 1.26 | 0.42 | - | 0.44 | 93.36 | - | - | - | - |
| | | | | | | 2.57 | 0.28 | 0.27 | 2.31 | - | 0.18 | 1.79 | 0.59 | - | 0.49 | 91.52 | - | - | - | - |
| 2006 | KEN | M | M2 (up) | 511 | 10255-2 | 4.02 | 0.36 | 0.49 | 1.64 | - | 0.07 | 1.24 | 0.36 | 0.26 | 0.54 | 91.01 | - | - | - | - |
| | | | | | | 2.67 | 0.26 | 0.35 | 1.16 | - | 0.12 | 1.38 | 0.33 | - | 0.53 | 93.19 | - | - | - | - |
| | | | | | | 3.12 | 0.31 | 0.46 | 1.38 | - | 0.11 | 2.18 | 0.52 | - | 0.63 | 91.29 | - | - | - | - |
| | | | | | | 2.85 | 0.21 | 0.36 | 1.62 | - | - | 1.12 | 0.24 | - | 0.58 | 93.02 | - | - | - | - |
| 2006 | KEN | M | M2 (up) | - | 10486 | 2.19 | 0.77 | 0.43 | 2.93 | - | 0.23 | 3.24 | - | 0.25 | 0.39 | 86.26 | - | - | 0.24 | 3.08 |
| | | | | | | 2.19 | 0.43 | 0.29 | 1.47 | - | - | 0.55 | 0.44 | 0.25 | 0.56 | 90.25 | - | - | - | 3.57 |
| | | | | | | 3.45 | 0.31 | 0.34 | 1.93 | - | - | 0.84 | 0.60 | 0.30 | 0.48 | 91.75 | - | - | - | - |
| | | | | | | 2.65 | 0.50 | 0.28 | 1.13 | - | 0.08 | 1.03 | 0.69 | 0.24 | 0.35 | 90.22 | 0.80 | - | - | 2.02 |
| | | | | | | 2.40 | 0.47 | 0.33 | 2.24 | - | 0.09 | 1.64 | 0.72 | 0.31 | 0.33 | 91.48 | - | - | - | - |
| | | | | | | 2.67 | 0.50 | 0.21 | 2.40 | - | - | 1.67 | 0.74 | 0.33 | 0.31 | 87.59 | - | - | - | 3.59 |
| 2006 | KEN | M | M2 | 602 | 10276 | 2.36 | 0.33 | 0.36 | 2.78 | - | - | 1.07 | 0.28 | 0.13 | 0.89 | 91.80 | - | - | - | - |
| | | | | | | 1.42 | - | 0.31 | 1.89 | - | - | 0.73 | - | - | 0.75 | 94.89 | - | - | - | - |
| | | | | | | 0.94 | - | 0.33 | 0.76 | - | 1.28 | 0.18 | - | - | 0.72 | 95.79 | - | - | - | - |
| | | | | | | 1.60 | 0.09 | 0.17 | 1.96 | - | 0.09 | 1.50 | 0.32 | - | 0.86 | 90.62 | - | - | - | 2.79 |
| | | | | | | 4.30 | 0.27 | 0.42 | 2.58 | - | - | 0.96 | 0.22 | 0.15 | 0.81 | 90.28 | - | - | - | - |
| | | | | | | 2.04 | 0.13 | 0.27 | 1.78 | - | - | 1.25 | 0.31 | - | 1.13 | 93.10 | - | - | - | - |
| | | | | | | 2.51 | 0.31 | 0.38 | 1.57 | - | 0.10 | 2.36 | 0.33 | - | 0.79 | 91.64 | - | - | - | - |
| 2006 | KEN | M | M2 | - | 10476 | 8.54 | - | 0.30 | 3.70 | - | 0.08 | 0.96 | - | - | - | 86.42 | - | - | - | - |
| | | | | | | 6.92 | - | 0.24 | 1.53 | - | 0.16 | 1.86 | 0.31 | - | - | 88.99 | - | - | - | - |
| | | | | | | - | 1.98 | 5.60 | 0.75 | 2.32 | 3.42 | 0.29 | 0.54 | 3.08 | 0.47 | 81.56 | - | - | - | - |
| | | | | | | 7.98 | - | 0.24 | 3.01 | - | 0.08 | 1.09 | 0.23 | - | - | 87.37 | - | - | - | - |
| | | | | | | 8.56 | - | 0.27 | 2.27 | - | - | 0.47 | 0.12 | - | - | 88.31 | - | - | - | - |
| | | | | | | 9.79 | - | 0.27 | 2.32 | 0.06 | 0.13 | 1.98 | 0.39 | - | - | 84.90 | - | - | 0.17 | - |
| | | | | | | 5.08 | 2.36 | 0.31 | 3.32 | - | 0.13 | 1.96 | 0.33 | - | - | 86.51 | - | - | - | - |
| 2006 | KEN | M | M2 | - | 10493 | 2.98 | - | 0.21 | 4.93 | - | 0.24 | 1.99 | 0.57 | - | - | 89.08 | - | - | - | - |
| | | | | | | 4.97 | - | 0.22 | 6.12 | - | 0.19 | 1.51 | 0.44 | - | - | 86.54 | - | - | - | - |
| | | | | | | 2.67 | - | 0.18 | 10.03 | - | 0.36 | 1.98 | 0.74 | - | - | 84.04 | - | - | - | - |
| | | | | | | 2.67 | - | 0.14 | 1.61 | - | 0.12 | 1.45 | 0.54 | - | - | 93.47 | - | - | - | - |
| | | | | | | 10.04 | 0.16 | 0.20 | 2.26 | - | - | 0.28 | 0.12 | - | - | 86.94 | - | - | - | - |
| | | | | | | 5.43 | 0.19 | - | 1.93 | - | 0.18 | 1.85 | 0.51 | - | - | 89.91 | - | - | - | - |
| | | | | | | 3.32 | 0.13 | 0.18 | 1.89 | 0.07 | 0.25 | 2.09 | 0.80 | - | - | 91.27 | - | - | - | - |

**Table 5.11:** SEM-EDX results for copper prills in the slag thin-sections. All results are presented in weight%. Double-bottom borders indicate a change in the excavation area, and the table was divided to avoid splitting any samples across two pages. The letter following the elemental symbol represents the electron shell. The first letter in the Stratum (Strat.) represents the excavation area. Samples that did not include copper prills are not included in this table (Continued).

| Complete Data for Copper Prills analyzed with SEM-EDS (Continued) | | | | | | | | | | | | | | | | | | | |
|---|---|---|---|---|---|---|---|---|---|---|---|---|---|---|---|---|---|---|---|
| Year | Site | Area | Strat. | Loc. | Sample | O-K | Al-K | Si-K | S-K | K-K | Ca-K | Mn-K | Fe-K | Co-K | Ni-K | Cu-K | Zn-K | As-K | Ba-L | Pb-L |
| 2006 | KEN | M | M2 | 606 | 606 | 4.98 | 0.37 | 0.43 | 7.88 | - | - | 0.66 | 0.22 | - | 0.50 | 84.96 | - | - | - | - |
| | | | | | | 2.50 | 0.18 | 0.15 | 1.49 | - | - | 0.30 | 0.48 | 0.22 | 0.48 | 94.20 | - | - | - | - |
| | | | | | | 3.31 | - | 0.19 | 2.57 | - | 0.06 | 0.64 | 0.30 | 0.21 | 0.41 | 92.31 | - | - | - | - |
| | | | | | | 2.08 | 0.16 | 0.24 | 1.25 | - | 0.08 | 1.12 | 0.38 | 0.29 | 0.43 | 93.98 | - | - | - | - |
| | | | | | | 2.65 | 0.12 | 0.13 | 2.42 | - | 0.07 | 0.67 | 0.50 | 0.33 | 0.46 | 92.65 | - | - | - | - |
| | | | | | | 3.64 | 0.19 | 0.26 | 0.82 | - | - | 0.50 | 0.22 | 0.46 | 0.27 | 93.64 | - | - | - | - |
| | | | | | | 2.49 | 0.19 | 0.31 | 1.27 | - | - | 0.48 | 0.31 | 0.21 | 0.50 | 94.24 | - | - | - | - |
| | | | | | | 1.84 | 0.26 | 0.22 | 2.43 | - | 0.15 | 2.08 | - | 0.23 | 0.80 | 91.52 | - | 0.46 | - | - |
| | | | | | | 1.52 | 0.34 | 0.27 | 0.51 | - | 0.14 | 1.73 | 0.39 | 0.20 | 0.41 | 89.57 | - | - | - | 4.92 |
| | | | | | | 2.61 | - | 0.15 | 2.63 | - | - | 0.28 | 0.44 | 0.24 | 0.41 | 93.25 | - | - | - | - |
| | | | | | | 2.30 | 0.14 | 0.17 | 1.45 | - | 0.10 | 1.13 | 0.44 | 0.24 | 0.41 | 93.62 | - | - | - | - |
| 2006 | KEN | M | M2 | 622 | 622 | 5.06 | 0.58 | 0.27 | 2.22 | - | - | 0.59 | 0.20 | - | - | 90.68 | - | 0.40 | - | - |
| | | | | | | 4.13 | - | 0.33 | 3.79 | - | - | 0.58 | 0.29 | - | - | 90.89 | - | - | - | - |
| | | | | | | 6.32 | 0.43 | 0.40 | 4.32 | - | 0.05 | 2.07 | 0.57 | - | - | 85.39 | - | 0.46 | - | - |
| 2006 | KEN | M | M2 | 602 | 9013 | 0.51 | 0.15 | 0.28 | 3.50 | - | 0.08 | 3.58 | - | - | 0.35 | 91.55 | - | - | - | - |
| | | | | | | 1.34 | 0.10 | 0.28 | 2.00 | - | 0.16 | 6.30 | - | 0.70 | 0.38 | 87.41 | 1.33 | - | - | - |
| | | | | | | 1.65 | 0.15 | 0.26 | 0.75 | - | - | 0.43 | 0.46 | 0.26 | 0.45 | 95.58 | - | - | - | - |
| | | | | | | 0.50 | 0.23 | 0.28 | 1.96 | - | 0.09 | 4.09 | - | 0.39 | 0.45 | 92.02 | - | - | - | - |
| | | | | | | 1.94 | 0.13 | 0.35 | 1.29 | 0.06 | 0.11 | 1.71 | 1.44 | 0.44 | 0.54 | 90.91 | 1.09 | - | - | - |
| 2006 | KEN | M | M2 | 602 | 10260 | 2.00 | 0.28 | 0.18 | - | - | 0.10 | 0.69 | 0.98 | 0.35 | 0.43 | 95.00 | - | - | - | - |
| | | | | | | 3.69 | 0.43 | 0.39 | 0.15 | - | 0.19 | 1.45 | 0.38 | - | 0.38 | 92.94 | - | - | - | - |
| 2006 | KEN | M | M2 | 627 | 10266 | 1.12 | 0.47 | 0.33 | 1.37 | - | 0.17 | 2.09 | - | 0.14 | 0.41 | 93.89 | - | - | - | - |
| | | | | | | 3.14 | 0.55 | 0.40 | 0.40 | - | 0.11 | 1.32 | 0.37 | - | 0.38 | 93.32 | - | - | - | - |
| | | | | | | 4.21 | 0.46 | 0.52 | 1.91 | - | 0.15 | 1.71 | 0.50 | - | 0.56 | 89.97 | - | - | - | - |
| | | | | | | 2.31 | - | 0.33 | 4.00 | - | - | 0.17 | - | - | 0.52 | 90.05 | - | 2.63 | - | - |
| | | | | | | 2.76 | 0.52 | 0.44 | - | - | - | 0.37 | 0.47 | - | 0.38 | 95.05 | - | - | - | - |
| | | | | | | 2.49 | 0.24 | 0.31 | - | - | - | 0.29 | 0.46 | 0.16 | - | 96.06 | - | - | - | - |
| | | | | | | 3.55 | 0.51 | 0.55 | 0.58 | - | 0.06 | 0.51 | 2.07 | 0.17 | - | 91.98 | - | - | - | - |
| | | | | | | 3.76 | - | 0.42 | 4.18 | - | 0.06 | 0.64 | 0.42 | 0.17 | 0.34 | 90.00 | - | - | - | - |
| | | | | | | 1.49 | 0.23 | 0.36 | 2.31 | - | - | 0.16 | - | - | 0.43 | 95.01 | - | - | - | - |
| 2006 | KEN | M | M2 | 629 | 629 | 3.73 | - | 0.27 | 4.32 | - | - | 0.49 | 0.16 | - | - | 91.03 | - | - | - | - |
| | | | | | | 6.69 | - | 0.36 | 2.75 | - | - | 0.76 | 0.27 | - | - | 89.18 | - | - | - | - |
| | | | | | | 3.35 | - | 0.28 | 3.20 | - | - | 0.86 | 0.30 | - | - | 92.00 | - | - | - | - |
| | | | | | | 4.36 | - | 0.30 | 2.80 | - | 0.09 | 1.06 | 0.31 | - | - | 91.09 | - | - | - | - |
| 2006 | KEN | M | M2/M3 | 641 | 10267 | 2.77 | 0.39 | 0.50 | 1.12 | - | 0.19 | 2.15 | 0.68 | - | 1.16 | 91.04 | - | - | - | - |
| | | | | | | 6.61 | 0.41 | 0.50 | - | - | - | 0.21 | 0.26 | 0.14 | 0.24 | 91.64 | - | - | - | - |
| | | | | | | 2.26 | - | 0.41 | 3.76 | - | 0.12 | 3.39 | - | - | 0.50 | 89.56 | - | - | - | - |
| | | | | | | 2.84 | - | 0.38 | 5.07 | 0.08 | 0.19 | 2.09 | - | - | 0.40 | 88.95 | - | - | - | - |
| | | | | | | 1.03 | - | 0.31 | 3.11 | 0.07 | 0.17 | 2.10 | - | - | 0.42 | 92.79 | - | - | - | - |
| | | | | | | 1.61 | 0.39 | 0.40 | 5.75 | 0.15 | 0.31 | 3.42 | - | - | 0.44 | 87.53 | - | - | - | - |
| | | | | | | 0.84 | - | 0.38 | - | 0.07 | 0.21 | 2.81 | - | - | 0.33 | 95.36 | - | - | - | - |
| 2006 | KEN | M | M2/M3 | 641 | 10465 | 2.59 | - | 0.29 | 4.03 | - | - | 3.01 | - | - | - | 90.08 | - | - | - | - |
| | | | | | | 2.74 | 0.12 | 0.39 | 4.54 | - | - | 1.45 | - | - | - | 90.77 | - | - | - | - |
| | | | | | | 2.63 | - | 0.37 | 4.22 | - | 0.09 | 2.71 | - | - | - | 89.98 | - | - | - | - |
| | | | | | | 5.64 | 0.53 | 1.09 | 5.58 | 0.26 | 0.18 | 2.52 | - | - | - | 83.68 | - | - | 0.52 | - |
| 2006 | KEN | M | M2/M3 | 641 | 10468 | 6.87 | - | 0.35 | 2.08 | 0.06 | 0.21 | 2.82 | - | - | 0.33 | 87.29 | - | - | - | - |
| | | | | | | 1.97 | 0.28 | - | 4.01 | - | 0.24 | 3.19 | - | - | 0.31 | 90.00 | - | - | - | - |
| | | | | | | 0.71 | - | 0.29 | 0.68 | 0.06 | 0.28 | 3.54 | - | - | 0.25 | 94.05 | - | - | 0.13 | - |
| | | | | | | 1.31 | - | 0.28 | 1.99 | - | 0.13 | 2.63 | - | - | 0.29 | 93.37 | - | - | - | - |

**Table 5.11:** SEM-EDX results for copper prills in the slag thin-sections. All results are presented in weight%. Double-bottom borders indicate a change in the excavation area, and the table was divided to avoid splitting any samples across two pages. The letter following the elemental symbol represents the electron shell. The first letter in the Stratum (Strat.) represents the excavation area. Samples that did not include copper prills are not included in this table (Continued).

| Complete Data for Copper Prills analyzed with SEM-EDS (Continued) | | | | | | | | | | | | | | | | | | | |
|---|---|---|---|---|---|---|---|---|---|---|---|---|---|---|---|---|---|---|---|
| Year | Site | Area | Strat. | Loc. | Sample | O-K | Al-K | Si-K | S-K | K-K | Ca-K | Mn-K | Fe-K | Co-K | Ni-K | Cu-K | Zn-K | As-K | Ba-L | Pb-L |
| 2006 | KEN | M | M3 (up) | - | 10268 | 3.56 | 0.49 | 0.33 | 4.44 | - | 0.11 | 1.45 | 1.16 | 0.89 | 0.35 | 87.22 | - | - | - | - |
| | | | | | | 2.91 | 0.52 | 0.36 | 4.49 | - | 0.12 | 2.29 | - | 0.28 | 0.41 | 88.62 | - | - | - | - |
| | | | | | | 2.87 | - | 0.27 | 2.01 | - | 0.12 | 1.73 | 0.83 | 1.13 | 0.30 | 90.73 | - | - | - | - |
| | | | | | | 2.93 | 0.33 | 0.26 | 2.29 | - | 0.10 | 1.51 | 1.65 | 0.81 | - | 90.12 | - | - | - | - |
| | | | | | | 2.85 | 0.64 | 0.31 | 2.58 | - | 0.09 | 1.31 | 0.80 | 0.37 | - | 91.04 | - | - | - | - |
| | | | | | | 2.16 | - | 0.26 | 10.49 | 0.06 | 0.18 | 1.77 | - | 0.13 | - | 84.96 | - | - | - | - |
| | | | | | | 1.45 | - | 0.29 | 1.74 | - | 0.07 | 1.13 | 0.29 | 0.28 | 0.42 | 94.32 | - | - | - | - |
| 2006 | KEN | M | M3 (up) | 647 | 10270 | 2.54 | - | 0.33 | 1.64 | - | - | 0.81 | 0.22 | - | 0.47 | 93.99 | - | - | - | - |
| | | | | | | 2.28 | 0.18 | 0.29 | 1.12 | - | 0.05 | 0.42 | 0.17 | - | 0.44 | 95.05 | - | - | - | - |
| 2006 | KEN | M | M3 (up) | 647 | 10269 | 2.19 | - | 0.25 | 0.92 | - | - | 1.87 | 0.33 | - | - | 94.45 | - | - | - | - |
| 2006 | KEN | M | M3 | 660 | 660 | 4.18 | 0.22 | 0.17 | 2.43 | - | 0.14 | 2.22 | 0.36 | 0.33 | 0.66 | 89.29 | - | - | - | - |
| | | | | | | 3.76 | 0.43 | 0.33 | 2.86 | - | 0.10 | 2.26 | - | 0.29 | 0.86 | 89.13 | - | - | - | - |
| | | | | | | 1.38 | - | 0.38 | 1.31 | 0.12 | 0.21 | 3.10 | - | - | 0.49 | 92.75 | - | - | 0.26 | - |
| 2006 | KEN | M | M3 | 665 | 665 | 5.05 | 0.49 | 0.40 | 0.87 | 0.08 | 0.21 | 2.31 | 0.58 | - | - | 90.00 | - | - | - | - |
| | | | | | | 3.37 | 0.34 | 0.27 | 1.19 | - | 0.13 | 2.06 | 0.49 | - | - | 92.15 | - | - | - | - |
| | | | | | | 7.33 | 0.52 | 0.42 | 1.70 | - | 0.17 | 2.17 | 0.43 | - | - | 87.25 | - | - | - | - |
| | | | | | | 12.16 | 0.48 | 0.48 | 1.11 | - | 0.13 | 1.75 | 0.43 | - | - | 83.45 | - | - | - | - |
| | | | | | | 1.94 | - | 0.34 | 1.52 | - | - | 0.18 | - | - | - | 96.01 | - | - | - | - |
| 2006 | KEN | M | M3 | 666 | 666 | 5.23 | 0.23 | 0.27 | 2.99 | - | - | 1.06 | - | - | - | 90.23 | - | - | - | - |
| | | | | | | 5.33 | 0.31 | 0.54 | 1.37 | 0.11 | 0.15 | 1.83 | 0.36 | - | - | 89.75 | - | - | 0.26 | - |
| | | | | | | 8.49 | 0.31 | 0.55 | 0.53 | - | 0.17 | 1.82 | 0.38 | - | - | 87.38 | - | - | 0.36 | - |
| | | | | | | 4.53 | 0.44 | 0.52 | 0.41 | 0.08 | 0.16 | 2.47 | 0.43 | - | - | 90.57 | - | - | 0.38 | - |
| | | | | | | 4.70 | 0.47 | 0.39 | 0.66 | 0.09 | 0.12 | 1.91 | 0.37 | - | - | 91.04 | - | - | 0.24 | - |
| | | | | | | 6.97 | 0.36 | 0.56 | 0.80 | 0.13 | 0.11 | 2.55 | 0.38 | - | - | 87.94 | - | - | 0.20 | - |
| | | | | | | 4.19 | - | 0.28 | 1.36 | - | - | - | - | - | 1.20 | 92.97 | - | - | - | - |
| | | | | | | 6.01 | 0.23 | 0.30 | 1.33 | - | - | 1.66 | - | - | - | 90.48 | - | - | - | - |
| | | | | | | 5.45 | 2.81 | 0.46 | 0.55 | 0.09 | 0.16 | 2.12 | 0.44 | - | - | 87.56 | - | - | 0.36 | - |
| | | | | | | 9.21 | 0.17 | 0.31 | 2.78 | - | - | 0.59 | 0.13 | - | - | 86.80 | - | - | - | - |
| 2006 | KEN | M | M3 | 666 | 10282 | 5.49 | 0.21 | 0.35 | 3.60 | - | 0.08 | 1.36 | - | - | - | 88.91 | - | - | - | - |
| | | | | | | 3.02 | 0.24 | 0.25 | 1.37 | - | 0.10 | 2.76 | - | - | - | 92.25 | - | - | - | - |
| | | | | | | 1.54 | 0.40 | 0.57 | 0.84 | - | 0.21 | 7.90 | - | - | - | 88.54 | - | - | - | - |
| | | | | | | 0.80 | - | 0.23 | 1.60 | - | - | 1.00 | - | - | - | 96.37 | - | - | - | - |
| | | | | | | 1.57 | 0.38 | 0.39 | 0.75 | - | 0.11 | 1.96 | - | - | - | 94.84 | - | - | - | - |
| | | | | | | 1.35 | - | 0.37 | 0.89 | - | 0.16 | 2.95 | - | - | - | 94.29 | - | - | - | - |
| | | | | | | 0.93 | 0.41 | 0.43 | 1.11 | 0.07 | 0.19 | 3.17 | - | - | - | 93.32 | - | - | 0.37 | - |
| | | | | | | 3.69 | 0.56 | 0.58 | 1.55 | - | 0.11 | 2.70 | - | - | - | 90.65 | - | - | 0.17 | - |
| 2006 | KEN | M | M3 (low) | 665 | 10277 | 3.00 | 0.18 | 0.30 | 2.64 | - | - | 0.81 | - | 0.22 | 0.39 | 92.47 | - | - | - | - |
| | | | | | | 2.66 | 0.27 | 0.30 | 1.89 | - | 0.16 | 2.00 | 0.63 | - | 0.71 | 91.37 | - | - | - | - |
| | | | | | | 1.39 | - | 0.23 | 2.87 | - | - | 0.94 | - | - | 0.73 | 93.57 | - | 0.28 | - | - |
| | | | | | | 2.63 | 0.11 | 0.20 | 2.69 | - | - | 1.95 | 0.31 | - | 0.82 | 91.30 | - | - | - | - |
| | | | | | | 2.48 | 0.30 | 0.36 | 1.47 | - | 0.09 | 1.64 | 0.80 | - | 0.68 | 92.17 | - | - | - | - |
| 2006 | KEN | M | M4 | 667 | 667 | 1.07 | - | 0.35 | 2.43 | - | - | - | - | - | - | 96.14 | - | - | - | - |
| 2006 | KEN | M | M4 | 670 | 670 | 1.02 | - | 0.36 | 3.81 | - | - | 2.59 | - | - | - | 92.22 | - | - | - | - |
| | | | | | | 4.99 | - | 0.44 | 1.53 | - | 0.07 | 1.53 | - | - | - | 91.45 | - | - | - | - |
| | | | | | | 0.89 | - | 0.35 | 2.07 | - | 0.06 | 1.57 | - | - | - | 95.06 | - | - | - | - |
| | | | | | | 2.15 | 0.55 | 0.41 | 4.43 | - | - | 1.62 | - | - | - | 90.85 | - | - | - | - |
| | | | | | | 3.66 | - | 0.34 | 8.78 | - | 0.08 | 1.96 | - | - | - | 85.19 | - | - | - | - |
| | | | | | | 1.18 | - | 0.31 | 2.87 | - | 0.10 | 3.08 | - | - | - | 92.46 | - | - | - | - |
| | | | | | | 1.98 | - | 0.38 | 6.17 | - | 0.15 | 3.02 | - | - | - | 88.31 | - | - | - | - |

**Table 5.11:** SEM-EDX results for copper prills in the slag thin-sections. All results are presented in weight%. Double-bottom borders indicate a change in the excavation area, and the table was divided to avoid splitting any samples across two pages. The letter following the elemental symbol represents the electron shell. The first letter in the Stratum (Strat.) represents the excavation area. Samples that did not include copper prills are not included in this table (Continued).

| Complete Data for Copper Prills analyzed with SEM-EDS (Continued) | | | | | | | | | | | | | | | | | | | | |
|---|---|---|---|---|---|---|---|---|---|---|---|---|---|---|---|---|---|---|---|---|
| Year | Site | Area | Strat. | Loc. | Sample | O-K | Al-K | Si-K | S-K | K-K | Ca-K | Mn-K | Fe-K | Co-K | Ni-K | Cu-K | Zn-K | As-K | Ba-L | Pb-L |
| 2006 | KEN | M | M5 | 674 | 674 | 5.89 | - | 0.21 | 1.63 | - | 0.25 | 1.94 | 2.40 | 0.50 | - | 87.18 | - | - | - | - |
| 2006 | KEN | M | - | - | 10253 | 4.69 | 0.51 | 0.42 | 1.16 | 0.07 | 0.81 | 3.15 | - | - | 0.45 | 88.73 | - | - | - | - |
| | | | | | | 3.18 | 0.51 | 0.56 | 1.03 | - | 0.12 | 2.40 | 0.49 | - | 0.34 | 89.96 | - | - | - | 1.40 |
| | | | | | | 1.11 | 0.18 | 0.28 | - | - | 0.09 | 2.13 | 0.43 | - | 0.39 | 91.08 | - | - | - | 4.31 |
| | | | | | | 2.94 | 1.21 | 0.41 | 0.66 | - | - | 0.64 | 0.16 | - | 0.36 | 93.62 | - | - | - | - |
| | | | | | | 2.15 | 0.41 | 0.43 | - | - | 0.10 | 2.39 | 0.56 | - | 0.36 | 93.60 | - | - | - | - |
| | | | | | | 2.66 | 0.37 | 0.29 | 1.80 | - | 0.10 | 2.04 | 0.44 | - | 0.35 | 91.95 | - | - | - | - |
| | | | | | | 2.46 | 0.55 | 0.53 | 0.39 | - | 0.05 | 0.96 | 0.28 | 0.29 | 0.39 | 94.10 | - | - | - | - |
| | | | | | | 2.53 | 0.39 | 0.31 | 2.77 | - | 0.10 | 2.51 | 0.47 | - | 0.22 | 90.71 | - | - | - | - |
| | | | | | | 2.91 | 0.38 | 0.43 | 0.74 | - | - | 1.06 | 0.24 | - | 0.38 | 93.86 | - | - | - | - |
| | | | | | | 1.62 | 0.45 | 0.30 | 0.63 | - | 0.08 | 2.08 | 0.46 | - | 0.35 | 94.02 | - | - | - | - |
| | | | | | | 2.13 | 0.54 | 0.54 | - | - | - | 1.74 | 0.32 | - | 0.32 | 94.42 | - | - | - | - |
| 2009 | KEN | R | R3 | 142 | 1496 | 1.30 | 0.54 | 0.80 | 2.41 | 0.09 | 0.17 | 4.99 | - | - | 0.51 | 89.19 | - | - | - | - |
| | | | | | | 0.64 | 0.47 | 0.30 | 1.60 | - | - | 0.92 | - | 0.23 | 0.50 | 95.33 | - | - | - | - |
| | | | | | | 2.48 | 0.44 | 0.22 | 1.89 | - | 0.11 | 4.61 | 1.02 | 0.50 | 0.65 | 88.08 | - | - | - | - |
| | | | | | | 2.78 | - | 0.22 | 2.06 | - | - | 0.61 | 1.10 | 0.61 | 0.47 | 90.70 | - | - | - | 1.47 |
| | | | | | | 1.67 | 0.45 | 0.18 | 1.57 | - | - | 0.57 | 0.98 | 0.34 | 0.58 | 93.67 | - | - | - | - |
| | | | | | | 0.70 | 0.33 | 0.20 | 1.89 | - | 0.07 | 3.45 | - | 0.27 | 0.61 | 91.09 | - | - | - | 1.39 |
| | | | | | | 2.41 | - | 0.26 | 4.02 | - | - | 3.56 | - | 0.30 | 0.93 | 88.52 | - | - | - | - |
| | | | | | | 3.11 | 0.54 | 0.41 | 2.70 | - | - | 2.26 | 0.75 | 0.28 | 0.43 | 89.51 | - | - | - | - |
| | | | | | | 6.67 | - | - | - | - | - | 1.18 | 1.16 | - | 0.28 | 85.29 | - | - | - | 5.42 |
| | | | | | | 1.69 | 0.31 | 0.18 | 2.97 | - | 0.10 | 3.27 | 1.00 | 0.31 | 0.22 | 89.95 | - | - | - | - |
| | | | | | | 2.27 | 0.32 | 0.14 | 1.63 | - | - | 1.18 | 2.35 | 1.03 | 0.48 | 90.60 | - | - | - | - |
| | | | | | | 1.47 | 0.30 | 0.23 | 1.08 | - | - | 0.33 | 0.97 | - | 0.58 | 95.03 | - | - | - | - |
| | | | | | | 1.82 | 0.19 | 0.19 | 1.62 | - | - | 2.22 | 0.87 | 0.26 | 0.41 | 92.43 | - | - | - | - |
| | | | | | | 2.95 | - | 0.22 | 3.79 | - | - | 1.62 | - | - | 1.42 | 90.00 | - | - | - | - |
| | | | | | | 1.24 | 0.16 | 0.24 | 3.26 | - | - | 2.08 | - | - | 0.63 | 92.39 | - | - | - | - |
| 2009 | KEN | R | R3 | 119 | 1270 | 3.02 | 1.03 | 0.50 | 3.71 | 0.13 | - | 0.73 | 3.15 | - | - | 87.72 | - | - | - | - |
| | | | | | | 1.85 | 0.42 | 0.41 | 2.18 | - | 0.09 | 0.70 | 3.02 | - | - | 91.32 | - | - | - | - |
| | | | | | | 2.03 | 0.56 | 0.89 | 1.79 | 0.17 | - | 0.84 | 1.86 | - | - | 91.84 | - | - | - | - |
| | | | | | | 1.43 | 0.26 | 0.33 | 2.39 | 0.14 | 0.08 | 0.76 | 0.86 | - | - | 93.76 | - | - | - | - |
| | | | | | | 2.71 | 0.42 | 0.41 | 3.41 | 0.06 | - | 0.66 | 3.17 | - | - | 89.15 | - | - | - | - |
| 2009 | KEN | R | R3 | 117 | 1323 | 3.12 | 0.37 | 0.32 | 1.18 | - | 0.38 | 2.69 | 0.34 | - | 0.16 | 91.46 | - | - | - | - |
| | | | | | | 1.73 | 0.17 | 0.23 | 0.87 | - | 0.23 | 2.00 | 0.35 | - | 0.27 | 94.14 | - | - | - | - |
| | | | | | | 3.89 | 0.51 | 0.57 | - | - | 0.41 | 3.05 | - | - | 0.29 | 91.29 | - | - | - | - |
| | | | | | | 4.09 | 0.20 | 0.22 | 2.20 | 0.32 | 0.10 | 1.70 | 0.31 | - | 0.47 | 90.39 | - | - | - | - |
| | | | | | | 4.04 | 0.41 | 0.51 | 4.48 | 0.35 | 0.09 | 1.64 | 0.28 | - | 0.35 | 87.86 | - | - | - | - |
| | | | | | | 5.91 | 0.50 | - | 3.48 | 0.34 | - | 2.56 | 1.08 | - | 0.37 | 85.76 | - | - | - | - |
| 2009 | KEN | R | R3 | 135 | 1468 | 1.74 | 0.40 | 0.30 | 2.50 | - | - | 0.47 | 0.57 | 0.64 | 0.71 | 92.67 | - | - | - | - |
| | | | | | | 6.14 | 0.20 | 0.34 | 3.99 | - | 0.10 | 2.37 | 0.43 | 0.20 | 0.78 | 85.46 | - | - | - | - |
| | | | | | | 2.92 | - | 0.90 | 2.03 | - | 0.27 | 5.15 | 0.72 | - | 0.76 | 87.25 | - | - | - | - |
| | | | | | | 1.70 | 0.21 | 0.32 | 1.83 | - | - | 0.68 | 0.52 | 0.68 | 0.74 | 93.34 | - | - | - | - |
| | | | | | | 2.25 | 0.19 | 0.35 | 1.46 | - | 0.09 | 2.04 | 0.66 | - | 0.65 | 92.31 | - | - | - | - |

**Table 5.11:** SEM-EDX results for copper prills in the slag thin-sections. All results are presented in weight%. Double-bottom borders indicate a change in the excavation area, and the table was divided to avoid splitting any samples across two pages. The letter following the elemental symbol represents the electron shell. The first letter in the Stratum (Strat.) represents the excavation area. Samples that did not include copper prills are not included in this table (Continued).

| Complete Data for Copper Prills analyzed with SEM-EDS (Continued) | | | | | | | | | | | | | | | | | | | |
|---|---|---|---|---|---|---|---|---|---|---|---|---|---|---|---|---|---|---|---|
| Year | Site | Area | Strat. | Loc. | Sample | O-K | Al-K | Si-K | S-K | K-K | Ca-K | Mn-K | Fe-K | Co-K | Ni-K | Cu-K | Zn-K | As-K | Ba-L | Pb-L |
| 2006 | KEN | F | F1a | 819 | 1248 | 2.56 | 0.12 | 0.19 | 3.07 | - | 0.07 | 2.29 | - | 0.22 | 0.71 | 90.77 | - | - | - | - |
| | | | | | | 5.48 | 0.14 | 0.16 | 3.70 | - | 0.09 | 2.01 | - | 0.13 | 1.20 | 85.56 | - | - | - | 1.54 |
| | | | | | | 1.44 | 0.16 | 0.16 | 3.12 | - | 0.06 | 1.38 | - | 0.22 | 0.68 | 92.79 | - | - | - | - |
| | | | | | | 1.56 | 0.30 | 0.20 | 7.24 | - | - | 0.66 | - | - | 1.34 | 87.90 | - | 0.81 | - | - |
| 2006 | KEN | F | F2a | 860 | 1303 | 2.53 | 0.16 | 0.29 | 1.50 | - | - | 0.27 | 0.75 | 0.47 | 0.45 | 93.58 | - | - | - | - |
| | | | | | | 2.15 | - | 0.34 | 2.39 | - | - | 0.66 | 0.17 | 0.36 | 0.44 | 93.48 | - | - | - | - |
| | | | | | | 2.29 | 0.21 | 0.30 | 1.91 | - | - | 2.44 | 0.30 | 0.40 | 0.40 | 91.76 | - | - | - | - |
| | | | | | | 4.65 | 0.17 | 0.31 | 3.20 | - | - | 2.39 | 0.91 | 1.11 | 0.38 | 86.88 | - | - | - | - |
| | | | | | | 2.08 | 0.29 | 0.25 | 2.21 | - | - | 0.71 | 0.14 | 0.31 | 0.50 | 93.51 | - | - | - | - |
| | | | | | | 4.29 | - | 0.34 | 3.41 | - | - | 1.04 | 0.22 | 0.29 | 0.51 | 89.91 | - | - | - | - |
| 2006 | KEN | F | F2a | 863 | 1195 | 5.82 | 0.35 | 0.35 | 2.97 | - | - | 1.68 | - | 0.26 | 0.25 | 88.33 | - | - | - | - |
| | | | | | | 3.54 | 0.35 | 0.47 | 5.69 | 0.08 | 0.20 | 2.94 | - | - | 0.22 | 86.51 | - | - | - | - |
| | | | | | | 6.83 | 2.83 | 0.74 | 2.38 | 0.10 | 0.15 | 2.86 | 0.36 | 0.22 | - | 83.52 | - | - | - | - |
| | | | | | | 1.58 | 0.37 | 0.39 | 5.66 | - | - | 1.15 | - | 0.21 | 0.28 | 90.36 | - | - | - | - |
| | | | | | | 2.70 | 0.18 | 0.21 | 4.33 | - | 0.08 | 1.53 | - | 0.25 | 0.30 | 90.42 | - | - | - | - |
| 2006 | KEN | F | F2b | 900 | 1461 | 7.14 | - | 0.47 | 3.43 | - | 0.11 | 2.24 | - | 0.43 | 0.52 | 85.67 | - | - | - | - |
| | | | | | | 2.42 | 0.35 | 0.29 | 3.50 | - | 0.06 | 1.18 | 0.83 | 0.41 | 0.41 | 90.56 | - | - | - | - |
| | | | | | | 6.38 | 0.39 | 0.41 | 3.54 | - | 0.10 | 2.21 | 0.50 | 0.38 | 0.44 | 85.65 | - | - | - | - |
| | | | | | | 1.91 | 0.32 | 0.28 | - | - | 0.06 | 1.84 | 0.56 | 0.25 | 0.42 | 94.35 | - | - | - | - |
| | | | | | | 4.62 | 1.96 | 0.32 | 3.69 | - | 0.08 | 2.11 | 1.06 | 0.35 | 0.43 | 85.38 | - | - | - | - |

**Table 5.12**: The average and standard deviation copper content of all prills per sample analyzed with SEM-EDX. All results are presented in weight%. The standard deviation is not provided for samples where only one prill was analyzed.

| Averages and Standard Deviations of Copper Content in Prills by Sample | | | | | | | | |
|---|---|---|---|---|---|---|---|---|
| Year | Site | Area | Stratum | Locus | Sample | N | Cu - Avg. | Cu - STDV |
| 2014 | KAJ | C | C1 | 533 | 10314 | 1 | 93.67 | - |
| 2014 | KAJ | C | C1 | 529 | 10338 | 1 | 91.66 | - |
| 2006 | KAJ | A | A1a | 100 | 3262 | 3 | 89.94 | 1.89 |
| 2006 | KAJ | A | A1a | 100 | 3278 | 11 | 93.09 | 2.96 |
| 2006 | KAJ | A | A1a | 100 | 3263 | 4 | 90.68 | 4.21 |
| 2006 | KAJ | A | A1a/A3 | 105 | 3265 | 7 | 92.06 | 2.88 |
| 2006 | KAJ | A | A1a/A3 | 105 | 3264 | 8 | 93.21 | 0.66 |
| 2006 | KAJ | A | A3 | 118 | 3283 | 11 | 92.76 | 2.83 |
| 2006 | KAJ | A | A3 | 118 | 3267 | 1 | 91.67 | - |
| 2006 | KAJ | A | A4 | 119 | 3281 | 5 | 89.69 | 3.67 |
| 2006 | KAJ | A | A5 | 119 | 3269 | 8 | 93.21 | 0.66 |
| 2006 | KAJ | A | A5 | 119 | 3282 | 5 | 90.11 | 1.47 |
| 2006 | KAJ | A | A5 | 121 | 3285 | 12 | 90.44 | 4.19 |
| 2006 | KAJ | A | A5 | 121 | 3279 | 9 | 90.11 | 3.77 |
| 2006 | KEN | M | M1 | 502/503 | 10250 | 11 | 91.77 | 2.42 |
| 2006 | KEN | M | M1 | 502/503 | 10250-2 | 6 | 93.52 | 1.46 |
| 2006 | KEN | M | M1 | - | 10482/10482-2 | 9 | 91.27 | 2.25 |
| 2006 | KEN | M | M1/M2 | - | 10484 | 4 | 91.73 | 3.46 |
| 2006 | KEN | M | M1/M2 | - | 10484-2 | 5 | 92.48 | 1.86 |
| 2006 | KEN | M | M1/M2 | - | 10485 | 13 | 92.05 | 1.35 |
| 2006 | KEN | M | M1/M2 | - | 10485-2 | 8 | 93.19 | 0.85 |
| 2006 | KEN | M | M1/M2 | - | 10487 | 6 | 89.17 | 1.32 |
| 2006 | KEN | M | M2 (upper) | - | 10488 | 3 | 89.7 | 4.24 |
| 2006 | KEN | M | M2 (upper) | - | 10489 | 8 | 87.44 | 4.24 |
| 2006 | KEN | M | M2 (upper) | 511 | 10255 | 7 | 91.6 | 2.43 |
| 2006 | KEN | M | M2 (upper) | 511 | 10255-2 | 4 | 92.13 | 1.14 |
| 2006 | KEN | M | M2 (upper) | - | 10486 | 6 | 89.59 | 2.20 |
| 2006 | KEN | M | M2 | - | 10493 | 7 | 88.75 | 3.17 |
| 2006 | KEN | M | M2 | 606 | - | 11 | 92.18 | 2.77 |
| 2006 | KEN | M | M2 | 622 | - | 3 | 88.99 | 3.12 |
| 2006 | KEN | M | M2 | - | 10476 | 7 | 86.29 | 2.48 |
| 2006 | KEN | M | M2 | 602 | 9013 | 5 | 91.49 | 2.92 |
| 2006 | KEN | M | M2 | 602 | 10260 | 2 | 93.97 | 1.46 |
| 2006 | KEN | M | M2 | 627 | 10266 | 9 | 92.82 | 2.40 |
| 2006 | KEN | M | M2 | 602 | 10276 | 7 | 92.59 | 2.10 |
| 2006 | KEN | M | M2 | 629 | - | 4 | 90.83 | 1.85 |
| 2006 | KEN | M | M2/M3 (M3 upper) | 641 | 10267 | 7 | 90.98 | 2.61 |
| 2006 | KEN | M | M2/M3 | 641 | 10268 | 7 | 89.57 | 3.00 |

**Table 5.12**: The average and standard deviation copper content of all prills per sample analyzed with SEM-EDX. All results are presented in weight%. The standard deviation is not provided for samples where only one prill was analyzed (Continued).

| Averages and Standard Deviations of Copper Content in Prills by Sample (Continued) | | | | | | | | |
|---|---|---|---|---|---|---|---|---|
| **Year** | **Site** | **Area** | **Stratum** | **Locus** | **Sample** | **N** | **Cu - Avg.** | **Cu - STDV** |
| 2006 | KEN | M | M3 (upper) | - | 10468 | 4 | 91.18 | 3.14 |
| 2006 | KEN | M | M3 (upper) | 647 | 10269 | 1 | 94.45 | - |
| 2006 | KEN | M | M3 (upper) | 647 | 10270 | 2 | 94.52 | 0.75 |
| 2006 | KEN | M | M3 | 666 | 10282 | 8 | 92.39 | 2.84 |
| 2006 | KEN | M | M3 | - | 10465 | 4 | 88.63 | 3.32 |
| 2006 | KEN | M | M3 | 660 | - | 3 | 90.39 | 2.05 |
| 2006 | KEN | M | M3 | 665 | - | 5 | 89.77 | 4.77 |
| 2006 | KEN | M | M3 | 666 | - | 10 | 89.47 | 1.97 |
| 2006 | KEN | M | M3 (lower) | 665 | 10277 | 5 | 92.18 | 0.93 |
| 2006 | KEN | M | M4 | 667 | - | 1 | 96.14 | - |
| 2006 | KEN | M | M4 | 670 | - | 7 | 90.79 | 3.19 |
| 2006 | KEN | M | M5 | 674 | - | 1 | 87.18 | - |
| 2006 | KEN | M | - | - | 10253 | 11 | 92.37 | 1.97 |
| 2009 | KEN | R | R3 | 117 | 1323 | 6 | 90.15 | 2.95 |
| 2009 | KEN | R | R3 | 119 | 1270 | 5 | 90.75 | 2.36 |
| 2009 | KEN | R | R3 | 142 | 1496 | 14 | 91.18 | 2.29 |
| 2009 | KEN | R | R3 | 135 | 1468 | 5 | 90.21 | 3.59 |
| 2006 | KEN | F | F1a | 819 | 1248 | 4 | 89.25 | 3.17 |
| 2006 | KEN | F | F2a | 863 | 1195 | 5 | 87.83 | 2.90 |
| 2006 | KEN | F | F2a | 860 | 1303 | 6 | 91.52 | 2.69 |
| 2006 | KEN | F | F2b | 900 | 1461 | 5 | 88.32 | 4.01 |

**Table 5.13**: The average and standard deviation copper content of all prills analyzed with SEM-EDX by stratigraphic layer. All results are presented in weight%. The standard deviation is not provided for layers where only one prill was analyzed.

| Average Copper Content of Prills by Stratum (Averages of all samples) | | | | | | |
|---|---|---|---|---|---|---|
| **Year** | **Site** | **Area** | **Stratum** | **N** | **Cu. - Avg.** | **Cu. - STDV** |
| 2014 | KAJ | C | C1 | 3 | 89.51 | 5.55 |
| 2006 | KAJ | A | A1a | 19 | 91.58 | 3.71 |
| 2006 | KAJ | A | A1a/A3 | 15 | 92.67 | 2.03 |
| 2006 | KAJ | A | A3 | 12 | 92.67 | 2.71 |
| 2006 | KAJ | A | A4 | 5 | 89.69 | 3.67 |
| 2006 | KAJ | A | A5 | 34 | 90.96 | 3.36 |
| 2006 | KEN | M | M1 | 26 | 92.00 | 2.27 |
| 2006 | KEN | M | M1/M2 | 36 | 91.94 | 1.92 |
| 2006 | KEN | M | M2 (upper) | 28 | 89.85 | 3.41 |
| 2006 | KEN | M | M2 | 55 | 90.88 | 3.30 |
| 2006 | KEN | M | M2/M3 | 15 | 90.41 | 2.940 |
| 2006 | KEN | M | M2/M3 (M3 upper) | 7 | 84.80 | 2.966 |
| 2006 | KEN | M | M3 (upper) | 10 | 91.05 | 3.420 |
| 2006 | KEN | M | M3 | 26 | 90.53 | 3.050 |
| 2006 | KEN | M | M3 (lower) | 5 | 92.18 | 0.930 |
| 2006 | KEN | M | M4 | 16 | 91.46 | 3.510 |
| 2006 | KEN | M | M5 | 1 | 87.18 | - |
| 2006 | KEN | F | F1a | 4 | 89.25 | 3.17 |
| 2006 | KEN | F | F2a | 11 | 89.84 | 3.27 |
| 2006 | KEN | F | F2b | 5 | 88.32 | 4.01 |
| 2006 | KEN | R | R3 | 31 | 90.56 | 2.71 |

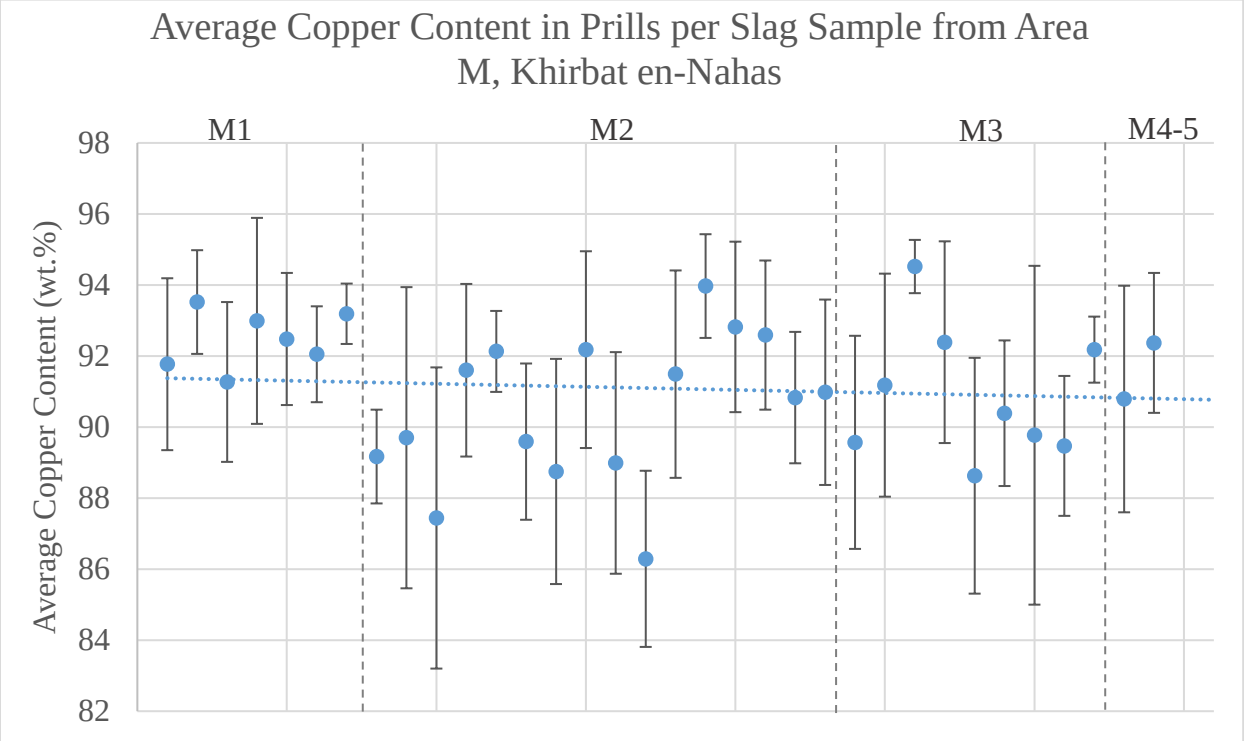


**Figure 5.26:** Graph of the average copper content in prills per slag sample from Area M at Khirbat en-Nahas. The top y-axis and vertical dashed lines depict the stratigraphic contexts. Moving left to right across the graph are the deeper layers of the slag mound with M4-5 being the bottommost layer. Vertical error bars represent the standard deviation of copper content, and the dotted blue line is the trend line for copper content.

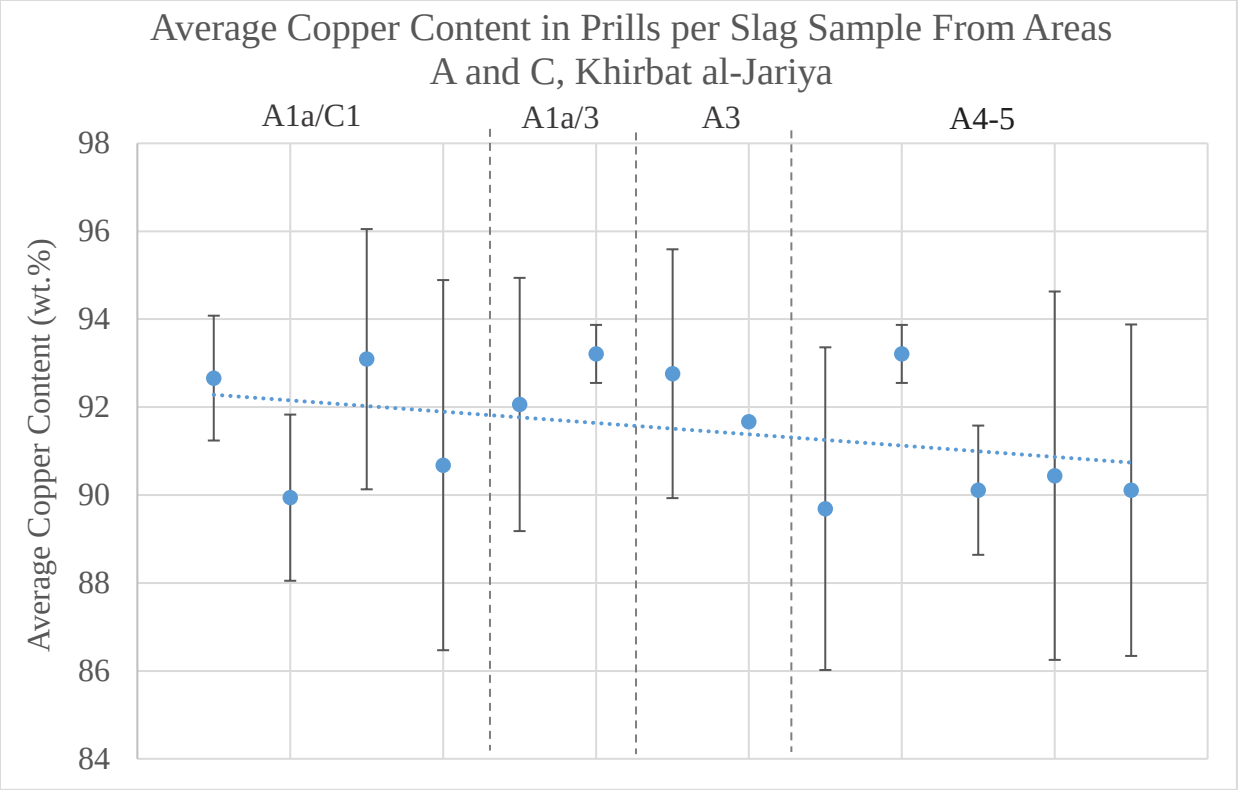


**Figure 5.27:** Graph of the average copper content in prills per slag sample from Areas A and C at Khirbat al-Jariya. The top y-axis and vertical dashed lines depict the stratigraphic contexts. Moving left to right across the graph are the deeper layers of the slag mound with A4-5 being the bottommost layer. Vertical error bars represent the standard deviation of copper content, and the dotted blue line is the trend line for copper content.

content and standard deviation in the uppermost later, M1, in comparison to the Area A slag mound at Khirbat al-Jariya which is more variable even in the top layers. This finding is reiterated by looking at just Area M and arranging the data according to average copper content by stratigraphical context; there is a somewhat consistent increase in the average copper content of prills and decrease in the standard deviation through time (Figure 5.28). As such, the copper content of metal produced during the Iron Age generally increased through time reaching a peak during the smelting associated with the uppermost layers of Area M at Khirbat en-Nahas (ca. $10^{th}$-$9^{th}$ centuries BCE).

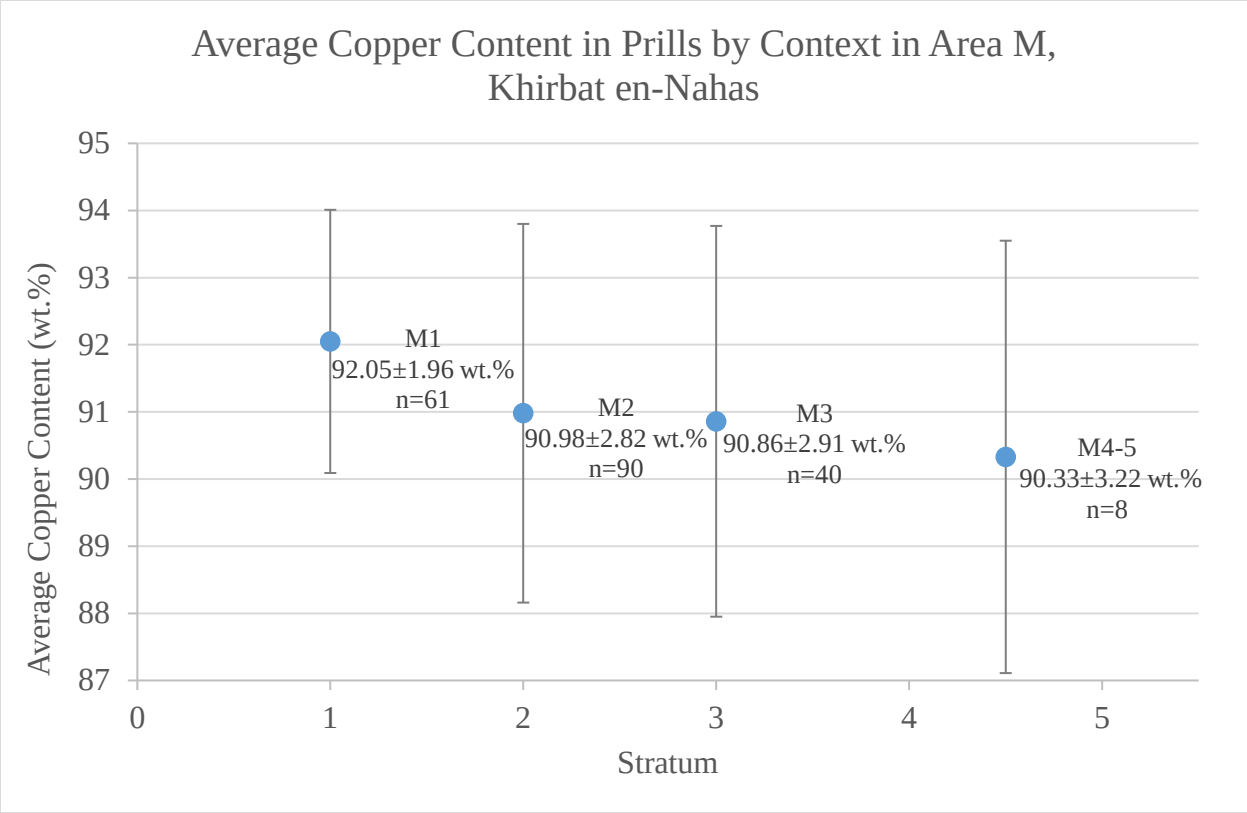


**Figure 5.28:** Graph of the average copper content in prills by stratigraphic context in Area M at Khirbat en-Nahas. Vertical error bars represent the standard deviation of copper content.

The results were also organized to match the copper production phase model developed by Ben-Yosef (2010, et al. 2019, see also Chapter 3) in Figure 5.29 and its associated data table. Ben-Yosef et al. (2019) grouped Khirbat al-Jariya Layer A3 with Layer A4 in Phase 1 and used a date towards the beginning of the maximum error range (the median date was used for all other contexts). Based on the results here, Layer A3 was included in Phase 2 as the average copper content is more in line with Phase 2 and using the median radiocarbon date of this layer still works with this adjustment. All other phase assignments for contexts are consistent with Ben-Yosef et al. 2019.

During analysis, it was found that many of the inclusions in the slags were copper-sulfides rather than pure copper metal. The presence of copper-sulfide in Iron Age slags from

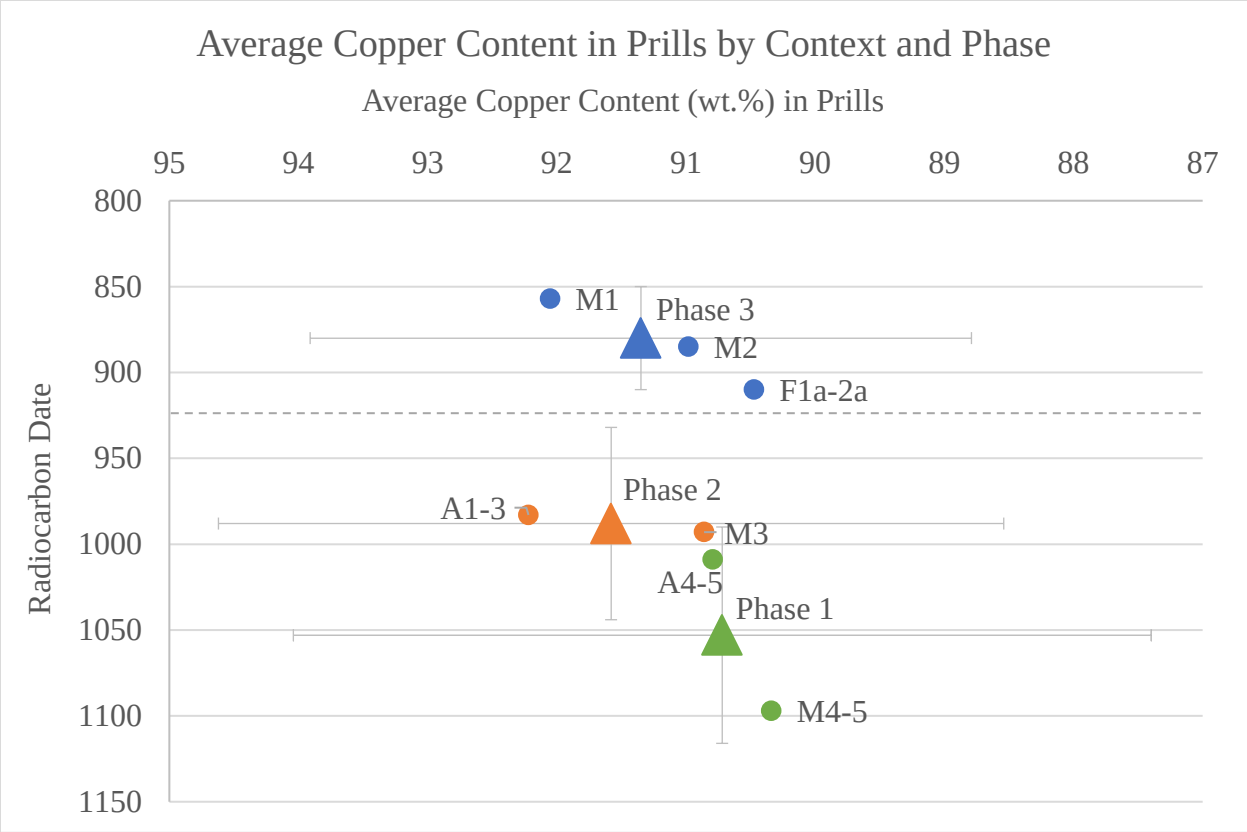


| | Contexts | Average Cu | Stdv | RC Date | n |
|---|---|---|---|---|---|
| ***Phase 3*** | M1, M2, F1a-2a | 91.35 wt.% | 2.56 | 880±30 BCE | 160 |
| ***Phase 2*** | A1-A3, M3 | 91.58 wt.% | 3.04 | 988±56 BCE | 86 |
| ***Phase 1*** | A4-6, M4-5 | 90.72 wt.% | 3.32 | 1053±63 BCE | 46 |

**Figure 5.29:** Graph and associated data table of the average Copper content in prills by context and Production Phase following the model developed by Ben-Yosef et al. 2019. Triangles represent the Phases and circles are individual contexts. The color of the symbol is consistent by phase (i.e., any context associated with Phase 1 is a green circle). Radiocarbon dates for Phases were determined by using an average of all the radiocarbon dates from its constituent contexts. The dashed gray line represents the punctuated leap and change in smelting technology identified by Ben-Yosef et al. 2019. For clarity, error bars were only included for the Phases. Vertical error bars represent the range for the radiocarbon dates, and the horizontal error bars are the standard deviation of the average copper content.

Faynan has been documented (Ben-Yosef 2010: Figure 8.37; Hauptmann 2007: 178-179). The large number of these inclusions was a surprising finding and created a methodological difficulty for the analysis. It was originally expected that most inclusions in the slag would be copper

metal; however, metallic copper prills were often difficult to identify and in much lower numbers than expected in comparison to the more abundant copper-sulfide inclusions. Moreover, copper-sulfide frequently surrounded metallic copper in crescent and halo shapes making the features difficult to distinguish (Figure 5.30). Not only did this limit the number of prills analyzed both per sample and total, but it also increased the amount of time spent on the SEM per sample. Each sample required much more careful consideration and examination to identify copper metal versus copper-sulfide inclusions as they look quite similar in the SEM (Figure 5.30). The number of copper prills analyzed per sample ranged from 0 to 15 with an average of about 5-6 per sample in slags that included prills. The number of prills analyzed per sample could also be impacted by using a small portion of the slag (sections were roughly 1x1 inch) and reusing previous samples from Ben-Yosef's research which limited the ability to select where from the slags to take a thin-section. Many copper-sulfide inclusions were analyzed with SEM-EDX for future consideration.

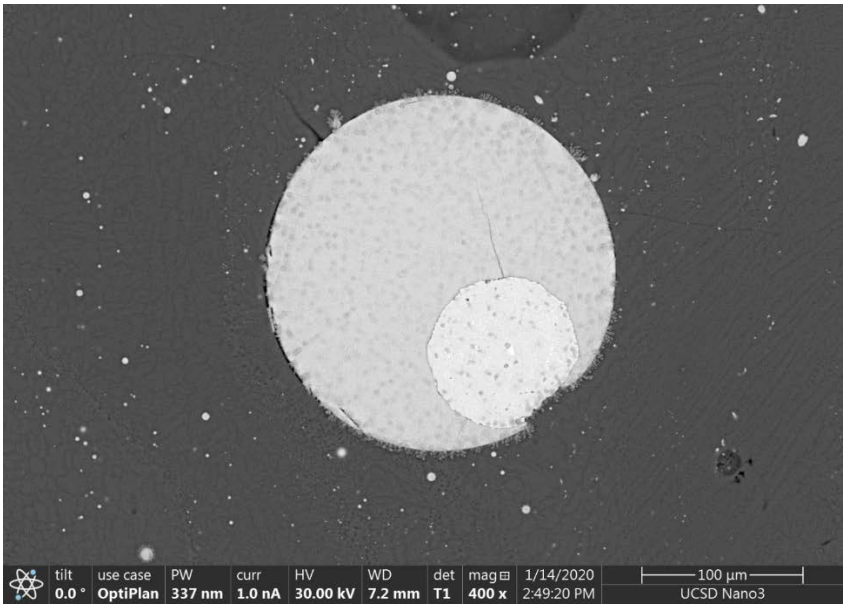


**Figure 5.30:** SEM image showing a copper prill encapsulated within a copper-sulfide inclusion (Sample 3281, Area A, Khirbat al-Jariya). The darker gray circle is copper-sulfide and the lighter gray is a relatively pure copper prill (89.20 wt.% Copper). This was a common phenomenon in the slag samples and required careful consideration during analysis.

#### 5.4.4.2 Other Elements in Copper Prills

It is also important to consider the other elements identified in the copper prills. Given the methodology and its limitations, some trace and minor elements were potentially undetected or inaccurate. With this in mind, the elements other than copper that were consistently identified are discussed here. Based on Table 5.11, these elements were oxygen, aluminum, silicon, sulfur, iron, and manganese. Lead, nickel, and zinc were less common (especially in comparison to previous studies, Hauptmann et al. 1992: 20, Table 6), with zinc and nickel often present in near or less than one wt.%. Lead was occasionally in the range of several wt.%, but it also frequently was undetected. Oxygen and sulfur occasionally appeared in high amounts, up to 10 wt.%, and aluminum and silicon almost always appeared as less than one wt.%, occasionally reaching up to 2 wt.%. Iron content was often less than 1 wt.% and only reaching 1-2 wt.% in a few instances; contrastingly, Iron was over 2 wt.% in seven of the 10 samples analyzed by Hauptmann (2007: Table A17). When looking at Area M from Khirbat en-Nahas, the iron content does generally increase over time (Figure 5.31). Finally, manganese was almost always present in the range of 1-3 wt.%.

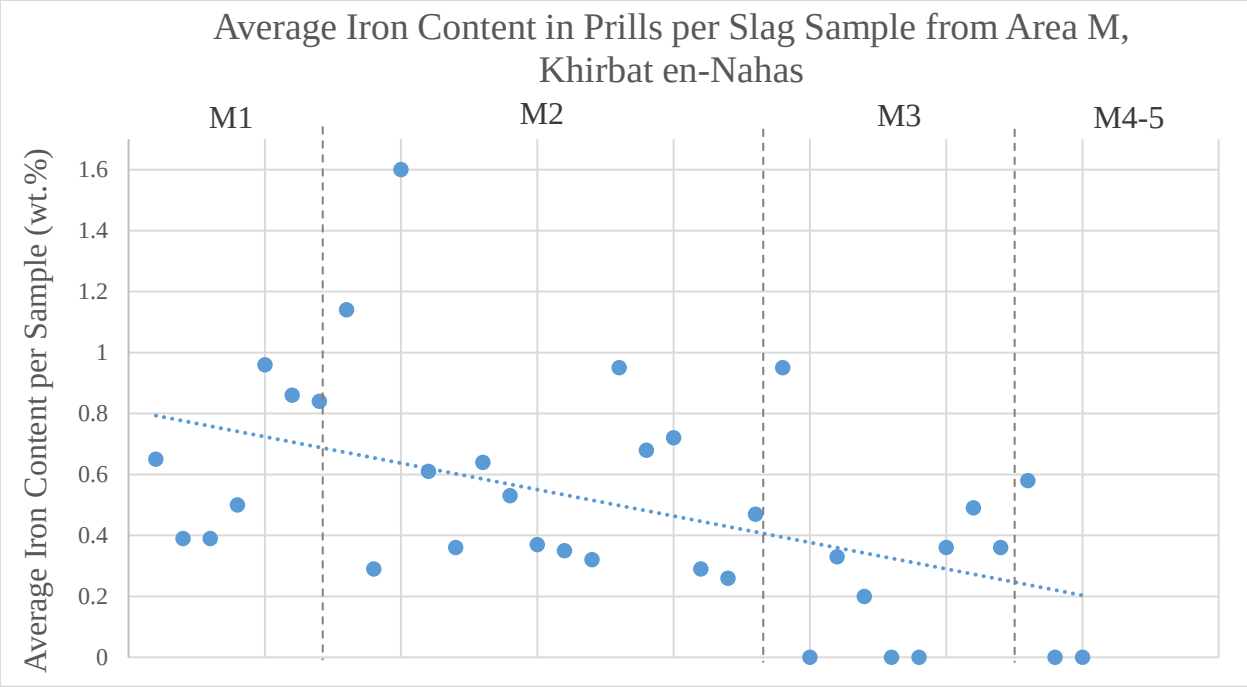


**Figure 5.31:** Graph of the average Iron content in prills by sample in Area M at Khirbat en-Nahas. The top y-axis and vertical dashed lines depict the stratigraphic contexts. Moving left to right across the graph are the deeper layers of the slag mound with M4-5 being the bottommost layer. The dotted blue line is the trend line for Iron content. Sample 675 from Layer M5 was not included as this data point appears to be anomalistic compared to the other data from Layers M4 and M5.

#### 5.4.4.3 Iron Inclusions

Along with the copper prills, iron inclusions were also occasionally identified during SEM-EDX analysis (Figure 5.32 and Table 5.14). In total, 46 iron inclusions were identified and analyzed in 11 different samples. Of the 11 samples, one was from Khirbat al-Jariya Area C, six originated in Area M at Khirbat en-Nahas, and four were excavated from Area R at Khirbat en-Nahas. The average iron content was 77.98 wt.%, and some inclusions contained over 90 wt.% iron (Table 5.14). The analyzed iron also contained phosphorous, copper, and manganese. The copper content was 4.25 wt.% on average, but it was often higher reaching 16.97 wt.% in one analysis from Sample 674 (Table 5.14). The phosphorous content was high with 13.66 wt.% on average. Based on the number of samples, iron inclusions were the most common in slags from

Area R at Khirbat en-Nahas being identified in four of the eight samples included in this study; however, this could be biased by the small samples size. Oxygen was only identified in 12 of the iron inclusions, and a high percentage of cobalt (6-13 wt.%) was found in eight samples; cobalt was also found in the iron-copper chunks analyzed above with LA-ICP-MS.

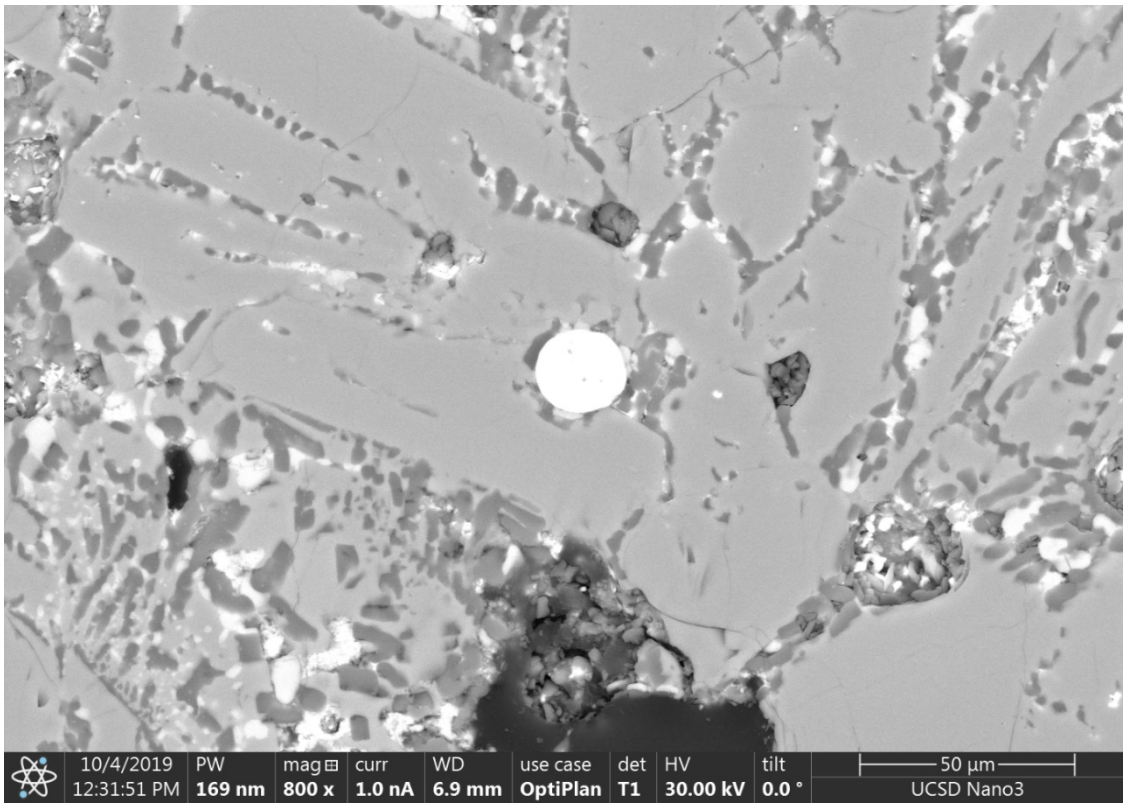


**Figure 5.32:** SEM image of an iron prill from Sample 10314, Area C, Khirbat al-Jariya (bright white circle). The prill contained 92.03 wt.% Iron.

**Table 5.14:** SEM-EDX results for iron prills and inclusions in the slag thin-sections. All results are presented in weight%. Phosphorous is included here as it is much higher than expected for simply a peak overlap with iridium from the sputter-coating; however, the value needs to be considered critically due to this phenomenon. Double-bottom borders indicate a change in the excavation area.

| Complete Data for Iron Inclusions/Prills analyzed with SEM-EDS | | | | | | | | | | | | | | | | | |
|---|---|---|---|---|---|---|---|---|---|---|---|---|---|---|---|---|---|
| Year | Site | Strat. | Locus | Sample | O-K | Mg-K | Al-K | Si-K | P-K | S-K | K-K | Ca-K | Mn-K | Fe-K | Co-K | Ni-K | Cu-K |
| 2014 | KAJ | C1 | 553 | 10314 | | | 0.34 | 0.17 | 2.45 | 0.19 | 0.10 | 0.34 | 1.84 | 88.24 | | | 6.32 |
| | | | | | | | 0.16 | 0.17 | 2.11 | 0.34 | 0.05 | 0.26 | 1.50 | 89.80 | | | 5.61 |
| | | | | | | | | 0.10 | 1.82 | 0.25 | | 0.26 | 1.25 | 93.77 | | | 2.54 |
| | | | | | | | | 0.17 | 14.66 | | | 0.07 | 0.40 | 83.34 | | | 1.36 |
| | | | | | | | | | 3.11 | | | 0.09 | 0.44 | 90.91 | | | 5.45 |
| | | | | | | | 0.31 | 0.15 | 3.51 | 0.24 | | 0.16 | 0.86 | 92.03 | | | 2.73 |
| | | | | | | | 0.34 | 0.16 | 2.05 | 0.24 | 0.08 | 0.26 | 1.25 | 92.96 | | | 2.65 |
| | | | | | | | | 0.24 | 1.78 | | | 0.23 | 2.02 | 85.92 | | | 9.81 |
| 2006 | KEN | M2 (up.) | | 10486 | | | | 0.19 | 25.34 | | | 0.13 | 1.76 | 72.57 | | | |
| | | | | | | | | 0.16 | 24.21 | | | | 1.59 | 73.65 | | | 0.39 |
| | | | | | | | | 0.13 | 25.25 | | | | 1.30 | 72.91 | | | 0.42 |
| | | | | | | | | 0.11 | 25.84 | | | 0.08 | 1.42 | 72.54 | | | |
| | | | | | | | | 0.12 | 24.95 | | | 0.07 | 3.76 | 70.43 | | | 0.67 |
| | | | | | | | | 0.15 | 24.99 | | 0.07 | 0.15 | 2.90 | 70.89 | | | 0.85 |
| | | | | | 6.88 | 0.49 | | 2.62 | 16.13 | | 0.42 | | 0.67 | 71.34 | | | 1.46 |
| | | | | | 1.12 | | | 0.13 | 19.07 | | 0.10 | | 0.52 | 77.79 | | | 1.27 |
| | | | | | | | | 0.19 | 18.94 | | 0.13 | | 0.79 | 77.70 | | | 2.25 |
| | | | | | | | | 0.08 | 25.80 | | | | 0.77 | 73.35 | | | |
| 2006 | KEN | M4 | 666 | 10282 | | | | 0.10 | 19.46 | | | | 0.73 | 78.63 | | | 1.07 |
| | | | | | | | | 0.10 | 25.84 | | | | 0.66 | 72.93 | | | 0.48 |
| 2006 | KEN | M2 | 602 | 9013 | | | | 0.24 | 3.19 | | 0.09 | 0.15 | 0.96 | 82.03 | 11.44 | | 1.90 |
| | | | | | | | | 0.20 | 12.42 | | | 0.17 | 2.08 | 76.65 | 6.87 | | 1.62 |
| | | | | | | | | 0.23 | 14.00 | | | | 0.81 | 82.65 | | | 2.31 |
| 2006 | KEN | M3 | | 659 | | | | 0.27 | 10.45 | 3.50 | 0.08 | 0.10 | 1.25 | 76.60 | | | 7.74 |
| | | | | | 0.84 | | 0.07 | 0.22 | 9.85 | 3.15 | 0.09 | 0.14 | 1.48 | 76.93 | | | 7.04 |
| | | | | | 8.41 | | 0.05 | 1.41 | 11.23 | 0.82 | 0.05 | 0.09 | 1.76 | 74.69 | | | 1.47 |
| | | | | | | | | 0.17 | 13.87 | | | 0.10 | 0.98 | 82.65 | | | 2.23 |
| | | | | | | | 0.06 | 0.28 | 3.25 | | | | 0.58 | 93.61 | | | 2.21 |
| | | | | | | | 0.13 | 0.21 | 6.12 | | | | 0.55 | 90.76 | | | 2.23 |
| 2006 | KEN | M5 | | 674 | 0.79 | | | 0.29 | 1.09 | 1.75 | | 0.23 | 1.59 | 65.96 | 13.33 | 1.06 | 13.15 |
| | | | | | 2.13 | | | 0.32 | 1.32 | 6.87 | 0.09 | 0.46 | 1.59 | 59.72 | 9.77 | 0.74 | 16.97 |
| 2006 | KEN | | | 9037 | 0.71 | | | 0.21 | 1.17 | | 0.12 | 0.28 | 1.32 | 91.55 | | 0.67 | 3.78 |
| | | | | | | | | 0.33 | 1.04 | | | 0.33 | 1.28 | 91.17 | | 0.71 | 5.14 |
| 2009 | KEN | R3 | | 1323 | 1.10 | | | 0.24 | 14.35 | 0.24 | 0.29 | 0.10 | 1.27 | 57.38 | 8.83 | | 16.18 |
| | | | | | | | | 0.21 | 24.75 | | 0.07 | 0.23 | 2.45 | 71.69 | | | 0.60 |
| | | | | | | | | 0.21 | 26.19 | | 0.06 | 0.31 | 1.15 | 71.81 | | | 0.27 |
| | | | | | | | | 0.24 | 15.18 | | 0.33 | | 1.15 | 63.99 | 9.28 | | 9.82 |
| | | | | | | | | 0.26 | 16.38 | | | 0.16 | 1.48 | 79.96 | | | 1.75 |
| | | | | | | | | 0.22 | 18.26 | | | 0.14 | 1.31 | 78.26 | | | 1.81 |
| 2009 | KEN | R3 | | 845 | | | | 0.10 | 19.35 | | 0.09 | 0.11 | 1.02 | 78.87 | | 0.45 | |
| | | | | | 6.70 | | | 0.23 | 18.17 | | 0.45 | 0.66 | 1.12 | 72.19 | | 0.49 | |
| | | | | | 0.14 | | | 0.21 | 24.26 | | 0.14 | 0.12 | 1.90 | 73.23 | | | |
| | | | | | | | | 0.12 | 25.66 | | 0.10 | 0.14 | 1.92 | 72.06 | | | |
| | | | | | 1.90 | | 1.07 | 2.13 | 16.59 | | 0.91 | 0.16 | 1.42 | 75.81 | | | |
| 2009 | KEN | R3 | | 1496 | | | 0.05 | 0.13 | 11.37 | | | 0.06 | 1.16 | 60.95 | 10.66 | 1.85 | 13.77 |
| 2009 | KEN | R3 | | 1270 | 1.28 | | 0.52 | 0.62 | 1.35 | | 0.20 | 0.08 | 0.68 | 84.12 | 11.15 | | |

#### 5.4.4.4 SEM-EDX and XRF Comparison

As not all of Ben-Yosef's original collection was analyzed here (Figures 5.19 and 5.20), and only some of the samples yielded copper prills, 35 of the slag samples have XRF data for their bulk composition and SEM-EDX data for their entrapped prills (the XRF data is available in Ben-Yosef et al. 2019: Table S3). This subsample still allows for comparison between the bulk compositions of the slag with the copper directly produced in association with that slag. To do so, the Pearson Correlation Coefficient was used to test for statistical correlations between the elements analyzed using XRF and the copper content of the prills determined via SEM-EDX. The Pearson Correlation Coefficient determines the correlation between variables which could realistically have a linear relationship[5]. Essentially, this statistical test draws a line of best fit between two datasets of variables and determines how close the data points fall near this line to find their correlation. The produced values range from -1 to 1; a correlation coefficient of 1 would suggest a positive linear relationship between two variables with all data points falling on the line of best fit (-1 is the same but in the opposite direction). As values approach 0, the correlation is less linear - the data points are more scattered around the line with 0 indicating no association between the variables. The Pearson Correlation Coefficient allows for a test to check for linear relationships/correlations between any of the elements in the slag and the copper content of the prills in the same slag samples. In doing so, it can provide greater insight on the

[5] The Pearson Correlation Coefficient assumes the data follows a normal distribution. To ensure this assumption, the kurtosis and skewness were calculated for all the elements analyzed with XRF and the copper content from SEM-EDX. While there is some debate concerning what "appropriate" skewness and kurtosis values for indicating a normal distribution, Kline (2016: 76-77) suggests the absolute value of skewness should be <3 and the absolute value kurtosis should be <10 to indicate a dataset is not "severely non-normal". Here, the skewness was <3 absolute value and the kurtosis was <5 absolute value for all elements from the XRF analysis and the copper content of prills from SEM-EDS.

how slag bulk composition is representative of metal produced, and which elements can provide the statistically significant correlations.

The results from Area M at Khirbat an-Nahas were used as a case study; 26 samples included XRF and SEM-EDX data (the other excavation areas had too few samples to warrant insightful statistical analyses e.g., only eight samples from Khirbat al-Jariya Area A had data from both methods). The Pearson Correlation Coefficient was determined for all elements analyzed with XRF in comparison to the copper content of the SEM-EDX data using Microsoft Excel's data analysis package (Table 5.15). The correlations range from 0.01 to 0.48 (absolute value – Table 5.15). While the interpretation of the Pearson Coefficient is somewhat variable by source, below 0.5 is generally considered a moderate correlation, and below 0.3 is considered weak to negligible. The only correlations above 0.3 in absolute value were silicon (0.48) and calcium (-0.36); iron was close at 0.29.

**Table 5.15:** Pearson Correlation Coefficient for the elemental contents of slags analyzed by XRF (Ben-Yosef et al. 2019: Table S3) and the copper content of prills from the same samples analyzed by SEM-EDS from Area M at Khirbat en-Nahas.

| | ***Al*** | ***Si*** | ***K*** | ***Ca*** | ***Ti*** | ***Mn*** | ***Fe*** | ***Ni*** | ***Cu*** | ***Zn*** | ***Ba*** | ***Pb*** | ***Cu Prills*** |
|---|---|---|---|---|---|---|---|---|---|---|---|---|---|
| **Al** | 1.00 | | | | | | | | | | | | |
| **Si** | 0.30 | 1.00 | | | | | | | | | | | |
| **K** | -0.14 | -0.15 | 1.00 | | | | | | | | | | |
| **Ca** | -0.26 | -0.47 | 0.58 | 1.00 | | | | | | | | | |
| **Ti** | -0.28 | -0.09 | -0.07 | -0.35 | 1.00 | | | | | | | | |
| **Mn** | -0.15 | -0.28 | -0.50 | -0.47 | 0.35 | 1.00 | | | | | | | |
| **Fe** | -0.20 | 0.69 | -0.14 | -0.21 | 0.03 | -0.27 | 1.00 | | | | | | |
| **Ni** | 0.36 | 0.23 | 0.02 | 0.11 | -0.51 | -0.14 | -0.02 | 1.00 | | | | | |
| **Cu** | 0.28 | 0.01 | -0.32 | -0.59 | 0.38 | 0.31 | -0.22 | -0.35 | 1.00 | | | | |
| **Zn** | 0.22 | 0.14 | -0.20 | -0.54 | 0.41 | 0.24 | -0.08 | -0.54 | 0.84 | 1.00 | | | |
| **Ba** | -0.10 | -0.30 | -0.06 | -0.26 | 0.79 | 0.44 | -0.26 | -0.30 | 0.31 | 0.35 | 1.00 | | |
| **Pb** | 0.21 | 0.12 | 0.02 | -0.56 | 0.53 | 0.24 | -0.12 | -0.35 | 0.74 | 0.82 | 0.46 | 1.00 | |
| **Cu Prills** | -0.14 | 0.48 | -0.08 | -0.36 | 0.01 | -0.05 | 0.29 | 0.16 | 0.02 | -0.01 | -0.16 | 0.04 | 1.00 |

In other words, only the silicon, calcium and iron content in slag showed a moderate correlation to the copper in the prills. With regards to silicon and iron, they showed a moderate positive trend suggesting they increased as copper in prills increased. In contrast, calcium in slag and copper in prills had a negative correlation; the calcium content in slag decreased as the copper in prills increased. These values may be influenced by outliers in the statistical sense, but "outliers" are also somewhat expected in this dataset; copper smelting was a variable process especially in the earlier phases of the Iron Age (Ben-Yosef et al. 2019: Figure 3). These four elements were further investigated with bivariate regression to determine the significance of the correlation (p-value). The p-values were 0.013 for silicon, 0.073 for calcium, 0.153 for iron, and 0.93 for copper. As such, the only statistically significant correlation ($p\text{-value}<0.05$) is silicon; the other p-values near 0.05 such as calcium may suggest a trend towards significance that is potentially limited due to the small sample size, but this would need further research to support. In other words, based on the current data set, the only identified statistically significant relationship between the bulk composition of slag and the copper content of prills from the same sample is based on the silicon content. For a visual representation, each bivariate regression was plotted to show the trend between copper in prills and the respective element (Figure 5.33).

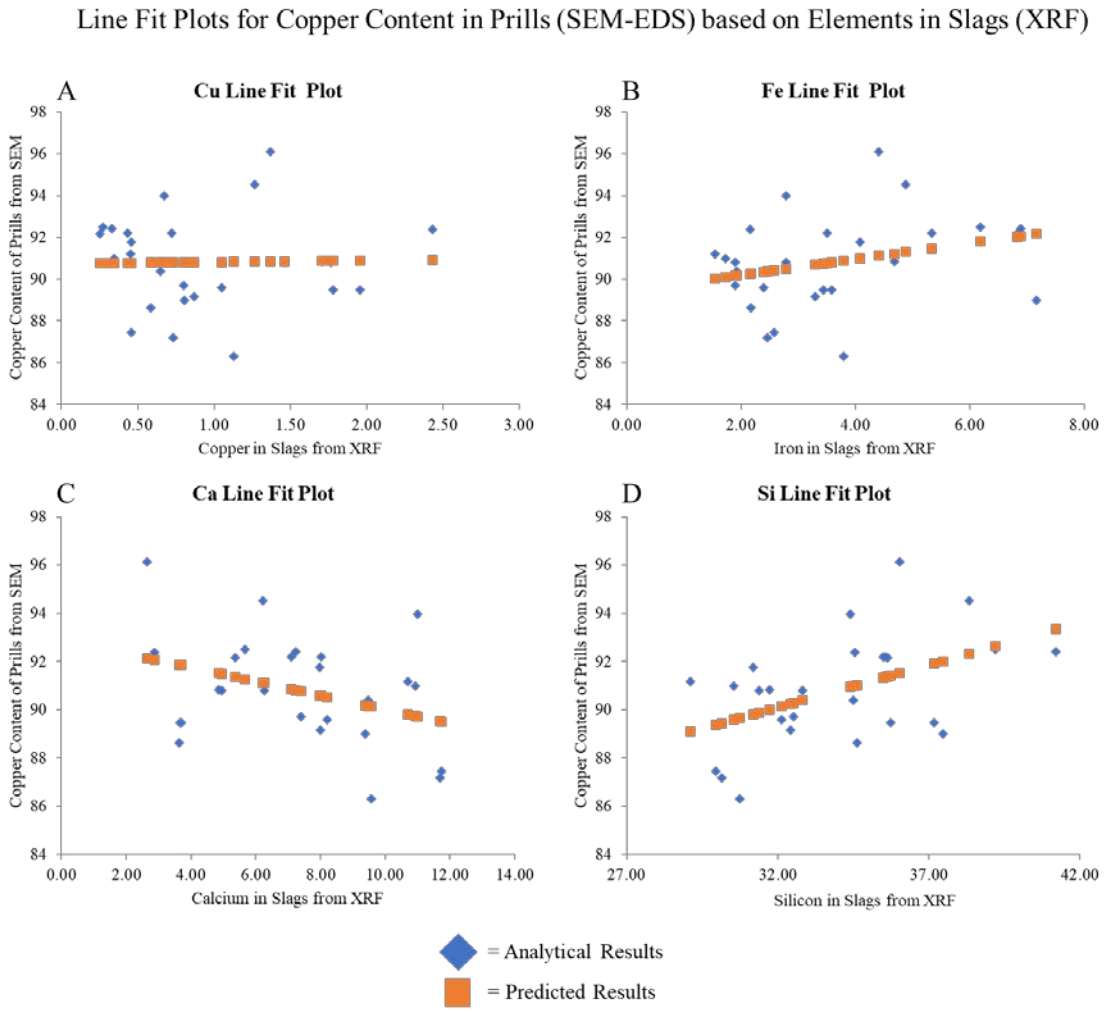


**Figure 5.33:** Line fit plots for the Copper content in prills (SEM-EDX) and bulk composition elements of slags (XRF) – A) Copper, B) Iron, C) Calcium, and D) Silicon. All results are in wt.%. The blue diamonds are the plotted results of each slag sample – copper content of prills versus element content in the same slag sample. The orange squares represent the best fit line based on the bivariate regression. The slope and direction of the best fit line is the Pearson Correlation Coefficient – Copper = 0.02, Iron = 0.29, Calcium = -0.36, and Silicon = 0.48.

### 5.4.5 Discussion

Overall, the results of the SEM-EDX analysis of metal prills in the slag fit with understandings of copper production in Iron Age Faynan. As best represented by Area M at Khirbat en-Nahas (Figures 5.26 and 5.28), the copper content in prills generally increased

overtime and the standard deviation decreased with the tightest clustering in Layer M1[6]. This finding suggests that metal produced during this phase was consistently high in copper and with less variation in comparison to other periods, matching with previous interpretations that metallurgy was at its peak during this period. Similarly, the results from Area A at Khirbat al-Jariya also showed a general increase in prill copper content over time, although the standard deviations were more variable (Figure 5.27). Thus, at the scale of individual contexts, the purity of copper produced in Faynan during the Iron Age improved over time, reaching a peak in the 10$^{th}$-9$^{th}$ century BCE.

However, these interpretations become somewhat convoluted when the SEM-EDX results are organized according to the metallurgical Phases identified by Ben-Yosef et al. (2019). Here, copper content in prills from Phase 2 was found to be higher on average than Phase 3, contrasting with the expectation that Phase 3 would produce the purest copper (Figure 5.29). This unexpected result is primarily due to the copper prills from Khribat al-Jariya Layers A1-3 (which is dated to Phase 2) having the highest copper content of any context. It is not clear why this is the case, but several factors are possible; 1) the high copper content was just a product of the inherent variability in ancient smelting practices; 2) a higher quality ore was used in these particular smelts; or 3) this phase of smelting used a uniquely efficient technology. Any of these explanations are possible; however, there is currently no archaeological evidence that a different technology was employed during the occupation of Khirbat al-Jariya. The variability of ancient smelting practices (which is loosely supported by the larger standard deviation of copper content

[6]Area R and F at Khirbat en-Nahas were expected to have the highest copper content in analyzed prills given these areas are associated with the most sophisticated smelting technologies during the final phases of production in the 10$^{th}$-9$^{th}$ centuries BCE, but the average copper content from the SEM-EDX analysis was the actually slightly lower in these areas (Area R = 90.56±2.71 wt.% (n=31), Area F = 89.34.12±3.32 wt.% (n=20) in comparison to the slag mounds. This finding could be the result of the small sample sizes, but it should be considered further.

in prills associated with this phase compared to Phase 3) is also possible, but difficult to concretely support. Finally, a change in ore source availability could be explained by the nearby Jabal al-Jariya minefields. Ben-Yosef (2010: 417) suggests the ore from these mines were "extremely high quality" and "completely exhausted in antiquity". Thus, it is possible this final phase of production at Khribat al-Jariya smelted the limited remaining high quality of ore of these mine fields prior to their exhaustion, and the abandonment of the site. Regardless, this phenomenon at Khirbat al-Jariya requires further investigation.

With that said, Phase 1 still yielded the lowest average copper content in prills as expected, and the standard deviation decreased with each phase, including from Phase 2 to Phase 3. As such, there is still some evidence to suggest a general improvement in the produced copper quality over time in Faynan, matching with the results of the XRF study by Ben-Yosef et al. (2019). Returning to the question raised in the introduction of this chapter, these results indicate that the quality of metal being produced generally improved through the Iron Age, likely as result of improved copper smelting technologies as identified and suggested by Ben-Yosef et al. 2019 and Hauptmann et al. 1992.

Looking at the other common elements found in the produced copper metal, the results reiterate that high quality copper was produced even in the final phases of Iron Age smelting. Concerning the iron content of the copper prills, an increase in iron content over time was identified here (Figure 5.32) and by Hauptmann et al. (1992: 25). This increase in iron corroborates the improvement in metallurgical technology during the Iron Age; the better controlled and more reducing smelting conditions resulted in the reduction of iron-oxides (Hauptmann 2007: 248). The iron content of the associated slags also slightly increased with the increased in copper content of prills (Pearson Correlation Coefficient of 0.29, $p=0.153$), perhaps

also connected to the improved smelting technologies (i.e., iron was being extracted from the furnace charge in larger amounts, some of which was lost in the slag). The iron inclusions found in the slags during SEM-EDX also contribute to this understanding. These inclusions confirm that the smelting technology of Iron Age Faynan could produce metallic iron which requires controlled reducing conditions. The high phosphorous content of some of these inclusions also matches previous studies. As discussed above, the DLS formation includes nodules and layers of phosphorite resulting in iron phosphide inclusions in Faynan copper associated with prills of α-Fe (Hauptmann 2007: 209 with similar composition to what is seen here – Table 5.14). Based on the current samples, there is no clear chronological component to the appearance of iron inclusions in the slags, but samples from Area R most consistently contained these iron features. Area R also yielded evidence for advanced copper smelting and the iron-copper chunks. To summarize, the iron content of copper prills (increasing over time) provides additional evidence for advancements in copper smelting during the Iron Age, the same advancements which likely resulted in higher quality copper metal (despite this increase in iron content). The appearance of metallic iron in slags potentially supports this understanding, but it requires further investigation to test for a chronological component. Regardless, it seems to confirm the capability of producing metallic iron in a copper smelting furnace as discussed earlier in this chapter.

The other elements consistently identified in the analysis of copper prills were oxygen, aluminum, silicon, sulfur, and manganese. Aluminum, silicon, and manganese were likely present due to the interaction volume of the SEM beam spilling into the slag matrix rather than components of the copper itself. Manganese is natural in the DLS ores or Faynan and results in a manganese-rich slag; however, this element readily incorporates into slag rather than copper metal during smelting (Tylecote, Ghaznavi, and Boydell 1977: 324). Similarly, silicon is a

primary elemental constituent of metallurgical slags along with aluminum. As such, while actions were taken to try to avoid the slag matrix influencing the analysis of copper metal, it seems this still happened at least on occasion (likely with the smaller copper prills). The sulfur content ranged from less than one to several wt.%, and it was likely a result of intergrown sulfidic ores in the oxidic ores of Faynan. Hauptmann et al. (1992: 23) suggest a low sulfur content is expected in the copper metal due to the low sulfur content of intergrown sulfidic ores in the DLS of Faynan, which are predominantly oxidic. The occasionally high sulfur content of the copper prills (average 2.12 wt.% across all analyzed samples) contrasts with Hauptmann's (2007: Table A17) results where sulfur was always less than one wt.% and occasionally undetectable. Copper prills with an elevated sulfur content are likely also a result of beam interaction volume; as mentioned above, copper-sulfide inclusions were often identified as crescents or halos around metallic copper (Figure 5.30). As Hauptmann mechanically extracted the copper from slags, it is possible he was able to avoid such copper-sulfide inclusions resulting in the much lower sulfur contents.

Oxygen was present in all analyses with an average of 3.29 wt.% and a standard deviation of 2.02 wt.%. Oxygen is to be expected due to oxidation of the metal into copper-oxides; this phenomenon is common, and Cuprite ($Cu_2O$) is a typical phase in slags from Faynan (Hauptmann 2007: 200, Table 6.1). It is difficult to determine if the present of copper-oxides was a result of post-depositional corrosion or weak reducing conditions at the time of smelting. However, given the sophistication of the copper smelting technology, the low average oxygen content, and the precipitation of iron metal, it seems more likely that the oxidation was post-depositional. This interpretation is potentially supported by the average oxygen content by excavation area; Area R at Khirbat en-Nahas had the lowest average oxygen in copper prills at

2.50 wt.% compared to 3.49 wt.% for all other areas. As mentioned, the copper smelting technology in Area R was identified by Ben-Yosef to be the most sophisticated, and the mixed iron-copper chunks from there further reiterated the strong reducing conditions of the furnaces. Thus, the low oxygen content of the copper prills analyzed from this area may corroborate this understanding.

In comparing the SEM-EDX results to the bulk composition of the slags from XRF, the Pearson Correlation Coefficient and the best fit prediction line (Figure 5.33) suggest there is no statistically significant relationship between the copper content of the slags and the copper content of the analyzed prills (0.02, p-value=0.93). It was expected that the copper content of slag would decrease with increased copper content in prills, a negative correlation, as the technology improved over time. However, the lack of a correlation between these variables suggests that the copper content of slags is not necessarily an indicator for the quality of produced metal based on these data. It is possible this is a result of the small sample size (n=26) or the data not having a normal distribution, impacting the validity of the correlation coefficient. Alternatively, it is possibly connected to a technological phenomenon such as increasing reducing conditions resulting in more efficient smelts, but also a greater precipitation of other elements such as iron in the copper metal (reiterated by the diachronically increasing iron content in analyzed prills). If this were the case however, a positive correlation would be expected – copper content in both slags and prills would decrease together. As such, the lack of a relationship between these variables is currently difficult to interpret. It is worth noting that in looking at Graph A in Figure 5.33, the residual (distance between the analytical results and the best fit line) seems to generally decrease and cluster as the copper content of the slag decreases. This phenomenon could provide additional evidence that slags with low copper contents are

associated with consistency efficient smelts, despite not being associated with higher copper content in prills. Hopefully future studies employing the methodology from this dissertation (analyzing both the bulk composition of slag and the elemental composition of the entrapped prills) will increase the size of the dataset and contribute further to this issue.

The statistical analysis of the iron content was discussed above, but calcium and silicon also showed correlations with the copper content of prills with Pearson Coefficients of -0.36 (p-value=0.013) and 0.48 (p-value=0.73) respectively (Table 5.15 and Figure 5.33). Calcium is a typical component of ancient copper slags, and it can be introduced to the furnace charge through a variety of pathways including the ore, flux, fuel, furnace lining, tuyères, etc. which can make it complicated to identify the exact source (Ben-Yosef and Yagel 2019: 71). As the ore, flux, and fuel sources were probably consistent through the Iron Age, the changing calcium content can most likely be attributed to technological equipment (furnaces, tuyères, etc.) or practices. If the calcium was introduced into the slag through melting technical ceramics such as tuyère tips and furnace linings, calcium content in slag would likely increase with improving technologies and higher firing temperatures (Ben-Yosef and Yagel 2019: 71), which is the opposite of the results presented here. In following, two possible explanations are adjustments to the furnace charge (such as flux:ore ratio) or beneficiation practices (extracting more gangue from the ores prior to charging the furnace). For example, Ben-Yosef and Yagel (2019: 73-74) suggest the decreasing calcium content found in Iron Age slags from Timna in comparison to the Late Bronze Age was a result of increasing the flux in the furnace charge for a more fuel-efficient smelt. However, as the manganese (the primary flux in Faynan) content in slag shows little change through the Iron Age, it doesn't seem that the amount of flux was changed. Thus, the identified correlation between a decreasing calcium content in slag and an increasing copper content in prills could be

caused by changing beneficiation practices, perhaps simply through different manual sorting/crushing (Hauptmann 2007: 71); ore with less gangue was entering the furnace resulting in purer metal and less calcium in slag. Again, the statistical results need to be considered critically given the correlation is only moderate and only near-statistically significant.

The only statistically significant correlation with copper content in prills was the silicon content of slag. Silicon is a primary gangue material in copper ores hence its high content in all ancient slags. The logical interpretation for the increasing silicon content in slag with higher copper content in prills is a better separation of gangue from metal resulting in a purer copper. However, the increasing silicon content runs counter to expectations given that silicon will increase the viscosity of the slag which is understood to impact the separation of slag and metal, i.e., slags with a higher viscosity will result in a less efficient smelt (Bachman 1980: 131, Figure 6). Two factors potentially play a role in allowing silicon to slightly increase while maintaining efficient separation of slag and metal. First, the silicon content for Iron Age slags was consistently within an expected range for efficient copper smelts as identified by Ben-Yosef et al. (2019: Figure 4). Second, it is possible that increasing furnace temperatures countered the impact of an elevated silicon content as viscosity is also a function of temperature. It is important to note the additional evidence from Ben-Yosef et al. (2019) that smelting efficiency improved through the Iron Age. As such, the correlation between silicon in slag and copper in prills was likely the result of efficient smelts that were successfully extracting gangue from the ores.

Finally, the current dataset does not indicate that copper ores were exhausted or overly degraded in the in the $10^{th}$-$9^{th}$ centuries BCE prior to the collapse of the copper smelting industry – there is no evidence for human driven natural resource degradation/exhaustion despite intense copper smelting using sophisticated technologies. The increasing copper content, even in the

uppermost layers of the Area M slag mound at Khirbat en-Nahas, indicate that high-quality copper metal was produced through the entirety of the Iron Age. The correlations between copper in prills and other elements in the bulk composition of the slag further reiterates that smelts were continuously efficient even in the final phases of production. In turn, these results provide evidence against overshoot as a possible driver in the collapse of the Iron Age Faynan cultural system (discussed further in Chapter 7), and also support Hauptmann's (2007: 69-71) claim that copper ore sources remained sufficient in Faynan in antiquity. In following, this collapse requires an alternative explanation; possibilities are discussed in Chapter 7.

#### 5.4.6 Future Directions

Some additional steps can be taken to further develop the results of this analysis. First, additional slag mounds could be sampled from Khirbat en-Nahas and Khirbat al-Jariya. While a representative collection was analyzed based on what was available, only three slag mounds were considered; Khirbat en-Nahas alone contains ca. 36 slag mounds. Additional slag mounds, particularly samples from the uppermost layers, could further contribute to understanding the final stages of copper production during the Iron Age. Second, additional smelting sites could be included in this study. In particular, Khirbat al-Ghuwayba and Khirbat Faynan were not sampled and would provide additional insight. Khirbat Faynan likely also produced copper for the entirety of the Iron Age and thus would be particularly relevant to this research. Moreover, as Khirbat Faynan resumed production in the Roman and Byzantine Period using a different ore body, analyzing slags from this period could provide an additional chronological component. Third, a collection of copper prills could be physically extracted from the slag and analyzed using other techniques such as ICP-MS to provide standards, consider trace elements with greater resolution,

and test the analytical quality/accuracy of the SEM-EDX. While the produced results are in line with the analysis by Hauptmann (2007: Table A17), his analysis of copper metal was somewhat limited for the Iron Age (n=10). A collection of copper analyzed with a highly accurate quantitative technique would provide a valuable baseline and standard. Fourth, increasing the sample size of the slags with both bulk composition and copper prills analyses would increase the power of the statistical methods introduced above. A larger dataset could be particularly insightful for deducing how bulk composition of the slag is indicative of the metal produced. Finally, producing samples of the limited copper artifacts excavated from Faynan and analyzing them with SEM-EDX could provide an additional and comparative dataset for the results produced here. It would be especially interesting to compare the results to determine how representative the prills within the slag are of the final copper products. It could also reveal additional steps of purification in the *chaîne opératoire*.

## 5.5 Summary

The goal of this chapter was to discuss the analytical methods and results used to address four research questions that provide the foundations for this dissertation as a whole: 1) was iron produced in Faynan as an adventitious byproduct of sophisticated copper smelting? 2) How can we interpret the mixed iron-copper chunks excavated from Khirbat en-Nahas? 3) Does the quality of copper produced in Faynan change through time? and 4) Does the quality of copper in the final phases of the Iron Age industry suggest the industry over-exploited the highest quality copper ores? To summarize this chapter, each question is answered below:

1. Based on the mass spectrometry analyses focusing on osmium isotopes and HSE abundances, the mixed copper-iron chunks excavated at Khirbat en-Nahas were not

further purified to extract iron metal and produce the excavated objects. As such, neither the copper-iron chunks nor the iron objects should be considered evidence for the adventitious production of iron from a sophisticated copper smelting technology. The iron objects were probably imported, possibly in exchange for copper. They likely represent a kind of wealth finance that supported the political economy of the Iron Age. While the sediment analysis did discover abundant magnetic material, the interpretation of these findings remains ambiguous and require further research. Based on the results of the isotope study, the magnetic material including potential hammerscales and prills could be the result of some experimentation of process of the iron-copper chunks.

2. The exact function of the copper-iron chunks is still open for interpretation, but they were possibly refined to collect the copper or were simply waste products from failed smelts as previously suggested by Ben-Yosef (2010) and Hauptmann (2007), respectively. However, the LA-ICP-MS and SEM results confirmed that these unique materials were likely the result of copper smelting rather than a geological mixture or other corroded mineral. In combination with the iron prills identified in the slags, these results show that raw iron metal was being produced during copper smelting in Iron Age Faynan – likely unintentionally from an iron-rich furnace charge. This also further reiterates the improvements in smelting technology identified by Ben-Yosef (2010; Ben-Yosef et al. 2019) as producing metal iron requires a controlled and reducing smelting environment. The majority of the copper-iron chunks and the iron prills identified in slags being from Area R at Khirbat en-Nahas also fits with previous studies as a sophisticated metallurgical technology was excavated from this area.

3. In general, the quality of the copper metal produced in Faynan seems to diachronically improve through the Iron Age. The SEM-EDX analysis of 360 copper prills embedded in slags showed a general increase in copper content through time. When the data is organized to match Ben-Yosef's (2010; Ben-Yosef et al. 2019: Figure 3) metallurgical phase scheme for Faynan, the results are complicated, but Phase 3 still has the highest average copper content and lowest standard deviation coinciding with the low copper content of Phase 3 slags. The statistical analyses comparing the copper content of the prills to the bulk composition of their associated slags also indicates improvements in copper smelting through time. As copper content in the prills increased, the silicon and iron content in the slag increased perhaps suggesting a greater separation of gangue from metal and stronger reducing conditions resulting in elevated iron contents.
4. In following, the quality of copper metal in the final phases of the Iron Age industry does not suggest the industry over-exploited or degraded the locally available copper ores. The results indicate high quality copper was produced during the entire smelting campaign during the Iron Age in Faynan. As such, overshoot should not currently be considered the cause for industrial and societal collapse in the 9$^{th}$ century BCE, and other explanations warrant further consideration and investigation (see also Chapter 7).

In summary, these four research questions and their associated analytical data inform current understandings of the trajectory of metal production and society in Iron Age Faynan. By systematically analyzing the iron artifacts collected form Khirbat en-Nahas, adventitious iron production from sophisticated copper smelting can be currently ruled out as a possibility in Iron Age Faynan. While iron production may have taken place, it was likely through direct smelting of local iron ores, rather than extraction from the mixed copper-iron chunks. The sediment

analysis with its limited discovery of iron prills and hammerscales lends further support to this conclusion. Furthermore, the SEM-EDX analysis of copper prills produced the largest dataset for copper produced during the Iron Age, and it revealed that the quality of the metal remained high even in the final phases of the industry. As such, diminishing availabilities of quality copper ores was likely not a factor in the abandonment of copper smelting in the 9$^{th}$ century BCE.

Chapter 5, in part, is a reprint of the material as it appears in Brady Liss, Thomas E. Levy, and James M.D. Day 2020 Origin of Iron Production in the Eastern Mediterranean: Osmium isotope and highly siderophile element evidence from Iron Age Jordan, *Journal of Archaeological Science* 122: 105227. The dissertation author was the primary investigator and author of this paper.

# Chapter 6 - Data Sharing and Record Keeping: 3-D Modeling at Khirbat al-Jariya and Khirbat en-Nahas

## 6.1 Introduction

The development of 3-D technologies facilitated what some have called a "revolution" in the digital humanities, cultural heritage, and archaeology (Magnani et al. 2020; Guery and Hautefort 2014; Howland 2018; Remondino and Campana 2014). Specifically, the advent of photogrammetry and Structure from Motion (SfM) or Image-Based Modeling have been fully integrated into modern archaeological research (Marín-Buzón et al. 2021; Magnani et al .2020; De Reu et al. 2014; Howland 2018; Howland, Kuester, and Levy 2014; Olson et al. 2013; Levy and Liss 2020; Knabb et al. 2014b). While debates are ongoing concerning the specific usefulness and analytical applications of 3-D modeling in archaeological research and discourse, their application as a visual aid and digital record of archaeological contexts is generally accepted (Magnani et al. 2020; Garstki 2017; Howland 2018). As mentioned in the excavations chapter, 3-D modeling in archaeology introduced new opportunities for creating and sharing photorealistic, three-dimensional models of archaeological sites, excavations, and even individual artifacts with wide audiences In an academic context, 3-D models are now occasionally included in conjunction with publications to provide an unprecedented view of the archaeological data, a practice that will hopefully continue to develop (see Liss et al. 2020: Figure 4 as an example – note that the 3-D model itself is also available in the link provided in the figure caption). Not only do these digital models serve academic and research functions as seen in Chapter 4, but they also provide exciting and attention-grabbing methods to inform the general public about archaeological information and practice (Howland et al. 2020; Earley-Spadoni 2017). Moreover, advancements in 3-D visualization have created new opportunities for people to engage with models ranging from fully-immersive experiences in CAVE (Cave

Automated Virtual Environment) environments to personal and affordable platforms like Oculus Rift and Google Cardboard (Levy et al. 2020; Knabb et al. 2014b; Schulze et al. 2015; Christofi et al. 2018). Finally, 3-D models also allow for preservation of the archaeological record[1]; every scale of an excavation or historical site can be recorded and preserved with a 3-D model (Levy et al. 2020; Lercari et al. 2016; Levy and Liss 2020; Olson et al. 2013). As such, a main goal of this dissertation was to integrate photogrammetry and 3-D models of the sites and excavations for data sharing, record keeping, and outreach.

While 3-D models are regularly being produced on archaeological projects, the best methods for sharing them with scholars, stakeholders, and the public are still under exploration (Ellenberger 2017; Scopigno et al. 2017; Earley-Spadoni 2017; Howland et al. 2020; Lloyd 2016). Along with the lowering costs of the equipment and software to produce models, tools for sharing and visualizing them are similarly becoming cheaper. As mentioned, some publications now provide opportunities for including 3-D models, but also many websites such as SketchFab, Google Poly, and ProjectMosul (an archaeological example) have also introduced 3-D visualization applications creating new opportunities for affordably viewing models (Scopigno et al. 2017: 3-4). In addition, the required equipment for viewing a 3-D model in virtual reality (VR) is increasingly affordable; for example, a Google Cardboard can be purchased for $15.00 and used with most smart phones for a personal VR experience. With this in mind, SketchFab was explored as a possible outlet for sharing 3-D models produced as part of this research.

SketchFab was selected for several reasons: 1) users can upload models for free (although paid subscriptions with additional capabilities are available); 2)the interface is user-friendly and intuitive; 3) models can be viewed on any device with internet access; 4) models can be easily

[1] While a valuable tool for site recording and preservation, 3-D models and their production are still conditioned by the biases and subjectivities of the archaeologist (Garstki 2017, see also Guery and Hautefort 2014 and Howland 2018).

shared using the URL link but still controlled by using passwords; 5) additional content can be added to the models through annotations such as text bubbles, images, and sounds; 6) models are downloadable with appropriate access/password; and 7) models can be viewed in 3-D using a personal VR viewer. SketchFab also allows the user to control subtle details such as the scale and position of the viewer when the model is opened in VR which can be important for orienting a lay audience to the archaeological record. Together, all of these functions allow the model to be appropriately contextualized within its archaeological and historical contexts for viewers with varying levels of knowledge and familiarity with archaeology (cf., Lloyd 2016). Although some drawbacks to SketchFab have been raised, such as the lack of data archives and limits on additional text, it's become a popular choice among archaeologists for some of the reasons noted above (Garstki et al. 2020).

Here, SketchFab was used for disseminating models from both KAJ and KEN (links to all models are provided in the respective figure captions and a general link is provided in the chapter conclusion). As KAJ was excavated in 2014 and 3-D modeling was intentionally included in the excavation process (see Chapter 4), using SketchFab was a straight-forward and intuitive process (discussed below). However, KEN required further consideration as some contexts were excavated in in 2002 and 2006, before the widespread use of photogrammetry on archaeological projects, and the size of the site produced much larger files which required additional steps to facilitate online sharing. A brief overview of the models produced and uploaded from KAJ is provided before moving into a more detailed discussion of KEN and the methods used to create 3-D models using archived photographs.

## 6.2 3-D Modeling at Khirbat al-Jariya

The role of 3-D modeling at KAJ in context of the 2014 excavation season has already been discussed and will only be briefly described here (see Chapter 4); this section will focus on using the 3-D models for data sharing and outreach. The model of the entire site played a critical role in making informed research decisions and in providing a significantly more detailed map of the site, but it also provides an unparalleled perspective of the site for dissemination (Liss et al. 2020; Howland et al. 2015). In addition, creating a 3-D model of every area and locus at several points throughout the excavation provided a large dataset of models to be created and shared in different research and outreach contexts (Howland et al. 2020). For this dissertation, models of the slag mound excavation and other slag mound features around the site were of particular interest and played an important role in the data collection and preservation. Specifically, photorealistic 3-D models of the slag mound excavations provided a critical record of the context and stratigraphic relationships of slag samples analyzed for this dissertation. Ideally, these models should be freely available to view in conjunction with the research presented here (the full site model is already available through Liss et al. 2020).

Six additional 3-D models from KAJ were uploaded to SketchFab including two models of Area C, one of a locus excavated in Area C, and three models of crushed slag mounds around the site (discussed in Chapter 4). The Area C models include a terrestrial model providing a detailed view of the slag mound probe and an aerial perspective of the entire slag mound with the surrounding area produced using the balloon platform. The terrestrial model provides a record of the excavation and its stratigraphy; the different layers of slag accumulation (including the upper most layer where the analyzed slag samples were collected) separated by an occupation layer can clearly be seen (Figure 6.1). There is a gap in one of the sections due to a lack of adequate

imagery, but this section was also cut by a mining road making it already damaged. The details of the excavation itself are blurred in the model of the entire area because of the height of the balloon and the depth of the excavation. However, the aerial perspective contextualizes the excavation probe; the size of the slag mound is made clear and the road running along its northern border is also visible (Figure 6.2).

**Figure 6.1**: Screenshot of the Khirbat al-Jariya Area C slag mound probe model. The stratigraphy is clearly visible showing the layers of crushed slag at the bottom, an occupation horizon (note the pottery sherd just to the right of the scale bar), and uppermost layer of large slag fragments. Model by Brady Liss and photography by Thomas E. Levy.

**Figure 6.2:** Screenshot of Khirbat al-Jariya Area C model produced using the balloon photography system. The model captures the entire slag mound and the modern mining road cutting its northern edge, providing context for the excavation probe (also visible). Note that the excavation pit is 1 meter by 1 meter for scale. Photography by Matthew D. Howland and model produced by Kendra Scheer.

The three crushed slag mound models provide an additional perspective of these features which are otherwise mainly on the outskirts of the site (Howland et al. 2015). In addition, some of the models include the bedrock mortars associated with the crushed heaps, giving some insight into the slag crushing *chaîne opératoire* (Figure 6.3).

All models discussed here were produced using Agisoft Metashape (using the standard workflow of aligning the photos to produce a point cloud, dense cloud, mesh, and then textured model) and exported as .obj files, a standard 3-D model file format which can be used in various editing programs and uploaded to 3-D databases such as SketchFab (see Howland, Kuester, and Levy 2014 for a detailed overview of the entire Structure from Motion process using

Metashape). Once uploaded, a descriptive note was added providing information about the history and archaeology as well as references for further reading. The models are accessible through general searches on the website including certain key words (e.g. Faynan, Cultural Heritage, History, archaeology, etc.) or by sharing the link directly, allowing for widespread dissemination; they can also be easily accessed by searching “Khirbat al-Jariya” or “Brady Liss”. Now, SketchFab provides a database of 3-D models from KAJ that are directly related to this research, freely available to view as is or in VR. Some of the additional functions of SketchFab were explored with the KEN models.

**Figure 6.3:** Screenshot of a model of a crushed slag mound on the southeastern outskirts of Khirbat al-Jariya (Locus 523). A bedrock mortar filled (ca. 30 centimeters in diameter) with crushed slag is visible in the center of the model (arrow). Photography by Thomas E. Levy and model produced by Kendra Scheer.

## 6.3 3-D Modeling at Khirbat en-Nahas

As has been shown, the Area M slag mound excavation and Khirbat en-Nahas played a significant role in this dissertation, and it was important to investigate possibly creating a 3-D model of this archaeological context as well. This goal raised a methodological issue: is it possible to construct a 3-D model of an excavation that was not intentionally recorded with these methods at the time? Moreover, when the site was visited during the 2014 ELRAP season, the edges of the slag mound had since eroded and collapsed due to its depth of over 6.5 meters, partially filling the excavation, destroying the stratigraphic sections, and preventing taking any new photographs (reiterating the importance of creating the 3-D model of Area C at KAJ) (Figure 6.4). To circumvent this issue, this dissertation tested an original methodology of using archived digital photographs from the excavation for photogrammetry.

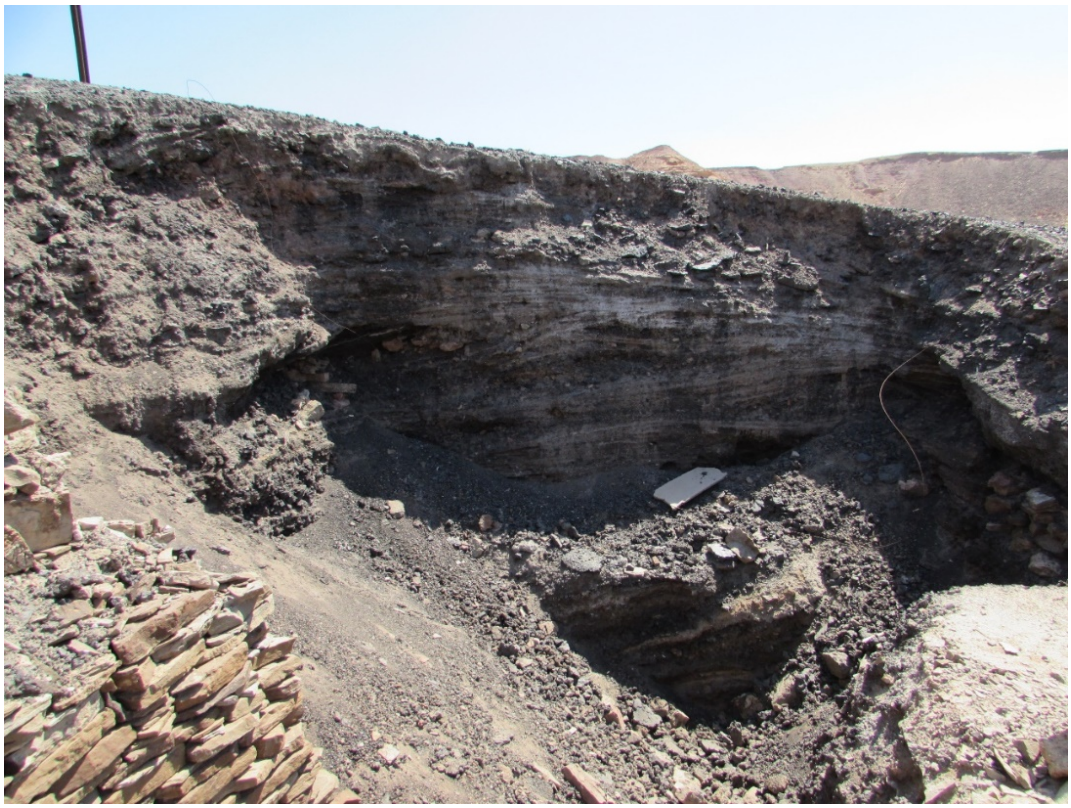

**Figure 6.4:** Photograph of the collapsed Area M excavation at Khirbat en-Nahas in 2014. Photograph credit: Brady Liss.

The Area M slag mound was not photographed specifically for SfM, but it was intensively recorded with digital photography throughout the excavation process following typical archaeological protocol and the *cyber-archaeology* methodology. Critically, many photographs were taken at the completion of the excavation both focused within the slag mound to capture the bottommost layers and from above using a boom system to record the entire area (see Levy et al. 2014: Figure 2.70a). By taking photographs from several angles around the excavation probe, the excavators also managed to create overlap between many of the images. In following the *cyber-archaeology* workflow, all of these digital photos were stored on the UCSD Levantine Archaeology Lab server allowing them to be easily accessed. These photographs were used as a dataset for possibly generating a 3-D model.

An added benefit of potentially constructing a photorealistic model of the slag mound excavation is the ability to generate orthophotos (typically an aerial image that has been geometrically corrected to remove distortion and create uniform scale). While orthophotos are often used to provide a top-down perspective of a site or excavation square/area for mapping purposes, they have also been used for generating images of stratigraphic sections (Vincent et al. 2015). An orthophoto of a section can provide an image of the entire stratigraphy, which is not always possible with a single photograph, with a perpendicular perspective. The orthophoto can be used for simply record keeping or also as a basis for section drawings (Vincent et al. 2015). While the sections of the Area M slag mound were recorded with detailed drawings (Ben-Yosef 2010: Figures 5.55 and 5.56), the depth of the excavation prevented capturing the sections with a single photo, and as mentioned, the sections eroded since the completion of excavation. Thus, generating orthophotos of the stratigraphy would be a valuable contribution that could return the sections to their original state at the time of excavation.

In addition to attempting to produce a model of the excavation area, this research also explored the possibility of contextualizing it within the site. When KEN was visited in 2014, a site-wide 3-D model was produced for the first time using the balloon photography system (Figure 6.5; Howland et al. 2020). The model provides a complete photorealistic depiction of the entire site; however, it inherently included the collapsed Area M. It was also tested here if a new model of Area M could be aligned with the site-wide model, to replace the collapsed portion. While there is value in the model capturing exactly what the site looked like at the time, it is archaeologically significant for data sharing to be able to include a complete depiction of the Area M excavation within the site in 3-D. Finally, one of the main incentives for producing the models was for wide-spread dissemination of the archaeological record as discussed above.

**Figure 6.5:** Screenshot of the 3-D model of Khirbat en-Nahas from 2014. For scale, the large square fortress on the left side of the models is ca. 73x73 meters. The photographs were taken using the ELRAP balloon platform. Photography and model by Matthew D. Howland.

### 6.3.1 Methods and Workflow

The first step was to test if a model of Area M could be produced using the archived digital photographs. In total, 251 photographs from throughout the excavation process were collected and stored on the server. As most of the images were in focus and the overlap between photographs was not intended for SfM, the entire collection was included to maximize coverage in the attempt to make a model. The digital photographs were converted to TIFs and imported into Agisoft Metashape. While there were artifact tags, measuring tapes, and a member of the ELRAP excavation team in some of the photographs, they were not masked out due to the limited number of images in these areas of the excavation. All 251 photographs taken by T.E. Levy were processed without masking in Metashape, and the produced model was exported as an .obj file[2].

Once the model was completed and saved, it was then used to generate orthophotos of the stratigraphic sections, also in Metashape. In order to find a perspective of the entire excavated sections, the orthophotos were produced one at a time by first cutting away the portion of the model that was not needed. For example, when making the orthophoto of the eastern section, the rest of the model was simply highlighted and deleted using the selection tool. This step allowed the model to be oriented correctly for a perpendicular viewpoint of the section and to only include the relevant material in the orthophoto. Once generated, there were some lighting differences and also some blurry portions in various areas of the orthophoto. To correct for this, the Image Assignment function within Metashape was used to select particular images with better focus/lighting. Image Assignment allows the user to draw a polygon around the

[2] A similar method was attempted for the Area A slag mound at KAJ from the 2006 excavation season, but it was unsuccessful likely due to a lack of photographs or insufficient overlap between the images.

problematic area of the orthophoto/model to see all of the photographs for that were used in generating that portion of the model. The images with the correct focus and lighting can then be selected, and only those photographs will be used in producing the final model/orthophoto, removing any photos that were blurry and improving the quality of the model. The same process was repeated for each relevant section of the slag mound excavation.

To integrate the produced Area M model and the site-wide KEN model, both .obj files were uploaded into Blender – a free software for creating, editing, and manipulating 3-D data. Once in Blender, the models could be viewed simultaneously in the same workspace and the model of Area M could be manually aligned with the site model using points of similarity, in this case, primarily the edges of the excavation pit and the corner of the excavated structure. Once aligned, the new Area M model was hidden, and the collapsed portion of the site model was cut away using the Blender tools to select and delete individual polygons from the mesh. Returning the Area M model, the intersections between the two models were smoothed by adjusting the polygons of the mesh to fill any gaps from deleted polygons or to reduce any unnatural edges (Figure 6.6). The file was then saved as a single .obj model, adjoining them into a single model.

The new combined model, given the high quality of the Area M model and the size of KEN, needed to be reduced in size for uploading online (SketchFab with a pro account has a limit of 200 megabytes). The model was decimated which reduces the number vertices or faces of a mesh without drastically impacting its shape to lessen the file size, and the high-resolution texture was “baked” onto the decimated model as a normal map. Texture baking essentially records the surface characteristics of a 3-D model into 2-D image textures which are “baked” on the geometry (the texture no longer needs to be rendered once baked) (McAvoy, personal communication).

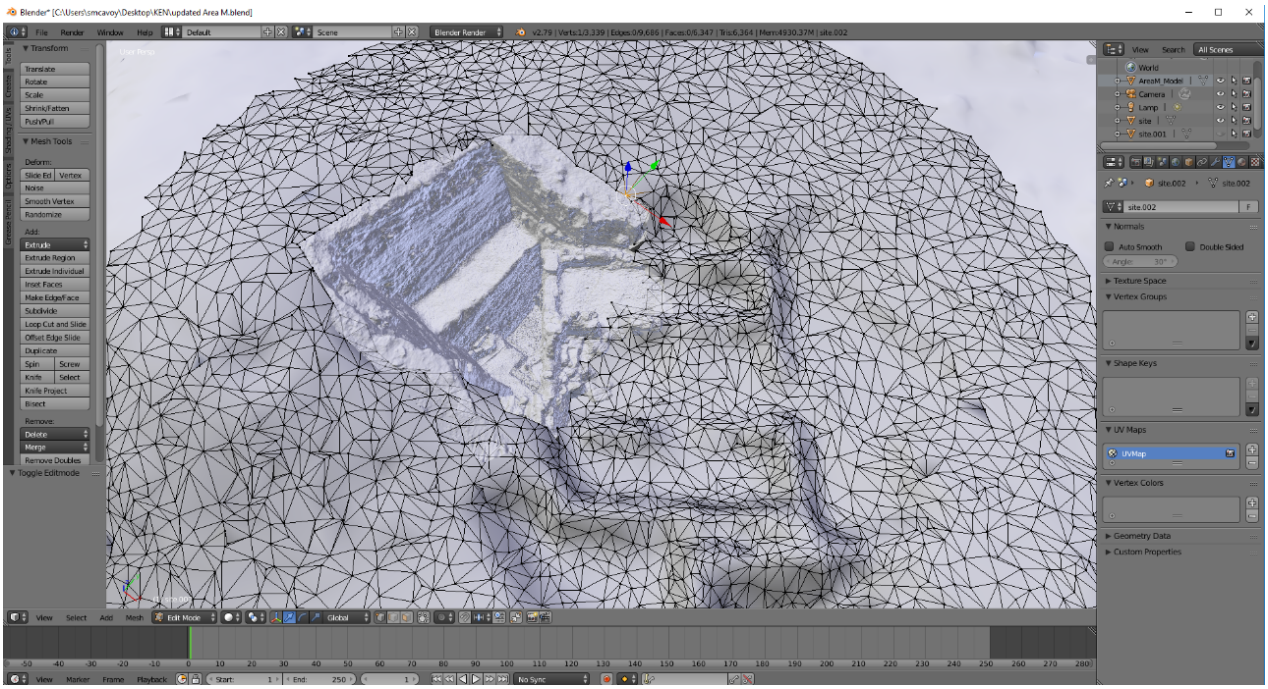

**Figure 6.6:** Screenshot of the Area M and Khirbat en-Nahas site model being aligned in Blender. The site model was cut down (circular portion) during this process to reduce computational strain. The corner of the building and the edges of the slag mound probe provided the main points of similarity for aligning the two models. Here, the individual polygons of the site model (black triangles) are being manually adjusted to smooth the intersections between the Area M model and the site. Screenshot by Scott McAvoy, UCSD Library.

Baking as a "normal map" reduces the number of polygons in comparison to the high-resolution model while maintaining geometric details; the normal map recreates topography using light/color rather than polygons ("Normal Map (Bump Mapping)" 2019). This process essentially allows the user to drape a high-resolution texture over a lower resolution mesh, drastically reducing file size while keeping detail as a texture layer to facilitate sharing online[3]. SketchFab was also used for sharing the models from KEN including the Area M excavation and

[3] Special thanks to Scott McAvoy of the UCSD Library for all his assistance with this stage of the research.

the combined Area M/site model[4]. An additional benefit of SketchFab is that models can be exported from Blender or Agisoft Metashape to your SketchFab account allowing the combined model to be uploaded directly. The added sound and point of interest functions within SketchFab were integrated into the Area M model (discussed further below).

### 6.3.2 Results and Discussion

The archived excavation photographs from Area M proved to be an excellent dataset for producing a 3-D model. The large number of photos created enough overlap between them to generate a high-quality model (Figure 6.7).

**Figure 6.7:** Screenshot of Khirbat en-Nahas Area M 3-D model produced using the original excavation photographs. Photography by Thomas E. Levy and the UCSD Levantine and Cyber Archaeology Lab. Model produced by Brady Liss and Matthew D. Howland.

[4] These steps to reduce the file sizes were not required for the other models such as the Area C model because they were produced at lower qualities in Metashape (medium versus very high). These models were simply exported directly to SketchFab from Metashape.

Most significantly, the model almost perfectly captures the excavation at the time of completion; the entire slag mound probe is visible down to the bedrock and the archaeologically significant stratigraphic sections are completely intact. The model now provides the best available record of the complete excavation, especially given that the slag mound has since collapsed. The only gaps in the model are in a corner of the excavation where an excavator was standing in some of the photographs. Unfortunately, these were the only available images covering this part of the excavation, so masking was not an option. However, the gaps are only in the corner of the excavation and are not overly detrimental to the model and its representation of the archaeology. Overall, the model is successful in reconstructing the archaeological excavation.

Because the stratigraphic sections were complete in the model (lacking any significant gaps), it could also be used to generate orthophotos of the stratigraphy. Using the methods above, orthophotos of the south and east sections were created (Figure 6.8); these are the sections where samples of slag, including those analyzed here, and charcoal were collected (Ben-Yosef 2010; Ben-Yosef et al. 2019). The orthophotos were able to capture the entire stratigraphic section from surface to bedrock despite the size of the excavation at over six meters deep, which was impossible with a single photograph. Moreover, the Image Assignment function allowed the entire image to be in focus and to have consistent lighting throughout. In conjunction with the drawing, these orthophotos provide the best visual record of the stratigraphy and provide critical preservation of the archaeological record.

The Area M model was also integrated into the full site model contextualizing the excavation area in 3-D for the first time. The collapsed portion in the original site model was successfully removed, and the new model of Area M was added in its place (Figure 6.9).

**Figure 6.8:** Orthophotographs of the south (left) and east (right) sections of the Area M slag mound excavation at Khirbat en-Nahas. The white lines are measuring tapes from the original excavation photos. The shifts in the measuring tapes and lighting in the southern section are due to the step that was left unexcavated (visible in Figure 6.7). Note that these sections are as deep as 6.5 meters but are entirely captured with a single image. Photography by Thomas E. Levy and the UCSD Levantine and Cyber Archaeology Lab. Orthophotos produced by Brady Liss, Matthew D. Howland, and Anthony Tamberino.

**Figure 6.9:** Comparison of Area M in the site model before (left) and after (right) the new Khirbat en-Nahas Area M model was integrated, and the collapsed portion was removed.

The combination of Agisoft Metashape and Blender allowed for easy production, editing, and combining of the models (while producing the models can take significant time depending on the quality and file size, the entire process of combining the models only took roughly an hour of work). However, as the two models were aligned manually and polygons were adjusted to fill gaps between them, there is some distortion in the model compared to reality around this excavation area[5]. These manual edits would only be impactful if using the model for research such as taking measurements or georeferencing artifact locations; the model still provides an excellent dataset for maintaining a record of the archaeology more generally and for outreach about KEN and Area M (as seen in Howland et al. 2020). There are also some lighting differences between the two models, but these are potentially beneficial in clearly showing the

[5] This step of the process could be improved and facilitated if both models are accurately georeferenced using control points; the Area M model was not georeferenced due to a lack of secure control points. In theory, the models could be automatically aligned if using the same coordinate system. This would also avoid some of the manual manipulation to align the two models and maintain the overall accuracy.

added Area M model (Figure 6.9). In general, the combined model provides a unique opportunity to explore the Area M excavation as one component of the entire site, providing its full context, in comparison to the stand-alone model.

Finally, both the Area M model and the combined KEN model were uploaded to SketchFab along with the models from KAJ[6]. The Area M model was used as a test case for the various features and customization available in SketchFab. For example, when VR is selected for Area M, the user is automatically positioned at the edge of the slag mound and at around the height of an average person (ca. five feet, five inches or 1.65 meters) (Figure 6.10).

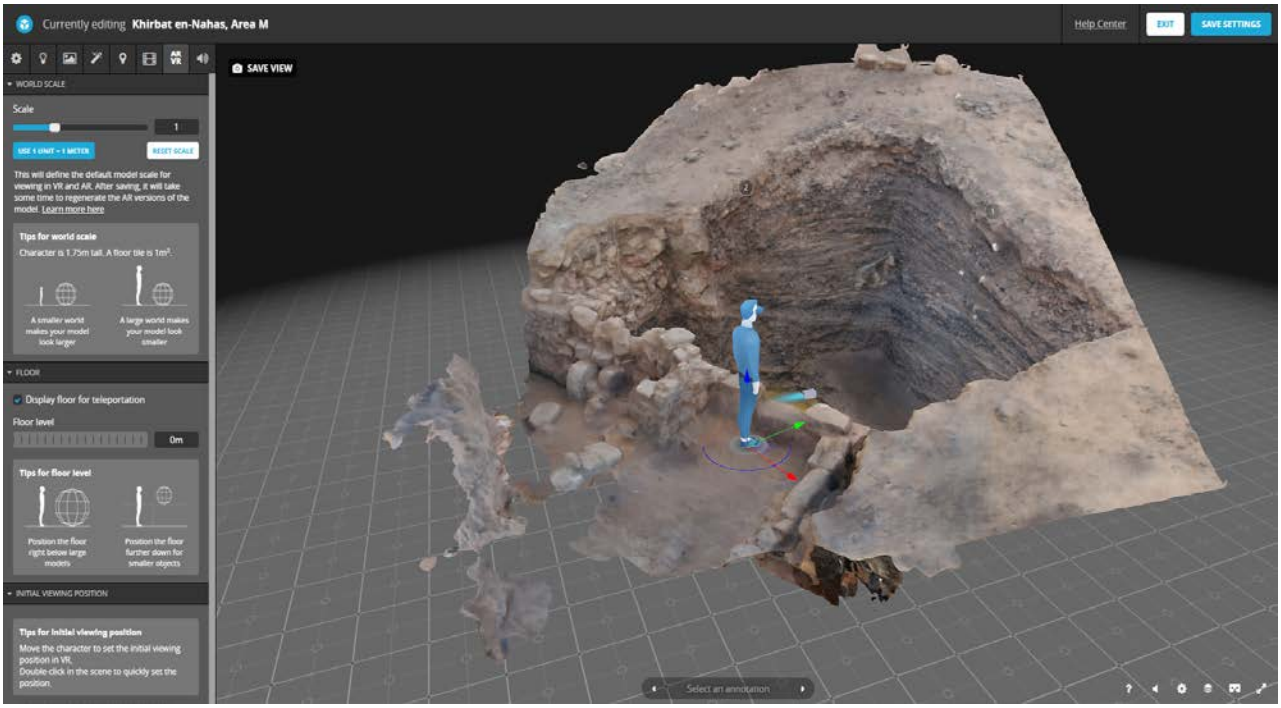


**Figure 6.10:** Screenshot of SketchFab showing the position and height of the viewer when they enter the virtual reality view on the Khirbat en-Nahas Area M model. This position orients the viewer towards the archaeological record and maintains a realistic experience by "standing" on the ground and looking down into the excavation.

[6] While not directly part of this research, the 3-D models produced from both KAJ and KEN were also included in an ArcGIS StoryMap which tells the history of Faynan providing another avenue of outreach and dissemination (see Howland et al. 2020).

This viewpoint orients the viewer for a direct perspective of the archaeological record, and also provides a realistic experience of standing at the edge looking down into the excavation. The viewer can still move freely around the model to explore its different features (which is particularly beneficial in the full site model) using the hand controls of the Oculus Rift or the touch control on a Google Cardboard. In this way, SketchFab provides an affordable and widely accessible VR experience of the archaeological excavations at KEN and KAJ.

The ability to include additional information and interactive components with the 3-D model within SketchFab proved particularly valuable as well. Specifically, when the Area M model is opened, a recorded Mp3 (sound file) begins with a voice over explanation of the archaeological context and the model[7]. The viewer can simply listen to the recording providing some of the basic information that may be of interest or helpful to audiences who are not familiar with archaeology; those not interested can simply mute it. A shortened version of the voice over recording is written in the note section of the model which also provides resources for further reading. In coordination with the automatic positioning, any viewer should be able to experience and understand the archaeological significance of the model passively but is also free to actively go further both virtually in the model and intellectually.

The annotation function allows highlighting specific components of the model where additional information is needed or beneficial. This function was used to create points of interest with scholars and researchers in mind, although they are accessible by anyone viewing the model. Two points of interest were added to the Area M model which provide links to the original section drawings by Ben-Yosef (2010: Figures 5.55-5.56). When clicked, the model is automatically positioned with a view of the section, and a text bubble appears with the link that

[7] SketchFab temporarily removed this feature from its models due to copyright issues. As such, the voice recording may not be available when viewing the model. However, the included text still provides sufficient overview of the model and its context.

opens directly to the relevant section drawing (Figure 6.11). The section drawings are particularly helpful for visualizing and identifying the stratigraphy of the slag mound, and also because they include the locations of all the samples collected by Ben-Yosef (2010) for his dissertation research (see also Ben-Yosef et al. 2019). As this dissertation also used the same slags and maintained the sample numbers, the section drawings also provide the locations of the samples analyzed here along with the 3-D model of their context. Furthermore, as the analyses conducted for this dissertation (as with archaeology more generally) were entirely dependent on the stratigraphic relationships between slag samples, the 3-D models ensure current understandings and interpretations of the stratigraphy in conjunction with the section drawings.


**Figure 6.11:** Screenshot of SketchFab showing the Khirbat en-Nahas Area M model with added annotation providing a link to the original section drawing. The annotation is selected so the model automatically oriented to view the section. The small "1" in the circle at the top of the section on the right side of the image is the second annotation with a link to that section drawing.

By using these functions, both the Area M model and the samples collected from the excavation are fully contextualized in their archaeological, historical, and research contexts. Finally, it is important to note that the Area M excavation continues to be a focus of debate in the archaeological discourse of the region. Specifically, the stratigraphy and dating of Area M have recently been emphasized/evaluated by Ben-Yosef (2019) and Tebes (2021), reiterating the importance of creating a digital record of this excavation. To easily access and view the models, search for “Khirbat en-Nahas” on SketchFab.

## 6.4 Summary

Overall, this research reiterated the value in creating 3-D models at various scales in the field and provided a proof of concept for reconstructing archaeological excavations using just excavation photographs. As most archaeological excavations have used rigorous digital photography recording strategies since its advent, these projects can potentially use archived images to construct 3-D models of previous excavations if needed. The determining factor for whether a model can be produced will likely be the number of photos taken and the amount of overlap between them. This method will be particularly pertinent for excavations and sites that have since been damaged as was the case for Area M (ProjectMosul uses a similar approach for restoring artifacts that have been damaged by looting and warfare) and can potentially make a significant contribution to the conservation of archaeological excavations and sites (e.g., Lercari et al. 2016). In addition, combining models proved a viable option for contextualizing smaller area models into the larger sites, and SketchFab provided an ideal outlet for disseminating the models due to its ease-of-use, affordability, and the ability to include additional information to assist unfamiliar audiences or provide more detail to scholars/researchers.

Critically, the contexts relevant to the samples analyzed in this dissertation are now accessible online. All models are freely available for viewing on SketchFab. As the majority of the samples came from Area M, this model provides an excellent contextual reference for this research. The combination of the photorealistic model along with the drawings of the stratigraphic sections allows researchers to see the context of any given sample analyzed here and also the relationships between samples. Finally, SketchFab also now functions as a database for preserving these archaeological contexts, and as a platform for learning about the archaeology of Faynan.

# Chapter 7 - Synthesis and Discussion: The Cycle and "Collapse" of Iron Age Copper Production in Faynan

## 7.1 Introduction

Considering both previous investigations and the new excavations and analysis presented here, the adaptive cycle can be applied for a holistic model of copper production and society in the Faynan region (the adaptive cycle and its various phases are detailed in Chapter 2, Figure 2.2, and Table 2.1). As this dissertation is primarily focused on the Late Bronze to Early Iron Ages, the adaptive cycle is chronologically constrained to the Middle Bronze through Late Iron Ages to facilitate a complete examination of the periods both preceding and following this intensive phase of copper production. Based on a combination of the archaeological record and the archaeometallurgical analysis, two complete cycles were identified, and each phase is discussed below in chronological order[1] (Figure 7.1 and Table 7.1). In addition, the culture system model is applied where relevant to parse out additional intricacies of the development and growth of a complex social-ecological system and to further elucidate the transitions between phases of the adaptive cycle. Political economy provides additional insight into the internal processes of individual phases and transitions. The role of a more nuanced understanding of collapse and the potential application of "overshoot" are integrated into the adaptive cycle to critically evaluate the important transition from the K to Ω phase in the Iron Age. Together, the application of these theoretical models with support from the new and robust analytical dataset provides valuable insight for understanding the cycle and collapse of Iron Age copper production in Faynan. Figure 7.1 provides the complete stylized adaptive cycles constructed through this research, and Table

[1] It should be noted that additional adaptive cycles can extend beyond the Late Bronze and Iron Ages. For a continuation of the adaptive cycle into a third iteration during the Roman and Byzantine periods, see Knabb 2015: Figure 4.16.

7.1 describes each phase along with their archaeological evidence and correlations to the phases of copper production from Ben-Yosef et al. 2019.

**Figure 7.1:** The complete adaptive cycles for roughly the Middle Bronze ($20^{th}$-$14^{th}$ centuries BCE) to Late Iron Ages ($7^{th}$-$6^{th}$ centuries BCE) for society and copper production in Faynan. The red arrows represent the "beginning" and "end" of the cycles from the perspective of this research. See Chapter 2 and Table 2.1 for detailed descriptions of each phase.

Adaptive Cycle of Iron Age Faynan

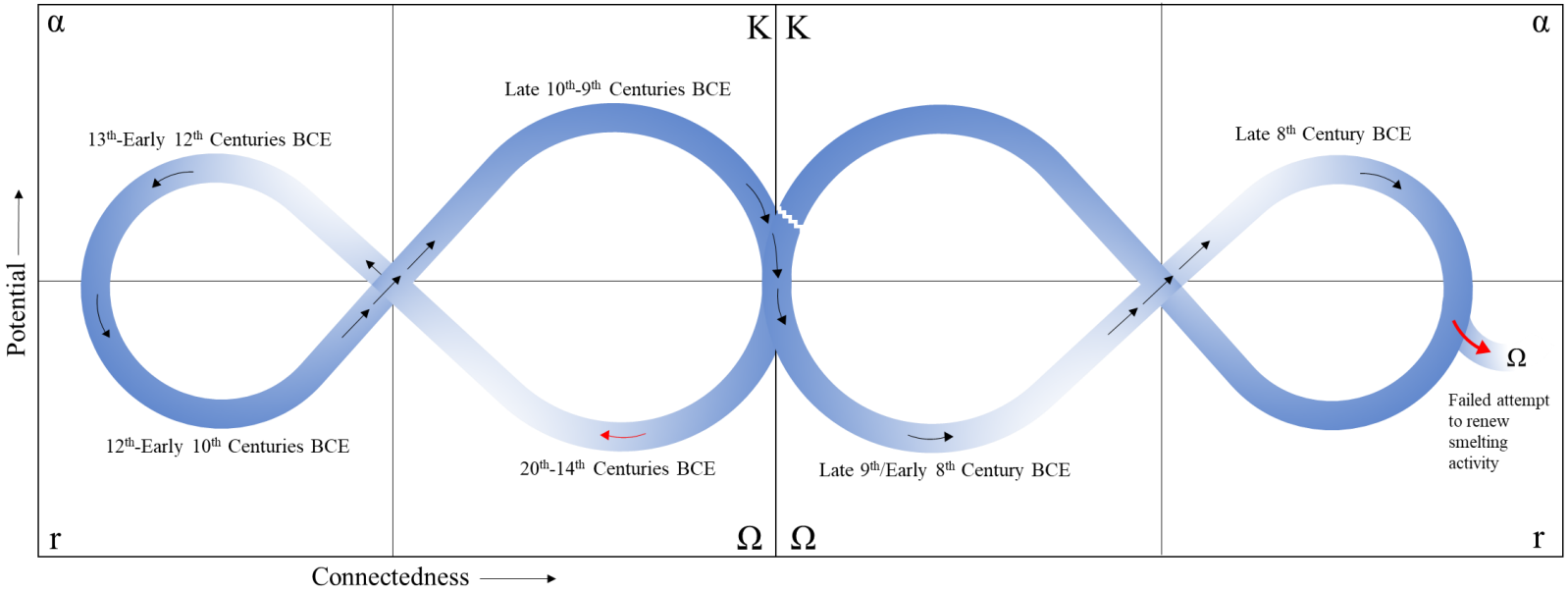

**Table 7.1:** Descriptions of each phase of the adaptive cycle for the social-ecological system of Faynan along with their archaeological evidence and correlation to Ben-Yosef's phases of copper production. See Figure 7.1 for the depiction of these phases as a cycle.

| Adaptive Cycle Phase | Ω | α | r | K | Ω | α |
|---|---|---|---|---|---|---|
| **Time Period** | 20th-14th Centuries BCE Middle Bronze – Late Bronze Age | 13th-12th Centuries BCE Late Bronze - Early Iron Age | 12th-Early 10th Centuries BCE Early Iron Age | Late 10th-9th Centuries BCE Early Iron Age | Late 9th/Early 8th Century BCE Late Iron Age | Late 8th-7th Centuries BCE Late Iron Age |
| **Description** | This time period lacks evidence of copper production and likely represents a release following the Early Bronze Age industry. | Reorganization of pastoral nomads to begin the earliest Late Bronze-Early Iron Age copper production in Faynan. Initial establishment and experimentation with copper production. | Pastoral nomadic tribes coalesced into an early chiefdom to intensively exploit local copper ores and produced metal on a more substantial scale. Captured opportunity following Late Bronze Age Collapse ("remember" process). | Following the campaigns of Sheshonq I, copper production reached an industrial peak centered at KEN. Local resources and capital controlled through structured industry, and efficiency improved through new smelting technology. | Copper production industry in Faynan was abandoned, and control over the local ores is released. Populations in Faynan returned to more pastoral nomadic lifeways ("revolt" cascade). | A failed attempt to reorganize and renew copper smelting activity. Center of Edomite polity shifted to the highlands. |
| **Archaeological Evidence** | -None | -Limited archaeological evidence but includes crushed slag and installations at the bottom of the Area M slag mound at KEN and possibly Wadi Dana 1.<br>-Egyptian texts reiterate the presence of *Shasu* nomads in the region in the Late Bronze Age.<br>-First mention of "Edom" in the Papyrus Anastasi VI, dated to the end of the 12th century BCE. | -Accumulation of slag at KEN (Layer M3-M4).<br>-Construction of KEN fortress and elite architecture in 10th century BCE.<br>-KAJ and KAG established in 11th century BCE.<br>-WF40 cemetery.<br>-RHI watchtower constructed.<br>-Legacies of past cycles reused at KHI, Ras en-Naqb, and Barqa el-Hetiye in the form of infrastructure and recycling of slags. | -Reorganization of fortress gatehouse at KEN.<br>-Flattening of Area M slag mound for building.<br>-Area R smelting complex and Area F constructed.<br>-Abandonment of KAJ and KAG (consolidation at KEN).<br>-RHI watchtower.<br>-New metallurgical technology including large tuyères and tap slags.<br>-Significant accumulation of slag in Area M at KEN (Layer M2-M1).<br>-Copper smelting at KF. | -Abandonment of KEN. | -RAM Archaeological Complex with incomplete fortress.<br>-RAM Mines.<br>-Small habitation at RHI.<br>-Absence of smelting sites.<br>-Buseirah, Umm el-Biyara, and Tawilan on the Edomite Plateau. |
| **Copper Production Phase** | -None | -Phase 0* and beginning of Phase 1 | -Phases 1-2 | -Phase 3 | -None | -Phase 4 |

*Phase 0 is currently identified by Late Bronze Age activity in Timna. The earliest material culture at the bottom of the Khirbat en-Nahas Area M slag mound and Wadi Dana 1 could represent Phase 0 in Faynan, but the record is limited and requires further investigation.

7.2 Release (Ω) in the Middle Bronze Age: 20th-16th Centuries BCE

Current archaeological evidence for copper smelting in Faynan during the Middle Bronze Age is largely lacking (Hauptmann 2007: Figure 5.2; Ben-Yosef 2010: Table 10.1; Hauptmann and Weisgerber 1992: 63). While there was potentially mining activity during this period based on an OSL date from the Jabal al-Jariya mines and possible Middle Bronze Age pottery sherds from the Wadi Khalid mines, there is no contemporaneous smelting sites in Faynan (Ben-Yosef 2010: 495, 513; Hauptmann 2007: 116-120). To date, there is only one site in the entire Wadi Arabah with evidence of Middle Bronze Age copper smelting - Be'er Ora Hill south of Timna (Avner 2002: 43, Table 9; Ben-Yosef 2010: 513, Table 10.1). Thus, from the perspective of copper production in Faynan, the Middle Bronze Age can be characterized as a release during which the local ores were free from any control; they were not bound within a social-ecological system. This understanding is reiterated by the evidence for substantial copper smelting during the preceding Early Bronze Age as evidenced at Khirbat Hamra Ifdan, Ras en-Naqb, and Barqa el-Hetiye - representative of a K-phase during this period. Finally, Cyprus is also generally considered a copper supplier to the Levant during the Middle Bronze Age based on archaeological evidence and ancient texts (Yahalom-Mack et al. 2014a). Ingots from Middle Bronze Age Hazor were sourced to Cyprus with lead isotope analysis (Yahalom-Mack et al. 2014a, 2014b), and the copper from the Bronze Age kingdom of "Alashiya" which appears in numerous Bronze Age texts including the Middle Bronze Age Mari Tablets is generally recognized as originating in Cyprus (Goren et al. 2003; Knapp 1985). Thus, while this release phase is primarily identified by an absence of evidence within Faynan, this absence is supported by substantial excavations and surveys, and the additional evidence from the greater Sothern Levant lend credence for this conclusion.

## 7.3 Reorganization (α) in the Late Bronze Age: 16th-Early 12th Centuries BCE

Most of the Late Bronze Age is missing from the archaeological record in Faynan like the Middle Bronze Age. However, there are some indications for copper smelting towards the end of the Late Bronze Age. While the archaeological record is somewhat limited for the 13th-Early 12th centuries BCE, this period should be considered a reorganization phase. Returning to the definition, reorganization is associated with innovation and experimentation during times of social transformation (Holling and Gunderson 2002: 35). Innovation draws on freely available resources to create a new system or for "the initial establishment of entities" dedicated to resource accumulation (Holling and Gunderson 2002: 41). The evidence for reorganization in Faynan can be seen in crushed slag layers at the bottom of the Area M slag mound at Khirbat en-Nahas which were radiocarbon dated to the 13th century BCE, suggesting copper production at the site could have begun as early as the end of the Late Bronze Age (Figure 7.1 and Table 7.1). Wadi Dana 1 also provides potential evidence of Late Bronze Age copper smelting, but as discussed, the site requires further investigation. Moreover, the archaeometallurgical *chaîne opértoire*, at least by the Iron Age and likely also during this early phase, is different from the preceding Early Bronze Age technological repertoire in Faynan (Ben-Yosef et al. 2019: 8). Early Bronze Age copper production relied on wind-based furnaces in contrast to furnaces operated by sack-bellows in the Iron Age (Ben-Yosef et al. 2019: 8; Hauptmann 2007: 228-239). This technological dissonance provides additional evidence that Faynan experienced a reorganization based on the "innovation" (or "introduction") of a new smelting technology in the region.

Additional support for a Late Bronze Age reorganization phase in Faynan can be drawn from the textual evidence. The *Shasu* nomads of Egyptian sources reiterate a presence of pastoral

nomads in the region during the Late Bronze Age, perhaps also providing an explanation for why archaeological sites dating to this period are largely lacking (Ben-Yosef 2021; Finkelstein 1992b). Furthermore, if the understanding that Faynan was within the borders of the Edomite territory is correct, the Papyrus Anastasi VI indicates an Edomite polity significant enough to draw the attention of Egyptian officials at this time (Levy and Najjar 2006a). As this is the first appearance of Edom in ancient texts, it potentially provides evidence of "social transformation" during this period. Thus, the archaeology and texts together suggest a presence of a significant population in the region beginning to produce copper (likely on a small-scale) in the 13$^{th}$ century BCE – the "initial establishment" of copper smelting for resource accumulation. Considering the absence of any evidence for copper production in the preceding Middle Bronze Age, the Late Bronze Age can be interpreted as a reorganization of the pastoral nomadic society in Faynan to (re)introduce copper smelting into their lifeway with a "substantial amount of potential available for future development" (Holling and Gunderson 2002: 41). From the perspective of the cultural system model, it is during this phase that "metallurgy" was added to the technology subsystem. This early production and reorganization correlate with Ben-Yosef's Phase 0 and the beginning of Phase 1.

## 7.4 The Nested Hierarchy: Faynan and the Late Bronze Age Collapse as an Example of "Revolt" and "Remember"

The Late Bronze age collapse plays a key role in the development of Iron Age Faynan and the transition from the Late Bronze reorganization phase to the Early Iron Age exploitation phase. However, the Late Bronze Age collapse was a large-scale phenomenon impacting the entire Eastern Mediterranean, and therefore needs to be considered in a separate adaptive cycle. The adaptive cycle can function on multiple interconnected scales through the "nested

hierarchy". As discussed in Chapter 2, the "nested hierarchy" allows researchers to "nest" adaptive cycles across time and space to investigate the interactions between them and the constraints created by these interactions (See Holling, Gunderson, and Peterson 2002: Table 3-1 for some examples). Holling, Gunderson, and Peterson (2002: 75-76) identified two main cross-scale interactions: "remember" and "revolt". To reiterate, "remember" is used to describe the process through which a smaller-scale adaptive cycle draws "on the potential that has been accumulated and stored in a larger, slower cycle" for renewal (Holling, Gunderson, and Peterson 2002: 75). As described by Holling, Gunderson, and Peterson (2002: 76), "Once a catastrophe is triggered at a level, the opportunities and constraints for the renewal of the cycle are strongly organized by the K-phase of the next larger and slower level". Said otherwise, smaller scale adaptive cycles can capitalize on opportunities maintained by the persisting K-phase of a larger adaptive cycle. Holling, Gunderson, and Peterson (2002: 76) connect the "remember" process from a large-scale K-phase to a middle-scale reorganization (Figure 7.2), but they also recognize that there are "potentially multiple connections between phases at one level and phases at another level". In contrast, "revolt" occurs when a collapse on a smaller scale cycle "cascades" into a larger cycle facilitating a multi-scalar collapse. Here, "revolt" can be directly applied to the Late Bronze Age collapse, and "remember", with some nuance, can aptly describe the growth of the copper production industry in Faynan during the Early Iron Age, the r-phase of the 12$^{th}$-Early 10$^{th}$ centuries BCE.

First, the nested hierarchy of adaptive cycles needs to be identified. Borrowing the language used by Rosen and Rivera-Collazo (2011: 2) in their application of the nested hierarchy, the three levels of adaptive cycles are referred to as micro-, meso-, and macro-scales from smallest to largest in geographical scales, and from fastest to slowest regarding the time to

**Figure 7.2:** The “nested hierarchies” of adaptive cycles situating the social-ecological system of Faynan in a larger geographical and temporal context in the Late Bronze (A) and Early Iron Ages (B). The Late Bronze Age collapse can be characterized by the “revolt” phenomenon (arrow) in which the collapse of empires “cascaded” into a larger scale collapse of the Eastern Mediterranean economic system which was in a conservation phase. As Faynan was on the margins of these empires and in a reorganization phase, society was likely not significantly impacted by the collapse (represented by the blue microscale adaptive cycle). The increase in copper production and societal complexity in Early Iron Age Faynan can be associated with the “remember” process through which society capitalized on new opportunities for production/exchange facilitated by the persisting demand for copper in the Eastern Mediterranean and the political vacuum created by the collapsing empires.

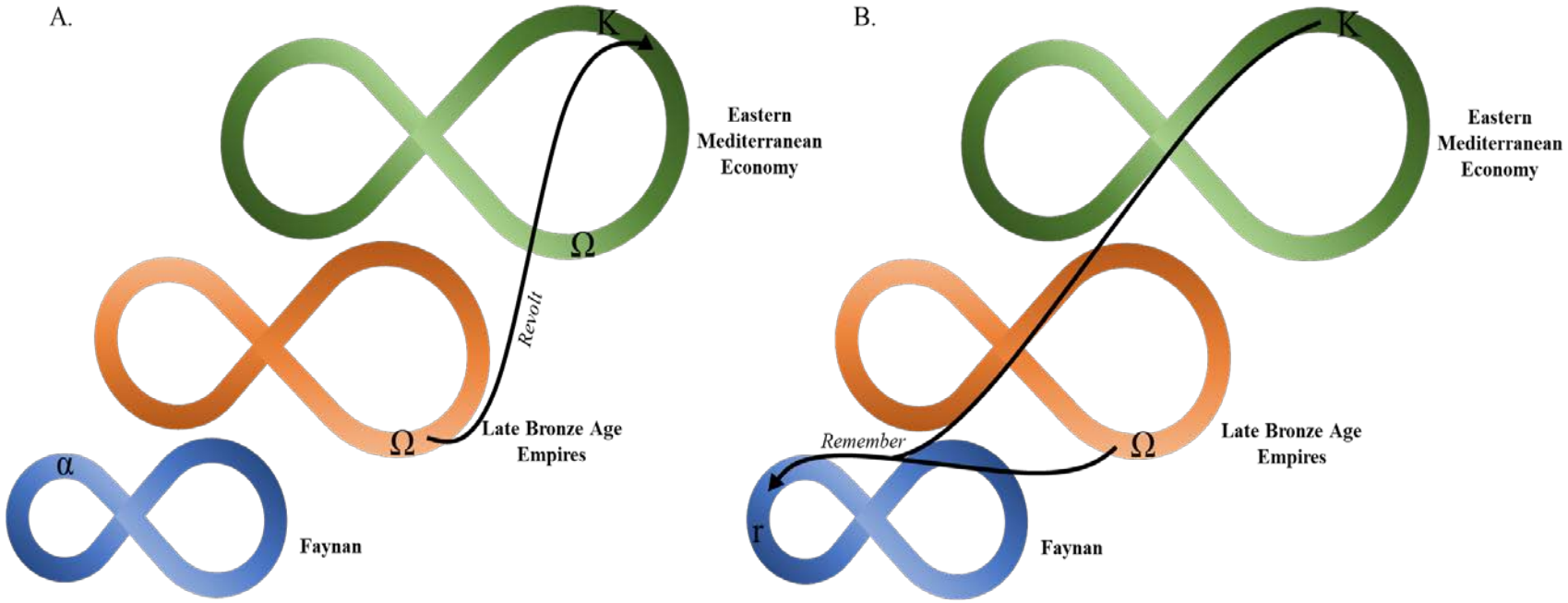


Late Bronze Age

Early Iron Age

proceed through a complete cycle, respectively. The Eastern Mediterranean world of the Late Bronze Age can be considered the largest and slowest level or macroscale adaptive cycle. This cycle will primarily be considered from an economic perspective as the commercial networks highlight the interconnectivity of the region, perhaps best represented by the international cargo of the Late Bronze Age Uluburun and Cape Gelidonya shipwrecks (Bass 2005; Pulak 2005; Cline 1994; Sherratt and Sherratt 1991). The Late Bronze Age empires that composed the Eastern Mediterranean and their localized territories can represent the next level down, the mesoscale. The phases of this mesoscale adaptive cycle can be identified by the organization, growth, development, and subsequent collapse of these empires[2]. At the smallest or microscale is the adaptive cycle of society and copper production in Faynan, which existed on the margins of these empires (Figure 7.2).

Beginning with the Late Bronze Age collapse, the revolt phenomenon provides an effective model. While the causes (or triggering agents) of the collapse are highly debated (see Chapter 2), the fall of multiple Eastern Mediterranean empires during this time is accepted and evidenced through the widespread destruction of sites (Cline 2014). Critically, the trade networks that connected the Mediterranean world similarly broke down, dismantling the economy of the time. In other words, the world system of the Late Bronze Age Eastern Mediterranean experienced a collapse phase on several scales. Returning to the designed nested hierarchy, there is a collapse at the mesoscale, the Late Bronze Age empires, and the macroscale, the Eastern Mediterranean and its interconnected economy (Figure 7.2). As the Late Bronze Age empires were likely one of the primary drivers of the economic system (Sherratt and Sherratt 1991: 370-375), this extensive collapse can be described as a “revolt”. The collapse of the local empires

[2] The individual phases of the meso- and macro-scale adaptive cycles are not described in detail here as they are beyond the scope of this dissertation.

cascaded up facilitating a larger scale collapse in the macroscale cycle of the Eastern Mediterranean system (Figure 7.2)[3].

From the perspective of Faynan and its nascent copper production (in the reorganization phase during this time), the Late Bronze Age collapse created "unlimited opportunity" (Holling and Gunderson 2002: 43). With the breakdown of the Late Bronze Age economic network, Cyprus no longer functioned as the main provider of copper to the Eastern Mediterranean (Kassianidou 2012, 2014; Yahalom-Mack et al. 2014a; Knauf 1991; Knauf-Belleri 1995). However, while the mechanisms for trade transitioned into a collapse phase, the demand for copper, which can be treated as the persisting K-phase at the macroscale, was sustained into the Iron Age[4]. In this way, the exploitation phase in Faynan and the growth of the copper smelting industry beginning in the 12th century BCE "aggressively captured" an "open market" through the process of "remember" (Holling and Gunderson 2002: 43). In addition, this dissertation suggests a slightly more complex "remember" process that simultaneously captured "potential" on both the meso- and macro-scales to facilitate a rapid transition from a reorganization to an exploitation phase (Figure 7.2). The collapse of the Eastern Mediterranean empires at the mesoscale created the necessary political vacuum for the emergence of a more complex tribal kingdom in Faynan (Knauf 1991; Knauf-Belleri 1995). As previously described, critical to the

[3] The destruction of sites during the Late Bronze Age collapse could potentially represent an additional microscale adaptive cycle, and a "revolt" cascading on two scales (the "collapse" of sites).

[4] The return of trade networks interconnecting the entire Mediterranean world during the Iron Age provides further evidence for the existence and persistence of a macroscale adaptive cycle driven by economic demand (Ben-Yosef 2019b and citations there within). For example, Faynan copper has been identified reaching as far as Greece during this period (Kiderlen et al. 2016). These economic networks also experienced what could be interpreted as a reorganization phase during the Iron Age. Sherratt and Sherratt (1991: 373) describe the "growth of *opportunistic* trading in small vessels by interstitial and peripheral groups" made possible by the "*released* dependent populations [due to the collapse of empires] and new configurations of economic activity" (emphasis added) in the Early Iron Age which fits well with the characteristics of a reorganization phase.

growth and development of this polity was the ability to convert the local copper ores resources into economic capital (political ecology) which was only made possible by the sustained demand for the metal at the macroscale. These corresponding "remember" processes allowed society in Faynan to transition into an exploitation phase to take control of the newly opened marked for copper by intensively developing the copper smelting industry.

## 7.5 Exploitation and Growth (r) in the Early Iron Age: 12th-Early 10th Centuries BCE

Following the Late Bronze Age collapse, the reorganization phase in Faynan moved rapidly into a full exploitation and growth phase starting in the 12th century BCE. The r-phase is connected to "intense activity…energized…by open opportunity" and it is "very much influenced by external variability" (Holling and Gunderson 2002: 43). As discussed, the Late Bronze Age collapse represents this "external variability" through creating a "newly opened market" for copper metal in the Levantine world. The archaeological record for the 12th-10th century BCE in Faynan fits with expectations of an exploitation phase; the evidence for copper production dramatically increases during the Early Iron Age in comparison to the Late Bronze Age, suggesting copper was being produced on a substantial scale ("intense activity"). Specifically, there is a more significant accumulation of slag in the Area M slag mound at Khirbat an-Nahas (Layer M4) indicative of an increasing scale of copper production. The earliest phases of Area S and Area W at Khirbat en-Nahas are also dated to the 11th century BCE, suggesting the site was expanding along with its associated industry. Critically, it is during the 11th century BCE that Khirbat al-Jariya and Khirbat al-Ghuwayba were established as satellite smelting centers and possibly a provisioning site in the case of Khirbat al-Ghuwayba. Khirbat al-Jariya encapsulates the "energy" and "intense activity" of an exploitation phase as it was

probably developed to expand the industry and to exploit additional copper ore resources up the Wadi al-Jariya (Chapter 4). This understanding is further reiterated by the significant accumulation of slag dated to the 11th century BCE at the bottom of the Area C slag mound; the site was capturing potential and exploiting resources from its outset. The 12th-11th century BCE and the development of a more regional smelting industry represent Phase 1 in Ben-Yosef's model.

The copper industry continued to grow in the Early 10th century BCE – ca. 1000-925 BCE (Ben-Yosef's Phase 2). Perhaps most representative of the continued expansion is that every ELRAP excavation area at Khirbat en-Nahas included layers dated to the Early 10th century BCE. Additionally, all these layers contained evidence connected to copper production either through direct indications for smelting activity or residual material such as crushed slag (see Levy et al. 2014: Table 2.1). Thus, based on the current archaeological evidence, Khirbat en-Nahas was likely reaching its full extent during this period. In addition, Layer M3 in the slag mound is dated to the Early 10th century BCE, and it is one of the most significant accumulations of copper production waste. It also correlates with the thickest accumulation of slag at Khirbat al-Jariya, Layer C2a. As the 10th century BCE continues, substantial and possibly elite architecture was also constructed at Khirbat en-Nahas. The first construction phases of the Area A gatehouse, the Area T tower/elite residence, the Area W complex, and the main elite structure in Area R are all dated to this period. The gatehouse and its associated fortress provided a clear expression of control over resources and exemplify the growth of the industry during this phase. Control over the region and its copper ores was also conveyed through the construction of the Rujm Hamra Ifdan watchtower. It is difficult to securely date its original construction due to limited radiocarbon dates, but it could have been built in the Early 10th century BCE. The

location of this watchtower at the entrance of the wadi indicates its purpose to watch and control movement in and out of industrial landscape – starting to "control external variability". In sum, society in Faynan experienced continued growth, and the exploited copper resources were becoming increasingly bound within the system (higher connectedness) as represented by constructing permanent and significant architecture.

Along with developing new smelting sites and the growth in production at Khirbat en-Nahas, there is also evidence for using the "legacies of past cycles" to accumulate additional resources during this exploitation phase (Holling and Gunderson 2002: 43). Smelting sites and materials from previous cycles, primarily the Early Bronze Age, were repurposed during the Early Iron Age. Specifically, excavations at Khirbat Hamra Ifdan yielded evidence for Iron Age copper smelting dating to the 12$^{th}$-10$^{th}$ centuries BCE despite being constructed and mainly used in the Early Bronze Age. Similarly, while Ras en-Naqb and Barqa el-Hetiye currently have less secure dating based on pottery, slag typologies, and a few radiocarbon dates, they likely represent a similar phenomenon; both these Early Bronze Age smelting sites contained evidence for activity during the Iron Age. Excavations at Barqa el-Hetiye discovered a possible Iron Age habitation based on a house structure dated to the Iron Age I, and an Iron Age slag mound (possibly Iron Age II based on pottery) was identified at Ras en-Naqb. Thus, all these sites likely represent repurposing "legacies" in the form of previous smelting sites/infrastructure in order to grow the copper smelting industry during the Iron Age. In addition, Hauptmann (2007: 104, 124) further suggests that Iron Age copper production could have recycled Early Bronze Age slag through re-smelting or crushing to extract its copper prills; the less efficient smelting technology of the Early Bronze Age resulted in slags abundant in copper content and prills. These slags

similarly represent the legacies of a past cycle, which could have contributed to the exploitation and growth of copper production during the Iron Age.

Society in Faynan more generally also experienced developments during this phase in conjunction with the expansion of the copper smelting industry. Along with the establishment of new sites at Khribat al-Jariya and Khirbat al-Ghuwayba, archaeologically identified connections between these sites and Khirbat en-Nahas suggest Faynan was developing a regional network and industrial landscape. The dating of Khirbat al-Jariya in the 11$^{th}$ century BCE after the start of the copper industry at Khirbat en-Nahas and consistencies in the metallurgical *chaîne opértoire* indicate that it was an expansion of the existing industry, possibly by a subset of workers from Khirbat en-Nahas. While Khirbat al-Ghuwayba contributed to the copper smelting on a smaller scale, its primary purpose was likely control over ‘Ain al-Ghuwayba and growing orchards for provisioning of foods and fuel to the other smelting centers and mining sites (Chapter 4). The botanical evidence at Khirbat al-Jariya including fruit seeds and wood from pomegranate, grape, and fig among others reiterates a connection between these sites and the role of Khirbat al-Ghuwayba in growing such trees. Finally, the Wadi Faynan 40 cemetery is contemporaneous with these developments, dated from the 11$^{th}$-9$^{th}$ centuries BCE. As the industry grew, Wadi Fidan 40 was established at the entrance of the Wadi Fidan possibly as an ethnographic and territorial marker complementing the Rujm Hamra Ifdan watchtower; this could also suggest a new ethnic identity was developed during this phase as a result of the coalescing tribal kingdom following Levy’s oscillating tribal segmentary system model. Through a combination of new smelting sites, elite architecture, a watchtower, and cemetery site, society in Faynan established an identity and exerted authority over local resources, allowing greater “control over external variability” to “reinforce their own expansion” (Holling and Gunderson 2002: 44).

### 7.5.1 Explaining Growth in the r-phase: The Multiplier Effect and Political Economy

While the phases of the adaptive cycle are applicable across complex systems, the drivers facilitating both the internal processes within and transitions between phases are contextual and idiosyncratic (Gunderson and Holling 2002). Coupling the adaptive cycle with additional theoretical perspectives, here the culture system model and political economy, can bolster its application to archaeological case studies. The growth and exploitation phase matches with the "multiplier effect" from the culture system model. Renfrew (1972: 23) suggests culture change is driven by a "multiplier effect" when "changes in one area of human experience lead to developments in another. In this way the created environment is enlarged in many dimensions, and itself becomes more complex". In looking at the archaeological evidence of the exploitation phase in Iron Age Faynan, the "multiplier effect" accurately describes the situation.

Along with the growth in the copper production industry, the technology subsystem, there were also identifiable changes in the social organization, trade, and symbolic subsystems[5]. The construction of elite architecture and the fortress at Khirbat en-Nahas show a clear transition in the social organization of Faynan compared to previous periods. It is difficult to securely identify the nature of this social organization, but the appearance of large-scale permanent architecture and sites is a discernible difference from the fully pastoral nomadic organization of the Late Bronze Age. The construction of possible elite residencies (particularly Area R at Khirbat en-Nahas and potentially Area B are Khirbat al-Jariya) could also indicate the development of a sociopolitical hierarchy. Concerning the trade/communication subsystem, the scale of copper

[5] It is possible that there were also changes in the subsistence subsystem as well based on the appearance of fruits at Khirbat al-Jariya or through possible trade for additional subsistence goods, but this is difficult to securely identify based on the archaeological record in comparison to previous phases.

production was beyond local consumption during the 12th-Early 10th centuries BCE, and metal was being traded. Iron Age I-IIA copper ingots from Faynan were discovered off the coast of Israel indicating the copper trade extended to at least the Mediterranean coast, and lead isotope analysis has identified Faynan copper in Greece and Egypt (Yahalom-Mack et al. 2014a; see also Martin and Finkelstein 2013; Martin et al. 2013; Kiderlen et al. 2016; Ben-Dor Evian et al. 2021; Ben-Dor Evian 2017; Vaelske, Bode, and Loeben 2019). Finally, changes in the symbolic subsystem are evidence by the Wadi Fidan 40 cemetery which is likely connected to an ethnic identity further established during this period. Furthermore, some of the excavated graves contained copper goods suggesting a connection between the symbolic and technology subsystems. This connection could also function on a figurative level; the Wadi Fidan 40 cemetery could be symbolically marking control over the mining and copper smelting region. As such, the cultural system of Iron Age Faynan was likely experiencing a multiplier effect during the 12th-Early 10th centuries BCE; the innovations within the metallurgical industry created positive feedback loops with the other subsystems of the Iron Age Faynan cultural system. In turn, the developments in these various impacted subsystems likely "favour[ed] the further development of the innovation [copper smelting]" as evidenced by the increasing scale of production (Renfrew 1972: 38). Moreover, as technology was impacting most if not all other subsystems, this phase could also be described as a "cultural take-off" in Faynan – all involved subsystems experienced "marked structural change" (Renfrew 1972: 39-43). In turn, the multiplier effect works in tandem with the adaptive cycle to provide additional explanation for how a complex system transitions from reorganization to exploitation phases.

The result of this cultural take-off was the emergence of a tribal kingdom or polity intimately connected to metallurgy. Returning to Levy's oscillating tribal segmentary system

model, cultural take-off aligns with the ethnogenesis process through which segmentary tribes identified with a new ethnic identity, possibly Edomite, to form a chiefly confederacy (Levy 2009: 158; Maeir 2021). The critical role of technology in this sociopolitical development, described here as the 'multiplier effect', is also highlighted by Levy as "political ecology" in suggesting the abundant copper ores of Faynan provided a main driver in sociopolitical complexity (Levy 2009: 158). From the perspective of punctuated equilibrium, Ben-Yosef et al. (2019: 11) also describe this phenomenon of "the formation of the tribal confederation of the Edomite Kingdom" which they suggest is "evident as early as the 11$^{th}$ century BCE". Using the archaeometallurgical record, they identified a "striking synchronous agreement between technology in Timna and Faynan" which provides evidence of "an overarching political body" (Ben-Yosef et al. 2019: 11). Ben-Yosef et al. (2019: 11) describe this period as a "quasi-stasis" associated with constant and deliberate efforts to improve the efficiency of the metallurgical industry. These efforts, identified in the analytical data, again fit with the multiplier effect – positive feedback loops between subsystems would "favour the further development" in the technology (Renfrew 1972: 8). The culture system model provides a theoretical perspective to holistically explain these interrelated processes.

Political economy likely also played an important role during the r-phase of Faynan (and the K-phase). The identified contemporaneous increases in copper production and sociopolitical complexity in the 12$^{th}$-Early 10$^{th}$ centuries BCE were probably a result of "unequal access to wealth and power" through control over both production and exchange of copper (Hirth 1996: 204-205). This unequal access is represented by the appearance of the elite structure of Area R and its stone seat at Khirbat en-Nahas. The central and elevated location of Area R would have allowed overseeing copper production across the site, possibly from the position of the stone

bench. The construction of the fortress was a further projection of control over production at the site, and it also could have provided control over exchange. The chambers of the gatehouse might have held finished copper products and ingots for trade, and its location at the northern end of Khirbat an-Nahas made it widely visible to anyone traveling along the wadi. Exchange and movement in and out of Faynan was further controlled and monitored by the Rujm Hamra Ifdan watchtower. The location of Rujm Hamra Ifdan reiterates its intended purpose; it was placed on an elevated outcrop at the western entrance to the region – the "gateway to Faynan" (Figure 4.1) (Levy et al. 2002). Finally, ceramic analysis from Area B at Khirbat al-Jariya indicate this large, central structure may also have served an elite function (Howland 2021). Howland (2021) suggests these elites may have gained their status through control of copper production and exchange at the site. In general, these architectural and site developments would allow greater control over copper industry, creating differential access to wealth.

Controlling the trade of copper would afford additional access to staple and wealth finance further supporting the existing political economy. Copper was likely traded via the Negev Highlands for staples including cereals/grains, and probably also "politically charged" goods such as iron objects (discussed below and in Chapter 5). As exotica is largely lacking from the current archaeological record, staple finance likely played a significant role. This could also support a more localized, or "agency-oriented", control of political power outside the realm of the projection of power from a political "core" which may be expressed through prestigious exotics (Goldstein 2000). The new localized ideational and social structures of the Iron Age also would have facilitated resource mobilization through their intimate connections to copper smelting i.e., the positive feedback loops between the symbolic, social organization, and technology subsystems of the culture system "provide the structure and justification" that

allowed the political economy to operate (Hirth 1996: 209). The Wadi Fidan 40 cemetery, graves with copper goods, a bronze figurine from the gatehouse, and a figurine casting mold from Khirbat en-Nahas all show that copper was integrated into the ideational structure of Iron Age society. Taken together, the "multiplier effect" and political economy provide modes for the growth and exploitation within the r-phase of the adaptive cycle, giving this theoretical approach additional explanatory power. Moreover, as has been shown, these processes can be identified in the archaeological record. The ensuing cultural take-off can be correlated to the transition period between the r- and K-phases as the system becomes further interconnected and expands.

## 7.6 Transition from r to K: A Punctuated Leap or Gradual Growth?

The transition from the growth and exploitation phase to the conservation and consolidation phase in Faynan leaves some room for debate. While it is presented as a clear divide in Table 7.1, this process could be considered more continuous and gradual; it is represented as such in the adaptive cycle. The "front loop" depicts a continuous and unbroken transition from r to K, and it is generally described as a slower process within the cycle (Holling and Gunderson 2002: 35, 47). However, in archaeological contexts, the "speed" associated with the adaptive cycle is probably more variable (compared to ecological applications) and "radical transformations" can occur "very quickly" (Redman 2005: 74). This discussion is in line with the theoretical considerations presented in Ben-Yosef et al. (2019) and Luria (2021) concerning applying phyletic gradualism versus punctuated equilibrium to the archaeological record; in other words, can technological/societal change be better characterized by episodic events (leaps) or more gradual and steady transformations? Either way, it is still important to identify changes in the archaeological record that possibly represent the progression from r to K.

This dissertation builds on Ben-Yosef et al. (2019) in suggesting that the "punctuated leap" identified in copper smelting technology and the centralization of the copper production industry at Khirbat en-Nahas in the Late 10th century BCE represents the transition from the r-phase to the K-phase in Iron Age Faynan. The "accumulation of capital" associated with a K-phase is attributed to the improved smelting technologies following the "punctuated leap" (discussed further below). This approach secures the shift from r to K within a small chronological window in the Late 10th century BCE, and arguably to a particular event – the campaigns of Sheshonq I. While Luria (2021) argues this transition is not a punctuated leap spurred by Egyptian involvement but rather a gradual and indigenous development facilitated through Egyptian demand for copper, his perspective still recognizes the technological developments and improvements used here to identify the transition to the K-phase. The analytical results from this dissertation complicate this narrative from the perspective of the produced copper (see Chapter 5), but the copper prills from the Area M slag mound, which provides the largest and most chronologically secured dataset, further support the identified pinnacle in metallurgy following the punctuation event.

Alternatively, the 10th century BCE and the growth of Khirbat en-Nahas during this period could represent a more steady and continuous transition between the phases. The expansion of the site and the appearance of elite architecture over the course of the 10th century BCE could characterize the transformation. The construction of the fortress, the largest and most substantial architecture in the region and emblematic of the control over resources, could represent the completion of the r-phase and the progression into the K-phase. Pushing this transition back to earlier in the 10th century BCE with the first construction of the fortress would then situate the technological developments of the Late 10th century BCE and the consolidation

of the industry at Khirbat en-Nahas within the K-phase, rather than the boundary between phases. Both approaches for characterizing the shift from r to K in Iron Age Faynan are viable (neither can be (dis)proven given the current state of the archaeological record), and perhaps could also be taken together as more generally representing this transition.

## 7.7 Conservation and Consolidation (K) in the Iron Age: Late 10th-9th Centuries BCE

In accepting the "punctuated leap" in smelting technology as the tipping point between the r and K phases, the evidence for Iron Age Faynan transitioning into the conservation and consolidation phase is largely derived from the archaeometallurgical record on both the macro- and micro-scales. Beginning around ca. 925 BCE and potentially connected the campaigns of Sheshonq I, copper production in Faynan reached a peak in terms of scale and efficiency (Ben-Yosef's Phase 3). It is only in the Late 10th-9th centuries BCE that excavations have identified the "large tuyères", larger furnaces, and massive tap slags associated with this technological zenith (Ben-Yosef et al. 2019: 10, Figure 5). The copper content in slags analyzed from this period is also the lowest on average and has the smallest range of standard deviation indicative of consistently efficient smelts (Ben-Yosef et al. 2019: Figure 3). The analysis of copper prills presented here similarly identified a consistently high copper content with lower standard deviation or variability in comparison to previous periods, indicative of consistently efficient smelts during this phase. At Khirbat en-Nahas, the high iron content found in the copper produced during the Late 10th-9th centuries BCE provides additional evidence for a sophisticated smelting technology, and Area F with its unique archaeometallurgical toolkit was potentially constructed for the purpose of refining this copper (discussed in Chapters 4 and 5). These technological improvements, while possibly initiated by an outside influence, represent the

"inward focus" on "increasing efficiency" and "streamlining operations" associated with the K-phase in the adaptive cycle (Holling and Gunderson 2002: 44). The K-phase is also described as a "climax" and a period of "equilibrium" within complex systems, which similarly applies to the situation with copper production during this period (Berkes and Folke 2002: 122, 125-126; Fath, Dean, and Katzmair 2015). Ben-Yosef et al. (2019: 11) in a similar fashion refer to the period following these changes in smelting technology as an "equilibrium" during which copper production continued "for more than a century with no discernible changes". Thus, the archaeometallurgical evidence indicates the industry reached its "climax", and copper was efficiently produced in a stable system.

In following, efforts were made to "conserve" the prevailing conditions. In the Late 10$^{th}$ century BCE, the copper smelting industry was consolidated and centralized at Khirbat en-Nahas (and potentially also Khirbat Faynan though further research is needed here), decommissioning Khirbat al-Jariya and possibly Khirbat al-Ghuwayba. In doing so, the number of "key nodes" in the industrial landscape was reduced (increasing connectedness), allowing Khirbat en-Nahas to have a "high concentration of influence" over copper smelting (Fath, Dean, and Katzmair 2015). The fortress at Khirbat en-Nahas was also repurposed for metallurgical functions, perhaps to ensure even greater control over production as it still maintained an inherently "defensive" functionality, even if just as a physical demarcation from the rest of the site. This understanding is further reiterated by the construction of the Area F refinery within the fortress walls, providing an additional level of authority and visibility over production. Ben-Yosef (2010: 333-334) suggests the fortress could have functioned as a "projection of social power" over the metallurgical industry based on the location of Area F, and in this way, resources were increasingly bound within the system. As such, the archaeological record compliments the

archaeometallurgical evidence, indicating society in Faynan transitioned into a conservation phase in the Late 10th century BCE.

### 7.7.1 Resilience and Rigidity: Copper Production as a Rigidity Trap

Another key component of the K-phase is the loss of resilience. The system becomes more interconnected, and more dependent on sustained production - it becomes more rigid and vulnerable to "triggering agents". While concentrating the copper smelting industry at Khirbat en-Nahas likely facilitated greater authority over production and an inward focus on streamlining, it also would have increased the rigidity of the system. By decommissioning other smelting centers, there was a "loss of redundancy" in Faynan creating a greater dependency on the accustomed conditions of Khirbat en-Nahas producing abundant copper (Fath, Dean, and Katzmair 2015). Redundancy in a complex system affords a "buffer" to disturbances; "loss of redundancy" can lead a complex system towards a "rigidity trap" – when a system is over "refined" leaving little room for diversity or innovation (Fath, Dean, and Katzmair 2015; Berkes and Folke 2002: 132-133; Holling, Gunderson, and Peterson 2002: 95-98). Thus, the complex social-ecological system in Late 10th-9th century BCE Faynan was likely existing in a stable climax, but also precariously vulnerable due to its intense focus on copper production with limited redundancy and diversity - entirely centralized at Khirbat en-Nahas, and potentially also Khirbat Faynan.

The idea of a rigidity trap also fits with current understandings of pastoral nomadism and desert populations. Returning to the question introduced in Chapter 2, "how do societies in marginal environments actually deal with risk in either a reactive or strategic sense?" (Smith et al. 2007: 2), society in Faynan likely used a unique combination of pastoral nomadism and

industrial-scale copper production. For subsistence, this “semi-nomadic pastoralism” or “mixed economy” was based on animal herding but included some horticulture as evidenced by the botanicals at Khirbat al-Jariya, possibly cultivation in the fields by Khirbat Faynan, and exchange for subsistence goods (Khazanov 1994: 20-21; Bar-Yosef and Khazanov 1992: 2; Marx 2006: 86; Beherec 2011: 129; Barker 2012). It is difficult to identify archaeologically due to the perishable nature of staple goods, but exchange of copper for food stuffs likely played a predominant role in “dealing with risk” in the marginalized environment of Faynan. Ethnographic studies have shown that even pastoral nomads practicing some agriculture often require additional grains from agricultural societies, especially in times of drought (Bar-Yosef and Khazanov 1992: 5). Khazanov (1994: 198-212) suggests pastoral nomadic populations “cannot function in isolation” of the settled world and production (of crafts or animal products connected to pastoral herds) within such societies can be “directed to quite a considerable extent towards exchange”. As such, society in Iron Age Faynan likely employed industrial copper production and exchange for staples as an adaptive strategy to deal with its marginalized environment and the more sedentary lifestyle associated with copper smelting.

New archaeological evidence from the Negev Highlands further supports the claim that the inhabitants in Faynan participated in exchange for additional subsistence. Martin and Finkelstein (2013; Martin et al. 2013) identified pottery originating in the Wadi Arabah and Faynan in the Negev Highlands. They suggest that this pottery was not a medium of exchange in itself based on the assemblage consisting primarily of handmade wares of household typologies (Martin and Finkelstein 2013: 35-36). Rather, this pottery was probably the result people moving and carrying pottery from the Wadi Arabah (Martin and Finkelstein 2013: 36). The movement of

people and pottery from Faynan was likely to exchange copper[6]; Martin and Finkelstein (2013: 36) believe "These people must have been employed in the Arabah copper districts as miners and smelters". They further suggest that the sites of the Negev Highlands participated in exchange with neighboring sedentary lands, primarily for cereals and grains to support their subsistence economy in the harsh climate (Martin and Finkelstein 2013: 37-38). In this way, an economic connection between Faynan, the Negev Highlands, and agricultural societies was established in the Iron Age which could have provided an avenue of exchange of copper for cereals/grains to be brought back to Faynan. This access to additional subsistence goods likely "released the pastoral nomads from their total dependence on animal husbandry", facilitated the increased focus on copper production, increased sedentarization at smelting centers, and possibly diminished the size of the pastoral herds (Martin and Finkelstein 2013: 38; Finkelstein 1995: 37-38). However, as has been seen in other pastoral-nomadic populations that specialize in a craft, this centralization and further concentration on copper smelting would have increased the dependency on sedentary populations for exchange (Khazanov 1998: 9; Bar-Yosef and Khazanov 1992: 5; Finkelstein 1995: 37-38). In other words, investing in non-subsistence practices can decrease resilience for pastoral nomads – creating a rigidity trap

Political economy could also have contributed to the decreasing resiliency of the K-phase. The consolidation and intensification of copper production at Khirbat en-Nahas was potentially another stage in asserting control over the production and exchange of copper by existing elites. Furthermore, economic relationships between pastoral and non-pastoral groups are not limited to only agricultural goods (staple finance); wealth objects are often also

[6] A similar model was proposed for the Early Bronze Age IV where "The copper mining in Feinan and the potential for amassing wealth from the profits must have contributed to the existence of settlement in the southern area of the Dead Sea and the Negev" (Haiman 1996: 24).

exchanged (Khazanov 1994: 204; Bar-Yosef and Khazanov 1992: 5; Marx 2006: 86). Wealth finance could have provided an additional incentive for elites to focus on copper production and exchange. While there is limited evidence for imports or foreign material culture in the archaeological record of Faynan[7], the iron objects from the Late 10th-9th centuries BCE could be an example of such wealth finance. The isotopic analysis of Chapter 5 suggests that iron objects in Faynan were the result of exchange (not locally produced) which could contribute to their value as foreign and imported. The appearance of iron jewelry in particularly wealthy graves of Wadi Fidan 40 reiterates a certain value was attached to the metal. In general, the increased focus on copper production during the consolidation phase in pursuit of likely both staple and wealth finance could have further increased the rigidity of the social-ecological system in Faynan.

## 7.8 Transition from K to Ω: Collapse or Abandonment?

As introduced in Chapter 2, this dissertation argues that society in Faynan experienced a "collapse" driven by a failure in the copper industry in the 9th century BCE. While it is possible the metallurgical industry was simply abandoned with a transition to the Edomite plateau and a renewed connection to Cypriot copper 8th-6th centuries BCE, in applying the adaptive cycle, the interruption in copper production should be interpreted as a "triggering agent" and the 8th century BCE in Faynan is more accurately characterized as a release or collapse (the role of Cypriot copper and how/why copper production in Faynan stopped is discussed further below). It is argued here that a failure in the copper production industry was a catalyst for a larger scale

[7] Recent excavations in Timna discovered textiles dyed in the famed royal purple associated with the Mediterranean Coast providing new evidence for a potential elite class and the possible exchange of copper with a focus on wealth finance (Sukenik et al. 2021). Unfortunately, the environmental conditions of Faynan do not preserve textiles, but these findings could more generally represent economic connections focused on wealth goods between Edom and the Mediterranean Coast. This evidence also further suggests a feedback loop existed between technology and the symbolic subsystem as well.

collapse in the cultural system of Iron Age Faynan, rather than a consequence. In other words, a collapse in the metal production industry was a triggering agent that facilitated the transition from K to Ω. Returning to the definitions introduced in Chapter 2, it is suggested that Faynan experienced a transformation in at least its economic complexity and likely also its social and political complexity[8].

As has been seen in the adaptive cycle thus far, copper production was a major driver in the increasing growth, exploitation, and complexity of the Iron Age Faynan cultural system. From the initial reorganization through the climax and equilibrium of the K-phase, copper smelting provided a primary means to exploit resources that could be converted into economic and sociopolitical capital with subsequent growth. The exchange of copper provided critical access to staple and wealth finance allowing for a combined carrying capacity and increasing sociopolitical complexity. The positive feedback loops between metal production and the other subsystems of the social-ecological system played a crucial role in the rapid development of

[8] On this topic specifically, Ben-Yosef (2021: 163-165) recently argued that the abandonment of copper production and the lack of archaeological visibility in Faynan during the late 9th-8th centuries BCE should *not* be interpreted as a "collapse". Rather, he claims "social complexity" was likely consistent through this period, and the "nomadic polity" simply transitioned "into a less archaeologically visible phase" (Ben-Yosef 2021: 165). He goes on to suggest "The change in the polity's economy, which was the result of external forces (Ben-Yosef and Sergi 2018), was undoubtedly dramatic; however, it cannot be directly translated into socio-political transformations" (Ben-Yosef 2021: 165). As such, while Ben-Yosef (2021) argues against a "collapse" in relation to social complexity, he also recognizes the economy experiences a "dramatic" transformation. Thus, this line of thinking can fit with the perspectives presented here; this research similarly argues that Faynan at the very least experienced an economic "collapse". However, given the significant role of copper production in the rise of an Edomite polity (Ben-Yosef et al. 2019; Maeir 2021), and in applying the culture system model and adaptive cycle, this dissertation does claim that the socio-political complexity of Faynan did experience a "collapse" transformation in the 9th century BCE (discussed in the following paragraphs). In other words, it is argued here the technological, economic, and social systems of culture are inextricably bound; transformations in one system will undoubtedly impact the others - "the social is indissolubly linked with the technological and the economic" (Hughes 1986: 112). This understanding is reiterated by applying political economy in which "economic control provides the material means to support political bureaucracies" (Hirth 1996: 209). It is unlikely that the existing political structures/complexity of the Early Iron Age (1200-800 BCE) could persist without the material means provided from industrial scale copper production.

society in Faynan, likely culminating in a “cultural take-off” and the emergence of the “kingdom” potentially connected to the Edomites. Because metallurgical technology and production was intimately interconnected to the other subsystems, maintaining this industry and likely also the exchange of metal was vital to sustaining the cultural system in a stable state, the equilibrium of the K-phase.

It is argued that the cultural system in Faynan became overly dependent on sustained copper production (the prevailing conditions allowing for equilibrium), lacked redundancy/diversity, and slipped into a rigidity trap – “an accident waiting to happen” (Holling and Gunderson 2002: 45). In following, a collapse within the industry would cause “strong destabilizing positive feedbacks” to the other subsystems; the collapse of the copper smelting industry functioned as a kind of triggering agent in an overly rigid social-ecological system (Holling and Gunderson 2002: 45). Returning to the definition of collapse, the situation of 8$^{th}$ century BCE in Faynan can be interpreted as such because the cultural system experienced a marked and “rapid transformation to a lower social, political, and economic complexity” along with the cessation of copper production (Tainter 1988: 4). Based on the abandonment of smelting centers and copper production, the inhabitants likely returned to predominantly pastoral nomadic lifeways. This understanding is reiterated by the lack of archaeological evidence for habitation during the 8$^{th}$ century BCE in Faynan, likely a result of the mobile nomadism and ephemeral settlements (Ben-Yosef 2019, 2021). This line of thinking also fits with Redman’s (2005: 74) applications of the adaptive cycle to archaeological contexts: “a triggering event causing release and collapse also can occur as the result of an internal change in the system, often having inadvertently developed as part of the strategy to maintain the system in K”. The “internal change” of a failing metallurgical industry which was intensively “developed as part of the

strategy to maintain the system" in equilibrium in the K-phase created a "triggering event causing release and collapse"[9]. However, the reason for the abandonment of copper production also requires consideration.

### 7.8.1 Overshoot or Otherwise? Identifying the Triggering Agent

A primary goal of this dissertation was to identify a possible cause or triggering agent in the collapse of the copper production industry, mainly from the perspective of "overshoot". Based on the trajectory of the adaptive cycle and the likely dependence on copper production/exchange for a sustainable social-ecological system in Faynan, it was hypothesized that "overshooting" the available copper ore resources could have been the triggering agent that resulted in the collapse of society at the end of the 9$^{th}$ century BCE. The pastoral-nomadic mixed economy of Iron Age Faynan gave this possibility additional support; exchange with sedentary agricultural societies likely provided critical access to additional staples to sustain the workforce in Faynan. From the perspective of overshoot and carrying capacity, this exchange with agricultural societies allowed society in Faynan to "enlarge its scope" and create a "combined carrying capacity" that extended beyond what was capable in the harsh climate and terrain of the region. The combined carrying capacity could have played a crucial role in the growing copper smelting industry by allowing larger work forces, or more dedicated specialization in metallurgy. However, with scope enlargement comes increased vulnerability, or decreased resilience, because any disruption to this trade can have significant repercussions on the social-ecological system (Catton 1980: 159). The breakdown of the combined carrying capacity could have

[9] It is also possible to treat copper production as a microscale adaptive cycle which then caused a cascading revolt, facilitating collapse in a mesoscale adaptive cycle representing society in Faynan more generally.

facilitated the collapse of the copper smelting industry by forcing a returned focus on pastoral nomadism. One possible catalyst for the loss of carrying capacity could have been an exhaustion or over degradation (overshoot) of available copper ores – the copper ores had become "indispensable but inadequate" – and in turn, a larger scale societal collapse (Catton 1980: 158).

However, as it discussed in Chapter 5, the analytical data does not suggest there were any significant changes in the elemental composition of the copper metal produced in Faynan through the Iron Age. There is currently no indication that the copper ores were exhausted or sufficiently degraded to impact the analyzed copper, providing evidence against the possibility that society in Faynan over-exploited the available copper ore resources in the Iron Age i.e., overshoot does not seem to be the triggering agent in the Iron Age collapse of the Faynan culture system. In following, other possible trigger agents require consideration. A standing theory is that copper production in Faynan could not be sustained after Cyprus began exporting copper to the Levant again in the Late Iron Age, likely over new Phoenician economic connections (Fantalkin and Finkelstein 2006: 25, 28-31; Yahalom-Mack et al. 2014a; Knauf 1991: 185; Knauf-Belleri 1995: 112-113; Bienkowski 2021). As mentioned, Knauf (1991: 185) suggested copper smelting in the Wadi Arabah only "flourished" when "the Cypro-Phoenician copper supply failed". Furthermore, Knauf (1991: 185) highlighted the "inherent logistic difficulties" of mining in the Wadi Arabah: "one had to get there, one had to sustain one's work-force when there, one had to get back from there with the copper". With the revival of the more economic and efficient Cypro-Phoenician copper supply to the Levant in the 9$^{th}$ century BCE, the industry in Faynan could have been out-competed, causing it to collapse (Fantalkin and Finkelstein 2006: 31). This understanding recently gained further support based on lead-isotope analysis of Iron Age copper ingots excavated in Israel and the Mediterranean coast (Yahalom-Mack et al. 2014a).

The chemical analysis suggests Cyprus provided copper to the Levant starting again in the 9th century BCE (Yahalom-Mack et al. 2014a: 174-175, Figure 17). Martin and Finkelstein (2013: 39) also suggested this shift in copper supply could have similarly caused the end of settlement in the Negev Highlands in the mid-9th century which would no longer be able to capitalize on copper moving through the highlands from the Wadi Arabah. The abandonment of settlement in the Negev Highlands would further cut off Faynan from the economic markets of the Levant and beyond. Following this model, the resumption of economic connections between Cyprus and the Levant would be considered the triggering agent in the collapse of the copper industry in Faynan.

Building on these ideas and a previous hypothesis proposed by Fantalkin and Finkelstein (2006; Finkelstein 2014), Ben-Yosef and Sergi (2018) recently suggested the abandonment of the copper industry in Faynan was connected to the contemporaneous destruction of Tell es-Safi. Similarly putting emphasis on the economic connections between Faynan and the Levant, they suggest Tell es-Safi likely functioned as a main hub for the export of copper produced in Faynan (Ben-Yosef and Sergi 2018)[10]. Copper was exported from Faynan via the Beersheba Valley and the Negev Highlands to Tell es-Safi and the Philistine Coast and beyond. With the destruction of Tell es-Safi at the end of the 9th century BCE (and potentially also related to the abandonment of the Negev Highlands settlements), Ben-Yosef and Sergi (2018: 474) believe Faynan was essentially disconnected from the markets of the Eastern Mediterranean, preventing an economic outlet for copper, and forcing an abandonment of the industry. In this case, the return of Cypriot copper in the Levant could be in response to the failure in the Wadi Arabah copper supply - in a similar fashion to the emergence of the Faynan industry following the Late Bronze Age collapse

[10] The iron objects excavated in Faynan could provide additional evidence for economic connections between Faynan and Tell es-Safi (Chapter 5) and further supporting this theory, but this requires further research.

(Ben-Yosef and Sergi 2018: 463-464). In other words, Ben-Yosef and Sergi are suggesting the destruction of Tell es-Safi could have been the triggering agent in the collapse of Faynan[11].

Looking at it generally, Ben-Yosef and Sergi's hypothesis is essentially based on critical economic networks providing opportunities for exchange of copper produced in Faynan. It is difficult to equate the destruction of one site with a complete cessation of copper exchange (cf., Bienkowski 2021); however, the destruction at Tell es-Safi may be emblematic of bigger issues in the exchange networks more generally. Without these trade connections, the social-ecological system of Iron Age Faynan and its industrial copper production could not sustain the prevailing conditions to remain in a stable equilibrium. This understanding is largely in line with the theoretical perspectives of this dissertation. It is further suggested here that these economic networks were vital to providing a combined carrying capacity for the industrial workforce in Faynan. The collapse of the economic networks with the destruction of Tell es-Safi could have prevented the exchange for subsistence goods and reduced the combined carrying capacity in Faynan (a reduction of scope). The data produced here could also provide additional support for this hypothesis. As it currently appears that copper was continually smelted at a consistent quality even in the latest stages of production, external triggering agents for the abandonment appear more likely. While the specific connections between Tell es-Safi and Faynan need further investigation, the current evidence suggests a breakdown in the economic connections between Faynan and the markets for copper was a primary driver in the collapse of the industry, and in turn, society in the 9$^{th}$ century BCE. For now, this can be considered the general triggering agent

[11] See Chapter 3 for a review and discussion of Bienkowski's (2021) recent critique of this theory. While plausible, it is suggested in Chapter 3 that his alternative model currently lacks the necessary archaeological support. In particular, the claim that the copper industry was abandoned due to a lack of administration is problematic (Bienkowski 2021: 5-7). Thus, Ben-Yosef and Sergi's (2018) model is given emphasis here.

rather than overshoot, and perhaps a more specific event (such as the destruction of Tell es-Safi) can be identified in future research.

### 7.9 Release or "Collapse" (Ω) in the Late Iron Age: Late 9th/Early 8th Century BCE

Similar to the Middle Bronze Age, the release phase of the Iron Age is largely characterized and identifiable by the lack of archaeological evidence for copper production or habitation in Faynan. By the Late 9th to Early 8th century BCE, the significant metallurgical industry of the Iron Age was no longer producing copper, indicating this transition from K to Ω. Specifically, there is no evidence for copper production at Khirbat en-Nahas[12] during the 8th century BCE, the only remaining production center from the K-phase. In other words, the "accumulated resources" of Faynan and the tribal kingdom were "released from their bound, sequestered, and controlled state" (Holling and Gunderson 2002: 45). There is potential evidence to suggest the release or collapse was already starting to some extent in the 9th century BCE. The gatehouse to the fortress at Khirbat en-Nahas was decommissioned based on the blocking of its southern entrance (though it was likely still used for copper production), and the walls of the fortress were potentially plundered for stone based on their low standing height when excavated and limited surrounding collapse (Ben-Yosef 2010: 334-335). Ben-Yosef (2010: 334-335) suggests the stones were repurposed for constructing nearby 9th century BCE buildings, perhaps implying a lack of available resources or labor to collect additional stone. Both phenomena could indicate the fortress and its associated authority were no longer able to exert the same control over the accumulated resources/industry.

[12] Khirbat Faynan also does not have evidence of continued production or habitation into the 7th century BCE, but due to the nature of the site, it cannot be conclusively said that a Late Iron Age phase does not exist. Further research is needed.

However, the use of the term “collapse” should not be associated with a catastrophe/calamity. As mentioned, and in line with Tainter (1988, 2016), this project suggests the collapse of Iron Age Faynan was the transformation or “fragmentation” in the socio-political and economic complexity; the copper industry was abandoned, and the tribal kingdom “disarticulated” with its constituent tribes returning to pastoral nomadic lifeways (following Levy’s oscillating tribal segmentary system model); this return to more mobile subsistence practices provided a “buffer mechanism” in response to the “variability” in food resources created by the collapse of exchange and the enlarged scope (the previously employed buffering mechanism) (Halstead and O’Shea 1989). In other words, society in Faynan experienced a “change in complexity” which manifested in its economic and sociopolitical structures (Tainter 1988: 4-5). The economic transformation is inherent to the collapse of copper production, but the sociopolitical transformation is more difficult to detect i.e., how do we identify/measure sociopolitical complexity? As Ben-Yosef (2019a, 2020) argues, the lack of stone architecture in the 8$^{th}$ century BCE shouldn’t be equated with a lack of complexity. The pastoral nomads of Faynan could have maintained significant sociopolitical complexity without architecture. However, while the existing elites in Faynan may have retained their status, this is difficult to determine and seems unlikely given the political economy; they would no longer have control over staple and wealth finance (discussed above). This is reiterated by the significant role copper production played in the development and formation of an Edomite polity; could this same level of sociopolitical complexity continued without the industry generating unequal access to wealth and power? This question is difficult to securely answer and requires further research. However, in following the adaptive cycle, the culture system model, and political economy, this dissertation suggests society in Faynan experienced a “collapse”.

The return to a predominantly pastoral nomadic lifeways during and after the release phase can also be characterized as a "remember" process. Following the study by Rosen and Rivera-Collazo (2012: 3640-3642) on applying the adaptive cycle to prehistoric foraging economies in the Levant, the identified transition to pastoral nomadism was likely a result of "long-term social memory of accumulated experiences" which can be treated as a macroscale cycle extending thousands of years. In other words, the populations in Faynan were able to "remember" previous subsistence practices and strategies, drawing on a larger cycle of social memory that "is kept alive at the microscale of generational memory" in response to more short-term problems "and the socially prescribed methods to survive them" (Rosen and Rivera-Collazo 2012: 3642). Rosen and Rivera-Collazo (2012: 3640) further suggest that this "long-term social memory of accumulated experiences is an important resource for preparing and responding to economic challenges". Here, the collapse of the Iron Age copper smelting industry can be perceived as a "short-term" economic challenge (on the microscale), and the "socially prescribed method to survive" was to return to the pastoral nomadism of the Late Bronze Age. In doing so, populations were able to create a broader-based diet with increased mobility in comparison to the increasingly rigid system dependent on copper production and exchange. Treating social memory as a macrocycle in this way can also explain other "archaeologically invisible" periods in Faynan such as the Middle Bronze Age (described above).

Finally, Faynan also contributes to the paradigmatic shift regarding collapse placing new emphasis on post-collapse continuity, regeneration, and reorganization as there is evidence for both continuity and regeneration/reorganization (McAnany and Yoffee 2010a; Faulseit 2016a; Schwartz and Nichols 2006; Gunderson and Holling 2002). As is suggested by the adaptive cycle, the release phase was brief; Faynan quickly transitioned into a second reorganization (or

regeneration) phase in the 8th-6th centuries BCE when there is again evidence for activity related to copper production (continuity).

## 7.10 A Failed Reorganization (α) in the Late Iron Age: Late 8th-6th Centuries BCE

Following the release phase of the 8th century BCE, there was a possible resumption of copper production in Faynan during the Late Iron Age in the late 8th/7th-6th centuries BCE. This attempt to renew copper smelting could then be considered a reorganization phase during the Iron Age. The main evidence for any activity related to copper production during this period is the Ras al-Miyah archaeological complex[13]. Ben-Yosef, Najjar, and Levy (2014a: 816-840) suggest the Ras al-Miyah fortresses and adjacent mines represent a period of intense mining activity in the Late Iron Age. However, and as they acknowledge, Faynan currently lacks any contemporaneous smelting sites (Ben-Yosef, Najjar, and Levy 2014a: 836-837; Ben-Yosef 2010: 420). In addition, the excavations of one of the fortresses indicated that its construction was never completed. Weisgerber (2006: 15) had previously suggested that this Late Iron Age metallurgical activity should be considered "unsuccessful" possibly because "the yield in copper ore there did not meet expectations". The analytical results here suggest high-quality ores were likely still available in the Late Iron Age based on the consistencies in the elemental composition of the metal produced during the previous production phase. However, the incomplete fortress and lack of associated smelting sites seem to indicate a copper smelting industry was not successfully renewed in the 7th-6th centuries BCE despite efforts to do so.

[13] There is also the small 7th century BCE habitation at Rujm Hamra Ifdan, but it does not seem to be connected to metal production, and generally requires further investigation (Smith, Najjar, and Levy 2014: 737).

In following, this period in Faynan can be considered a failed reorganization phase from the perspective of the copper smelting industry. The adaptive cycle accounts for "leaking" away of potential during a reorganization, which can describe the situation in Faynan (Figure 2.2). The loss of potential during an α-phase is attributed to the low connectedness; potential is lost until the "reorganization is consolidated" and the available resources are exploited (Holling and Gunderson 2002: 45-46). Moreover, the loss or leaking of potential can result in "a flip into a less productive and organized system" and an "exit from the cycle" – the system does not transition into the next exploitation phase (Holling and Gunderson 2002: 34). While the inhabitants of Late Iron Age Faynan attempted to reorganize copper production in the region, the failure to establish a new industry represents a "flip" to a less productive system perhaps due to Cyprus' renewed control over the copper market[14]. This system was short-lived, as evidenced by the incomplete fortress, and likely exited the cycle into a second release phase within Faynan. It is worth noting that during the 7$^{th}$-6$^{th}$ centuries BCE, the center of the Edomite polity was shifted to the plateau, and Faynan lacks archaeological evidence for Late Iron Age habitation outside of the Ras al-Miyah complex and Rujm Hamra Ifdan. The shift to the highlands also represents a reorganization away from copper smelting to a new social-ecological system (following the exit from the previous cycle), possibly to exploit the Arabian trade (Bienkowski and van der Steen 2001). In interpreting the shift to the highlands as a "reorganization", it also fits with novel ideas of post-collapse continuity more generally and the possibility of socio-political continuity within the Edomites specifically, from the Early to Late Iron Ages (Ben-Yosef 2021: 166). Thus, Faynan seems to have experienced simultaneous reorganizations; an attempt to reorganize

[14] It could also be interpreted as a "failed experiment" which Holling and Gunderson (2002: 41) predict for the reorganization phase. They describe the reorganization phase as a "welcoming environment for experiments" but "many will fail" (Holling and Gunderson 2002: 41).

copper smelting which like failed resulting in an exit from the cycle and a more successful transition to the Edomite Plateau with an entirely reorganized economic structure.

Based on the current archaeological record, the copper production and the region of Faynan remained in a release phase along with the shift to the highlands, characterized by primarily pastoral nomadic activities (if any) rather than copper production until the Roman Period. Copper mining and smelting were successfully renewed then, but mining in this period exploited a different ore source (Weisgerber 2006: 21; Hauptmann 2007: 155). Here, the adaptive cycle begins again with a new reorganization to exploit the available resources in the Massive Brown Sandstone geological unit.

# Chapter 8 - Conclusion

As indicated by the title, this dissertation was primarily concerned with three components of Iron Age Faynan: copper, culture, and collapse. In particular, this study examined the interrelationships between these components with a new analytical dataset and through an original theoretical lens, contributing to our understandings of Iron Age Faynan specifically and collapse processes more generally. The holistic examination presented here affords new insight on each, and how they come together to reveal a cyclical cultural system in the archaeological record of Faynan. In doing so, this research functions as a case study for the innovative methodological approaches for diachronically examining copper production (Chapter 5) and the application of combined theoretical perspectives from diverse fields (Chapters 2 and 7). The results contribute to anthropological archaeology more generally by highlighting the value of the adaptive cycle for investigating collapse, a primary focus of anthropological and archaeological research, with particular emphasis on the preceding conditions/causes, the collapse processes, and post-collapse continuity. Furthermore, integrating the adaptive cycle with anthropological theory including the anthropology of technology, the culture system model, and political economy bolstered its explanatory power and exemplified its application in anthropological archaeology investigations. Copper, culture, and collapse are each discussed below, summarizing the previous chapters along with highlighting the specific contributions of this research.

## 8.1 Copper

While Iron Age Faynan and its metallurgical industry have been the subject of numerous archaeological/archaeometallurgical studies and publications (e.g., Levy, Ben-Yosef and Najjar 2014; Barker et al. 2007; Hauptmann 2007; Ben-Yosef 2010), most previous research has

focused on slag, other constituents of the metallurgical *chaîne opératoire* (e.g., Ben-Yosef 2010; Ben-Yosef et al. 2019), or only included limited investigations concerning the copper metal (e.g., Hauptmann 2007; Ben-Yosef 2010). The lack of research on the produced copper was detrimental to a complete understanding of the technological, economic, and socio-political trajectory of Iron Age society. In turn, creating a new dataset focused on the copper metal from Iron Age Faynan was a crucial goal of this dissertation.

The primary obstacle in analyzing copper metal from Faynan was the limited collection available. Excavations thus far had discovered few copper artifacts or raw metal affording only a narrow corpus of material. In addition, the excavated metal was not completely representative of the entire Iron Age sequence, and it was difficult to situate chronologically. In order to circumvent these issues, this research employed an innovative methodology using a combination of SEM-EDX and the slag mound excavations at major smelting sites. While using SEM-EDX for archaeometallurgical analyses is common practice, stratigraphical excavation of slag mounds is less frequent (the Area M excavation at Khirbat en-Nahas was the first excavation of its kind in Faynan). Moreover, prills embedded in slag were an ideal sample material as it afforded both a larger collection of copper and secure chronological control through the rigorous radiocarbon dating of the slag mound excavations. Furthermore, the slag mound section functioned as a chronological scaffold, allowing for a diachronic examination of produced copper. In tandem with the analytical power of the SEM-EDX, this methodology resulted in the largest systematic investigation and dataset for copper metal produced in Iron Age Faynan to date, covering the entire sequence from the $12^{th}$-$9^{th}$ centuries BCE.

This research also makes a methodological contribution in reusing slag samples previously analyzed by Ben-Yosef (2010; Ben-Yosef et al. 2019). In doing so, all the copper

prills analyzed here also have bulk compositional data of the slag via XRF. This combination of datasets afforded new opportunities to test for relationships between the elemental composition of the slag and the associated copper metal. By applying statistical analyses, the data raised new questions and insights for using the bulk composition of slag as a proxy to predict the quality of metal produced. While this mathematical examination currently lacks statistical significance, this is potentially a product of the small sample size. Further application of these statistical techniques could reveal additional understanding of these correlations and enhance the predicative value of using slag to evaluate smelting technology.

Along with the produced copper, the appearance of copper-iron mixtures in the $10^{th}$-$9^{th}$ centuries BCE of Faynan was a similarly understudied feature of the archaeological record. The significance of these artifacts extends beyond Faynan as they are often referenced in scholarly discussions concerned with the origins of iron production (Erb-Satullo 2019). Again, an innovative methodological approach of applying a suite of mass spectrometry techniques allowed new insight concerning the nature of the iron-copper chunks. By examining the osmium isotopic signatures and HSE abundances of the iron in the mixed chunks compared to the select iron objects excavated at Khirbat en-Nahas, this research offers a new line of evidence against the adventitious discovery of iron production from sophisticated copper smelting. While the iron-copper chunks and iron inclusions discovered in the slags reiterate that copper metallurgy in Faynan created the necessary reducing conditions to produce raw metallic iron, the results currently suggest this iron was not further manipulated to produce objects and should not be interpreted as iron production. In following, the metal mixtures were likely either waste products of failed smelts or required further purification to extract copper metal, rather than iron. The iron objects were likely imports contributing to the political economy of the Iron Age, providing new

evidence for the exchange of copper metal. The discovery of potential iron prills and hammerscales in the sediment analysis is somewhat confounding given the current lack of evidence for iron smithing/secondary smelting; however, these materials could be the product of some experimentation or processing to extract copper from the metal mixtures. In sum, the iron-copper chunks still require further consideration, but the results helped eliminate the possibility that they represent an intermediate step towards the origins of iron production in this case and further provide proof of concept in using these methodologies to examine similar material culture in other contexts (e.g., Schwab et al. 2022).

Along with the analytical data, these methods and results afforded new opportunities to critically evaluate the intersections of metal production and society in Faynan more generally – particularly from the perspective of culture and collapse.

## 8.2 Culture

As discussed, society in Faynan witnessed dual technological and cultural revolutions during the Iron Age with the development of industrial scale metallurgy (Levy et al. 2008; Ben-Yosef 2010; Ben-Yosef et al. 2019). While copper was recognized as a key driver in the development of the Iron Age sociopolitical structure (Ben-Yosef 2010), this dissertation further investigated this relationship through the application of new theoretical perspectives using a combined approach based in anthropology, ecology, and sociology. Specifically, the adaptive cycle from Resilience Theory in ecology provided a heuristic model for examining the trajectory of society and copper production across the entire Iron Age sequence. The adaptive cycle was bolstered with the culture system approach and political economy from anthropology/archaeology to provide greater insight into the internal processes of individual

phases as well as the transitions between them. Finally, the overshoot theory from sociology, while primarily focuses on the societal collapse, helped frame copper as an "indispensable" resource of Faynan's carrying capacity and highlighted the critical role of economic connections in a pastoral nomadic society especially given the precarity of desert lifeways. By correlating these theoretical perspectives with the archaeological record, the connections between copper and culture in Iron Age Faynan could be holistically modeled.

In order to examine the beginnings of copper production and associated sociopolitical developments during the Iron Age, the adaptive cycle was chronologically "started" with the Middle Bronze Age (Chapters 2 and 7). This period is largely void of archaeological evidence for copper smelting, and thus was characterized as a release phase (Ω-phase) – the local ores were free from any form of control. The Late Bronze Age represented a reorganization stage (α-phase) with the "initial establishment" of copper smelting for resource accumulation. From the perspective of a cultural system, metallurgy was (re)introduced to the technology subsystem during this phase, but pastoral nomadism remained the predominant lifeway. The archaeological evidence is somewhat limited (the bottom layers of the Area M slag mound at Khirbat en-Nahas and possibly Wadi Dana 1) for this phase, but it is further supported by contemporaneous Egyptian texts. Following the Late Bronze Age collapse (a possible example of "revolt" in the wider Eastern Mediterranean), society in Faynan rapidly transitioned a period of exploitation and growth (r-phase). The pastoral nomadic tribes of Faynan practicing limited and opportunistic copper production during the Late Bronze Age coalesced into a regional polity to intensively smelt copper and capture economic opportunities following the collapse. This new focus and emphasis on metallurgy likely correlated with increased sedentarization at smelting centers, and possibly diminished the size of the pastoral herds placing additional reliance on economic

connections for subsistence (scope enlargement and combined carrying capacity). The archaeological evidence for this phase is abundant including all excavations areas at Khirbat en-Nahas, the establishment additional smelting centers at Khirbat al-Jariya and Khirbat al-Ghuwayba, and new territorial/ethnic markers at the Rujm Hamra Ifdan watchtower and Wadi Fidan 40 cemetery. The industrial focus on copper smelting created feedback loops between technology and the other subsystems within the cultural system (social organization, trade, and symbolic), likely causing a multiplier effect. The resulting cultural take-off was probably supported by a new political economy driven by the exchange of copper for both staple and wealth finance such as the iron objects.

The transition from a period of growth and exploitation to conservation and consolidation (K-phase) is connected to the "punctuated leap" in copper smelting technology in the 10$^{th}$ century BCE (Ben-Yosef et al. 2019). Following the campaigns of Sheshonq I, local resources and capital were controlled through a structured industry, and the efficiency was improved through new smelting technology. The "inward focus" on "increasing efficiency" and "streamlining operations" associated with the K-phase in the adaptive cycle was similarly identified in the copper prill analysis with metal from this period having the highest copper content. Along with the analytical data, the archaeological record matches the expectations of conservation and consolidation: the industry was reorganized and centralized at Khirbat en-Nahas and potentially Khirbat Faynan (Khirbat al-Jariya and Khirbat al-Ghuwayba were decommissioned) with an improved metallurgical technology characterized by larger tap slags, furnaces, and tuyères. However, this inward focus on copper production created a more interconnected system (critical feedback loops were increasingly established between technology and the other subsystems) dependent on sustained production.

The system was slipping into a rigidity trap exacerbated by the desert environment - it became more vulnerable to "triggering agents" that could induce a transition to an Ω-phase or a collapse.

## 8.3 Collapse

Collapse is of particular interest in anthropological archaeology but understanding why/how societies collapse is convoluted and debated within anthropological discourse (e.g., Tainter 1988; Renfrew 1984; McAnany and Yoffee 2010a; Faulseit 2016a). Explanations of collapse are somewhat elusive partially due to the significant variation between cultural and environmental contexts. As such, developing a collection of comparative models and examples is critical for interpreting the archaeological record, anthropologically investigating living societies/cultures, and evaluating trends in modern society. Archaeology can provide a means to this end. This project archaeologically constructed a case study of collapse investigating the preceding conditions, the collapse processes, and post-collapse reorganization. The results of this research can contribute to current understandings of collapse in the archaeological record, providing a comparative case study for archaeological and anthropological contexts more generally, particularly in cases examining the possible role of natural resource exhaustion and/or post-collapse phenomena.

Furthermore, in the case of Faynan, a possible connection between the collapse of the cultural system and intensive metallurgy has been largely unexamined (cf., Ben-Yosef and Sergi 2018; Ben-Yosef 2010: 984; Ben-Yosef 2021; Bienkowski 2021). By combining a robust analytical dataset of elemental compositions from copper prills with theoretical approaches from anthropology, ecology, and sociology, this project helps to fill this lacuna concerning society and

culture in Iron Age Faynan. The results suggest "overshoot" was *not* a primary driver of the collapse in Iron Age Faynan as originally hypothesized; however, it can still generally contribute to the conviction that society inherently exists enmeshed within larger complex systems with inextricable ecological and technological components. By drawing on Resilience Theory, this research emphasized and investigated the dynamics of social-ecological systems (i.e., the significance of copper production in the cultural system of Faynan and its movement through the various stages of the adaptive cycle) while avoiding the limitations of environmental determinism (Faulseit 2016b: 12-14) and the mechanistic nature of General Systems Theory (Hodder and Hutson 2004: 42-44), further validating its application in anthropological contexts.

Critically, the abandonment of the copper smelting industry of Faynan in the 9$^{th}$ century BCE was reinterpreted here as a collapse in line with the more nuanced approaches of recent research (cf., Ben-Yosef 2021). Through highlighting the essential role of copper smelting in maintaining a functioning cultural system (i.e., feedback loops and multiplier effect), economic connections (i.e., combined carrying capacity, scope enlargement, and staple finance), and sociopolitical structures (i.e., political economy and wealth/staple finance), the failure of the copper production industry can be viewed as a "triggering agent" in the collapse of Iron Age society more broadly. The evidence against "overshoot" further suggests the initial collapse of the industry was driven by economic factors (one possibility suggested by Ben-Yosef and Sergi 2018) rather than the exhaustion of available resources, which similarly places emphasis on the precarity of pastoral nomadism in desert contexts, their reliance on connections with the settled world, and the possibility of a rigidity trap. It is also important to *not* associate the application of "collapse" with a catastrophic event and complete abandonment of the region; rather, the collapse in the 9$^{th}$ century BCE likely resulted in a return to predominantly pastoral nomadic life

ways – a “rapid transformation to a lower social, political, and economic complexity” or a “disarticulation” of the “particular political apparatus” (Tainter 1988: 4; Faulseit 2016b: 5). Moreover, this release or collapse was brief as the cultural system transitioned quickly into a phase of reorganization and regeneration.

The adaptive cycle provided a new perspective on these post-collapse processes in Faynan during the Late Iron Age. The attempted resumption of copper smelting in the 8th/7th-6th centuries BCE further reiterates the continued presence of pastoral nomadic communities in Faynan following the 9th century BCE collapse; however, the evidence for mining activity without contemporaneous smelting sites during this period was perplexing (Ben-Yosef 2010: 420; Weisgerber 2006: 15). Interpreting this event as a failed reorganization and an exit from the existing adaptive cycle provides a new understanding – the reorganized system was less productive and unsustainable, perhaps again highlighting the need for strong economic connections with the settled world when pastoral nomads invest in non-subsistence practices (Cyprus now captured this economic market). Moreover, it affords additional explanation for the shift of the Edomite polity to the highlands as a reorganization away from copper smelting to a new social-ecological system (following the exit from the previous cycle) focused on the Arabian trade. Unable to reorganize a productive copper smelting industry, focus shifted to new opportunities for economic growth on the plateau, and the cycle began again.

**References**


Ababsa, Myriam

2013 Aridity. In *Atlas of Jordan: History, Territories and Society*, edited by Myriam Ababsa, pp.64-67. Presses de l'ifpo, Beyrouth.

Adams, Russell B.

1999 The Development of Copper Metallurgy during the Early Bronze Age of the Southern Levant: Evidence from the Faynan Region, Southern Jordan. Ph.D. Dissertation, University of Sheffield, Sheffield, United Kingdom.

Adams, Russell B.

1992 Romancing the stones: new light on Glueck's 1934 survey of Eastern Palestine as a result of recent work by the Wadi Fidan Project. In Early *Edom and Moab: The beginning of the Iron Age in Southern Jordan*, edited by P. Bienkowski, pp. 177-86. J.R. Collis Publications, Sheffield.

Adams, Russell B.

1991 The Wadi Fidan Project, Jordan, 1989. *Levant* 23(1): 181-186.

Aerial Photographic Archive of Archaeology in the Middle East (APAAME), archive accessible from: www.humanities.uwa.edu.au/research/cah/aerial-archaeology.

Althusser, Louis

1969[1965] *For Marx.* Translated by Ben Brewster. Allen Lane, Great Britain.

Anfinset, Nils

2010 *Metal, Nomads and Culture Contact: The Middle East and North Africa*. Equinox, London.

Avery, Donald H.

1982 The Iron Bloomery. In *Early Pyrotechnology: The Evolution of the First Fire-Using Industries*, edited by T.A. Wertime and S. F. Wertime, pp. 205-214.Smithsonian Institution Press, Washington D.C.

Avishur, Isaac

2007 Edom. In *Encyclopedia Judaica, Volume 6, 2nd Edition*, edited by F. Skolnik, pp. 151-158. Keter, Jerusalem.

Avner, Uzi

2021 The Desert's Role in the Formation of Early Israel and the Origin of Yhwh. *Entangled Religions* 12(2).

Avner, Uzi

2002 *Studies in the Material and Spiritual Culture of the Negev and Sinai Populations, During the 6th-3rd Millennia B.C.* Ph.D. dissertation, Hebrew University of Jerusalem, Jerusalem.

Bachmann, Hans-Gert
1980 Early copper smelting techniques in Sinai and in the Negev as deduced from slag investigations. In *Scientific Studies in Early Mining and Extractive Metallurgy*, edited by Paul T. Craddock, pp. 103-134. British Museum Occasional Papers, London.

Bar-Matthews, Miryam, Avner Ayalon, and Aaron Kaufman
1997 Late Quaternary Paleoclimate in the Eastern Mediterranean Region from Stable Isotope Analysis of Speleothems at Soreq Cave, Israel. *Quaternary Research* 47: 155-168.

Barker, Graeme
2012 The desert and the sown: Nomad-farmer interactions in the Wadi Faynan, southern Jordan. *Journal of Arid Environments* 86:82-96.

Barker, Graeme, David Gilbertson, and David Mattingly
2007 *Archaeology and Desertification: The Wadi Faynan Landscape Survey, Southern Jordan*. Oxbow Books, Oxford.

Barker, Graeme, O.H. Creighton, David D. Gilbertson, Christopher O. Hunt, D.J. Mattingly, S.J. McLaren, D.C. Thomas, and G.C. Morgan
1997 The Wadi Faynan Project, Southern Jordan: a Preliminary Report on Geomorphology and Landscape Archaeology. *Levant* 29: 19-40.

Bartlett, John R.
1992 Biblical Sources for the Early Iron Age Edom. In *Early Edom and Moab: The Beginning of the Iron Age in Southern Jordan*, edited by Piotr Bienkowski, pp. 21-34. J. R. Collis, Sheffield.

Bartlett, John R.
1989 *Edom and the Edomites*. Continuum International, New York.

Bartlett, John R.
1972 The Rise and Fall of the Kingdom of Edom. *Palestine Exploration Quarterly* 104: 26-37.

Bar-Yosef, Ofer and Anatoly Khazanov
1992 Introduction. In *Pastoralism in the Levant: Archaeological Materials in Anthropological Perspectives*, edited by Ofer Bar-Yosef and Anatoly Khazanov, pp. 1-10. Prehistory Press, Wisconsin.

Bass, George F.
2005 Cargo from the Age of Bronze: Cape Gelidonya, Turkey. In *Beneath the Seven Seas: Adventures with the Institute of Nautical Archaeology*, pp. 48-55, edited by G. F. Bass. Thames & Hudson Ltd, London.

Basta, E.Z. and B.F. Sunna

1972 The Manganese Mineralisation at Feinan District, Jordan. *Bulletin of Faculty of Science* 44:111-126.

Bayley, Justine, David Dungworth, and Sarah Paynter
2001 *Centre for Archaeology Guidelines: Archaeometallurgy.* English Heritage, London.

Beherec, Marc A.
2011 *Nomads in Transition: Mortuary Archaeology in the Lowlands of Edom (Jordan).* Ph.D. dissertation, Department of Anthropology, University of California, San Diego, La Jolla.

Beherec, Marc A., Mohammad Najjar, and Thomas E. Levy
2014 Wadi Fidan 40 and Mortuary Archaeology in the Edom Lowlands. In *New Insights into the Iron Age Archaeology of Edom, Southern Jordan (Volume 2)*, edited by Thomas E. Levy, Mohammad Najjar and Erez Ben-Yosef, pp. 665-721. UCLA Cotsen Institute of Archaeology Press, Los Angeles.

Beherec, Marc A., Thomas E. Levy, Ofir Tirosh, Mohammad Najjar, Kyle A. Knabb, and Yigal Erel
2016 Iron Age Nomads and their relation to copper smelting in Faynan (Jordan): Trace metal and Pb and Sr isotopic measurements form the Wadi Fidan 40 cemetery. *Journal of Archaeological Science* 65: 70-83.

Ben-Dor Evian, Shirly
2017 Follow the Negebite Ware Road. In *Rethinking Israel: Studies in the History and Archaeology of Ancient Israel in Honor of Israel Finkelstein*, edited by Oded Lipschits, Yuval Gadot, and Matthew J. Adams, pp. 19-27. Eisenbrauns, Winona Lake.

Ben-Dor Evian, Shirly, Omri Yagel, Yehudit Harlavan, Hadas Seri, Jessica Lewinsky, and Erez Ben-Yosef
2021 Pharaoh's copper: The provenance of copper in bronze artifacts from post-imperial Egypt at the end of the second millennium BCE. *Journal of Archaeological Science: Reports* 38: 103025.

Bennett, Crystal-M.
1966 'Fouilles d"Umm el-Biyara: Rapport Preliminaire'. *Revue Biblique* 73: 372-403.

Bennett, Crystal-M.
1977 Excavations in Buseirah, Southern Jordan. *Levant* 9: 1-10.

Bennett, Crystal-M.
1983 Excavations at Buseirah (Biblical Bozrah). In *Midian, Moab and Edom: The History and Archaeology of Late Bronze and Iron Age Jordan and North-West Arabia*, edited by John F. Sawyer and David J.A. Clines, pp. 9-17. JSOT Press, Sheffield.

Ben-Yosef, Erez

2021 Rethinking the Social Complexity of Early Iron Age Nomads. *Jerusalem Journal of Archaeology* 1: 155-179.

Ben-Yosef, Erez
2020 And Yet, A Nomadic Error: A Reply to Israel Finkelstein. *Antiguo Oriente* 18: 33-60.

Ben-Yosef, Erez
2019a The Architectural Bias in Current Biblical Archaeology. *Vestus Testamentum* 69(3): 361-387.

Ben-Yosef, Erez
2019b Archaeological science brightens Mediterranean dark age. *Proceedings of the National Academy of Sciences* 116(13): 5843-5845.

Ben-Yosef, Erez
2016 Back to Solomon's Era: Results of the First Excavations at “Slaves' Hill” (Site 34, Timna, Israel). *Bulletin of the American Schools of Oriental Research* 376:169-198.

Ben-Yosef, Erez
2010 *Technology and Social Process: Oscillations in Iron Age Copper Production and Power in Southern Jordan.* Ph.D. dissertation, Department of Anthropology, University of California San Diego, La Jolla.

Ben-Yosef, Erez and Omri A. Yagel
2019 Calcium Content in Metallurgical Slag as a Proxy for Fuel Efficiency of Ancient Copper Smelting Technologies. *The Journal of the International Union for Prehistoric and Protohistoric Sciences* 2(1): 66-76.

Ben-Yosef, Erez, and Omer Sergi
2018 The Destruction of Gath by Hazael and the Arabah Copper Industry: A Reassessment.” In *Tell it in Gath: Studies in the History and Archaeology of Israel: Essays in Honor of Aren M. Maeir on the Occasion of his Sixtieth Birthday*, edited by Itzhaq Shai, Jeffrey R. Chadwick, Louise Hitchcock, Amit Dagan, Chris McKinny, and Joe Uziel, pp. 461-480. Zaphon, Munster.

Ben-Yosef, Erez and Thomas E. Levy
2014a A “Small Town” Discovered Twice: A Forgotten Report of Major H. H. Kitchener. *Palestine Exploration Quarterly* 146(3): 179-184.

Ben-Yosef, Erez and Thomas E. Levy
2014b The Material Culture of Iron Age Copper Production in Faynan. In *New Insights into the Iron Age Archaeology of Edom, Southern Jordan (Volume 2)*, edited by Thomas E. Levy, Mohammad Najjar and Erez Ben-Yosef, pp. 887-960. UCLA Cotsen Institute of Archaeology Press, Los Angeles.

Ben-Yosef, Erez, Mohammad Najjar, and Thomas E. Levy
2014a New Iron Age Excavations at Copper Production Sites, Mines, and Fortresses in Faynan. In *New Insights into the Iron Age Archaeology of Edom, Southern Jordan (Volume 2)*, edited by Thomas E. Levy, Mohammad Najjar and Erez Ben-Yosef, pp. 767-886. UCLA Cotsen Institute of Archaeology Press, Los Angeles.

Ben-Yosef, Erez, Mohammad Najjar, and Thomas E. Levy
2014b Local Iron Age Trade Routes in Northern Edom From the Faynan Copper Ore District to the Highlands. In *New Insights into the Iron Age Archaeology of Edom, Southern Jordan (Volume 2)*, edited by Thomas E. Levy, Mohammad Najjar and Erez Ben-Yosef, pp. 493-576. UCLA Cotsen Institute of Archaeology Press, Los Angeles.

Ben-Yosef, Erez, Thomas E. Levy, and Mohammad Najjar
2009a Ras al-Miyah Fortresses: New Discoveries at One of the Gateways to the Iron Age Copper Production District of Faynan, Jordan. *Studies in the History and Archaeology of Jordan* X: 823-842.

Ben-Yosef, Erez, Thomas E. Levy, and Mohammad Najjar
2009b New Iron Age Copper Mine Fields Discovered in Southern Jordan. *Near Eastern Archaeology* 72(2): 98-101.

Ben-Yosef, Erez, Brady Liss, Omri A. Yagel, Ofir Tirosh, Mohammad Najjar, and Thomas E. Levy
2019 Ancient technology and punctuated change: Detecting the emergence of the Edomite Kingdom in the Southern Levant. *PLoS ONE* 14(9): e0221967.

Ben-Yosef, Erez, Aaron Gidding, Lisa Tauxe, Uri Davidovich, Mohammad Najjar, and Thomas E. Levy
2016 Early Bronze Age copper production systems in the northern Arabah Valley: New Insights from archaeomagnetic study of slag deposits in Jordan and Israel. *Journal of Archaeological Science* 72: 71-84.

Ben-Yosef, Erez, Ron Shaar, Lisa Tauxe, and Hagai Ron
2012 A New Chronological Framework for Iron Age Copper Production at Timna (Israel). *Bulletin of the American Schools of Oriental Research* 367: 31-71.

Ben-Yosef, Erez, Thomas E. Levy, Thomas Higham, Mohammad Najjar, and Lisa Tauxe
2010 The beginning of Iron Age copper production in the southern Levant: new evidence from Khirbat al-Jariya, Faynan, Jordan. *Antiquity* 84 (325): 724-746.

Ben-Yosef, Erez, Lisa Tauxe, Thomas E. Levy, Ron Shaar, Hagai Ron, and Mohammad Najjar
2009 Geomagnetic intensity spike recorded in high resolution slag deposit in southern Jordan. *Earth and Planetary Science Letters* 287: 529-39.

Ben-Yosef, Erez, Lisa Tauxe, Hagai Ron, Amotz Agnon, Uzi Avner, Mohammad Najjar,

Thomas E. Levy
2008 A New Approach for Geomagnetic Archaeointensity Research: Insights on Ancient Metallurgy in the Southern Levant. *Journal of Archaeological Science* 35: 2863-2879.

Berkes, Fikret and Carl Folke
2002 Back to the Future: Ecosystem Dynamics and Local Knowledge. In *Panarchy: Understanding Transformation in Human and Natural Systems*, edited by L.H. Gunderson and C.S. Holling, pp. 121-146. Island Press, Washington D.C.

Bienkwoski, Piotr
2021 The End of Arabah Copper Production and the Destruction of Gath: A Critique and an Alternative Interpretation. *Palestine Exploration Quarterly.*

Bienkowski, Piotr
1995 The Edomites: The Archaeological Evidence from Transjordan. In *You Shall not Abhor an Edomite for He is Your Brother: Edom and Seir in History and Tradition*, edited by Diana Vikander Edelman, pp. 41-92. Scholars Press, Atlanta.

Bienkowski, Piotr
1992a The Date of Sedentary Occupation in Edom: Evidence from Umm el-Biyara, Tawilan and Buseirah. In *Early Edom and Moab: The Beginning of the Iron Age in Southern Jordan*, edited by Piotr Bienkowski, pp. 99-112. J. R. Collis, Sheffield.

Bienkowski, Piotr
1992b The Beginning of the Iron Age in Edom: A Reply to Finkelstein. *Levant* 24: 167-169.

Bienkowski, Piotr
1990 Umm el-Biyara, Tawilan and Buseirah in Retrospect. *Levant* 22:91-109.

Bienkowski, Piotr and Eveline van der Steen
2001 Tribes, Trade, and Towns: A New Framework for the Late Iron Age in Southern Jordan and the Negev. *Bulletin of the American Schools of Oriental Research* 323: 21-47.

Bietak, Manfred
2007 Egypt and the Levant. In *The Egyptian World*, edited by T. Wilkinson, pp. 417-448. Taylor & Francis, London.

Binford, Lewis
1965 Archaeological Systematics and the Study of Culture Process. *American Antiquity* 31(2): 203-210.

Bloch, Lindsay
2015 Use of Handheld XRF Bruker Tracer III-SD. Research Laboratories of Archaeology, University of North Carolina at Chapel Hill.

Bradtmöller, Marcel, Sonja Grimm, and Julien Riel-Salvatore
2017 Resilience theory in archaeological practice – An annotated review. *Quaternary International* 446(2): 3-16.

Brauns, Michael, Naama Yahalom-Mack, Ivan Stepanov, Lee Sauder, Jake Keen, and Adi Eliyahu-Behar
2020 Osmium isotope analysis as an innovative tool for provenancing ancient iron: A systematic approach. *PLoS ONE* 15(3): e0229623.

Brauns, Michael, Roland Schwab, Guntram Gassmann, Günther Wieland, Ernst Pernicka
2013 Provenance of Iron Age iron in southern Germany: a new approach. *Journal of Archaeological Science* 40: 841-849.

Bruins, H.J.
2006 Desert Environment and Geoarchaeology of the Wadi Arabah. In *Crossing the Rift: Resources, Routes, Settlement Patterns and Interaction in the Wadi Arabah*, edited by Piotr Bienkowski and Katharina Galor, pp. 29-44. Oxbow Books with the Council for British Research in the Levant, Oxford.

Brumfiel, Elizabeth and Timothy Earle
1987 Specialization, exchange, and complex societies: An introduction. In *Specialization, Exchange, and Complex Societies*, edited by Elizabeth Brumfiel and Timothy Earle, pp. 1-9. Cambridge University Press, Cambridge.

Bruker AXS Handheld
2013 Art & Archaeology Market: Reality and Potential. Bruker, Washington.

Butzer, Karl W.
2012 Collapse, environment, and society. *Proceedings of the National Academy of Sciences* 109(10): 3632-3639.

Carpenter, Rhys
1966 *Discontinuity in Greek Civilisation*. Cambridge University Press, Cambridge.

Catton, William R. Jr.
1980 *Overshoot: The Ecological Basis of Revolutionary Change*. University of Illinois Press, Urbana and Chicago.

Charles, James A.
1980 The Coming of Copper and Copper-Base Alloys and Iron: A Metallurgical Sequence. In *The Coming of the Age of Iron*, edited by T.A. Wertime and J.D. Muhly, pp. 151-181. Yale University Press, New Haven.

Chew, Sing C.
2001 *World Ecological Degradation: Accumulation, Urbanization, and Deforestation.* University of Illinois Press, Urbana.

Christofi, Maria, Christos Kyrlitsias, Desphina Michael-Grigoriou, Zoe Anastasiadou, Maria Michaelidou, Ioanna Papamichael, and Katerina Pieri
2018 A Tour in the Archaeological Site of Choirokoitia Using Virtual Reality: A Learning Performance and Interest Generation Assessment. In *Advances in Digital Cultural Heritage*, edited by Marinos Ioannides, João Martins, Roko Žarnić, and Veranika Lim, pp. 208-217. Springer, Cham.

Cline, Eric
2014 *1177 BC: The Year Civilization Collapsed*. Princeton University Press, Princeton.

Cline, Eric
1994 Sailing the Wine Dark Sea: International Trade and the Late Bronze Age Aegean, BAR International Serie 591. Tempus Reparatum, Oxford.

Cooke, Strathmore R.B. and Stanley Aschenbrenner
1975 The Occurrence of Metallic Iron in Ancient Copper. *Journal of Field Archaeology* 2 (3): 251-266.

Cordova, Carlos E.
2007 *Millennial Landscape Change in Jordan: Geoarchaeology and Cultural Ecology*. The University of Arizona Press, Tucson.

Costin, Cathy
1991 Craft Specialization: Issues in Defining, Documenting, and Explaining the Organization of Production. *Archaeological Method and Theory* 3: 1-56.

Costin, Cathy
1998. Introduction. In *Craft and Social Identity*, edited by Cathy Costin and R. Wright, pp. 3-18. American Anthropological Association, Washington D.C.

Costin, Cathy
2001 Craft Production Systems. In *Archaeology at the millennium: A Sourcebook*, edited by G.M. Feinman and D.T. Price, pp. 273-327. Plenum Publishers, New York.

Cowgill, George L.
1988 Onward and Upward with Collapse. In *The Collapse of Ancient States and Civilizations*, edited by Norman Yoffee and George L. Cowgill, pp. 244-276. University of Arizona Press, Tucson.

Craddock, Paul T.
1995 *Early Metal Mining and Production*. Edinburgh University Press, Edinburgh.

Craddock, Paul T.

1988 The composition of the metal finds. In *The Egyptian Mining Temple at Timna, Researches in the Arabah 1959-1984, Vol. 1,* edited by Beno Rothenberg, pp. 169-180. Institute for Archaeo-Metallurgical Studies, London.

Craddock, Paul T. and N.D. Meeks
1987 Iron in ancient copper. *Archaeometry* 29(2):187-204.

Day, James M.D.
2019 Determining the source of silcrete sarsen stones. *Journal of Archaeological Science: Reports* 28: 102051.

Day, James M.D., Jennifer Maria-Benavides, Francis M. McCubbin, and Ryan A. Zeigler
2018 The potential for metal contamination during Apollo lunar sample curation. *Meteoritics & Planetary Science* 53(6): 1238-1291.

Day, James M.D., Alan D. Brandon, and Richard J. Walker
2016 Highly Siderophile Elements in Earth, the Moon, Mars, and Asteroids. *Reviews in Mineralogy and Geochemistry* 81(1): 161-238.

Day, James M.D., Christopher L. Waters, Bruce F. Schaefer, Richard J. Walker, Simon Turner
2016 Use of Hydrofluoric Acid Desilicification in the Determination of Highly Siderophile Element Abundances and Re-Pt-Os Isotope Systematics in Mafic-Ultramafic Rocks. *Geostandards and Geoanalytical Research* 40(1): 49-65.

Diamond, Jared D.
2005 *Collapse: How Societies Choose to Fail or Succeed.* Viking, New York.

De Reu, Jeroen, Philippe De Smedt, Davy Herremans, Marc Van Meirvenne, Pieter Laloo, and Wim De Clercq
2014 On Introducing an Image-Based 3D Reconstruction Method in Archaeological Excavation Practice. *Journal of Archaeological Science* 41:251-262.

Drake, Brandon L.
2012 The influence of climate change on the Late Bronze Age Collapse and the Greek Dark Ages. *Journal of Archaeological Science* 39(6):1862-1870.

Drews, Robert
1993 *The End of the Bronze Age: Changes in Warfare and the Catastrophe ca.1200 B.C.* Princeton University Press, Princeton.

Dungworth, David and Roger Wilkes
2007 An Investigation of Hammerscale: Technology Report. *English Heritage Research Department Report Series* 26: 1-36.

Earley-Spadoni, Tiffany

2017 Spatial History, Deep Mapping, and Digital Storytelling: Archaeology's Future Imagined through an Engagement with the Digital Humanities. *Journal of Archaeological Science* 84: 95-102.

Edelman, Diana V.
1995 Edom: A Historical Geography. In *You Shall Not Abhor an Edomite For He is Your Brother: Edom and Seir in History and Tradition*, edited by Diana V. Edelman, pp. 1-12. Scholars Press, Atlanta.

Eliyahu-Behar, Adi and Naama Yahalom-Mack
2018a Metallurgical Investigations at Tell es-Safi/Gath. In *Tell it in Gath: Studies in the History and Archaeology of Israel – Essays in Honor of Aren M. Maeir on the Occasion of his Sixtieth Birthday*, edited by Itzhaq Shair, Jeffrey R. Chadwick, Louise Hitchcock, Amit Dagan, Chris McKinny, and Joe Uziel, pp. 811-815. Münster, Zaphon.

Eliyahu-Behar, Adi and Naama Yahalom-Mack
2018b Reevaluating early iron-working skills in the Southern Levant through microstructure analysis. *Journal of Archaeological Science: Reports* 18: 447-462.

Eliyahu-Behar, Adi, Naama Yahalom-Mack, Yucal Gadot, and Israel Finkelstein
2013 Iron Smelting and Smithing in Major Urban Centers in Israel during the Iron Age. *Journal of Archaeological Science* 40: 4319-4330.

Eliyahu-Behar, Adi, Naama Yahalom-Mack, Sana Shilstein, Alexander Zukerman, Cynthia Shafer-Elliott, Aren M. Maeir, Elisabetta Boaretto, Israel Finkelstein, and Steve Weiner
2012 Iron and bronze production in Iron Age IIA Philistia: new evidence for Tell es-Safi/Gath, Israel. *Journal of Archaeological Science* 39: 255-267.

Ellenberger, Kate
2017 Virtual and Augmented Reality in Public Archaeology Teaching. *Advances in Archaeological Practice* 5(3): 305-309.

Eisenstadt, Shmuel N.
1988 Beyond Collapse. In *The Collapse of Ancient States and Civilizations*, edited by Norman Yoffee and George L. Cowgill, pp. 236-243. University of Arizona Press, Tucson.

el-Rishi, Hwedi A., Chris O. Hunt, David D. Gilberston, John Grattan, Sue McLaren, Brian Pyatt, Geoff Duller, Gavin Gilmore, and Paul Philips
2007 The past and present landscapes of the Wadi Faynan: geoarchaeological approaches and frameworks. In *Archaeology and Desertification: The Wadi Faynan Landscape Survey, Southern Jordan*, edited by Graeme Barker, David Gilbertson, and David Mattingly, pp. 59-96. Oxbow Books, Oxford.

Engel, T.

1993 Charcoal Remains from an Iron Age Copper Smelting Slag Hear at Feinan, Wadi Arabah (Jordan). *Vegetation History and Archaeobotany* 2: 205-211.

Engels, Friedrich
1934[1890] A Letter to Hans Starkenburg. *The New International* 1(3): 84.

Erb-Satullo, Nathaniel L.
2021 Technological rejection in regions of early gold innovation revealed by geospatial analysis. *Scientific Reports* 11: 20255.

Erb-Satullo, Nathaniel L.
2019 The Innovation and Adoption of Iron in the Ancient Near East. *Journal of Archaeological Research* 27: 557–607.

Erb-Satullo, Nathaniel L. and Joshua T. Walton
2017 Iron and copper production at Iron Age Ashkelon: Implications for the organization of Levantine metal production. *Journal of Archaeological Science: Reports* 15: 8-19.

Erb-Satullo, Nathaniel L., Dimitri Jachvliani, Kakha Kakhiani, and Richard Newman
2020 Direct evidence for the co-manufacturing of early iron and copper-alloy artifacts in the Caucasus. *Journal of Archaeological Science* 123: 105220.

Fantalkin, Alexander and Israel Finkelstein
2006 The Sheshonq I Campaign and the 8th Century BCE Earthquake – More on the Archaeology and History of the South in the Iron I-IIA. *Tel Aviv* 33: 18-42.

Fath, Brian D., Carly A. Dean, and Harald Katzmair
2015 Navigating the adaptive cycle: an approach to managing the resilience of social systems. *Ecology and Society* 20(2): 24.

Faulseit, Ronald K.
2016a *Beyond Collapse: Archaeological Perspectives on Resilience, Revitalization, and Transformation in Complex Societies.* Southern Illinois University Press, Carbondale.

Faulseit, Ronald K.
2016b Collapse, Resilience, and Transformation in Complex Societies: Modeling Trends and Understanding Diversity. In *Beyond Collapse: Archaeological Perspectives on Resilience, Revitalization, and Transformation in Complex Societies*, edited by Ronald Faulseit, pp. 3-26. Southern Illinois University Press, Carbondale.

Faust, Avraham
2006 *Israel's Ethnogenesis: Settlement, Interaction, Expansion and Resistance*. Equinox, London.

FEI Apreo SEM
2020 FEI Apreo SEM Operation Procedure. *UCSD Nano3.*

Fick, S.E. and R.J. Hijmans
2017 WorldClim 2: new 1km spatial resolution climate surfaces for global land areas. *International Journal of Climatology* 37(12): 4302-4315.

Finkelstein, Israel
2020 The Arabah Copper Polity and the Rise of Iron Age Edom: A Bias in Biblical Archaeology? *Antiguo Oriente* 18: 11-32.

Finkelstein, Israel
2014 The Southern Steppe of the Levant ca. 1050-750 BCE: A Framework for a Territorial History. *Palestine Exploration Quarterly* 146(2): 89–104

Finkelstein, Israel
2005a A Low Chronology Update: Archaeology, history and bible. In *The Bible and Radiocarbon Dating: Archaeology, Text and Science*, edited by T. E. Levy and T. Higham, pp. 31-42. Equinox, Oakville.

Finkelstein, Israel
2005b Khirbat en-Nahas, Edom and Biblical History. *Tel Aviv* 32, 119-125.

Finkelstein, Israel
1995 *Living on the Fringe: The Archaeology and History of the Negev, Sinai and Neighbouring Regions in the Bronze and Iron Ages* (Monographs in Mediterranean Archaeology 6). Sheffield Academic Press, Sheffield.

Finkelstein, Israel
1992a Edom in the Iron I. *Levant* 24: 159-166.

Finkelstein, Israel
1992b Invisible Nomads – A Rejoinder. *Bulletin of the American Schools of Oriental Research* 287: 87–88.

Finkelstein, Israel
1988 *The Archaeology of the Israelite Settlement*. Brill, Jerusalem.

Finkelstein, Israel and Eli Piasetzky
2011 The Iron Age chronology debate: Is the gap narrowing? *Near Eastern Archaeology* 74(1): 50-54.

Finkelstein, Israel and Neil A. Silberman
2002 *The Bible Unearthed: Archaeology's New Vision on Ancient Israel and the Origin of its Sacred Texts*. Touchstone, New York.

Finlayson, Bill and Steven Mithen (eds.)

2007 *The Early Prehistory of Wadi Faynan, Southern Jordan, Archaeological survey of Wadis Faynan, Ghuwayr and al-Bustan and evaluation of the Pre-Pottery Neolithic A site of WF16*, Wadi Faynan Series Volume 1, Levant Supplementary Series Volume 4, Council for British Research in the Levant and Oxbow Books, Oxford

Finné, Martin, Karin Holmgren, Hanna S. Sundqvist, Erika Weiberg, and Michael Lindblom
2011 Climate in the eastern Mediterranean, and adjacent regions, during the past 6000 years – A review. *Journal of Archaeological Science* 38: 3153-3173.

Frank, Fritz
1934 Aus der ‘Araba I. Reiseberichte. *Zeitschrift des Deutschen Palästina-Vereins* 57(3/4): 191-280.

Friedman, Hannah, Russell B. Adams, Keitgh Haylock, and Marta D’Andrea
2020 Deeper Understandings: A Trench Through the Bronze Age Deposits at Khirbat Hamra Ifdan. In *New Horizons in the Study of the Early Bronze III and Early Bronze IV of the Levant*, edited by Suzanne Richard, pp. 265-279. Eisenbrauns, University Park.

Frumkin, Amos and Yoel Elitzur
2002. Historic Dead Sea Level Fluctuations Calibrated with Geological and Archaeological Evidence. *Quaternary Research* 57: 334-342.

Gale, Noel H., Hans G. Bachmann, Beno Rothenberg, Zofia A. Stos-Gale, and Ronald F. Tylcote
1990 The Adventitious Production of Iron in the Smelting of Copper. In *The Ancient Metallurgy of Copper, Researches in the Arabah 1959-1984, Vol. 2*, edited by Beno Rothenberg, pp. 182-190. Institute for Archaeo-Metallurgical Studies, London.

Garstki, Kevin
2017 Virtual representation: the production of 3-D digital artifacts. *Journal of Archaeological Method and Theory* 24(3): 726-750.

Garstki, Kevin, Derek B. Counts, Erin Walcek Averett, Sarah Whitcher Kansa, and Eric C. Kansa
2020 A Square Peg in a Round Hole: Rethinking Archaeological Publication. *Near Earthern Archaeology* 83(4): 264-269.

Gidding, Aaron, and Thomas E. Levy
2020 Manufacturing Copper in the Periphery: Radiocarbon and the Question of Urbanism During the Early Bronze Age III-IV Transition. In *New Horizons in the Study of the Early Bronze III and Early Bronze IV of the Levant*, edited by Suzanne Richard, pp. 312-326. Eisenbrauns, University Park.

Gidding, Aaron, Thomas E. Levy, and Thomas A. DeFanti
2014 ArchaeoSTOR: The Development and Utilization of a Web-Based Database for the Field and Lab. *Near Eastern Archaeology* 77: 198-202.

Gidding, Aaron, Y. Matsui, Thomas E. Levy, Thomas A. DeFanti, and Falko Kuester
2013 ArchaeoSTOR: A Data Curation System for Research on the Archeological Frontier. *Future Generation Computer Systems* 29: 2117-2127.

Gilberston, David, Graeme Barker, David Mattingly, Carol Palmer, John Grattan, and Brian Pyatt
2007 Archaeology and desertification: the landscapes of the Wadi Faynan. In *Archaeology and Desertification: The Wadi Faynan Landscape Survey, Southern Jordan*, edited by Graeme Barker, David Gilbertson, and David Mattingly, pp. 397-424.Oxbow Books, Oxford.

Glueck, Nelson
1940a *The Other Side of the Jordan*. American Schools of Oriental Research, New Haven.

Glueck, Nelson
1940b The Pittsburgh of Old Palestine. *Scientific American* January: 22-24.

Glueck, Nelson
1936a The Boundaries of Edom. *Hebrew Union College Annual* 11: 141-157.

Glueck, Nelson
1936b The Recently Discovered Ore Deposits in Eastern Palestine. *Bulletin of the American Schools of Oriental Research* 63: 4-8.

Glueck, Nelson
1935 Explorations in Eastern Palestine, II. *Annual of the American Schools of Oriental Research* 15: 1-288.

Glueck, Nelson
1934 Explorations in Eastern Palestine and the Negeb. *Bulletin of the American Schools of Oriental Research* 55: 3-21.

Glueck, Nelson and William F. Albright
1938 The First Campaign at Tell el-Kheleifeh (Ezion-geber). *Bulletin of the American Schools of Oriental Research* 71: 3-18.

Godelier, Maurice
1978 The Object and Method of Economic Anthropology. In *Relations of Production: Marxist Approaches to Economic Anthropology*, edited by David Seddon, pp. 49-126. Frank Cass and Company Limited, Totowa.

Goldstein, Paul S.
2000 Exotic Goods and Everyday Chiefs: Long-Distance Exchange and Indigenous Sociopolitical Development in the South Central Andes. *Latin American Antiquity* 11(4): 335-361.

Goldstein, Joseph I., Dale E. Newbury, Joseph R. Michael, Nicholas W.M. Ritchie, John Henry J. Scott, and David C. Joy
2018 *Scanning Electron Microscopy and X-Ray Microanalysis. Fourth Edition.* Springer, New York.

Goren, Yuval, Shlomo Bunimovitz, Israel Finkelstein, and Nadav Na'Aman
2003 The Location of Alashiya: New Evidence from Petrographic Investigation of Alashiyan Tablets from El-Amarna and Ugarit. *American Journal of Archaeology* 107(2): 233-255.

Gottlieb, Yulia
2010 The Advent of the Age of Iron in the Land of Israel: A Review and Reassessment. *Tel Aviv* 37: 89-110.

Grattan, J.P., D.D. Gilberston, and C.O. Hunt
2007 The local and global dimensions of metalliferous pollution derived from a reconstruction of an eight thousand year record of copper smelting and mining at a desert-mountain frontier in southern Jordan. *Journal of Archaeological Science* 34(1): 83-110.

Gross, Jürgen P.
2011 *Mass Spectrometry: A Textbok, 2nd Edition*. Springer, Berlin.

Guery, Julien and Raphael Hautefort
2014 Perception and Representation; The 3D Revolution. In *EVA Berlin: Elektronische Medien & Kunst, Kultur und Historie*, edited by Andreas Bienert and Pedro Santos, pp. 78-84. Staatliche Museen zu Berlin - Preußischer Kulturbesitz, Fraunhofer-Institut für Graphische Datenverarbeitung IGD und Autoren.

Gunderson, Lance H. and C.S. Holling (eds.)
2002 *Panarchy: Understanding Transformations in Human and Natural Systems*. Island Press, Washington D.C.

Hadas, Gideon
2006 Fritz Frank, A Templar, Surveyor of the 'Arava Valley and Cucumber Grower in 'Ein Gedi, Israel. *Bulletin of the Anglo-Israel Archaeological Society* 24: 77-83.

Haiman, Mordechai
1996 Early Bronze Age IV Settlement Pattern of the Negev and Sinai Deserts: A View from Small Marginal Temporary Sites. *Bulletin of the American Schools of Oriental Research* 303: 1-32.

Halstead, P and J O'Shea

1989 Introduction: cultural responses to risk and uncertainty. In *Bad Year Economics: Cultural Responses to Risk and Uncertainty*, edited by Paul Halstead and John O'Shea, pp. 1-7. Cambridge University Press, Cambridge.

Hamilton, Elizabeth G.
1996 *Technology and Social Change in Belgic Gaul: Copper Working at the Titelberg, Luxembourg, 125 B.C.-A.D. 300.* University of Pennsylvania Museum of Archaeology and Anthropology, Philadelphia.

Hauptmann, Andreas
2007 *The Archaeometallurgy of Copper: Evidence from Faynan, Jordan*. Springer, Berlin.

Hauptmann, Andreas
2006 Mining Archaeology and Archaeometallurgy in the Wadi Arabah: The Mining Districts of Faynan and Timna. In *Crossing the Rift: Resources, Routes, Settlement Patterns and Interaction in the Wadi Arabah*. Edited by Piotr Bienkowski and K. Galor, pp. 125-134. Oxbow Books, Oxford.

Hauptmann, Andreas
1989 The earliest periods of copper metallurgy in Feinan, Jordan. In *Old World Archaeometallurgy*. Edited by Andreas Hauptmann, Ernst Pernicka, and G.A Wagner, pp. 119-135. Deutsche Bergbau-Museum, Bochum.

Hauptmann, Andreas, and I. Löffler
2013 Technological Innovations and Organisational Structures of Prehistoric Mining and Metal Production – Examples from Faynan, Jordan. In *Metal Matters: Innovative Technologies and Social Change in Prehistory and Antiquity*, edited by S. Burmeister, S. Hansen, M. Kunst, and N. Müller-Scheeßel, pp. 65-89. Rahden: Verlag Marie Leidorf.

Hauptmann, Andreas and Gerd Weisgerber
1992 Periods of Ore Exploitation and Metal Production in the Area of Feinan, Wadi 'Arabah, Jordan. In *Studies in the History and Archaeology of Jordan IV*, edited by M. Zaghloul, K. 'Amir, F. Zayadine, and R. Nabeel. Department of Antiquities of Jordan, Amman.

Hauptmann, Andreas and Gerd Weisgerber
1987 Archaeometallurgical and mining-archaeological investigations in the area of Feinan, Wadi Arabah (Jordan). *Annual of the Department of Antiquities of Jordan* 31: 419-435.

Hauptmann, Andreas, Friedrich Begeman, Ekkehard Heitkemper, Ernst Pernicka, and Sigrid Schmitt-Strecker
1992 Early Copper Produced at Feinan, Wadi Araba, Jordan: The Composition of Ores and Copper. *Archaeomaterials* 6:1-33.

Herr, Larry G. and Mohammad Najjar

2001 The Iron Age. In *The Archaeology of Jordan*, edited by Burton MacDonald, Russell Adams, and Piotr Bienkowski, pp. 323-345. Sheffield Academic, Sheffield.

Heu, Rod, Sina Shahbazmohamdi, John Yorston, and Patrick Capeder
2019 Target Material Selection for Sputter Coating of SEM Samples. *Microscopy Today* 27(4): 32-36.

Higham, Thomas, Johannes van der Plicht, Christopher Bronk Ramsey, Hendrik J. Bruins, Mark Robinson, and Thomas E. Levy
2005 Radiocarbon dating of the Khirbat-en Nahas site (Jordan) and Bayesian modeling of the results. In *The Bible and Radiocarbon Dating - Archaeology, Text and Science*, edited by T.E. Levy and T Higham, pp. 164 - 178. Equinox, London.

Hirth, Kenneth G.
1996 Political Economy and Archaeology: Perspectives on Exchange and Production. *Journal of Archaeological Research* 4(3): 203-239.

Hodder, Ian
1994 Theoretical Archaeology: a reactionary view. In *Interpreting Objects and Collections*, edited by S.M. Pearce, pp.48-52. Routledge, London.

Hodder, Ian, and Scott Hutson
2004 *Reading the Past: Current Approaches to Interpretation in Archaeology*. 3rd ed. Cambridge University Press, Cambridge.

Hoggarth, Julie A. and Jamie J. Awe
2016 Household Adaptation and Reorganization in the Aftermath of the Classic Maya Collapse at Baking Pot, Belize. In *Beyond Collapse: Archaeological Perspectives on Resilience, Revitalization, and Transformation in Complex Societies*, edited by Ronald Faulseit, pp. 504-527. Southern Illinois University Press, Carbondale.

Holling, C.S.
2001 Understanding the Complexity of Economic, Ecological, and Social Systems. *Ecosystems* 4: 390-405.

Holling, C. S.
1973 Resilience and stability of ecological systems. *Annual Review of Ecology and Systematics* 4: 1-23.

Holling, C.S. and Lance H. Gunderson
2002 Resilience and Adaptive Cycles. In *Panarchy: Understanding Transformation in Human and Natural Systems*, edited by Lance H. Gunderson and C.S. Holling, pp.25-62. Island Press, Washington D.C.

Holling, C.S., Lance H. Gunderson, and Donald Ludwig

2002 In Quest of a Theory of Adaptive Change. In *Panarchy: Understanding Transformation in Human and Natural Systems*, edited by L.H. Gunderson and C.S. Holling, pp. 3-24. Island Press, Washington D.C.

Holling, C.S., Lance H. Gunderson, and Garry D. Peterson
2002 Sustainability and Panarchies. In *Panarchy: Understanding Transformation in Human and Natural Systems*, edited by Lance H. Gunderson and C.S. Holling, pp. 63-102. Island Press, Washington D.C.

Howland, Matthew D.
2021 *Long-Distance Trade and Social Complexity in Iron Age Faynan, Jordan*. Ph.D. dissertation, Department of Anthropology, University of California, San Diego, La Jolla.

Howland, Matthew D.
2018 3D Recording in the Field: Style without Substance? In *Cyber-Archaeology and Grand Narratives: Digital Technology and Deep-Time Perspectives on Culture Change in the Middle East*, edited by Ian W. N. Jones and Thomas E. Levy, pp. 19-33. Springer, Cham.

Howland, Matthew D., Falko Kuester, and Thomas E. Levy
2014 Structure from Motion: Twenty-First Century Field Recording with 3D Technology. *Near Eastern Archaeology* 77:187-191.

Howland, Matthew D., Brady Liss, Mohammad Najjar, and Thomas E. Levy
2020 Integrating Digital Datasets into Public Engagement through ArcGIS StoryMaps. *Advances in Archaeological Practice* 8(4): 351-360.

Howland, Matthew D., Brady Liss, Mohammad Najjar, and Thomas E. Levy
2015 GIS-Based Mapping of Archaeological Sites with Low-Altitude Aerial Photography and Structure from Motion: a Case Study from Southern Jordan. In *Proceedings of the 2015 Digital Heritage International Conference (Volume 1)*, edited by G. Guidi, R. Scopigno, J. Carlos Torres, and H. Graf, 91-94. IEEE.

Hughes, Thomas P.
1986 The Seamless Web: Technology, Science, Etcetera, Etcetera. *Social Studies of Science* 16: 281-292.

Hughes, J. Donald and J. V. Thirgood
1982 Deforestation, Erosion, and Forest Management in Ancient Greece and Rome. *Journal of Forest History* 26(2): 60-75.

Hunt, Chris O., David D. Gilbertson, and Hwedi A. El-Rishi
2007 An 8000-year history of landscape, climate, and copper exploitation in the Middle East: the Wadi Faynan and the Wadi Dana National Reserve in southern Jordan. *Journal of Archaeological Science* 34(8): 1306-1338.

Hunt, Chris O., Hwedi A. el-Rishi, David D. Gilbertson, John Grattan, Sue McLaren, F. Brian Pyatt, G. Rushworth, and Graeme W. Barker
2004 Early-holocene environments in the Wadi Faynan, Jordan. *Holocene* 14(6): 921-930

Hyde, Brendt C., James M.D. Day, Kimberly T. Tait, Richard D. Ash, David D. Holdsworth, Desmond E. Moser
2014 Characterization of weathering and heterogeneous mineral phase distribution in brachinite Northwest Africa 4872. *Meteoritics & Planetary Science* 49(7): 1141-1156.

Ilani, Shimon, Zvi Lederman, and Shlomo Bunimovitz
2020 Iron oxide concretions as raw material for iron IIA iron metallurgy in the southern Levant: New evidence from Tel Beth-Shemesh, Israel. *Journal of Archaeological Science: Reports* 34: 102570.

Isaar, Arie S. and Mattanyah Zohar
2007 *Climate Change – Environment and History of the Near East, 2nd Edition*. Springer, Berlin.

Jacobsen, Thorkild and Robert M. Adams
1958 Salt and silt in ancient Mesopotamian agriculture. *Science* 128: 1251-1258.

Jevons, W. Stanley
1906 *The Coal Question: An Inquiry Concerning the Progress of the Nation, and the Probable Exhaustion of out Coal-mines*. Augustus M. Kelley, New York.

Joffe, Alexander H.
2002 The Rise of Secondary States in the Iron Age Levant. *Journal of the Economic and Social History of the Orient* 45(4): 425-467.

Jones, Ian W.N. and Thomas E. Levy
2018 Cyber-archaeology and Grand Narratives: Where Do We Currently Stand? In *Cyber-Archaeology and Grand-Narratives: Digital technology and Deep-Time Perspectives on Cultural Change in the Middle East*, edited by Ian W.N Jones and Thomas E. Levy, pp. 1-18. Springer, Cham.

Jones, Ian W.N., Thomas E. Levy, and Mohammad Najjar
2012 Khirbat Nuqayb al-Asaymir and Middle Islamic Metallurgy in Faynan: Surveys of Wadi al-Ghuwayb and Wadi al-Jariya in Faynan, Southern Jordan. *Bulletin of the American Schools of Oriental Research* 368: 67-102.

Kafafi, Zeidan, A.
2014 New Insights on the Copper Mines of Wadi Faynan/Jordan. *Palestine Exploration Quartelry* 146(4): 263-280.

Kaiser, Bruce

2010 Draft of Bruker XRF spectroscopy user guide: spectral interpretation and sources of interference. Bruker AXS.

Kaniewski, David, Nick Marriner, Rachid Cheddadi, Peter M. Fischer, Thierry Otto, Frédéric, and Elise Van Campo
2020 Climate Change and Social Unrest: A 6,000-Year Chronicle from the Eastern Mediterranean.

Kaniewski, David, Nick Marriner, Joachim Bretschneider, Greta Jans, Christophe Morhange, Rachid Cheddadi, Thierry Otto, Frédéric, and Elise Van Campo
2019 300-year drought frames Late Bronze Age to Early Iron Age transition in the Near East: new palaeoecological data from Cyprus and Syria. *Regional Environmental Change*.

Kaniewski, David, Elise Van Campo, Joel Guiot, Sabine Le Burel, Thierry Otto, and Cecile Baeteman
2013 Environmental Roots of the Late Bronze Age Crisis. *PLoS ONE* 8(8): 1-10.

Kaniewski, David, E. Paulissen, Elise Van Campo, H. Weiss, Thierry Otto, J. Bretschneider, and K. Van Lerberghe
2010 Late second-early first millennium BC abrupt climate changes in coastal Syria and their possible significance on the history of the Eastern Mediterranean. *Journal of Archaeological Science* 74: 207-215.

Kassianidou, Vasiliki
2014 Cypriot Copper for the Iron Age World of the Eastern Mediterranean. In *Structure, Measurement and Meaning: Insights into the Prehistory of Cyprus. Studies on Prehistoric Cyprus in Honour of David Frankel*, edited by J. M. Webb, pp. 261-271. Åström Editions, Uppsala.

Kassianidou, Vasiliki
2013 The Exploitation of the Landscsape: Metal Resources and the Copper Trade during the Age of the Cypriot City-Kingdoms. *Bulletin of the American Schools of Oriental Research* 370: 49-82.

Kassianidou, Vasiliki
2012 The Origin and Use of Metals in Iron Age Cyprus. In *Cyprus and the Aegean in the Early Iron Age: The Legacy of Nicolas Coldstream*, edited by M. Iacovou, pp. 229-259. Bank of Cyprus Cultural Foundation, Nicosia.

Kassianidou, Vasiliki
1994 Could Iron have been Produced in Cyprus(?). *Report of the Department of Antiquities, Cyprus* 73-81.

Kassianidou, Vasiliki and A. Bernard Knapp

2005 Archaeometallurgy in the Mediterranean: the social context of mining, technology and trade. In *The Archaeology of Mediterranean Prehistory*, edited by E. Blake and A.B. Knapp, pp. 215-251. Blackwell, Oxford.

Khazanov, Anatoly M.
1998 Pastoralists in the Contemporary World: The Problem of Survival. In *Changing Nomads in a Changing World*, edited by Joseph Ginat and Anatoly M. Khazanov, pp.7-23. Sussex Academic Press, Brighton.

Khazanov, Anatoly M.
1994 *Nomads and the Outside World.* University of Wisconsin Press, Madison.

Kiderlen, Moritz, Michael Bode, Andreas Hauptmann, and Yannis Bassiakos
2016 Tripod Cauldrons Produced at Olympia Give Evidence of Trade with Copper from Faynan (Jordan) to South West Greece, c. 950-750 BCE. *Journal of Archaeological Science: Reports* 8: 303-313.

Killebrew, Ann E.
2005 *Biblical Peoples and Ethnicity: An Archaeological Study of Egyptians, Canaanites, Philistines and Early Israel, 1300-1100 B.C.E.* Society of Biblical Literature, Atlanta.

Kitchen, K.A.
1992 The Egyptian Evidence on Ancient Jordan. In *Early Edom and Moab: The Beginning of the Iron Age in Southern Jordan*, edited by Piotr Bienkowski, pp. 21-34. J. R. Collis, Sheffield.

Kitchener, Horatio H.
1884 Major Kitchener's Report. *Palestine Exploration Quarterly* 16: 202-221.

Kline, Rex B.
2016 *Principles and Practice of Structural Equation Modeling, 4th Edition*. The Guilford Press, New York and London.

Knabb, Kyle A.
2015 Long-term Socioeconomic Strategies in Ancient Jordan: Rural Perspectives from the Iron Age through the Roman Period. Ph.D. dissertation, Department of Anthropology, University of California, San Diego, La Jolla.

Knabb, Kyle A., Yigal Erel, Ofir Tirosh, Tammy Rittenour, Sofia Laparidou, Mohammad Najjar, and Thomas E. Levy
2016 Environmental impacts of ancient copper mining and metallurgy: Multi-proxy investigation of human-landscape dynamics in the Faynan valley, southern Jordan. *Journal of Archaeological Science* 74: 85-101.

Knabb, Kyle A., Ian W. N. Jones, Mohammad Najjar, and Thomas E. Levy

2014a Patterns of Iron Age Mining and Settlement in Jordan's Faynan District. In *New Insights into the Iron Age Archaeology of Edom, Southern Jordan (Volume 2)*, edited by Thomas E. Levy, Mohammad Najjar, and Erez Ben-Yosef, pp. 577-625. UCLA Cotsen Institute of Archaeology Press, Los Angeles.

Knabb, Kyle A., Jürgen P. Schulze, Falko Kuester, Thomas E. DeFanti, and Thomas E. Levy
2014b Scientific Visualization, 3D Immersive Virtual Reality Environments, and Archaeology in Jordan and the Near East. Near Eastern Archaeology 77(3): 228-232.

Knapp, A. Bernard
1985 Alashiya, Caphtor/Keftiu, and Eastern Mediterranean Trade: Recent Studies in Cypriote Archaeology and History. *Journal of Field Archaeology* 12(2): 231-250.

Knapp, A. Bernard and Sturt W. Manning
2016 Crisis in Context: The End of the Late Bronze Age in the Eastern Mediterranean. *American Journal of Archaeology* 120(1): 99-149.

Knauf-Belleri, Ernst A.
1995 Edom: The Social and Economic History. In *You Shall Not Abhor an Edomite for He is Your Brother: Edom and Seir in History and Tradition*, edited by Diana V. Edelman, pp. 93-118. Scholars Press, Atlanta.

Knauf, Ernst A.
1991 King Solomon's Copper Supply. In *Phoenicia and the Bible*, edited by E. Lepiński, pp. 167-186. Peeters Press, Leuven.

Knauf, Ernst A., and C. Lenzen
1987 Edomite Copper Industry. In *Studies in the History and Archaeology of Jordan III*, edited by A. Hadidi, pp. 83-88. Department of Antiquities of Jordan, Amman.

LaBianca, Oystein S. and Younker, Randall W.
1995 The Kingdoms of Ammon, Moab, and Edom: The Archaeology of Society in Late Bronze/Iron Age TransJordan (ca. 1400-500 BCE). In *The Archaeology of Society in the Holy Land*, edited by Thomas E. Levy, pp. 399-415. Leicester University Press, London.

Langgut, Dafna, Israel Finkelstein, Thomas Litt, Frank H. Neumann, and Mordechai Stein
2015 Vegetation and Climate Changes during the Bronze and Iron Ages (~3600-600 BCE) in the Southern Levant based on Palynological Record. *Radiocarbon* 57(2): 217-235.

Langgut, Dafna, Israel Finkelstein, and Thomas Litt
2013 Climate and the Late Bronze Collapse: New Evidence from the Southern Levant. *Tel Aviv* 40: 149-175.

Lee, Sharen, Christopher Bronk Ramsey, and Amihai Mazar
2013 Iron Age Chronology in Israel: Results from Modeling with a Trapezoidal Bayesian Framework. *Radiocarbon* 55(2-3): 731-740.

Lechtman, Heather and Arthur Steinberg
1979 The History of Technology: An Anthropological Point of View. In *The History and Philosophy of Science*, edited by George Bugliarello and Dean B. Doner, pp. 135-162. University of Illinoi Press, Urbana.

Lemonnier, Pierre
1992 *Elements for an Anthropology of Technology*. University of Michigan, Ann Arbor.

Lemonnier, Pierre
1989 Bark Capes, Arrowheads and Concord: On Social Representations of Technology. In *The Meaning of Things: Material Culture and Symbolic Expression*, edited by Ian Hodder, pp. 156-171. Unwin Hyman, Boston.

Lemonnier, Pierre
1986 The Study of Material Culture Today: Toward an Anthropology of Technical Systems. *Journal of Anthropological Archaeology* 5:147-186. Cambridge.

Lercari, Nicola, Jürgen P. Schulze, Willike Wendrich, Benjamin Porter, Margie Burton, and Thomas E. Levy
2016 3-D Digital Preservation of At-Risk Global Cultural Heritage. In *Proceedings of Eurographics Workshop on Graphics and Cultural Heritage (GCH), Genova, Italy, Oct 5-7*, edited by C.E. Catalano and L. De Luca, pp. 123-126. The Eurographics Association.

Levy, Thomas E.
2017 The Future of the Past: At-risk World Heritage, Cyber-Archaeology, and Transdisciplinary Research. In *Rethinking Israel: Studies in the History and Archaeology of Ancient Israel in Honor of Israel Finkelstein*, edited by Oded Lipschits, Yuval Gadot, and Matthew J. Adams, 221-232. Eisenbrauns, Winona Lake.

Levy, Thomas E.
2015 The Past Forward. *Biblical Archaeology Review Special Issue: "40 Futures: Experts Predict What's Next for Biblical Archaeology"* 81-87.

Levy, Thomas E.
2013 Cyber-Archaeology and World Cultural Heritage: Insights from the Holy Land. *Bulletin of the American Academy of Arts and Sciences* 66: 26–33.

Levy, Thomas E.
2010 The New Pragmatism: Integrating Anthropological, Digital, and Historical Biblical Archaeologies. In *Historical Biblical Archaeology and the Future: The New Pragmatism*, edited by Thomas E. Levy, pp. 3-42. Equinox, London.

Levy, Thomas E.

2009 Pastoral Nomads and Iron Age Metal Production in Ancient Edom. In *Nomads, Tribes, and the State in the Ancient Near East: Cross Disciplinary Perspectives*, edited by Jeffrey Szuchman, pp. 147-178. University of Chicago Press, Chicago.

Levy, Thomas E.
2008 "You Shall Make for Yourself No Molten Gods": Some Thoughts on Archaeology and Edomite Ethnic Identity. In *Sacred History, Sacred Literature: Essays on Ancient Israel, the Bible, and Religion in Honor of R. E. Friedman on His Sixtieth Birthday*, edited by Shawna Dolanksy, pp.239-255. Eisenbrauns, Winona Lake.

Levy, Thomas E. and Brady Liss
2020 Cyber-Archaeology. In *Encyclopedia of Global Archaeology*, edited by C. Smith. Springer, New York.

Levy, Thomas E. and Mohammad Najjar
2006a Edom & Copper: The Emergence of Ancient Israel's Rival. *Biblical Archaeology Review* 32(4): 16-35, 70.

Levy, Thomas E. and Mohammad Najjar
2006b Some Thoughts on Khirbet en-Nahas, Edom, Biblical History and Anthropology - a Response to Israel Finkelstein. *Tel Aviv* 33: 3-17.

Levy, Thomas E. and A.F.C. Holl
2002 Migrations, ethnogenesis, and settlement dynamics: Israelites in Iron Age Canaan and Shuwa-Arabs in the Chad Basin. *Journal of Anthropological Archaeology* 21(1): 83-118.

Levy, Thomas E., Erez Ben-Yosef, and Mohammad Najjar
2018 Intensive Surveys, Large- Scale Excavation Strategies and Iron Age Industrial Metallurgy in Faynan, Jordan: Fairy Tales Don't Come True. In *Mining for Ancient Copper: Essays in Honor of Beno Rothenberg*, edited by Erez Ben-Yosef, pp. 245-258. Eisenbrauns, Winona Lake.

Levy, Thomas E., Megan Bettilyon, and Margie M. Burton
2016 The Iron Age Copper Industrial Complex: A Preliminary Study of the Role of Ground Stone Tools at Khirbat en-Nahas, Jordan. *Journal of Lithic Studies* 3(3): 1-23.

Levy, Thomas E., Mohammad Najjar, and Erez Ben-Yosef (eds.)
2014 *New Insights in the Iron Age Archaeology of Edom, Southern Jordan*. UCLA Cotsen Institute of Archaeology Press, Los Angeles.

Levy, Thomas E., Erez Ben-Yosef, and Mohammad Najjar
2014 The Iron Age Edom Lowlands Regional Archaeology Project: Research, Design, and Methodology. In *New Insights in the Iron Age Archaeology of Edom, Southern Jordan (Volume 1)*, edited by Thomas E. Levy, Mohammad Najjar, and Erez Ben-Yosef, pp. 1-88. UCLA Cotsen Institute of Archaeology Press, Los Angeles.

Levy, Thomas E., Stefan Münger, and Mohammad Najjar
2014 A newly discovered scarab of Sheshonq I: recent Iron Age explorations in southern Jordan. *Antiquity*: on-line http://journal.antiquity.ac.uk/projgall/levy341.

Levy, Thomas E., Mohammad Najjar, and Thomas Higham
2007 Iron Age Complex Societies, Radiocarbon Dates and Edom: Working the Data and Debates. *Antiguo Oriente* 5: 13-34.

Levy, Thomas E., Russell B. Adams, and Adolfo Muniz
2004 Archaeology and the Shasu Nomads: Recent Excavations in the Jabal Hamrat Fidan, Jordan. In *Le-David Maskil: A Birthday Tribute for David Noel Freedman*, edited by Richard E. Friedman and William H. Propp, pp. 63-89. Eisenbrauns, Winona Lake.

Levy, Thomas E., Russel B. Adams and Mohammad Najjar
2001 Jabal Hamrat Fidan. *American Journal of Archaeology* 105: 442-443.

Levy, Thomas E., Russell B. Adams and Rula Shafiq
1999 The Jabal Hamrat Fidan Project: Excavations at the Wadi Fidan 40 Cemetery, Jordan. *Levant* 31: 293-308.

Levy, Thomas E., Connor Smith, Kristin Agcaoili, Anish Kannan, Avner Goren, Jürgen P. Schulze, and Glenn Yago
2020 At-Risk World Heritage and Virtual Reality Visualization for Cyber-Archaeology. In *Digital Cities: Between History and Archaeology*, edited by Maurizio Forte and Helena Murteira, pp. 151-171. Oxford University Press, New York.

Levy, Thomas E., Mohammad Najjar, Thomas Higham, Yoav Arbel, Adolfo Muniz, Erez Ben-Yosef, Neil G. Smith, Marc Beherec, Aaron Gidding, Ian W. Jones, Daniel Frese, Craig Smitheram, and Mark Robinson
2014 Excavations at Khirbat en-Nahas, 2002-2009: An Iron Age Copper Production Center in the Lowlands of Edom. In *New Insights into the Iron Age Archaeology of Edom, Southern Jordan*, edited by T. E. Levy, M. Najjar and E. Ben-Yosef, pp. 89-245. UCLA Cotsen Institute of Archaeology Press, Los Angeles.

Levy, Thomas E., Neil G. Smith, Mohammad Najjar, Thomas A. DeFanti, Albert Y-M. Lin, and Falko Kuester
2012 *Cyber-Archaeology in the Holy Land: The Future of the Past.* Washington, DC: The Biblical Archaeology Society.

Levy, Thomas E., Thomas Higham, Christopher Bronk Ramsey, Neil G. Smith, Erez Ben-Yosef, Mark Robinson, Stefan Münger, Kyle Knabb, Jürgen P. Schulze, Mohammad Najjar and Lisa Tauxe.
2008 High-precision radiocarbon dating and historical biblical archaeology in southern Jordan. *Proceedings of the National Academy of Science* 105: 16460-16465.

Levy, Thomas E., Mohammad Najjar, Johannes van der Plicht, Neil Smith, Hendrik J. Bruins, and Thomas Higham
2005 Lowland Edom and the High and Low Chronologies. In *The Bible and Radiocarbon Dating – Archaeology, Text and Science*, edited by Thomas E. Levy and Thomas Higham, pp. 129-163. Equinox, London.

Levy, Thomas E., Russell B. Adams, Mohammad Najjar, Andreas Hauptmann, James D. Anderson, Baruch Brandl, Mark A. Robinson, and Thomas Higham
2004 Reassessing the chronology of Biblical Edom: new excavations a 14C dates from Khirbat en-Nahas (Jordan). *Antiquity* 78: 865-879.

Levy, Thomas E., Russell B. Adams, James D. Anderson, Mohammad Najjar, Neil Smith, Yoav Arbel, Lisa Soderbaum, and Adolfo Muniz
2003 An Iron Age Landscape in the Edomite Lowlands: Archaeological Surveys along Wadi al-Ghuwayb and Wadi al-Jariya, Jabal Hamrat Fidan, Jordan, 2002. *Annual of the Department of Antiquities of Jordan* 47: 247-277.

Levy, Thomas E., Russell B. Adams, Andreas Hauptmann, Michael Prange, Sigrid Schmitt-Strecker, and Mohammad Najjar
2002 Early Bronze Age metallurgy: a newly discovered copper manufactory in southern Jordan. *Antiquity* 76: 423-437.

Liss, Brady
2015 Reconstructing the Metallurgical Narrative of an Iron Age Smelting Site: New Excavations and Archaeometallurgical Investigations at Khirbat al-Jariya, Southern Jordan. M.A. Thesis, Department of Anthropology, University of California, San Diego, La Jolla.

Liss, Brady and Thomas E. Levy
2018 Metallurgy in the World of the Bible. In *Behind the Scenes of the Old Testament: Cultural, Social, and Historical Contexts*, edited by Jonathan S. Greer, John W. Hilber, and John H. Walton, pp. 438-445. Baker Academic, Grand Rapids.

Liss, Brady and Samantha Stout
2017 Materials Characterization for Cultural Heritage: XRF Case Studies in Archaeology and Art. In *Heritage and Archaeology in the Digital Age: Acquisition, Curation, and Dissemination of Spatial Cultural Heritage Data*, edited by Matthew L. Vincent, Victor Manuel Lopez-Menchero Bendicho, Marinos Ioannides, and Thomas E. Levy, pp. 49-65. Springer, Cham.

Liss, Brady and Thomas E. Levy
2015 One Man's Trash: Using XRF to Recreate Ancient Narratives from Metallurgical Waste Heaps in Southern Jordan. In *Proceedings of the 2015 Digital Heritage International Conference (Volume 1)*, edited by G. Guidi, R. Scopigno, J. Carlos Torres, and H. Graf, pp. 27-34. IEEE.

Liss, Brady, Thomas E. Levy, and James M.D. Day
2020 Origin of iron production in the Eastern Mediterranean: Osmium isotope and highly siderophile element evidence from Iron Age Jordan. *Journal of Archaeological Science* 144: 105227.

Liss, Brady, Matthew D. Howland, Brita Lorentzen, Craig Smitheram, Mohammad Najjar, and Thomas E. Levy
2020 Up the Wadi: Development of an Iron Age Industrial Landscape in Faynan, Jordan. *Journal of Field Archaeology* 45(6): 413-427.

Lloyd, James
2016 Contextualizing 3D Cultural Heritage. In *Digital Heritage: Progress in Cultural Heritage: Documentation, Preservation, and Protection*, edited by Marinos Ioannides, Eleanor Fink, Antonia Moropoulou, Monika Hagedorn-Saupe, Antonella Fresa, Gunnar Liestøl, Vlatka Rajcic, and Pierre Grussenmeyer, pp. 859–868. Springer, Cham.

Lo Schiavo, Fulvia, James D. Muhly, Robert Maddin, and Alessandra Giumlia-Mair (eds.)
2009 *Oxhide Ingots in the Central Mediterranean*. A.G. Leventis Foundation, Roma.

Luria, David
2021 Copper technology in the Arabah during the Iron Age and the role of the indigenous population in the industry. *PLoS ONE* 16(12): e0260518.

MacDonald, Burton
1992 *The Southern Ghors and Northeast 'Arabah Archaeological Survey.* J.R. Collis Publications, Sheffield.

Maeir, Aren M.
2021 Identity Creation and Resource Controlling Strategies: Thoughts on Edomite Ethnogenesis and Development. *Bulletin of ASOR* 386.

Maddin, Robert
1982 Early Iron Technology in Cyprus. . In *Early Metallurgy in Cyprus, 4000-500 BC*, edited by James D. Muhly, Robert Maddin, and Vassos Karageorghis, pp. 303-314. Pierides Foundation, Nicosia.

Magnani, Matthew, Matthew Douglass, Whittaker Schroder, Jonathan Reeves, and David R. Braun
2020 The Digital Revolution to Come: Photogrammetry in Archaeological Practice. *American Antiquity* 85(4): 737-760.

Malthus, Thomas R.
1798 *An Essay on the Principle of Population*. Joseph Johnson, London.

Manning, Sturt W., Brita Lorentzen, Lynn Welton, Stephen Batiuk, and Timothy P. Harrison

2020 Beyond megadrought and collapse in the Northern Levant: The chronology of Tell Tayinat and two historical inflection episodes, around 4.2ka BP, and following 3.2KA BP. *PLoS ONE* 15(10): e0240799.

Marcus, Joyce and Gary M. Feinman
1998 Introduction. In *Archaic States*, edited by G.M. Feinman and J. Marcus, pp. 3-13. School of American Research Press, Santa Fe.

Marín-Buzón, Carmen, Antonio Pérez-Romero, José López-Castro, Imed B. Jerbania, and Francisco Manzano-Agugliaro
2021 Photogrammetry as a New Scientific Tool in Archaeology: Worldwide Research Trends. *Sustainability*, 13(9): 5319.

Martin, Mario A. S., and Israel Finkelstein
2013 Iron IIA Pottery from the Negev Highlands: Petrographic Investigation and Historical Implications. *Tel Aviv* 40: 6-45.

Martin, Mario A. S., Adi Eliyahu-Behar, M. Anenburg, Yuval Goren, and Israel Finkelstein
2013 Iron IIA Slag-Tempered Pottery in the Negev Highlands, Israel. *Journal of Archaeological Science* 40: 3777-3792.

Marx, Emmanuel
2006 The Political Economy of Middle Eastern and North African Pastoral Nomads. In *Nomadic Societies in the Middle East and North Africa: Entering the 21st Century*, edited by Dawn Chatty, pp. 78-98. Brill, Leiden.

Marx, Karl
1904[1859] *A Contribution to the Critique of Political Economy*. Translated by N.I. Stone. Charles H. Kerr & Company, Chicago.

Marx, Karl and Friedrich Engels
1947 *The German Ideology: Parts I & III*. International Publishers, New York.

Mattingly, David, Paul Newson, John Grattan, Roberta Tomber, Graeme Barker, David Gilbertson, and Chris Hunt
2007 The making of early states: the Iron Age and Nabatean periods. In *Archaeology and Desertification: The Wadi Faynan Landscape Survey, Southern Jordan*, edited by Graeme Barker, David Gilbertson, and David Mattingly, pp. 271-303. Oxbow Books, Oxford.

Mazar, Amihai
2011 The Iron Age chronology debate: Is the gap narrowing? Another viewpoint. *Near Eastern Archaeology* 74(2): 105-111.

Mazar Amihai

2005 The debate over the chronology of the Iron Age in the Southern Levant. In T*he Bible and Radiocarbon Dating: Archaeology, Text and Science,* edited by Thomas E. Levy and Thomas Higham, pp. 15-30. Equinox, London.

McAnany, Patricia A. and Norman Yoffee
2010a *Questioning Collapse: Human Resilience, Ecological Vulnerability, and the Aftermath of Empire*. Cambridge University Press, Cambridge.

McAnany, Patricia A. and Norman Yoffee
2010b Why We Question Collapse and Study Human Resilience, Ecological Vulnerability, and the Aftermath of Empire. In *Questioning Collapse: Human Resilience, Ecological Vulnerability, and the Aftermath of Empire*, edited by Patricia A. McAnany and Norman Yoffee, pp. 1-20. Cambridge University Press, New York.

McDonough, W.F. and S-S. Sun
1995 The composition of the Earth. *Chemical Geology* 120: 223-253.

McGovern, Thomas H.
1980 Cows, Harp Seals, and Churchbells: Adaptation and Extinction in Norse Greenland. *Human Ecology* 8(3): 245-275.

Méndez, Pablo F., Nicola Isendahl, Jaime M. Amezaga, and Luis Santamaría
2012 Facilitating transitional processes in rigid institutional regimes for water management and wetland conservation: experience from the Guadalquivir Estuary. *Ecology and Society* 17(1): 26.

Merkel, J. and K. Barrett
2000 'The adventitious production of iron in the smelting of copper' revisited: metallographic evidence against a tempting model. *Historical Metallurgy* 34(2): 59-66.

Migowski, Claudia, Mordechai Stein, Sushma Prasad, Jörg F.W. Negendank, and Amotz Agnon
2006 Holocene Climate Variability and Cultural Evolution in the near East from the Dead Sea Sedimentary Record. *Quaternary Research* 66: 421-431.

Mithen, Steven and Emily Black
2011 *Water, Life and Civilization: Climate, Environment and Society in the Jordan Valley*. Cambridge University Press, Cambridge.

Moorey, P.R.S.
1994 *Ancient Mesopotamian Materials and Industries*. Clarendon Press, Oxford.

Mourad, Anna-Latifa
2021 Strategies of survival? Change, continuity and the adaptive cycle across the middle to early late bronze age at Tell el-Dab'a, Egypt. *Journal of Anthropological Archaeology* 64: 101367.

Muhly, James D.
1989 The organization of the copper industry in Late Bronze Age Cyprus. In *Early Society in Cyprus*, edited by Edgar Peltenburg, pp. 298-314. Edinburgh University Press, Edinburgh.

Muhly, James D.
1987 Solomon, the Copper King: A Twentieth Century Myth. *Expedition* 29(2): 38-47.

Muhly, James D. and Vasiliki Kassianidou
2012 Parallels and diversities in the production, trade and use of copper and iron in Crete and Cyprus from the Bronze Age to the Iron Age. In *Parallel Lives: Ancient Island Societies in Crete and Cyprus*, edited by Getald Cadogan, Maria Iacovou, Katerina Kopaka, and James Whitley, pp. 119-140. The British School at Athens, Great Britain

Musil, Alois
1907 *Arabia Petraea II. Edom: Topograhischere Reisebericht*. Alfred Hölder, Vienna.

Najjar, Mohammad
2015 Solomonic Phobia or 10th Century BCE Phobia? Response to Zeidan A. Kafafi, "New Insights on the Copper Mines of Wadi Faynan/Jordan". *Palestine Exploration Quarterly* 147(3): 247-253.

Najjar, Mohammad and Thomas E. Levy
2011 Condemned to the Mines: Copper Production and Christian Persecution. *Biblical Archaeology Review* 37(6): 30-39, 71.

"Normal Map (Bump Mapping)".
2019 *Unity User Manual 2019.4*. Unity Technologies.
https://docs.unity3d.com/Manual/StandardShaderMaterialParameterNormalMap.html

Olson, Brandon R., Ryan A. Placchetti, Jamie Quartermaine, and Ann E. Killebrew
2013 The Tel Akko Total Archaeology Project (Akko, Israel): Assessing the suitability of multi-scale 3D field recording in archaeology. *Journal of Field Archaeology* 38(3): 244-262.

O'Shea, John
1989 The role of wild resources in small-scale agricultural systems: tales from the Lakes and the Plains. In *Bad Year Economics: Cultural Responses to Risk and Uncertainty*, edited by Paul Halstead and John O'Shea, pp. 57-67. Cambridge University Press, Cambridge.

Palmer, Carol, David Gilbertson, Hwedi el-Rishi, Chris Hunt, John Grattan, Sue McLaren, and Brian Pyatt
2007 The Wadi Faynan Today: Landscape, Environment, People. In *Archaeology and Desertification: The wadi Faynan Landscape Survey, Southern* Jordan, edited by Graeme Barker, David Gilbertson, and David Mattingly, pp. 27-57. Oxbow Books, Oxford.

Papadimitriou, G.
2001 Simulation Study of Ancient Bronzes: Their Mechanical and Metalworking Properties. In *Archaeometric Issues in Greek Prehistory and Antiquity*, eds. Y. Bassiakos, E. Aloupi, and Y. Facorellis, pp.713-733. Hellenic Society for Archaeometry, Athens.

Pfaffenberger, Bryan
1992 Social Anthropology of Technology. *Annual Review of Anthropology* 21: 491-516.

Pfaffenberger, Bryan
1988 Fetishised Objects and Humanised Nature: Towards an Anthropology of Technology. *Man* 23: 236-252.

Pickles, Sydney and Edgar Peltenburg
1998 Metallurgy, Society and the Bronze/Iron Transition in the East Mediterranean and the Near East. *Report of the Department of Antiquities, Cyprus* 67-100.

Pigott, Vincent C.
1982 The Innovation of Iron: Cultural Dynamics in Technological Change. *Expedition* 25: 20-25.

Pleiner, Radomir
1979 The technology of three Assyrian iron artifacts from Khorsabad. *Journal of Near Eastern Studies* 38: 83-91.

Polanyi, Karl
1944 *The Great Transformation*. Beacon Press, Boston.

Pratico, Gary D.
1985 Nelson Glueck's 1938-1940 Excavations at Tell el-Kheleifeh: A Reappraisal. *Bulletin of the American Schools of Oriental Research* 259: 1-32.

Pulak, Cemal
2005 Discovering a Royal Ship from the Age of King Tut: Uluburun, Turkey. In *Beneath the Seven Seas: Adventures with the Institute of Nautical Archaeology*, pp. 34-47, edited by G. F. Bass. Thames & Hudson Ltd, London.

Rabba', I.
1991 *The Geology of the Al Qurayqira (Jabal Hamra Faddan) Map Sheet No. 3051 II*. Geological Mapping Division Bulletin 28. Geology Directorate, Amman.

Rabinovich, Alla, Naama Yahalom-Mack, Yosef Garfinkel, Saar Ganor, and Michael G. Hasel
2019 The Metal Assemblage from Early Iron Age IIA Khirbet Qeiyafa and Its Implications for the Inception of Iron Production and Use. *Bulletin of the American Schools of Oriental Research* 382: 89-110.

Raikes, Thomas
1980 Notes on Some Neolithic and Later Sites in Wadi Araba and the Dead Sea Valley. *Levant* 12: 40-60.

Rainey, Anson F. and R. Steven Notley
2006 *The Sacred Bridge: Carta's Atlas of the Biblical World*. Carta, Jerusalem.

Rambeau, Claire and Stuart Black
2011 Paleoenvironments of the southern Levant 5,000 BP to present: linking the geological and archaeological records. In *Water, Live and Civilisation: Climate, Environment and Society in the Jordan Valley*, edited by Steven Mithen and Emily Black, pp. 94-104. Cambridge University Press, Cambridge

Redman, Charles L.
2005 Resilience Theory in Archaeology. *American Anthropologist* 107(1): 70-77.

Rees, William E.
2002 Carrying Capacity and Sustainability: Waking Malthus' Ghost. In *Introduction to Sustainable* Development, edited by David V.J. Bell, and Y. Annie Cheung. In *Encyclopedia of Life Support Systems*. Eolss Publishers, Oxford. http://www.eolss.net.

Remondino, Fabio and Stefano Campana (eds.)
2014 *3D Recording and Modelling in Archaeology and Cultural Heritage: Theory and best practices.* Bar International Series 2598. BAR Publishing, Oxford.

Renfrew, Colin
1984 *Approaches to Social Archaeology*. Edinburgh University Press, Edinburgh.

Renfrew, Colin
1972 *The Emergence of Civilization: The Cyclades and the Aegean in the Third Millennium B.C.* Methuen & Co. Ltd, London.

Rivera-Collazo, Isabel C., Cristina Rodríguez-Franco, and José Julián Garay-Vázquez
2018 A Deep-Time Socioecosystem Framework to Understand Social Vulnerability on a Tropical Island. *Environmental Archaeology* 23(1): 97-108.

Roman, Itzhak
1990 The Copper Ingots. In *The Ancient Metallurgy of Copper, Researches in the Arabah 1959-1984, Vol. 2*, edited by Beno Rothenberg, pp. 176-181. Institute for Archaeo-Metallurgical Studies, London.

Roseberry, William
1989 *Anthropologies and Histories: Essays in Culture, History, and Political Economy*. Rutgers University Press, New Brunswick.

Rosen, Arlene

2007 *Civilizing Climate: Social Responses to Climate Change in the Ancient Near East*. Rowan & Littlefield Publishers, Lanham.

Rosen, Arlene and Isabel Rivera-Collazo
2012 Climate change, adaptive cycles, and the persistence of foraging economies during the late Pleistocene/Holocene transition in the Levant. *Proceedings of the National Academy of Sciences* 109(10): 3640-3645.

Rothenberg, Beno
1996-1997 Researches in the Southern Arabah 1959–1990: Summary of Thirty Years of Archaeo-Metallurgical Field Work in the Timna Valley, the Wadi Amram and the Southern Arabah (Israel). *Arx* 2-3: 5-42.

Rothenberg, Beno (ed.)
1990a *The Ancient Metallurgy of Copper*. Researches in the Arabah 1959–1984 2; Metal in History 3. Institute for Archaeo-Metallurgical Studies, London.

Rothenberg, Beno
1990b Copper Smelting Furnaces, Tuyeres, Slags, Ingot-Moulds and Ingots in the Arabah: The Archaeological Data. In *The Ancient Metallurgy of Copper*. Edited by B. Rothenberg, pp. 1–77. Researches in the Arabah 1959–1984 2; Metal in History 3. Institute for Archaeo-Metallurgical Studies, London.

Rothenberg, Beno (ed.)
1988 *The Egyptian Mining Temple at Timna.* Researches in the Arabah 1959–1984 1; Metal in History 2. Institute for Archaeo-Metallurgical Studies, London.

Rothenberg, Beno
1972 *Were These King Solomon's Mines? Excavations in the Timna Valley*. Stein and Day, New York.

Salmon, Merrilee H.
1978 What Can Systems Theory Do for Archaeology? *American Antiquity* 43(2): 174-183.

Sauer, James A.
1986 Transjordan in the Bronze and Iron Ages: A Critique of Glueck's Synthesis. *Bulletin of the American Schools of Oriental Research* 263: 1-26.

Schilman, Bettina, Miryam Bar-Matthews, Ahuva Almogi-Labi, and Boaz Luz
2001 Global climate instability reflected by Eastern Mediterranean marine records during the Late Holocene. *Paleogeography, Paleoclimatology, Paleoecology* 176: 157-176.

Schulze, Jürgen P., Jessica Block, Philip Weber, Thomas E. Levy, Gregory L, Dawe, Brad C. Sparks, and Thomas A. DeFanti

2015 The WAVE and 3D: How the Waters Might Have Parted - Visualizing Evidence for a Major Volcanic Eruption in the Mediterranean and Its Impact on Exodus Models. In *Israel's Exodus in Transdisciplinary Perspective - Text, Archaeology, Culture, and Geoscience*, edited by Thomas E. Levy, Thomas Schneider, and William Propp, pp. 161-172. Springer International Publishing.

Schwab, Ronald, Michael Brauns, Walter Fasnacht, Susan Womer Katzev, Nicole Lockhoff, and Helena Wylde Swiny
2022 From Cyprus, or to Cyprus? A pilot study with osmium isotopy and siderophile trace elements to reconstruct the origin of corroded iron billets from the Kyrenia shipwreck. *Journal of Archaeological Science: Reports* 103365.

Schwartz, Glenn M. and John J. Nichols (eds.)
2006 *After Collapse: The Regeneration of Complex Societies*. University of Arizona Press, Tucson.

Scopigno, Roberto, Marco Callieri, Matteo Dellepiane, Federico Ponchio, and Marco Potenziani
2017 Delivering and Using 3D Models on the Web: Are We Ready? *Virtual Archaeology Review* 8(17): 1-9.

Shaar, Ron, Hagai Ron, Lisa Tauxe, Ronit Kessel, Amotz Agnon, Erez Ben-Yosef, and Joshua M. Feinberg
2010 Testing the accuracy of absolute intensity estimates of the ancient geomagnetic field using copper slag material. *Earth and Planetary Science Letters* 209: 201-213.

Sherratt, Susan, and Andrew Sherratt
1991 From Luxuries to Commodities: The Nature of Mediterranean Bronze Age Trading Systems. In *Bronze Age Trade in the Mediterranean*, pp. 351- 386, edited by N. H. Gale. Paul Åströms Förlag, Jonsered.

Simon, Herbert
1962 The Architecture of Complexity. *Proceedings of the American Philosophical Society* 106(6): 467-482.

Smith, Mike, Peter Veth, Peter Hiscock, and Lynley A. Wallis
2007 Global Deserts in Perspective. In *Desert Peoples: Archaeological Perspectives*, edited by Peter Veth, Mike Smith, and Peter Hiscock, pp. 1-14. Blackwell Publishing, Malden.

Smith, Neil G. and Thomas E. Levy
2014 ArchField in Jordan: Real-time GIS Data Recording for Archaeological Excavations. *Near Eastern Archaeology* 77: 166-170

Smith, Neil G. and Thomas E. Levy

2012 Real-Time 3D Archaeological Field Recording: ArchField, An Open-Source GIS System Pioneered in Jordan. *Antiquity* 85: on-line http://antiquity.ac.uk/projgall/smith331/.

Smith, Neil G., and Thomas E. Levy
2008 The Iron Age Pottery from Khirbat en-Nahas, Jordan: A Preliminary Study. *Bulletin of the American Schools of Oriental Research* 352: 41-91.

Smith, Neil G., Yuval Goren, and Thomas E. Levy
2014 The Petrography of Iron Age Edom: From the Lowlands to the Highlands. In *New Insights into the Iron Age Archaeology of Edom, Southern Jordan (Volume 1)*, edited by Thomas E. Levy, Mohammad Najjar, and Erez Ben-Yosef, pp. 461-491. UCLA Cotsen Institute of Archaeology Press, Los Angeles.

Smith, Neil G., Mohammad Najjar, and Thomas E. Levy
2014 A Picture of the Early and Late Iron Age II in the Lowlands: Preliminary Soundings at Rujm Hamra Ifdan. In *New Insights into the Iron Age Archaeology of Edom, Southern Jordan (Volume 2)*, edited by Thomas E. Levy, Mohammad Najjar and Erez Ben-Yosef, pp. 723-739. UCLA Cotsen Institute of Archaeology Press, Los Angeles.

Snodgrass, Anthony M.
1982 Cyprus and the Beginnngs of Iron Technology in the Eastern Mediterranean. In *Early Metallurgy in Cyprus, 4000-500 BC*, edited by James D. Muhly, Robert Maddin, and Vassos Karageorghis, pp. 285-295. Pierides Foundation, Nicosia.

Starley, David
1995 Hammerscale. *The Historical Metallurgy Society: Archaeology Datasheet* 10.

Stöllner, Thomas R.
2014 Methods in Mining Archaeology (Montanarchäologie). In *Archaeometallurgy in Global Perspective: Methods and Syntheses*, edited by Benjamin W. Roberts and Christopher P. Thornton, pp. 133-159. Springer, New York.

Sukenik, Naama, David Iluz, Zohar Amar, Alexander Varvak, Orit Shamir, and Erez Ben-Yosef
2021 Early evidence of royal purple dyed textile from Timna Valley (Israel). *PLoS ONE* 16(1): e0245897.

Tainter, Joseph
2016 Why Collapse is so Difficult to Understand. In *Beyond Collapse: Archaeological Perspectives on Resilience, Revitalization, and Transformation in Complex Societies*, edited by Ronald Faulseit, pp. 27-39. Southern Illinois University Press, Carbondale.

Tainter, Joseph
2014 Collapse and Sustainability: Rome, the Maya, and the Modern World. *Archaeological Papers of the American Anthropological Association* 24: 210-214.

Tainter, Joseph
2012 Theories of the Collapse of States. In *The Oxford Companion to Archaeology, Second Edition*, edited by Neil A. Silberman, Alex B. Bauer, Margarita Diaz-Andreu, Cornelius Holtorf, and Emma Waterron, pp. 221-224. Oxford University Press, Oxford.

Tainter, Joseph
2006 Archaeology of Overshoot and Collapse. *Annual Review of Anthropology* 35: 59-74.

Tainter, Joseph
1988 *The Collapse of Complex Societies*. Cambridge University Press, Cambridge.

Tebes, Juan Manuel
2021 A Reassessment of the Chronology of the Iron Age Site of Khirbat en-Nahas, Southern Jordan. *Palestine Exploration Quarterly*.

Tylecote, Ronald F.
1992 *A History of Metallurgy, 2 ed*. Maney, London.

Tylecote, Ronald F. and P.J. Boydell
1978 Experiments on Copper Smelting Based on Early Furnaces Found at Timna. In *Chalcolithic Copper Smelting, Excavations and* Experiments, edited by Beno Rothenberg, pp. 27-49. Institute for Archaeo-Metallurgical Studies, London.

Tylecote, Ronald F., H.A. Ghaznavi, and P.J. Boydell
1977 Partitioning of Trace Elements Between the Ores, Fluxes, Slags and Metal During the Smelting of Copper. *Journal of Archaeological Science* 4: 305-333.

Vaelske, Veit, Michael Bode, and Christian E. Loeben
2019 Early Iron Age Copper Trail Between Wadi Arabah and Egypt During the 21st Dynasty: First Results from Tanis, ca. 1000 BC. *Zeitschrift für Orient-Archäologie* 12: 184-203.

Veldhuijzen, Harald Alexander
2009 Red hot: the smithy at Tel Beth-Shemesh. *Near Eastern Archaeology* 72: 129-131.

Veldhuijzen, Harald Alexander and Thilo Rehren
2007 Slags and the city: early iron production at Tell Hammeh, Jordan, and Tel Beth-Shemesh, Israel. In *Metals and Mines – Studies in Archaeometallurgy*, edited by S. La Niece, D.R. Hook, and P.T. Craddock, pp. 189-201. Archetype Publications, London.

Vincent, Monique, Matthew L. Vincent, and Jillian R. Logee
2015 Balking at Balks: New Approaches to Section Drawings. Poster. *American Schools of Oriental Research Annual Meeting.*

Waldbaum, Jane C.

1999 Copper, Iron, Tin, Wood: The Starts of the Iron Age in the Eastern Mediterranean. *Archaeomaterials* 3: 111-122.

Waldbaum, Jane C.
1980 The First Archaeological Appearance of Iron. In *The Coming of the Age of Iron,* edited by T. Wertime and J. Muhly, pp. 69-98. Yale University Press, New Haven.

Ward, William A.
1992 Shasu. In *The Anchor Bible Dictionary: Volume 5*, edited by David Noel Freedman, pp. 1165-1167. Doubleday, New York.

Wassilkowska, Anna, Anna Czaplicka-Kotas, Michał Zielina, and Andrzej Bielski
2014 An analysis of the elemental composition of micro-samples using EDS technique. *Technical Transactions* 111(1-Ch): 133-148.

Weik, T.M.
2014 The Archaeology of Ethnogenesis. *Annual Review of Anthropology* 43: 291-305.

Wiener, M.H.
2018 The Collapse of Civilizations. *Belfer Center for Science and International Affairs Harvard Kennedy School Paper* 1-22.

Weippert, Manfred
1982 Remarks on the History of Settlement in Southern Jordan during the Early Iron Age. *Studies in the History and Archaeology of Jordan* I: 153-162.

Weisgerber, Gerd
2006 The mineral wealth of ancient Arabia and its use IL Copper mining and smelting at Feinan and Timna – comparison and evaluation of techniques, production, and strategies. *Arabian Archaeology and Epigraphy* 17(1): 1-30

Wertime, Theodore A.
1980 The Pyrotechnological Background. In *The Coming of the Age of Iron*, edited by T.A. Wertime and J.D. Muhly, pp. 1-24. Yale University Press, New Haven.

Wertime, Theodore A., and James D. Muhly
1980 *The Coming of the Age of Iron*. Yale University Press, New Haven.

"What's In a Name? The Many Names of Feynan"
2014 *Feynan Ecolodge*, https://ecohotels.me/news-and-promotions/whats-name-many-names-feynan.

Wilson, John A.
1969 Egyptian Historical Texts. In *Ancient Near Eastern Texts Relating to the Old Testament, 3rd Edition with Supplement,* edited by James B. Pritchard, pp. 227-264. Princeton University Press, Princeton.

Workman, Vanessa, Aren M. Maeir, Amit Dagan, Johanna Regev, Elisabetta Boaretto, and Adi Eliyahu-Behar.
2020 An Iron IIA Iron and Bronze Workshop in the Lower City of Tell es-Safi/Gath. *Tel Aviv* 47(2): 208-36.

Yagel, Omri A., Erez Ben-Yosef, and Paul T. Craddock
2016 Late Bronze Age copper production in Timna: new evidence from Site 3. *Levant* 48(1): 33-51.

Yahalom-Mack, Naama, and Irina Segal
2018 The Origin of Copper Used in Canaan during the Late Bronze/Iron Age Transition. In *Mining for Ancient Copper: Essays in Honor of Beno Rothenberg*, edited by Erez Ben-Yosef, pp. 313-331. Eisenbrauns, Winona Lake.

Yahalom-Mack, Naama and Adi Eliyahu-Behar
2015 The Transition from Bronze to Iron in Canaan: Chronology, Technology, and Context. *Radiocarbon* 57: 285-305.

Yahalom-Mack, Naama, D.M. Finn, Yigal Erel, Ofir Tirosh, Ehud Galili, and Assaf Yasur-Landau
2022 Incised Late Bronze Age lead ingots from the southern anchorage of Caesarea. *Journal of Archaeological Science: Reports* 41: 103321.

Yahalom-Mack, Naama, Ehud Galili, Irina Segal, Adi Eliyahu-Behar, Elisabetta Boaretto, Sana Shilstein, and Israel Finkelstein
2014a New Insights into Levantine Copper Trade: Analysis of Ingots from the Bronze and Iron Ages in Israel. *Journal of Archaeological Science* 45: 159-177.

Yahalom-Mack, Naama, Yuval Gadot, Adi Eliyahu-Behar, Shlomit Bechar, Sana Shilstein, and Israel Finkelstein
2014b Metalworking at Hazor: A Long-Term Perspective. *Oxford Journal of Archaeology* 33(1): 19-45.

Yakar, Jak
2006 Dating the Sequence of the Final Destruction/Abandonment of LBA Settlements: Towards a Better Understanding of Events that led to the Collapse of the Hittite Kingdom. In *Strukturierung und datierung in der hethitischen Archaeologie/Structure and dating in Hittite Archaeology*, edited by D.P. Mielke, U.D. Schoop, and J. Seeher, pp. 33-51. BYZAS 4, Istanbul.

Yoffee, Norman.
2005 *Myths of the Archaic State: Evolution of the Earliest Cities, States, and Civilizations*. Cambridge University Press, Cambridge.

Yoffee, Norman

1988 Orienting Collapse. In *The Collapse of Ancient States and Civilizations*, edited by Norman Yoffee and George L. Cowgill, pp. 1-19. University of Arizona Press, Tucson.

Yoffee, Norman, and George L. Cowgill.
1988 *The Collapse of Ancient States and Civilizations*. University of Arizona Press, Tucson.

Zaccagnini, Carlo
1990 The Transition from Bronze to Iron in the Near East and in the Levant: Marginal Notes. *Journal of the American Oriental Society* 110: 493-502.

Zucconi, Laura M.
2007 From the Wilderness of Zin alongside Edom: Edomite Territory in the Eastern Negev during the Eight-Sixth Centuries B.C.E. In *Milk and Honey: Essays on Ancient Israel and the Bible in Apreciation of the Judaic Studies Program at the University of California, San Diego*, edited by Sarah Malena and David Miano, pp. 241-256. Eisenbrauns, Winona Lake.